(12) INTERNATIONAL APPLICATION PUBLISHED UNDER THE PATENT COOPERATION TREATY (PCT)

(19) World Intellectual Property Organization
International Bureau

(43) International Publication Date
09 December 2021 (09.12.2021)

WIPO | PCT

(10) International Publication Number
WO 2021/247925 A1

(51) International Patent Classification:
A61P 31/14 (2006.01) *C07K 16/10* (2006.01)

(21) International Application Number:
PCT/US2021/035782

(22) International Filing Date:
03 June 2021 (03.06.2021)

(25) Filing Language: English

(26) Publication Language: English

(30) Priority Data:

63/034,326	03 June 2020 (03.06.2020)	US
63/055,861	23 July 2020 (23.07.2020)	US
63/058,368	29 July 2020 (29.07.2020)	US
63/066,093	14 August 2020 (14.08.2020)	US
63/070,803	26 August 2020 (26.08.2020)	US
63/078,157	14 September 2020 (14.09.2020)	US
63/166,874	26 March 2021 (26.03.2021)	US

(71) Applicants: **VIR BIOTECHNOLOGY, INC.** [US/US]; 499 Illinois Street, Suite 500, San Francisco, California 94158 (US). **UNIVERSITY OF WASHINGTON** [US/US]; 4545 Roosevelt Way NE, Suite 400, Seattle, Washington 98105 (US). **HUMABS BIOMED SA** [CH/CH]; Via dei Gaggini 3, 6500 Bellinzona (CH).

(72) Inventors; and

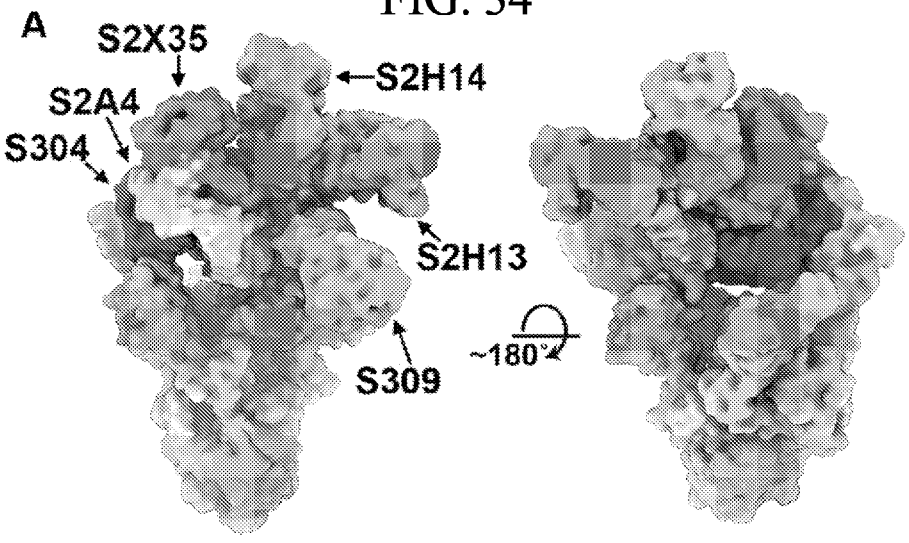
(71) Applicants: **CORTI, Davide** [IT/CH]; Via dei Gaggini 3, 6500 Bellinzona (CH). **SNELL, Gyorgy** [US/US]; 499 Illinois Street, Suite 500, San Francisco, California 94158 (US). **CZUDNOCHOWSKI, Nadine** [DE/US]; 499 Illinois Street, Suite 500, San Francisco, California 94158 (US). **VEESLER, David** [FR/US]; 4545 Roosevelt Way NE, Suite 400, Seattle, Washington 98105 (US). **WALLS, Alexandra C.** [US/US]; 4545 Roosevelt Way NE, Suite 400, Seattle, Washington 98105 (US). **PARK, Young-Jun** [KR/US]; 4545 Roosevelt Way NE, Suite 400, Seattle, Washington 98105 (US). **TORTORICI, M. Alejandra** [US/US]; 4545 Roosevelt Way NE, Suite 400, Seattle, Washington 98105 (US).

(74) Agent: **MORGAN, John, A.** et al.; Seed Intellectual Property Law Group LLP, Suite 5400, 701 Fifth Avenue, Seattle, Washington 98104-7064 (US).

(81) Designated States *(unless otherwise indicated, for every kind of national protection available)*: AE, AG, AL, AM, AO, AT, AU, AZ, BA, BB, BG, BH, BN, BR, BW, BY, BZ, CA, CH, CL, CN, CO, CR, CU, CZ, DE, DJ, DK, DM, DO, DZ, EC, EE, EG, ES, FI, GB, GD, GE, GH, GM, GT, HN, HR, HU, ID, IL, IN, IR, IS, IT, JO, JP, KE, KG, KH, KN, KP, KR, KW, KZ, LA, LC, LK, LR, LS, LU, LY, MA, MD, ME, MG, MK, MN, MW, MX, MY, MZ, NA, NG, NI, NO, NZ, OM, PA, PE, PG, PH, PL, PT, QA, RO, RS, RU, RW,

(54) Title: STRUCTURE-GUIDED IMMUNOTHERAPY AGAINST SARS-COV-2

FIG. 34



(57) Abstract: The instant disclosure provides antibodies and antigen-binding fragments thereof that can bind in certain regions of a SARS-CoV-2 S glycoprotein and can neutralize a SARS-CoV-2 infection. Also provided are immunogenic compositions that comprise a SARS-CoV-2 S glycoprotein or a portion thereof that is capable of being bound by an antibody or antigen-binding fragment.

WO 2021/247925 A1

[Continued on next page]

SA, SC, SD, SE, SG, SK, SL, ST, SV, SY, TH, TJ, TM, TN, TR, TT, TZ, UA, UG, US, UZ, VC, VN, WS, ZA, ZM, ZW.

(84) **Designated States** *(unless otherwise indicated, for every kind of regional protection available)*: ARIPO (BW, GH, GM, KE, LR, LS, MW, MZ, NA, RW, SD, SL, ST, SZ, TZ, UG, ZM, ZW), Eurasian (AM, AZ, BY, KG, KZ, RU, TJ, TM), European (AL, AT, BE, BG, CH, CY, CZ, DE, DK, EE, ES, FI, FR, GB, GR, HR, HU, IE, IS, IT, LT, LU, LV, MC, MK, MT, NL, NO, PL, PT, RO, RS, SE, SI, SK, SM, TR), OAPI (BF, BJ, CF, CG, CI, CM, GA, GN, GQ, GW, KM, ML, MR, NE, SN, TD, TG).

Published:

— *with international search report (Art. 21(3))*
— *before the expiration of the time limit for amending the claims and to be republished in the event of receipt of amendments (Rule 48.2(h))*
— *with sequence listing part of description (Rule 5.2(a))*

STRUCTURE-GUIDED IMMUNOTHERAPY AGAINST SARS-COV-2

STATEMENT REGARDING SEQUENCE LISTING

The Sequence Listing associated with this application is provided in text format in lieu of a paper copy, and is hereby incorporated by reference into the specification. The name of the text file containing the Sequence Listing is 930585_412WO_SEQUENCE_LISTING.txt. The text file is 206 KB, was created on June 2, 2021, and is being submitted electronically via EFS-Web.

BACKGROUND

A novel betacoronavirus emerged in Wuhan, China, in late 2019. As of May 29, 2021, approximately 169,600,000 cases of infection by this virus (termed, among other names, SARS-CoV-2 and Wuhan coronavirus), were confirmed worldwide, and had resulted in approximately 3,500,000 deaths. Therapies for preventing or treating SARS-CoV-2 infection are needed.

BRIEF DESCRIPTION OF THE DRAWINGS

Figures 1A and 1B show data from a neutralization of infection assay using SARS-CoV-2 virus. Serial dilutions of human monoclonal antibodies were incubated with 10^2 focus-forming units of SARS-CoV-2 strain 2019n-CoV/USA_WA1/2020 (obtained from the CDC) for 1 hour at 37 °C. SARS-CoV-2-infected cell foci were visualized using TruBlue peroxidase substrate (KPL) and quantitated on an ImmunoSpot microanalyzer (Cellular Technologies). Data were processed using Prism software (GraphPad Prism 8.0). Figure 1A shows results for four exemplary antibodies and comparator antibody S309. Figure 1B shows results for six exemplary antibodies, with calculated EC50 values to the right of the graph.

Figure 2 shows neutralization of SARS-CoV-2 infection by monoclonal antibodies S309, S2H14, and S2X2. The antibodies were tested individually (left

panel), in two-antibody combinations (center panel), and in a three-antibody combination (right panel). For combinations, antibodies were used at 1:1 and 1:1:1 ratios. Calculated EC50 values for each antibody or antibody combination are shown below each graph.

Figure 3 shows neutralization of SARS-CoV-2 infection by monoclonal antibodies S309, S2H14, and S2A4. The antibodies were tested individually, in two antibody combinations, and in a three-antibody combination, as shown in the legend. For combinations, S2H14 and/or S2A4 were used at a concentration of 5 μg/ml and S309 was used at the concentrations indicated on the x-axis.

Figure 4 summarizes results of quantitative epitope-specific serology studies using monoclonal antibody S309 and other anti-Spike antibodies, as determined by binding competition, cryo-EM, and crystallography data. Underlined and bolded antibodies are cross-reactive with SARS-CoV-1.

Figures 5A-5C show data from a neutralization of infection assay using SARS-CoV-2 virus. Serial dilutions of human monoclonal antibodies were incubated with 102 focus-forming units of SARS-CoV-2 strain 2019n-CoV/USA_WA1/2020 (obtained from the CDC) for 1 hour at 37 °C. SARS-CoV-2-infected cell foci were visualized using TruBlue peroxidase substrate (KPL) and quantitated on an ImmunoSpot microanalyzer (Cellular Technologies). Data were processed using Prism software (GraphPad Prism 8.0). Figure 5A shows results for antibody S2X190 and four comparator antibodies. Figure 5B shows results for antibody S2X129 and four comparator antibodies. Figure 5C shows results for antibodies S2X132 and S2X127, along with 4 comparator antibodies. Calculated EC50 values are shown to the right of each graph.

Figure 6 shows a cryoEM structure of the prefusion SARS-CoV-2 S ectodomain trimer with three S2X259 Fab fragments bound to three open RBDs viewed along two orthogonal orientations. N-linked glycans are rendered as dark grey spheres. As discussed further herein, S2X259 recognizes a glycan-free, cryptic epitope within antigenic site IIa, which was defined based on the S2X35 mAb isolated from the same donor (See Piccoli *et al*. Mapping Neutralizing and Immunodominant Sites on the

SARS-CoV-2 Spike Receptor-Binding Domain by Structure-Guided High-Resolution Serology. *Cell* 183, 1024-1042.e21 (2020)). S2X259 binding appears to require opening of two RBDs to grant access to the Fab in the context of the S trimer. S2X259 contacts the RBD using both heavy and light chains, which contribute approximately two thirds and one third of the ~950 Å2 paratope surface buried upon binding, respectively. S2X259 uses complementary determining regions (CDRs) H1-H3, L1 and L3 to contact RBD residues 369-386, which form two α-helices and an intervening β-strand belonging to the structurally conserved RBD β-sheet, as well as the residues 404-411 and 499-508 which form a continuous surface made up of an α-helix and a loop followed by an α-helix, respectively.

Figure 7 shows a model of S2X259 binding with SARS-CoV-2 RBD. The binding pose involves contacts with multiple RBD regions. Residues corresponding to prevalent RBD mutations are shown as light grey spheres. N-linked glycans are rendered as dark grey spheres.

Figure 8 shows selected interactions formed between S2X259 and the SARS-CoV-2 RBD.

Figure 9 shows a map of mutations reducing S2X259 binding using DMS. Mean mutation effect on ACE2 affinity, RBD folding, and predicted contribution to S2X259 binding for substitutions at each position in the S2X259 epitope is shown. Mutations introducing a N-linked glycosylation sites that may not be tolerated in full spike are indicated with *.

Figure 10 shows selection of the G504D mutation as single neutralization escape mutant using a replicating SARS-CoV-2 S VSV system.

Figure 11 shows a detailed view of the S2X259/RBD interface showing G504D in RBD.

Figures 12A and 12B show data from neutralization tests with S2E12 and S230 control mAbs against VSV pseudotypes harbouring the S glycoprotein of SARS-CoV-1 and SARS-CoV-2 related strains and VOCs. Figure 12A shows data for SARS-CoV-2 and SARS-CoV-2 variants. Figure 12B shows data for SARS-CoV-1 and related strains.

Figure 13 shows representative electron micrographs (upper panels) and class averages (lower panels) of SARS-CoV-2 S in complex with the S2X259 Fab.

Figure 14 shows gold-standard Fourier shell correlation curves for the S trimer bound to three S2X259 Fabs (solid black line) and the locally refined reconstruction of the RBD/S2X259 variable domains. The 0.143 cutoff is indicated by horizontal dashed lines.

Figure 15 shows a local resolution map for the open S trimer bound to three S2X259 (left panel) and the locally refined reconstruction of the RBD/S2X259 variable domains (right panel).

Figure 16 shows the cryoEM data processing flow-chart.

Figure 17 shows a ribbon diagram showing a superimposition of the S2X259-bound and S2A4-bound (PDB 7JVA) SARS-CoV-2 RBD (Piccoli et al 2020). The SARS-CoV glycan at position N357 was modelled based on the S230-bound SARS-CoV S structure (PDB 6NB630) and is predicted to sterically hinder S2A4 binding (red star) but not S2X259. A portion of the mAb heavy chains are indicated with arrows; S2X259 light chain is adjacent the S2X259 heavy chain and shown at the upper left portion of the figure; a portion of the S2A4 light chain is shown generally beneath the S2X259 light chain portion. N-linked glycans are rendered as dark spheres.

Figure 18 shows S2X259 Fc-mediated activation of FcγRIIa and FcγRIIIa *in vitro*. NFAT-driven luciferase signal induced in Jurkat cells stably expressing FcγRIIa H131 (left panel) variant or FcγRIIIa V158 (right panel) variant by S2X259 binding to full-length wild-type SARS-CoV-2 S on ExpiCHO target cells. SE12, S2M11, S309, S309-GRLR mAbs are included as controls.

Figure 19 shows S2X259 Fc-mediated activation of FcγRIIa and FcγRIIIa in vitro. NFAT-driven luciferase signal induced in Jurkat cells stably expressing FcγRIIa H131 (left panel) variant or FcγRIIIa V158 (right panel) variant by S2X259 binding to uncleavable full-length pre-fusion stabilized SARS-CoV-2 S (unable to release the S1 subunit) transiently expressed in ExpiCHO cells. SE12, S2M11, S309, and S309-GRLR mAbs are included as controls.

Figure 20 shows site I-targeting SE12, site II-targeting S2X259, and site IV-targeting S309 mAb binding to immobilized SARS-CoV-2 RBD.

Figure 21 shows RBD binding to S2X259 and ACE2. S2X259 and ACE2 bind partially overlapping binding sites on the SARS-CoV-2 RBD.

Figures 22A and 22B show biolayer interferometry binding analysis of the S2X259 Fab to wildtype or VOC SARS-CoV-2 biotinylated RBDs immobilized at the surface of SA biosensors. Figure 22A shows analysis of S2X259 Fab binding to SARS-CoV-2 wildtype RBD (left graph) and SARS-CoV-2 variant B.1.1.7 RBD (right graph). Figure 22B shows analysis of S2X259 Fab binding to SARS-CoV-2 variant B.1.351 (left graph) and SARS-CoV-2 variant P.1 (right graph).

Figures 23A-23C show description of cohorts of SARS-CoV-2-infected individuals. (A) Summary of patient demographics. (B) Age distribution of hospitalized, symptomatic and asymptomatic individuals. (C) Time interval between the date of sample collection and the date of symptom onset.

Figures 24A-24G show analysis of serum/plasma IgG binding titers to SARS-CoV-2 and SARS-CoV antigens. (A–C) IgG (A), IgA (B) and IgM (C) binding titers to SARS-CoV-2 S, RBD and N from 67 and 154 samples collected from hospitalized and symptomatic individuals, respectively, whose date of symptom onset was known. (D) Correlation between SARS-CoV-2 S- and N-specific IgG binding titers (ED50). (E and F) IgG binding titers to SARS-CoV-2 and SARS-CoV S (E) and RBD (F) from 19 hospitalized, 130 symptomatic and 8 asymptomatic individuals. (G) Ratios of SARS-CoV-2/SARS-CoV S and RBD IgG binding titers.

Figures 25A-25J show characteristics of six probe monoclonal antibodies used for structural and epitope-mapping studies. (A) V(D)J usage, percentage identity to germline, number of somatic mutations, source and time interval between sample collection and mAb isolation, RBD site recognized and neutralization potency of the 6 mAbs. B mem, memory B cell; PC, plasma cells. (B) Binding of the 6 mAbs to the SARS-CoV-2 (up) or SARS-CoV (down) RBD analyzed by ELISA. (C) Competition matrix for binding of each of the six mAbs in presence of another mAb evaluated by biolayer interferometry. (D) mAb-mediated inhibition of RBD binding to ACE2

analyzed by ELISA. (E) mAb-mediated S1 subunit shedding from cell-surface expressed SARS-CoV-2 S as determined by flow-cytometry. (F) Conservation of RBM and epitope residues in ~74,000 SARS-CoV-2 sequences (GISAID, August 11th, 2020). RBM and epitope residues are shown as gray bars. Black bars indicate variant prevalence for epitope residues with at least 2 variants. RBM residues were determined from PDB 6M0J using a 5.0A° distance cutoff between RBD and ACE2 residues using MOE. (G) Western-blot analysis (top) of the prefusion-stabilized SARS-CoV-2 S ectodomain trimer in presence of S2A4, S304 or S2X35 Fab after incubation for the indicated amount of times. Red ponceau staining (bottom) of the SDS-PAGE gel used for carrying out the western blot confirming the presence of added Fabs when indicated. (H) Analysis of activation of FcγRIIIa (V158 allele) expressed on Jurkat cells by SARS-CoV-2 S stably transfected CHO cells incubated with mAbs. GRLR indicates an antibody Fc variant carrying mutations that abolish binding to FcγRs. (I) Analysis of activation of FcγRIIa (H131 allele), expressed on Jurkat cells by SARS-CoV-2 S stably transfected CHO cells incubated with mAbs. (J) Killing of SARS-CoV-2 S stably transfected CHO cells by mAbs in the presence of complement (CDC assay).

Figures 26A-26B show conservation analysis across Clades of Sarbecoviruses. (A-1-A-4) S glycoprotein residues making contact with S304, S2H13, S2H14 or S2A4 across sarbecovirus clades. Residue numbers for both SARS-CoV-2 S and SARS-CoV S are shown. Multiple sequence alignment was performed using MAFFT. A dash represents the same residue, a strikethrough represents a gap. Asterisk (*) indicates manually aligned residues. Civet SARS-CoV is SARS-CoV HC/SZ/61/03 and raccoon dog SARS-CoV is SARS-CoV A031G. (B) Identity and similarity of SARS-CoV-2 S, RBD, RBM and mAb epitopes across select sequences of the 3 sarbecovirus clades. Values were calculated using EMBOSS Needle. The insertion in the S2A4 epitope for the Clade 1 sarbecoviruses was not included in the calculation.

Figures 27A and 27B show analysis of Fab and IgG binding to the prefusion SARS-CoV-2 S ectodomain trimer and recombinant RBD at neutral and acidic pH analyzed by surface plasmon resonance. (A and B) SARS-CoV-2 S or RBD was captured on the sensor chip surface and binding at multiple mAb concentrations was

measured. Neutral pH measurements were performed in multi-cycle format (A) and acidic pH measurements in single-cycle format (B). All data have been fit to a 1:1 binding model, which is an approximation for the S-binding data, since the kinetics incorporate conformational dynamics between open and closed RBD states, and because IgG binding involves avidity. The solid gray horizontal line gives the predicted maximum signal (saturation) based on each fit; the dashed line shows the S309 maximum binding for comparison. Asterisk indicates where a high concentration of S304 IgG was binding to the reference surface (fit was to the first two concentrations only). All mAbs bind similarly to the RBD at both pHs, but the mAbs that bind to only open RBD show a maximum below S309 in the context of the S trimer. This difference is dramatic at acidic pH where RBDs are primarily in the closed state (Zhou et al., 2020b). S2X35 was an exception, likely because its very slow off rate allows it to bias the S equilibrium toward open RBD.

Figures 28A-28I shows analysis of the specificity of IgG, IgA, and IgM serum/plasma Abs from a panel of 647 hospitalized, symptomatic, and asymptomatic SARS-CoV-2-infected individuals. (A–C) Binding titers (ED50) of antigen-specific IgG (A), IgA (B), or IgM (C) were measured in plasma or sera from convalescent SARS-CoV-2 patients (47 hospitalized, 556 symptomatic, and 44 asymptomatic) and from pre-pandemic healthy donors (n = 32). A cut-off of 30 was determined based on signal of prepandemic samples and binding to uncoated ELISA plates. (D) Binding titers (ED50) of S- and N-specific IgGs measured in sera from symptomatic and asymptomatic SARS-CoV-2-infected individuals from the Ticino healthcare workers cohort (n = 459) categorized according to symptoms severity, as described in the methods. (E) IgG binding titers to SARS-CoV-2 RBD (left) and SARS-CoV-2 S pseudovirus neutralizing titers (ID80, center) before and after depletion of RBD-specific Abs from 21 SARS-CoV-2 immune plasma samples. The percentage of depletion of binding and neutralizing Abs (right) for each sample tested is shown on the right. (F) Ab-mediated inhibition of SARS-CoV-2 RBD binding to solid phase ACE2, as determined by ELISA. Shown is the reciprocal plasma or serum dilution that blocks 80% binding (BD80) of RBD to human ACE2. (G) Ab-mediated inhibition of SARS-

CoV-2 RBD binding to solid phase ACE2 in the Ticino healthcare workers cohort determined as in (F). A cut-off of 10 was used to separate neutralizing from non-neutralizing titers. (H) Correlation analysis between levels of plasma/serum RBD-specific IgG (ED50) and the titers of Abs blocking RBD attachment to ACE2 (BD80). (I) Correlation analysis between plasma/serum neutralizing Ab titers (ID80) and the titers of Abs blocking RBD attachment to ACE2 (BD80).

Figures 29A-29H show kinetics of IgG Responses Specific for the SARS-CoV-2 RBD and Blocking RBD Attachment to ACE2. (A) Binding titers (ED50) of serum or plasma IgG to the SARS-CoV-2 RBD measured at two time points separated by an average time of 44 days in 368 subjects. T1, time of first blood draw; T2, time of second blood draw. (B) Variation of RBD-specific IgG binding titers from T1 to T2. (C) Kinetics of RBD- and N-specific IgG responses in serum or plasma from 24 convalescent individuals (red, hospitalized; blue, symptomatic non-hospitalized). The starting time point corresponds to the date of collection of the first sample. (D) Model predicted longitudinal decline of RBD- and N-specific IgG binding titers from 18 convalescent individuals with respect to the onset of symptoms from infection. Symbols, observations; shaded region, 90% prediction interval; line, median prediction. (E) Serum or plasma titers of Abs blocking RBD attachment to ACE2 (BD80) measured at T1 and T2. (F) Variation of RBD-specific IgG binding titers and titers of Abs blocking RBD attachment to ACE2 (BD80) from T1 to T2. (G) Avidity index of serum IgG binding to RBD (%) measured at T1 and T2. (H) Variation of avidity index of IgG binding to RBD (%) from T1 to T2.

Figures 30A-30H show that S2H13 mAb inhibits SARS-CoV-2 by blocking attachment to ACE2 via recognition of an epitope accessible in the open and closed S conformations. (A) SARS-CoV-2 S pseudovirus neutralization assay indicating an IC50 of 500 ng/mL. (B and C) Molecular surface representation of the SARS-CoV-2 S/S2H13 Fab complex structure with three RBDs closed shown in two orthogonal orientations. (D) Molecular surface representation of the SARS-CoV-2 S/S2H13 Fab complex structure with one RBD open. Each SARS-CoV-2 protomer of the trimer is shaded differently, and N-linked glycans are rendered as dark spheres. The S2H13 light

and heavy chain variable domains are identified – light chain variable domain with lighter shading, heavy chain variable domain with darker shading. (E) S2H13 recognizes a crevice formed by the SARS-CoV-2 RBM. Selected side chains at the interface are shown. (F) S2H13 and ACE2 (dark green) bind overlapping RBM epitope. The star indicates steric clashes. (G) BLI binding competition between S2H13 and ACE2 for binding to the SARS-CoV-2 RBD. (H) Molecular surface representation of the SARS-CoV-2 RBD (gray) with the S2H13 epitope colored by residue conservation across SARS-CoV-2 isolates and SARS-CoV.

Figures 31A-31I show that S2H14 mAb inhibits SARS-CoV-2 by blocking attachment to the ACE2 receptor. (A) SARS-CoV-2 S pseudovirus neutralization assay indicating an IC50 of 900 ng/mL. (B and C) Molecular surface representation of the SARS-CoV-2 S/S2H14 Fab complex structure with two RBDs open and one RBD closed viewed along two orthogonal orientations. (D and E) Molecular surface representation of the SARS-CoV-2 S/S2H14 Fab complex structure with three RBDs open shown in two orthogonal orientations. Each SARS-CoV-2 protomer is shaded distinctly, and N-linked glycans are rendered as dark spheres. The S2H14 light and heavy chain variable domains are shaded distinctly. (F) S2H14 binds to an epitope within the SARS-CoV-2 RBM. (G) S2H14 and ACE2 bind overlapping RBM epitope. The red star indicates steric clashes. (H) BLI binding competition between S2H14 and ACE2 for binding to the SARS-CoV-2 RBD. (I) Molecular surface representation of the SARS-CoV-2 RBD (gray) with the S2H14 epitope colored by residue conservation across SARS-CoV-2 isolates and SARS-CoV.

Figures 32A-32H show that S2A4 mAb promotes SARS-CoV-2 S opening through binding to a cryptic epitope. (A) SARS-CoV-2 S pseudovirus neutralization assay indicating an IC50 of 3.5 mg/mL. (B and C) Molecular surface representation of the SARS-CoV-2 S/S2A4 Fab complex cryo-EM structure with three RBDs open viewed along two orthogonal orientations. Each SARS-CoV-2 protomer is shaded distinctly, and N-linked glycans are rendered as dark spheres. The S2A4 light and heavy chain variable domains are shaded differently, as shown in the figure key. (D and E) Detailed views of the contacts formed between S2A4 and the RBD with selected

side chains shown. (F) S2A4 and ACE2 bind distinct RBD epitopes but would clash via steric hindrance. The star indicates steric clashes. (G) BLI binding competition between S2A4 and ACE2 for binding to the SARS-CoV-2 RBD. (H) Molecular surface representation of the SARS-CoV-2 RBD (gray) with the S2A4 epitope colored by amino acid residue conservation with SARS-CoV. The position of the SARS-CoV N357 glycan is indicated with red dotted lines.

Figures 33A-33H show that S304 mAb promotes SARS CoV-2 S Opening through binding to a cryptic epitope conserved within the Sarbecovirus subgenus. (A and B) Molecular surface representation of the SARS-CoV-2 S/S304 Fab complex cryo-EM structure with three RBDs opened viewed along two orthogonal orientations. Each SARS-CoV-2 S protomer is shaded distinctly (see figure key), and N-linked glycans are rendered as dark spheres. The S304 light and heavy chains are shaded differently, as shown in the figure key. (C) Cryo-EM reconstruction of the S1 subunit trimer (with disordered S2) bound to three S304 Fabs viewed along two orthogonal orientations and the corresponding atomic model fit in density. Each SARS-CoV-2 S1 protomer is shaded distinctly. The S304 light and heavy chain variable domains are shaded distinctly. (D) Ribbon diagram of the crystal structure of S304, S2H14, and S309 in complex with the SARS-CoV-2 RBD. Only the S304 variable domains are shown, whereas S2H14 and S309 were omitted for clarity. (E) Positioning of ACE2 relative to the S304 Fab bound to the SARS-CoV-2 RBD. ACE2 N-linked glycans at position N322 and N546 are indicated, as they could putatively clash with S304. (F) Molecular surface representation of the SARS CoV-2 RBD (gray) with the S304 epitope colored by residue conservation with SARS-CoV. (G and H) Positioning of ACE2 (relative to the S2A4 (G) and S2X35 (H) Fabs bound to the SARS-CoV-2 RBD. The stars indicate steric clashes.

Figures 34A-34L show structure-guided high-resolution serology. (A) Composite model of the SARS-CoV-2 S trimer with three open RBDs viewed along two orientations with all six mAbs used for competition ELISA shown bound to one RBD. (B–G) Epitopes recognized by each mAb are shown on the surface of the RBD for S2H14 (teal, B), S2H13 (orange, C), S2X35 (red, D), S2A4 (yellow, E), S304

(magenta, F), and S309 (purple, G). The glycan at position N343 is rendered as blue spheres and the RBM is shown as a black outline. (H–J) Competition ELISA (blockade-of-binding) between individual mAbs and sera or plasma from hospitalized (H), symptomatic (I), and asymptomatic (J) COVID-19 convalescent subjects. Each plot shows the magnitude of inhibition of binding to immobilized RBD in the presence of each mAb, expressed as reciprocal sera or plasma dilution blocking 80% of the maximum binding response. (K) Correlation analysis of titers of serum Abs blocking RBD binding to ACE2 and Abs blocking each of the six probe mAbs. (L) Comparison of RBD-specific IgG titers between sera containing Ab blocking at least one probe mAb and sera that do not contain Ab blocking any of the six probe mAbs.

Figures 35A-35G show that S2E12 and S2M11 neutralize SARS-CoV-2 via targeting the RBD. A-B. Neutralization of authentic SARS-CoV-2 (SARS-CoV-2-Nluc) by S2E12 (A) and S2M11 (B) IgG or Fab. Symbols are means±SD of triplicates. Dotted lines indicate IC_{50} and IC_{90} values. Average IC_{50} values are indicated in parentheses below the graphs (determined from two independent experiments). **C-F.** ELISA binding of S2M11, S2E12 or S309 mAbs to immobilized SARS-CoV-2 RBD (C), SARS-CoV-2 S (D), SARS-CoV RBD (E) or SARS-CoV S (F). Symbols show means of duplicates. **G.** SPR analysis of S2E12 and S2M11 Fab binding to the SARS-CoV-2 RBD or S ectodomain trimer. Experiments were carried out at pH 7.4 (orange) and pH 5.4 (green) and were repeated twice with similar results (one experiment is shown). The apparent equilibrium dissociation constants at pH7.4 are indicated. White and gray stripes indicate association and dissociation phases, respectively. S2M11 binding to S was fit to two parallel kinetic phases and the resulting $K_{D,\,app\,\#1}$ and $K_{D,\,app\,\#2}$ were interpreted as apparent affinity for open RBDs (tertiary epitope) and closed RBDs (quaternary epitope), respectively, as supported by the similar binding kinetics and affinity observed for S2M11 binding to the isolated RBD .

Figures 36A-36D show that S2E12 neutralizing mAb recognizes the SARS-CoV-2 RBM. (A-B) CryoEM structure of the prefusion SARS-CoV-2 S ectodomain trimer with three S2E12 Fab fragments bound to three open RBDs viewed along two orthogonal orientations. (C) The S2E12 concave paratope recognizes the convex RBM

tip. (D) Close-up views showing selected interactions formed between S2E12 and the SARS-CoV-2 RBD. In (A)-(D), each SARS-CoV-2 S protomer is shaded distinctly whereas the S2E12 light and heavy chain variable domains are also shaded differently from one another. N-linked glycans are rendered as dark spheres in (A)-(C).

Figures 37A-37F show that S2M11 neutralizing mAb recognizes a quaternary epitope spanning two RBDs and stabilizes S in the closed state. (A-B) CryoEM structure of the prefusion SARS-CoV-2 S ectodomain trimer bound to three S2M11 Fab fragments viewed along two orthogonal orientations. (C-D) The S2M11 binding pose, which involves a quaternary epitope spanning two neighboring RBDs. (E-F) Close-up views showing selected interactions formed between S2M11 and the SARS-CoV-2 RBDs. In (A)-(F), each SARS-CoV-2 S protomer is shaded distinctly whereas the S2M11 light and heavy chain variable domains are also shaded distinctly. N-linked glycans are rendered as dark spheres in (A)-(D) and as sticks in (E)-(F). FR: framework.

Figures 38A-38I show that S2E12 and S2M11 prevent SARS-CoV-2 S attachment to ACE2, inhibit membrane fusion and S2M11 triggers effector functions. (A) S2E12 and ACE2 bind overlapping binding sites on the SARS-CoV-2 RBD. (B) S2M11 and ACE2 bind overlapping binding sites on the SARS-CoV-2 RBD. The stars indicate steric clashes. (C-D) Binding of the SARS-CoV-2 RBD (C) or S ectodomain trimer (D) alone (grey) or precomplexed with the S2M11 (red), S2E12 (blue) or S309* (yellow) mAbs to the ACE2 ectodomain immobilized at the surface of biosensors analyzed by biolayer interferometry. "S309*" in the figure is an engineered version of the parent S309 mAb , and comprises the VH amino acid sequence of SEQ ID NO.:93 and the VL amino acid sequence of SEQ ID NO.:97. KB: kinetic buffer (negative control). (E) Binding of varying concentrations of S2E12 (blue), S2M11 (red) or S309 (yellow) mAbs to full-length S expressed at the surface of CHO cells in the presence of 20 μg/mL of the ACE2 ectodomain analyzed by flow cytometry (one measurement per condition). (F) Cell-cell fusion inhibition assay with VeroE6 cells transfected with SARS-CoV-2 S and incubated with varying concentrations of S2E12 (blue), S2M11 (red) or S309 (yellow) mAbs and a control mAb. The values are normalized to the percentage of fusion without mAb and to the percentage of fusion of non-transfected

cells. (G) FcγRIIIa (high affinity variant V158) signaling induced by individual mAbs or mAb cocktails. For mAb cocktails, the concentration of the constant mAb was 5 μg/ml. The concentration of the diluted mAb is indicated on the x axis. (H) ADCC using primary NK cells as effectors and SARS-CoV-2 S-expressing CHO cells as targets. The magnitude of NK cells-mediated killing is expressed as the area under the curve (AUC) for each mAb used at concentrations ranging between 0.1 ng/ml and 20 μg/ml. For mAb cocktails, the mAb listed first was kept constant at 5 μg/ml. Each symbol represents one donor, data are combined from two individual experiments. (I) ADCP using PBMCs as a source of phagocytic cells (monocytes) and PKH67-fluorescently labelled S-expressing CHO cells as target cells. The y axis indicates % of monocytes double-positive for anti-CD14 (monocyte) marker and PKH67. The dashed line indicates the signal detected in the presence of target and effector cells but without mAb (baseline). Each line indicates the data for one PBMC donor. Symbols are means of duplicates. Data are from one experiment.

Figures 39A-39C show in vivo protection of S2E12, S2M11 or cocktails of these two mAbs against SARS-CoV-2 challenge. Syrian hamsters were injected with the indicated amount of mAb 48 h before intra-nasal challenge with SARS-CoV-2. (A) Quantification of viral RNA in the lungs 4 days post infection. (B) The concentration of mAbs measured in the serum before infection (day 0) inversely correlates with the viral RNA load in the lung 4 days post infection. (C) Quantification of replicating virus in lung homogenates harvested 4 days post infection using a TCID50 assay. For mAb cocktails, the total dose of an equimolar mixture of both mAbs is indicated.

Figures 40A-40C show neutralization of SARS-CoV-2 S pseudotyped and authentic viruses by S2E12 and S2M11. (A) Neutralization assay with SARS-CoV-2 S-VSV. Symbols represent means±SD of triplicates. (B) Neutralization assay with SARS-CoV-2 S-MLV. Symbols represent means of duplicates. (C) Neutralization of authentic virus using a focus-forming-assay. The determined mean and range of IC_{50} and IC_{90} values for each mAb tested are indicated. Symbols represent means of duplicates. Results are combined from one to seven individual experiments for each mAb and (pseudotyped) virus.

Figures 41A-41C show binding analysis of monoclonal antibodies (mAbs) S2M11, S2E12 and S309. (A) mAb binding to the immobilized SARS-CoV-2 RBD or the S ectodomain trimer was evaluated by SPR at pH7.4 and pH5.4. The order of addition of the first and second mAb is indicated above and below the graph, respectively. The experiment was performed once. (B). mAb binding to SARS-CoV-2 S expressed at the surface of ExpiCHO cells analyzed by flow cytometry. The mAbs indicated in the legend below the graphs (first mAb) was serially diluted and incubated with cells before addition of biotinylated mAbs at a concentration that achieved 80% maximal binding (when analyzed in the absence of competitors). Symbols show means±SEM. Data are combined from three independent experiments. (C) Surface plasmon resonance analysis of S2E12 and S2M11 IgG binding to the SARS-CoV-2 RBD or the S ectodomain trimer. Experiments were carried out at pH 7.4 (orange) and at pH 5.4 (green) and were performed twice with similar results (one representative experiment is shown). White and gray stripes indicate association and dissociation phases, respectively.

Figures 42A-42G show cryo-electron microscopy data processing and validation of the S/S2E12 complex dataset. (A-B) Representative electron micrograph (A) and class averages (B) of SARS-CoV-2 S in complex with the S2E12 Fab embedded in vitreous ice. Scale bar: 500 Å. (C) Gold-standard Fourier shell correlation curves for the open S trimer bound to three S2E12 Fabs (solid black line) and the locally refined reconstruction of the RBD/S2E12 variable domains. The 0.143 cutoff is indicated by horizontal dashed lines. (D-E) Local resolution map calculated using cryoSPARC for the open S trimer bound to three S2E12 Fabs (D) and the locally refined reconstruction of the RBD/S2E12 variable domains (E). (F) Close-up view showing selected interactions formed between S2E12 (light and heavy chain are shaded lighter and darker, respectively) and the SARS-CoV-2 RBD with the corresponding region of cryoEM density (transparent grey surface). (G) CryoEM data processing flow-chart.

Figures 43A-43D show epitopes targeted by S2E12 and S2M11 on the SARS-CoV-2 S trimer. (A-B) The S2E12 footprint is shown in purple on one protomer of the

closed (A) or open (B) SARS-CoV-2 S trimer. (C-D) The quaternary S2M11 footprint is shown in purple on two neighboring protomers of the closed (A) or open (B) SARS-CoV-2 S trimer. In (A)-(D), the SARS-CoV-2 S is rendered as a molecular surface colored distinctly for each protomer (cyan, pink and gold).

Figures 44A-44G show cryo-electron microscopy data processing and validation of the S/S2M11 complex dataset. (A-B) Representative electron micrograph (A) and class averages (B) of SARS-CoV-2 S in complex with the S2M11 Fab embedded in vitreous ice. Scale bar: 500 Å. (C) Gold-standard Fourier shell correlation curves for the closed S2M11-bound trimer. The 0.143 cutoff is indicated by horizontal dashed lines. (D) Local resolution map calculated using cryoSPARC. (E) Close-up view showing selected interactions formed between S2M11 (light and heavy chain portions are colored magenta and purple, respectively) and the SARS-CoV-2 RBDs (cyan and gold) with the corresponding region of cryoEM density (transparent grey surface). (F) CryoEM data processing flow-chart. (G) Comparison of the orientation of the SARS-CoV-2 glycan at position N343 in the S2M11-bound (blue) and the S309-bound (grey) structures (PDB ID 6WPS) reveal a rotation of ~45°.

Figures 45A-45E show effector functions of individual monoclonal antibodies and monoclonal antibody cocktails. (A-B) Binding of S2E12, S2M11 and S309 to the surface of VeroE6 cells infected with authentic SARS-CoV-2. Flow cytometry graphs showing the binding of mAbs at a concentration of 10 μg/ml or the secondary Ab only as a negative control (2ry Ab only) (A). Data for the binding of mAbs at 0.1, 1 and 10μg/ml (B). Results are from one out of two independent experiments with similar results. (C) FcγRIIIa low affinity variant F158 and FcγRIIa (high affinity variant H) signaling induced by individual S2E12 or S2M11 mAbs and the S2E12/S2M11 mAb cocktail. Results are shown as fold increase over background (RLU at mAb conc. x/RLU without mAb). (D) FcγRIIIa high affinity variant V158, low affinity variant F158 and FcγRIIa (high affinity variant H) signaling induced by S2M11, S309 or the S2M11/S309 cocktail. (E) Representative mAb dose-dependent NK-mediated killing for a donor heterozygous for F158 and V158 FcγRIIIa. For C-E: Symbols show means of duplicates. For mAb cocktails, the concentration of the constant mAb was 5 μg/ml.

The concentration of the diluted mAb, starting at 5 μg/ml, is indicated on the x axis. Experiments in C-D were conducted two to three times with similar results.

Figures 46A-46J shows neutralization of known SARS-CoV-2 S variants by monoclonal antibody cocktails. (A-F) S2M11 (A and B) and S2E12 (C and D)-mediated neutralization of SARS-CoV-2 S-VSV variants. SARS-CoV-2 S mutations in the variants tested are indicated in the legend. Symbols show means±SD of triplicates for A-D and means of duplicates for E and F. (G) Variant prevalence of amino acids targeted by S2M11 based on 90,287 complete genome sequences reported by GISAID as of September 12th 2020. At least 4 supporting sequences were required to define a variant. (H-J) Neutralization of SARS-CoV-2 S-VSV variants by mAb cocktails, mixed at 1:1 equimolar ratio for S2E12+S2M11 (G), S2M11+S309 (H), S2E12+S309 (I). The x axis indicates the total mAb concentration. Symbols show means±SD of triplicates. Dashed lines indicated the IC_{50} and IC_{90}. A constraint of <100 was used for all curve fit analysis. All experiments were repeated at least once with similar results.

Figure 47 shows ACE2 binding to variant SARS-CoV-2 S corresponding to circulating isolates. Binding of fluorescently labeled recombinant ACE2 ectodomain to ExpiCHO cells transiently transfected with SARS-CoV-2 S variants. The experiment was performed twice with similar results.

Figures 48A-48F shows data evaluating neutralization potency of monoclonal antibody cocktails. (A) Neutralization matrix to assess the synergistic activity of S2M11 and S2E12 mAb cocktails *in vitro* with authentic SARS-CoV-2-Nluc. (B-C) Neutralization matrix for S2M11 in combination with S2E12 tested with SARS-CoV-2 VSV (B) and SARS-CoV-2 MLV (C). (D-E) Neutralization matrix for S309 in combination with S2M11 tested with SARS-CoV-2-MLV (D) and SARS-CoV-2 VSV (E). (F) Neutralization matrix for S309 in combination with S2E12, tested with SARS-CoV-2 VSV. Data for authentic SARS-CoV-2-Nluc are from one representative experiment out of two, done in triplicate each. All SARS-CoV-2 S-VSV assays were performed twice with similar results, each from triplicate plates. Data for SARS-CoV-2 S-MLV are from quadruplicate plates from one experiment.

Figure 49 shows kinetics and affinity parameters of S2E12 (Fab and IgG) and S2M11 (Fab and IgG) to RBD and S glycoprotein, as determined by surface plasmon resonance.

Figure 50 shows cryoEM data collection and refinement statistics for investigating binding of S2M11 and S2E12 to S glycoprotein.

Figure 51 shows x-ray crystallography data collection and refinement statistics for investigating binding of S2E12 Fab to S glycoprotein.

Figure 52 shows binding of S2M11, S2E12 and S309 mAbs to SARS-CoV-2 S variants expressed at the surface of CHO cells and assessed by flow cytometry +: no loss of binding. -: loss of binding.

Figures 53A-53K show cryo-EM data processing and validation of the S/S2H13 and S/S2H14 complex datasets. (A and B) Representative electron micrograph (A) and class averages (B) of SARS-CoV-2 S in complex with the S2H13 Fab embedded in vitreous ice. Scale bar: 400Å. (C) Gold-standard Fourier shell correlation curves for the closed S2H13-bound trimer (black solid line), partially open S2H13-bound trimer (gray solid line) and locally refined RBM/S2H13 variable domains (black dashed line). The 0.143 cutoff is indicated by horizontal dashed lines. (D and F) Local resolution maps calculated using cryoSPARC for the closed (D) and partially open (E) reconstructions as well as for the locally refined RBM/S2H13 variable domains (F). (G and H) Representative electron micrograph (G) and class averages (H) of SARS-CoV-2 S in complex with the S2H14 Fab embedded in vitreous ice. Scale bar: 400Å. (I) Gold-standard Fourier shell correlation curves for the S2H14-bound trimer with one RBD closed (black solid line) or three RBDs open (gray solid line). The 0.143 cutoff is indicated by horizontal dashed lines. (J and K) Local resolution maps calculated using cryoSPARC for the reconstructions with one RBD closed (J) and three RBDs open (K).

Figures 54A-54O show cryo-EM data processing and validation of the S/S2A4 and S/S304 complex datasets. (A and B) Representative electron micrograph (A) and class averages (B) of SARS-CoV-2 S in complex with the S2A4 Fab embedded in vitreous ice. Scale bar: 400Å. A 2D class average corresponding to an S1 subunit trimer (with disordered S2) bound to three S2A4 Fabs is highlighted in red. (C) Gold-standard

Fourier shell correlation curves for the S2A4-bound trimer (black solid line) and locally refined RBD/S2A4 variable domains (black dashed line). The 0.143 cutoff is indicated by a horizontal dashed line. (D and E) Local resolution maps calculated using cryoSPARC for the whole reconstruction (D) as well as for the locally refined RBD/S2A4 variable domains (E). (F) Superimposition of the three distinct open conformations of the S trimer, with three bound S2A4 Fabs and RBDs swung out to various extent. The arrows indicate the distinct positions of the Fabs in the maps. (G and H) CryoEM reconstruction of the S1 subunit trimer (with disordered S2) bound to three S2A4 Fabs viewed along two orthogonal orientations and the corresponding atomic model fit in density. Each SARS-CoV-2 S1 protomer is colored distinctly (cyan, pink and gold). The S2A4 light and heavy chains are colored magenta and purple, respectively. (I and J) Representative electron micrograph (I) and class averages (J) of SARS-CoV-2 S in complex with the S304 Fab embedded in vitreous ice. Scale bar: 400Å. (K) Gold-standard Fourier shell correlation curve for the S304-bound S trimer reconstruction. The 0.143 cutoff is indicated by a horizontal dashed line. (L) Local resolution map calculated using cryoSPARC. (M) Superimposition of the three distinct open conformations of the S trimer, with three bound S304 Fabs and RBDs swung out to various extent. The arrows indicate the distinct positions of the Fabs in the maps. (N and O) CryoEM reconstruction of the S1 subunit trimer (with disordered S2) bound to three S304 Fabs viewed along two orthogonal orientations and the corresponding atomic model fit in density. Each SARS-CoV-2 S1 protomer is colored distinctly (cyan, pink and gold). The S304 light and heavy chains are colored magenta and purple, respectively.

DETAILED DESCRIPTION

Provided herein are antibodies and antigen-binding fragments that are capable of binding to a SARS-CoV-2 S glycoprotein, for example, a S glycoprotein of a S glycoprotein trimer. Presently disclosed antibodies and antigen-binding fragments can, for example, bind by contacting one or more amino acid residues of the S glycoprotein or trimer, recognize an epitope formed by specified amino acid residues of the S

glycoprotein or trimer, and/or bind to a S glycoprotein of a trimer wherein the three RBDs of a trimer comprise various conformations (*e.g.*, one RBD up ("open") and two RBDs down ("closed"), two RBDs up and one RBD down, three RBDs up, and/or three RBDs down). Accordingly, presently disclosed antibodies and antigen-binding fragments are useful to target SARS-CoV-2 S glycoprotein in a variety of conformations. Presently disclosed antibodies and antigen-binding fragments include those that compete with a specified antibody or antigen-binding fragment for binding to a SARS-CoV-2 S glycoprotein.

Antibodies were isolated from survivors of SARS-CoV or SARS-CoV-2 and used to elucidate different antigenic sites and epitopes in SARS-CoV-2 S glycoprotein. Mechanisms for binding to and/or neutralizing SARS-CoV-2 infection (*e.g.*, by binding to SARS-CoV-2 S glycoprotein receptor binding domain (RBD) in open, closed, or open and closed conformations; by interfering with S glycoprotein interaction with human ACE2; by locking S glycoprotein RBDs (of a trimer) in a closed conformation) were determined. High-resolution serology studies of the human antibody response to SARS-CoV-2 infection were performed.

Also provided are compositions and combinations that comprise any two or more of the presently disclosed antibodies or antigen-binding fragments. Theantibodies or antigen-binding fragments, compositions, and combinations can, in certain embodiments, provide multiple mechanisms for binding to and, optionally, neutralizing, a SARS-CoV-2. Antibody or antigen-binding fragment-encoding polynucleotides and vectors are also provided, as well as host cells that comprise the same and/or that express an antibody or antigen-binding fragment. Also provided are uses of the presently disclosed antibodies or antigen-binding fragments, combinations, and compositions for treating or diagnosing a SARS-CoV-2 infection, or for testing a vaccine composition (*e.g.*, based on the S glycoprotein) to determine whether the vaccine comprises an epitope in a correct conformation.

Also provided are immunogenic compositions comprising a SARS-CoV-2 S polypeptide (*i.e.*, a complete S glycoprotein or a portion thereof, optionally which is comprised in a multimer such as a trimer or a dimer) that is capable of being bound by a

presently disclosed antibody or antigen-binding fragment, as well as immunogenic compositions that comprise two or more different such S polypeptides (*e.g.*, such that two or more different presently disclosed antibodies or antigen-binding fragments can bind to the immunogenic composition). Methods of using the immunogenic compositions are also provided.

Prior to setting forth this disclosure in more detail, it may be helpful to an understanding thereof to provide definitions of certain terms to be used herein. Additional definitions are set forth throughout this disclosure.

As used herein, "SARS-CoV-2", also referred to herein as "Wuhan seafood market phenomia virus", or "Wuhan coronavirus" or "Wuhan CoV", or "novel CoV", or "nCoV", or "2019 nCoV", or "Wuhan nCoV" is a betacoronavirus believed to be of lineage B (sarbecovirus). SARS-CoV-2 was first identified in Wuhan, Hubei province, China, in late 2019 and spread within China and to other parts of the world by early 2020. Symptoms of SARS-CoV-2 infection include fever, dry cough, and dyspnea.

The genomic sequence of SARS-CoV-2 isolate Wuhan-Hu-1 is provided in SEQ ID NO.:1 (*see also* GenBank MN908947.3, January 23, 2020), and the amino acid translation of the genome is provided in SEQ ID NO.:2 (*see also* GenBank QHD43416.1, January 23, 2020). Like other coronaviruses (*e.g.*, SARS- CoV-1), SARS-CoV-2 comprises a "spike" or surface ("S") type I transmembrane glycoprotein containing a receptor binding domain (RBD). RBD is believed to mediate entry of the lineage B SARS coronavirus to respiratory epithelial cells by binding to the cell surface receptor angiotensin-converting enzyme 2 (ACE2). In particular, a receptor binding motif (RBM) in the virus RBD is believed to interact with ACE2.

It will be understood that SARS CoV-2 S glycoproteins naturally form trimers. The RBDs can undergo hinge-like conformational movements between an "open" (receptor-accessible) conformation that generally points "up", away from the C-terminal end of the S glycoprotein, and a "closed" (receptor-inaccessible) conformation. RBDs of a trimer in an open conformation are depicted in, for example, Figures 33A-33C and 36A-36B. RBDs of a trimer in a closed conformation are depicted in, for example, Figures 37A and 37B. Figures 43A and 43B shown top-down

views of a closed S trimer and an open S trimer, respectively. Figures 43C and 43D show top-down views of a closed S trimer and an open S trimer, respectively.

As taught herein, certain epitopes may be available for binding only when an RBD is in an open conformation. Certain other epitopes may be available for binding only when an RBD is in a closed conformation. Some epitopes may be available for binding only when one or more RBDs of a trimer is present in an open conformation. Some other epitopes may be available for binding only when one or more RBDs of a trimer is present in a closed conformation. Some epitopes are available when an RBD is in an open conformation or a closed conformation.

The amino acid sequence of the Wuhan-Hu-1 surface glycoprotein is provided in SEQ ID NO.:3. The amino acid sequence of SARS-CoV-2 RBD is provided in SEQ ID NO.:4. SARS-CoV-2 S protein has approximately 73% amino acid sequence identity with SARS-CoV-1. The amino acid sequence of SARS-CoV-2 RBM is provided in SEQ ID NO.:5. SARS-CoV-2 RBD has approximately 75% to 77% amino acid sequence similarity to SARS–CoV-1 RBD, and SARS-CoV-2 RBM has approximately 50% amino acid sequence similarity to SARS-CoV-1 RBM.

SARS-CoV-2 includes a virus comprising the amino acid sequence set forth in any one or more of SEQ ID NOs.:2, 3, and 4, optionally with the genomic sequence set forth in SEQ ID NO.:1. There have been a number of emerging SARS-CoV-2 variants. Some SARS-CoV-2 variants contain an N439K mutation, which has enhanced binding affinity to the human ACE2 receptor (Thomson, E.C., et al., The circulating SARS-CoV-2 spike variant N439K maintains fitness while evading antibody-mediated immunity. bioRxiv, 2020). Some SARS-CoV-2 variants contain an N501Y mutation, which is associated with increased transmissibility, including the lineages B.1.1.7 (also known as 20I/501Y.V1 and VOC 202012/01; (del69-70, del144, N501Y, A570D, D614G, P681H, T716I, S982A, and D1118H mutations)) and B.1.351 (also known as 20H/501Y.V2; L18F, D80A, D215G, R246I, K417N, E484K, N501Y, D614G, and A701V mutations), which were discovered in the United Kingdom and South Africa, respectively (Tegally, H., et al., Emergence and rapid spread of a new severe acute respiratory syndrome-related coronavirus 2 (SARS-CoV-2) lineage with multiple spike

mutations in South Africa. medRxiv, 2020: p. 2020.12.21.20248640; Leung, K., et al., Early empirical assessment of the N501Y mutant strains of SARS-CoV-2 in the United Kingdom, October to November 2020. medRxiv, 2020: p. 2020.12.20.20248581). B.1.351 also include two other mutations in the RBD domain of SARS-CoV2 spike protein, K417N and E484K (Tegally, H., et al., Emergence and rapid spread of a new severe acute respiratory syndrome-related coronavirus 2 (SARS-CoV-2) lineage with multiple spike mutations in South Africa. medRxiv, 2020: p. 2020.12.21.20248640). Other SARS-CoV-2 variants include the Lineage B.1.1.28, which was first reported in Brazil; the Variant P.1, lineage B.1.1.28 (also known as 20J/501Y.V3), which was first reported in Japan; Variant L452R, which was first reported in California in the United States (Pan American Health Organization, Epidemiological update: Occurrence of variants of SARS-CoV-2 in the Americas, January 20, 2021, available at reliefweb.int/sites/reliefweb.int/files/resources/2021-jan-20-phe-epi-update-SARS-CoV-2.pdf). Other SARS-CoV-2 variants include a SARS CoV-2 of clade 19A; SARS CoV-2 of clade 19B; a SARS CoV-2 of clade 20A; a SARS CoV-2 of clade 20B; a SARS CoV-2 of clade 20C; a SARS CoV-2 of clade 20D; a SARS CoV-2 of clade 20E (EU1); a SARS CoV-2 of clade 20F; a SARS CoV-2 of clade 20G; and SARS CoV-2 B1.1.207; and other SARS CoV-2 lineages described in Rambaut, A., et al., A dynamic nomenclature proposal for SARS-CoV-2 lineages to assist genomic epidemiology. Nat Microbiol 5, 1403–1407 (2020). The foregoing SARS-CoV-2 variants, and the amino acid and nucleotide sequences thereof, are incorporated herein by reference.

SARS-CoV is another betacoronavirus of lineage B (sarbecovirus) that causes respiratory symptoms in infected individuals. The genomic sequence of SARS-CoV Urbani strain has GenBank accession number AAP13441.1.

In the present description, any concentration range, percentage range, ratio range, or integer range is to be understood to include the value of any integer within the recited range and, when appropriate, fractions thereof (such as one tenth and one hundredth of an integer), unless otherwise indicated. Also, any number range recited herein relating to any physical feature, such as polymer subunits, size or thickness, are to be understood to include any integer within the recited range, unless otherwise

indicated. As used herein, the term "about" means ± 20% of the indicated range, value, or structure, unless otherwise indicated. It should be understood that the terms "a" and "an" as used herein refer to "one or more" of the enumerated components. The use of the alternative (*e.g.*, "or") should be understood to mean either one, both, or any combination thereof of the alternatives. As used herein, the terms "include," "have," and "comprise" are used synonymously, which terms and variants thereof are intended to be construed as non-limiting.

"Optional" or "optionally" means that the subsequently described element, component, event, or circumstance may or may not occur, and that the description includes instances in which the element, component, event, or circumstance occurs and instances in which they do not.

In addition, it should be understood that the individual constructs, or groups of constructs, derived from the various combinations of the structures and subunits described herein, are disclosed by the present application to the same extent as if each construct or group of constructs was set forth individually. Thus, selection of particular structures or particular subunits is within the scope of the present disclosure.

The term "consisting essentially of" is not equivalent to "comprising" and refers to the specified materials or steps of a claim, or to those that do not materially affect the basic characteristics of a claimed subject matter. For example, a protein domain, region, or module (e.g., a binding domain) or a protein "consists essentially of" a particular amino acid sequence when the amino acid sequence of a domain, region, module, or protein includes extensions, deletions, mutations, or a combination thereof (e.g., amino acids at the amino- or carboxy-terminus or between domains) that, in combination, contribute to at most 20% (e.g., at most 15%, 10%, 8%, 6%, 5%, 4%, 3%, 2% or 1%) of the length of a domain, region, module, or protein and do not substantially affect (i.e., do not reduce the activity by more than 50%, such as no more than 40%, 30%, 25%, 20%, 15%, 10%, 5%, or 1%) the activity of the domain(s), region(s), module(s), or protein (e.g., the target binding affinity of a binding protein).

As used herein, "amino acid" refers to naturally occurring and synthetic amino acids, as well as amino acid analogs and amino acid mimetics that function in a manner

similar to the naturally occurring amino acids. Naturally occurring amino acids are those encoded by the genetic code, as well as those amino acids that are later modified, *e.g.*, hydroxyproline, γ-carboxyglutamate, and O-phosphoserine. Amino acid analogs refer to compounds that have the same basic chemical structure as a naturally occurring amino acid, *i.e.*, an α-carbon that is bound to a hydrogen, a carboxyl group, an amino group, and an R group, *e.g.*, homoserine, norleucine, methionine sulfoxide, methionine methyl sulfonium. Such analogs have modified R groups (*e.g.*, norleucine) or modified peptide backbones, but retain the same basic chemical structure as a naturally occurring amino acid. Amino acid mimetics refer to chemical compounds that have a structure that is different from the general chemical structure of an amino acid, but that functions in a manner similar to a naturally occurring amino acid.

As used herein, "mutation" refers to a change in the sequence of a nucleic acid molecule or polypeptide molecule as compared to a reference or wild-type nucleic acid molecule or polypeptide molecule, respectively. A mutation can result in several different types of change in sequence, including substitution, insertion or deletion of nucleotide(s) or amino acid(s).

A "conservative substitution" refers to amino acid substitutions that do not significantly affect or alter binding characteristics of a particular protein. Generally, conservative substitutions are ones in which a substituted amino acid residue is replaced with an amino acid residue having a similar side chain. Conservative substitutions include a substitution found in one of the following groups: Group 1: Alanine (Ala or A), Glycine (Gly or G), Serine (Ser or S), Threonine (Thr or T); Group 2: Aspartic acid (Asp or D), Glutamic acid (Glu or Z); Group 3: Asparagine (Asn or N), Glutamine (Gln or Q); Group 4: Arginine (Arg or R), Lysine (Lys or K), Histidine (His or H); Group 5: Isoleucine (Ile or I), Leucine (Leu or L), Methionine (Met or M), Valine (Val or V); and Group 6: Phenylalanine (Phe or F), Tyrosine (Tyr or Y), Tryptophan (Trp or W). Additionally or alternatively, amino acids can be grouped into conservative substitution groups by similar function, chemical structure, or composition (*e.g.*, acidic, basic, aliphatic, aromatic, or sulfur-containing). For example, an aliphatic grouping may include, for purposes of substitution, Gly, Ala, Val, Leu, and Ile. Other conservative

substitutions groups include: sulfur-containing: Met and Cysteine (Cys or C); acidic: Asp, Glu, Asn, and Gln; small aliphatic, nonpolar or slightly polar residues: Ala, Ser, Thr, Pro, and Gly; polar, negatively charged residues and their amides: Asp, Asn, Glu, and Gln; polar, positively charged residues: His, Arg, and Lys; large aliphatic, nonpolar residues: Met, Leu, Ile, Val, and Cys; and large aromatic residues: Phe, Tyr, and Trp. Additional information can be found in Creighton (1984) Proteins, W.H. Freeman and Company.

As used herein, "protein" or "polypeptide" refers to a polymer of amino acid residues. Proteins apply to naturally occurring amino acid polymers, as well as to amino acid polymers in which one or more amino acid residue is an artificial chemical mimetic of a corresponding naturally occurring amino acid, and non-naturally occurring amino acid polymers. Variants of proteins, peptides, and polypeptides of this disclosure are also contemplated. In certain embodiments, variant proteins, peptides, and polypeptides comprise or consist of an amino acid sequence that is at least 70%, 75%, 80%, 85%, 90%, 91%, 92%, 93%, 94%, 95%, 96%, 97%, 98%, 99%, or 99.9% identical to an amino acid sequence of a defined or reference amino acid sequence as described herein.

"Nucleic acid molecule" or "polynucleotide" or "polynucleic acid" refers to a polymeric compound including covalently linked nucleotides, which can be made up of natural subunits (*e.g.*, purine or pyrimidine bases) or non-natural subunits (*e.g.*, morpholine ring). Purine bases include adenine, guanine, hypoxanthine, and xanthine, and pyrimidine bases include uracil, thymine, and cytosine. Nucleic acid molecules include polyribonucleic acid (RNA), which includes mRNA, microRNA, siRNA, viral genomic RNA, and synthetic RNA, and polydeoxyribonucleic acid (DNA), which includes cDNA, genomic DNA, and synthetic DNA, either of which may be single or double stranded. If single-stranded, the nucleic acid molecule may be the coding strand or non-coding (anti-sense) strand. A nucleic acid molecule encoding an amino acid sequence includes all nucleotide sequences that encode the same amino acid sequence. Some versions of the nucleotide sequences may also include intron(s) to the extent that the intron(s) would be removed through co- or post-transcriptional mechanisms. In

other words, different nucleotide sequences may encode the same amino acid sequence as the result of the redundancy or degeneracy of the genetic code, or by splicing.

Variants of nucleic acid molecules of this disclosure are also contemplated. Variant nucleic acid molecules are at least 70%, 75%, 80%, 85%, 90%, and are preferably 95%, 96%, 97%, 98%, 99%, or 99.9% identical a nucleic acid molecule of a defined or reference polynucleotide as described herein, or that hybridize to a polynucleotide under stringent hybridization conditions of 0.015M sodium chloride, 0.0015M sodium citrate at about 65-68°C or 0.015M sodium chloride, 0.0015M sodium citrate, and 50% formamide at about 42°C. Nucleic acid molecule variants retain the capacity to encode a binding domain thereof having a functionality described herein, such as binding a target molecule.

"Percent sequence identity" refers to a relationship between two or more sequences, as determined by comparing the sequences. Preferred methods to determine sequence identity are designed to give the best match between the sequences being compared. For example, the sequences are aligned for optimal comparison purposes (*e.g.*, gaps can be introduced in one or both of a first and a second amino acid or nucleic acid sequence for optimal alignment). Further, non-homologous sequences may be disregarded for comparison purposes. The percent sequence identity referenced herein is calculated over the length of the reference sequence, unless indicated otherwise. Methods to determine sequence identity and similarity can be found in publicly available computer programs. Sequence alignments and percent identity calculations may be performed using a BLAST program (*e.g.*, BLAST 2.0, BLASTP, BLASTN, or BLASTX). The mathematical algorithm used in the BLAST programs can be found in Altschul *et al.*, *Nucleic Acids Res. 25*:3389-3402, 1997. Within the context of this disclosure, it will be understood that where sequence analysis software is used for analysis, the results of the analysis are based on the "default values" of the program referenced. "Default values" mean any set of values or parameters which originally load with the software when first initialized.

The term "isolated" means that the material is removed from its original environment (*e.g.*, the natural environment if it is naturally occurring). For example, a

naturally occurring nucleic acid or polypeptide present in a living animal is not isolated, but the same nucleic acid or polypeptide, separated from some or all of the co-existing materials in the natural system, is isolated. Such nucleic acid could be part of a vector and/or such nucleic acid or polypeptide could be part of a composition (*e.g.*, a cell lysate), and still be isolated in that such vector or composition is not part of the natural environment for the nucleic acid or polypeptide.

The term "gene" means the segment of DNA or RNA involved in producing a polypeptide chain; in certain contexts, it includes regions preceding and following the coding region (*e.g.*, 5' untranslated region (UTR) and 3' UTR) as well as intervening sequences (introns) between individual coding segments (exons).

A "functional variant" refers to a polypeptide or polynucleotide that is structurally similar or substantially structurally similar to a parent or reference compound of this disclosure, but differs slightly in composition (e.g., one base, atom or functional group is different, added, or removed), such that the polypeptide or encoded polypeptide is capable of performing at least one function of the parent polypeptide with at least 50% efficiency, preferably at least 55%, 60%, 70%, 75%, 80%, 85%, 90%, 95%, 96%, 97%, 98%, 99%, 99.9%, or 100% level of activity of the parent polypeptide. In other words, a functional variant of a polypeptide or encoded polypeptide of this disclosure has "similar binding," "similar affinity" or "similar activity" when the functional variant displays no more than a 50% reduction in performance in a selected assay as compared to the parent or reference polypeptide, such as an assay for measuring binding affinity (e.g., Biacore® or tetramer staining measuring an association (Ka) or a dissociation (K_D) constant).

As used herein, a "functional portion" or "functional fragment" refers to a polypeptide or polynucleotide that comprises only a domain, portion or fragment of a parent or reference compound, and the polypeptide or encoded polypeptide retains at least 50% activity associated with the domain, portion or fragment of the parent or reference compound, preferably at least 55%, 60%, 70%, 75%, 80%, 85%, 90%, 95%, 96%, 97%, 98%, 99%, 99.9%, or 100% level of activity of the parent polypeptide, or provides a biological benefit (*e.g.*, effector function). A "functional portion" or

"functional fragment" of a polypeptide or encoded polypeptide of this disclosure has "similar binding" or "similar activity" when the functional portion or fragment displays no more than a 50% reduction in performance in a selected assay as compared to the parent or reference polypeptide (preferably no more than 20% or 10%, or no more than a log difference as compared to the parent or reference with regard to affinity).

As used herein, the term "engineered," "recombinant," or "non-natural" refers to an organism, microorganism, cell, nucleic acid molecule, or vector that includes at least one genetic alteration or has been modified by introduction of an exogenous or heterologous nucleic acid molecule, wherein such alterations or modifications are introduced by genetic engineering (*i.e.*, human intervention). Genetic alterations include, for example, modifications introducing expressible nucleic acid molecules encoding functional RNA, proteins, fusion proteins or enzymes, or other nucleic acid molecule additions, deletions, substitutions, or other functional disruption of a cell's genetic material. Additional modifications include, for example, non-coding regulatory regions in which the modifications alter expression of a polynucleotide, gene, or operon.

As used herein, "heterologous" or "non-endogenous" or "exogenous" refers to any gene, protein, compound, nucleic acid molecule, or activity that is not native to a host cell or a subject, or any gene, protein, compound, nucleic acid molecule, or activity native to a host cell or a subject that has been altered. Heterologous, non-endogenous, or exogenous includes genes, proteins, compounds, or nucleic acid molecules that have been mutated or otherwise altered such that the structure, activity, or both is different as between the native and altered genes, proteins, compounds, or nucleic acid molecules. In certain embodiments, heterologous, non-endogenous, or exogenous genes, proteins, or nucleic acid molecules (*e.g.*, receptors, ligands, etc.) may not be endogenous to a host cell or a subject, but instead nucleic acids encoding such genes, proteins, or nucleic acid molecules may have been added to a host cell by conjugation, transformation, transfection, electroporation, or the like, wherein the added nucleic acid molecule may integrate into a host cell genome or can exist as extra-chromosomal genetic material (*e.g.*, as a plasmid or other self-replicating vector). The term "homologous" or

"homolog" refers to a gene, protein, compound, nucleic acid molecule, or activity found in or derived from a host cell, species, or strain. For example, a heterologous or exogenous polynucleotide or gene encoding a polypeptide may be homologous to a native polynucleotide or gene and encode a homologous polypeptide or activity, but the polynucleotide or polypeptide may have an altered structure, sequence, expression level, or any combination thereof. A non-endogenous polynucleotide or gene, as well as the encoded polypeptide or activity, may be from the same species, a different species, or a combination thereof.

In certain embodiments, a nucleic acid molecule or portion thereof native to a host cell will be considered heterologous to the host cell if it has been altered or mutated, or a nucleic acid molecule native to a host cell may be considered heterologous if it has been altered with a heterologous expression control sequence or has been altered with an endogenous expression control sequence not normally associated with the nucleic acid molecule native to a host cell. In addition, the term "heterologous" can refer to a biological activity that is different, altered, or not endogenous to a host cell. As described herein, more than one heterologous nucleic acid molecule can be introduced into a host cell as separate nucleic acid molecules, as a plurality of individually controlled genes, as a polycistronic nucleic acid molecule, as a single nucleic acid molecule encoding a fusion protein, or any combination thereof. When

As used herein, the term "endogenous" or "native" refers to a polynucleotide, gene, protein, compound, molecule, or activity that is normally present in a host cell or a subject.

The term "expression", as used herein, refers to the process by which a polypeptide is produced based on the encoding sequence of a nucleic acid molecule, such as a gene. The process may include transcription, post-transcriptional control, post-transcriptional modification, translation, post-translational control, post-translational modification, or any combination thereof. An expressed nucleic acid molecule is typically operably linked to an expression control sequence (e.g., a promoter).

The term "operably linked" refers to the association of two or more nucleic acid molecules on a single nucleic acid fragment so that the function of one is affected by the other. For example, a promoter is operably linked with a coding sequence when it is capable of affecting the expression of that coding sequence (i.e., the coding sequence is under the transcriptional control of the promoter). "Unlinked" means that the associated genetic elements are not closely associated with one another and the function of one does not affect the other.

As described herein, more than one heterologous nucleic acid molecule can be introduced into a host cell as separate nucleic acid molecules, as a plurality of individually controlled genes, as a polycistronic nucleic acid molecule, as a single nucleic acid molecule encoding a protein (*e.g.*, a heavy chain of an antibody), or any combination thereof. When two or more heterologous nucleic acid molecules are introduced into a host cell, it is understood that the two or more heterologous nucleic acid molecules can be introduced as a single nucleic acid molecule (*e.g.*, on a single vector), on separate vectors, integrated into the host chromosome at a single site or multiple sites, or any combination thereof. The number of referenced heterologous nucleic acid molecules or protein activities refers to the number of encoding nucleic acid molecules or the number of protein activities, not the number of separate nucleic acid molecules introduced into a host cell.

The term "construct" refers to any polynucleotide that contains a recombinant nucleic acid molecule (or, when the context clearly indicates, a fusion protein of the present disclosure). A (polynucleotide) construct may be present in a vector (e.g., a bacterial vector, a viral vector) or may be integrated into a genome. A "vector" is a nucleic acid molecule that is capable of transporting another nucleic acid molecule. Vectors may be, for example, plasmids, cosmids, viruses, a RNA vector or a linear or circular DNA or RNA molecule that may include chromosomal, non-chromosomal, semi-synthetic or synthetic nucleic acid molecules. Vectors of the present disclosure also include transposon systems (*e.g.*, Sleeping Beauty, *see, e.g., Geurts et al., Mol. Ther. 8*:108, 2003: Mátés *et al., Nat. Genet. 41*:753, 2009). Exemplary vectors are those capable of autonomous replication (episomal vector), capable of delivering a

polynucleotide to a cell genome (e.g., viral vector), or capable of expressing nucleic acid molecules to which they are linked (expression vectors).

As used herein, "expression vector" or "vector" refers to a DNA construct containing a nucleic acid molecule that is operably linked to a suitable control sequence capable of effecting the expression of the nucleic acid molecule in a suitable host. Such control sequences include a promoter to effect transcription, an optional operator sequence to control such transcription, a sequence encoding suitable mRNA ribosome binding sites, and sequences which control termination of transcription and translation. The vector may be a plasmid, a phage particle, a virus, or simply a potential genomic insert. Once transformed into a suitable host, the vector may replicate and function independently of the host genome, or may, in some instances, integrate into the genome itself or deliver the polynucleotide contained in the vector into the genome without the vector sequence. In the present specification, "plasmid," "expression plasmid," "virus," and "vector" are often used interchangeably.

The term "introduced" in the context of inserting a nucleic acid molecule into a cell, means "transfection", "transformation," or "transduction" and includes reference to the incorporation of a nucleic acid molecule into a eukaryotic or prokaryotic cell wherein the nucleic acid molecule may be incorporated into the genome of a cell (*e.g.*, chromosome, plasmid, plastid, or mitochondrial DNA), converted into an autonomous replicon, or transiently expressed (*e.g.*, transfected mRNA).

In certain embodiments, polynucleotides of the present disclosure may be operatively linked to certain elements of a vector. For example, polynucleotide sequences that are needed to effect the expression and processing of coding sequences to which they are ligated may be operatively linked. Expression control sequences may include appropriate transcription initiation, termination, promoter, and enhancer sequences; efficient RNA processing signals such as splicing and polyadenylation signals; sequences that stabilize cytoplasmic mRNA; sequences that enhance translation efficiency (*i.e.*, Kozak consensus sequences); sequences that enhance protein stability; and possibly sequences that enhance protein secretion. Expression control sequences may be operatively linked if they are contiguous with the gene of interest and

expression control sequences that act in *trans* or at a distance to control the gene of interest.

In certain embodiments, the vector comprises a plasmid vector or a viral vector (*e.g.*, a lentiviral vector or a γ-retroviral vector). Viral vectors include retrovirus, adenovirus, parvovirus (*e.g.*, adeno-associated viruses), coronavirus, negative strand RNA viruses such as ortho-myxovirus (*e.g.*, influenza virus), rhabdovirus (*e.g.*, rabies and vesicular stomatitis virus), paramyxovirus (*e.g.*, measles and Sendai), positive strand RNA viruses such as picornavirus and alphavirus, and double-stranded DNA viruses including adenovirus, herpesvirus (*e.g.*, Herpes Simplex virus types 1 and 2, Epstein-Barr virus, cytomegalovirus), and poxvirus (*e.g.*, vaccinia, fowlpox, and canarypox). Other viruses include, for example, Norwalk virus, togavirus, flavivirus, reoviruses, papovavirus, hepadnavirus, and hepatitis virus. Examples of retroviruses include avian leukosis-sarcoma, mammalian C-type, B-type viruses, D type viruses, HTLV-BLV group, lentivirus, spumavirus (Coffin, J. M., Retroviridae: The viruses and their replication, In Fundamental Virology, Third Edition, B. N. Fields et al., Eds., Lippincott-Raven Publishers, Philadelphia, 1996).

"Retroviruses" are viruses having an RNA genome, which is reverse-transcribed into DNA using a reverse transcriptase enzyme, the reverse-transcribed DNA is then incorporated into the host cell genome. "Gammaretrovirus" refers to a genus of the retroviridae family. Examples of gammaretroviruses include mouse stem cell virus, murine leukemia virus, feline leukemia virus, feline sarcoma virus, and avian reticuloendotheliosis viruses.

"Lentiviral vectors" include HIV-based lentiviral vectors for gene delivery, which can be integrative or non-integrative, have relatively large packaging capacity, and can transduce a range of different cell types. Lentiviral vectors are usually generated following transient transfection of three (packaging, envelope, and transfer) or more plasmids into producer cells. Like HIV, lentiviral vectors enter the target cell through the interaction of viral surface glycoproteins with receptors on the cell surface. On entry, the viral RNA undergoes reverse transcription, which is mediated by the viral reverse transcriptase complex. The product of reverse transcription is a double-stranded

linear viral DNA, which is the substrate for viral integration into the DNA of infected cells.

In certain embodiments, the viral vector can be a gammaretrovirus, *e.g.*, Moloney murine leukemia virus (MLV)-derived vectors. In other embodiments, the viral vector can be a more complex retrovirus-derived vector, *e.g.*, a lentivirus-derived vector. HIV-1-derived vectors belong to this category. Other examples include lentivirus vectors derived from HIV-2, FIV, equine infectious anemia virus, SIV, and Maedi-Visna virus (ovine lentivirus). Methods of using retroviral and lentiviral viral vectors and packaging cells for transducing mammalian host cells with viral particles containing transgenes are known in the art and have been previous described, for example, in: U.S. Patent 8,119,772; Walchli *et al.*, *PLoS One 6*:327930, 2011; Zhao *et al.*, *J. Immunol. 174*:4415, 2005; Engels *et al.*, *Hum. Gene Ther. 14*:1155, 2003; Frecha *et al.*, *Mol. Ther. 18*:1748, 2010; and Verhoeyen *et al.*, *Methods Mol. Biol. 506*:97, 2009. Retroviral and lentiviral vector constructs and expression systems are also commercially available. Other viral vectors also can be used for polynucleotide delivery including DNA viral vectors, including, for example adenovirus-based vectors and adeno-associated virus (AAV)-based vectors; vectors derived from herpes simplex viruses (HSVs), including amplicon vectors, replication-defective HSV and attenuated HSV (Krisky *et al.*, *Gene Ther. 5*:1517, 1998).

Other vectors that can be used with the compositions and methods of this disclosure include those derived from baculoviruses and α-viruses. (Jolly, D J. 1999. Emerging Viral Vectors. pp 209-40 in Friedmann T. ed. The Development of Human Gene Therapy. New York: Cold Spring Harbor Lab), or plasmid vectors (such as sleeping beauty or other transposon vectors).

When a viral vector genome comprises a plurality of polynucleotides to be expressed in a host cell as separate transcripts, the viral vector may also comprise additional sequences between the two (or more) transcripts allowing for bicistronic or multicistronic expression. Examples of such sequences used in viral vectors include internal ribosome entry sites (IRES), furin cleavage sites, viral 2A peptide, or any combination thereof.

Plasmid vectors, including DNA-based antibody or antigen-binding fragment-encoding plasmid vectors for direct administration to a subject, are described further herein.

As used herein, the term "host" refers to a cell or microorganism targeted for genetic modification with a heterologous nucleic acid molecule to produce a polypeptide of interest (*e.g.*, an antibody of the present disclosure).

A host cell may include any individual cell or cell culture which may receive a vector or the incorporation of nucleic acids or express proteins. The term also encompasses progeny of the host cell, whether genetically or phenotypically the same or different. Suitable host cells may depend on the vector and may include mammalian cells, animal cells, human cells, simian cells, insect cells, yeast cells, and bacterial cells. These cells may be induced to incorporate the vector or other material by use of a viral vector, transformation via calcium phosphate precipitation, DEAE-dextran, electroporation, microinjection, or other methods. *See*, for example, Sambrook *et al.*, *Molecular Cloning: A Laboratory Manual* 2d ed. (Cold Spring Harbor Laboratory, 1989).

In the context of a SARS-CoV-2 infection, a "host" refers to a cell or a subject infected with the SARS-CoV-2 coronavirus.

"Antigen" or "Ag", as used herein, refers to an immunogenic molecule that provokes an immune response. This immune response may involve antibody production, activation of specific immunologically-competent cells, activation of complement, antibody dependent cytotoxicicity, or any combination thereof. An antigen (immunogenic molecule) may be, for example, a peptide, glycopeptide, polypeptide, glycopolypeptide, polynucleotide, polysaccharide, lipid, or the like. It is readily apparent that an antigen can be synthesized, produced recombinantly, or derived from a biological sample. Exemplary biological samples that can contain one or more antigens include tissue samples, stool samples, cells, biological fluids, or combinations thereof. Antigens can be produced by cells that have been modified or genetically engineered to express an antigen. Antigens can also be present in a SARS-CoV-2

coronavirus (*e.g.*, a surface glycoprotein or portion thereof), such as present in a virion, or expressed or presented on the surface of a cell infected by SARS-CoV-2.

The term "epitope" or "antigenic epitope" includes any molecule, structure, amino acid sequence, or protein determinant that is recognized and specifically bound by a cognate binding molecule, such as an immunoglobulin, or other binding molecule, domain, or protein. Epitopic determinants generally contain chemically active surface groupings of molecules, such as amino acids or sugar side chains, and can have specific three-dimensional structural characteristics, as well as specific charge characteristics. Where an antigen is or comprises a peptide or protein, the epitope can comprise consecutive amino acids (*e.g.*, a linear epitope), or can comprise amino acids from different parts or regions of the protein that are brought into proximity by protein folding (*e.g.*, a discontinuous or conformational epitope), or non-contiguous amino acids that are in close proximity irrespective of protein folding.

Antibodies, Antigen-Binding Fragments, and Antibody Combinations

In one aspect, the present disclosure provides an isolated antibody, or an antigen-binding fragment thereof, that is capable of binding to a surface glycoprotein of SARS-CoV-2. In certain embodiments, the antibody or antigen-binding fragment is capable of binding to a surface glycoprotein of SARS-CoV-2 expressed on a cell surface of a host cell and/or on a SARS-CoV-2 virion.

In certain embodiments, an antibody or antigen-binding fragment of the present disclosure associates with or unites with a SARS-CoV-2 surface glycoprotein epitope or antigen comprising the epitope, while not significantly associating or uniting with any other molecules or components in a sample.

In certain embodiments, an antibody or antigen-binding fragment of the present disclosure associates with or unites (*e.g.*, binds) to a SARS-CoV-2 surface glycoprotein epitope, and can also associate with or unite with an epitope from another coronavirus (*e.g.*, SARS-CoV-1) present in the sample, but not significantly associating or uniting with any other molecules or components in the sample. In other words, in certain embodiments, an antibody or antigen binding fragment of the present disclosure is cross-reactive for SARS-CoV-2 and one or more additional coronavirus.

Binding comprises "contacting" a S glycoprotein feature, such as an amino acid, a glycan, or the like. In this context, contacting encompasses, for example, electrostatic interactions, hydrophobic interactions, hydrophobic contacts, formation of a chemical bond (*e.g.*, a hydrogen bond), formation of a water molecule, van der Waals interactions, and/or interactions due to shape complementarity (*e.g.*, inserting or burying an antibody (or antigen-binding fragment) amino acid residue in a recess formed by the S glycoprotein; antibody amino acids encompassing a S glycoprotein amino acid residue or residues), and combinations of these.

In some contexts, binding to a S glycoprotein or trimer thereof is described with reference to herein-disclosed cryo-electron microscopy techniques and/or x-ray crystallography techniques and/or crystal structures. In some embodiments, binding interactions are resolved to a resolution of 10 angstroms or less, 5 angstroms or less, 4 angstroms or less, 3.9 angstroms or less, 3.8 angstroms or less, 3.7 angstroms or less, 3.6 angstroms or less, 3.5 angstroms or less, 3.4 angstroms or less, 3.3 angstroms or less, 3.2 angstroms or less, 3.1 angstroms or less, 3.0 angstroms or less, 2.9 angstroms or less, 2.8 angstroms or less, 2.7 angstroms or less, 2.65 angstroms or less, 2.6 angstroms or less, or 2.5 angstroms or less. In some embodiments, contacting comprises a distance between an antibody (or antigen-binding fragment) amino acid residue and a S glycoprotein amino acid residue of 3.6 angstroms or less, 3.5 angstroms or less, 3.4 angstroms or less, 3.3 angstroms or less, 3.2 angstroms or less, 3.1 angstroms or less, 3.0 angstroms or less, 2.9 angstroms or less, 2.8 angstroms or less, 2.7 angstroms or less, 2.65 angstroms or less, 2.6 angstroms or less, or 2.5 angstroms or less. Settings and techniques for performing x-ray crystallography and cryo-electron microscopy include those disclosed in the present Examples, and principles of these are known in the art.

In some contexts, binding of an antibody or antigen-binding fragment comprises recognizing (*i.e.*, specifically recognizing, as opposed to non-specific sticking) an epitope formed by certain amino acids and/or glycan structures. An epitope that is formed by the recited amino acids and/or structures is comprised in, and can be comprised of some or all of, the recited amino acids and/or structures. For example, in

an amino acid sequence comprising residues 1-10, an epitope that is formed by residues 1-10 can comprise from 1 to 10 amino acids that contact an amino acid of an antibody or antigen-binding fragment. Other amino acids forming the epitope may not contact an amino acid of an antibody or antigen-binding fragment, but may contribute to the overall structure of the epitope; *e.g.*, supporting the position of an epitope amino acid that does contact an amino acid of an antibody or antigen-binding fragment.

In certain embodiments, an antibody or antigen-binding fragment is capable of the recited binding when the S glycoprotein is present as a monomer and/or in a trimer. Unless expressly stated otherwise, the ability to bind to a S glycoprotein monomer is not exclusive of the ability to bind to the S glycoprotein when present in a trimer. In certain embodiments, an antibody or antigen-binding fragment is capable of binding to an epitope that comprises amino acids in two adjacent RBDs in a trimer.

In certain embodiments, an antibody or antigen-binding fragment of the present disclosure specifically binds to a SARS-CoV-2 surface glycoprotein. As used herein, "specifically binds" refers to an association or union of an antibody or antigen-binding fragment to an antigen with an affinity or K_a (*i.e.*, an equilibrium association constant of a particular binding interaction with units of 1/M) equal to or greater than 10^5 M^{-1} (which equals the ratio of the on-rate [K_{on}] to the off rate [K_{off}] for this association reaction), while not significantly associating or uniting with any other molecules or components in a sample. Alternatively, affinity may be defined as an equilibrium dissociation constant (K_d) of a particular binding interaction with units of M (*e.g.*, 10^{-5} M to 10^{-13} M). Antibodies may be classified as "high-affinity" antibodies or as "low-affinity" antibodies. "High-affinity" antibodies refer to those antibodies having a K_a of at least 10^7 M^{-1}, at least 10^8 M^{-1}, at least 10^9 M^{-1}, at least 10^{10} M^{-1}, at least 10^{11} M^{-1}, at least 10^{12} M^{-1}, or at least 10^{13} M^{-1}. "Low-affinity" antibodies refer to those antibodies having a K_a of up to 10^7 M^{-1}, up to 10^6 M^{-1}, up to 10^5 M^{-1}. Alternatively, affinity may be defined as an equilibrium dissociation constant (K_d) of a particular binding interaction with units of M (*e.g.*, 10^{-5} M to 10^{-13} M).

A variety of assays are known for identifying antibodies of the present disclosure that bind a particular target, as well as determining binding domain or

binding protein affinities, such as Western blot, ELISA (*e.g.*, direct, indirect, or sandwich), analytical ultracentrifugation, spectroscopy, and surface plasmon resonance (Biacore®) analysis (*see, e.g.,* Scatchard *et al.*, *Ann. N.Y. Acad. Sci. 51*:660, 1949; Wilson, *Science 295*:2103, 2002; Wolff *et al.*, *Cancer Res. 53*:2560, 1993; and U.S. Patent Nos. 5,283,173, 5,468,614, or the equivalent). Assays for assessing affinity or apparent affinity or relative affinity are also known.

In certain examples, binding can be identified by recombinantly expressing a SARS-CoV-2 antigen in a host cell (*e.g.*, by transfection) and immunostaining the (*e.g.*, fixed, or fixed and permeabilized) host cell with antibody and assessing presence or absence of binding by flow cytometery (*e.g.*, using a ZE5 Cell Analyzer (BioRad®) and FlowJo software (TreeStar). In some embodiments, positive binding can be defined by differential staining by antibody of SARS-CoV-2 -expressing cells versus control (*e.g.*, mock) cells.

In some embodiments an antibody or antigen-binding fragment of the present disclosure binds to SARS-CoV-2 S protein, as measured using biolayer interferometry.

In certain embodiments, an antibody or antigen-binding fragment of the present disclosure is capable of neutralizing infection by SARS-CoV-2. As used herein, a "neutralizing antibody" is one that can neutralize, *i.e.*, prevent, inhibit, reduce, impede, or interfere with, the ability of a pathogen to initiate and/or perpetuate an infection in a host. The terms "neutralizing antibody" and "an antibody that neutralizes" or "antibodies that neutralize" are used interchangeably herein. In any of the presently disclosed embodiments, the antibody or antigen-binding fragment is capable of preventing and/or neutralizing a SARS-CoV-2 infection in an *in vitro* model of infection and/or in an *in vivo* animal model of infection and/or in a human.

Terms understood by those in the art of antibody technology are each given the meaning acquired in the art, unless expressly defined differently herein. For example, the term "antibody" refers to an intact antibody comprising at least two heavy (H) chains and two light (L) chains inter-connected by disulfide bonds, as well as any antigen-binding portion or fragment of an intact antibody that has or retains the ability to bind to the antigen target molecule recognized by the intact antibody, such as an

scFv, Fab, or Fab'2 fragment. Thus, the term "antibody" herein is used in the broadest sense and includes polyclonal and monoclonal antibodies, including intact antibodies and functional (antigen-binding) antibody fragments thereof, including fragment antigen binding (Fab) fragments, F(ab')2 fragments, Fab' fragments, Fv fragments, recombinant IgG (rIgG) fragments, single chain antibody fragments, including single chain variable fragments (scFv), and single domain antibodies (*e.g.*, sdAb, sdFv, nanobody) fragments. The term encompasses genetically engineered and/or otherwise modified forms of immunoglobulins, such as intrabodies, peptibodies, chimeric antibodies, fully human antibodies, humanized antibodies, and heteroconjugate antibodies, multispecific, *e.g.*, bispecific antibodies, diabodies, triabodies, tetrabodies, tandem di-scFv, and tandem tri-scFv. Unless otherwise stated, the term "antibody" should be understood to encompass functional antibody fragments thereof. The term also encompasses intact or full-length antibodies, including antibodies of any class or sub-class, including IgG and sub-classes thereof (IgG1, IgG2, IgG3, IgG4), IgM, IgE, IgA, and IgD.

The terms "V_L" or "VL" and "V_H" or "VH" refer to the variable binding region from an antibody light chain and an antibody heavy chain, respectively. In certain embodiments, a VL is a kappa (κ) class (also "VK" herein). In certain embodiments, a VL is a lambda (λ) class. The variable binding regions comprise discrete, well-defined sub-regions known as "complementarity determining regions" (CDRs) and "framework regions" (FRs). The terms "complementarity determining region," and "CDR," are synonymous with "hypervariable region" or "HVR," and refer to sequences of amino acids within antibody variable regions, which, in general, together confer the antigen specificity and/or binding affinity of the antibody, wherein consecutive CDRs (*i.e.*, CDR1 and CDR2, CDR2 and CDR3) are separated from one another in primary structure by a framework region. There are three CDRs in each variable region (HCDR1, HCDR2, HCDR3; LCDR1, LCDR2, LCDR3; also referred to as CDRHs and CDRLs, respectively). In certain embodiments, an antibody VH comprises four FRs and three CDRs as follows: FR1-HCDR1-FR2-HCDR2-FR3-HCDR3-FR4; and an antibody VL comprises four FRs and three CDRs as follows: FR1-LCDR1-FR2-

LCDR2-FR3-LCDR3-FR4. In general, the VH and the VL together form the antigen-binding site through their respective CDRs.

As used herein, a "variant" of a CDR refers to a functional variant of a CDR sequence having up to 1-3 amino acid substitutions (*e.g.*, conservative or non-conservative substitutions), deletions, or combinations thereof.

Numbering of CDR and framework regions may be according to any known method or scheme, such as the Kabat, Chothia, EU, IMGT, and AHo numbering schemes (*see*, *e.g.*, Kabat *et al.*, "Sequences of Proteins of Immunological Interest, US Dept. Health and Human Services, Public Health Service National Institutes of Health, 1991, 5th ed.; Chothia and Lesk, *J. Mol. Biol. 196*:901-917 (1987)); Lefranc *et al.*, *Dev. Comp. Immunol. 27*:55, 2003; Honegger and Plückthun, *J. Mol. Bio. 309*:657-670 (2001)). Equivalent residue positions can be annotated and for different molecules to be compared using Antigen receptor Numbering And Receptor Classification (ANARCI) software tool (2016, Bioinformatics 15:298-300). Accordingly, identification of CDRs of an exemplary variable domain (VH or VL) sequence as provided herein according to one numbering scheme is not exclusive of an antibody comprising CDRs of the same variable domain as determined using a different numbering scheme.

Exemplary antibodies of the present disclosure include those summarized in Table 1.

Table 1. Features of certain Antibodies

Antibody	VH SEQ ID NO.	CDRH1-CDRH3 SEQ ID NOs.	VL SEQ ID NO.	CDRL1-CDRL3 SEQ ID NOs.	Binds in Antigenic Site
S2H14	47	48, 49, 50	51	52, 53, 54	Ia
S2H13	31	32, 33, 34	35	36, 37, 38	Ib
S2X259	16	10, 12, 15	26	23-25	IIa
S2X35	72	73, 74, 75	76	77, 78, 79	IIa
S2A4	64	65, 66, 67	68	69, 70, 71	IIb

Antibody	VH SEQ ID NO.	CDRH1-CDRH3 SEQ ID NOs.	VL SEQ ID NO.	CDRL1-CDRL3 SEQ ID NOs.	Binds in Antigenic Site
S304	150	151, 152, 153	154	155, 156, 157	IIc
S309	101	102, 103, 104	105	106, 107, 108	IV
S2E12	123	109, 110, 111	138	133, 134, 135	Tertiary epitope
S2M11	142	143, 144, 145	146	147, 148, 149	Quaternary epitope comprised of two adjacent closed RBDs

Herein, "S2H14" refers to an antibody that comprises the VH amino acid sequence of SEQ ID NO.:47 and the VL amino acid sequence of SEQ ID NO.:51. Herein, "S2H13" refers to an antibody that comprises the VH amino acid sequence of SEQ ID NO.:31 and the VL amino acid sequence of SEQ IDNO.:35. Herein, "S2X259" refers to an antibody that comprises the VH amino acid sequence of SEQ ID NO.:16 and the VL amino acid sequence of SEQ IDNO.:26. Herein, "S2X35" refers to an antibody that comprises the VH amino acid sequence of SEQ ID NO.:72 and the VL amino acid sequence of SEQ IDNO.:76. Herein, "S2A4" refers to an antibody that comprises the VH amino acid sequence of SEQ ID NO.:64 and the VL amino acid sequence of SEQ IDNO.:68. Herein, "S304" refers to an antibody that comprises the VH amino acid sequence of SEQ ID NO.:150 and the VL amino acid sequence of SEQ IDNO.:154. Herein, "S309" refers to an antibody that comprises the VH amino acid sequence of SEQ ID NO.:101 and the VL amino acid sequence of SEQ IDNO.:105. Herein, "S2E12" refers to an antibody that comprises the VH amino acid sequence of SEQ ID NO.:123 and the VL amino acid sequence of SEQ ID NO.:138. Herein, "S2M11" refers to an antibody that comprises the VH amino acid sequence of SEQ ID NO.:142 and the VL amino acid sequence of SEQ IDNO.:146.

Presently disclosed antibodies and antigen-binding fragments bind in an antigenic Site as described herein. For example, Site Ia (containing the S2H14 epitope) largely overlaps with the ACE2-binding site and is only accessible in the open S state (*e.g.* Figure 34B), whereas Site Ib (containing the S2H13 epitope; Figure 34C) partially overlaps with the ACE2 footprint and is accessible in both the open and closed S states (Figure 34C). Site II is divided into Site IIa (containing the S2X35 epitope, *e.g.* Figure 34D), which partially overlaps with the ACE2-binding site, Site IIb (containing the S2A4 epitope, proximal to the N343 glycan, *e.g.* Figure 34E), which does not overlap with the ACE2-binding site, and Site IIc (containing the S304 epitope, proximal to the N343 glycan, *e.g.* Figure 34F). Site IV does not overlap with the ACE-2 binding site and contains the S309 proteoglycan epitope (*e.g.* Figure 34G).

The S2X259 epitope is formed by amino acid residues 369-386, 404-411, and 499-508 of SEQ ID NO: 3. The S2H13 epitope is formed by amino acid residues 444-449 and 472-498 of SEQ ID NO: 3. The S2H14 epitope is formed by amino acid residues 403, 444-456, 475, and 485-505 of SEQ ID NO: 3. The S2A4 epitope is formed by amino acid residues 368-388 and 407-414 of SEQ ID NO: 3. The S304 epitope is formed by amino acid residues 369-392, 411-414, 427-430, and 515-517 of SEQ ID NO: 3. The S2E12 epitope is formed by amino acid residues 417, 453, 455, 456, 473, 475-480, 484-489, and 493 of SEQ ID NO: 3. The S2M11 epitope is formed by: (i) on a first RBD, amino acid residues 339, 342, 343, 367, 368, 371, 372, 373, 374, 436, 440, and 441, and, (ii) on a second RBD, amino acid residues 446, 447, 449, 452, 455, 456, 484, 485, 486, 487, 489, 490, 492, 493, 494, 496, and 498, wherein the amino acid numbering is according to SEQ ID NO.:3.

In certain embodiments, presently disclosed immunogenic compositions comprise a Site Ia polypeptide, a Site Ib polypeptide, a Site IIa polypeptide, a Site IIb polypeptide, a Site IIc polypeptide, and/or a Site IV polypeptide; these polypeptides comprise at least a portion of a RBD or S glycoprotein, wherein the at least a portion includes the Site Ia, Ib, IIa, IIb, IIc, or IV; *i.e.*, comprises amino acid sequence and a structure such that a herein disclosed antibody is capable of binding thereto.

Variants of S2H14 include those that comprise the VH amino acid sequence of any one of SEQ ID NOs:55, 57, 59, 61, and 62.

Variants of S2H13 include those that comprise the VH amino acid sequence of any one of SEQ ID NOs.:39, 41, 43, 44, and 45.

Variants of S2X259 include those that comprise the VH amino acid sequence of any one of SEQ ID NOs.:17-22 and/or the VL amino acid sequence of any one of SEQ ID NOs.:27-29.

Variants of S2X35 include those that comprise: the VH amino acid sequence of SEQ ID NO.:83, SEQ ID NO.:85, or SEQ ID NO.:88.

The S304 epitope (in Antigenic site IIc) partially overlaps with the epitopes of S315 (VH of SEQ ID NO.:162, VL of SEQ ID NO.:163), S2A4, S2X35, S2D22 (VH of SEQ ID NO.:166, VL of SEQ ID NO.:167), and CR3022 (heavy chain of SEQ ID NO.: 158, light chain of SEQ ID NO.:159).

S309 is described in, for example, Pinto *et al.*, *Nature* 583, pages 290–295 (2020). Amino acid residues 333-337, 339-341, 343-346, 354, 356-361, 440, 441, and 509 of SEQ ID NO.:3 contribute to the S309 proteoglycan epitope, with amino acid residues 340, 343, 345, 346, and 356 contributing significantly to antigen-antibody binding energy. A non-limiting variant of S309 comprises the VH amino acid sequence of SEQ ID NO.:93 (comprising a N55Q mutation in CDRH2 relative to S309) and the VL amino acid sequence of SEQ ID NO.:97.

The antibodies S303 (VH of SEQ ID NO.:164, VL of SEQ ID NO.:165) and S2A10 (VH of SEQ ID NO.:168, VL of SEQ ID NO.:169) bind in the same antigenic region as S309.

Variants of S2E12 include those that comprise the VH amino acid sequence of any one of SEQ ID NOs.:124-132 and/or the VL amino acid sequence of any one of SEQ ID NOs.:140-141.

Other antibodies that have been reported to bind to an epitope comprising two neighboring RBDs and stabilize the S glycoprotein in a closed conformation include the nanobody Nb6 and its engineered derivatives (M. Schoof *et al.*, An ultra-potent synthetic nanobody neutralizes SARS-CoV-2 by locking Spike into an inactive

conformation. *bioRxiv* 2020.2008.2008.238469 [Preprint]. (17 August 2020)) and the human antibody C144 (C. O. Barnes et al., Structural classification of neutralizing antibodies against the SARS-CoV-2 spike receptor-binding domain suggests vaccine and therapeutic strategies. bioRxiv 2020.2008.2030.273920 [Preprint] (30 August 2020). Nb6 and the engineered derivatives thereof, and C144, are incorporated herein by reference.

In some embodiments, an antibody, or an antigen-binding fragment thereof, is provided that competes with an antibody or antigen-binding fragment comprising a VH amino acid sequence according to SEQ ID NO: 16 and a VL amino acid sequence according to SEQ ID NO: 26 for binding to a SARS-CoV-2 S glycoprotein of a S glycoprotein trimer.

In some embodiments, an antibody, or an antigen-binding fragment thereof, is provided that is capable of binding to a SARS CoV-2 S glycoprotein of a S glycoprotein trimer, wherein: (a) binding comprises contacting one or more of amino acid residues 369-386, 404-411, and 499-508 of SEQ ID NO: 3; and/or (b) binding comprises binding an epitope formed by amino acid residues 369-386, 404-411, and 499-508 of SEQ ID NO: 3. In certain embodiments, the antibody or antigen-binding fragment does not contact one or more of amino acids 406, 409, 410, 411, 499, 500, 505, and 507 of SEQ ID NO.:3 when binding to the S glycoprotein.

In some embodiments, the antibody or antigen-binding fragment is capable of binding to a SARS-CoV-2 S glycoprotein of a S glycoprotein trimer wherein two or three receptor binding domains (RBDs) of the trimer are in an open conformation and one or zero RBDs of the trimer is in a closed conformation, and optionally is not capable of binding to the S glycoprotein when only one RBD of the trimer is in an open conformation and two RBDs of the trimer are in a closed conformation.

In certain embodiments, an antibody, or an antigen-binding fragment thereof, is provided which is capable of binding to a SARS-CoV-2 S glycoprotein of a S glycoprotein trimer wherein two or three receptor binding domains (RBDs) of the trimer are in an open conformation and one or zero RBDs of the trimer is in a closed conformation, and optionally is not capable of binding to the S protein when only one

RBD of the trimer is in an open conformation and two RBDs of the trimer are in a closed conformation.

In certain embodiments, an antibody, or an antigen-binding fragment thereof, is provided that competes with an antibody or antigen-binding fragment comprising a VH amino acid sequence according to SEQ ID NO: 31 and a VL amino acid sequence according to SEQ ID NO: 35 for binding to a SARS-CoV-2 S glycoprotein of a S glycoprotein trimer.

In some embodiments, an antibody, or an antigen-binding fragment thereof, is provided that is capable of binding to a SARS CoV-2 S glycoprotein of a S glycoprotein trimer, wherein: (a) binding comprises contacting one or more of amino acid residues 444-449 and 472-498 of SEQ ID NO: 3; and/or (b) the antibody or antigen-binding fragment recognizes an epitope formed by amino acid residues 444-449 and 472-498 of SEQ ID NO: 3; and/or (c) binding comprises binding within a crevice formed by a receptor binding motif (RBM) β-hairpin in a receptor binding domain (RBD) of the S glycoprotein. In ceratin embodiments, antibody or antigen-binding fragment does not contact one or more of amino acids 448, 473-478, 487, 491, 492, 495, 496, and 497 of SEQ ID NO.:3 when binding to the SARS-CoV-2 S glycoprotein.

In certain embodiments, the antibody or antigen-binding fragment is capable of binding to a SARS-CoV-2 S glycoprotein of a S glycoprotein trimer wherein one or zero receptor binding domains (RBDs) of the trimer are in an open conformation and two or three RBDs of the trimer are in a closed conformation.

In some embodiments, an antibody, or an antigen-binding fragment thereof, is provided which is capable of binding to a SARS-CoV-2 S glycoprotein protein of a S glycoprotein trimer wherein one or zero receptor binding domains (RBDs) of the trimer are in an open conformation and two or three RBDs of the trimer are in a closed conformation.

In some embodiments, an antibody, or an antigen-binding fragment thereof, is provided that competes with an antibody or antigen-binding fragment comprising a VH amino acid sequence according to SEQ ID NO: 47 and a VL amino acid sequence

according to SEQ ID NO: 51 for binding to a SARS-CoV-2 S glycoprotein of a S glycoprotein trimer.

In some embodiments, an antibody, or an antigen-binding fragment thereof, is provided that is capable of binding to a SARS CoV-2 S glycoprotein, wherein: (a) binding comprises contacting one or more of amino acid residues 403, 444-456, 475, and 485-505 of SEQ ID NO: 3; and/or (b) the antibody or antigen-binding fragment recognizes an epitope formed by amino acid residues 403, 444-456, 475, and 485-505 of SEQ ID NO: 3. In certain embodiments, the antibody or antigen-binding fragment does not contact one or more of amino acids 448, 450, 451, 452, 454, 486, 488, 490, 491, 492, 497, 503, and 504 of SEQ ID NO.:3 when binding to the S glycoprotein.

In some embodiments, the antibody or antigen-binding fragment is capable of binding to a SARS-CoV-2 S glycoprotein of a S glycoprotein trimer wherein one, two, or three receptor binding domains (RBDs) of the trimer are in an open conformation.

In some embodiments, an antibody, or an antigen-binding fragment thereof, is provided that competes with an antibody or antigen-binding fragment comprising a VH amino acid sequence according to SEQ ID NO: 64 and a VL amino acid sequence according to SEQ ID NO: 58 for binding to a SARS-CoV-2 S glycoprotein of a S glycoprotein trimer.

In some embodiments, an antibody, or an antigen-binding fragment thereof, is provided that is capable of binding to a SARS CoV-2 S glycoprotein of a S glycoprotein trimer, wherein: (a) binding comprises contacting one or more of amino acid residues 368-388 and 407-414 of SEQ ID NO: 3; and/or (b) the antibody or antigen-binding fragment recognizes an epitope formed by amino acid residues 368-388 and 407-414 of SEQ ID NO: 3.

In certain embodiments, the antibody or antigen-binding fragment is capable of binding to a SARS-CoV-2 S glycoprotein of a S glycoprotein trimer wherein two or three receptor binding domains (RBDs) of the trimer are in an open conformation and zero or one RBDs of the trimer is in a closed conformation.

In some embodiments, an antibody, or an antigen-binding fragment thereof, is provided that competes with an antibody or antigen-binding fragment comprising a VH

amino acid sequence according to SEQ ID NO: 150 and a VL amino acid sequence according to SEQ ID NO: 154 for binding to a SARS-CoV-2 S glycoprotein of a S glycoprotein trimer.

In some embodiments, an antibody, or an antigen-binding fragment thereof, is provided that is capable of binding to a SARS CoV-2 S glycoprotein of a S glycoprotein trimer, wherein: (a) binding comprises contacting one or more of amino acid residues 369-392, 411-414, 427-430, and 515-517 of SEQ ID NO: 3; and/or (b) the antibody or antigen-binding fragment recognizes an epitope formed by amino acid residues 369-392, 411-414, 427-430, and 515-517 of SEQ ID NO: 3. In certain embodiments, the antibody or antigen-binding fragment is capable of binding to a SARS-CoV-2 S protein of a S protein trimer wherein two or three receptor binding domains (RBDs) of the trimer are in an open conformation and zero or one RBDs of the trimer is in a closed conformation.

In ceratin embodiments, binding of the antibody or antigen-binding fragment to the S glycoprotein promotes or leads to release of the S1 subunit from the S glycoprotein.

In some embodiments, an antibody, or an antigen-binding fragment thereof, is provided that competes with an antibody or antigen-binding fragment comprising a VH amino acid sequence according to SEQ ID NO: 123 and a VL amino acid sequence according to SEQ ID NO: 138 for binding to a SARS-CoV-2 S glycoprotein of a S glycoprotein trimer.

In some embodiments, an antibody, or an antigen-binding fragment thereof, is provided that is capable of binding to a SARS CoV-2 S glycoprotein of a S glycoprotein trimer, wherein: (a) binding comprises contacting one or more of amino acid residues 417, 453, 455, 456, 473, 475-480, 484-489, and 493 of SEQ ID NO: 3; and/or (b) the antibody or antigen-binding fragment recognizes an epitope formed by amino acid residues 417, 453, 455, 456, 473, 475-480, 484-489, and 493of SEQ ID NO.: 3.

In certain embodiments, the antibody or antigen-binding fragment capable of binding to a SARS-CoV-2 S glycoprotein of a S glycoprotein trimer wherein one, two,

or three receptor binding domains (RBDs) of the trimer are in an open conformation and zero, one, or two RBDs of the trimer are in a closed conformation.

In some embodiments, an antibody, or an antigen-binding fragment thereof, is provided that competes with an antibody or antigen-binding fragment comprising a VH amino acid sequence according to SEQ ID NO: 142 and a VL amino acid sequence according to SEQ ID NO: 146 for binding to a SARS-CoV-2 S glycoprotein trimer.

In some embodiments, an antibody, or an antigen-binding fragment thereof, is provided that is capable of binding to a SARS CoV-2 S glycoprotein trimer, wherein: (a) binding comprises contacting one or more of amino acid residues on each of two receptor binding domains (RBDs), wherein binding comprises contacting, on a first RBD, one or more of amino acid residues 339, 342, 343, 367, 368, 371, 372, 373, 374, 436, 440, and 441, and, on a second RBD, one or more of amino acid residues 446, 447, 449, 452, 455, 456, 484, 485, 486, 487, 489, 490, 492, 493, 494, 496, and 498, wherein the amino acid numbering is according to SEQ ID NO.:3; and/or (b) the antibody or antigen-binding fragment recognizes an epitope formed by the following: (b)(i) on a first RBD, amino acid residues 339, 342, 343, 367, 368, 371, 372, 373, 374, 436, 440, and 441, and, (b)(ii) on a second RBD, amino acid residues 446, 447, 449, 452, 455, 456, 484, 485, 486, 487, 489, 490, 492, 493, 494, 496, and 498, wherein the amino acid numbering is according to SEQ ID NO.:3.

In certain embodiments, the antibody or antigen-binding fragment of is capable of binding to the S glycoprotein trimer wherein three receptor binding domains (RBDs) of the trimer are in a closed conformation.

In certain embodiments, binding of the antibody or antigen-binding fragment to the S glycoprotein trimer inhibits or prevents an RBD of the trimer from assuming an open conformation.

In certain embodiments, binding of the antibody or antigen-binding fragment to the S glycoprotein or S glycoprotein trimer, respectively, blocks an interaction between the S glycoprotein and a human ACE2.

In certain embodiments, binding of the antibody or antigen-binding fragment to the S glycoprotein or S glycoprotein trimer, respectively, does not block an interaction between the S glycoprotein and a human ACE2.

In certain embodiments, the antibody or antigen-binding fragment is capable of neutralizing an infection by a SARS-CoV-2.

The term "CL" refers to an "immunoglobulin light chain constant region" or a "light chain constant region," *i.e.*, a constant region from an antibody light chain. The term "CH" refers to an "immunoglobulin heavy chain constant region" or a "heavy chain constant region," which is further divisible, depending on the antibody isotype into CH1, CH2, and CH3 (IgA, IgD, IgG), or CH1, CH2, CH3, and CH4 domains (IgE, IgM). The Fc region of an antibody heavy chain is described further herein. In any of the presently disclosed embodiments, an antibody or antigen-binding fragment of the present disclosure comprises any one or more of CL, a CH1, a CH2, and a CH3. In certain embodiments, a CL comprises an amino acid sequence having 90%, 91%, 92%, 93%, 94%, 95%, 96%, 975, 98%, 99%, or 100% identity to the amino acid sequence of SEQ ID NO.:8 or SEQ ID NO.: 9. In certain embodiments, a CH1-CH2-CH3 comprises an amino acid sequence having 90%, 91%, 92%, 93%, 94%, 95%, 96%, 97%, 98%, 99%, or 100% identity to the amino acid sequence of SEQ ID NO.:6 or SEQ ID NO.:6 or 7.

A "Fab" (fragment antigen binding) is the part of an antibody that binds to antigens and includes the variable region and CH1 of the heavy chain linked to the light chain via an inter-chain disulfide bond. Each Fab fragment is monovalent with respect to antigen binding, *i.e.*, it has a single antigen-binding site. Pepsin treatment of an antibody yields a single large F(ab')2 fragment that roughly corresponds to two disulfide linked Fab fragments having divalent antigen-binding activity and is still capable of cross-linking antigen. Both the Fab and F(ab')2 are examples of "antigen-binding fragments." Fab' fragments differ from Fab fragments by having additional few residues at the carboxy terminus of the CH1 domain including one or more cysteines from the antibody hinge region. Fab'-SH is the designation herein for Fab' in which the cysteine residue(s) of the constant domains bear a free thiol group. F(ab')2 antibody

fragments originally were produced as pairs of Fab' fragments that have hinge cysteines between them. Other chemical couplings of antibody fragments are also known.

Fab fragments may be joined, *e.g.*, by a peptide linker, to form a single chain Fab, also referred to herein as "scFab." In these embodiments, an inter-chain disulfide bond that is present in a native Fab may not be present, and the linker serves in full or in part to link or connect the Fab fragments in a single polypeptide chain. A heavy chain-derived Fab fragment (*e.g.*, comprising, consisting of, or consisting essentially of VH + CH1, or "Fd") and a light chain-derived Fab fragment (*e.g.*, comprising, consisting of, or consisting essentially of VL + CL) may be linked in any arrangement to form a scFab. For example, a scFab may be arranged, in N-terminal to C-terminal direction, according to (heavy chain Fab fragment – linker – light chain Fab fragment) or (light chain Fab fragment – linker – heavy chain Fab fragment). Peptide linkers and exemplary linker sequences for use in scFabs are discussed in further detail herein.

"Fv" is a small antibody fragment that contains a complete antigen-recognition and antigen-binding site. This fragment generally consists of a dimer of one heavy- and one light-chain variable region domain in tight, non-covalent association. However, even a single variable domain (or half of an Fv comprising only three CDRs specific for an antigen) has the ability to recognize and bind antigen, although typically at a lower affinity than the entire binding site.

"Single-chain Fv" also abbreviated as "sFv" or "scFv", are antibody fragments that comprise the V_H and V_L antibody domains connected into a single polypeptide chain. In some embodiments, the scFv polypeptide comprises a polypeptide linker disposed between and linking the V_H and V_L domains that enables the scFv to retain or form the desired structure for antigen binding. Such a peptide linker can be incorporated into a fusion polypeptide using standard techniques well known in the art. For a review of scFv, see Pluckthun in The Pharmacology of Monoclonal Antibodies, vol. 113, Rosenburg and Moore eds., Springer-Verlag, New York, pp. 269-315 (1994); Borrebaeck 1995, *infra*. In certain embodiments, the antibody or antigen-binding fragment comprises a scFv comprising a VH domain, a VL domain, and a peptide linker linking the VH domain to the VL domain. In particular embodiments, a scFv comprises

a VH domain linked to a VL domain by a peptide linker, which can be in a VH-linker-VL orientation or in a VL-linker-VH orientation. Any scFv of the present disclosure may be engineered so that the C-terminal end of the VL domain is linked by a short peptide sequence to the N-terminal end of the VH domain, or vice versa (i.e., (N)VL(C)-linker-(N)VH(C) or (N)VH(C)-linker-(N)VL(C). Alternatively, in some embodiments, a linker may be linked to an N-terminal portion or end of the VH domain, the VL domain, or both.

Peptide linker sequences may be chosen, for example, based on: (1) their ability to adopt a flexible extended conformation; (2) their inability or lack of ability to adopt a secondary structure that could interact with functional epitopes on the first and second polypeptides and/or on a target molecule; and/or (3) the lack or relative lack of hydrophobic or charged residues that might react with the polypeptides and/or target molecule. Other considerations regarding linker design (*e.g.*, length) can include the conformation or range of conformations in which the VH and VL can form a functional antigen-binding site. In certain embodiments, peptide linker sequences contain, for example, Gly, Asn and Ser residues. Other near neutral amino acids, such as Thr and Ala, may also be included in a linker sequence. Other amino acid sequences which may be usefully employed as linker include those disclosed in Maratea et al., Gene 40:39 46 (1985); Murphy et al., Proc. Natl. Acad. Sci. USA 83:8258 8262 (1986); U.S. Pat. No. 4,935,233, and U.S. Pat. No. 4,751,180. Other illustrative and non-limiting examples of linkers may include, for example, Glu-Gly-Lys-Ser-Ser-Gly-Ser-Gly-Ser-Glu-Ser-Lys-Val-Asp (Chaudhary et al., Proc. Natl. Acad. Sci. USA 87:1066-1070 (1990)) and Lys-Glu-Ser-Gly-Ser-Val-Ser-Ser-Glu-Gln-Leu-Ala-Gln-Phe-Arg-Ser-Leu-Asp (Bird et al., Science 242:423-426 (1988)) and the pentamer Gly-Gly-Gly-Gly-Ser when present in a single iteration or repeated 1 to 5 or more times, or more. Any suitable linker may be used, and in general can be about 3, 4, 5, 6, 7, 8, 9, 10, 11, 12, 13, 14, 15, 16, 17, 18, 19, 20, 21, 22, 15 23, 24, 25, 26, 27, 28, 29, 30, 40, 50, 60, 70, 80, 90, 100 amino acids in length, or less than about 200 amino acids in length, and will preferably comprise a flexible structure (can provide flexibility and room for conformational movement between two regions, domains, motifs, fragments, or modules connected by the linker),

and will preferably be biologically inert and/or have a low risk of immunogenicity in a human.

scFv can be constructed using any combination of the VH and VL sequences or any combination of the CDRH1, CDRH2, CDRH3, CDRL1, CDRL2, and CDRL3 sequences disclosed herein.

In some embodiments, linker sequences are not required; for example, when the first and second polypeptides have non-essential N-terminal amino acid regions that can be used to separate the functional domains and prevent steric interference.

During antibody development, DNA in the germline variable (V), joining (J), and diversity (D) gene loci may be rearranged and insertions and/or deletions of nucleotides in the coding sequence may occur. Somatic mutations may be encoded by the resultant sequence, and can be identified by reference to a corresponding known germline sequence. In some contexts, somatic mutations that are not critical to a desired property of the antibody (*e.g.*, binding to a SARS-CoV-2 antigen), or that confer an undesirable property upon the antibody (*e.g.*, an increased risk of immunogenicity in a subject administered the antibody), or both, may be replaced by the corresponding germline-encoded amino acid, or by a different amino acid, so that a desirable property of the antibody is improved or maintained and the undesirable property of the antibody is reduced or abrogated. Thus, in some embodiments, the antibody or antigen-binding fragment of the present disclosure comprises at least one more germline-encoded amino acid in a variable region as compared to a parent antibody or antigen-binding fragment, provided that the parent antibody or antigen binding fragment comprises one or more somatic mutations. Variable region and CDR amino acid sequences of exemplary anti-SARS-CoV-2 antibodies of the present disclosure are provided in Table 1 herein.

In certain embodiments, an antibody or antigen-binding fragment comprises an amino acid modification (*e.g.*, a substitution mutation) to remove an undesired risk of oxidation, deamidation, and/or isomerization.

Also provided herein are variant antibodies that comprise one or more amino acid alterations in a variable region (*e.g.*, VH, VL, framework or CDR) as compared to

a presently disclosed ("parent") antibody, wherein the variant antibody is capable of binding to a SARS-CoV-2 antigen.

In certain embodiments, an antibody or antigen-binding fragment of the present disclosure is monospecific (*e.g.*, binds to a single epitope) or is multispecific (*e.g.*, binds to multiple epitopes and/or target molecules). Antibodies and antigen binding fragments may be constructed in various formats. Exemplary antibody formats disclosed in Spiess et al., Mol. Immunol. 67(2):95 (2015), and in Brinkmann and Kontermann, mAbs 9(2):182-212 (2017), which formats and methods of making the same are incorporated herein by reference and include, for example, Bispecific T cell Engagers (BiTEs), DARTs, Knobs-Into-Holes (KIH) assemblies, scFv-CH3-KIH assemblies, KIH Common Light-Chain antibodies, TandAbs, Triple Bodies, TriBi Minibodies, Fab-scFv, scFv-CH-CL-scFv, F(ab')2-scFv2, tetravalent HCabs, Intrabodies, CrossMabs, Dual Action Fabs (DAFs) (two-in-one or four-in-one), DutaMabs, DT-IgG, Charge Pairs, Fab-arm Exchange, SEEDbodies, Triomabs, LUZ-Y assemblies, Fcabs, κλ-bodies, orthogonal Fabs, DVD-Igs (*e.g.*, US Patent No. 8,258,268, which formats are incorporated herein by reference in their entirety), IgG(H)-scFv, scFv-(H)IgG, IgG(L)-scFv, scFv-(L)IgG, IgG(L,H)-Fv, IgG(H)-V, V(H)-IgG, IgG(L)-V, V(L)-IgG, KIH IgG-scFab, 2scFv-IgG, IgG-2scFv, scFv4-Ig, Zybody, and DVI-IgG (four-in-one), as well as so-called FIT-Ig (*e.g.*, PCT Publication No. WO 2015/103072, which formats are incorporated herein by reference in their entirety), so-called WuxiBody formats (*e.g.*, PCT Publication No. WO 2019/057122, which formats are incorporated herein by reference in their entirety), and so-called In-Elbow-Insert Ig formats (IEI-Ig; *e.g.*, PCT Publication Nos. WO 2019/024979 and WO 2019/025391, which formats are incorporated herein by reference in their entirety).

In certain embodiments, the antibody or antigen-binding fragment comprises two or more of VH domains, two or more VL domains, or both (*i.e.*, two or more VH domains and two or more VL domains). In particular embodiments, an antigen-binding fragment comprises the format (N-terminal to C-terminal direction) VH-linker-VL-linker-VH-linker-VL, wherein the two VH sequences can be the same or different and the two VL sequences can be the same or different. Such linked scFvs can include any

combination of VH and VL domains arranged to bind to a given target, and in formats comprising two or more VH and/or two or more VL, one, two, or more different eptiopes or antigens may be bound. It will be appreciated that formats incorporating multiple antigen-binding domains may include VH and/or VL sequences in any combination or orientation. For example, the antigen-binding fragment can comprise the format VL-linker-VH-linker-VL-linker-VH, VH-linker-VL-linker-VL-linker-VH, or VL-linker-VH-linker-VH-linker-VL.

Monospecific or multispecific antibodies or antigen-binding fragments of the present disclosure constructed comprise any combination of the VH and VL sequences and/or any combination of the CDRH1, CDRH2, CDRH3, CDRL1, CDRL2, and CDRL3 sequences disclosed herein. A bispecific or multispecific antibody or antigen-binding fragment may, in some embodiments, comprise one, two, or more antigen-binding domains (*e.g.*, a VH and a VL) of the instant disclosure. Two or more binding domains may be present that bind to the same or a different SARS-CoV-2 epitope, and a bispecific or multispecific antibody or antigen-binding fragment as provided herein can, in some embodiments, comprise a further SARS-CoV-2 binding domain, and/or can comprise a binding domain that binds to a different antigen or pathogen altogether.

In any of the presently disclosed embodiments, the antibody or antigen-binding fragment can be multispecific; *e.g.*, bispecific, trispecific, or the like.

In certain embodiments, the antibody or antigen-binding fragment comprises a Fc polypeptide, or a fragment thereof. The "Fc" fragment or Fc polypeptide comprises the carboxy-terminal portions (*i.e.*, the CH2 and CH3 domains of IgG) of both antibody H chains held together by disulfides. Antibody “effector functions” refer to those biological activities attributable to the Fc region (a native sequence Fc region or amino acid sequence variant Fc region) of an antibody, and vary with the antibody isotype. Examples of antibody effector functions include: C1q binding and complement dependent cytotoxicity; Fc receptor binding; antibody-dependent cell-mediated cytotoxicity (ADCC); phagocytosis; down regulation of cell surface receptors (e.g., B cell receptor); and B cell activation. As discussed herein, modifications (*e.g.*, amino acid substitutions) may be made to an Fc domain in order to modify (*e.g.*, improve,

reduce, or ablate) one or more functionality of an Fc-containing polypeptide (*e.g.*, an antibody of the present disclosure). Such functions include, for example, Fc receptor (FcR) binding, antibody half-life modulation (e.g., by binding to FcRn), ADCC function, protein A binding, protein G binding, and complement binding. Amino acid modifications that modify (e.g., improve, reduce, or ablate) Fc functionalities include, for example, the T250Q/M428L, M252Y/S254T/T256E (also referred-to as "YTE"), H433K/N434F, M428L/N434S (also referred-to as "LS" or "MLNS"), E233P/L234V/L235A/G236 + A327G/A330S/P331S, E333A, S239D/A330L/I332E, P257I/Q311, K326W/E333S, S239D/I332E/G236A, N297Q, K322A, S228P, L235E + E318A/K320A/K322A, L234A/L235A (also referred to herein as "LALA"), and L234A/L235A/P329G mutations, which mutations are summarized and annotated in "Engineered Fc Regions", published by InvivoGen (2011) and available online at invivogen.com/PDF/review/review-Engineered-Fc-Regions-invivogen.pdf?utm_source=review&utm_medium=pdf&utm_campaign=review&utm_content=Engineered-Fc-Regions, and are incorporated herein by reference. Unless specifically stated otherwise, numbering of Fc residues is according to the EU numbering system as set forth in Kabat.

For example, to activate the complement cascade, the C1q protein complex can bind to at least two molecules of IgG1 or one molecule of IgM when the immunoglobulin molecule(s) is attached to the antigenic target (Ward, E. S., and Ghetie, V., *Ther. Immunol.* 2 (1995) 77-94). Burton, D. R., described (*Mol. Immunol.* 22 (1985) 161-206) that the heavy chain region comprising amino acid residues 318 to 337 is involved in complement fixation. Duncan, A. R., and Winter, G. (*Nature* 332 (1988) 738-740), using site directed mutagenesis, reported that Glu318, Lys320 and Lys322 form the binding site to C1q. The role of Glu318, Lys320 and Lys 322 residues in the binding of C1q was confirmed by the ability of a short synthetic peptide containing these residues to inhibit complement mediated lysis.

For example, FcR binding can be mediated by the interaction of the Fc moiety (of an antibody) with Fc receptors (FcRs), which are specialized cell surface receptors on cells including hematopoietic cells. Fc receptors belong to the immunoglobulin

superfamily, and shown to mediate both the removal of antibody-coated pathogens by phagocytosis of immune complexes, and the lysis of erythrocytes and various other cellular targets (e.g. tumor cells) coated with the corresponding antibody, via antibody dependent cell mediated cytotoxicity (ADCC; Van de Winkel, J. G., and Anderson, C. L., *J. Leukoc. Biol.* 49 (1991) 511-524). FcRs are defined by their specificity for immunoglobulin classes; Fc receptors for IgG antibodies are referred to as FcγR, for IgE as FcεR, for IgA as FcαR and so on and neonatal Fc receptors are referred to as FcRn. Fc receptor binding is described for example in Ravetch, J. V., and Kinet, J. P., *Annu. Rev. Immunol.* 9 (1991) 457-492; Capel, P. J., et al., *Immunomethods* 4 (1994) 25-34; de Haas, M., et al., *J Lab. Clin. Med.* 126 (1995) 330-341; and Gessner, J. E., et al., *Ann. Hematol.* 76 (1998) 231-248.

Cross-linking of receptors by the Fc domain of native IgG antibodies (FcγR) triggers a wide variety of effector functions including phagocytosis, antibody-dependent cellular cytotoxicity, and release of inflammatory mediators, as well as immune complex clearance and regulation of antibody production. Fc moieties providing cross-linking of receptors (e.g., FcγR) are contemplated herein. In humans, three classes of FcγR have been characterized to-date, which are: (i) FcγRI (CD64), which binds monomeric IgG with high affinity and is expressed on macrophages, monocytes, neutrophils and eosinophils; (ii) FcγRII (CD32), which binds complexed IgG with medium to low affinity, is widely expressed, in particular on leukocytes, is believed to be a central player in antibody-mediated immunity, and which can be divided into FcγRIIA, FcγRIIB and FcγRIIC, which perform different functions in the immune system, but bind with similar low affinity to the IgG-Fc, and the ectodomains of these receptors are highly homologuous; and (iii) FcγRIII (CD16), which binds IgG with medium to low affinity and has been found in two forms: FcγRIIIA, which has been found on NK cells, macrophages, eosinophils, and some monocytes and T cells, and is believed to mediate ADCC; and FcγRIIIB, which is highly expressed on neutrophils.

FcγRIIA is found on many cells involved in killing (e.g. macrophages, monocytes, neutrophils) and seems able to activate the killing process. FcγRIIB seems to play a role in inhibitory processes and is found on B-cells, macrophages and on mast

cells and eosinophils. Importantly, it has been shown that 75% of all FcγRIIB is found in the liver (Ganesan, L. P. et al., 2012: "FcγRIIb on liver sinusoidal endothelium clears small immune complexes," Journal of Immunology 189: 4981–4988). FcγRIIB is abundantly expressed on Liver Sinusoidal Endothelium, called LSEC, and in Kupffer cells in the liver and LSEC are the major site of small immune complexes clearance (Ganesan, L. P. et al., 2012: FcγRIIb on liver sinusoidal endothelium clears small immune complexes. Journal of Immunology 189: 4981–4988).

In some embodiments, the antibodies disclosed herein and the antigen-binding fragments thereof comprise an Fc polypeptide or fragment thereof for binding to FcγRIIb, in particular an Fc region, such as, for example IgG-type antibodies. Moreover, it is possible to engineer the Fc moiety to enhance FcγRIIB binding by introducing the mutations S267E and L328F as described by Chu, S. Y. et al., 2008: Inhibition of B cell receptor-mediated activation of primary human B cells by coengagement of CD19 and FcgammaRIIb with Fc-engineered antibodies. Molecular Immunology 45, 3926–3933. Thereby, the clearance of immune complexes can be enhanced (Chu, S., et al., 2014: Accelerated Clearance of IgE In Chimpanzees Is Mediated By Xmab7195, An Fc-Engineered Antibody With Enhanced Affinity For Inhibitory Receptor FcγRIIb. Am J Respir Crit, American Thoracic Society International Conference Abstracts). In some embodiments, the antibodies of the present disclosure, or the antigen binding fragments thereof, comprise an engineered Fc moiety with the mutations S267E and L328F, in particular as described by Chu, S. Y. et al., 2008: Inhibition of B cell receptor-mediated activation of primary human B cells by coengagement of CD19 and FcgammaRIIb with Fc-engineered antibodies. Molecular Immunology 45, 3926–3933.

On B cells, FcγRIIB may function to suppress further immunoglobulin production and isotype switching to, for example, the IgE class. On macrophages, FcγRIIB is thought to inhibit phagocytosis as mediated through FcγRIIA. On eosinophils and mast cells, the B form may help to suppress activation of these cells through IgE binding to its separate receptor.

Regarding FcγRI binding, modification in native IgG of at least one of E233-G236, P238, D265, N297, A327 and P329 reduces binding to FcγRI. IgG2 residues at positions 233-236, substituted into corresponding positions IgG1 and IgG4, reduces binding of IgG1 and IgG4 to FcγRI by 10^3-fold and eliminated the human monocyte response to antibody-sensitized red blood cells (Armour, K. L., et al. *Eur. J. Immunol.* 29 (1999) 2613-2624).

Regarding FcγRII binding, reduced binding for FcγRIIA is found, e.g., for IgG mutation of at least one of E233-G236, P238, D265, N297, A327, P329, D270, Q295, A327, R292 and K414.

Two allelic forms of human FcγRIIA are the "H131" variant, which binds to IgG1 Fc with high affinity, and the "R131" variant, which binds to IgG1 Fc with low affinity. *See, e.g.*, Bruhns *et al.*, *Blood 113*:3716-3725 (2009).

Regarding FcγRIII binding, reduced binding to FcγRIIIA is found, e.g., for mutation of at least one of E233-G236, P238, D265, N297, A327, P329, D270, Q295, A327, S239, E269, E293, Y296, V303, A327, K338 and D376. Mapping of the binding sites on human IgG1 for Fc receptors, the above-mentioned mutation sites, and methods for measuring binding to FcγRI and FcγRIIA, are described in Shields, R. L., et al., *J. Biol. Chem.* 276 (2001) 6591-6604.

Two allelic forms of human FcγRIIIA are the "F158" variant, which binds to IgG1 Fc with low affinity, and the "V158" variant, which binds to IgG1 Fc with high affinity. *See, e.g.*, Bruhns *et al.*, *Blood 113*:3716-3725 (2009).

Regarding binding to FcγRII, two regions of native IgG Fc appear to be involved in interactions between FcγRIIs and IgGs, namely (i) the lower hinge site of IgG Fc, in particular amino acid residues L, L, G, G (234 – 237, EU numbering), and (ii) the adjacent region of the CH2 domain of IgG Fc, in particular a loop and strands in the upper CH2 domain adjacent to the lower hinge region, *e.g.* in a region of P331 (Wines, B.D., et al., J. Immunol. 2000; 164: 5313 – 5318). Moreover, FcγRI appears to bind to the same site on IgG Fc, whereas FcRn and Protein A bind to a different site on IgG Fc, which appears to be at the CH2-CH3 interface (Wines, B.D., et al., J. Immunol. 2000; 164: 5313 – 5318).

Also contemplated are mutations that increase binding affinity of an Fc polypeptide or fragment thereof of the present disclosure to a (*i.e.*, one or more) Fcγ receptor (*e.g.*, as compared to a reference Fc polypeptide or fragment thereof or containing the same that does not comprise the mutation(s)). *See, e.g.*, Delillo and Ravetch, Cell 161(5):1035-1045 (2015) and Ahmed et al., J. Struc. Biol. 194(1):78 (2016), the Fc mutations and techniques of which are incorporated herein by reference.

In any of the herein disclosed embodiments, an antibody or antigen-binding fragment can comprise a Fc polypeptide or fragment thereof comprising a mutation selected from G236A; S239D; A330L; and I332E; or a combination comprising any two or more of the same; *e.g.*, S239D/I332E; S239D/A330L/I332E; G236A/S239D/I332E; G236A/A330L/I332E (also referred to herein as "GAALIE"); or G236A/S239D/A330L/I332E. In some embodiments, the Fc polypeptide or fragment thereof does not comprise S239D. In some embodiments, the Fc polypeptide or fragment thereof comprises a native amino acid (*e.g.*, serine) at position 239.

In certain embodiments, the Fc polypeptide or fragment thereof may comprise or consist of at least a portion of an Fc polypeptide or fragment thereof that is involved in binding to FcRn binding. In certain embodiments, the Fc polypeptide or fragment thereof comprises one or more amino acid modifications that improve binding affinity for (*e.g.*, enhance binding to) FcRn (*e.g.*, at a pH of about 6.0) and, in some embodiments, thereby extend *in vivo* half-life of a molecule comprising the Fc polypeptide or fragment thereof (*e.g.*, as compared to a reference Fc polypeptide or fragment thereof or antibody that is otherwise the same but does not comprise the modification(s)). In certain embodiments, the Fc polypeptide or fragment thereof comprises or is derived from a IgG Fc and a half-life-extending mutation comprises any one or more of: M428L; N434S; N434H; N434A; N434S; M252Y; S254T; T256E; T250Q; P257I Q311I; D376V; T307A; E380A (EU numbering). In certain embodiments, a half-life-extending mutation comprises M428L/N434S (also referred to herein as "MLNS"). In certain embodiments, a half-life-extending mutation comprises M252Y/S254T/T256E. In certain embodiments, a half-life-extending mutation comprises T250Q/M428L. In certain embodiments, a half-life-extending mutation

comprises P257I/Q311I. In certain embodiments, a half-life-extending mutation comprises P257I/N434H. In certain embodiments, a half-life-extending mutation comprises D376V/N434H. In certain embodiments, a half-life-extending mutation comprises T307A/E380A/N434A.

In some embodiments, an antibody or antigen-binding fragment includes a Fc moiety that comprises the substitution mtuations M428L/N434S. In some embodiments, an antibody or antigen-binding fragment includes a Fc polypeptide or fragment thereof that comprises the substitution mtuations G236A/A330L/I332E. In certain embodiments, an antibody or antigen-binding fragment includes a (e.g., IgG) Fc moiety that comprises a G236A mutation, an A330L mutation, and a I332E mutation (GAALIE), and does not comprise a S239D mutation (e.g., comprises a native S at position 239). In particular embodiments, an antibody or antigen-binding fragment includes an Fc polypeptide or fragment thereof that comprises the substitution mutations: M428L/N434S and G236A/A330L/I332E, and optionally does not comprise S239D. In certain embodiments, an antibody or antigen-binding fragment includes a Fc polypeptide or fragment thereof that comprises the substitution mutations: M428L/N434S and G236A/S239D/A330L/I332E.

In certain embodiments, the antibody or antigen-binding fragment comprises a mutation that alters glycosylation, wherein the mutation that alters glycosylation comprises N297A, N297Q, or N297G, and/or the antibody or antigen-binding fragment is partially or fully aglycosylated and/or is partially or fully afucosylated. Host cell lines and methods of making partially or fully aglycosylated or partially or fully afucosylated antibodies and antigen-binding fragments are known (*see*, *e.g.*, PCT Publication No. WO 2016/181357; Suzuki *et al. Clin. Cancer Res. 13*(6):1875-82 (2007); Huang *et al. MAbs 6*:1-12 (2018)).

In certain embodiments, the antibody or antigen-binding fragment is capable of eliciting continued protection *in vivo* in a subject even once no detectable levels of the antibody or antigen-binding fragment can be found in the subject (*i.e.*, when the antibody or antigen-binding fragment has been cleared from the subject following administration). Such protection is referred to herein as a vaccinal effect. Without

wishing to be bound by theory, it is believed that dendritic cells can internalize complexes of antibody and antigen and thereafter induce or contribute to an endogenous immune response against antigen. In certain embodiments, an antibody or antigen-binding fragment comprises one or more modifications, such as, for example, mutations in the Fc comprising G236A, A330L, and I332E, that are capable of activating dendritic cells that may induce, *e.g.*, T cell immunity to the antigen.

In any of the presently disclosed embodiments, the antibody or antigen-binding fragment comprises a Fc polypeptide or a fragment thereof, including a CH2 (or a fragment thereof, a CH3 (or a fragment thereof), or a CH2 and a CH3, wherein the CH2, the CH3, or both can be of any isotype and may contain amino acid substitutions or other modifications as compared to a corresponding wild-type CH2 or CH3, respectively. In certain embodiments, a Fc polypeptide of the present disclosure comprises two CH2-CH3 polypeptides that associate to form a dimer.

In any of the presently disclosed embodiments, the antibody or antigen-binding fragment can be monoclonal. The term "monoclonal antibody" (mAb) as used herein refers to an antibody obtained from a population of substantially homogeneous antibodies, *i.e.*, individual antibodies comprising the population are identical except for possible naturally occurring mutations that may be present, in some cases in minor amounts. Monoclonal antibodies are highly specific, being directed against a single antigenic site. Furthermore, in contrast to polyclonal antibody preparations that include different antibodies directed against different epitopes, each monoclonal antibody is directed against a single epitope of the antigen. In addition to their specificity, the monoclonal antibodies are advantageous in that they may be synthesized uncontaminated by other antibodies. The term "monoclonal" is not to be construed as requiring production of the antibody by any particular method. For example, monoclonal antibodies useful in the present invention may be prepared by the hybridoma methodology first described by Kohler *et al.*, *Nature 256*:495 (1975), or may be made using recombinant DNA methods in bacterial, eukaryotic animal, or plant cells (*see*, *e.g.*, U.S. Pat. No. 4,816,567). Monoclonal antibodies may also be isolated from phage antibody libraries using the techniques described in Clackson *et al.*, *Nature*,

352:624-628 (1991) and Marks *et al.*, *J. Mol. Biol.*, *222*:581-597 (1991), for example. Monoclonal antibodies may also be obtained using methods disclosed in PCT Publication No. WO 2004/076677A2.

Antibodies and antigen-binding fragments of the present disclosure include "chimeric antibodies" in which a portion of the heavy and/or light chain is identical with or homologous to corresponding sequences in antibodies derived from a particular species or belonging to a particular antibody class or subclass, while the remainder of the chain(s) is identical with or homologous to corresponding sequences in antibodies derived from another species or belonging to another antibody class or subclass, as well as fragments of such antibodies, so long as they exhibit the desired biological activity (*see,* U.S. Pat. Nos. 4,816,567; 5,530,101 and 7,498,415; and Morrison *et al.*, Proc. Natl. Acad. Sci. USA, *81*:6851-6855 (1984)). For example, chimeric antibodies may comprise human and non-human residues. Furthermore, chimeric antibodies may comprise residues that are not found in the recipient antibody or in the donor antibody. These modifications are made to further refine antibody performance. For further details, see Jones *et al.*, *Nature* 321:522-525 (1986); Riechmann *et al.*, *Nature* 332:323-329 (1988); and Presta, *Curr. Op. Struct. Biol. 2*:593-596 (1992). Chimeric antibodies also include primatized and humanized antibodies.

A "humanized antibody" is generally considered to be a human antibody that has one or more amino acid residues introduced into it from a source that is non-human. These non-human amino acid residues are typically taken from a variable domain. Humanization may be performed following the method of Winter and co-workers (Jones *et al.*, *Nature*, 321:522-525 (1986); Reichmann *et al.*, *Nature*, 332:323-327 (1988); Verhoeyen *et al.*, *Science*, 239:1534-1536 (1988)), by substituting non-human variable sequences for the corresponding sequences of a human antibody. Accordingly, such "humanized" antibodies are chimeric antibodies (U.S. Pat. Nos. 4,816,567; 5,530,101 and 7,498,415) wherein substantially less than an intact human variable domain has been substituted by the corresponding sequence from a non-human species. In some instances, a “humanized” antibody is one which is produced by a non-human cell or animal and comprises human sequences, *e.g.*, Hc domains.

A "human antibody" is an antibody containing only sequences that are present in an antibody that is produced by a human. However, as used herein, human antibodies may comprise residues or modifications not found in a naturally occurring human antibody (*e.g.*, an antibody that is isolated from a human), including those modifications and variant sequences described herein. These are typically made to further refine or enhance antibody performance. In some instances, human antibodies are produced by transgenic animals. For example, *see* U.S. Pat. Nos. 5,770,429; 6,596,541 and 7,049,426.

In certain embodiments, an antibody or antigen-binding fragment of the present disclosure is chimeric, humanized, or human.

Presently disclosed antibodies and antigen-binding fragments can be obtained by, for example, introducing into a host (*e.g.*, a mouse, a rabbit, a camelid, or a human) a SARS-CoV-2 spike protein or an immunogenic polypeptide as provided herein, and, in accordance with known methods, identifying from the host antibodies that bind to a presently disclosed epitope or epitope portion. Antigen-binding fragments can be produced from an antibody using known means. Presently disclosed antibodies can also be obtained by screening B cells, plasma cells, or sera from a subject that is or has been infected with a SARS-CoV-2 and identifying antibodies that bind to a presently disclosed epitope or epitope portion. Techniques for determining epitope-binding can include, for example, X-ray crystallography, alanine scanning mutagenesis, and cryo-electron microscopy.

Also provided are antibody compositions and combinations that comprise any two or more (*i.e.*, any two, any three, any four, any five, any six, or the like) antibodies or antigen-binding fragments of the present disclosure.

Immunogenic Compositions

Also provided herein are immunogenic compositions that comprise or encode a SARS-CoV-2 polypeptide (*e.g.*, RBD, S glycoprotein, nucleoprotein, or fragment thereof) or polypeptide multimer (*e.g.*, a S polypeptide trimer) that is capable of being bound by (*e.g.*, comprises, retains, or substantially retains an epitope or antigenic

region) a presently disclosed antibody or antigen-binding fragment and are capable of inducing a host immune response against the polypeptide or multimer that may involve, for example, production of antibodies, activation of specific immunologically competent cells, production of inflammatory cytokines, activation of complement, antibody dependent cytotoxicity, or any combination thereof. An immunogenic composition can include a polypeptide comprising an amino acid sequence that is at least 80%, at least 85%, at least 90%, at least 91%, at least 92%, at least 93%, at least 94%, at least 95%, at least 96%, at least 97%, at least 98%, at least 99%, or 100% identical to a corresponding S polypeptide, RBD, or portion thereof that comprises the epitope or antigenic region, provided that the subject epitope or antigen region is completely retained or is at least substantially retained as compared to the reference S polypeptide or RBD sequence and structure. For example, in some embodiments, an immunogenic composition comprises an S polypeptide amino acid sequence that is at least 80%, at least 85%, at least 90%, at least 91%, at least 92%, at least 93%, at least 94%, at least 95%, at least 96%, at least 97%, at least 98%, at least 99%, or 100% identical to SEQ ID NO.:3, or to a portion of SEQ ID NO.:3 that comprises the subject epitope or antigenic site. In some embodiments, an immunogenic composition comprises a RBD amino acid sequence that is at least least 80%, at least 85%, at least 90%, at least 91%, at least 92%, at least 93%, at least 94%, at least 95%, at least 96%, at least 97%, at least 98%, at least 99%, or 100% identical to SEQ ID NO.:4, or to a portion of SEQ ID NO.:4 that comprises the subject epitope or antigenic site. In some embodiments, an immunogenic composition comprises a RBM amino acid sequence that is at least least 80%, at least 85%, at least 90%, at least 91%, at least 92%, at least 93%, at least 94%, at least 95%, at least 96%, at least 97%, at least 98%, at least 99%, or 100% identical to SEQ ID NO.:5, or to a portion of SEQ ID NO.:5 that comprises the subject epitope or antigenic site.

It will also be understood that any one two or more immunogenic amino acid sequences each comprising all or a portion of a presently disclosed epitope or antigenic site can be present in, for example, an isolated fragment of a SARS-CoV-2 S protein or RBD, in a fusion protein (e.g., fused or linked to a different portion, sequence or

fragment of SARS-CoV-2 RBD, or as a Fc fusion or antibody fusion protein), as a recombinant protein, in a mixture of immunogenic polypeptides, or the like. Two or more immunogenic polypeptides each comprising all or a portion of a presently disclosed epitope or target region can also be present as separate molecules in a composition.

S glycoprotein and RBD polypeptides can be engineered to comprise one or more mutations that can, for example, bias the S glycoprotein and/or RBD in a conformation of interest. Such mutations include, for example, D614G, replacement of the residues 682-685 with the sequence G-S-A-S, V987P, and K986P, as well as the other mutations and alterations disclosed in Xiong *et al.*, *Nature Strutural & Molecular Biology 27* (934-941 (2020)), which mutations and other alterations are incorporated herein by reference.

S glycoprotein polypeptides can be provided in monomeric form, or as a multimer (*e.g.*, a trimer). In certain embodiments, S glycoprotein polypeptides (in monomeric or multimeric form) can be present as monomers or can be comprised in disposed on or at a surface of a host cell or on a carrier molecule, such as a substrate polypeptide, lipid, or surface (*e.g.*, a nanobead).

In some embodiments, an immunogenic composition is provided that comprises: (a) a SARS-CoV-2 nucleocapsid (N) protein (SEQ ID NO.:170), or an immunogenic fragment thereof; (b) a SARS-CoV-2 S glycoprotein polypeptide or multimer thereof comprising (i) one, two, or three Receptor Binding Domains (RBDs) in an open conformation and (ii) a Site Ia polypeptide, the Site Ia polypeptide capable of being bound by antibody S2H14; (c) a SARS-CoV-2 Spike (S) polypeptide comprising (i) a RBD in an open conformation or in a closed conformation and (ii) a Site Ib polypeptide, the Site Ib polypeptide capable of being bound by antibody S2H13; (d) a SARS-CoV-2 S polypeptide or multimer thereof comprising (i) two or three Receptor Binding Domains (RBDs) in an open conformation and (ii) a Site IIa polypeptide, the Site IIa polypeptide capable of being bound by antibody S2X35; (e) a SARS-CoV-2 S polypeptide or multimer thereof comprising (i) two adjacent RBDs in an open conformation and (ii) a Site IIb polypeptide, the Site IIb polypeptide capable of being

bound by antibody S2A4; (f) a SARS-CoV-2 S polypeptide or multimer thereof comprising (i) two adjacent RBDs in an open conformation and (ii) a Site IIc polypeptide, the Site IIc polypeptide capable of being bound by antibody S304; (g) a SARS-CoV-2 S polypeptide capable of being bound by antibody CR3022; (h) a SARS-CoV-2 Spike (S) polypeptide or multimer thereof comprising (i) a RBD in an open conformation or in a closed conformation and (ii) a Site IV polypeptide, the Site IV polypeptide capable of being bound by antibody S309; (i) a polynucleotide encoding the SARS-CoV-2 N or S protein polypeptide of any one or more of (a)-(h); or (j) any combination of (a)-(i) above.

In further embodiments, the immunogenic composition further comprises a pharmaceutically acceptable carrier, excipient, or diluent, and/or comprising an adjuvant.

In some embodiments, the SARS-COV-2 S glycoprotein polypeptide comprises a prefusion-stabilized S ectodomain and/or does not comprise a C-terminal domain, such as a R1 domain, a CH domain, a CD domain, a HR1 domain, a HR2 domain, a TM domain, and/or a CT domain. In some embodiments, a SARS-CoV-2 S glycoprotein comprises one or more mutations and/or is missing one or more domains as compared to a native, full-length SARS-CoV-2 S glycoprotein.

In some embodiments, an immunogenic composition is provided that comprises: (a) a SARS-CoV-2 S polypeptide or multimer thereof that comprises two or three receptor binding domains (RBDs) in a closed-conformation, wherein two adjacent RBDs are in a closed conformation; (b) a SARS-CoV-2 S polypeptide or multimer thereof capable of being bound by an antibody or antigen-binding fragment thereof comprising a CDRH1 comprising the sequence set forth in SEQ ID NO: 143, a CDRH2 comprising the sequence set forth in SEQ ID NO:144, a CDRH3 comprising the sequence set forth in SEQ ID NO:145, a CDRL1 comprising the sequence set forth in SEQ ID NO:147, a CDRL2 comprising the sequence set forth in SEQ ID NO:148, and a CDRL3 comprising the sequence set forth in SEQ ID NO:149; (c) a SARS-CoV-2 S polypeptide or multimer thereof capable of being bound by an antibody or antigen-binding fragment thereof comprising a CDRH1 comprising the sequence set forth in

SEQ ID NO: 109, a CDRH2 comprising the sequence set forth in SEQ ID NO:110, a CDRH3 comprising the sequence set forth in SEQ ID NO:111, a CDRL1 comprising the sequence set forth in SEQ ID NO:133, a CDRL2 comprising the sequence set forth in SEQ ID NO:134, and a CDRL3 comprising the sequence set forth in SEQ ID NO:135; or any combination of (a)-(c).

In further embodiments, the immunogenic composition comprises: (d) a SARS-CoV-2 S polypeptide or multimer thereof capable of being bound by an antibody or antigen-binding fragment thereof comprising a CDRH1 comprising the sequence set forth in SEQ ID NO: 102, a CDRH2 comprising the sequence set forth in SEQ ID NO:103, a CDRH3 comprising the sequence set forth in SEQ ID NO:104, a CDRL1 comprising the sequence set forth in SEQ ID NO:106, a CDRL2 comprising the sequence set forth in SEQ ID NO:107, and a CDRL3 comprising the sequence set forth in SEQ ID NO:108; (e) a SARS-CoV-2 S polypeptide or multimer thereof capable of being bound by an antibody or antigen-binding fragment thereof comprising a CDRH1 comprising the sequence set forth in SEQ ID NO:94, a CDRH2 comprising the sequence set forth in SEQ ID NO:95, a CDRH3 comprising the sequence set forth in SEQ ID NO:96, a CDRL1 comprising the sequence set forth in SEQ ID NO:98, a CDRL2 comprising the sequence set forth in SEQ ID NO:99, and a CDRL3 comprising the sequence set forth in SEQ ID NO:100; or a combination thereof.

In certain embodiments, an immunogenic composition is provided that comprises: (a) a SARS-CoV-2 S polypeptide or multimer thereof capable of being bound by an antibody or antigen-binding fragment thereof comprising a VH comprising the sequence set forth in SEQ ID NO:142 and a VL comprising the sequence set forth in SEQ ID NO:146; (b) a SARS-CoV-2 S polypeptide or multimer thereof capable of being bound by an antibody or antigen-binding fragment thereof comprising a VH comprising the sequence set forth in SEQ ID NO:123 and a VL comprising the sequence set forth in SEQ ID NO:138; or a combination thereof.

In further embodiments, the immunogenic composition comprises: (c) a SARS-CoV-2 S protein polypeptide capable of being bound by an antibody or antigen-binding fragment thereof comprising a CDRH1 comprising the sequence set forth in SEQ ID

NO: 102, a CDRH2 comprising the sequence set forth in SEQ ID NO:103, a CDRH3 comprising the sequence set forth in SEQ ID NO:104, a CDRL1 comprising the sequence set forth in SEQ ID NO:106, a CDRL2 comprising the sequence set forth in SEQ ID NO:107, and a CDRL3 comprising the sequence set forth in SEQ ID NO:108; (d) a SARS-CoV-2 S protein polypeptide capable of being bound by an antibody or antigen-binding fragment thereof comprising a CDRH1 comprising the sequence set forth in SEQ ID NO: 94, a CDRH2 comprising the sequence set forth in SEQ ID NO:95, a CDRH3 comprising the sequence set forth in SEQ ID NO:96, a CDRL1 comprising the sequence set forth in SEQ ID NO:98, a CDRL2 comprising the sequence set forth in SEQ ID NO:99, and a CDRL3 comprising the sequence set forth in SEQ ID NO:100; or a combination thereof.

In some embodiments, an immunogenic composition is provided that comprises: (a) a SARS-CoV-2 S polypeptide capable of being bound by antibody S2M11, or an antigen-binding fragment thereof; (b) a SARS-CoV-2 S polypeptide capable of being bound by antibody S2E12, or an antigen-binding fragment thereof; (c) a SARS-CoV-2 S polypeptide capable of being bound by antibody S309, or an antigen-binding fragment thereof; or (d) any combination of (a)-(c) above.

In some embodiments, the immunogenic composition further comprises a pharmaceutically acceptable carrier, excipient, or diluent, and/or comprising an adjuvant.

In some embodiments, an immunogenic composition comprises a polynucleotide that encodes a presently disclosed RBD or S glycoprotein polypeptide (or multimer), and/or a vector that comprises the polynucleotide.

In certain embodiments, the immunogenic composition further comprises an adjuvant. Examples of adjuvants include, for example, poly-ICLC, poly I:C, GLA, CpG, GM-CSF, alum, Delta Inulin, aluminum hydroxide, alhydrogel, aluminum phosphate, MF59, AS03, TLR agonists, resiquimod, and saponins.

In some embodiments, an immunogenic polypeptide is provided with a carrier, such as, for example, a further polypeptide (e.g., an antibody or an antibody Fc that is conjugated to or fused to the immunogenic polyeptide), a liposome, a polysaccharide, a

polylactic acid, a polyglycolic acid, polymeric amino acids, an amino acid copolymer, an inactive virus particle, a microbead, a nanobead, or the like.

Polynucleotides, Vectors, and Host cells

In another aspect, the present disclosure provides isolated polynucleotides that encode any of the presently disclosed antibodies or an antigen-binding fragment thereof, or a portion thereof (*e.g.*, a CDR, a VH, a VL, a heavy chain, or a light chain), and/or that encode a presently disclosed immunogenic composition. In certain embodiments, the polynucleotide is codon-optimized for expression in a host cell. Once a coding sequence is known or identified, codon optimization can be performed using known techniques and tools, *e.g.*, using the GenScript® OptimiumGene™ tool; *see also* Scholten *et al.*, *Clin. Immunol. 119*:135, 2006). Codon-optimized sequences include sequences that are partially codon-optimized (*i.e.*, one or more codon is optimized for expression in the host cell) and those that are fully codon-optimized.

It will also be appreciated that polynucleotides encoding antibodies, antigen-binding fragments and/or immunogenic compositions of the present disclosure may possess different nucleotide sequences while still encoding a same antibody or antigen-binding fragment or immunogenic composition due to, for example, the degeneracy of the genetic code, splicing, and the like.

In any of the presently disclosed embodiments, the polynucleotide can comprise deoxyribonucleic acid (DNA) or ribonucleic acid (RNA). In some embodiments, the RNA comprises messenger RNA (mRNA).

Vectors are also provided, wherein the vectors comprise or contain a polynucleotide as disclosed herein (*e.g.*, a polynucleotide that encodes an antibody or antigen-binding fragment that binds to SARS-CoV-2). A vector can comprise any one or more of the vectors disclosed herein. In particular embodiments, a vector is provided that comprises a DNA plasmid construct encoding the antibody or antigen-binding fragment, or a portion thereof (*e.g.*, so-called "DMAb"; *see*, *e.g.*, Muthumani *et al.*, *J Infect Dis. 214*(3):369-378 (2016); Muthumani *et al.*, *Hum Vaccin Immunother 9*:2253-2262 (2013)); Flingai *et al.*, *Sci Rep. 5*:12616 (2015); and Elliott *et al.*, *NPJ Vaccines* 18 (2017), which antibody-coding DNA constructs and related methods of use,

including administration of the same, are incorporated herein by reference). In certain embodiments, a DNA plasmid construct comprises a single open reading frame encoding a heavy chain and a light chain (or a VH and a VL) of the antibody or antigen-binding fragment, wherein the sequence encoding the heavy chain and the sequence encoding the light chain are optionally separated by polynucleotide encoding a protease cleavage site and/or by a polynucleotide encoding a self-cleaving peptide. In some embodiments, the substituent components of the antibody or antigen-binding fragment are encoded by a polynucleotide comprised in a single plasmid. In other embodiments, the substituent components of the antibody or antigen-binding fragment are encoded by a polynucleotide comprised in two or more plasmids (*e.g.*, a first plasmid comprises a polynucleotide encoding a heavy chain, VH, or VH+CH, and a second plasmid comprises a polynucleotide encoding the cognate light chain, VL, or VL+CL). In certain embodiments, a single plasmid comprises a polynucleotide encoding a heavy chain and/or a light chain from two or more antibodies or antigen-binding fragments of the present disclosure. An exemplary expression vector is pVax1, available from Invitrogen®. A DNA plasmid of the present disclosure can be delivered to a subject by, for example, electroporation (*e.g.*, intramuscular electroporation), or with an appropriate formulation (*e.g.*, hyaluronidase).

In a further aspect, the present disclosure also provides a host cell expressing an antibody or antigen-binding fragment or immunogenic composition according to the present disclosure; or comprising or containing a vector or polynucleotide according the present disclosure.

Examples of such cells include but are not limited to, eukaryotic cells, *e.g.*, yeast cells, animal cells, insect cells, plant cells; and prokaryotic cells, including *E. coli*. In some embodiments, the cells are mammalian cells. In certain such embodiments, the cells are a mammalian cell line such as CHO cells (*e.g.*, DHFR- CHO cells (Urlaub *et al., PNAS 77*:4216 (1980)), human embryonic kidney cells (*e.g.*, HEK293T cells), PER.C6 cells, Y0 cells, Sp2/0 cells. NS0 cells, human liver cells, e.g. Hepa RG cells, myeloma cells or hybridoma cells. Other examples of mammalian host cell lines include mouse sertoli cells (*e.g.*, TM4 cells); monkey kidney CV1 line transformed by

SV40 (COS-7); baby hamster kidney cells (BHK); African green monkey kidney cells (VERO-76); monkey kidney cells (CV1); human cervical carcinoma cells (HELA); human lung cells (W138); human liver cells (Hep G2); canine kidney cells (MDCK; buffalo rat liver cells (BRL 3A); mouse mammary tumor (MMT 060562); TRI cells; *MRC* 5 cells; and FS4 cells. Mammalian host cell lines suitable for antibody production also include those described in, for example, Yazaki and Wu, *Methods in Molecular Biology*, Vol. 248 (B. K. C. Lo, ed., Humana Press, Totowa, N.J.), pp. 255-268 (2003).

In certain embodiments, a host cell is a prokaryotic cell, such as an *E. coli.* The expression of peptides in prokaryotic cells such as *E. coli* is well established (*see*, *e.g.*, Pluckthun, A. *Bio/Technology 9:*545-551 (1991). For example, antibodies may be produced in bacteria, in particular when glycosylation and Fc effector function are not needed. For expression of antibody fragments and polypeptides in bacteria, *see, e.g.*, U.S. Pat. Nos. 5,648,237; 5,789,199; and 5,840,523.

In particular embodiments, the cell may be transfected with a vector according to the present description with an expression vector. The term "transfection" refers to the introduction of nucleic acid molecules, such as DNA or RNA (e.g. mRNA) molecules, into cells, such as into eukaryotic cells. In the context of the present description, the term "transfection" encompasses any method known to the skilled person for introducing nucleic acid molecules into cells, such as into eukaryotic cells, including into mammalian cells. Such methods encompass, for example, electroporation, lipofection, *e.g.*, based on cationic lipids and/or liposomes, calcium phosphate precipitation, nanoparticle based transfection, virus based transfection, or transfection based on cationic polymers, such as DEAE-dextran or polyethylenimine, *etc*. In certain embodiments, the introduction is non-viral.

Moreover, host cells of the present disclosure may be transfected stably or transiently with a vector according to the present disclosure, *e.g.* for expressing an antibody, antigen-binding fragment, or immunogenic composition according to the present disclosure. In such embodiments, the cells may be stably transfected with the vector as described herein. Alternatively, cells may be transiently transfected with a

vector according to the present disclosure encoding an antibody, antigen-binding fragment, or immunogenic composition as disclosed herein. In any of the presently disclosed embodiments, a polynucleotide may be heterologous to the host cell.

Accordingly, the present disclosure also provides recombinant host cells that heterologously express an antibody, antigen-binding fragment, or immunogenic composition of the present disclosure. For example, the cell may be of a species that is different to the species from which the antibody was fully or partially obtained (*e.g.*, CHO cells expressing a human antibody or an engineered human antibody). In some embodiments, the cell type of the host cell does not express the antibody or antigen-binding fragment in nature. Moreover, the host cell may impart a post-translational modification (PTM; *e.g.*, glysocylation or fucosylation) on the antibody or antigen-binding fragment that is not present in a native state of the antibody or antigen-binding fragment (or in a native state of a parent antibody from which the antibody or antigen binding fragment was engineered or derived). Such a PTM may result in a functional difference (*e.g.*, reduced immunogenicity). For example, an antibody or antigen-binding fragment of the present disclosure that is produced by a host cell as disclosed herein may include one or more post-translational modification that is distinct from the antibody (or parent antibody) in its native state (*e.g.*, a human antibody produced by a CHO cell can comprise a more post-translational modification that is distinct from the antibody when isolated from the human and/or produced by the native human B cell or plasma cell).

Insect cells useful expressing an antibody or antigen-binding fragment of the present disclosure are known in the art and include, for example, *Spodoptera frugipera* Sf9 cells, Trichoplusia ni BTI-TN5B1-4 cells, and *Spodoptera frugipera* SfSWT01 "Mimic™" cells. *See*, *e.g.*, Palmberger *et al.*, *J. Biotechnol. 153*(3-4):160-166 (2011). Numerous baculoviral strains have been identified which may be used in conjunction with insect cells, particularly for transfection of *Spodoptera frugiperda* cells.

Eukaryotic microbes such as filamentous fungi or yeast are also suitable hosts for cloning or expressing protein-encoding vectors, and include fungi and yeast strains with "humanized" glycosylation pathways, resulting in the production of an antibody

with a partially or fully human glycosylation pattern. *See* Gerngross, *Nat. Biotech.* 22:1409-1414 (2004); Li *et al.*, *Nat. Biotech.* 24:210-215 (2006).

Plant cells can also be utilized as hosts for expressing a binding protein of the present disclosure. For example, PLANTIBODIES™ technology (described in, for example, U.S. Pat. Nos. 5,959,177; 6,040,498; 6,420,548; 7,125,978; and 6,417,429) employs transgenic plants to produce antibodies.

In certain embodiments, the host cell comprises a mammalian cell. In particular embodiments, the host cell is a CHO cell, a HEK293 cell, a PER.C6 cell, a Y0 cell, a Sp2/0 cell, a NS0 cell, a human liver cell, a myeloma cell, or a hybridoma cell.

In a related aspect, the present disclosure provides methods for producing an antibody, antigen-binding fragment, or immunogenic composition, wherein the methods comprise culturing a host cell of the present disclosure under conditions and for a time sufficient to produce the antibody, antigen-binding fragment, or immunogenic composition. Methods useful for isolating and purifying recombinantly produced antibodies, by way of example, may include obtaining supernatants from suitable host cell/vector systems that secrete the recombinant antibody into culture media and then concentrating the media using a commercially available filter. Following concentration, the concentrate may be applied to a single suitable purification matrix or to a series of suitable matrices, such as an affinity matrix or an ion exchange resin. One or more reverse phase HPLC steps may be employed to further purify a recombinant polypeptide. These purification methods may also be employed when isolating an immunogen from its natural environment. Methods for large scale production of one or more of the isolated/recombinant antibody, antigen-binding fragment, or immunogenic composition described herein include batch cell culture, which is monitored and controlled to maintain appropriate culture conditions. Purification of soluble antibodies may be performed according to methods described herein and known in the art and that comport with laws and guidelines of domestic and foreign regulatory agencies.

Additional Compositions

Also provided herein are compositions that comprise any one or more of the presently disclosed antibodies, antigen-binding fragments, polynucleotides, vectors, host cells, or immunogenic compositions, singly or in any combination, and can further comprise a pharmaceutically acceptable carrier, excipient, or diluent. Carriers, excipients, and diluents are discussed in further detail herein.

In certain embodiments, a composition comprises two or more different antibodies, antigen-binding fragments, or immunogenic compositions according to the present disclosure. In certain embodiments, antibodies or antigen-binding fragments to be used in a combination each independently have one or more of the following characteristics: neutralize naturally occurring SARS-CoV-2 variants; do not compete with one another for Spike protein binding; bind distinct Spike protein epitopes; have a reduced formation of resistance to SARS-CoV-2; when in a combination, have a reduced formation of resistance to SARS-CoV-2; potently neutralize live SARS-CoV-2 virus; exhibit additive or synergistic effects on neutralization of live SARS-CoV-2 virus when used in combination; exhibit effector functions; are protective in relevant animal model(s) of infection; are capable of being produced in sufficient quantities for large-scale production.

In certain embodiments, a composition comprises a first vector comprising a first plasmid, and a second vector comprising a second plasmid, wherein the first plasmid comprises a polynucleotide encoding a heavy chain, VH, or VH+CH, and a second plasmid comprises a polynucleotide encoding the cognate light chain, VL, or VL+CL of the antibody or antigen-binding fragment thereof. In certain embodiments, a composition comprises a polynucleotide (*e.g.*, mRNA) coupled to a suitable delivery vehicle or carrier. Exemplary vehicles or carriers for administration to a human subject include a lipid or lipid-derived delivery vehicle, such as a liposome, solid lipid nanoparticle, oily suspension, submicron lipid emulsion, lipid microbubble, inverse lipid micelle, cochlear liposome, lipid microtubule, lipid microcylinder, or lipid nanoparticle (LNP) or a nanoscale platform (*see*, *e.g.*, Li *et al. Wilery Interdiscip Rev. Nanomed Nanobiotechnol. 11*(2):e1530 (2019)). Principles, reagents, and techniques

for designing appropriate mRNA and and formulating mRNA-LNP and delivering the same are described in, for example, Pardi *et al.* (*J Control Release 217*345-351 (2015)); Thess *et al.* (*Mol Ther 23*: 1456-1464 (2015)); Thran *et al.* (*EMBO Mol Med 9*(10):1434-1448 (2017); Kose *et al.* (*Sci. Immunol. 4* eaaw6647 (2019); and Sabnis *et al.* (*Mol. Ther. 26*:1509-1519 (2018)), which techniques, include capping, codon optimization, nucleoside modification, purification of mRNA, incorporation of the mRNA into stable lipid nanoparticles (*e.g.*, ionizable cationic lipid/phosphatidylcholine/cholesterol/PEG-lipid; ionizable lipid:distearoyl PC:cholesterol:polyethylene glycol lipid), and subcutaneous, intramuscular, intradermal, intravenous, intraperitoneal, and intratracheal administration of the same, are incorporated herein by reference.

Methods and Uses

Also provided herein are methods for use of an antibody or antigen-binding fragment, nucleic acid, vector, cell, immunogenic composition, or composition of the present disclosure in the diagnosis of SARS-CoV-2 infection (*e.g.*, in a human subject, or in a sample obtained from a human subject).

Methods of diagnosis (*e.g., in vitro, ex vivo*) may include contacting an antibody, antibody fragment (e.g., antigen binding fragment) with a sample. Such samples may be isolated from a subject, for example an isolated tissue sample taken from, for example, nasal passages, sinus cavities, salivary glands, lung, liver, pancreas, kidney, ear, eye, placenta, alimentary tract, heart, ovaries, pituitary, adrenals, thyroid, brain, skin or blood. The methods of diagnosis may also include the detection of an antigen/antibody complex, in particular following the contacting of an antibody or antibody fragment with a sample. Such a detection step can be performed at the bench, *i.e.* without any contact to the human or animal body. Examples of detection methods are well-known to the person skilled in the art and include, *e.g.*, ELISA (enzyme-linked immunosorbent assay), including direct, indirect, and sandwich ELISA.

Also provided herein are methods of treating a subject using an antibody or antigen-binding fragment, nucleic acid, vector, cell, immunogenic composition, or composition, wherein the subject has, is believed to have, or is at risk for having an

infection by SARS-CoV-2. "Treat," "treatment," or "ameliorate" refers to medical management of a disease, disorder, or condition of a subject (*e.g.*, a human or non-human mammal, such as a primate, horse, cat, dog, goat, mouse, or rat). In general, an appropriate dose or treatment regimen comprising an antibody or composition of the present disclosure is administered in an amount sufficient to elicit a therapeutic or prophylactic benefit. Therapeutic or prophylactic/preventive benefit includes improved clinical outcome; lessening or alleviation of symptoms associated with a disease; decreased occurrence of symptoms; improved quality of life; longer disease-free status; diminishment of extent of disease, stabilization of disease state; delay or prevention of disease progression; remission; survival; prolonged survival; or any combination thereof. In certain embodiments, therapeutic or prophylactic/preventive benefit includes reduction or prevention of hospitalization for treatment of a SARS-CoV-2 infection (i.e., in a statistically significant manner). In certain embodiments, therapeutic or prophylactic/preventive benefit includes a reduced duration of hospitalization for treatment of a SARS-CoV-2 infection (i.e., in a statistically significant manner). In certain embodiments, therapeutic or prophylactic/preventive benefit includes a reduced or abrogated need for respiratory intervention, such as intubation and/or the use of a respirator device. In certain embodiments, therapeutic or prophylactic/preventive benefit includes reversing a late-stage disease pathology and/or reducing mortality.

A "therapeutically effective amount" or "effective amount" of an antibody, antigen-binding fragment, polynucleotide, vector, host cell, composition, or immunogenic composition of this disclosure refers to an amount of the composition or molecule sufficient to result in a therapeutic effect, including improved clinical outcome; lessening or alleviation of symptoms associated with a disease; decreased occurrence of symptoms; improved quality of life; longer disease-free status; diminishment of extent of disease, stabilization of disease state; delay of disease progression; remission; survival; or prolonged survival in a statistically significant manner. When referring to an individual active ingredient, administered alone, a therapeutically effective amount refers to the effects of that ingredient or cell expressing that ingredient alone. When referring to a combination, a therapeutically effective

amount refers to the combined amounts of active ingredients or combined adjunctive active ingredient with a cell expressing an active ingredient that results in a therapeutic effect, whether administered serially, sequentially, or simultaneously. A combination may comprise, for example, two or more different antibodies that specifically bind a SARS-CoV-2 antigen, which in certain embodiments, may be the same or different SARS-CoV-2 antigen, and/or can comprise the same or different epitopes.

Accordingly, in certain embodiments, methods are provided for treating a SARS-CoV-2 infection in a subject, wherein the methods comprise administering to the subject an effective amount of an antibody, antigen-binding fragment, polynucleotide, vector, host cell, immunogenic composition, or composition as disclosed herein.

Subjects that can be treated by the present disclosure are, in general, human and other primate subjects, such as monkeys and apes for veterinary medicine purposes. Other model organisms, such as mice and rats, may also be treated according to the present disclosure. In any of the aforementioned embodiments, the subject may be a human subject. The subjects can be male or female and can be any suitable age, including infant, juvenile, adolescent, adult, and geriatric subjects.

A number of criteria are believed to contribute to high risk for severe symptoms or death associated with a SARS CoV-2 infection. These include, but are not limited to, age, occupation, general health, pre-existing health conditions, and lifestyle habits. In some embodiments, a subject treated according to the present disclosure comprises one or more risk factors.

In certain embodiments, a human subject treated according to the present disclosure is an infant, a child, a young adult, an adult of middle age, or an elderly person. In certain embodiments, a human subject treated according to the present disclosure is less than 1 year old, or is 1 to 5 years old, or is between 5 and 125 years old (*e.g.*, 5, 10, 15, 20, 25, 30, 35, 40, 45, 50, 55, 60, 65, 70, 75, 80, 85, 90, 95, 100, 105, 110, 115, or 125 years old, including any and all ages therein or therebetween). In certain embodiments, a human subject treated according to the present disclosure is 0-19 years old, 20-44 years old, 45-54 years old, 55-64 years old, 65-74 years old, 75-84 years old, or 85 years old, or older. Persons of middle, and especially of elderly age are

believed to be at particular risk. In particular embodiments, the human subject is 45-54 years old, 55-64 years old, 65-74 years old, 75-84 years old, or 85 years old, or older. In some embodiments, the human subject is male. In some embodiments, the human subject is female.

In certain embodiments, a human subject treated according to the present disclosure is a resident of a nursing home or a long-term care facility, is a hospice care worker, is a healthcare provider or healthcare worker, is a first responder, is a family member or other close contact of a subject diagnosed with or suspected of having a SARS-CoV-2 infection, is overweight or clinically obese, is or has been a smoker, has or had chronic obstructive pulmonary disease (COPD), is asthmatic (*e.g.*, having moderate to severe asthma), has an autoimmune disease or condition (*e.g.*, diabetes), and/or has a compromised or depleted immune system (*e.g.*, due to AIDS/HIV infection, a cancer such as a blood cancer, a lymphodepleting therapy such as a chemotherapy, a bone marrow or organ transplantation, or a genetic immune condition), has chronic liver disease, has cardiovascular disease, has a pulmonary or heart defect, works or otherwise spends time in close proximity with others, such as in a factory, shipping center, hospital setting, or the like.

In certain embodiments, a subject treated according to the present disclosure has received a vaccine for SARS-CoV-2 and the vaccine is determined to be ineffective, *e.g.*, by post-vaccine infection or symptoms in the subject, by clinical diagnosis or scientific or regulatory criteria.

In certain embodiments, treatment is administered as peri-exposure prophylaxis. In certain embodiments, treatment is administered to a subject with mild-to-moderate disease, which may be in an outpatient setting. In certain embodiments, treatment is administered to a subject with moderate-to-severe disease, such as requiring hospitalization.

Typical routes of administering the presently disclosed compositions thus include, without limitation, oral, topical, transdermal, inhalation, parenteral, sublingual, buccal, rectal, vaginal, and intranasal. The term "parenteral", as used herein, includes subcutaneous injections, intravenous, intramuscular, intrasternal injection or infusion

techniques. In certain embodiments, administering comprises administering by a route that is selected from oral, intravenous, parenteral, intragastric, intrapleural, intrapulmonary, intrarectal, intradermal, intraperitoneal, intratumoral, subcutaneous, topical, transdermal, intracisternal, intrathecal, intranasal, and intramuscular. In particular embodiments, a method comprises orally administering the antibody, antigen-binding fragment, polynucleotide, vector, host cell, or composition to the subject.

Pharmaceutical compositions according to certain embodiments of the present invention are formulated so as to allow the active ingredients contained therein to be bioavailable upon administration of the composition to a patient. Compositions that will be administered to a subject or patient may take the form of one or more dosage units, where for example, a tablet may be a single dosage unit, and a container of a herein described an antibody or antigen-binding in aerosol form may hold a plurality of dosage units. Actual methods of preparing such dosage forms are known, or will be apparent, to those skilled in this art; for example, *see* Remington: The Science and Practice of Pharmacy, 20th Edition (Philadelphia College of Pharmacy and Science, 2000). The composition to be administered will, in any event, contain an effective amount of an antibody or antigen-binding fragment, polynucleotide, vector, host cell, , or composition of the present disclosure, for treatment of a disease or condition of interest in accordance with teachings herein.

A composition may be in the form of a solid or liquid. In some embodiments, the carrier(s) are particulate, so that the compositions are, for example, in tablet or powder form. The carrier(s) may be liquid, with the compositions being, for example, an oral oil, injectable liquid or an aerosol, which is useful in, for example, inhalatory administration. When intended for oral administration, the pharmaceutical composition is preferably in either solid or liquid form, where semi solid, semi liquid, suspension and gel forms are included within the forms considered herein as either solid or liquid.

As a solid composition for oral administration, the pharmaceutical composition may be formulated into a powder, granule, compressed tablet, pill, capsule, chewing gum, wafer or the like. Such a solid composition will typically contain one or more inert diluents or edible carriers. In addition, one or more of the following may be

present: binders such as carboxymethylcellulose, ethyl cellulose, microcrystalline cellulose, gum tragacanth or gelatin; excipients such as starch, lactose or dextrins, disintegrating agents such as alginic acid, sodium alginate, Primogel, corn starch and the like; lubricants such as magnesium stearate or Sterotex; glidants such as colloidal silicon dioxide; sweetening agents such as sucrose or saccharin; a flavoring agent such as peppermint, methyl salicylate or orange flavoring; and a coloring agent. When the composition is in the form of a capsule, for example, a gelatin capsule, it may contain, in addition to materials of the above type, a liquid carrier such as polyethylene glycol or oil.

The composition may be in the form of a liquid, for example, an elixir, syrup, solution, emulsion or suspension. The liquid may be for oral administration or for delivery by injection, as two examples. When intended for oral administration, preferred compositions contain, in addition to the present compounds, one or more of a sweetening agent, preservatives, dye/colorant and flavor enhancer. In a composition intended to be administered by injection, one or more of a surfactant, preservative, wetting agent, dispersing agent, suspending agent, buffer, stabilizer and isotonic agent may be included.

Liquid pharmaceutical compositions, whether they be solutions, suspensions or other like form, may include one or more of the following adjuvants: sterile diluents such as water for injection, saline solution, preferably physiological saline, Ringer's solution, isotonic sodium chloride, fixed oils such as synthetic mono or diglycerides which may serve as the solvent or suspending medium, polyethylene glycols, glycerin, propylene glycol or other solvents; antibacterial agents such as benzyl alcohol or methyl paraben; antioxidants such as ascorbic acid or sodium bisulfite; chelating agents such as ethylenediaminetetraacetic acid; buffers such as acetates, citrates or phosphates and agents for the adjustment of tonicity such as sodium chloride or dextrose. The parenteral preparation can be enclosed in ampoules, disposable syringes or multiple dose vials made of glass or plastic. Physiological saline is a preferred adjuvant. An injectable pharmaceutical composition is preferably sterile.

A liquid composition intended for either parenteral or oral administration should contain an amount of an antibody or antigen-binding fragment as herein disclosed such that a suitable dosage will be obtained. Typically, this amount is at least 0.01% of the antibody or antigen-binding fragment in the composition. When intended for oral administration, this amount may be varied to be between 0.1 and about 70% of the weight of the composition. Certain oral pharmaceutical compositions contain between about 4% and about 75% of the antibody or antigen-binding fragment. In certain embodiments, pharmaceutical compositions and preparations according to the present invention are prepared so that a parenteral dosage unit contains between 0.01 to 10% by weight of antibody or antigen-binding fragment prior to dilution.

The composition may be intended for topical administration, in which case the carrier may suitably comprise a solution, emulsion, ointment or gel base. The base, for example, may comprise one or more of the following: petrolatum, lanolin, polyethylene glycols, bee wax, mineral oil, diluents such as water and alcohol, and emulsifiers and stabilizers. Thickening agents may be present in a composition for topical administration. If intended for transdermal administration, the composition may include a transdermal patch or iontophoresis device. The pharmaceutical composition may be intended for rectal administration, in the form, for example, of a suppository, which will melt in the rectum and release the drug. The composition for rectal administration may contain an oleaginous base as a suitable nonirritating excipient. Such bases include, without limitation, lanolin, cocoa butter and polyethylene glycol.

A composition may include various materials which modify the physical form of a solid or liquid dosage unit. For example, the composition may include materials that form a coating shell around the active ingredients. The materials that form the coating shell are typically inert, and may be selected from, for example, sugar, shellac, and other enteric coating agents. Alternatively, the active ingredients may be encased in a gelatin capsule. The composition in solid or liquid form may include an agent that binds to the antibody or antigen-binding fragment of the disclosure and thereby assists in the delivery of the compound. Suitable agents that may act in this capacity include monoclonal or polyclonal antibodies, one or more proteins or a liposome. The

composition may consist essentially of dosage units that can be administered as an aerosol. The term aerosol is used to denote a variety of systems ranging from those of colloidal nature to systems consisting of pressurized packages. Delivery may be by a liquefied or compressed gas or by a suitable pump system that dispenses the active ingredients. Aerosols may be delivered in single phase, bi phasic, or tri phasic systems in order to deliver the active ingredient(s). Delivery of the aerosol includes the necessary container, activators, valves, subcontainers, and the like, which together may form a kit. One of ordinary skill in the art, without undue experimentation, may determine preferred aerosols.

It will be understood that compositions of the present disclosure also encompass carrier molecules for polynucleotides, as described herein (*e.g.*, lipid nanoparticles, nanoscale delivery platforms, and the like).

The pharmaceutical compositions may be prepared by methodology well known in the pharmaceutical art. For example, a composition intended to be administered by injection can be prepared by combining a composition that comprises an antibody, antigen-binding fragment thereof, or antibody conjugate as described herein and optionally, one or more of salts, buffers and/or stabilizers, with sterile, distilled water so as to form a solution. A surfactant may be added to facilitate the formation of a homogeneous solution or suspension. Surfactants are compounds that non-covalently interact with the peptide composition so as to facilitate dissolution or homogeneous suspension of the antibody or antigen-binding fragment thereof in the aqueous delivery system.

In general, an appropriate dose and treatment regimen provide the composition(s) in an amount sufficient to provide therapeutic and/or prophylactic benefit (such as described herein, including an improved clinical outcome (*e.g.*, a decrease in frequency, duration, or severity of diarrhea or associated dehydration, or inflammation, or longer disease-free and/or overall survival, or a lessening of symptom severity). For prophylactic use, a dose should be sufficient to prevent, delay the onset of, or diminish the severity of a disease associated with disease or disorder. Prophylactic benefit of the compositions administered according to the methods

described herein can be determined by performing pre-clinical (including *in vitro* and *in vivo* animal studies) and clinical studies and analyzing data obtained therefrom by appropriate statistical, biological, and clinical methods and techniques, all of which can readily be practiced by a person skilled in the art.

Compositions are administered in an effective amount (*e.g.*, to treat a Wuhan coronavirus infection), which will vary depending upon a variety of factors including the activity of the specific compound employed; the metabolic stability and length of action of the compound; the age, body weight, general health, sex, and diet of the subject; the mode and time of administration; the rate of excretion; the drug combination; the severity of the particular disorder or condition; and the subject undergoing therapy. In certain embodiments, tollowing administration of therapies according to the formulations and methods of this disclosure, test subjects will exhibit about a 10% up to about a 99% reduction in one or more symptoms associated with the disease or disorder being treated as compared to placebo-treated or other suitable control subjects.

Generally, a therapeutically effective daily dose of an antibody or antigen binding fragment is (for a 70 kg mammal) from about 0.001 mg/kg (*i.e.*, 0.07 mg) to about 100 mg/kg (*i.e.,* 7.0 g); preferably a therapeutically effective dose is (for a 70 kg mammal) from about 0.01 mg/kg (*i.e.*, 0.7 mg) to about 50 mg/kg (*i.e.*, 3.5 g); more preferably a therapeutically effective dose is (for a 70 kg mammal) from about 1 mg/kg (*i.e.*, 70 mg) to about 25 mg/kg (*i.e.*, 1.75 g). For polynucleotides, vectors, host cells, and related compositions of the present disclosure, a therapeutically effective dose may be different than for an antibody or antigen-binding fragment.

In certain embodiments, a method comprises administering the antibody, antigen-binding fragment, polynucleotide, vector, host cell, or composition to the subject at 2, 3, 4, 5, 6, 7, 8, 9, 10 times, or more.

In certain embodiments, a method comprises administering the antibody, antigen-binding fragment, or composition to the subject a plurality of times, wherein a second or successive administration is performed at about 6, about 7, about 8, about 9,

about 10, about 11, about 12, about 24, about 48, about 74, about 96 hours, or more, following a first or prior administration, respectively.

In certain embodiments, a method comprises administering the antibody, antigen-binding fragment, polynucleotide, vector, host cell, immungenuc composition, or composition at least one time prior to the subject being infected by SARS-CoV-2.

Compositions comprising an antibody, antigen-binding fragment, polynucleotide, vector, host cell, immunogenic composition, or composition of the present disclosure may also be administered simultaneously with, prior to, or after administration of one or more other therapeutic agents. Such combination therapy may include administration of a single pharmaceutical dosage formulation which contains a compound of the invention and one or more additional active agents, as well as administration of compositions comprising an antibody or antigen-binding fragment of the disclosure and each active agent in its own separate dosage formulation. For example, an antibody or antigen-binding fragment thereof as described herein and the other active agent can be administered to the patient together in a single oral dosage composition such as a tablet or capsule, or each agent administered in separate oral dosage formulations. Similarly, an antibody or antigen-binding fragment as described herein and the other active agent can be administered to the subject together in a single parenteral dosage composition such as in a saline solution or other physiologically acceptable solution, or each agent administered in separate parenteral dosage formulations. Where separate dosage formulations are used, the compositions comprising an antibody or antigen-binding fragment and one or more additional active agents can be administered at essentially the same time, *i.e.*, concurrently, or at separately staggered times, *i.e.*, sequentially and in any order; combination therapy is understood to include all these regimens.

In certain embodiments, a combination therapy is provided that comprises one or more anti-SARS-CoV-2 antibody (or one or more nucleic acid, host cell, vector, or composition) of the present disclosure and one or more anti-inflammatory agent and/or one or more anti-viral agent. In particular embodiments, the one or more anti-inflammatory agent comprises a corticosteroid such as, for example, dexamethasone,

prednisone, or the like. In some embodiments, the one or more anti-inflammatory agents comprise a cytokine antagonist such as, for example, an antibody that binds to IL6 (such as siltuximab), or to IL-6R (such as tocilizumab), or to IL-1β, IL-7, IL-8, IL-9, IL-10, FGF, G-CSF, GM-CSF, IFN-γ, IP-10, MCP-1, MIP-1A, MIP1-B, PDGR, TNF-α, or VEGF. In some embodiments, anti-inflammatory agents such as leronlimab, ruxolitinib and/or anakinra are used. In some embodiments, the one or more anti-viral agents comprise nucleotide analogs or nucelotide analog prodrugs such as, for example, remdesivir, sofosbuvir, acyclovir, and zidovudine. In particular embodiments, an anti-viral agent comprises lopinavir, ritonavir, favipiravir, or any combination thereof. Other anti-inflammatory agents for use in a combination therapy of the present disclosure include non-steroidal anti-inflammatory drugs (NSAIDS). It will be appreciated that in such a combination therapy, the one or more antibody (or one or more nucleic acid, host cell, vector, or composition) and the one or more anti-inflammatory agent and/or one or the more antiviral agent can be administered in any order and any sequence, or together.

In some embodiments, an antibody (or one or more nucleic acid, host cell, vector, or immunogenic composition, composition) is administered to a subject who has previously received one or more anti-inflammatory agent and/or one or more antiviral agent. In some embodiments, one or more anti-inflammatory agent and/or one or more antiviral agent is administered to a subject who has previously received an antibody (or one or more nucleic acid, host cell, vector, immunogenic composition, or composition).

In certain embodiments, a combination therapy is provided that comprises two or more anti-SARS-CoV-2 antibodies of the present disclosure. A method can comprise administering a first antibody to a subject who has received a second antibody, or can comprise administering two or more antibodies together. For example, in particular embodiments, a method is provided that comprises administering to the subject (a) a first antibody or antigen-binding fragment, when the subject has received a second antibody or antigen-binding fragment; (b) the second antibody or antigen-binding fragment, when the subject has received the first antibody or antigen-binding

fragment; or (c) the first antibody or antigen-binding fragment, and the second antibody or antigen-binding fragment.

In a related aspect, uses of the presently disclosed antibodies, antigen-binding fragments, vectors, host cells, and compositions are provided.

In certain embodiments, an antibody, antigen-binding fragment, polynucleotide, vector, host cell, immunogenic composition, or composition is provided for use in a method of preventing or treating a SARS-CoV-2 infection in a subject.

In certain embodiments, an antibody, antigen-binding fragment, immunogenic composition, or composition is provided for use in a method of manufacturing or preparing a medicament for preventing or treating a SARS-CoV-2 coronavirus infection in a subject.

The present disclosure also provides the following Embodiments.

Embodiment 1. An antibody, or an antigen-binding fragment thereof, that competes with an antibody or antigen-binding fragment comprising a VH amino acid sequence according to SEQ ID NO: 16 and a VL amino acid sequence according to SEQ ID NO: 26 for binding to a SARS-CoV-2 S glycoprotein of a S glycoprotein trimer.

Embodiment 2. An antibody, or an antigen-binding fragment thereof, that is capable of binding to a SARS CoV-2 S glycoprotein of a S glycoprotein trimer, wherein:

(a) binding comprises contacting one or more of amino acid residues 369-386, 404-411, and 499-508 of SEQ ID NO: 3; and/or

(b) binding comprises binding an epitope formed by amino acid residues 369-386, 404-411, and 499-508 of SEQ ID NO: 3.

Embodiment 3. The antibody or antigen-binding fragment of Embodiment 2, which does not contact one or more of amino acids 406, 409, 410, 411, 499, 500, 505, and 507 of SEQ ID NO.:3 when binding to the S glycoprotein.

Embodiment 4. The antibody or antigen-binding fragment of any one of Embodiments 1-3, which is capable of binding to a SARS-CoV-2 S glycoprotein of a S glycoprotein trimer wherein two or three receptor binding domains (RBDs) of the trimer are in an open conformation and one or zero RBDs of the trimer is in a closed conformation, and optionally is not capable of binding to the S glycoprotein when only one RBD of the trimer is in an open conformation and two RBDs of the trimer are in a closed conformation.

Embodiment 5. An antibody, or an antigen-binding fragment thereof, which is capable of binding to a SARS-CoV-2 S glycoprotein of a S glycoprotein trimer wherein two or three receptor binding domains (RBDs) of the trimer are in an open conformation and one or zero RBDs of the trimer is in a closed conformation, and optionally is not capable of binding to the S protein when only one RBD of the trimer is in an open conformation and two RBDs of the trimer are in a closed conformation.

Embodiment 6. An antibody, or an antigen-binding fragment thereof, that competes with an antibody or antigen-binding fragment comprising a VH amino acid sequence according to SEQ ID NO: 31 and a VL amino acid sequence according to SEQ ID NO: 35 for binding to a SARS-CoV-2 S glycoprotein of a S glycoprotein trimer.

Embodiment 7. An antibody, or an antigen-binding fragment thereof, that is capable of binding to a SARS CoV-2 S glycoprotein of a S glycoprotein trimer, wherein:

(a) binding comprises contacting one or more of amino acid residues 444-449 and 472-498 of SEQ ID NO: 3; and/or

(b) the antibody or antigen-binding fragment recognizes an epitope formed by amino acid residues 444-449 and 472-498 of SEQ ID NO: 3; and/or

(c) binding comprises binding within a crevice formed by a receptor binding motif (RBM) β-hairpin in a receptor binding domain (RBD) of the S glycoprotein.

Embodiment 8. The antibody or antigen-binding fragment of Embodiment 7, which does not contact one or more of amino acids 448, 473-478, 487, 491, 492, 495, 496, and 497 of SEQ ID NO.:3 when binding to the SARS-CoV-2 S glycoprotein.

Embodiment 9. The antibody or antigen-binding fragment of any one of Embodiments 6-8, which is capable of binding to a SARS-CoV-2 S glycoprotein of a S glycoprotein trimer wherein one or zero receptor binding domains (RBDs) of the trimer are in an open conformation and two or three RBDs of the trimer are in a closed conformation.

Embodiment 10. An antibody, or an antigen-binding fragment thereof, which is capable of binding to a SARS-CoV-2 S glycoprotein protein of a S glycoprotein trimer wherein one or zero receptor binding domains (RBDs) of the trimer are in an open conformation and two or three RBDs of the trimer are in a closed conformation.

Embodiment 11. An antibody, or an antigen-binding fragment thereof, that competes with an antibody or antigen-binding fragment comprising a VH amino acid sequence according to SEQ ID NO: 47 and a VL amino acid sequence according to SEQ ID NO: 51 for binding to a SARS-CoV-2 S glycoprotein of a S glycoprotein trimer.

Embodiment 12. An antibody, or an antigen-binding fragment thereof, that is capable of binding to a SARS CoV-2 S glycoprotein, wherein:

(a) binding comprises contacting one or more of amino acid residues 403, 444-456, 475, and 485-505 of SEQ ID NO: 3; and/or

(b) the antibody or antigen-binding fragment recognizes an epitope formed by amino acid residues 403, 444-456, 475, and 485-505 of SEQ ID NO: 3.

Embodiment 13. The antibody or antigen-binding fragment of Embodiment 12, which does not contact one or more of amino acids 448, 450, 451, 452, 454, 486, 488, 490, 491, 492, 497, 503, and 504 of SEQ ID NO.:3 when binding to the S glycoprotein.

Embodiment 14. The antibody or antigen-binding fragment of any one of Embodiments 11-13, which is capable of binding to a SARS-CoV-2 S glycoprotein of a S glycoprotein trimer wherein one, two, or three receptor binding domains (RBDs) of the trimer are in an open conformation.

Embodiment 15. An antibody, or an antigen-binding fragment thereof, that competes with an antibody or antigen-binding fragment comprising a VH amino acid sequence according to SEQ ID NO: 64 and a VL amino acid sequence according to SEQ ID NO: 68 for binding to a SARS-CoV-2 S glycoprotein of a S glycoprotein trimer.

Embodiment 16. An antibody, or an antigen-binding fragment thereof, that is capable of binding to a SARS CoV-2 S glycoprotein of a S glycoprotein trimer, wherein:

(a) binding comprises contacting one or more of amino acid residues 368-388 and 407-414 of SEQ ID NO: 3; and/or

(b) the antibody or antigen-binding fragment recognizes an epitope formed by amino acid residues 368-388 and 407-414 of SEQ ID NO: 3.

Embodiment 17. The antibody or antigen-binding fragment of Embodiment 15 or 16, which is capable of binding to a SARS-CoV-2 S glycoprotein of a S glycoprotein trimer wherein two or three receptor binding domains (RBDs) of the trimer are in an open conformation and zero or one RBDs of the trimer is in a closed conformation.

Embodiment 18. An antibody, or an antigen-binding fragment thereof, that competes with an antibody or antigen-binding fragment comprising a VH amino acid sequence according to SEQ ID NO: 150 and a VL amino acid sequence according to SEQ ID NO: 154 for binding to a SARS-CoV-2 S glycoprotein of a S glycoprotein trimer.

Embodiment 19. An antibody, or an antigen-binding fragment thereof, that is capable of binding to a SARS CoV-2 S glycoprotein of a S glycoprotein trimer, wherein:

(a) binding comprises contacting one or more of amino acid residues 369-392, 411-414, 427-430, and 515-517 of SEQ ID NO: 3; and/or

(b) the antibody or antigen-binding fragment recognizes an epitope formed by amino acid residues 369-392, 411-414, 427-430, and 515-517 of SEQ ID NO: 3.

Embodiment 20. The antibody or antigen-binding fragment of Embodiment 18 or 19, which is capable of binding to a SARS-CoV-2 S protein of a S protein trimer wherein two or three receptor binding domains (RBDs) of the trimer are in an open conformation and zero or one RBDs of the trimer is in a closed conformation.

Embodiment 21. The antibody or antigen-binding fragment of any one of Embodiments 15-20, wherein binding of the antibody or antigen-binding fragment to the S glycoprotein promotes or leads to release of the S1 subunit from the S glycoprotein.

Embodiment 22. An antibody, or an antigen-binding fragment thereof, that competes with an antibody or antigen-binding fragment comprising a VH amino acid sequence according to SEQ ID NO: 123 and a VL amino acid sequence according to SEQ ID NO: 138 for binding to a SARS-CoV-2 S glycoprotein of a S glycoprotein trimer.

Embodiment 23. An antibody, or an antigen-binding fragment thereof, that is capable of binding to a SARS CoV-2 S glycoprotein of a S glycoprotein trimer, wherein:

(a) binding comprises contacting one or more of amino acid residues 417, 453, 455, 456, 473, 475-480, 484-489, and 493 of SEQ ID NO: 3; and/or

(b) the antibody or antigen-binding fragment recognizes an epitope formed by amino acid residues 417, 453, 455, 456, 473, 475-480, 484-489, and 493of SEQ ID NO.: 3.

Embodiment 24. The antibody or antigen-binding fragment of Embodiment 22 or 23, which is capable of binding to a SARS-CoV-2 S glycoprotein of a S glycoprotein trimer wherein one, two, or three receptor binding domains (RBDs) of the trimer are in an open conformation and zero, one, or two RBDs of the trimer are in a closed conformation.

Embodiment 25. An antibody, or an antigen-binding fragment thereof, that competes with an antibody or antigen-binding fragment comprising a VH amino acid sequence according to SEQ ID NO: 142 and a VL amino acid sequence according to SEQ ID NO: 146 for binding to a SARS-CoV-2 S glycoprotein trimer.

Embodiment 26. An antibody, or an antigen-binding fragment thereof, that is capable of binding to a SARS CoV-2 S glycoprotein trimer, wherein:

(a) binding comprises contacting one or more of amino acid residues on each of two receptor binding domains (RBDs), wherein binding comprises contacting, on a first RBD, one or more of amino acid residues 339, 342, 343, 367, 368, 371, 372, 373, 374, 436, 440, and 441, and, on a second RBD, one or more of amino acid residues 446, 447, 449, 452, 455, 456, 484, 485, 486, 487, 489, 490, 492, 493, 494, 496, and 498, wherein the amino acid numbering is according to SEQ ID NO.:3; and/or

(b) the antibody or antigen-binding fragment recognizes an epitope formed by the following:

(b)(i) on a first RBD, amino acid residues 339, 342, 343, 367, 368, 371, 372, 373, 374, 436, 440, and 441, and,

(b)(ii) on a second RBD, amino acid residues 446, 447, 449, 452, 455, 456, 484, 485, 486, 487, 489, 490, 492, 493, 494, 496, and 498, wherein the amino acid numbering is according to SEQ ID NO.:3.

Embodiment 27. The antibody or antigen-binding fragment of Embodiment 25 or 26, which is capable of binding to the S glycoprotein trimer wherein three receptor binding domains (RBDs) of the trimer are in a closed conformation.

Embodiment 28. The antibody or antigen-binding fragment of any one of Embodiments 25-27, wherein binding of the antibody or antigen-binding fragment to the S glycoprotein trimer inhibits or prevents an RBD of the trimer from assuming an open conformation.

Embodiment 29. The antibody or antigen-binding fragment of any one of Embodiments 1-28, wherein binding of the antibody or antigen-binding fragment to the S glycoprotein or S glycoprotein trimer, respectively, blocks an interaction between the S glycoprotein and a human ACE2.

Embodiment 30. The antibody or antigen-binding fragment of any one of Embodiments 1-28, wherein binding of the antibody or antigen-binding fragment to the S glycoprotein or S glycoprotein trimer, respectively, does not block an interaction between the S glycoprotein and a human ACE2.

Embodiment 31. The antibody or antigen-binding fragment of any one of Embodiments 1-30, which is capable of neutralizing an infection by a SARS-CoV-2.

Embodiment 32. An isolated polynucleotide encoding the antibody or antigen-binding fragment of any one of Embodiments 1-31.

Embodiment 33. A vector comprising the polynucleotide of Embodiment 32.

Embodiment 34. A recombinant host cell that: (i) expresses the antibody or antigen-binding fragment of any one of Embodiments 1-31; (ii) comprises the polynucleotide of Embodiment 32; and/or (iii) comprises the vector of Embodiment 33.

Embodiment 35. A composition comprising:

(i) the antibody or antigen-binding fragment of any one of Embodiments 1-31;

(ii) the polynucleotide of Embodiment 32;

(iii) the vector of Embodiment 33; and/or

(iv) the host cell of Embodiment 34, and

a pharmaceutically acceptable carrier, excipient, or diluent.

Embodiment 36. A combination comprising (i) any two or more of the antibodies or antigen-binding fragments of any of Embodiments 1-31 or (ii) a first antibody or antigen-binding fragment of any of Embodiments 1-31 and a second antibody that is antibody S309 or that competes with antibody S309 for binding to a SARS-CoV-2 S glycoprotein.

Embodiment 37. A composition comprising (i) any two or more of the antibodies or antigen-binding fragments of any of Embodiments 1-31 or (ii) a first antibody or antigen-binding fragment of any of Embodiments 1-31 and a second antibody or antigen-binding fragment that is antibody S309 or that competes with antibody S309 for binding to a SARS-CoV-2 S glycoprotein, and a pharmaceutically acceptable carrier, excipient, or diluent.

Embodiment 38. A method for treating a SARS-CoV-2 infection in a subject, the method administering to the subject an effective amount of:

(i) the antibody or antigen-binding fragment of any one of Embodiments 1-31;

(ii) the polynucleotide of Embodiment 32;

(iii) the vector of Embodiment 33;

(iv) the host cell of Embodiment 34;

(v) the composition of Embodiment 35;

(vi) the combination of Embodiment 36;

(vii) the composition of Embodiment 37;

(viii) any two or more of the antibodies or antigen-binding fragments of any of Embodiments 1-31; or

(ix) any combination of (i)-(viii).

Embodiment 39. The antibody or antigen-binding fragment of any one of Embodiments 1-31, the polynucleotide of Embodiment 32, the vector of Embodiment 33, the host cell of Embodiment 34, the composition of Embodiment 35, the combination of Embodiment 36, the composition of Embodiment 37, and/or the any two or more of the antibodies or antigen-binding fragments of Embodiments 1-31, for use in a method of treating a SARS-CoV-2 infection in a subject.

Embodiment 40. An immunogenic composition comprising:

(a) a SARS-CoV-2 nucleocapsid (N) protein (SEQ ID NO.:170), or an immunogenic fragment thereof;

(b) a SARS-CoV-2 S polypeptide or multimer thereof comprising (i) one, two, or three Receptor Binding Domains (RBDs) in an open conformation and (ii) a Site Ia polypeptide, the Site Ia polypeptide capable of being bound by antibody S2H14;

(c) a SARS-CoV-2 Spike (S) polypeptide comprising (i) a RBD in an open conformation or in a closed conformation and (ii) a Site Ib polypeptide, the Site Ib polypeptide capable of being bound by antibody S2H13;

(d) a SARS-CoV-2 S polypeptide or multimer thereof comprising (i) two or three Receptor Binding Domains (RBDs) in an open conformation and (ii) a Site IIa polypeptide, the Site IIa polypeptide capable of being bound by antibody S2X35;

(e) a SARS-CoV-2 S polypeptide or multimer thereof comprising (i) two adjacent RBDs in an open conformation and (ii) a Site IIb polypeptide, the Site IIb polypeptide capable of being bound by antibody S2A4;

(f) a SARS-CoV-2 S polypeptide or multimer thereof comprising (i) two adjacent RBDs in an open conformation and (ii) a Site IIc polypeptide, the Site IIc polypeptide capable of being bound by antibody S304;

(g) a SARS-CoV-2 S polypeptide capable of being bound by antibody CR3022;

(h) a SARS-CoV-2 Spike (S) polypeptide or multimer thereof comprising (i) a RBD in an open conformation or in a closed conformation and (ii) a Site IV polypeptide, the Site IV polypeptide capable of being bound by antibody S309;

(i) a polynucleotide encoding the SARS-CoV-2 N or S protein polypeptide of any one or more of (a)-(h); or

(j) any combination of (a)-(i) above.

Embodiment 41. The immunogenic composition of Embodiment 40, further comprising a pharmaceutically acceptable carrier, excipient, or diluent, and/or comprising an adjuvant.

Embodiment 42. The immunogenic composition of Embodiment 40 or Embodiment 41, wherein the SARS-COV-2 S polypeptide comprises a prefusion-stabilized S ectodomain and/or does not comprise a R1 domain, a CH domain, a CD domain, a HR1 domain, a HR2 domain, a TM domain, and/or a CT domain.

Embodiment 43. A method comprising administering the immunogenic composition or composition of any one of Embodiments 40-42 to a subject having, suspected of having, or at risk for having a SARS-CoV-2 infection.

Embodiment 44. Use of:

(a) (a)(i) antibody S2H14, or an antigen-binding fragment thereof, or (a)(ii) an antibody or antigen-binding fragment thereof that competes with (a)(i) for binding to a SARS-CoV-2 S glycoprotein;

(b) (b)(i) antibody S2H13, or an antigen-binding fragment thereof, or (b)(ii) an antibody or antigen-binding fragment thereof that competes with (b)(i) for binding to a SARS-CoV-2 S glycoprotein;

(c) (c)(i) antibody S2X35, or an antigen-binding fragment thereof, or (c)(ii) an antibody or antigen-binding fragment thereof that competes with (i) for binding to a SARS-CoV-2 S glycoprotein;

(d) (d)(i) antibody S2A4 or an antigen-binding fragment thereof, or (d)(ii) an antibody or antigen-binding fragment thereof that competes with (d)(i) for binding to a SARS-CoV-2 S glycoprotein;

(e) (e)(i) antibody S304 or an antigen-binding fragment thereof, or (e)(ii) an antibody or antigen-binding fragment thereof that competes with (e)(i) for binding to a SARS-CoV-2 S glycoprotein;

(f) (f)(i) antibody S309 or an antigen-binding fragment thereof, or (f)(ii) an antibody or antigen-binding fragment thereof that competes with (f)(i) for binding to a SARS-CoV-2 S glycoprotein; and/or

(g) (g)(i) antibody CR3022, or an antigen-binding fragment thereof, or (g)(ii) an antibody or antigen-binding fragment thereof that competes with (g)(i) for binding to a SARS-CoV-2 S glycoprotein,

in the diagnosis of a SARS-CoV-2 infection, wherein the diagnosis comprises contacting the antibody or antigen-binding fragment thereof with a sample from a subject, and detecting the presence or absence of a complex comprising the antibody or antigen-binding fragment with an antigen.

Embodiment 45. Use of:

(a) (a)(i) antibody S2H14, or an antigen-binding fragment thereof, or (a)(ii) an antibody or antigen-binding fragment thereof that competes with (a)(i) for binding to a SARS-CoV-2 S glycoprotein;

(b) (b)(i) antibody S2H13, or an antigen-binding fragment thereof, or (b)(ii) an antibody or antigen-binding fragment thereof that competes with (b)(i) for binding to a SARS-CoV-2 S glycoprotein;

(c) (c)(i) antibody S2X35, or an antigen-binding fragment thereof, or (c)(ii) an antibody or antigen-binding fragment thereof that competes with (c)(i) for binding to a SARS-CoV-2 S glycoprotein;

(d) (d)(i) antibody S2A4 or an antigen-binding fragment thereof, or (d)(ii) an antibody or antigen-binding fragment thereof that competes with (d)(i) for binding to a SARS-CoV-2 S glycoprotein;

(e) (e)(i) antibody S304 or an antigen-binding fragment thereof, or (e)(ii) an antibody or antigen-binding fragment thereof that competes with (e)(i) for binding to a SARS-CoV-2 S glycoprotein;

(f) (f)(i) antibody S309 or an antigen-binding fragment thereof, or (f)(ii) an antibody or antigen-binding fragment thereof that competes with (f)(i) for binding to a SARS-CoV-2 Spike S glycoprotein; and/or

(g) (g)(i) antibody CR3022, or an antigen-binding fragment thereof, or (g)(ii) an antibody or antigen-binding fragment thereof that competes with (g)(i) for binding to a SARS-CoV-2 S glycoprotein,

in determining whether a SARS-CoV-2 vaccine composition comprises an epitope in a correct conformation for binding by the antibody or antigen-binding fragment thereof.

Embodiment 46. A method comprising detecting, in sera from one or more subject having (hospitalized, symptomatic, or asymptomatic) or recovered from a SARS-CoV-2 infection:

(a) the titer of antibody (e.g., IgG, IgA, and/or IgM) that binds to SARS-CoV-2 S glycoprotein;

(b) the titer of antibody that binds to SARS-CoV-2 RBD and optionally neutralizes the SARS-CoV-2 infection;

(c) the titer of antibody that binds to SARS-CoV-2 Domain A and optionally neutralizes the SARS CoV-2 infection;

(d) the titer of antibody that binds to SARS-CoV-2 S2 and optionally neutralizes the SARS CoV-2 infection; and/or

(e) the titer of antibody that binds to SARS-CoV-2 N protein and optionally neutralizes the SARS-CoV-2 infection.

Embodiment 47. The method of Embodiment 45, further comprising preparing an immunogenic composition comprising whichever of SARS-CoV-2 S glycoprotein, RBD, Domain A, or N protein that resulted in the highest titer of antibody.

Embodiment 48. The method of Embodiment 46 or 47, wherein the sera is from a subject who experienced a symptom of a SARS-CoV-2 infection and the method further comprises preparing an immunogenic composition comprising whichever of the SARS-CoV-2 S protein, RBD, Domain A, or N protein against which the highest titer of antibody is detected at 25, preferably 50, more preferably 75, still more preferably 100, even more preferably 125, still more preferably 150 days after the onset of the symptom.

Embodiment 49. A composition or combination comprising any two, any three, or all four of (a)-(d):

(a) (a)(i) an antibody or antigen-binding fragment thereof (*e.g.*, Fv, scFv, Fab, scFab, or the like) that is capable of binding to a SARS CoV-2 S glycoprotein and comprises a CDRH1 comprising the sequence set forth in SEQ ID NO: 143, a CDRH2 comprising the sequence set forth in SEQ ID NO:144, a CDRH3 comprising the sequence set forth in SEQ ID NO:145, a CDRL1 comprising the sequence set forth in SEQ ID NO:147, a CDRL2 comprising the sequence set forth in SEQ ID NO:148, and a

CDRL3 comprising the sequence set forth in SEQ ID NO:149, or (a)(ii) an antibody or antigen-binding fragment thereof that competes with the antibody or antigen-binding fragment of (a)(i) for binding to the SARS CoV-2 S glycoprotein;

(b) (b)(i) an antibody or antigen-binding fragment thereof that is capable of binding to a SARS CoV-2 S glycoprotein and comprises a CDRH1 comprising the sequence set forth in SEQ ID NO: 109, a CDRH2 comprising the sequence set forth in SEQ ID NO:110, a CDRH3 comprising the sequence set forth in SEQ ID NO:111, a CDRL1 comprising the sequence set forth in SEQ ID NO:133, a CDRL2 comprising the sequence set forth in SEQ ID NO:134, and a CDRL3 comprising the sequence set forth in SEQ ID NO:135, or (b)(ii) an antibody or antigen-binding fragment thereof that competes with the antibody or antigen-binding fragment of (b)(i) for binding to the SARS CoV-2 S glycoprotein;

(c) (c)(i) an antibody or antigen-binding fragment thereof that is capable of binding to a SARS CoV-2 S glycoprotein and comprises a CDRH1 comprising the sequence set forth in SEQ ID NO: 102, a CDRH2 comprising the sequence set forth in SEQ ID NO:103, a CDRH3 comprising the sequence set forth in SEQ ID NO:104, a CDRL1 comprising the sequence set forth in SEQ ID NO:106, a CDRL2 comprising the sequence set forth in SEQ ID NO:107, and a CDRL3 comprising the sequence set forth in SEQ ID NO:108, or (c)(ii) an antibody or antigen-binding fragment thereof that competes with the antibody or antigen-binding fragment of (c)(i) for binding to the SARS CoV-2 S glycoprotein;

(d) (d)(i) an antibody or antigen-binding fragment thereof that is capable of binding to a SARS CoV-2 S glycoprotein and comprises a CDRH1 comprising the sequence set forth in SEQ ID NO: 94, a CDRH2 comprising the sequence set forth in SEQ ID NO:95, a CDRH3 comprising the sequence set forth in SEQ ID NO:96, a CDRL1 comprising the sequence set forth in SEQ ID NO:98, a CDRL2 comprising the sequence set forth in SEQ ID NO:99, and a CDRL3 comprising the sequence set forth in SEQ ID NO:100, or (d)(ii) an antibody or antigen-binding fragment thereof that competes with the antibody or antigen-binding fragment of (d)(i) for binding to the SARS CoV-2 S glycoprotein.

Embodiment 50. The composition of Embodiment 49, further comprising a pharmaceutically acceptable carrier, excipient, or diluent.

Embodiment 51. The composition of Embodiment 49 or 50, wherein:

(1) the antibody or antigen-binding fragment of (a)(i) comprises a VH comprising or consisting of an amino acid sequence having at least 80%, 85%, 90%, 91%, 92%, 93%, 94%, 95%, 96,%, 97%, 98%, or 99% identity (*e.g.*, as determined using BLAST) (*e.g.*, 100% identity) to the amino acid sequence set forth in SEQ ID NO:142 and a VL comprising or consisting of an amino acid sequence having at least 80%, 85%, 90%, 91%, 92%, 93%, 94%, 95%, 96,%, 97%, 98%, or 99% identity to the amino acid sequence set forth in SEQ ID NO:146;

(2) the antibody or antigen-binding fragment thereof of (b)(i) comprises a VH comprising or consisting of an amino acid sequence having at least 80%, 85%, 90%, 91%, 92%, 93%, 94%, 95%, 96,%, 97%, 98%, or 99% identity to the amino acid sequence set forth in SEQ ID NO:123 and a VL comprising or consisting of an amino acid sequence having at least 80%, 85%, 90%, 91%, 92%, 93%, 94%, 95%, 96,%, 97%, 98%, or 99% identity to the sequence set forth in SEQ ID NO:138;

(3) the antibody or antigen-binding fragment thereof of (c)(i) comprises a VH comprising or consisting of an amino acid sequence having at least 80%, 85%, 90%, 91%, 92%, 93%, 94%, 95%, 96,%, 97%, 98%, or 99% identity to the amino acid sequence set forth in SEQ ID NO:101 and a VL comprising or consisting of an amino acid sequence having at least 80%, 85%, 90%, 91%, 92%, 93%, 94%, 95%, 96,%, 97%, 98%, or 99% identity to the amino acid sequence set forth in SEQ ID NO:105; and/or

(4) the antibody or antigen-binding fragment thereof of (d)(i) comprises a VH comprising or consisting of an amino acid sequence having at least 80%, 85%, 90%, 91%, 92%, 93%, 94%, 95%, 96,%, 97%, 98%, or 99% identity to the amino acid sequence set forth in SEQ ID NO:93 and a VL comprising or consisting of an amino acid sequence having at least 80%, 85%, 90%, 91%, 92%, 93%, 94%, 95%, 96,%, 97%, 98%, or 99% identity to the amino acid sequence set forth in SEQ ID NO:97.

Embodiment 52. A composition comprising:

(a) (a)(i) antibody S2M11, or an antigen-binding fragment thereof, or (a)(ii) an antibody or antigen-binding fragment thereof that competes with (a)(i) for binding to a SARS-CoV-2 S glycoprotein;

(b) (b)(i) antibody S2E12, or an antigen-binding fragment thereof, or (b)(ii) an antibody or antigen-binding fragment thereof that competes with (b)(i) for binding to a SARS-CoV-2 S glycoprotein;

(c) (c)(i) antibody S309, or an antigen-binding fragment thereof, or (c)(ii) an antibody or antigen-binding fragment thereof that competes with (c)(i) for binding to a SARS-CoV-2 S glycoprotein; or

(d) any combination of (a)-(c) above.

Embodiment 53. The composition of Embodiment 52, further comprising a pharmaceutically acceptable carrier, excipient, or diluent.

Embodiment 54. The antibody or antigen-binding fragment of any one of Embodiments 1-31, the combination of Embodiment 36, or the composition of any one of Embodiments 37, 38, and 49-53, wherein any one or more of the antibodies or antigen binding fragments comprises a Fc polypeptide comprising:

(i) a mutation that enhances binding to a human FcRn and/or extends an *in vivo* half-life of antibody or antigen-binding fragment, optionally a M428L mutation, a N434S mutation, YTE mutation, or any combination thereof; and/or

(ii) a mutation that that enhances binding to a human FcγR, optionally a G236A mutation, a A330L mutation, a I332E, a S239D mutation, or any combination thereof.

Embodiment 55. The composition of any one of Embodiments 49-54 for use in treating or preventing SARS-CoV-2 infection.

Embodiment 56. A method of treating or preventing SARS-CoV-2 infection in a subject, comprising administering to the subject an effective amount of the composition of any one of Embodiments 49-54.

Embodiment 57. A method of treating or preventing a SARS-CoV-2 infection in a subject, comprising administering to the subject an effective amount of any one or more of:

(a) (i) an antibody or antigen-binding fragment thereof (*e.g.*, Fv, scFv, Fab, scFab, or the like) that is capable of binding to a SARS CoV-2 S protein and comprises a CDRH1 comprising the sequence set forth in SEQ ID NO: 143, a CDRH2 comprising the sequence set forth in SEQ ID NO:144, a CDRH3 comprising the sequence set forth in SEQ ID NO:145, a CDRL1 comprising the sequence set forth in SEQ ID NO:147, a CDRL2 comprising the sequence set forth in SEQ ID NO:148, and a CDRL3 comprising the sequence set forth in SEQ ID NO:149, or (ii) an antibody or antigen-binding fragment thereof that competes with the antibody or antigen-binding fragment of (i) for binding to the SARS CoV-2 S protein;

(b) (i) an antibody or antigen-binding fragment thereof that is capable of binding to a SARS CoV-2 S protein and comprises a CDRH1 comprising the sequence set forth in SEQ ID NO: 109, a CDRH2 comprising the sequence set forth in SEQ ID NO:110, a CDRH3 comprising the sequence set forth in SEQ ID NO:111, a CDRL1 comprising the sequence set forth in SEQ ID NO:133, a CDRL2 comprising the sequence set forth in SEQ ID NO:134, and a CDRL3 comprising the sequence set forth in SEQ ID NO:135, or (ii) an antibody or antigen-binding fragment thereof that competes the antibody or antigen-binding fragment of (i) for binding to the SARS CoV-2 S protein;

(c) (i) an antibody or antigen-binding fragment thereof that is capable of binding to a SARS CoV-2 S protein and comprises a CDRH1 comprising the sequence set forth in SEQ ID NO: 102, a CDRH2 comprising the sequence set forth in SEQ ID NO:103, a CDRH3 comprising the sequence set forth in SEQ ID NO:104, a CDRL1 comprising the sequence set forth in SEQ ID NO:106, a CDRL2 comprising the

sequence set forth in SEQ ID NO:107, and a CDRL3 comprising the sequence set forth in SEQ ID NO:108, or (ii) an antibody or antigen-binding fragment thereof that competes the antibody or antigen-binding fragment of (i) for binding to the SARS CoV-2 S protein;

(d) (i) an antibody or antigen-binding fragment thereof that is capable of binding to a SARS CoV-2 S protein and comprises a CDRH1 comprising the sequence set forth in SEQ ID NO: 94, a CDRH2 comprising the sequence set forth in SEQ ID NO:95, a CDRH3 comprising the sequence set forth in SEQ ID NO:96, a CDRL1 comprising the sequence set forth in SEQ ID NO:98, a CDRL2 comprising the sequence set forth in SEQ ID NO:99, and a CDRL3 comprising the sequence set forth in SEQ ID NO:100, or (ii) an antibody or antigen-binding fragment thereof that competes the antibody or antigen-binding fragment of (i) for binding to the SARS CoV-2 S protein.

Embodiment 58. The method of Embodiment 57, wherein:

(1) the antibody or antigen-binding fragment of (a)(i) comprises a VH comprising or consisting of an amino acid sequence having at least 80%, 85%, 90%, 91%, 92%, 93%, 94%, 95%, 96,%, 97%, 98%, or 99% identity (*e.g.*, as determined using BLAST) (*e.g.*, 100% identity) to the amino acid sequence set forth in SEQ ID NO:142 and a VL comprising or consisting of an amino acid sequence having at least 80%, 85%, 90%, 91%, 92%, 93%, 94%, 95%, 96,%, 97%, 98%, or 99% identity to the amino acid sequence set forth in SEQ ID NO:146;

(2) the an antibody or antigen-binding fragment thereof of (b)(i) comprises a VH comprising or consisting of an amino acid sequence having at least 80%, 85%, 90%, 91%, 92%, 93%, 94%, 95%, 96,%, 97%, 98%, or 99% identity to the amino acid sequence set forth in SEQ ID NO:123 and a VL comprising or consisting of an amino acid sequence having at least 80%, 85%, 90%, 91%, 92%, 93%, 94%, 95%, 96,%, 97%, 98%, or 99% identity to the sequence set forth in SEQ ID NO:138;

(3) the an antibody or antigen-binding fragment thereof of (c)(i) comprises a VH comprising or consisting of an amino acid sequence having at least 80%, 85%,

90%, 91%, 92%, 93%, 94%, 95%, 96,%, 97%, 98%, or 99% identity to the amino acid sequence set forth in SEQ ID NO:101 and a VL comprising or consisting of an amino acid sequence having at least 80%, 85%, 90%, 91%, 92%, 93%, 94%, 95%, 96,%, 97%, 98%, or 99% identity to the amino acid sequence set forth in SEQ ID NO:105; and/or

(4) the antibody or antigen-binding fragment thereof of (d)(i) comprises a VH comprising or consisting of an amino acid sequence having at least 80%, 85%, 90%, 91%, 92%, 93%, 94%, 95%, 96,%, 97%, 98%, or 99% identity to the amino acid sequence set forth in SEQ ID NO:93 and a VL comprising or consisting of an amino acid sequence having at least 80%, 85%, 90%, 91%, 92%, 93%, 94%, 95%, 96,%, 97%, 98%, or 99% identity to the amino acid sequence set forth in SEQ ID NO:97.

Embodiment 59. A method of treating or preventing a SARS-CoV-2 infection in a subject, comprising administering to the subject an effective amount of one of (a)-(d):

(a) (i) an antibody or antigen-binding fragment thereof (*e.g.*, Fv, scFv, Fab, scFab, or the like) that is capable of binding to a SARS CoV-2 S protein and comprises a CDRH1 comprising the sequence set forth in SEQ ID NO: 143, a CDRH2 comprising the sequence set forth in SEQ ID NO:144, a CDRH3 comprising the sequence set forth in SEQ ID NO:145, a CDRL1 comprising the sequence set forth in SEQ ID NO:147, a CDRL2 comprising the sequence set forth in SEQ ID NO:148, and a CDRL3 comprising the sequence set forth in SEQ ID NO:149, or (ii) an antibody or antigen-binding fragment thereof that competes with the antibody or antigen-binding fragment of (i) for binding to the SARS CoV-2 S protein;

(b) (i) an antibody or antigen-binding fragment thereof that is capable of binding to a SARS CoV-2 S protein and comprises a CDRH1 comprising the sequence set forth in SEQ ID NO:109, a CDRH2 comprising the sequence set forth in SEQ ID NO:110, a CDRH3 comprising the sequence set forth in SEQ ID NO:111, a CDRL1 comprising the sequence set forth in SEQ ID NO:133, a CDRL2 comprising the sequence set forth in SEQ ID NO:134, and a CDRL3 comprising the sequence set forth in SEQ ID NO:135, or (ii) an antibody or antigen-binding fragment thereof that

competes the antibody or antigen-binding fragment of (i) for binding to the SARS CoV-2 S protein;

(c) (i) an antibody or antigen-binding fragment thereof that is capable of binding to a SARS CoV-2 S protein and comprises a CDRH1 comprising the sequence set forth in SEQ ID NO: 102, a CDRH2 comprising the sequence set forth in SEQ ID NO:103, a CDRH3 comprising the sequence set forth in SEQ ID NO:104, a CDRL1 comprising the sequence set forth in SEQ ID NO:106, a CDRL2 comprising the sequence set forth in SEQ ID NO:107, and a CDRL3 comprising the sequence set forth in SEQ ID NO:108, or (ii) an antibody or antigen-binding fragment thereof that competes the antibody or antigen-binding fragment of (i) for binding to the SARS CoV-2 S protein;

(d) (i) an antibody or antigen-binding fragment thereof that is capable of binding to a SARS CoV-2 S protein and comprises a CDRH1 comprising the sequence set forth in SEQ ID NO:94, a CDRH2 comprising the sequence set forth in SEQ ID NO:95, a CDRH3 comprising the sequence set forth in SEQ ID NO:96, a CDRL1 comprising the sequence set forth in SEQ ID NO:98, a CDRL2 comprising the sequence set forth in SEQ ID NO:99, and a CDRL3 comprising the sequence set forth in SEQ ID NO:100, or (ii) an antibody or antigen-binding fragment thereof that competes the antibody or antigen-binding fragment of (i) for binding to the SARS CoV-2 S protein;

wherein the subject has received, or is receiving, any one or more of the other of (a)-(d) (*e.g.*, administering an effective amount of (a) to a subject who has received or is receiving (b), (c), and/or (d).

Embodiment 60. The method of Embodiment 59, wherein:

(1) the antibody or antigen-binding fragment of (a)(i) comprises a VH comprising or consisting of an amino acid sequence having at least 80%, 85%, 90%, 91%, 92%, 93%, 94%, 95%, 96,%, 97%, 98%, or 99% identity (*e.g.*, as determined using BLAST) (*e.g.*, 100% identity) to the amino acid sequence set forth in SEQ ID NO:142 and a VL comprising or consisting of an amino acid sequence having at least

80%, 85%, 90%, 91%, 92%, 93%, 94%, 95%, 96,%, 97%, 98%, or 99% identity to the amino acid sequence set forth in SEQ ID NO:146;

(2) the antibody or antigen-binding fragment thereof of (b)(i) comprises a VH comprising or consisting of an amino acid sequence having at least 80%, 85%, 90%, 91%, 92%, 93%, 94%, 95%, 96,%, 97%, 98%, or 99% identity to the amino acid sequence set forth in SEQ ID NO:123 and a VL comprising or consisting of an amino acid sequence having at least 80%, 85%, 90%, 91%, 92%, 93%, 94%, 95%, 96,%, 97%, 98%, or 99% identity to the sequence set forth in SEQ ID NO:138;

(3) the antibody or antigen-binding fragment thereof of (c)(i) comprises a VH comprising or consisting of an amino acid sequence having at least 80%, 85%, 90%, 91%, 92%, 93%, 94%, 95%, 96,%, 97%, 98%, or 99% identity to the amino acid sequence set forth in SEQ ID NO:101 and a VL comprising or consisting of an amino acid sequence having at least 80%, 85%, 90%, 91%, 92%, 93%, 94%, 95%, 96,%, 97%, 98%, or 99% identity to the amino acid sequence set forth in SEQ ID NO:105; and/or

(4) the antibody or antigen-binding fragment thereof of (d)(i) comprises a VH comprising or consisting of an amino acid sequence having at least 80%, 85%, 90%, 91%, 92%, 93%, 94%, 95%, 96,%, 97%, 98%, or 99% identity to the amino acid sequence set forth in SEQ ID NO:93 and a VL comprising or consisting of an amino acid sequence having at least 80%, 85%, 90%, 91%, 92%, 93%, 94%, 95%, 96,%, 97%, 98%, or 99% identity to the amino acid sequence set forth in SEQ ID NO:97.

Embodiment 61. The method of any one of Embodiments 57-60, wherein an antibody or antigen-binding fragment administered to the subject comprises a Fc polypeptide comprising:

(i) a mutation that enhances binding to a human FcRn and/or extends an *in vivo* half-life of antibody or antigen-binding fragment, optionally a M428L mutation, a N434S mutation, YTE mutation, or any combination thereof; and/or

(ii) a mutation that that enhances binding to a human FcγR, optionally a G236A mutation, a A330L mutation, a I332E, a S239D mutation, or any combination thereof.

Embodiment 62. A method of diagnosing a SARS-CoV-2 infection, comprising contacting the composition of any one of Embodiments 49-54 with a sample from a subject and detecting the presence or absence of a complex comprising the antibody or antigen-binding fragment and an antigen.

Embodiment 63. The composition of any one of Embodiments 49-54 for use in determining whether a SARS-CoV-2 vaccine composition comprises an epitope in a correct conformation for binding by the antibody(ies) or antigen-binding fragment(s) thereof.

Embodiment 64. An immunogenic composition comprising:

(a) a SARS-CoV-2 S polypeptide or multimer thereof that comprises two or three receptor binding domains (RBDs) in a closed-conformation, wherein two adjacent RBDs are in a closed conformation;

(b) a SARS-CoV-2 S polypeptide or multimer thereof capable of being bound by an antibody or antigen-binding fragment thereof comprising a CDRH1 comprising the sequence set forth in SEQ ID NO: 143, a CDRH2 comprising the sequence set forth in SEQ ID NO:144, a CDRH3 comprising the sequence set forth in SEQ ID NO:145, a CDRL1 comprising the sequence set forth in SEQ ID NO:147, a CDRL2 comprising the sequence set forth in SEQ ID NO:148, and a CDRL3 comprising the sequence set forth in SEQ ID NO:149;

(c) a SARS-CoV-2 S polypeptide or multimer thereof capable of being bound by an antibody or antigen-binding fragment thereof comprising a CDRH1 comprising the sequence set forth in SEQ ID NO: 109, a CDRH2 comprising the sequence set forth in SEQ ID NO:110, a CDRH3 comprising the sequence set forth in SEQ ID NO:111, a CDRL1 comprising the sequence set forth in SEQ ID NO:133, a CDRL2 comprising the sequence set forth in SEQ ID NO:134, and a CDRL3 comprising the sequence set forth in SEQ ID NO:135;

or any combination of (a)-(c).

Embodiment 65. The immunogenic composition of Embodiment 64, further comprising:

(d) a SARS-CoV-2 S polypeptide or multimer thereof capable of being bound by an antibody or antigen-binding fragment thereof comprising a CDRH1 comprising the sequence set forth in SEQ ID NO: 102, a CDRH2 comprising the sequence set forth in SEQ ID NO:103, a CDRH3 comprising the sequence set forth in SEQ ID NO:104, a CDRL1 comprising the sequence set forth in SEQ ID NO:106, a CDRL2 comprising the sequence set forth in SEQ ID NO:107, and a CDRL3 comprising the sequence set forth in SEQ ID NO:108;

(e) a SARS-CoV-2 S polypeptide or multimer thereof capable of being bound by an antibody or antigen-binding fragment thereof comprising a CDRH1 comprising the sequence set forth in SEQ ID NO:94, a CDRH2 comprising the sequence set forth in SEQ ID NO:95, a CDRH3 comprising the sequence set forth in SEQ ID NO:96, a CDRL1 comprising the sequence set forth in SEQ ID NO:98, a CDRL2 comprising the sequence set forth in SEQ ID NO:99, and a CDRL3 comprising the sequence set forth in SEQ ID NO:100;

or a combination thereof.

Embodiment 66. An immunogenic composition comprising:

(a) a SARS-CoV-2 S polypeptide or multimer thereof capable of being bound by an antibody or antigen-binding fragment thereof comprising a VH comprising the sequence set forth in SEQ ID NO:142 and a VL comprising the sequence set forth in SEQ ID NO:146;

(b) a SARS-CoV-2 S polypeptide or multimer thereof capable of being bound by an antibody or antigen-binding fragment thereof comprising a VH comprising the sequence set forth in SEQ ID NO:123 and a VL comprising the sequence set forth in SEQ ID NO:138;

or a combination thereof.

Embodiment 67. The immunogenic composition of Embodiment 66, further comprising:

(c) a SARS-CoV-2 S protein polypeptide capable of being bound by an antibody or antigen-binding fragment thereof comprising a CDRH1 comprising the sequence set forth in SEQ ID NO: 102, a CDRH2 comprising the sequence set forth in SEQ ID NO:103, a CDRH3 comprising the sequence set forth in SEQ ID NO:104, a CDRL1 comprising the sequence set forth in SEQ ID NO:106, a CDRL2 comprising the sequence set forth in SEQ ID NO:107, and a CDRL3 comprising the sequence set forth in SEQ ID NO:108;

(d) a SARS-CoV-2 S protein polypeptide capable of being bound by an antibody or antigen-binding fragment thereof comprising a CDRH1 comprising the sequence set forth in SEQ ID NO: 94, a CDRH2 comprising the sequence set forth in SEQ ID NO:95, a CDRH3 comprising the sequence set forth in SEQ ID NO:96, a CDRL1 comprising the sequence set forth in SEQ ID NO:98, a CDRL2 comprising the sequence set forth in SEQ ID NO:99, and a CDRL3 comprising the sequence set forth in SEQ ID NO:100;

or a combination thereof.

Embodiment 68. An immunogenic composition comprising:

(a) a SARS-CoV-2 S polypeptide capable of being bound by antibody S2M11, or an antigen-binding fragment thereof;

(b) a SARS-CoV-2 S polypeptide capable of being bound by antibody S2E12, or an antigen-binding fragment thereof;

(c) a SARS-CoV-2 S polypeptide capable of being bound by antibody S309, or an antigen-binding fragment thereof; or

(d) any combination of (a)-(c) above.

Embodiment 69. The immunogenic composition of any one of Embodiments 64-68, further comprising a pharmaceutically acceptable carrier, excipient, or diluent, and/or comprising an adjuvant.

Table 2. Sequences

Sequence Description	SEQ ID NO.	Sequence
SARS-CoV-2 Wuhan seafood market pneumonia virus isolate Wuhan-Hu-1 genomic sequence (GenBank: MN908947.3; January 23, 2020)	1	1 attaaaggtt tataccttcc caggtaacaa accaaccaac tttcgatctc ttgtagatct 61 gttctctaaa cgaactttaa aatctgtgtg gctgtcactc ggctgcatgc ttagtgcact 121 cacgcagtat aattaataac taattactgt cgttgacagg acacgagtaa ctcgtctatc 181 ttctgcaggc tgcttacggt ttcgtccgtg ttgcagccga tcatcagcac atctaggttt 241 cgtccgggtg tgaccgaaag gtaagatgga gagccttgtc cctggtttca acgagaaaac 301 acacgtccaa ctcagtttgc ctgttttaca ggttcgcgac gtgctcgtac gtggctttgg 361 agactccgtg gaggaggtct tatcagaggc cgtcaacat cttaaagatg gcacttgtgg 421 cttagtagaa gttgaaaaag gcgttttgcc tcaacttgaa cagccctatg tgttcatcaa 481 acgttcggat gctcgaactg cacctcatgg tcatgttatg gttgagctgg tagcagaact 541 cgaaggcatt cagtacggtc gtagtggtga gacacttggt gtccttgtcc ctcatgtggg 601 cgaaatacca gtggcttacc gcaaggttct tcttcgtaag aacggtaata aaggagctgg 661 tggccatagt tacggcgccg atctaaagtc atttgactta ggcgacgagc ttggcactga 721 tccttatgaa gattttcaag aaaactggaa cactaaacat agcagtggtg ttacccgtga 781 actcatgcgt gagcttaacg gaggggcata cactcgctat gtcgataaca acttctgtgg 841 ccctgatggc taccctcttg agtgcattaa agaccttcta gcacgtgctg gtaaagcttc 901 atgcactttg tccgaacaac tggactttat tgacactaag aggggtgtat actgctgccg 961 tgaacatgag catgaaattg cttggtacac ggaacgttct gaaaagagct atgaattgca 1021 gacacctttt gaaattaaat tggcaaagaa atttgacacc ttcaatgggg aatgtccaaa 1081 ttttgtattt cccttaaatt ccataatcaa gactattcaa ccaagggttg aaaagaaaaa 1141 gcttgatggc tttatgggta gaattcgatc tgtctatcca gttgcgtcac caaatgaatg 1201 caaccaaatg tgcctttcaa ctctcatgaa gtgtgatcat tgtggtgaaa cttcatggca 1261 gacgggcgat tttgttaaag ccacttgcga attttgtggc actgagaatt tgactaaaga 1321 aggtgccact acttgtggtt acttacccca aaatgctgtt gttaaaattt attgtccagc 1381 atgtcacaat tcagaagtag gacctgagca tagtcttgcc gaataccata atgaatctgg 1441 cttgaaaacc attcttcgta agggtggtcg cactattgcc tttggaggct gtgtgttctc

Sequence Description	SEQ ID NO.	Sequence
		1501 ttatgttggt tgccataaca agtgtgccta ttgggttcca cgtgctagcg ctaacatagg 1561 ttgtaaccat acaggtgttg ttggagaagg ttccgaaggt cttaatgaca accttcttga 1621 aatactccaa aaagagaaag tcaacatcaa tattgttggt gactttaaac ttaatgaaga 1681 gatcgccatt attttggcat ctttttctgc ttccacaagt gcttttgtgg aaactgtgaa 1741 aggtttggat tataaagcat tcaaacaaat tgttgaatcc tgtggtaatt ttaaagttac 1801 aaaaggaaaa gctaaaaaag gtgcctggaa tattggtgaa cagaaatcaa tactgagtcc 1861 tctttatgca tttgcatcag aggctgctcg tgttgtacga tcaatttct cccgcactct 1921 tgaaactgct caaaattctg tgcgtgtttt acagaaggcc gctataacaa tactagatgg 1981 aatttcacag tattcactga gactcattga tgctatgatg ttcacatctg atttggctac 2041 taacaatcta gttgtaatgg cctacattac aggtggtgtt gttcagttga cttcgcagtg 2101 gctaactaac atctttggca ctgtttatga aaaactcaaa cccgtccttg attggcttga 2161 agagaagttt aaggaaggtg tagagtttct tagagacggt tgggaaattg ttaaatttat 2221 ctcaacctgt gcttgtgaaa ttgtcggtgg acaaattgtc acctgtgcaa aggaaattaa 2281 ggagagtgtt cagacattct ttaagcttgt aaataaattt ttggctttgt gtgctgactc 2341 tatcattatt ggtggagcta aacttaaagc cttgaattta ggtgaaacat ttgtcacgca 2401 ctcaaaggga ttgtacagaa agtgtgttaa atccagagaa gaaactggcc tactcatgcc 2461 tctaaaagcc ccaaaagaaa ttatcttctt agagggagaa acacttccca cagaagtgtt 2521 aacagaggaa gttgtcttga aaactggtga tttacaacca ttagaacaac ctactagtga 2581 agctgttgaa gctccattgg ttggtacacc agtttgtatt aacgggctta tgttgctcga 2641 aatcaaagac acagaaaagt actgtgccct tgcacctaat atgatggtaa caaacaatac 2701 cttcacactc aaaggcggtg caccaacaaa ggttacttttt ggtgatgaca ctgtgataga 2761 agtgcaaggt tacaagagtg tgaatatcac ttttgaactt gatgaaagga ttgataaagt 2821 acttaatgag aagtgctctg cctatacagt tgaactcggt acagaagtaa atgagttcgc 2881 ctgtgttgtg gcagatgctg tcataaaaac tttgcaacca gtatctgaat tacttacacc 2941 actgggcatt gatttagatg agtggagtat ggctacatac tacttatttg atgagtctgg 3001 tgagtttaaa ttggcttcac atatgtattg ttctttctac cctccagatg aggatgaaga 3061 agaaggtgat tgtgaagaag aagagtttga gccatcaact caatatgagt atggtactga 3121 agatgattac caaggtaaac ctttggaatt tggtgccact tctgctgctc ttcaacctga 3181 agaagagcaa gaagaagatt ggttagatga tgatagtcaa caaactgttg gtcaacaaga 3241 cggcagtgag gacaatcaga caactactat tcaaacaatt gttgaggttc aacctcaatt 3301 agagatggaa cttacaccag ttgttcagac tattgaagtg aatagtttta gtggttattt 3361 aaaacttact gacaatgtat acattaaaaa tgcagacatt gtggaagaag ctaaaaaggt 3421

Sequence Description	SEQ ID NO.	Sequence
		aaaaccaaca gtggttgtta atgcagccaa tgtttacctt aaacatggag gaggtgttgc 3481 aggagcctta aataaggcta ctaacaatgc catgcaagtt gaatctgatg attacatagc 3541 tactaatgga ccacttaaag tgggtggtag ttgtgtttta agcggacaca atcttgctaa 3601 acactgtctt catgttgtcg gcccaaatgt taacaaaggt gaagacattc aacttcttaa 3661 gagtgcttat gaaaatttta atcagcacga agttctactt gcaccattat tatcagctgg 3721 tatttttggt gctgacccta tacattcttt aagagtttgt gtagatactg ttcgcacaaa 3781 tgtctactta gctgtctttg ataaaaatct ctatgacaaa cttgtttcaa gctttttgga 3841 aatgaagagt gaaaagcaag ttgaacaaaa gatcgctgag attcctaaag aggaagttaa 3901 gccatttata actgaaagta aaccttcagt tgaacagaga aaacaagatg ataagaaaat 3961 caaagcttgt gttgaagaag ttacaacaac tctggaagaa actaagttcc tcacagaaaa 4021 cttgttactt tatattgaca ttaatggcaa tcttcatcca gattctgcca ctcttgttag 4081 tgacattgac atcactttct taaagaaaga tgctccatat atagtgggtg atgttgttca 4141 agagggtgtt ttaactgctg tggttatacc tactaaaaag gctggtggca ctactgaaat 4201 gctagcgaaa gctttgagaa aagtgccaac agacaattat ataaccactt acccgggtca 4261 gggtttaaat ggttacactg tagaggaggc aaagacagtg cttaaaaagt gtaaaagtgc 4321 cttttacatt ctaccatcta ttatctctaa tgagaagcaa gaaattcttg gaactgtttc 4381 ttggaatttg cgagaaatgc ttgcacatgc agaagaaaca cgcaaattaa tgcctgtctg 4441 tgtggaaact aaagccatag tttcaactat acagcgtaaa tataagggta ttaaaataca 4501 agagggtgtg gttgattatg gtgctagatt ttacttttac accagtaaaa caactgtagc 4561 gtcacttatc aacacactta acgatctaaa tgaaactctt gttacaatgc cacttggcta 4621 tgtaacacat ggcttaaatt tggaagaagc tgctcggtat atgagatctc tcaaagtgcc 4681 agctacagtt tctgtttctt cacctgatgc tgttacagcg tataatggtt atcttacttc 4741 ttcttctaaa acacctgaag aacattttat tgaaaccatc tcacttgctg gttcctataa 4801 agattggtcc tattctggac aatctacaca actaggtata gaatttctta agagaggtga 4861 taaaagtgta tattacacta gtaatcctac cacattccac ctagatggtg aagttatcac 4921 ctttgacaat cttaagacac ttctttcttt gagagaagtg aggactatta aggtgtttac 4981 aacagtagac aacattaacc tccacacgca agttgtggac atgtcaatga catatggaca 5041 acagtttggt ccaacttatt tggatggagc tgatgttact aaaataaaac ctcataattc 5101 acatgaaggt aaaacatttt atgttttacc taatgatgac actctacgtg ttgaggcttt 5161 tgagtactac cacacaactg atcctagttt tctgggtagg tacatgtcag cattaaatca 5221 cactaaaaag tggaaatacc cacaagttaa

Sequence Description	SEQ ID NO.	Sequence
		tggtttaact tctattaaat gggcagataa 5281 caactgttat cttgccactg cattgttaac actccaacaa atagagttga agtttaatcc 5341 acctgctcta caagatgctt attacagagc aagggctggt gaagctgcta acttttgtgc 5401 acttatctta gcctactgta ataagacagt aggtgagtta ggtgatgtta gagaaacaat 5461 gagttacttg tttcaacatg ccaatttaga ttcttgcaaa agagtcttga acgtggtgtg 5521 taaaacttgt ggacaacagc agacaaccct taagggtgta gaagctgtta tgtacatggg 5581 cacactttct tatgaacaat ttaagaaagg tgttcagata ccttgtacgt gtggtaaaca 5641 agctacaaaa tatctagtac aacaggagtc acctttgtt atgatgtcag caccacctgc 5701 tcagtatgaa cttaagcatg gtacatttac ttgtgctagt gagtacactg gtaattacca 5761 gtgtggtcac tataaacata taacttctaa agaaactttg tattgcatag acggtgcttt 5821 acttacaaag tcctcagaat acaaaggtcc tattacggat gttttctaca aagaaaacag 5881 ttacacaaca accataaaac cagttactta taaattggat ggtgttgttt gtacagaaat 5941 tgaccctaag ttggacaatt attataagaa agacaattct tatttcacag agcaaccaat 6001 tgatcttgta ccaaaccaac catatccaaa cgcaagcttc gataatttta agtttgtatg 6061 tgataatatc aaatttgctg atgatttaaa ccagttaact ggttataaga aacctgcttc 6121 aagagagctt aaagttacat ttttccctga cttaaatggt gatgtggtgg ctattgatta 6181 taaacactac acaccctctt ttaagaaagg agctaaattg ttacataaac ctattgtttg 6241 gcatgttaac aatgcaacta ataaagccac gtataaacca aatacctggt gtatacgttg 6301 tctttggagc acaaaaccag ttgaaacatc aaattcgttt gatgtactga agtcagagga 6361 cgcgcaggga atggataatc ttgcctgcga agatctaaaa ccagtctctg aagaagtagt 6421 ggaaaatcct accatacaga aagacgttct tgagtgtaat gtgaaaacta ccgaagttgt 6481 aggagacatt atacttaaac cagcaaataa tagtttaaaa attacagaag aggttggcca 6541 cacagatcta atggctgctt atgtagacaa ttctagtctt actattaaga aacctaatga 6601 attatctaga gtattaggtt tgaaaaccct tgctactcat ggtttagctg ctgttaatag 6661 tgtcccttgg gatactatag ctaattatgc taagcctttt cttaacaaag ttgttagtac 6721 aactactaac atagttacac ggtgtttaaa ccgtgtttgt actaattata tgccttattt 6781 ctttacttta ttgctacaat tgtgtacttt tactagaagt acaaattcta gaattaaagc 6841 atctatgccg actactatag caaagaatac tgttaagagt gtcggtaaat tttgtctaga 6901 ggcttcattt aattatttga agtcacctaa tttttctaaa ctgataaata ttataatttg 6961 gtttttacta ttaagtgttt gcctaggttc tttaatctac tcaaccgctg ctttaggtgt 7021 tttaatgtct aatttaggca tgccttctta ctgtactggt tacagagaag gctatttgaa 7081 ctctactaat gtcactattg caacctactg tactggttct ataccttgta

Sequence Description	SEQ ID NO.	Sequence
		gtgtttgtct 7141 tagtggttta gattctttag acacctatcc ttctttagaa actatacaaa ttaccatttc 7201 atcttttaaa tgggatttaa ctgcttttgg cttagttgca gagtggtttt tggcatatat 7261 tcttttcact aggtttttct atgtacttgg attggctgca atcatgcaat tgtttttcag 7321 ctattttgca gtacatttta ttagtaattc ttggcttatg tggttaataa ttaatcttgt 7381 acaaatggcc ccgatttcag ctatggttag aatgtacatc ttctttgcat cattttatta 7441 tgtatggaaa agttatgtgc atgttgtaga cggttgtaat tcatcaactt gtatgatgtg 7501 ttacaaacgt aatagagcaa caagagtcga atgtacaact attgttaatg gtgttagaag 7561 gtccttttat gtctatgcta atggaggtaa aggcttttgc aaactacaca attggaattg 7621 tgttaattgt gatacattct gtgctggtag tacatttatt agtgatgaag ttgcgagaga 7681 cttgtcacta cagtttaaaa gaccaataaa tcctactgac cagtcttctt acatcgttga 7741 tagtgttaca gtgaagaatg gttccatcca tctttacttt gataaagctg gtcaaaagac 7801 ttatgaaaga cattctctct ctcattttgt taacttagac aacctgagag ctaataacac 7861 taaaggttca ttgcctatta atgttatagt ttttgatggt aaatcaaaat gtgaagaatc 7921 atctgcaaaa tcagcgtctg tttactacag tcagcttatg tgtcaaccta tactgttact 7981 agatcaggca ttagtgtctg atgttggtga tagtgcggaa gttgcagtta aaatgtttga 8041 tgcttacgtt aatacgtttt catcaacttt taacgtacca atggaaaaac tcaaaacact 8101 agttgcaact gcagaagctg aacttgcaaa gaatgtgtcc ttagacaatg tcttatctac 8161 ttttatttca gcagctcggc aagggtttgt tgattcagat gtagaaacta aagatgttgt 8221 tgaatgtctt aaattgtcac atcaatctga catagaagtt actggcgata gttgtaataa 8281 ctatatgctc acctataaca aagttgaaaa catgacaccc cgtgaccttg gtgcttgtat 8341 tgactgtagt gcgcgtcata ttaatgcgca ggtagcaaaa agtcacaaca ttgctttgat 8401 atggaacgtt aaagatttca tgtcattgtc tgaacaacta cgaaaacaaa tacgtagtgc 8461 tgctaaaaag aataacttac cttttaagtt gacatgtgca actactagac aagttgttaa 8521 tgttgtaaca acaaagatag cacttaaggg tggtaaaatt gttaataatt ggttgaagca 8581 gttaattaaa gttacacttg tgttcctttt tgttgctgct attttctatt taataacacc 8641 tgttcatgtc atgtctaaac atactgactt ttcaagtgaa atcataggat acaaggctat 8701 tgatggtggt gtcactcgtg acatagcatc tacagatact tgttttgcta acaaacatgc 8761 tgattttgac acatggttta gccagcgtgg tggtagttat actaatgaca aagcttgccc 8821 attgattgct gcagtcataa caagagaagt gggttttgtc gtgcctggtt tgcctggcac 8881 gatattacgc acaactaatg gtgacttttt gcatttctta cctagagttt ttagtgcagt 8941 tggtaacatc tgttacacac catcaaaact

Sequence Description	SEQ ID NO.	Sequence
		tatagagtac actgactttg caacatcagc 9001 ttgtgttttg gctgctgaat gtacaatttt taaagatgct tctggtaagc cagtaccata 9061 ttgttatgat accaatgtac tagaaggttc tgttgcttat gaaagtttac gccctgacac 9121 acgttatgtg ctcatggatg gctctattat tcaatttcct aacacctacc ttgaaggttc 9181 tgttagagtg gtaacaactt ttgattctga gtactgtagg cacggcactt gtgaaagatc 9241 agaagctggt gtttgtgtat ctactagtgg tagatgggta cttaacaatg attattacag 9301 atctttacca ggagttttct gtggtgtaga tgctgtaaat ttacttacta atatgtttac 9361 accactaatt caacctattg gtgctttgga catatcagca tctatagtag ctggtggtat 9421 tgtagctatc gtagtaacat gccttgccta ctattttatg aggtttagaa gagcttttgg 9481 tgaatacagt catgtagttg cctttaatac tttactattc cttatgtcat tcactgtact 9541 ctgtttaaca ccagtttact cattcttacc tggtgtttat tctgttattt acttgtactt 9601 gacattttat cttactaatg atgtttcttt tttagcacat attcagtgga tggttatgtt 9661 cacaccttta gtacctttct ggataacaat tgcttatatc atttgtattt ccacaaagca 9721 tttctattgg ttctttagta attacctaaa gagacgtgta gtctttaatg gtgtttcctt 9781 tagtactttt gaagaagctg cgctgtgcac ctttttgtta aataaagaaa tgtatctaaa 9841 gttgcgtagt gatgtgctat tacctcttac gcaatataat agatacttag ctctttataa 9901 taagtacaag tattttagtg gagcaatgga tacaactagc tacagagaag ctgcttgttg 9961 tcatctcgca aaggctctca atgacttcag taactcaggt tctgatgttc tttaccaacc 10021 accacaaacc tctatcacct cagctgtttt gcagagtggt tttagaaaaa tggcattccc 10081 atctggtaaa gttgagggtt gtatggtaca agtaacttgt ggtacaacta cacttaacgg 10141 tctttggctt gatgacgtag tttactgtcc aagacatgtg atctgcacct ctgaagacat 10201 gcttaaccct aattatgaag atttactcat tcgtaagtct aatcataatt tcttggtaca 10261 ggctggtaat gttcaactca gggttattgg acattctatg caaaattgtg tacttaagct 10321 taaggttgat acagccaatc ctaagacacc taagtataag tttgttcgca ttcaaccagg 10381 acagactttt tcagtgttag cttgttacaa tggttcacca tctggtgttt accaatgtgc 10441 tatgaggccc aatttcacta ttaagggttc attccttaat ggttcatgtg gtagtgttgg 10501 ttttaacata gattatgact gtgtctcttt ttgttacatg caccatatgg aattaccaac 10561 tggagttcat gctggcacag acttagaagg taacttttat ggacctttg ttgacaggca 10621 aacagcacaa gcagctggta cggacacaac tattacagtt aatgttttag cttggttgta 10681 cgctgctgtt ataaatggag acaggtggtt tctcaatcga tttaccacaa ctcttaatga 10741 ctttaacctt gtggctatga agtacaatta tgaacctcta acacaagacc atgttgacat 10801 actaggacct ctttctgctc aaactggaat tgccgtttta gatatgtgtg cttcattaaa 10861

Sequence Description	SEQ ID NO.	Sequence
		agaattactg caaaatggta tgaatggacg taccatattg ggtagtgctt tattagaaga 10921 tgaatttaca ccttttgatg ttgttagaca atgctcaggt gttactttcc aaagtgcagt 10981 gaaaagaaca atcaagggta cacaccactg gttgttactc acaattttga cttcactttt 11041 agttttagtc cagagtactc aatggtcttt gttcttttt ttgtatgaaa atgccttttt 11101 acctttgct atgggtatta ttgctatgtc tgcttttgca atgatgtttg tcaaacataa 11161 gcatgcattt ctctgtttgt ttttgttacc ttctcttgcc actgtagctt attttaatat 11221 ggtctatatg cctgctagtt gggtgatgcg tattatgaca tggttggata tggttgatac 11281 tagtttgtct ggttttaagc taaaagactg tgttatgtat gcatcagctg tagtgttact 11341 aatccttatg acagcaagaa ctgtgtatga tgatggtgct aggagagtgt ggacacttat 11401 gaatgtcttg acactcgttt ataaagttta ttatggtaat gctttagatc aagccatttc 11461 catgtgggct cttataatct ctgttacttc taactactca ggtgtagtta caactgtcat 11521 gtttttggcc agaggtattg tttttatgtg tgttgagtat tgccctattt tcttcataac 11581 tggtaataca cttcagtgta taatgctagt ttattgtttc ttaggctatt tttgtacttg 11641 ttactttggc ctcttttgtt tactcaaccg ctactttaga ctgactcttg gtgtttatga 11701 ttacttagtt tctacacagg agtttagata tatgaattca cagggactac tcccacccaa 11761 gaatagcata gatgccttca aactcaacat taaattgttg ggtgttggtg gcaaaccttg 11821 tatcaaagta gccactgtac agtctaaaat gtcagatgta aagtgcacat cagtagtctt 11881 actctcagtt ttgcaacaac tcagagtaga atcatcatct aaattgtggg ctcaatgtgt 11941 ccagttacac aatgacattc tcttagctaa agatactact gaagcctttg aaaaaatggt 12001 ttcactactt tctgttttgc tttccatgca gggtgctgta gacataaaca agctttgtga 12061 agaaatgctg gacaacaggg caaccttaca agctatagcc tcagagttta gttcccttcc 12121 atcatatgca gcttttgcta ctgctcaaga agcttatgag caggctgttg ctaatggtga 12181 ttctgaagtt gttcttaaaa agttgaagaa gtctttgaat gtggctaaat ctgaatttga 12241 ccgtgatgca gccatgcaac gtaagttgga aaagatggct gatcaagcta tgacccaaat 12301 gtataaacag gctagatctg aggacaagag ggcaaaagtt actagtgcta tgcagacaat 12361 gcttttcact atgcttagaa agttggataa tgatgcactc aacaacatta tcaacaatgc 12421 aagagatggt tgtgttccct tgaacataat acctcttaca acagcagcca aactaatggt 12481 tgtcatacca gactataaca catataaaaa tacgtgtgat ggtacaacat ttacttatgc 12541 atcagcattg tgggaaatcc aacaggttgt agatgcagat agtaaaattg ttcaacttag 12601 tgaaattagt atggacaatt cacctaattt agcatggcct cttattgtaa cagctttaag 12661 ggccaattct gctgtcaaat tacagaataa tgagcttagt cctgttgcac tacgacagat 12721 gtcttgtgct

Sequence Description	SEQ ID NO.	Sequence
		gccggtacta cacaaactgc ttgcactgat gacaatgcgt tagcttacta 12781 caacacaaca aagggaggta ggtttgtact tgcactgtta tccgatttac aggatttgaa 12841 atgggctaga ttccctaaga gtgatggaac tggtactatc tatacagaac tggaaccacc 12901 ttgtaggttt gttacagaca cacctaaagg tcctaaagtg aagtatttat actttattaa 12961 aggattaaac aacctaaata gaggtatggt acttggtagt ttagctgcca cagtacgtct 13021 acaagctggt aatgcaacag aagtgcctgc caattcaact gtattatctt tctgtgcttt 13081 tgctgtagat gctgctaaag cttacaaaga ttatctagct agtgggggac aaccaatcac 13141 taattgtgtt aagatgttgt gtacacacac tggtactggt caggcaataa cagttacacc 13201 ggaagccaat atggatcaag aatcctttgg tggtgcatcg tgttgtctgt actgccgttg 13261 ccacatagat catccaaatc ctaaaggatt ttgtgactta aaaggtaagt atgtacaaat 13321 acctacaact tgtgctaatg accctgtggg ttttacactt aaaaacacag tctgtaccgt 13381 ctgcggtatg tggaaaggtt atggctgtag ttgtgatcaa ctccgcgaac ccatgcttca 13441 gtcagctgat gcacaatcgt ttttaaacgg gtttgcggtg taagtgcagc ccgtcttaca 13501 ccgtgcggca caggcactag tactgatgtc gtatacaggg cttttgacat ctacaatgat 13561 aaagtagctg gttttgctaa attcctaaaa actaattgtt gtcgcttcca agaaaaggac 13621 gaagatgaca atttaattga ttcttacttt gtagttaaga gacacacttt ctctaactac 13681 caacatgaag aaacaattta taatttactt aaggattgtc cagctgttgc taaacatgac 13741 ttctttaagt ttagaataga cggtgacatg gtaccacata tatcacgtca acgtcttact 13801 aaatacacaa tggcagacct cgtctatgct ttaaggcatt ttgatgaagg taattgtgac 13861 acattaaaag aaatacttgt cacatacaat tgttgtgatg atgattattt caataaaaag 13921 gactggtatg attttgtaga aaacccagat atattacgcg tatacgccaa cttaggtgaa 13981 cgtgtacgcc aagctttgtt aaaaacagta caattctgtg atgccatgcg aaatgctggt 14041 attgttggtg tactgacatt agataatcaa gatctcaatg gtaactggta tgatttcggt 14101 gatttcatac aaaccacgcc aggtagtgga gttcctgttg tagattctta ttattcattg 14161 ttaatgccta tattaacctt gaccagggct ttaactgcag agtcacatgt tgacactgac 14221 ttaacaaagc cttacattaa gtgggatttg ttaaaatatg acttcacgga agagaggtta 14281 aaactctttg accgttattt taaatattgg gatcagacat accacccaaa ttgtgttaac 14341 tgtttggatg acagatgcat tctgcattgt gcaaacttta atgttttatt ctctacagtg 14401 ttcccaccta caagttttgg accactagtg agaaaaatat ttgttgatgg tgttccattt 14461 gtagtttcaa ctggatacca cttcagagag ctaggtgttg tacataatca ggatgtaaac 14521 ttacatagct ctagacttag ttttaaggaa ttacttgtgt atgctgctga ccctgctatg 14581 cacgctgctt ctggtaatct		

Sequence Description	SEQ ID NO.	Sequence
		attactagat aaacgcacta cgtgcttttc agtagctgca 14641 cttactaaca atgttgcttt tcaaactgtc aaacccggta attttaacaa agacttctat 14701 gactttgctg tgtctaaggg tttctttaag gaaggaagtt ctgttgaatt aaaacacttc 14761 ttctttgctc aggatggtaa tgctgctatc agcgattatg actactatcg ttataatcta 14821 ccaacaatgt gtgatatcag acaactacta tttgtagttg aagttgttga taagtacttt 14881 gattgttacg atggtggctg tattaatgct aaccaagtca tcgtcaacaa cctagacaaa 14941 tcagctggtt ttccatttaa taaatggggt aaggctagac tttattatga ttcaatgagt 15001 tatgaggatc aagatgcact tttcgcatat acaaaacgta atgtcatccc tactataact 15061 caaatgaatc ttaagtatgc cattagtgca aagaatagag ctcgcaccgt agctggtgtc 15121 tctatctgta gtactatgac caatagacag tttcatcaaa aattattgaa atcaatagcc 15181 gccactagag gagctactgt agtaattgga acaagcaaat tctatggtgg ttggcacaac 15241 atgttaaaaa ctgtttatag tgatgtagaa aaccctcacc ttatgggttg ggattatcct 15301 aaatgtgata gagccatgcc taacatgctt agaattatgg cctcacttgt tcttgctcgc 15361 aaacatacaa cgtgttgtag cttgtcacac cgtttctata gattagctaa tgagtgtgct 15421 caagtattga gtgaaatggt catgtgtggc ggttcactat atgttaaacc aggtggaacc 15481 tcatcaggag atgccacaac tgcttatgct aatagtgttt ttaacatttg tcaagctgtc 15541 acggccaatg ttaatgcact tttatctact gatggtaaca aaattgccga taagtatgtc 15601 cgcaatttac aacacagact ttatgagtgt ctctatagaa atagagatgt tgacacagac 15661 tttgtgaatg agttttacgc atatttgcgt aaacatttct caatgatgat actctctgac 15721 gatgctgttg tgtgtttcaa tagcacttat gcatctcaag gtctagtggc tagcataaag 15781 aactttaagt cagttcttta ttatcaaaac aatgttttta tgtctgaagc aaaatgttgg 15841 actgagactg accttactaa aggacctcat gaattttgct ctcaacatac aatgctagtt 15901 aaacagggtg atgattatgt gtaccttcct tacccagatc catcaagaat cctaggggcc 15961 ggctgttttg tagatgatat cgtaaaaaca gatggtacac ttatgattga acggttcgtg 16021 tctttagcta tagatgctta cccacttact aaacatccta atcaggagta tgctgatgtc 16081 tttcatttgt acttacaata cataagaaag ctacatgatg agttaacagg acacatgtta 16141 gacatgtatt ctgttatgct tactaatgat aacacttcaa ggtattggga acctgagttt 16201 tatgaggcta tgtacacacc gcatacagtc ttacaggctg ttggggcttg tgttctttgc 16261 aattcacaga cttcattaag atgtggtgct tgcatacgta gaccattctt atgttgtaaa 16321 tgctgttacg accatgtcat atcaacatca cataaattag tcttgtctgt taatccgtat 16381 gtttgcaatg ctccaggttg tgatgtcaca gatgtgactc aactttactt aggaggtatg 16441 agctattatt gtaaatcaca taaaccaccc

Sequence Description	SEQ ID NO.	Sequence
		attagttttc cattgtgtgc taatggacaa 16501 gtttttggtt tatataaaaa tacatgtgtt ggtagcgata atgttactga ctttaatgca 16561 attgcaacat gtgactggac aaatgctggt gattacattt tagctaacac ctgtactgaa 16621 agactcaagc tttttgcagc agaaacgctc aaagctactg aggagacatt taaactgtct 16681 tatggtattg ctactgtacg tgaagtgctg tctgacagag aattacatct ttcatgggaa 16741 gttggtaaac ctagaccacc acttaaccga aattatgtct ttactggtta tcgtgtaact 16801 aaaaacagta aagtacaaat aggagagtac acctttgaaa aaggtgacta tggtgatgct 16861 gttgtttacc gaggtacaac aacttacaaa ttaaatgttg gtgattattt tgtgctgaca 16921 tcacatacag taatgccatt aagtgcacct acactagtgc cacaagagca ctatgttaga 16981 attactggct tatacccaac actcaatatc tcagatgagt tttctagcaa tgttgcaaat 17041 tatcaaaagg ttggtatgca aaagtattct acactccagg gaccacctgg tactggtaag 17101 agtcattttg ctattggcct agctctctac tacccttctg ctcgcatagt gtatacagct 17161 tgctctcatg ccgctgttga tgcactatgt gagaaggcat taaaatattt gcctatagat 17221 aaatgtagta gaattatacc tgcacgtgct cgtgtagagt gttttgataa attcaaagtg 17281 aattcaacat tagaacagta tgtcttttgt actgtaaatg cattgcctga gacgacagca 17341 gatatagttg tctttgatga aatttcaatg gccacaaatt atgatttgag tgttgtcaat 17401 gccagattac gtgctaagca ctatgtgtac attggcgacc ctgctcaatt acctgcacca 17461 cgcacattgc taactaaggg cacactagaa ccagaatatt tcaattcagt gtgtagactt 17521 atgaaaacta taggtccaga catgttcctc ggaacttgtc ggcgttgtcc tgctgaaatt 17581 gttgacactg tgagtgcttt ggtttatgat aataagctta aagcacataa agacaaatca 17641 gctcaatgct ttaaaatgtt ttataagggt gttatcacgc atgatgtttc atctgcaatt 17701 aacaggccac aaataggcgt ggtaagagaa ttccttacac gtaaccctgc ttggagaaaa 17761 gctgtcttta tttcacctta taattcacag aatgctgtag cctcaaagat tttgggacta 17821 ccaactcaaa ctgttgattc atcacagggc tcagaatatg actatgtcat attcactcaa 17881 accactgaaa cagctcactc ttgtaatgta aacagattta atgttgctat taccagagca 17941 aaagtaggca tactttgcat aatgtctgat agagaccttt atgacaagtt gcaatttaca 18001 agtcttgaaa ttccacgtag gaatgtggca actttacaag ctgaaaatgt aacaggactc 18061 tttaaagatt gtagtaaggt aatcactggg ttacatccta cacaggcacc tacacacctc 18121 agtgttgaca ctaaattcaa aactgaaggt ttatgtgttg acatacctgg catacctaag 18181 gacatgacct atagaagact catctctatg atgggtttta aaatgaatta tcaagttaat 18241 ggttacccta acatgtttat cacccgcgaa gaagctataa gacatgtacg tgcatggatt 18301 ggcttcgatg tcgaggggtg

Sequence Description	SEQ ID NO.	Sequence
		tcatgctact agagaagctg ttggtaccaa tttaccttta 18361 cagctaggtt tttctacagg tgttaaccta gttgctgtac ctacaggtta tgttgataca 18421 cctaataata cagatttttc cagagttagt gctaaaccac cgcctggaga tcaatttaaa 18481 cacctcatac cacttatgta caaaggactt ccttggaatg tagtgcgtat aaagattgta 18541 caaatgttaa gtgacacact taaaaatctc tctgacagag tcgtatttgt cttatgggca 18601 catggctttg agttgacatc tatgaagtat tttgtgaaaa taggacctga gcgcacctgt 18661 tgtctatgtg atagacgtgc cacatgcttt tccactgctt cagacactta tgcctgttgg 18721 catcattcta ttggatttga ttacgtctat aatccgttta tgattgatgt tcaacaatgg 18781 ggttttacag gtaacctaca aagcaaccat gatctgtatt gtcaagtcca tggtaatgca 18841 catgtagcta gttgtgatgc aatcatgact aggtgtctag ctgtccacga gtgctttgtt 18901 aagcgtgttg actggactat tgaatatcct ataattggtg atgaactgaa gattaatgcg 18961 gcttgtagaa aggttcaaca catggttgtt aaagctgcat tattagcaga caaattccca 19021 gttcttcacg acattggtaa ccctaaagct attaagtgtg tacctcaagc tgatgtagaa 19081 tggaagttct atgatgcaca gccttgtagt gacaaagctt ataaaataga agaattattc 19141 tattcttatg ccacacattc tgacaaattc acagatggtg tatgcctatt ttggaattgc 19201 aatgtcgata gatatcctgc taattccatt gtttgtagat ttgacactag agtgctatct 19261 aaccttaact tgcctggttg tgatggtggc agtttgtatg taaataaaca tgcattccac 19321 acaccagctt ttgataaaag tgcttttgtt aatttaaaac aattaccatt tttctattac 19381 tctgacagtc catgtgagtc tcatggaaaa caagtagtgt cagatataga ttatgtacca 19441 ctaaagtctg ctacgtgtat aacacgttgc aatttaggtg gtgctgtctg tagacatcat 19501 gctaatgagt acagattgta tctcgatgct tataacatga tgatctcagc tggctttagc 19561 ttgtgggttt acaaacaatt tgatacttat aacctctgga acacttttac aagacttcag 19621 agtttagaaa atgtggcttt taatgttgta aataagggac actttgatgg acaacagggt 19681 gaagtaccag tttctatcat taataacact gtttacacaa aagttgatgg tgttgatgta 19741 gaattgtttg aaaataaaac aacattacct gttaatgtag catttgagct ttgggctaag 19801 cgcaacatta aaccagtacc agaggtgaaa atactcaata atttgggtgt ggacattgct 19861 gctaatactg tgatctggga ctacaaaaga gatgctccag cacatatatc tactattggt 19921 gtttgttcta tgactgacat agccaagaaa ccaactgaaa cgatttgtgc accactcact 19981 gtctttttg atggtagagt tgatggtcaa gtagacttat ttagaaatgc ccgtaatggt 20041 gttcttatta cagaaggtag tgttaaaggt ttacaaccat ctgtaggtcc caaacaagct 20101 agtcttaatg gagtcacatt aattggagaa gccgtaaaaa cacagttcaa ttattataag 20161 aaagttgatg gtgttgtcca acaattacct

Sequence Description	SEQ ID NO.	Sequence
		gaaacttact ttactcagag tagaaattta 20221 caagaattta aacccaggag tcaaatggaa attgatttct tagaattagc tatggatgaa 20281 ttcattgaac ggtataaatt agaaggctat gccttcgaac atatcgttta tggagatttt 20341 agtcatagtc agttaggtgg tttacatcta ctgattggac tagctaaacg ttttaaggaa 20401 tcacctttg aattagaaga ttttattcct atggacagta cagttaaaaa ctatttcata 20461 acagatgcgc aaacaggttc atctaagtgt gtgtgttctg ttattgattt attacttgat 20521 gattttgttg aaataataaa atcccaagat ttatctgtag tttctaaggt tgtcaaagtg 20581 actattgact atacagaaat ttcatttatg ctttggtgta aagatggcca tgtagaaaca 20641 ttttacccaa aattacaatc tagtcaagcg tggcaaccgg gtgttgctat gcctaatctt 20701 tacaaaatgc aaagaatgct attagaaaag tgtgaccttc aaaattatgg tgatagtgca 20761 acattaccta aaggcataat gatgaatgtc gcaaaatata ctcaactgtg tcaatattta 20821 aacacattaa cattagctgt accctataat atgagagtta tacattttgg tgctggttct 20881 gataaaggag ttgcaccagg tacagctgtt ttaagacagt ggttgcctac gggtacgctg 20941 cttgtcgatt cagatcttaa tgactttgtc tctgatgcag attcaacttt gattggtgat 21001 tgtgcaactg tacatacagc taataaatgg gatctcatta ttagtgatat gtacgaccct 21061 aagactaaaa atgttacaaa agaaaatgac tctaaagagg gttttttcac ttacatttgt 21121 gggtttatac aacaaaagct agctcttgga ggttccgtgg ctataaagat aacagaacat 21181 tcttggaatg ctgatcttta taagctcatg ggacacttcg catggtggac agcctttgtt 21241 actaatgtga atgcgtcatc atctgaagca tttttaattg gatgtaatta tcttggcaaa 21301 ccacgcgaac aaatagatgg ttatgtcatg catgcaaatt acatattttg gaggaataca 21361 aatccaattc agttgtcttc ctattcttta tttgacatga gtaaatttcc ccttaaatta 21421 aggggtactg ctgttatgtc tttaaaagaa ggtcaaatca atgatatgat tttatctctt 21481 cttagtaaag gtagacttat aattagagaa aacaacagag ttgttatttc tagtgatgtt 21541 cttgttaaca actaaacgaa caatgtttgt ttttcttgtt ttattgccac tagtctctag 21601 tcagtgtgtt aatcttacaa ccagaactca attacccccct gcatacacta attctttcac 21661 acgtggtgtt tattaccctg acaaagtttt cagatcctca gttttacatt caactcagga 21721 cttgttctta cctttctttt ccaatgttac ttggttccat gctatacatg tctctgggac 21781 caatggtact aagaggtttg ataaccctgt cctaccattt aatgatggtg tttattttgc 21841 ttccactgag aagtctaaca taataagagg ctggattttt ggtactactt tagattcgaa 21901 gacccagtcc ctacttattg ttaataacgc tactaatgtt gttattaaag tctgtgaatt 21961 tcaattttgt aatgatccat ttttgggtgt ttattaccac aaaaacaaca aaagttggat 22021 ggaaagtgag

Sequence Description	SEQ ID NO.	Sequence
		ttcagagttt attctagtgc gaataattgc acttttgaat atgtctctca 22081 gccttttctt atggaccttg aaggaaaaca gggtaatttc aaaaatctta gggaatttgt 22141 gtttaagaat attgatggtt attttaaaat atattctaag cacacgccta ttaatttagt 22201 gcgtgatctc cctcagggtt tttcggcttt agaaccattg gtagatttgc caataggtat 22261 taacatcact aggtttcaaa ctttacttgc tttacataga agttatttga ctcctggtga 22321 ttcttcttca ggttggacag ctggtgctgc agcttattat gtgggttatc ttcaacctag 22381 gacttttcta ttaaaatata atgaaaatgg aaccattaca gatgctgtag actgtgcact 22441 tgaccctctc tcagaaacaa agtgtacgtt gaaatccttc actgtagaaa aaggaatcta 22501 tcaaacttct aactttagag tccaaccaac agaatctatt gttagatttc ctaatattac 22561 aaacttgtgc ccttttggtg aagtttttaa cgccaccaga tttgcatctg tttatgcttg 22621 gaacaggaag agaatcagca actgtgttgc tgattattct gtcctatata attccgcatc 22681 attttccact tttaagtgtt atggagtgtc tcctactaaa ttaaatgatc tctgctttac 22741 taatgtctat gcagattcat ttgtaattag aggtgatgaa gtcagacaaa tcgctccagg 22801 gcaaactgga aagattgctg attataatta taaattacca gatgatttta caggctgcgt 22861 tatagcttgg aattctaaca atcttgattc taaggttggt ggtaattata attacctgta 22921 tagattgttt aggaagtcta atctcaaacc ttttgagaga gatatttcaa ctgaaatcta 22981 tcaggccggt agcacacctt gtaatggtgt tgaaggtttt aattgttact ttcctttaca 23041 atcatatggt ttccaaccca ctaatggtgt tggttaccaa ccatacagag tagtagtact 23101 ttcttttgaa cttctacatg caccagcaac tgtttgtgga cctaaaaagt ctactaattt 23161 ggttaaaaac aaatgtgtca atttcaactt caatggttta acaggcacag gtgttcttac 23221 tgagtctaac aaaaagtttc tgcctttcca acaatttggc agagacattg ctgacactac 23281 tgatgctgtc cgtgatccac agacacttga gattcttgac attacaccat gttcttttgg 23341 tggtgtcagt gttataacac caggaacaaa tacttctaac caggttgctg ttctttatca 23401 ggatgttaac tgcacagaag tccctgttgc tattcatgca gatcaactta ctcctacttg 23461 gcgtgtttat tctacaggtt ctaatgtttt tcaaacacgt gcaggctgtt taataggggc 23521 tgaacatgtc aacaactcat atgagtgtga catacccatt ggtgcaggta tatgcgctag 23581 ttatcagact cagactaatt ctcctcggcg ggcacgtagt gtagctagtc aatccatcat 23641 tgcctacact atgtcacttg gtgcagaaaa ttcagttgct tactctaata actctattgc 23701 catacccaca aattttacta ttagtgttac cacagaaatt ctaccagtgt ctatgaccaa 23761 gacatcagta gattgtacaa tgtacatttg tggtgattca actgaatgca gcaatctttt 23821 gttgcaatat ggcagttttt gtacacaatt aaaccgtgct ttaactggaa tagctgttga 23881 acaagacaaa aacacccaag

Sequence Description	SEQ ID NO.	Sequence
		aagtttttgc acaagtcaaa caaatttaca aaacaccacc 23941 aattaaagat tttggtggtt ttaatttttc acaaatatta ccagatccat caaaaccaag 24001 caagaggtca tttattgaag atctactttt caacaaagtg acacttgcag atgctggctt 24061 catcaaacaa tatggtgatt gccttggtga tattgctgct agagacctca tttgtgcaca 24121 aaagtttaac ggccttactg ttttgccacc tttgctcaca gatgaaatga ttgctcaata 24181 cacttctgca ctgttagcgg gtacaatcac ttctggttgg acctttggtg caggtgctgc 24241 attacaaata ccatttgcta tgcaaatggc ttataggttt aatggtattg gagttacaca 24301 gaatgttctc tatgagaacc aaaaattgat tgccaaccaa tttaatagtg ctattggcaa 24361 aattcaagac tcactttctt ccacagcaag tgcacttgga aaacttcaag atgtggtcaa 24421 ccaaaatgca caagctttaa acacgcttgt taaacaactt agctccaatt ttggtgcaat 24481 ttcaagtgtt ttaaatgata tcctttcacg tcttgacaaa gttgaggctg aagtgcaaat 24541 tgataggttg atcacaggca gacttcaaag tttgcagaca tatgtgactc aacaattaat 24601 tagagctgca gaaatcagag cttctgctaa tcttgctgct actaaaatgt cagagtgtgt 24661 acttggacaa tcaaaaagag ttgatttttg tggaaagggc tatcatctta tgtccttccc 24721 tcagtcagca cctcatggtg tagtcttctt gcatgtgact tatgtccctg cacaagaaaa 24781 gaacttcaca actgctcctg ccatttgtca tgatggaaaa gcacactttc ctcgtgaagg 24841 tgtctttgtt tcaaatggca cacactggtt tgtaacacaa aggaattttt atgaaccaca 24901 aatcattact acagacaaca catttgtgtc tggtaactgt gatgttgtaa taggaattgt 24961 caacaacaca gtttatgatc ctttgcaacc tgaattagac tcattcaagg aggagttaga 25021 taaatatttt aagaatcata catcaccaga tgttgattta ggtgacatct ctggcattaa 25081 tgcttcagtt gtaaacattc aaaaagaaat tgaccgcctc aatgaggttg ccaagaattt 25141 aaatgaatct ctcatcgatc tccaagaact tggaaagtat gagcagtata taaaatggcc 25201 atggtacatt tggctaggtt ttatagctgg cttgattgcc atagtaatgg tgacaattat 25261 gctttgctgt atgaccagtt gctgtagttg tctcaagggc tgttgttctt gtggatcctg 25321 ctgcaaattt gatgaagacg actctgagcc agtgctcaaa ggagtcaaat tacattacac 25381 ataaacgaac ttatggattt gtttatgaga atcttcacaa ttggaactgt aactttgaag 25441 caaggtgaaa tcaaggatgc tactccttca gattttgttc gcgctactgc aacgataccg 25501 atacaagcct cactcccttt cggatggctt attgttggcg ttgcacttct tgctgttttt 25561 cagagcgctt ccaaaatcat aaccctcaaa aagagatggc aactagcact ctccaagggt 25621 gttcactttg tttgcaactt gctgttgttg tttgtaacag tttactcaca ccttttgctc 25681 gttgctgctg gccttgaagc ccctttctc tatctttatg ctttagtcta cttcttgcag 25741 agtataaact ttgtaagaat aataatgagg ctttggcttt gctggaaatg

Sequence Description	SEQ ID NO.	Sequence
		ccgttccaaa 25801 aacccattac tttatgatgc caactatttt ctttgctggc atactaattg ttacgactat 25861 tgtatacctt acaatagtgt aacttcttca attgtcatta cttcaggtga tggcacaaca 25921 agtcctattt ctgaacatga ctaccagatt ggtggttata ctgaaaaatg ggaatctgga 25981 gtaaaagact gtgttgtatt acacagttac ttcacttcag actattacca gctgtactca 26041 actcaattga gtacagacac tggtgttgaa catgttacct tcttcatcta caataaaatt 26101 gttgatgagc ctgaagaaca tgtccaaatt cacacaatcg acggttcatc cggagttgtt 26161 aatccagtaa tggaaccaat ttatgatgaa ccgacgacga ctactagcgt gcctttgtaa 26221 gcacaagctg atgagtacga acttatgtac tcattcgttt cggaagagac aggtacgtta 26281 atagttaata gcgtacttct ttttcttgct ttcgtggtat tcttgctagt tacactagcc 26341 atccttactg cgcttcgatt gtgtgcgtac tgctgcaata ttgttaacgt gagtcttgta 26401 aaaccttctt tttacgttta ctctcgtgtt aaaaatctga attcttctag agttcctgat 26461 cttctggtct aaacgaacta aatattatat tagtttttct gtttggaact ttaattttag 26521 ccatggcaga ttccaacggt actattaccg ttgaagagct taaaaagctc cttgaacaat 26581 ggaacctagt aataggtttc ctattcctta catggatttg tcttctacaa tttgcctatg 26641 ccaacaggaa taggtttttg tatataatta agttaatttt cctctggctg ttatggccag 26701 taactttagc ttgttttgtg cttgctgctg tttacagaat aaattggatc accggtggaa 26761 ttgctatcgc aatggcttgt cttgtaggct tgatgtggct cagctacttc attgcttctt 26821 tcagactgtt tgcgcgtacg cgttccatgt ggtcattcaa tccagaaact aacattcttc 26881 tcaacgtgcc actccatggc actattctga ccagaccgct tctagaaagt gaactcgtaa 26941 tcggagctgt gatccttcgt ggacatcttc gtattgctgg acaccatcta ggacgctgtg 27001 acatcaagga cctgcctaaa gaaatcactg ttgctacatc acgaacgctt tcttattaca 27061 aattgggagc ttcgcagcgt gtagcaggtg actcaggttt tgctgcatac agtcgctaca 27121 ggattggcaa ctataaatta aacacagacc attccagtag cagtgacaat attgctttgc 27181 ttgtacagta agtgacaaca gatgtttcat ctcgttgact ttcaggttac tatagcagag 27241 atattactaa ttattatgag gacttttaaa gtttccattt ggaatcttga ttacatcata 27301 aacctcataa ttaaaaattt atctaagtca ctaactgaga ataaatattc tcaattagat 27361 gaagagcaac caatggagat tgattaaacg aacatgaaaa ttattctttt cttggcactg 27421 ataacactcg ctacttgtga gctttatcac taccaagagt gtgttagagg tacaacagta 27481 cttttaaaag aaccttgctc ttctggaaca tacgagggca attcaccatt tcatcctcta 27541 gctgataaca aatttgcact gacttgcttt agcactcaat ttgcttttgc ttgtcctgac 27601 ggcgtaaaac acgtctatca gttacgtgcc agatcagttt cacctaaact gttcatcaga

Sequence Description	SEQ ID NO.	Sequence
		27661 caagaggaag ttcaagaact ttactctcca atttttctta ttgttgcggc aatagtgttt 27721 ataacacttt gcttcacact caaaagaaag acagaatgat tgaactttca ttaattgact 27781 tctatttgtg ctttttagcc tttctgctat tccttgtttt aattatgctt attatctttt 27841 ggttctcact tgaactgcaa gatcataatg aaacttgtca cgcctaaacg aacatgaaat 27901 ttcttgtttt cttaggaatc atcacaactg tagctgcatt tcaccaagaa tgtagtttac 27961 agtcatgtac tcaacatcaa ccatatgtag ttgatgaccc gtgtcctatt cacttctatt 28021 ctaaatggta tattagagta ggagctagaa aatcagcacc tttaattgaa ttgtgcgtgg 28081 atgaggctgg ttctaaatca cccattcagt acatcgatat cggtaattat acagtttcct 28141 gtttaccttt tacaattaat tgccaggaac ctaaattggg tagtcttgta gtgcgttgtt 28201 cgttctatga agacttttta gagtatcatg acgttcgtgt tgttttagat ttcatctaaa 28261 cgaacaaact aaaatgtctg ataatggacc ccaaaatcag cgaaatgcac cccgcattac 28321 gtttggtgga ccctcagatt caactggcag taaccagaat ggagaacgca gtggggcgcg 28381 atcaaaacaa cgtcggcccc aaggtttacc caataatact gcgtcttggt tcaccgctct 28441 cactcaacat ggcaaggaag accttaaatt ccctcgagga caaggcgttc caattaacac 28501 caatagcagt ccagatgacc aaattggcta ctaccgaaga gctaccagac gaattcgtgg 28561 tggtgacggt aaaatgaaag atctcagtcc aagatggtat ttctactacc taggaactgg 28621 gccagaagct ggacttccct atggtgctaa caaagacggc atcatatggg ttgcaactga 28681 gggagccttg aatacaccaa aagatcacat tggcacccgc aatcctgcta acaatgctgc 28741 aatcgtgcta caacttcctc aaggaacaac attgccaaaa ggcttctacg cagaagggag 28801 cagaggcggc agtcaagcct cttctcgttc ctcatcacgt agtcgcaaca gttcaagaaa 28861 ttcaactcca ggcagcagta ggggaacttc tcctgctaga atggctggca atggcggtga 28921 tgctgctctt gctttgctgc tgcttgacag attgaaccag cttgagagca aaatgtctgg 28981 taaaggccaa caacaacaag gccaaactgt cactaagaaa tctgctgctg aggcttctaa 29041 gaagcctcgg caaaaacgta ctgccactaa agcatacaat gtaacacaag ctttcggcag 29101 acgtggtcca gaacaaaccc aaggaaattt tggggaccag gaactaatca gacaaggaac 29161 tgattacaaa cattggccgc aaattgcaca atttgccccc agcgcttcag cgttcttcgg 29221 aatgtcgcgc attggcatgg aagtcacacc ttcgggaacg tggttgacct acacaggtgc 29281 catcaaattg gatgacaaag atccaaattt caaagatcaa gtcattttgc tgaataagca 29341 tattgacgca tacaaaacat tcccaccaac agagcctaaa aaggacaaaa agaagaaggc 29401 tgatgaaact caagccttac cgcagagaca gaagaaacag caaactgtga ctcttcttcc 29461 tgctgcagat ttggatgatt tctccaaaca attgcaacaa tccatgagca gtgctgactc 29521 aactcaggcc taaactcatg cagaccacac

Sequence Description	SEQ ID NO.	Sequence
		aaggcagatg ggctatataa acgttttcgc 29581 ttttccgttt acgatatata gtctactctt gtgcagaatg aattctcgta actacatagc 29641 acaagtagat gtagttaact ttaatctcac atagcaatct ttaatcagtg tgtaacatta 29701 gggaggactt gaaagagcca ccacattttc accgaggcca cgcggagtac gatcgagtgt 29761 acagtgaaca atgctaggga gagctgccta tatggaagag ccctaatgtg taaaattaat 29821 tttagtagtg ctatccccat gtgattttaa tagcttctta ggagaatgac aaaaaaaaaa 29881 aaaaaaaaaa aaaaaaaaaa aaa
SARS-CoV-2 Wuhan seafood market pneumonia virus isolate Wuhan-Hu-1 genomic sequence (GenBank: MN908947.3; January 23, 2020) – amino acid translation	2	MESLVPGFNEKTHVQLSLPVLQVRDVLVRGFGDS VEEVLSEARQHLKDGTCGLVEVEKGVLPQLEQPY VFIKRSDARTAPHGHVMVELVAELEGIQYGRSGE TLGVLVPHVGEIPVAYRKVLLRKNGNKGAGGHS YGADLKSFDLGDELGTDPYEDFQEN WNTKHSSGVTRELMRELNGGAYTRYVDNNFCGP DGYPLECIKDLLARAGKASCTLSEQLDFIDTKRGV YCCREHEHEIAWYTERSEKSYELQTPFEIKLAKKF DTFNGECPNFVFPLNSIIKTIQPRVEKKKLDGFMG RIRSVYPVASPNECNQMCLSTLMKCDHCGETSWQ TGDFVKATCEFCGTENLTKEGATTCGYLPQNAVV KIYCPACHNSEVGPEHSLAEYHNESGLKTILRKGG RTIAFGGCVFSYVGCHNKCAYWVPRASANIGCNH TGVVGEGSEGLNDNL LEILQKEKVNINIVGDFKLNEEIAIILASFSASTSAF VETVKGLDYKAFKQIVESCGNFKVTKGKAKKGA WNIGEQKSILSPLYAFASEAARVVRSIFSRTLETAQ NSVRVLQKAAITILDGISQYSLRLIDAMMFTSDLA TNNLVVMAYITGGVVQLTSQWLTNIFGTVYEKLK PVLDWLEEKFKEGVEFLRDGWEIVKFISTCACEIV GGQIVTCAKEIKESVQTFFKLVNKFLALCADSIIIG GAKLKALNLGETFVTHSKGLYRKCVKSREETGLL MPLKAPKEIIFLEGETLPTEVLTEEVVLKTGDLQPL EQPTSEAVEAPLVGTPVCINGLMLLEIKDTEKYCA LAPNMMVTNNTFTLKGGAPTKVTFGDDTVIEVQ GYKSVNITFELDERIDKVLNEKCSAYTVELGTEVN EFACVVADAVIKTLQPVSELLTPLGIDLDEWSMA TYYLFDESGEFKLASHMYCSFYPPDEDEEEGDCE EEEFEPSTQYEYGTEDDYQGKPLEFGATSAALQPE EEQEEDWLDDDSQQTVGQQDGSEDNQTTTIQTIV EVQPQLEMELTPVVQTIEVNSFSGYLKLTDNVYIK NADIVEEAKKVKPTVVVNAANVYLKHGGGVAG ALNKATNNAMQVESDDYIATNGPLKVGGSCVLS GHNLAKHCLHVVGPNVNKGEDIQLLKSAYENFN QHEVLLAPLLSAGIFGADPIHSLRVCVDTVRTNVY

Sequence Description	SEQ ID NO.	Sequence
		LAVFDKNLYDKLVSSFLEMKSEKQVEQKIAEIPKE EVKPFITESKPSVEQRKQDDKKIKACVEEVTTTLE ETKFLTENLLLYIDINGNLHPDSATLVSDIDITFLK KDAPYIVGDVVQEGVLTAVVIPTKKAGGTTEMLA KALRKVPTDNYITTYPGQGLNGYTVEEAKTVLKK CKSAFYILPSIISNEKQEILGTVSWNLREMLAHAEE TRKLMPVCVETKAIVSTIQRKYKGIKIQEGVVDYG ARFYFYTSKTTVASLINTLNDLNETLVTMPLGYVT HGLNLEEAARYMRSLKVPATVSVSSPDAVTAYN GYLTSSSKTPEEHFIETISLAGSYKDWSYSGQSTQL GIEFLKRGDKSVYYTSNPTTFHLDGEVITFDNLKT LLSLREVRTIKVFTTVDNINLHTQVVDMSMTYGQ QFGPTYLDGADVTKIKPHNSHEGKTFYVLPNDDT LRVEAFEYYHTTDPSFLGRYMSALNHTKKWKYP QVNGLTSIKWADNNCYLATALLTLQQIELKFNPP ALQDAYYRARAGEAANFCALILAYCNKTVGELG DVRETMSYLFQHANLDSCKRVLNVVCKTCGQQQ TTLKGVEAVMYMGTLSYEQFKKGVQIPCTCGKQ ATKYLVQQESPFVMMSAPPAQYELKHGTFTCASE YTGNYQCGHYKHITSKETLYCIDGALLTKSSEYK GPITDVFYKENSYTTTIKPVTYKLDGVVCTEIDPK LDNYYKKDNSYFTEQPIDLVPNQPYPNASFDNFK FVCDNIKFADDLNQLTGYKKPASRELKVTFFPDL NGDVVAIDYKHYTPSFKKGAKLLHKPIVWHVNN ATNKATYKPNTWCIRCLWSTKPVETSNSFDVLKS EDAQGMDNLACEDLKPVSEEVVENPTIQKDVLEC NVKTTEVVGDIILKPANNSLKITEEVGHTDLMAA YVDNSSLTIKKPNELSRVLGLKTLATHGLAAVNS VPWDTIANYAKPFLNKVVSTTTNIVTRCLNRVCT NYMPYFFTLLLQLCTFTRSTNSRIKASMPTTIAKN TVKSVGKFCLEASFNYLKSPNFSKLINIIIWFLLLS VCLGSLIYSTAALGVLMSNLGMPSYCTGYREGYL NSTNVTIATYCTGSIPCSVCLSGLDSLDTYPSLETI QITISSFKWDLTAFGLVAEWFLAYILFTRFFYVLG LAAIMQLFFSYFAVHFISNSWLMWLIINLVQMAPI SAMVRMYIFFASFYYVWKSYVHVVDGCNSSTCM MCYKRNRATRVECTTIVNGVRRSFYVYANGGKG FCKLHNWNCVNCDTFCAGSTFISDEVARDLSLQF KRPINPTDQSSYIVDSVTVKNGSIHLYFDKAGQKT YERHSLSHFVNLDNLRANNTKGSLPINVIVFDGKS KCEESSAKSASVYYSQLMCQPILLLDQALVSDVG DSAEVAVKMFDAYVNTFSSTFNVPMEKLKTLVA TAEAELAKNVSLDNVLSTFISAARQGFVDSDVET KDVVECLKLSHQSDIEVTGDSCNNYMLTYNKVE NMTPRDLGACIDCSARHINAQVAKSHNIALIWNV

Sequence Description	SEQ ID NO.	Sequence
		KDFMSLSEQLRKQIRSAAKKNNLPFKLTCATTRQ VVNVVTTKIALKGGKIVNNWLKQLIKVTLVFLFV AAIFYLITPVHVMSKHTDFSSEIIGYKAIDGGVTRD IASTDTCFANKHADFDTWFSQRGGSYTNDKACPL IAAVITREVGFVVPGLPGTILRTTNGDFLHFLPRVF SAVGNICYTPSKLIEYTDFATSACVLAAECTIFKD ASGKPVPYCYDTNVLEGSVAYESLRPDTRYVLM DGSIIQFPNTYLEGSVRVVTTFDSEYCRHGTCERS EAGVCVSTSGRWVLNNDYYRSLPGVFCGVDAVN LLTNMFTPLIQPIGALDISASIVAGGIVAIVVTCLA YYFMRFRRAFGEYSHVVAFNTLLFLMSFTVLCLT PVYSFLPGVYSVIYLYLTFYLTNDVSFLAHIQWM VMFTPLVPFWITIAYIICISTKHFYWFFSNYLKRRV VFNGVSFSTFEEAALCTFLLNKEMYLKLRSDVLLP LTQYNRYLALYNKYKYFSGAMDTTSYREAACCH LAKALNDFSNSGSDVLYQPPQTSITSAVLQSGFRK MAFPSGKVEGCMVQVTCGTTTLNGLWLDDVVY CPRHVICTSEDMLNPNYEDLLIRKSNHNFLVQAG NVQLRVIGHSMQNCVLKLKVDTANPKTPKYKFV RIQPGQTFSVLACYNGSPSGVYQCAMRPNFTIKGS FLNGSCGSVGFNIDYDCVSFCYMHHMELPTGVHA GTDLEGNFYGPFVDRQTAQAAGTDTTITVNVLA WLYAAVINGDRWFLNRFTTTLNDFNLVAMKYNY EPLTQDHVDILGPLSAQTGIAVLDMCASLKELLQN GMNGRTILGSALLEDEFTPFDVVRQCSGVTFQSA VKRTIKGTHHWLLLTILTSLLVLVQSTQWSLFFFL YENAFLPFAMGIIAMSAFAMMFVKHKHAFLCLFL LPSLATVAYFNMVYMPASWVMRIMTWLDMVDT SLSGFKLKDCVMYASAVVLLILMTARTVYDDGA RRVWTLMNVLTLVYKVYYGNALDQAISMWALII SVTSNYSGVVTTVMFLARGIVFMCVEYCPIFFITG NTLQCIMLVYCFLGYFCTCYFGLFCLLNRYFRLTL GVYDYLVSTQEFRYMNSQGLLPPKNSIDAFKLNI KLLGVGGKPCIKVATVQSKMSDVKCTSVVLLSVL QQLRVESSSKLWAQCVQLHNDILLAKDTTEAFEK MVSLLSVLLSMQGAVDINKLCEEMLDNRATLQAI ASEFSSLPSYAAFATAQEAYEQAVANGDSEVVLK KLKKSLNVAKSEFDRDAAMQRKLEKMADQAMT QMYKQARSEDKRAKVTSAMQTMLFTMLRKLDN DALNNIINNARDGCVPLNIIPLTTAAKLMVVIPDY NTYKNTCDGTTFTYASALWEIQQVVDADSKIVQL SEISMDNSPNLAWPLIVTALRANSAVKLQNNELSP VALRQMSCAAGTTQTACTDDNALAYYNTTKGGR FVLALLSDLQDLKWARFPKSDGTGTIYTELEPPCR FVTDTPKGPKVKYLYFIKGLNNLNRGMVLGSLAA

Sequence Description	SEQ ID NO.	Sequence
		TVRLQAGNATEVPANSTVLSFCAFAVDAAKAYK DYLASGGQPITNCVKMLCTHTGTGQAITVTPEAN MDQESFGGASCCLYCRCHIDHPNPKGFCDLKGKY VQIPTTCANDPVGFTLKNTVCTVCGMWKGYGCS CDQLREPMLQSADAQSFLNRVCGVSAARLTPCGT GTSTDVVYRAFDIYNDKVAGFAKFLKTNCCRFQE KDEDDNLIDSYFVVKRHTFSNYQHEETIYNLLKD CPAVAKHDFFKFRIDGDMVPHISRQRLTKYTMAD LVYALRHFDEGNCDTLKEILVTYNCCDDDYFNKK DWYDFVENPDILRVYANLGERVRQALLKTVQFC DAMRNAGIVGVLTLDNQDLNGNWYDFGDFIQTT PGSGVPVV
		DSYYSLLMPILTLTRALTAESHVDTDLTKPYIKWD LLKYDFTEERLKLFDRYFKYWDQTYHPNCVNCL DDRCILHCANFNVLFSTVFPPTSFGPLVRKIFVDG VPFVVSTGYHFRELGVVHNQDVNLHSSRLSFKEL LVYAADPAMHAASGNLLLDKRTTCFSVAALTNN VAFQTVKPGNFNKDFYDFAVSKGFFKEGSSVELK HFFFAQDGNAAISDYDYYRYNLPTMCDIRQLLFV VEVVDKYFDCYDGGCINANQVIVNNLDKSAGFPF NKWGKARLYYDSMSYEDQDALFAYTKRNVIPTIT QMNLKYAISAKNRARTVAGVSICSTMTNRQFHQ KLLKSIAATRGATVVIGTSKFYGGWHNMLKTVYS DVENPHLMGWDYPKCDRAMPNMLRIMASLVLA RKHTTCCSLSHRFYRLANECAQVLSEMVMCGGS LYVKPGGTSSGDATTAYANSVFNICQAVTANVNA LLSTDGNKIADKYVRNLQHRLYECLYRNRDVDT DFVNEFYAYLRKHFSMMILSDDAVVCFNSTYASQ GLVASIKNFKSVLYYQNNVFMSEAKCWTETDLT KGPHEFCSQHTMLVKQGDDYVYLPYPDPSRILGA GCFVDDIVKTDGTLMIERFVSLAIDAYPLTKHPNQ EYADVFHLYLQYIRKLHDELTGHMLDMYSVMLT NDNTSRYWEPEFYEAMYTPHTVLQAVGACVLCN SQTSLRCGACIRRPFLCCKCCYDHVISTSHKLVLS VNPYVCNAPGCDVTDVTQLYLGGMSYYCKSHKP PISFPLCANGQVFGLYKNTCVGSDNVTDFNAIATC DWTNAGDYILANTCTERLKLFAAETLKATEETFK LSYGIATVREVLSDRELHLSWEVGKPRPPLNRNY VFTGYRVTKNSKVQIGEYTFEKGDYGDAVVYRG TTTYKLNVGDYFVLTSHTVMPLSAPTLVPQEHYV RITGLYPTLNISDEFSSNVANYQKVGMQKYSTLQ GPPGTGKSHFAIGLALYYPSARIVYTACSHAAVD ALCEKALKYLPIDKCSRIIPARARVECFDKFKVNS TLEQYVFCTVNALPETTADIVVFDEISMATNYDLS VVNARLRAKHYVYIGDPAQLPAPRTLLTKGTLEP

Sequence Description	SEQ ID NO.	Sequence
		EYFNSVCRLMKTIGPDMFLGTCRRCPAEIVDTVSA LVYDNKLKAHKDKSAQCFKMFYKGVITHDVSSAI NRPQIGVVREFLTRNPAWRKAVFISPYNSQNAVA SKILGLPTQTVDSSQGSEYDYVIFTQTTETAHSCN VNRFNVAITRAKVGILCIMSDRDLYDKLQFTSLEI PRRNVATLQAENVTGLFKDCSKVITGLHPTQAPT HLSVDTKFKTEGLCVDIPGIPKDMTYRRLISMMGF KMNYQVNGYPNMFITREEAIRHVRAWIGFDVEG CHATREAVGTNLPLQLGFSTGVNLVAVPTGYVDT PNNTDFSRVSAKPPPGDQFKHLIPLMYKGLPWNV VRIKIVQMLSDTLKNLSDRVVFVLWAHGFELTSM KYFVKIGPERTCCLCDRRATCFSTASDTYACWHH SIGFDYVYNPFMIDVQQWGFTGNLQSNHDLYCQ VHGNAHVASCDAIMTRCLAVHECFVKRVDWTIE YPIIGDELKINAACRKVQHMVVKAALLADKFPVL HDIGNPKAIKCVPQADVEWKFYDAQPCSDKAYKI EELFYSYATHSDKFTDGVCLFWNCNVDRYPANSI VCRFDTRVLSNLNLPGCDGGSLYVNKHAFHTPAF DKSAFVNLKQLPFFYYSDSPCESHGKQVVSDIDY VPLKSATCITRCNLGGAVCRHHANEYRLYLDAYN MMISAGFSLWVYKQFDTYNLWNTFTRLQSLENV AFNVVNKGHFDGQQGEVPVSIINNTVYTKVDGV DVELFENKTTLPVNVAFELWAKRNIKPVPEVKILN NLGVDIAANTVIWDYKRDAPAHISTIGVCSMTDIA KKPTETICAPLTVFFDGRVDGQVDLFRNARNGVLI TEGSVKGLQPSVGPKQASLNGVTLIGEAVKTQFN YYKKVDGVVQQLPETYFTQSRNLQEFKPRSQMEI DFLELAMDEFIERYKLEGYAFEHIVYGDFSHSQLG GLHLLIGLAKRFKESPFELEDFIPMDSTVKNYFITD AQTGSSKCVCSVIDLLLDDFVEIIKSQDLSVVSKV VKVTIDYTEISFMLWCKDGHVETFYPKLQSSQAW QPGVAMPNLYKMQRMLLEKCDLQNYGDSATLP KGIMMNVAKYTQLCQYLNTLTLAVPYNMRVIHF GAGSDKGVAPGTAVLRQWLPTGTLLVDSDLNDF VSDADSTLIGDCATVHTANKWDLIISDMYDPKTK NVTKENDSKEGFFTYICGFIQQKLALGGSVAIKITE HSWNADLYKLMGHFAWWTAFVTNVNASSSEAF LIGCNYLGKPREQIDGYVMHANYIFWRNTNPIQLS SYSLFDMSKFPLKLRGTAVMSLKEGQINDMILSLL SKGRLIIRENNRVVISSDVLVNN
surface glycoprotein [SARS-CoV-2 Wuhan seafood	3	mfvflvllpl vssqcvnltt rtqlppaytn sftrgvyypd kvfrssvlhs tqdlflpffs 61 nvtwfhaihv sgtngtkrfd npvlpfndgv yfasteksni irgwifgttl dsktqslliv 121 nnatnvvikv cefqfcndpf lgvyyhknnk swmesefrvy ssannctfey vsqpflmdle181 gkqgnfknlr efvfknidgy fkiyskhtpi

Sequence Description	SEQ ID NO.	Sequence
market pneumonia virus]; GenBank: QHD43416.1; January 23, 2020		nlvrdlpqgf saleplvdlp iginitrfqt 241 llalhrsylt pgdsssgwta gaaayyvgyl qprtfllkyn engtitdavd caldplsetk 301 ctlksftvek giyqtsnfrv qptesivrfp nitnlcpfge vfnatrfasv yawnrkrisn 361 cvadysvlyn sasfstfkcy gvsptklndl cftnvyadsf virgdevrqi apgqtgkiad 421 ynyklpddft gcviawnsnn ldskvggnyn ylyrlfrksn lkpferdist eiyqagstpc 481 ngvegfncyf plqsygfqpt ngvgyqpyrv vvlsfellha patvcgpkks tnlvknkcvn 541 fnfngltgtg vltesnkkfl pfqqfgrdia dttdavrdpq tleilditpc sfggvsvitp 601 gtntsnqvav lyqdvnctev pvaihadqlt ptwrvystgs nvfqtragcl igaehvnnsy 661 ecdipigagi casyqtqtns prrarsvasq siiaytmslg aensvaysnn siaiptnfti 721 svtteilpvs mtktsvdctm yicgdstecs nlllqygsfc tqlnraltgi aveqdkntqe 781 vfaqvkqiyk tppikdfggf nfsqilpdps kpskrsfied llfnkvtlad agfikqygdc 841 lgdiaardli caqkfngltv lpplltdemi aqytsallag titsgwtfga gaalqipfam 901 qmayrfngig vtqnvlyenq klianqfnsa igkiqdslss tasalgklqd vvnqnaqaln 961 tlvkqlssnf gaissvlndi lsrldkveae vqidrlitgr lqslqtyvtq qliraaeira 1021 sanlaatkms ecvlgqskrv dfcgkgyhlm sfpqsaphgv vflhvtyvpa qeknfttapa 1081 ichdgkahfp regvfvsngt hwfvtqrnfy epqiittdnt fvsgncdvvi givnntvydp 1141 lqpeldsfke eldkyfknht spdvdlgdis ginasvvniq keidrlneva knlneslidl 1201 qelgkyeqyi kwpwyiwlgf iagliaivmv timlccmtsc csclkgccsc gscckfdedd 1261 sepvlkgvkl hyt
surface glycoprotein RBD [SARS-CoV-2 Wuhan seafood market pneumonia virus]; GenBank: QHD43416.1; January 23, 2020	4	nitnlcpfgevfnatrfasvyawnrkrisncvadysvlynsasfstfkcygvs ptklndlcftnvyadsfvirgdevrqiapgqtgkiadynyklpddftgcvia wnsnnldskvggnynylyrlfrksnlkpferdisteiyqagstpcngvegfn cyfplqsygfqptngvgyqpyrvvvlsfellhapatvcgpkkstnlvknkc vnfnfngltgtg
Receptor Binding Motif (RBM) in surface glycoprotein RBD [SARS-	5	Nsnnldskvggnynylyrlfrksnlkpferdisteiyqagstpcngvegfnc yfplqsygfqptngvgyqpy

Sequence Description	SEQ ID NO.	Sequence
CoV-2 Wuhan seafood market pneumonia virus]; GenBank: QHD43416.1; January 23, 2020		
SARS-CoV-2 CH1-CH3 LS G1m17 IgHG1*01 (aa)	6	ASTKGPSVFPLAPSSKSTSGGTAALGCLVKDYFPE PVTVSWNSGALTSGVHTFPAVLQSSGLYSLSSVV TVPSSSLGTQTYICNVNHKPSNTKVDKKVEPKSC DKTHTCPPCPAPELLGGPSVFLFPPKPKDTLMISRT PEVTCVVVDVSHEDPEVKFNWYVDGVEVHNAKT KPREEQYNSTYRVVSVLTVLHQDWLNGKEYKCK VSNKALPAPIEKTISKAKGQPREPQVYTLPPSRDEL TKNQVSLTCLVKGFYPSDIAVEWESNGQPENNYK TTPPVLDSDGSFFLYSKLTVDKSRWQQGNVFSCS VLHEALHSHYTQKSLSLSPGK
SARS-CoV-2 CH1-CH3 LS, ALE G1m17 IgHG1*01 (aa)	7	ASTKGPSVFPLAPSSKSTSGGTAALGCLVKDYFPE PVTVSWNSGALTSGVHTFPAVLQSSGLYSLSSVV TVPSSSLGTQTYICNVNHKPSNTKVDKKVEPKSC DKTHTCPPCPAPELLAGPSVFLFPPKPKDTLMISRT PEVTCVVVDVSHEDPEVKFNWYVDGVEVHNAKT KPREEQYNSTYRVVSVLTVLHQDWLNGKEYKCK VSNKALPLPEEKTISKAKGQPREPQVYTLPPSRDE LTKNQVSLTCLVKGFYPSDIAVEWESNGQPENNY KTTPPVLDSDGSFFLYSKLTVDKSRWQQGNVFSC SVLHEALHSHYTQKSLSLSPGK
SARS-CoV-2 CL IgLC*01 (aa)	8	GQPKAAPSVTLFPPSSEELQANKATLVCLISDFYP GAVTVAWKADSSPVKAGVETTTPSKQSNNKYAA SSYLSLTPEQWKSHRSYSCQVTHEGSTVEKTVAP TECS
SARS-CoV-2 CL (CK) k1m3 IgKC*01 (aa)	9	RTVAAPSVFIFPPSDEQLKSGTASVVCLLNNFYPR EAKVQWKVDNALQSGNSQESVTEQDSKDSTYSL SSTLTLSKADYEKHKVYACEVTHQGLSSPVTKSF NRGEC

Sequence Description	SEQ ID NO.	Sequence
S2X259 CDRH1	10	GGIFNTYT
S2X259 variant_1 CDRH1	11	GGIFSTYT
S2X259 CDRH2	12	IILMSGMA
S2X259 variant_1 CDRH2	13	IILISGIA
S2X259 variant_2 CDRH2	14	IILMSGKA
S2X259 CDRH3	15	ARGFNGNYYGWGDDDAFDI
S2X259 VH	16	QVQLVQSGAEVKKPGSSVKVSCKAS**GGIFNTYT** ISWVRQAPGQGLEWMGR**IILMSGMA**NYAQKIQ GRVTITADKSTSTAYMELTSLRSDDTAVYYC**AR GFNGNYYGWGDDDAFDI**SGQGTLVTVYS
S2X259 VH_v1	17	QVQLVQSGAEVKKPGSSVKVSCKAS**GGIFNTYT** ISWVRQAPGQGLEWMGR**IILMSGMA**NYAQKIQ GRVTITADKSTSTAYMELTSLRSDDTAVYYC**AR GFNGNYYGWGDDDAFDI**WGQGTLVTVYS
S2X259 VH_v2	18	QVQLVQSGAEVKKPGSSVKVSCKAS**GGIFNTYT** ISWVRQAPGQGLEWMGR**IILISGIA**NYAQKIQGR VTITADKSTSTAYMELTSLRSDDTAVYYC**ARGF NGNYYGWGDDDAFDI**SGQGTLVTVYS
S2X259 VH_v3	19	QVQLVQSGAEVKKPGSSVKVSCKAS**GGIFSTYT**I SWVRQAPGQGLEWMGR**IILMSGMA**NYAQKIQG RVTITADKSTSTAYMELTSLRSDDTAVYYC**ARG FNGNYYGWGDDDAFDI**SGQGTLVTVYS
S2X259 VH_v4	20	QVQLVQSGAEVKKPGSSVKVSCKAS**GGIFNTYT** ISWVRQAPGQGLEWMGR**IILMSGMA**NYAQKIQ GRVTITADKSTSTAYMELTSLRSDDTAVYYC**AR GFNGNYYGWGDDDAFDI**WGQGTLVTVSS
S2X259 VH_v5	21	QVQLVQSGAEVKKPGSSVKVSCKAS**GGIFNTYT** ISWVRQAPGQGLEWMGR**IILMSGKA**NYAQKIQ GRVTITADKSTSTAYMELTSLRSDDTAVYYC**AR**

Sequence Description	SEQ ID NO.	Sequence
		GFNGNYYGWGDDDAFDIWGQGTLVTVSS
S2X259 VH_v6	22	QVQLVQSGAEVKKPGSSVKVSCKAS**GGIFNTYT** ISWVRQAPGQGLEWMGR**IILISGIA**NYAQKIQGR VTITADKSTSTAYMELTSLRSDDTAVYYC**ARGF NGNYYGWGDDDAFDI**WGQGTLVTVSS
S2X259 CDRL1	23	NSNIGAGYD
S2X259 CDRL2	24	GNS
S2X259 CDRL3	25	QSYDSSLSGPNWV
S2X259 VL	26	QTVLTQPPSVSGAPGQRVTISCTGSNSNIGAGYD VHWYQQLPGTAPKLLICGNSNRPSGVPDRFSGSK SGTSASLAITGLQAEDEADYYCQSYDSSLSGPN WVFGGGTKLTVL
S2X259 VL_v1	27	QTVLTQPPSVSGAPGQRVTISCTGS**NSNIGAGYD** VHWYQQLPGTAPKLLIS**GNS**NRPSGVPDRFSGSK SGTSASLAITGLQAEDEADYYC**QSYDSSLSGPN WV**FGGGTKLTVL
S2X259 VL_v2	28	QTVLTQPPSVSGAPGQRVTISCTGS**NSNIGAGYD** VHWYQQLPGTAPKLLIA**GNS**NRPSGVPDRFSGSK SGTSASLAITGLQAEDEADYYC**QSYDSSLSGPN WV**FGGGTKLTVL
S2X259 VL_v3	29	QTVLTQPPSVSGAPGQRVTISCTGS**NSNIGAGYD** VHWYQQLPGTAPKLLIY**GNS**NRPSGVPDRFSGSK SGTSASLAITGLQAEDEADYYC**QSYDSSLSGPN WV**FGGGTKLTVL
S2X259 VL_v4	30	QTVLTQPPSVSGAPGQRVTISCTGS**NSNIGAGYD** VHWYQQLPGTAPKLLIV**GNS**NRPSGVPDRFSGSK SGTSASLAITGLQAEDEADYYC**QSYDSSLSGPN WV**FGGGTKLTVL
S2H13-v1 mAb VH	31	EVQLVESGGDSVQPGGSLRLSCAAA**GFTFSSYW** MNWVRQAPGKGLEWVAN**IKQDGSEK**YYVDSV KGRFTISRDNAKNSLYLQMNSLRAEDTAVYYC**AL SSGYSGYAGNY**WGQGTLVTVSS
S2H13-v1 mAb CDRH1	32	GFTFSSYW
S2H13-v1	33	IKQDGSEK

Sequence Description	SEQ ID NO.	Sequence
mAb CDRH2		
S2H13-v1 mAb CDRH3	34	ALSSGYSGYAGNY
S2H13-v1 mAb VL	35	QAVVTQEPSLTVSPGGTVTLTCGSS**TGAVTSGH** **Y**PYWFQQKPGQAPRTLIY**DTS**NKHSWTPARFSG SLLGGKAALTLSGA<u>R</u>PEDEAEYYC**LLSYSGARG** **V**FGGGTKLTVL
S2H13-v1 mAb CDRL1	36	TGAVTSGHY
S2H13-v1 mAb CDRL2	37	DTS
S2H13-v1 mAb CDRL3	38	LLSYSGARGV
S2H13-v2 mAb VH	39	EVQLVESGGDSVQPGGSLRLSCAAA**GFTFSSYFM** **N**WVRQAPGKGLEWVA**NIKQDGSEKYYVDSVKG** RFTISRDNAKNSLYLQMNSLRAEDTAVYYCAL**SS** **GYSGYAGNY**WGQGTLVTVSS
S2H13-v2 mAb CDRH1	40	GFTFSSYFMN
S2H13-v3 mAb VH	41	EVQLVESGGDSVQPGGSLRLSCAAA**GFTFSSYW** **MN**WVRQAPGKGLEWVA**NIKQEGSEKYYVDSV** **KG**RFTISRDNAKNSLYLQMNSLRAEDTAVYYCA L**SSGYSGYAGNY**WGQGTLVTVSS
S2H13-v3 mAb CDRH2	42	NIKQEGSEKYYVDSVKG
S2H13-v4 mAb VH	43	EVQLVESGGDSVQPGGSLRLSCAAA**GFTFSSYFM** **N**WVRQAPGKGLEWVA**NIKQEGSEKYYVDSVKG** RFTISRDNAKNSLYLQMNSLRAEDTAVYYCAL**SS** **GYSGYAGNY**WGQGTLVTVSS
S2H13-v5 mAb VH	44	EVQLVESGGDSVQPGGSLRLSCAAA**GFTFSSYFM** **N**WVRQAPGKGLEWVA**NIKQDASEKYYVDSVKG** RFTISRDNAKNSLYLQMNSLRAEDTAVYYCAL**SS** **GYSGYAGNY**WGQGTLVTVSS
S2H13-v5 mAb CDRH2	45	EVQLVESGGDSVQPGGSLRLSCAAA**GFTFSSYYM** **N**WVRQAPGKGLEWVA**NIKQEGSEKYYVDSVKG** RFTISRDNAKNSLYLQMNSLRAEDTAVYYCAL**SS** **GYSGYAGNY**WGQGTLVTVSS
S2H13-v6 mAb CDRH1	46	GFTFSSYYMN

Sequence Description	SEQ ID NO.	Sequence
S2H14-v1 mAb VH	47	EVQLVESGGGLVKPGGSLRLSCAAS**GFTFSNAW MS**WVRQAPGKGLEWVG**RIKSKTDGGTTDYAAP VKG**RFTISRDDSKNTLYLQMNSLKTEDTAVYYCT T**GSETYYYDSSGPFDY**WGQGTLVTVSS
S2H14-v1 mAb CDRH1	48	GFTFSNAWMS
S2H14-v1 mAb CDRH2	49	RIKSKTDGGTTDYAAPVKG
S2H14-v1 mAb CDRH3	50	GSETYYYDSSGPFDY
S2H14-v1 mAb VL	51	NFMLTQPHSVSESPGKTVTISC**TRSSGSIASNYVQ** WYQQRPGSSPTTVIY**EDNQRPS**GVPDRFSGSIDSS SNSASLTISGLKTEDEADYYC**QSYDSSNQV**FGGG TKLTVL
S2H14-v1 mAb CDRL1	52	TRSSGSIASNYVQ
S2H14-v1 mAb CDRL2	53	EDNQRPS
S2H14-v1 mAb CDRL3	54	QSYDSSNQV
S2H14-v2 mAb VH	55	EVQLVESGGGLVKPGGSLRLSCAAS**GFTFSNAFM S**WVRQAPGKGLEWVG**RIKSKTDGGTTDYAAPV KG**RFTISRDDSKNTLYLQMNSLKTEDTAVYYCTT **GSETYYYDSSGPFDY**WGQGTLVTVSS
S2H14-v2 mAb CDRH1	56	GFTFSNAFMS
S2H14-v3 mAb VH	57	EVQLVESGGGLVKPGGSLRLSCAAS**GFTFSNAW MS**WVRQAPGKGLEWVG**RIKSKTEGGTTDYAAP VKG**RFTISRDDSKNTLYLQMNSLKTEDTAVYYCT T**GSETYYYDSSGPFDY**WGQGTLVTVSS
S2H14-v3 mAb CDRH2	58	RIKSKTEGGTTDYAAPVKG
S2H14-v4	59	EVQLVESGGGLVKPGGSLRLSCAAS**GFTFSNAFM S**WVRQAPGKGLEWVG**RIKSKTDAGTTDYAAPV**

Sequence Description	SEQ ID NO.	Sequence
mAb VH		**KG**RFTISRDDSKNTLYLQMNSLKTEDTAVYYCTT **GSETYYYDSSGPFDY**WGQGTLVTVSS
S2H14-v4 mAb CDRH2	60	RIKSKTDAGTTDYAAPVKG
S2H14-v5 mAb VH	61	EVQLVESGGGLVKPGGSLRLSCAAS**GFTFSNAFM** SWVRQAPGKGLEWVG**RIKSKTEGGTTDYAAPV** **KG**RFTISRDDSKNTLYLQMNSLKTEDTAVYYCTT **GSETYYYDSSGPFDY**WGQGTLVTVSS
S2H14-v6 mAb VH	62	EVQLVESGGGLVKPGGSLRLSCAAS**GFTFSNAY** **MS**WVRQAPGKGLEWVG**RIKSKTEGGTTDYAAP** **VKG**RFTISRDDSKNTLYLQMNSLKTEDTAVYYCT T**GSETYYYDSSGPFDY**WGQGTLVTVSS
S2H14-v6 mAb CDRH1	63	GFTFSNAYMS
S2A4-v1 mAb VH	64	EVQLVESGGGLVQPGGSLRLSCAAS**GFTFSSYW** M<u>N</u>WVRQAPGKGLEWVAN**IKQDGSEK**YYVDSV KGRFTISRDNAKNSL<u>F</u>LQMNSLRAEDTAVYYC**AR** **VWWLRGSFDY**WGQGTLVTVSS
S2A4-v1 mAb CDRH1	65	GFTFSSYW
S2A4-v1 mAb CDRH2	66	IKQDGSEK
S2A4-v1 mAb CDRH3	67	ARVWWLRGSFDY
S2A4-v1 mAb VL	68	NFMLTQPHSVSESPGKTVTISCTGS**SGSIASNY**VQ WYQQRPGSAPTTVIY**EDN**QRPSGVPDRFSGSIDSS SNSASLTISGLKTEDEADYYC**QSYDSSNHVV**FGG GTKLTVL
S2A4-v1 mAb CDRL1	69	SGSIASNY
S2A4-v1 mAb CDRL2	70	EDN

Sequence Description	SEQ ID NO.	Sequence
S2A4-v1 mAb CDRL3	71	QSYDSSNHVV
S2X35-v1 VH	72	QVQLVQSGAEVKKPGASVKVSCKAS**GYTFT NYG**ISWVRQAPGQGLEWMGW**ISAYKGNT**N YAQKLQGRVTMTTDTSTSTAYMELRSLRSDD TAVYYC**ARPDYQVLGYDFWIGYYGMDV**W GQGTTVIVSS
S2X35-v1 CDRH1	73	**GYTFTNYG**
S2X35-v1 CDRH2	74	**ISAYKGNT**
S2X35-v1 CDRH3	75	**ARPDYQVLGYDFWIGYYGMDV**
S2X35-v1 VL	76	QSVLTQPPSVSGAPGQRVTISCTG**SSSNIGAGYD**V HWYQQLPGTAPKLLIY**GNT**NRPSGVPDRFSGSKS GTSASLAITGLQAEDEADYYC**QSYDSSLSGSEVV** FGGGTKLTVL
S2X35-v1 CDRL1	77	**SSNIGAGYD**
S2X35-v1 CDRL2	78	**GNT**
S2X35-v1 CDRL3	79	**QSYDSSLSGSEVV**
S2X35-v2 CDRH1	80	**GYTFTNYGIS**
S2X35-v2 CDRH2	81	**WISAYKGNTNYAQKLQG**
S2X35-v2 mAb CDRH3	82	**PDYQVLGYDFWIGYYGMDV**
S2X35-v3 VH	83	QVQLVQSGAEVKKPGASVKVSCKAS**GYTFTNYG** ISWVRQAPGQGLEWMGF**ISAYKGNT**NYAQKLQG RVTMTTDTSTSTAYMELRSLRSDDTAVYYC**ARP DYQVLGYDFWIGYYGMDV**WGQGTTVIVSS

Sequence Description	SEQ ID NO.	Sequence
S2X35-v3 CDRH1	84	**FISAYKGNTNYAQKLQG**
S2X35-v4 VH	85	QVQLVQSGAEVKKPGASVKVSCKAS**GYTFTNYG** ISWVRQAPGQGLEWMGW**ISAYKGNT**NYAQKLQ GRVTMTTDTSTSTAYMELRSLRSDDTAVYYC**AR PDYQVLGYDFFIGYYGMDV**WGQGTTVIVSS
S2X35-v4 CDRH3	86	**ARPDYQVLGYDFFIGYYGMDV**
S2X35-v5 CDRH3	87	**PDYQVLGYDFFIGYYGMDV**
S2X35-v6 VH	88	QVQLVQSGAEVKKPGASVKVSCKAS**GYTFTNYG** ISWVRQAPGQGLEWMGF**ISAYKGNT**NYAQKLQG RVTMTTDTSTSTAYMELRSLRSDDTAVYYC**ARP DYQVLGYDFFAGYYGMDV**WGQGTTVIVSS
S2X35-v6 CDRH3	89	**ARPDYQVLGYDFFAGYYGMDV**
S2X35-v7 CDRH3	90	**PDYQVLGYDFFAGYYGMDV**
S2X35-v8 CDRL1	91	**TGSSSNIGAGYDVH**
S2X35-v8 CDRL2	92	**GNTNRPS**
S309-v2 VH	93	QVQLVQSGAEVKKPGASVKVSCKAS**GYPFTSYG**I SWVRQAPGQGLEWMGW**ISTYQGNT**NYAQKFQG RVTMTTDTSTTTGYMELRRLRSDDTAVYYC**ARD YTRGAWFGESLIGGFDN**WGQGTLVTVSS
S309-v2 CDRH1	94	**GYPFTSYG**
S309-v2 CDRH2	95	**ISTYQGNT**
S309-v2 CDRH3	96	**ARDYTRGAWFGESLIGGFDN**
S309-v2 VL	97	EIVLTQSPGTLSLSPGERATLSCRASQTVSSTSLAW YQQKPGQAPRLLIYGASSRATGIPDRFSGSGSGTD FTLTISRLEPEDFAVYYCQQHDTSLTFGGGTKVEI

Sequence Description	SEQ ID NO.	Sequence
		K
S309-v2 CDRL1	98	QTVSSTS
S309-v2 CDRL2	99	GAS
S309-v2 CDRL3	100	QQHDTSLT
S309 VH	101	QVQLVQSGAEVKKPGASVKVSCKAS**GYPFTSYG**I SWVRQAPGQGLEWMGW**ISTYNGNT**NYAQKFQG RVTMTTDTSTTTGYMELRRLRSDDTAVYYC**ARD YTRGAWFGESLIGGFDN**WGQGTLVTVSS
S309 CDRH1	102	GYPFTSYG
S309 CDRH2	103	ISTYNGNT
S309 CDRH3	104	ARDYTRGAWFGESLIGGFDN
S309 VL	105	EIVLTQSPGTLSLSPGERATLSCRAS**QTVSSTS**LA WYQQKPGQAPRLLIY**GAS**SRATGIPDRFSGSGSGT DFTLTISRLEPEDFAVYYC**QQHDTSLT**FGGGTKV EIK
S309 CDRL1	106	QTVSSTS
S309 CDRL2	107	GAS
S309 CDRL3	108	QQHDTSLT
S2E12 CDRH1	109	GFTFTSSA
S2E12 CDRH2	110	IVVGSGNT
S2E12 CDRH3	111	PYCSGGSCSDGFDI
S2E12 CDRH3 variant 1	112	PYCSGGSCSDAFDI
S2E12 CDRH3 variant 2	113	PYSSGGSSSDGFDI
S2E12 CDRH3	114	PYPSGGSPSDGFDI

Sequence Description	SEQ ID NO.	Sequence
variant 3		
S2E12 CDRH3 variant 4	115	PYASGGSASDGFDI
S2E12 CDRH3 variant 5	116	PYCSGGSCSEGFDI
S2E12 CDRH3 with N-terminal adjacent alanine and serine amino acids	117	ASPYCSGGSCSDGFDI
S2E12 CDRH3 variant 1 with N-terminal adjacent alanine and serine amino acids	118	ASPYCSGGSCSDAFDI
S2E12 CDRH3 variant 2 with N-terminal adjacent alanine and serine amino acids	119	ASPYSSGGSSSDGFDI
S2E12 CDRH3 variant 3 with N-terminal adjacent alanine and serine amino acids	120	ASPYPSGGSPSDGFDI
S2E12 CDRH3 variant 4 with N-terminal	121	ASPYASGGSASDGFDI

Sequence Description	SEQ ID NO.	Sequence
adjacent alanine and serine amino acids		
S2E12 CDRH3 variant 5 with N-terminal adjacent alanine and serine amino acids	122	ASPYCSGGSCSEGFDI
S2E12 VH	123	QVQLVQSGPEVKKPGTSVRVSCKASGFTFTSSAV QWVRQARGQRLEWVGWIVVGSGNTNYAQKFHE RVTITRDMSTSTAYMELSSLRSEDTAVYYCASPY CSGGSCSDGFDIWGQGTMVTVSS
S2E12 VH_v1	124	QVQLVQSGPEVKKPGTSVRVSCKASGFTFTSSAV QWVRQARGQRLEWVGFIVVGSGNTNYAQKFHER VTITRDMSTSTAYMELSSLRSEDTAVYYCASPYCS GGSCSDGFDIWGQGTMVTVSS
S2E12 VH_v2	125	QVQLVQSGPEVKKPGTSVRVSCKASGFTFTSSAV QWVRQARGQRLEWVGYIVVGSGNTNYAQKFHE RVTITRDMSTSTAYMELSSLRSEDTAVYYCASPY CSGGSCSDGFDIWGQGTMVTVSS
S2E12 VH_v3	126	QVQLVQSGPEVKKPGTSVRVSCKASGFTFTSSAV QWVRQARGQRLEWVGWIVVGSGNTNYAQKFHE RVTITRDMSTSTAYMELSSLRSEDTAVYYCASPY CSGGSCSDAFDIWGQGTMVTVSS
S2E12 VH_v4	127	QVQLVQSGPEVKKPGTSVRVSCKASGFTFTSSAV QWVRQARGQRLEWVGWIVVGSGNTNYAQKFHE RVTITRDMSTSTAYMELSSLRSEDTAVYYCASPYS SGGSSSDGFDIWGQGTMVTVSS
S2E12 VH_v5	128	QVQLVQSGPEVKKPGTSVRVSCKASGFTFTSSAV QWVRQARGQRLEWVGWIVVGSGNTNYAQKFHE RVTITRDMSTSTAYMELSSLRSEDTAVYYCASPYP SGGSPSDGFDIWGQGTMVTVSS
S2E12 VH_v6	129	QVQLVQSGPEVKKPGTSVRVSCKASGFTFTSSAV QWVRQARGQRLEWVGWIVVGSGNTNYAQKFHE RVTITRDMSTSTAMELSSLRSEDTAVYYCASPYAS GGSASDGFDIWGQGTMVTVSS

Sequence Description	SEQ ID NO.	Sequence
S2E12 VH_v7	130	QVQLVQSGPEVKKPGTSVRVSCKASGFTFTSSAV QWVRQARGQRLEWVGFIVVGSGNTNYAQKFHER VTITRDMSTSTAYMELSSLRSEDTAVYYCASPYCS GGSCSEGFDIWGQGTMVTVSS
S2E12 VH_v8	131	QVQLVQSGPEVKKPGTSVRVSCKASGFTFTSSAV QWVRQARGQRLEWVGWIVVGSGNTNYAQKFHE RVTITRDMSTSTAYMELSSLRSEDTAVYYCASPY CSGGSCSEGFDIWGQGTMVTVSS
S2E12 VH_v9	132	QVQLVQSGPEVKKPGTSVRVSCKASGFTFTSSAV QWVRQARGQRLEWVGAIVVGSGNTNYAQKFHE RVTITRDMSTSTAYMELSSLRSEDTAVYYCASPY CSGGSCSDGFDIWGQGTMVTVSS
S2E12 CDRL1	133	QSVSSSY
S2E12 CDRL2	134	GAS
S2E12 CDRL3	135	QQYVGLTGWT
S2E12 CDRL3 variant 1	136	QQYVGLTGFT
S2E12 CDRL3 variant 2	137	QQYVGLTGYT
S2E12 VL	138	DIVLTQTPGTLSLSPGERATLSCRASQSVSSSYLA WYQQKPGQAPRLLIYGASSRATGIPDRFSGSGSGT DFTLTISRLEPEDFAVYYCQQYVGLTGWTFGQGT KVEIK
S2E12 VL_v1	139	DIVLTQTPGTLSLSPGERATLSCRASQSVSSSYLA WYQQKPGQAPRALIYGASSRATGIPDRFSGSGSGT DFTLTISRLEPEDFAVYYCQQYVGLTGWTFGQGT KVEIK
S2E12 VL_v2	140	DIVLTQTPGTLSLSPGERATLSCRASQSVSSSYLA WYQQKPGQAPRLLIYGASSRATGIPDRFSGSGSGT DFTLTISRLEPEDFAVYYCQQYVGLTGFTFGQGTK VEIK
S2E12 VL_v3	141	DIVLTQTPGTLSLSPGERATLSCRASQSVSSSYLA WYQQKPGQAPRLLIYGASSRATGIPDRFSGSGSGT DFTLTISRLEPEDFAVYYCQQYVGLTGYTFGQGT

Sequence Description	SEQ ID NO.	Sequence
		KVEIK
S2M11-v1 VH	142	EVQLVQSGAEVKKPGASVKVSCKAS**GYTFTGYY**MHWVRQAPGQGLEWMGW**INPISSGT**SYAQTFQGRVTMTSDTSITTAYMELSRLRSDDTAVYYC**ARAAPFYDFWSGYSYFDY**WGQGTLVTVSS
S2M11-v1 CDRH1	143	**GYTFTGYY**
S2M11-v1 CDRH2	144	**INPISSGT**
S2M11-v1 CDRH3	145	**ARAAPFYDFWSGYSYFDY**
S2M11-v1 VL	146	EIVMMQSPGTLSLSPGERATLSCRAS**QSVSSSY**LAWYQQKPGQAPRLLIY**GAS**SRATGIPDRFSGSGSGTDFTLTISRLEPEDFAVYYC**QQYGSSAWT**FGQGTKVEIK
S2M11-v1 CDRL1	147	**QSVSSSY**
S2M11-v1 CDRL2	148	**GAS**
S2M11-v1 CDRL3	149	**QQYGSSAWT**
S304 VH	150	EVQLVESGGGLVQPGGSLRLSCAAS**GFTFSSYD**MHWVRQTTGKGLEWVST**IGTAGDT**YYPDSVKGRFTISREDAKNSLYLQMNSLRAGDTAVYYC**ARGDSSGYYYYFDY**WGQGTLLTVSS
S304 CDRH1	151	**GFTFSSYD**
S304 CDRH2	152	**IGTAGDT**
S304 CDRH3	153	**ARGDSSGYYYYFDY**
S304 VL	154	DIQMTQSPSSLSAAVGDRVTITCRAS**QSIGSY**LNWYQQKPGKAPKLLIY**AAS**SLQSGVPSRFSGSGSGTDFTLTISSLQPEDFAIYYC**QQSYVSPTYT**FGPGTKVDIK
S304 CDRL1	155	**QSIGSY**
S304 CDRL2	156	**AAS**

Sequence Description	SEQ ID NO.	Sequence
S304 CDRL3	157	**QQSYVSPTYT**
CR3022 VH	158	QMQLVQSGTEVKKPGESLKISCKGSGYGFITYWI GWVRQMPGKGLEWMGIIYPGDSETRYSPSFQGQ VTISADKSINTAYLQWSSLKASDTAIYYCAGGSGI STPMDVWGQGTTVTVSS
CR3022 VL	159	DIQLTQSPDSLAVSLGERATINCKSSQSVLYSSINK NYLAWYQQKPGQPPKLLIYWASTRESGVPDRFSG SGSGTDFTLTISSLQAEDVAVYYCQQYYSTPYTFG QGTKVEIK
Signal peptide from Mu-phosphatase	160	MGILPSPGMPALLSLVSLLSVLLMGCVAETGT
Synthetic C-terminal extension sequence of SARS-CoV-2 S ectodomain	161	GSGRENLYFQGGGGSGYIPEAPRDGQAYVRKDGE WVLLSTFLGSGGLNDIFEAQKIEWHEGSGHHHHH HHH
S315 VH	162	EVQLVESGGGLVQPGGSLRLSCAASGFTFSNYWM TWVRQAPGKGLEWVANIKQDGSEKYYVDSVKG RFTISRDNAKNSLYLQMNSLRAEDTAVYYCARDL WWNDQAHYYGMDVWGQGTTVTVSS
S315 VL	163	SYELTQPPSVSVSPGQTARITCSGDAFPNQYAYW YQQKPGQAPVMLIYKDSERPSGIPERFFGSSSGTT VTLTIRGVQAEDEADYYCQSADSSGTVFGGGTKL TVL
S303 VH	164	EVQLVESGGGLVKPGGSLRLSCAASGFTFLTYSM NWVRQTPGKRLQWVSAISGSGGATYYADSVKGR FTISRDNSKNTLYLQMNTVTADDTAIYFCARERD DIFPMGLNAFDIWGQGAMVIVSS
S303 VL	165	DIQMTQSPSTLSASVGDRVTITCRASQSISNWLAW YQQKPGKAPKLLIYKASSLESGVPSRFSGSGSGTE FTLTISSLQPDDSATYYCQQYDTYSWTFGQGTKV EIK
S2D22 VH	166	EVHLVESGGGLVQPGGSLKLSCAASGFTFSGSAM HWVRQASGKGLEWVGRIRTKANTYATAYAASV KGRFTISRDDSKNTAYLQMNSLKTEDTAVYYCTR PAPYDFLSDYYTGEQLDYWGQGTLVTVSS
S2D22 VL	167	QSVLTQPPSVSGAPGQRVTISCTGSSSNIGAGYDV HWYQQLPGAAPKLLIYGNSNRPSGVPDRFSGSKS

Sequence Description	SEQ ID NO.	Sequence
		GTSASLAITGLQAEDEADYYCQSYDSSLSGPEVFG TGTKVTVL
S2A10 VH	168	QVQLQESGPGLVKPSQTLSLTCTVSGGSISSGDYY WSWIRQPPGKGLEWIGYIYYSGSTYYNPSLKSRV TISVDSSKNQFSLRLSSVTAADTAVYYCARGIKDA YCGGDCYHAFDIWGQGTMVTVSS
S2A10 VL	169	SYVLTQPPSVSVAPGQTARITCGGNNIGSKSVHW YQQKPGQAPVLVVYDDSDRPSGIPERFSGSNSGN TATLTISRVEAGDEADYYCQVWDSTSDHPNVFGT GTKVTVL
SARS-CoV-2 nucleocapsid polypeptide	170	MSDNGPQNQRNAPRITFGGPSDSTGSNQNGERSG ARSKQRRPQGLPNNTASWFTALTQHGKEDLKFPR GQGVPINTNSSPDDQIGYYRRATRRIRGGDGKMK DLSPRWYFYYLGTGPEAGLPYGANKDGIIWVATE GALNTPKDHIGTRNPANNAAIVLQLPQGTTLPKGF YAEGSRGGSQASSRSSSRSRNSSRNSTPGSSRGTSP ARMAGNGGDAALALLLLDRLNQLESKMSGKGQ QQQGQTVTKKSAAEASKKPRQKRTATKAYNVTQ AFGRRGPEQTQGNFGDQELIRQGTDYKHWPQIAQ FAPSASAFFGMSRIGMEVTPSGTWLTYTGAIKLDD KDPNFKDQVILLNKHIDAYKTFPPTEPKKDKKKK ADETQALPQRQKKQQTVTLLPAADLDDFSKQLQ QSMSSADSTQA

EXAMPLES

EXAMPLE 1

NEUTRALIZING ANTIBODIES AGAINST SARS-COV-2

Human monoclonal antibodies isolated from patients who recovered from SARS-CoV-2 infection were expressed recombinantly and were tested in neutralization

assays against SARS-CoV-2 virus. SARS-CoV-2 strain 2019 n-CoV/USA_WA1/2020 was obtained from the United States Centers for Disease Control and Prevention. Virus was passaged once in Vero CCL81 cells (ATCC) and titrated by focus-forming assay on Vero E6 cells. Serial dilutions of indicated mAbs were incubated with 10^2 FFU of SARS-CoV-2 for 1 hour at 37 °C. Antibody-virus complexes were added to Vero E6 cell monolayers in 96-well plates and incubated at 37 °C for 1 hour. Subsequently, cells were overlaid with 1% (w/v) methylcellulose in MEM supplemented with 2% FBS. Plates were harvested 30 hours later by removing overlays and fixed with 4% PFA in PBS for 20 minutes at room temperature. Plates were washed and sequentially incubated with 1 µg/mL of CR3022 anti-S antibody and HRP-conjugated goat anti-human IgG in PBS supplemented with 0.1% saponin and 0.1% BSA. SARS-CoV-2-infected cell foci were visualized using TrueBlue peroxidase substrate (KPL) and quantitated on an ImmunoSpot microanalyzer (Cellular Technologies). Data were processed using Prism software (GraphPad Prism 8.0).

Results are shown in Figures 1A and 1B. Calculated IC50 values (ng/ml) for Figure 1A are shown in Table 3. Calculated EC50 values (ng/ml) for Figure 1B are listed to the right of the graph in Figure 1B. Figure 1A includes comparator antibody S309, isolated from a patient who recovered from SARS-CoV-1 infection.

Table 3. Calculated IC50 values for Antibodies shown in Figure 1A

	S2H7	S2H13	S2H14	S2A4	S309
IC50	4332	1900	1955	18817	124.4

Neutralization assays were carried out using additional monoclonal antibodies using similar methods. Results are shown in Figures 5A-5C. Figure 5A shows results for antibody S2X190 and four comparator antibodies. Figure 5B shows results for antibody S2X129 and four comparator antibodies. Figure 5C shows results for antibodies S2X132 and S2X127, along with 4 comparator antibodies. Calculated EC50 values are shown to the right of each graph.

Neutralization of SARS-CoV-2 Infection by Antibody Combinations

Neutralization of SARS-CoV-2 infection by combinations of monoclonal antibodies was assessed using a SARS-CoV-2 live virus assay.

SARS-CoV-2 strain 2019n-CoV/USA_WA1/2020 was obtained from the Centers for Disease Control and Prevention. The virus was passaged once in Vero CCL81 cells (ATCC) and titrated by focus-forming assay on Vero E6 cells. Neutralization assays were carried out as follows. Serial dilutions of monoclonal antibodies were incubated with 10^2 FFU of SARS-CoV-2 for one hour at 37°C. Antibody-virus complexes were added to Vero E6 cell monolayers in 96-well plates and incubated at 37°C for one hour. Subsequently, cells were overlaid with 1% (w/v) methylcellulose in MEM supplemented with 2% FBS. Plates were harvested 30 hours later by removing overlays and fixed with 4% PFA in PBS for 20 minutes at room temperature. Plates were washed and sequentially incubated with one μg/mL of CR3022 (Yuan et al, 2020) anti-S antibody and HRP-conjugated goat anti-human IgG in PBS supplemented with 0.1% saponin and 0.1% BSA. SARS-CoV-2-infected cell foci were visualized using TrueBlue peroxidase substrate (KPL) and quantitated on an ImmunoSpot microanalyzer (Cellular Technologies). Data were processed using Prism software (GraphPad Prism 8.0).

Neutralization of SARS-CoV-2 infection by monoclonal antibodies S309, S2H14, and S2X2 alone or in combination was assessed. S309, S2H14, and S2X2 were tested individually, S2H14 and S2X2 were each tested in combination with S309, and the combination of all three of S309, S2H14, and S2X2 was tested. Results are shown in Figure 2. Calculated EC50 values are shown below each graph. Additionally, S309, S2H14, and S2A4 were tested individually, S2H14 and S2A4 were each tested in combination with S309, and the combination of all three of S309, S2H14, and S2A4 was tested. Results are shown in Figure 3.

Quantitative Epitope-Specific Serology of SARS-CoV-2 Spike Protein

SARS-CoV-2 Spike protein binding by various antibodies was analyzed by antibody competition assays, cryo-EM data, and crystallography data. From this analysis, Spike RBD antigenic Sites Ia, Ib, Ic, Id, II, and IV were identified. A map

showing these sites and exemplary antibodies that bind within each site is shown in Figure 4.

Further Characterization of Antibodies

Antibodies were further studied to assess function and structure. Data from these experiments is shown in Figures 6-22B. S2X259 binding was evaluated at 3.1-angstrom and 2.65-angstrom resolution. From these studies, the S2X259 epitope is formed by amino acid residues 369-386, 404-411, and 499-508 of the S glycoprotein (SEQ ID NO: 3). S2X259 does not appear to contact amino acids 406, 409, 410, 411, 499, 500, 505, and 507.

Materials and Methods

Flow-cytometry based screening for binding to CoV S protein expressed on mammalian cells

ExpiCHO cells were transfected with S protein of SARS-CoV-2, SARS-CoV and MERS-CoV, or with an empty plasmid as a negative control. The monoclonal antibodies were then tested by flow-cytometry at 10 μg/ml for their ability to stain ExpiCHO cells expressing the S protein of 2019-nCoV, SARS-CoV, MERS-CoV or Mock cell transfectants.

Transient expression of recombinant SARS-CoV-2 protein

The full-length S gene of SARS-CoV-2 strain (2019-nCoV-S) isolate BetaCoV/Wuhan-Hu-1/2019 (accession number MN908947) was codon optimized for human cell expression and cloned into the phCMV1 expression vector (Genlantis). Expi-CHO cells were transiently transfected with phCMV1-SARS-CoV-2-S, phCMV1-MERS-CoV-S (London1/2012), SARS-spike_pcDNA.3 (strain SARS) or the empty phCMV1 (Mock) using Expifectamine CHO Enhancer. Two days after transfection, cells were collected, fixed, or fixed and permeabilized with saponin for immunostaining with a panel of monoclonal antibodies reactive to SARS-CoV Receptor Binding Domain (RBD). An Alexa647-labelled secondary antibody anti-human IgG Fc was used for detection. Binding of antibodies to transfected cells was analyzed by flow-

cytometry using a ZE5 Cell Analyzer (Biorard) and FlowJo software (TreeStar). Positive binding was defined by differential staining of CoV-S-transfectants versus mock-transfectants.

Competition experiments using Octet (BLI, biolayer interferometry)

Unless otherwise indicated herein, anti-His sensors (BIOSENSOR ANTI-PENTA-HIS (HIS1K)) were used to immobilize the S1 subunit protein of SARS-CoV (Sino Biological Europe GmbH). Sensors were hydrated for 10 min with Kinetics Buffer (KB; 0.01% endotoxin-free BSA, 0.002^ Tween-20, 0.005% NaN3 in PBS). SARS-CoV S1 subunit protein was then loaded for 8 min at a concentration of 10 µg/ml in KB. Antibodies were associated for 6 min at 15 µg/ml for full length mAbs nCoV-10 and nCov-6 mAbs or 5 µg/ml for Fab nCoV-4, and in a subsequent experiment comprising nCoV-1 all at 10 µg/ml. Competing antibodies were then associated at the same concentration for additional 6 mins.

Competition experiments using Octet (BLI, biolayer interferometry)

For ACE2 competition experiments, ACE2-His (Bio-Techne AG) was loaded for 30 minutes at 5 µg/ml in KB onto anti-HIS (HIS2) biosensors (Molecular Devices-ForteBio). SARS-CoV-1 RBD-rabbitFc or SARS-CoV-2 RBD-mouseFc (Sino Biological Europe GmbH) at 1 µg/ml was associated for 15 minutes, after a preincubation with or without antibody (30 µg/ml, 30 minutes). Dissociation was monitored for 5 minutes.

Affinity determination using Octet (BLI, biolayer interferometry)

For K_D determination of full-length antibodies, protein A biosensors (Pall ForteBio) were used to immobilize recombinant antibodies at 2.7 µg/ml for 1 minute, after a hydration step for 10 minutes with Kinetics Buffer. Association curves were recorded for 5min by incubating the antibody-coated sensors with different concentration of SARS-CoV-1 RBD (Sino Biological) or SARS-CoV-2 RBD (produced in house; residues 331-550 of spike from BetaCoV/Wuhan-Hu-1/2019, accession number MN908947). Highest RBD concentration tested was 10ug/ml, then 1:2.5 serially diluted. Dissociation was recorded for 9min by moving the sensors to wells

containing KB. K_D values were calculated using a global fit model (Octet). Octet Red96 (ForteBio) equipment was used.

For K_D determination of full-length antibodies compared to Fab fragments, His-tagged RBD of SARS-CoV-1 or SARS-CoV-2 were loaded at 3 μg/ml in KB for 15 minutes onto anti-HIS (HIS2) biosensors (Molecular Devices, ForteBio). Association of full-length antibody and Fab was performed in KB at 15 ug/ml and 5 ug/ml respectively for 5 minutes. Dissociation in KB was measured for 10min.

ELISA binding

The reactivities of mAbs with SARS-CoV Spike S1 Subunit Protein (strain WH20) protein were determined by enzyme-linked immunosorbent assays (ELISA). Briefly, 96-well plates were coated with 3 μg/ml of recombinant SARS-CoV Spike S1 Subunit Protein (Sino. Biological). Wells were washed and blocked with PBS+1%BSA for 1 h at room temperature and were then incubated with serially diluted mAbs for 1 h at room temperature. Bound mAbs were detected by incubating alkaline phosphatase-conjugated goat anti-human IgG (Southern Biotechnology: 2040-04) for 1 h at room temperature and were developed by 1 mg/ml p-nitrophenylphosphate substrate in 0.1 M glycine buffer (pH 10.4) for 30 min at room temperature. The optical density (OD) values were measured at a wavelength of 405 nm in an ELISA reader (Powerwave 340/96 spectrophotometer, BioTek).

Neutralization assay

Unless otherwise indicated, Murine leukemia virus (MLV) pseudotyped with SARS-CoV-2 Spike protein (SARS-CoV-2pp) or SARS-CoV-1 Spike protein (SARS-CoV-1pp) were used. DBT cells stably transfected with ACE2 (DBT-ACE2) were used as target cells. SARS-CoV-2pp or SARS-CoV-1pp was activated with trypsin TPCK at 10ug/ml. Activated SARS-CoV-2pp or SARS-CoV-1pp was added to a dilution series of antibodies (starting 50ug/ml final concentration per antibody, 3-fold dilution). DBT-ACE2 cells were added to the antibody-virus mixtures and incubated for 48h. Luminescence was measured after aspirating cell culture supernatant and adding steady-GLO substrate (Promega).

Unless otherwise indicated, pseudoparticle neutralization assays use a VSV-based luciferase reporter pseudotyping system (Kerafast). VSV pseudoparticles and antibody are mixed in DMEM and allowed to incubate for 30 minutes at 37C. The infection mixture is then allowed to incubate with Vero E6 cells for 1h at 37C, followed by the addition of DMEM with Pen-Strep and 10% FBS (infection mixture is not removed). The cells are incubated at 37C for 18-24 hours. Luciferase is measured using an Ensight Plate Reader (Perkin Elmer) after the addition of Bio-Glo reagent (Promega).

SPR single-cycle kinetics

SPR experiments were carried out with a Biacore T200 instrument using a single-cycle kinetics approach. S309 IgG was captured on the surface and increasing concentrations of purified SARS-CoV-2 RBD, either glycosylated or deglycosylated, were injected. Association and dissociation kinetics were monitored and fit to a binding model to determine affinity.

Expression of recombinant antibodies

Recombinant antibodies were expressed in ExpiCHO cells transiently co-transfected with plasmids expressing the heavy and light chain as previously described. (Stettler *et al.* (2016) Specificity, cross-reactivity, and function of antibodies elicited by Zika virus infection. Science, 353(6301), 823–826) Monoclonal antibodies S303, S304, S306, S309, S310, and S315 were expressed as rIgG-LS antibodies. The LS mutation confers a longer half-life in vivo. (Zalevsky *et al.* (2010) Enhanced antibody half-life improves in vivo activity. Nature Biotechnology, 28(2), 157–159)

Sequence alignment

SARS-CoV-2 genomics sequences were downloaded from GISAID on March 29th 2020, using the "complete (>29,000 bp)" and "low coverage exclusion" filters. Bat and pangolin sequences were removed to yield human-only sequences. The spike ORF was localized by performing reference protein (YP_009724390.1)-genome alignments with GeneWise2. Incomplete matches and indel-containing ORFs were rescued and included in downstream analysis. Nucleotide sequences were translated *in silico* using seqkit. Sequences with more than 10% undetermined aminoacids (due to N basecalls)

were removed. Multiple sequence alignment was performed using MAFFT. Variants were determined by comparison of aligned sequences (n=2,229) to the reference sequence using the R/Bioconductor package Biostrings. A similar strategy was used to extract and translate spike protein sequences from SARS-CoV genomes sourced from ViPR (search criteria: SARS-related coronavirus, full-length genomes, human host, deposited before December 2019 to exclude SARS-CoV-2, n=53). Sourced SARS-CoV genome sequences comprised all the major published strains, such as Urbani, Tor2, TW1, P2, Frankfurt1, among others. Pangolin sequences as shown by Tsan-Yuk Lam *et al* were sourced from GISAID. Bat sequences from the three clades of Sarbecoviruses as shown by Lu *et al* (Lancet 2020) were sourced from Genbank. Civet and racoon dog sequences were similarly sourced from Genbank.

EXAMPLE 2

MAPPING NEUTRALIZING AND IMMUNODOMINANT SITES ON THE SARS-COV-2 SPIKE RECEPTOR-BINDING DOMAIN BY STRUCTURE-GUIDED HIGH-RESOLUTION SEROLOGY

Analysis of the specificity and kinetics of neutralizing antibodies (Abs) elicited by SARS-CoV-2 infection is important for understanding immune protection. In a cohort of 647 SARS-CoV-2-infected subjects, it was found that both the magnitude of Ab responses to SARS-CoV-2 spike (S) and nucleoprotein and nAb titers correlate with clinical scores. Based on these studies, the receptor-binding domain (RBD) is immunodominant and is the target of 90% of the neutralizing activity present in SARS-CoV-2 immune sera. Whereas overall RBD-specific serum IgG titers waned with a half-life of 49 days, titers and avidity of blocking antibodies increased over time for some individuals, consistent with affinity maturation. An RBD antigenic map was structurally defined and serum Abs specific for distinct RBD epitopes were serologically quantified, leading to the identification of two major receptor-binding motif antigenic sites.

IgG, IgA and IgM response to SARS-CoV-2 infection

Plasma or serum samples collected between March and July 2020 from 647 SARS-CoV-2-infected individuals, as determined by PCR (n=271) or by diagnosis based on signs and symptoms (n=392), were analyzed. A total of 1,078 samples, including multiple time points, were collected from 5 different cohorts in Italy, Switzerland and the US, which comprised 47 hospitalized, 556 symptomatic and 44 asymptomatic individuals, as well as 32 pre-pandemic healthy donors (Figures 23A-23C). For each sample, IgG, IgA, and IgM binding titers to the SARS-CoV-2 prefusion-stabilized S ectodomain (Walls et al., 2020), the RBD, domain A (residues 14-302), the S_2 subunit (residues 685-1211) and the N protein, were evaluated by ELISA.

The IgG responses were on average 1-2 orders of magnitude higher in hospitalized relative to non-hospitalized individuals and varied across SARS-CoV-2 antigens and among subjects (Figures 28A and 24A). Males had higher Ab titers than females, although no correlation with age was observed. Levels of SARS-CoV-2 S- and N-specific IgG correlated within each individual (p value <0.0001) (Figure 24D). SARS-CoV-2 RBD-specific Abs dominated IgG responses whereas much lower titers were observed to the S_2 subunit or domain A (Figure 28A). These findings might be related to the more extensive N-glycan shielding of domain A and the S_2 subunit, which respectively harbor 8 and 9 oligosaccharides, relative to the RBD that only possesses 2 N-linked glycans (Walls et al., 2020; Watanabe et al., 2020). The majority of samples contained IgG cross-reactive to the SARS-CoV prefusion-stabilized S ectodomain (Walls et al., 2019) and RBD with 3-fold and 15-fold lower binding titers than those for the corresponding SARS-CoV-2 antigens, respectively (Figures 24E-24G). The observed cross-reactivity between these two viruses are consistent with the 76% sequence identity shared between the two S glycoprotein ectodomains and recent findings (Barnes et al., 2020).

IgA responses to SARS-CoV-2 S and N were detected almost exclusively in hospitalized patients (Figures 28B and 24B) whereas IgM responses were limited to S and undetectable for N (Figures 28C and 24C). In addition, SARS-CoV-2 S- and RBD-specific IgM were detectable up to 60 days after symptom onset, suggesting that

detection of IgM antibodies is not associated with an ongoing or recent infection (Figure 24C). Finally, in the 459 individuals of the Ticino healthcare workers cohort, for which a symptom score was available, SARS-CoV-2 RBD-specific IgG, IgA and IgM and SARS-CoV-2 N-specific IgG binding titers were proportional to the severity of symptoms (Figure 28D). This serological analysis indicates that the responses varied amongst different individuals and amongst groups, with binding titers proportional to the severity of symptoms, possibly due to a prolonged exposure to large amounts of viral antigens during the course of viral disease.

Function of Antibodies in blocking S interactions with ACE2

To determine if the RBD is the primary target of neutralizing Abs in COVID-19 convalescent plasma in this study, neutralizing titers were measured before and after Ab depletion using RBD-coated beads. An almost complete depletion of RBD-specific Abs from 21 plasma samples reduced SARS-CoV-2 neutralizing titers by ~90% on average (Figure 28E and other data not shown). It was then evaluated whether RBD-specific Abs in patient serum or plasma samples inhibit binding of the SARS-CoV-2 RBD to ACE2. Although 77% of hospitalized individuals had Ab titers that blocked SARS-CoV-2 RBD binding to ACE2 efficiently (BD80 > 10), only 18% and 11% of non-hospitalized symptomatic and asymptomatic individuals had Abs strongly interfering with ACE2 binding, respectively (Figure 28F). The proportion of non-hospitalized individuals with ACE2-blocking Abs correlated with the anti-RBD Ab binding titers which parallel symptom severity (Figures 28D, 28G and other data not shown). These results suggest that although all SARS-CoV-2-infected individuals can produce RBD-specific Abs, they may not be endowed with enough avidity or are not present at a sufficiently high concentration to block RBD binding to ACE2 effectively. This is illustrated by the large fraction of samples with RBD binding titers ranging between 10^2 to 10^3 and which did not block RBD binding to ACE2 efficiently (Figure 28H). A positive correlation between the titers of Abs inhibiting RBD binding to ACE2 and neutralizing serum Ab titers (ID80) (Figure 28I) was observed, suggesting that the blockade-of-binding approach could be implemented as a high-throughput, alternative

method to measuring serum neutralizing Ab titers, as recently suggested (Tan et al., 2020).

Collectively, these findings indicate that the Ab responses to SARS-CoV-2 S were dominated by anti-RBD Abs and that the majority of the neutralizing activity against SARS-CoV-2 was mediated by RBD-specific Abs interfering with binding to ACE2.

Kinetics of Ab responses upon natural SARS-CoV-2 infection

To characterize persistence of potentially protective Abs, a longitudinal analysis of IgG titers specific for SARS-CoV-2 antigens at two time points (average of 44 days between samples) in 368 individuals tested within 3 months of infection was performed. RBD-specific IgG titers declined by 35% on average between the two time points tested (Figures 29A-29B), with a monthly average decay of approximately 25%, and this trend was independent of the magnitude of the initial binding titers. Kinetics of RBD- and N-specific serum IgG were also followed over a period of up to 126 days from the collection of the first sample (approximately 150 days after onset of symptoms) for a subset of 24 individuals (Figure 29C). This analysis revealed an average decay of RBD-specific IgGs of 67% over four months (21% per month), consistent with the above finding with a larger cohort. To further characterize the decay kinetics of the RBD- and N-specific IgG following onset of disease symptoms, a longitudinal mixed effects model was employed in a subset of 18 convalescent, hospitalized and symptomatic, individuals who had available data on symptom onset from the start of infection (Figure 29D). The model predicted a half-life of 49 days for RBD-specific IgG Abs and 75 days for S- and N-specific IgG Abs (Figure 29D and data not shown), respectively. No significant differences were observed in the decay kinetics in the hospitalized compared to symptomatic individuals.

The kinetics of anti-RBD Ab titers blocking attachment to ACE2 did not mirror the overall decay observed for RBD-specific IgG. In the same samples, an increase in Ab titers blocking attachment to ACE2 for 47% of the individuals who made this type of Abs (which account for 20% of subjects analyzed) as observed (Figures 29E-29F). This increase, which is not influenced by the initial titer of RBD-specific Abs, might

result from the development of Abs with increasingly higher affinity, in the context of an overall waning of Abs titers targeting the RBD. Indeed, an overall increased avidity of RBD-specific Abs between the two time points tested was measured (Figures 29G-29H).

Although a progressive decay of Ab titers was observed, these results demonstrate a change in the quality of the Ab responses that may result in increased neutralizing activity based on the aforementioned correlation with blocking ACE2 attachment.

Structural characterization of the S2H13 RBM-specific neutralizing mAb recognizing multiple RBD conformers

Given the heterogeneity of the humoral responses across individuals and the fact the RBD is the prime target of neutralizing Abs, the fine specificity of RBD-targeting Abs elicited in SARS-CoV-2-exposed individuals (Figures 25A-25B) was investigated. To understand SARS-CoV-2 neutralization, six mAbs with distinct function and epitope recognition (Figures 25A-25C) were selected from a large panel of RBD-specific Abs for structural characterization of their Fab fragments in complex with the SARS-CoV-2 S ectodomain trimer by cryoEM.

S2H13, a neutralizing mAb, was isolated from plasma cells of a SARS-CoV-2 infected individual 17 days after disease onset (Figures 30A and 25A**)**. CryoEM characterization led to the identification of two conformational states corresponding to a closed S trimer and a trimer with one RBD open, each with three S2H13 Fabs bound, for which 3D reconstructions at 3.0 Å (with 3-fold symmetry) and 3.4 Å (asymmetric) resolution, respectively, were determined (Figures 30B-30D and 53A-53E; other data not shown). To improve the resolvability of the S2H13 density, which was much lower than most other regions of the map, local refinement was used to determine a reconstruction at ~3.5 Å resolution enabling building the S2H13 variable domains and its epitope (Figure 53F, other data not shown).

S2H13 recognizes an epitope located within the crevice formed by the receptor binding motif (RBM) β-hairpin of the RBD, which is accessible in both the closed and open S states, thereby explaining the stoichiometric binding of Fab to each protomer of

the S trimer (Figures 30B-30D and 27A). S2H13 recognition of the SARS-CoV-2 RBM is mediated by electrostatic interactions and shape complementarity, and is dominated by unusual contacts involving CDRL2/FRL3, accounting for 55% of the ~700Å^2 of surface area buried by the Fab, in addition to the 13-residue long CDRH3, CDRH1, FRL1 and the heavy chain N-terminal end. Specifically, S2H13 FRL1 and CDRL2/FRL3 interacts with the SARS-CoV-2 residues 444-449 whereas the heavy chain N-terminus, CDRH1, CDRH3 and CDRL2/FRL3 recognize the tip of the RBM spanning residues 472-498 (Figure 30E). Further analysis (3.0 angstrom resolution) indicated that S2H13 does not contact amino acids 448, 473-478, 487, 491, 492, 495, 496, and 497.

Superimposition of the SARS-CoV-2 RBD/ACE2 structures (Lan et al., 2020; Shang et al., 2020; Wang et al., 2020b; Yan et al., 2020) onto the SARS-CoV-2 S/S2H13 complex reveals that S2H13 and ACE2 would clash upon binding to S and that they share partially overlapping binding sites although they have almost orthogonal orientations relative to the RBD (Figure 30F). These findings were confirmed using biolayer interferometry and ELISA to show that S2H13 competes with ACE2 for recognition of the SARS-CoV-2 RBD (Figures 30G and 25D). Therefore, S2H13 may neutralize SARS-CoV-2 by preventing viral attachment to host cells via recognition of an S epitope that remains accessible in both open and closed S states, which is not the case for the ACE2-binding site.

Only 6 out of 20 residues within the S2H13 epitope are conserved across SARS-CoV-2 and SARS-CoV, explaining the lack of binding to the latter virus (Figures 30H, 25B and 26A-26B). Substitutions of 7 epitope residues have been reported among the ~74,000 SARS-CoV-2 isolates sequenced to date, indicating that potential escape mutants might have already emerged to this site (Figures 30H and 25F; other data not shown).

Structural characterization of the neutralizing S2H14 mAb targeting an RBM epitope accessible uniquely in the open S state

The S2H14 neutralizing mAb was isolated from the plasma cells from the same SARS-CoV-2 convalescent individual from which S2H13 was obtained and does not

carry somatic hypermutations in the heavy or light chain variable regions (Figures 31A and 25A).

CryoEM analysis showed that a subset of the selected particle images corresponded to an S trimer with one RBD closed and two RBDs open (Figures 31B and 31C), whereas the rest of the data featured an S trimer with all three RBDs open (Figures 31D and 31E). In agreement with ELISA data, S2H14 recognizes the RBD (Figures 25B and 27A) and each of the three RBDs interacted with an S2H14 Fab in both conformational states. Asymmetric 3D reconstructions for each of the two conformational states were determined at 7.8 Å and 8.5 Å resolution, respectively, along with crystal structures of the S2H14 Fab and the RBD bound to the S2H14, S309 and S304 Fabs at 2.5Å and 2.65Å resolution, respectively (Figures 31B-31E and 53G-53K; other data not shown).

The observation of SARS-CoV-2 S trimers with two and three RBDs open suggest that S2H14 binding conformationally selects open RBDs in a way reminiscent of the SARS-CoV S230 (Walls et al., 2019) and of the SARS-CoV-2 C105 (Barnes et al., 2020) neutralizing mAbs. Indeed, these findings differ from what those observed for SARS-CoV-2 S without (Walls et al., 2020) or with bound Fabs, such as S309 (Pinto et al., 2020) or S2H13, which recognize epitopes accessible in all prefusion S states, hence no conformational selection occurred. Although the S2H14 epitope is masked in the closed S trimer, the present cryoEM data show that opening of two RBDs is enough to allow three Fabs to bind to an S trimer, as the remaining closed RBD can engage a Fab due to its angle of approach (Figures 26B and 26C).

S2H14 recognizes an epitope overlapping with the RBM which is inaccessible in the closed S state but becomes exposed upon RBD opening (Figures 26B-26E), similar to the ACE2-binding site (Walls et al., 2020; Wrapp et al., 2020). The crystal structure of the RBD bound to the S2H14, S309 and S304 Fabs show that CDRH1-H3 and CDRL1-L3 participate in the CDRH3-dominated S2H14 paratope which buries 900Å^2 at the interface with the RBM. The epitope spans the entire RBM crevice and involves SARS-CoV-2 S residues 403, 444-456, 475 and 485-505 that interact with S2H14 via hydrogen-bonding and shape complementarity (Figure 26A). Further

analysis indicated that S2H14 does not contact amino acids 448, 450, 451, 452, 454, 486, 488, 490, 491, 492, 497, 503, and 504.

The structures show that S2H14 and ACE2 bind to largely overlapping sites in the RBM (Figure 4F) and would be sterically incompatible with simultaneous binding to a single SARS-CoV-2 RBD (Figure 4G). This observation was validated using biolayer interferometry and ELISA to show that S2H14 competed with ACE2 for recognition of the SARS-CoV-2 RBD (Figures 4H and 25D), indicating that S2H14 likely neutralizes SARS-CoV-2 through inhibition of virus/host cell interaction.

13 out of 23 epitopes residues are substituted between SARS-CoV-2 and SARS-CoV, thereby rationalizing the lack of cross-reactivity of S2H14 with the latter virus (Figure 4I, Figures 25B and 26A-26B; other data not shown). Moreover, SARS-CoV-2 variants have already been detected for 13 epitope residues which suggests that some of the viruses currently circulating in humans might be able to escape S2H14-mediated neutralization (Figure 25F).

The S2A4 mAb recognizes a cryptic epitope leading to release of the S_1 subunit

The S2A4 mAb was isolated from memory B cells of a hospitalized patient 24 days after disease onset and was found to weakly neutralize SARS-CoV-2 infection (Figures 32A and 25A).

2D and 3D classification of the cryoEM dataset revealed the presence of three distinct open conformations of the S trimer, with three bound S2A4 Fabs and RBDs swung out to various extent, as well as an S_1 subunit trimer class (Figures 32B-32C and 54A-54H). 3D reconstructions of the three open conformations of the S/S2A4 complex at 3.3 Å resolution (applying 3-fold symmetry) and at 3.8Å and 3.9Å resolution (asymmetric) were determined (Figures 32B, 32C and 54A-54H; other data not shown). To improve the resolution of the S2A4 density, which was lower than the overall map resolution, local refinement was used to yield a reconstruction at 3.6 Å resolution allowing to build the S2A4 variable domains, which was subsequently validated by determining a crystal structure of the S2A4 Fab at 2.5Å resolution (Figures 54D-54E; other data not shown). Furthermore, a low-resolution reconstruction of the S_1 subunit trimer bound to three S2A4 Fabs was obtained (Figures 54G and 54H).

S2A4 binds to a cryptic epitope (distinct from the RBM) requiring opening of two adjacent RBDs to be unmasked and allow Fab binding (Figures 32B-32C). This finding along with the detection of an S_1 subunit trimer class, which may be triggered S with a disordered fusion machinery remaining covalently linked (Figure 25G), suggest that S2A4 acts as a molecular ratchet biasing the SARS-CoV-2 S conformational equilibrium towards opened RBDs. These results were confirmed by showing that S2A4 promoted shedding of the S_1 subunit from cell-surface expressed full-length wild-type S, as was the case with the RBM-targeted S2H14 (Figure 25E). These data are also in line with previous reports of the SARS-CoV neutralizing mAb S230- and ACE2-mediated transition of SARS-CoV S from the prefusion to the postfusion states (Song et al., 2018; Walls et al., 2019), the cryoEM observation of S_1 subunit trimers released from the MERS-CoV S ectodomain upon cleavage at S_1/S_2 (Yuan et al., 2017) and the fact that S spontaneously refolds to the postfusion state in the absence of the S_1 subunit (Walls et al., 2017).

S2A4 binding to the RBD buries an average surface of ~850Å^2 using all six CDR loops along with contributions from FRH3 and FRL3. CDRH3 and CDRL1 dominate the interface which involve electrostatic and hydrophobic interactions (Figures 32D and 32E). The S2A4 epitope comprises residues 368-388, which form two α-helices and an intervening β-strand participating in the formation of the structurally conserved RBD β-sheet, and residues 407-414 forming an α-helix followed by a loop segment (Figures 32D, 32E and Figure 26A).

S2A4 recognizes an epitope distinct from the RBM and its footprint does not overlap with the ACE2-binding site (Figure 32F). However, the present cryoEM structure indicates that upon binding S2A4 would sterically clash with ACE2 interacting with the same protomer within an S trimer. Biolayer interferometry and ELISA were used to validate these structural findings and demonstrated that S2A4 and ACE2 compete for binding to the SARS-CoV-2 RBD indicating that the neutralizing activity of this Ab likely results from preventing viral attachment to its host cell receptor, albeit with moderate efficiency (Figures 32G and 25D).

Sixteen out of 19 epitope residues are conserved across SARS-CoV-2 and SARS-CoV S glycoproteins (Figures 32H, 26A-26B and 25F; other data not shown). However, S2A4 does not cross-react with the SARS-CoV RBD putatively due to steric hindrance with a glycan at position N357 which is absent in the SARS-CoV-2 RBD (Figures 32H, 25B and 26A).

Identification of a SARS-CoV-2 S cryptic supersite defined by the cross-reactive S304 mAb along with S2A4, S2X35 and CR3022 mAbs

Previously isolated from a SARS survivor were two weakly neutralizing, cross-reactive mAbs (S304 and S315) that bind the RBD at sites distinct from both the RBM and the S309 epitope (Figures 25A-25C) (Pinto et al., 2020). Cocktails containing either of these two mAbs with S309 led to synergistic enhancement of the S309 neutralization potency against SARS-CoV-2 (Pinto et al., 2020).

Similar to S2A4, 3D classification of the cryoEM data for the S/S304 complex revealed the presence of three distinct open conformations of the S trimer, with three bound Fabs and RBDs swung out to various extent, as well as an S_1 subunit trimer class bound to three S304 Fabs (Figures 33A-33C and 54I-54O; other data not shown). A 3D reconstruction at 4.3 Å resolution (applying 3-fold symmetry) for one of the open S states and at 8 Å resolution (asymmetric) for the other two classes was determined (Figures 33A-33B and 54I-54M; other data not shown). Furthermore, 10Å resolution cryoEM reconstruction of the S_1 subunit trimer with 3 bound S304 Fabs was obtained (Figures 33C, 547N-54O).

S304 recognizes a cryptic epitope, which is buried in the closed S conformation but is distinct from the RBM, with one S304 Fab bound to each of the three open RBDs (Figures 33A-33B). CDRH1-H3, CDRL1 and CDRL3 interact with SARS-CoV-2 S through burial of an average surface area of 900$Å^2$ at the epitope/paratope interface involving electrostatic interactions and shape complementarity (Figure 33D). Based on the crystal structure of the RBD/S304/S309/S2H14 complex, the S304 epitope comprises residues 366-392, which form two α-helices and an intervening β-strand, as well as residues 515-517 (both regions participating in the formation of the structurally conserved RBD β-sheet), and loop residues 411-414 and 427-430 (Figure 33D and

Figure 26A). Although S304 binds away from the RBM, partial competition between S304 and ACE2 for binding to the SARS-CoV-2 RBD was observed, which might be explained by steric hindrance with the ACE2 N322 glycan and/or with the ACE2 N-terminus (through the heavy chain constant domain of S304 bound to a neighboring protomer) (Figures 33E and 25D).

Cross-reactivity of S304 with SARS-CoV-2 S and SARS-CoV S is explained by the conservation of 23 out of 25 epitope residues with neither of the two substitutions ($P_{SARS\text{-}CoV\text{-}2}384A_{SARS\text{-}CoV}$ and $T_{SARS\text{-}CoV\text{-}2}430M_{SARS\text{-}CoV}$) predicted to affect binding in light of structural data (Figures 33F, 25B and 26A). The conserved nature of the S304 epitope among the 74,000 SARS-CoV-2 isolates sequenced to date along with the high amino acid sequence identity within the epitope among sarbecoviruses indicate that S304 is likely to cross-react with other related sarbecoviruses (Figures 25F, 26B and other data not shown).

The S304 epitope partially overlaps with the epitopes of the weakly neutralizing mAb CR3022 (Huo et al., 2020; Joyce et al., 2020; ter Meulen et al., 2006; Tian et al., 2020; Yuan et al., 2020) and of the neutralizing mAb S2A4 (Figure 33G). It also overlaps with the mAb S2X35 which was isolated from the memory B cells of a COVID-19 convalescent symptomatic individual 48 days after disease onset and which neutralizes entry of SARS-CoV-2 pseudovirus into cells with IC_{50} values of 500 ng/ml (Figures 33H, 25A-25C and other data not shown). Although these mAbs have distinct angles of approach (Figures 33E, 33G and 33H), they conformationally select for open RBDs through recognition of cryptic epitopes requiring opening of at least two RBDs for binding, and lead to release of the S_1 subunit (Figure 25E). Comparison of the binding poses of these mAbs relative to the SARS-CoV-2 RBD reveal that their neutralization potencies correlate with the Fab proximity to the RBM. Both S2X35 and S2A4 Fabs sterically clash with ACE2 and are more potent neutralizers than S304, which putatively only partially overlap with ACE2 (Figures 33E, 33G, 33H and 25D). Collectively, these data suggest that the ability to hinder ACE2 binding by some mAbs recognizing this cryptic supersite largely explain their neutralization potencies.

Fc-mediated effector activation mechanisms by RBD-specific neutralizing mAbs

Natural killer-dependent mAb-mediated cell cytotoxicity (ADCC) or macrophage/dendritic cell-dependent mAb-mediated cellular phagocytosis (ADCP) can participate in controlling infections by clearing viruses and infected cells and by stimulating T cell response via presentation of viral antigens (DiLillo and Ravetch, 2015; He et al., 2017). Among the 6 mAbs structurally characterized in this study, S2H13 and S309 promoted ADCC as measured by FcγRIIIa (V158 allele) activation (Figure 25H). A weak activation of FcγRIIa, which is a reporter for ADCP, was observed for S2H13, S2H14 and S2X35, as compared to the robust activation previously observed with mAb S309 (Pinto et al., 2020) (Figure 25I). Similarly to what observed in ADCC, only S2H13 and S309 promoted complement-dependent cytotoxicity (Figure 25J). These findings may result from the different orientation and/or positioning of the S-bound mAb Fc fragments relative to FcγRIIIa and FcγRIIa receptors, as well as to the C1q subcomponent of the classical complement pathway, and suggests that only a fraction of RBD-specific Abs can recruit Fc-dependent protective mechanisms *in vivo*, as previously shown for other antiviral Abs (Corti et al., 2011; Hessell et al., 2007; Pinto et al., 2020).

Definition of humoral immunodominant responses in SARS-CoV-2 infected individuals

The epitopes recognized by the 5 aforementioned structurally characterized human mAbs along with S309 cover a large fraction of the SARS-CoV-2 RBD surface and collectively define an RBD antigenic map (Figures 34A and 25C). S2H14 and S2H13 define two classes of RBM-targeting mAbs recognizing sites that are referred to here as Ia and Ib, respectively. Site Ia largely overlaps with the ACE2-binding site and is only accessible in the open S state (Figure 34B), whereas site Ib partially overlaps with the ACE2 footprint and is accessible in both the open and closed S states (Figure 34C). These epitopes are SARS-CoV-2-specific and harbor several naturally occurring mutations among circulating viral isolates (Figure 25F andother data not shown). The S2X35, S2A4 and S304 mAbs recognize overlapping cryptic epitopes, that are only accessible when at least two RBDs are open, respectively termed sites IIa, IIb and IIc, which are positioned increasingly further away from the ACE2-binding site (Figures

34D-34F). Finally, S309 binds to a conserved epitope termed site IV, which is accessible independently of the RBD conformation, and neutralizes SARS-CoV-2 without interfering with ACE2 binding (Figure 34G) (Pinto et al., 2020).

S309 and S2H13 are set apart from the other mAbs studied here as they recognize epitopes accessible in both the closed and open S states. Consistent with a recent report that the closed S state is favored at endosomal pH (Zhou et al., 2020b), binding of all mAbs to the S ectodomain was dampened at pH 5.4, except for S309 and S2H13, whereas binding of all these mAbs to the free RBD was not affected at pH 5.4 (Figures 27A and 27B). S309 and S2H13 do not select for a specific S conformation nor promote S_1 shedding, which are specific features of site Ia- and site II-targeted mAbs (Figure 25E). Based on these data, high-density binding of S309 or S2H13 to multiple S conformations may explain their unique ability to trigger Fc-mediated effector functions efficiently among the panel of mAbs tested.

To characterize the fine specificity of Ab responses to the RBD in SARS-CoV-2 infected individuals, a quantitative blockade-of-binding assay was developed using the 6 structurally defined mAbs as probes for the corresponding antigenic sites (Figures 34B-34G). Abs against sites Ia and Ib were found at high titers in hospitalized donors and in a fraction of non-hospitalized symptomatic and asymptomatic subjects, and correlated with the titer of Abs blocking binding of the RBD to ACE2 (Figures 34H-34K). The serological response to the other RBD antigenic sites was overall lower (or null) but showed distinct signatures in different individuals. In particular, Abs to any RBD sites were not detected in 22% of non-hospitalized individuals. Although the possible existence of additional antigenic sites cannot be ruled out, a plausible explanation is that these individuals possess low level of RBD-specific Abs (Figures 34K-34L), putatively with low avidity, compounding their detection in the blockade-of-binding assay. In addition, the overall decline of the total anti-RBD Abs was paralleled by a similar decay of Abs directed to each RBD site (data not shown). Collectively, these results demonstrate that the SARS-CoV-2 RBD is the main target of neutralizing Abs and that sites Ia and Ib are prime antigenic sites.

Discussion

This study provides an extensive analysis of Ab responses to SARS-CoV-2 S, RBD and N in more than 600 SARS-CoV-2 infected individuals with different clinical outcomes. Collectively, these data define the immunodominance of the RBD and highlight qualitative and quantitative differences in the serological response of different individuals. The SARS-CoV-2 RBD is immunodominant in terms of total Abs elicited and is the target of 90% of the neutralizing activity present in the sera or plasma of most individuals evaluated. The remaining neutralizing activity observed in certain individuals may be accounted for by Abs targeting domain A (Chi et al., 2020), quaternary epitopes on the S trimer or the S_2 subunit (Liu et al., 2020a).

Information gained from 6 different mAb structures to develop a high-resolution serological epitope-mapping approach and define a blueprint of polyclonal Ab responses to the SARS-CoV-2 RBD. These data present a quantitative antigenic map of the epitopes targeted by neutralizing mAbs that explains immunodominance, neutralization properties and activation of effector functions. These studies showed that the RBM is immunodominant and comprises two partially overlapping antigenic sites (Ia and Ib defined by mAbs S2H14 and S2H13, respectively) targeted by neutralizing Abs inhibiting ACE2 attachment. Whereas site Ia coincides with the ACE2 binding site and is accessible only in the open S conformation, site Ib is also exposed in the closed S conformation and is targeted by Abs with both neutralizing activity and effector function. In contrast, the remaining RBD sites, IIa, IIb, IIc and IV, are subdominant and generate lower and variable Ab responses in different individuals. The immunodominance of sites Ia and Ib may be related to their greater accessibility compared to sites IIa, IIb and IIc, as the latter epitopes become exposed only after opening of two RBDs, which is a rare event (Ke et al., 2020; Walls et al., 2020; Wrapp et al., 2020). Although site IV is accessible in both open and closed S conformations, its subdominance may result from the masking effect of a conserved glycan (at position N343) within this antigenic site (Pinto et al., 2020). Overall, the observed increase in Ab titers blocking RBD attachment to ACE2 in the context of waning Ab titers is consistent with the putative production of higher affinity RBD-specific Abs, most of them targeting sites Ia and Ib.

Numerous amino acid substitutions have been detected in the RBD, with several of them found in the RBM (including the S2H13 and S2H14 epitopes), of the 74,000 SARS-CoV-2 isolates available to date in the GISAID database (Elbe and Buckland-Merrett, 2017). As sites Ia and Ib within the RBM are prime targets of neutralizing Abs, mutations leading to viral escape from mAb neutralization might have been selected, possibly during prolonged infections, eventually resulting in antigenic drift similar to influenza A viruses (Hensley et al., 2009). This is supported by the fact that naturally occurring RBD mutations were recently associated with escape from mAb binding and with reduced recognition by immune sera (Li et al., 2020b).

Fc-mediated effector functions are key antiviral pathways *in vivo* that can be profoundly affected by the epitope specificities of the mAbs (DiLillo et al., 2014; Hessell et al., 2007). The finding that only S309 and S2H13 (out of the six mAbs evaluated in this study) efficiently activated effector functions underscores the importance of the orientation and distance of the Fc fragment from the plasma membrane (DiLillo et al., 2016; Pinto et al., 2020; Tang et al., 2019) and the requirement for a high density binding of mAbs for efficient Fc receptors cross-linking and engagement of the hexameric C1q. Both S309 and S2H13 mAbs recognize epitopes accessible independent of the RBD conformation and are therefore expected to reach high occupancy on S trimers (Ortiz et al., 2016). Instead, Abs targeting site Ia and site II promote shedding of the S_1 subunit which may limit their ability to trigger effector functions. Further studies are performed to address whether bivalent binding by IgG molecules within a single S is possible and what could be role of cross-linking neighboring S proteins on virions or between virions.

Table 3.

STAR METHODS

REAGENT or RESOURCE	**SOURCE**	**IDENTIFIER**
Antibodies		

S304	(Pinto et al., 2020)	N/A
S309	(Pinto et al., 2020)	N/A
S304 Fab	ATUM	N/A
S309 Fab	ATUM	N/A
S2H14 Fab	ATUM	N/A
Goat F(ab')2 Anti-Mouse IgG(H+L), Human ads-AP	Southern Biotech	Cat. No. 1030-04
Goat Anti-Human IgG-AP	Southern Biotech	Cat. No. 2040-04
Goat Anti-Human IgA-AP	Southern Biotech	Cat. No. 2050-04
Goat Anti-Human IgM-AP	Southern Biotech	Cat. No. 2020-04
Alexa Fluor® 647-AffiniPure F(ab')2 Fragment Goat Anti-Human IgG, Fcγ Fragment Specific	Jackson ImmunoResearch	Cat. No. 109-606-098
Avi-tag Antibody, pAb, Rabbit	Genscript	Cat. No. A00674
Bacterial strains and pseudotype viruses		
NEB® 10-beta Competent E. coli	New England Biolabs	Cat. No. C3019

VSV-SARS-CoV-2 S-glycoprotein-pseudotyped virus	(Ou et al., 2020)	N/A
MLV-based SARS-CoV-2 S-glycoprotein-pseudotyped virus	(Walls et al., 2020)	N/A
Biological samples		
Serum and plasma of SARS-CoV-2 infected individuals	This paper	N/A
Serum and plasma of pre-pandemic healthy donors	This paper	N/A
PBMCs of donors S2A, S2H, S2X	This paper	N/A
Chemicals and Recombinant Proteins		
10% Igepal CA-630	Sigma-Aldrich	Cat. No. I8896
25 mM dNTPs	Cytiva	Cat. No. 28406560
RNase OUT	Life Technologies	Cat. No. 10777-019
Superscript III RT	Life Technologies	Cat. No. 18080-044
DNase/RNase free water	Life Technologies	Cat. No. 10977-035
10 mM dNTPs	Cytiva	Cat. No. 28406564

mix		
Q5 high fidelity DNA polymerase	Bioconcept	Cat. No. M0493S
AgeI-HF	New England Biolabs	Cat. No. R3552
SalI-HF	New England Biolabs	Cat. No. R3138
XhoI	New England Biolabs	Cat. No. R0146
BsiWI	New England Biolabs	Cat. No. R3553
NotI	New England Biolabs	Cat. No. R0189
KpnI	New England Biolabs	Cat. No. R0142
Cutsmart	New England Biolabs	Cat. No. B7204S
T4 DNA ligase	New England Biolabs	Cat. No. M0202
T4 ligase buffer	New England Biolabs	Cat. No. B0202S
293fectin	ThermoFisher Scientific	Cat. No. 12347019
PEI MAX	Polysciences	Cat. No. POL24765-1
4-Nitrophenyl phosphate disodium salt hexahydrate (pNPP)	Sigma-Aldrich	Cat. No. N2765-100TAB
ExpiFectamine	ThermoFisher	Cat. No. 14524

293 Transfection Kit	Scientific	
RBD mouse Fc-tagged	Sino Biological	Cat. No. 40592-V05H
Streptavidin-alkaline phosphatase conjugated	Jackson ImmunoResearch	Cat. No. 016-050-084
ACE2 Protein, Human	Sino Biological	Cat. No. 10108-H08H
Blocker Casein (1%) in PBS	ThermoFisher Scientific	Cat. No. 37528
Tween 20	Sigma Aldrich	Cat. No. 93773
SARS-CoV-2 S_2 sheep Fc-tagged	The Native Antigen Company	Cat. No. REC31807
Bovine Serum Albumine	Sigma	Cat. No. 3059
Trypsin, TPCK-Treated	Bioconcept	Cat. No. LS003741
Strep-Tactin XT	IBA GmbH	https://www.iba-lifesciences.com
SARS-CoV-2 Nucleoprotein, His-tagged (E. coli)	The Native Antigen Company	Cat. No. REC31812-500
Human SARS-CoV RBD His-tagged	Sino Biological	Cat. No. 40150-V08B2
Sodium thiocyanate	Sigma-Aldrich	Cat. No. 251410

(NaSCN)		
BioLock Biotin blocking solution	IBA GmbH	Cat. No. 2-0205-050
Cell lines		
Expi-CHO-S	ThermoFisher Scientific	Cat. No. A29127
HEK293T	ATCC	Cat. No. CRL-11268
Expi293F	ThermoFisher Scientific	Cat. No. A14527
CHO stably expressing WT SARS-CoV-2 S	This study	N/A
Commercial assays, kits and products		
EZ-Link™ NHS-PEG Solid-Phase Biotinylation Kit - Mini-Spin Columns	ThermoFisher	Cat. No. 21450
Pierce™ NHS-Activated Magnetic Beads	ThermoFisher	Cat. No. 88826
Streptavidin, Alexa Fluor™ 647 conjugate	Life Technologies	Cat. No. S21374
HiTrap Protein A columns (HiTrap Mab select Xtra)	Cytiva	Cat. No. 28-4082-61
HiTrap Fast desalting columns	Cytiva	Cat. No. 17-5087-01
XT Superflow®	IBA GmbH	Cat. No. 2-4026-001

high capacity cartridge		
HisTALON Superflow Cartridge, 5 ml	Takara Bio	Cat. No. 635683
HisTALON Superflow Cartridge, 1 ml	Takara Bio	Cat. No. 635650
Superdex 200 Increase 10/300 GL	Cytiva	Cat. No. 28-9909-44
Superose 6 Increase 10/300 GL	Cytiva	Cat. No. 29091596
StrepTrap HP column, 1 ml	Cytiva	Cat. No. 28-9075-46
Kifunensine	Cayman Chemical	10009437
EndoH	New England BioLabs	Cat. No. P0702L
Polyvalan Crystallophore No°1	Molecular Dimensions	Cat. No. MD2-82
Spectraplate-384 with high protein binding	Perkin Elmer	Cat. No. CUSG83093
Bio-Glo™ Luciferase Assay System	Promega AG	Cat. No. G7940
ExpiFectamine™	Life	Cat. No. A29130

CHO Transfection Kit	Technologies	
ExpiFectamine 293 ™ Transfection Kit	Thermo Fisher Scientific	Cat. No. A14524
CaptureSelect CH1-XL MiniChrom column	ThermoFisher Scientific	Cat. No. 5943462005
HiPrep™ 26/10 desalting columns	Cytiva	Cat. No. 17-5087-02
Zeba ™ Spin Desalting Columns	Thermo Scientific	Cat. No. 89892
Recombinant DNA		
Human antibody expression vectors (IgG1, Igl, Igk)	Tiller et al., 2008	N/A
Plasmid encoding SARS-CoV-2 2P S ectodomain (amino acids 14-1211) with C-terminal 8xHis-Tag	(Walls et al., 2020)	GenBank: NC_045512.2
Plasmid encoding SARS-CoV-2 RBD (amino acids 328-531)	This study	GenBank: NC_045512. 2

with C-terminal 8xHis-Tag		
Plasmid encoding SARS-CoV-2 RBD (amino acids 328-531) with C-terminal Thrombin-linker-Strep-8xHis-tag	This study	GenBank: NC_045512.2
Plasmid encoding SARS-CoV 2P S ectodomain (residues 14-1211) with C-terminal Avi and 8xHis-Tag	This study	GenBank: NC_045512.2
Plasmid encoding SARS-CoV-2 domain A (amino acids 14-302) with C-terminal 8xHis-Tag	This study	GenBank: NC_045512.2
Plasmid encoding SARS-CoV 2P S ectodomain (residues 14-1193) with C-terminal 8xHis-Tag	(Walls et al., 2020)	GenBank: XXXXXXX
Plasmid encoding	This study	UniProt: Q9BYF1

human ACE2 receptor (amino acids 19-615) plus C-terminal thrombin cleavage site, Twin-Strep-10xHis-Tag		
phCMV1 expression vector	Genlantis	Cat. No. P003100
NFAT-driven luciferase gene	Promega AG	Cat. No. G9798, G7018 and G9995
Software and Algorithms		
Prism 8	GraphPad	https://www.graphpad.com/
UNICORN (v7.3)	Cytiva	https://www.cytivalifesciences.com/
OpenLAB CDS (v2.5)	Agilent Technologies	https://www.agilent.com/
Biacore T200 Evaluation Software (v3.1)	Cytiva	https://www.cytivalifesciences.com/
Coot (v0.9)	(Emsley et al., 2010)	https://www2.mrc-lmb.cam.ac.uk/personal/pemsley/coot/
MOE (v2019.0102)	Chemical Computing Group	www.chemcomp.com
Refmac5 (v5.8.0258)	(Murshudov et al., 2011)	www2.mrc-lmb.cam.ac.uk/groups/murshudov/content/refmac/refmac.html
Phaser (v2.8.3)	(McCoy et al., 2007)	www.phaser.cimr.cam.ac.uk/index.php
XDS	(Kabsch, 2010)	http://xds.mpimf-heidelberg.mpg.de/

Relion	(Scheres, 2012a)	
Warp	(Tegunov and Cramer, 2019)	
Cryosparc	(Punjani et al., 2017)	
Leginon	(Suloway et al., 2005)	
NONMEM (v7.4)	Icon Development Solutions, Hanover MD, USA	https://www.iconplc.com/innovation/nonmem/
R 4.0.2	R Studio for Statistical Computing	https://rstudio.com/products/rstudio/
Igor Pro 8 (v8.00)	WaveMetrics, Inc.	https://www.wavemetrics.com/software/igor-pro-8
MAFFT (v7.471)	(Katoh et al., 2019), (Kuraku et al., 2013)	https://mafft.cbrc.jp/alignment/server/
EMBOSS Needle	(Needleman and Wunsch, 1970)	https://www.ebi.ac.uk/Tools/psa/emboss_needle/
Instruments		
BD FACSAria III	BD Biosciences	https://www.bdbiosciences.com/
ÄKTA Xpress FPLC	Cytiva	https://www.cytivalifesciences.com/
ÄKTA Pure 25	Cytiva	https://www.cytivalifesciences.com/
Synergy H1 Hybrid Multi-Mode plate reader	Biotek	https://www.biotek.com/

EL406 washer/dispenser BSL2 M	Biotek	https://www.biotek.com/
Powerwave 340/96 spectrophotometer	Biotek	https://www.biotek.com/
Biacore T200	Cytiva	https://www.cytivalifesciences.com/
Octet Red96	Pall ForteBio	https://www.fortebio.com/
ZE5 Cell Analyzer (FACS) BSL2 M	Bio-rad	http://www.bio-rad.com/

EXPERIMENTAL MODEL AND SUBJECT DETAILS

Cell lines

Cell lines used in this study were obtained from ATCC (HEK293T, Vero-E6), Thermo-Fisher Scientific (HEK293F, Expi293F) or Invitrogen (Expi-CHO-S cells). All cell lines used in this study (except HEK293F and Expi293F) were routinely tested for mycoplasma and found to be mycoplasma-free.

Sample donors and collection

Samples were obtained from 5 cohorts of SARS-CoV-2 infected individuals under study protocols approved by the local Institutional Review Boards (Canton Ticino Ethics Committee, Switzerland, the Ethical committee of Luigi Sacco Hospital, Milan, Italy, and WCG North America, Princeton, NJ, US). All donors provided written informed consent for the use of blood and blood components (such as PBMCs, sera or plasma) and were recruited at hospitals or as outpatients. Based on their availability, participants were enrolled and allocated to either single blood draws or longitudinal follow-up. Donors were categorized as symptomatic if they reported any COVID-19-related symptoms (a, fever; b, respiratory distress; c, cough; d, throat pain; e, common cold; f, taste loss/smell loss; g, diarrhea; h, fatigue; i, muscle bone pain; j, headache).

Donors from the Ticino healthcare workers cohort were further categorized based on symptom severity as follows: asymptomatic (declaration of no symptom experience), low symptomatic (1 or 2 symptoms of a-f and any of g-j), mild symptomatic (any 3 symptoms of a-f); high symptomatic (any 4 symptoms of a-f), severe symptomatic (any 4 symptoms of a-f, including b), atypical (all the remaining cases).

METHOD DETAILS

Isolation of peripheral blood mononuclear cells (PBMCs), plasma and sera

PBMCs and plasma were isolated from blood draw performed using tubes or syringes pre-filled with heparin, followed by Ficoll density gradient centrifugation. Sera were obtained from blood collected using tubes containing clot activator, followed by centrifugation. PBMCs, plasma and sera were stored in liquid nitrogen and -80°C freezers until use, respectively.

Ab discovery and recombinant expression

S2H13, S2H14 and S2A4 mAbs were isolated from memory B cells or plasma cells as previously described (Corti et al., 2011; Pinto et al., 2020). S2X35 was isolated from SARS-CoV-2 S-specific $CD19^+$ IgG^+ B cells sorted using a C-terminal biotinylated SARS-CoV-2 S ectodomain trimer conjugated to Streptavidin, Alexa Fluor™ 647 (Life Technologies).

Recombinant antibodies were expressed as IgG1 or Fab in ExpiCHO-S cells transiently co-transfected with plasmids expressing the heavy and light chain, as previously described (Stettler et al., 2016). Recombinant Abs were affinity purified using HiTrap Protein A columns (Cytiva) followed by desalting against phosphate-buffered saline (PBS) using HiTrap Fast desalting columns (Cytiva). All liquid chromatography purification steps were performed on a ÄKTA express FPLC (Cytiva). The final products were sterilized by filtration through 0.22 μm filters and stored at 4°C.

Fabs were expressed using transient transfection of ExpiCHO-S cells with ExpiCHO expression medium and ExpiFectamine™ CHO Transfection Kit (Life Technologies), purified by affinity chromatography on AKTA Xpress Mab System (Cytiva) with UNICORN 5.11 software version (Build 407) using CaptureSelect CH1-

XL MiniChrom column (ThermoFisher Scientific), buffer exchanged to PBS using a HiPrep™ 26/10 desalting columns (Cytiva) and sterilized through a 0.2 μm filter.

Recombinant glycoprotein production

The SARS-CoV-2 and SARS-CoV prefusion S ectodomain trimers were previously described (Walls et al., 2020; Walls et al., 2019). Briefly, the SARS-CoV-2 and SARS-CoV S ectodomains were synthesized by Genscript or GeneArt, respectively, with a mu-phosphatase signal peptide, 2P stabilizing mutation (Kirchdoerfer et al., 2018; Pallesen et al., 2017), a TEV cleavage site, foldon, and 8X His-tag. The SARS-CoV-2 domain A construct (residue 14-302) was synthesized by Genscript into pcDNA3.1- with an N-terminal mu-phosphatase signal peptide and a C-terminal octa-histidine tag (GSS(H)8). All constructs were produced in HEK293F cells grown in suspension using FreeStyle 293 expression medium (Life technologies) at 37˚C in a humidified 8% CO_2 incubator rotating at 130 rpm. The cultures were transfected using PEI (9 μg/ml) with cells grown to a density of 2.5 million cells per mL and cultivated for 3-4 days. The supernatants were harvested and cells resuspended for another 3-4 days in fresh media, yielding two harvests. Proteins were purified from clarified supernatants using a 5mL Cobalt affinity column (Takara Bio), concentrated and flash frozen in a buffer containing 20 mM Tris pH 8.0 and 150 mM NaCl prior to analysis. SDS-PAGE or negative stain EM was run to check purity.

For SPR experiments, a SARS-CoV-2 prefusion stabilized S ectodomain with an Avi-tag between the foldon domain and the 8x His-tag was codon optimized, synthesized and cloned into the phCMV1 vector by ATUM. For protein expression, Expi293F cells were transfected using ExpiFectamine according to Thermo Fisher's Expi293 expression system user guide. Supernatants were harvested after 4 days of expression and purified over a 5 mL Cobalt affinity column (Takara Bio). IMAC elution peak was pooled concentrated and injected onto a Superose 6 Increase 10/300 GL size exclusion chromatography column (Cytiva) using 1x PBS pH 7.4 as a running

buffer. SEC fractions corresponding to the main protein peak were pooled, flash frozen in liquid nitrogen and stored at -80°C.

RBD protein for ELISA was produced in Expi293 cells using the phCMV1 SARS-CoV-2 RBD plasmid, which encodes for an N-terminal mu-phosphatase signal peptide, an 'ETGT' linker, SARS-CoV-2 residues 328-531, a linker sequence and Strep-8xHis-tag. Supernatants were harvested five days after transfection, equilibrated with 0.1 M Tris-HCl, 0.15 M NaCl, 10 mM EDTA, pH 8.0 and supplemented with a biotin blocking solution (IBA Lifesciences). RBD was purified by affinity chromatography on a Strep-Trap HP 5 ml column followed by elution with 50 mM biotin and buffer exchange into PBS.

To produce SARS-CoV-2 RBD for crystallization, the phCMV1 SARS-CoV-2 RBD expression plasmid was used, which encodes for an N-terminal mu-phosphatase signal peptide, an 'ETGT' linker, SARS-CoV-2 residues 328-531 and a C-terminal 8xHis-tag. Protein was expressed in Expi293F cells in the presence of 10 μM kifunensine at 37°C and 8% CO_2 in a humidified incubator. Transfection was performed using ExpiFectamine 293 reagent (Thermo Fisher Scientific) and 1 μg plasmid per ml of cell culture. Cell culture supernatant was collected after three days, filtered through a 0.22 μm filter and supplemented with EDTA-free Protease Inhibitor (Thermo Scientific Pierce) and PBS to a final concentration of 2.5x (342.5 mM NaCl, 6.75 mM KCl and 29.75 mM phosphate). After a second filtration, SARS-CoV-2 RBD was purified using a 5 ml HisTALON Superflow cartridge (Takara Bio) and subsequently dialyzed against 50 mM Tris-HCl pH 7.5, 150 mM NaCl. SARS-CoV-2 RBD was deglycosylated by overnight incubation with EndoH glycosidase at 4°C.

For SPR, SARS-CoV-2 RBD (residues 328-531) with a C-terminal Thrombin-Twin-Strep-8xHis-tag was expressed in Expi293F cells at 37°C and 8% CO2 in a humidified incubator. Transfection was performed using ExpiFectamine 293 reagent (Thermo Fisher Scientific) and 1 μg plasmid per ml of cell culture. The protein was purified by affinity chromatography using a 1 ml HisTALON Superflow cartridge as described above (Takara Bio) and subsequently buffer exchanged using a Zeba spin desalting column into Cytiva 1x HBS-N buffer.

Antibody Fab fragments for mAbs S304, S309 and S2H14 were obtained from ATUM. To form the quaternary SARS-CoV-2 RBD-S304-S309-S2H14 Fab complex, the deglycosylated SARS-CoV-2 RBD was mixed with a 1.3-fold molar excess of S304 Fab, S309 Fab and S2H14 Fab. The complex was purified on a Superdex 200 Increase 10/300 GL column pre-equilibrated with 20 mM Tris-HCl pH 7.5, 150 mM NaCl, and concentrated to 4 mg/ml. 100 µl of the protein solution were mixed with 0.3 mg Polyvalan Crystallophore N°1 and this solution was used for setting up crystallization trays.

Recombinant ACE2 was expressed in ExpiCHO-S cells transiently transfected with a plasmid encoding ACE2 residues 19-615, a C-terminal thrombin cleavage site, Twin-Strep-tag and 10xHis-tag. Cell culture supernatant was collected after nine days, filtered through a 0.22 µm filter, supplemented with buffer to a final concentration of 80 mM Tris-HCl pH 8.0, 100 mM NaCl, and then incubated with BioLock solution for one hour. After a second filtration, ACE2 was purified using a 1 ml StrepTrap High Performance column (Cytiva) followed by size exclusion chromatography using a Superdex 200 Increase 10/300 GL column pre-equilibrated in 20 mM Tris-HCl pH 7.5, 150 mM NaCl.

Enzyme-linked immunosorbent assay (ELISA)

Spectraplate-384 with high protein binding treatment (custom made from Perkin Elmer) were coated overnight at 4°C with 1 µg/ml of SARS-CoV-2 S, domain A (in-house produced), N (The Native Antigen company), S2 (The Native Antigen company), SARS-CoV S (in-house produced) or 5 µg/ml of SARS-CoV-2/SARS-CoV RBD (in-house produced) in PBS, pH 7.2, and plates were subsequently blocked with Blocker Casein (1%) in PBS (Thermo Fisher Scientific) supplemeted with 0.05% Tween 20 (Sigma Aldrich). The coated plates were incubated with serial dilutions of human monoclonal antibodies or human plasma or sera for 1 h at room temperature. The plates were then washed with PBS containing 0.1 % Tween-20 (PBS-T), and Alkaline Phosphatase-conjugated Goat Anti-Human IgG, IgM or IgA (Southern Biotech) were added and incubated for 1 h. Plates were washed three times with PBS-T, and 4-NitroPhenyl Phosphate (pNPP, Sigma-Aldrich) substrate was added and incubated for 1

h (IgG) or 2 h (IgA and IgM). The absorbance of 405 nm was measured by a microplate reader (Biotek), and the data was plotted with Graph Prism software.

In the depletion experiments, the efficiency was calculated based on the ratio of the binding titers before and after depletion and is expressed as a percentage: (1-(ED50(after)/ED50(before))*100.

For chaotropic ELISA, after incubation with sera, plates were washed and incubated with 1 M solution of sodium thiocyanate (NaSCN) for 1 h. Avidity Index was calculated as the ratio (%) between the ED50 in presence and the ED50 in absence of NaSCN.

Depletion of RBD-specific Abs from plasma or serum samples

Magnetic beads (Pierce) were washed with ice-cold 1 mM HCl solution. 1 mg/ml RBD solution was coupled to magnetic beads in 50 mM borate buffer, pH 8.5, with a 2h incubation at room temperature. Beads were washed 3 times with 0.1 M glycine, pH 2.0, followed by a wash with purified water. Beads were then incubated with quenching buffer (3 M ethanolammine, pH 9.0) for 2 h. Beads were washed with purified water and resuspended in storage buffer (50 mM borate buffer, pH 8.5, with 0.05% sodium azide). Serum or plasma were diluted to 1/50 in 500 µl PBS containing 1/20 (25 µl) of RBD-magnetic beads and incubated for 1 h at room temperature, rotating. Tubes were placed on a magnetic holder and supernatants were collected.

Pseudovirus neutralization assays

VSV-based SARS-CoV-2 S-glycoprotein-pseudotyped viruses were used to test the neutralizing activity of serum or plasma from COVID-19 recovered patients. Briefly, HEK293T cells were transfected with a SARS-CoV-2 S glycoprotein-encoding plasmid harboring the Δ19 C-terminal truncation (Ou et al., 2020) using the X-tremeGENE HP DNA transfection reagent (Merck) according to the manufacturer's instructions and then incubated at 37 °C with 8% CO_2 for 24 h. Next, the transfected cells were infected with Delta-G-VSV-Luc in DMEM and incubated 1h at 37 °C with 5% CO_2. After removing the infection medium, the cells were washed twice with PBS

and DMEM containing 10% FBS and 1% penicillin–streptomycin was added. Infected cells were further incubated for 24 hours at 37°C before the supernatant containing the VSV-SARS-CoV-2 pseudoviruses was collected, cleaned from cellular debris by centrifugation, and stored at -80°C. VSV-SARS-CoV-2 pseudovirus was incubated with serial dilution of serum or plasma for 1 h in white culture 96 well plate at 37°C. Next, VeroE6 at 20 000 cells/well were added to the mix and incubated 2 h at 37°C. After 2 h, MEM supplemented with 40% FBS and 4% penicillin–streptomycin was added to the cells for additional 24h. Culture medium was then removed from the cells and 50 µL/well of Bio-Glo (Promega) diluted 1:2 with PBS $Ca^{2+}Mg^{2+}$ was added. After 5 minutes incubation in the dark the luminescence signal was measured using a Synergy H1 Hybrid Multi-Mode plate reader (Biotek). Measurements were performed in duplicate and relative luciferase units (RLU) were converted into neutralization percentages and plotted with a nonlinear regression curve fit in Graph Prism.

In the depletion experiments, the efficiency was calculated based on the ratio of the neutralizing titers before and after depletion and is expressed as a percentage: (1-(ID80(after)/ID80(before))*100.

MLV-based SARS-CoV-2 S-glycoprotein-pseudotyped viruses were used to test the neutralizing activity of recombinant mAbs. MLV-based SARS-CoV-2 S pseudotyped viruses were prepared as previously described (Walls et al., 2020). HEK293T cells were co-transfected with a SARS-CoV-2 S glycoprotein-encoding-plasmid harboring the Δ19 C-terminal truncation, an MLV Gag-Pol packaging construct and the MLV transfer vector encoding a luciferase reporter using the X-tremeGENE HP DNA transfection reagent (Merck) according to the manufacturer's instructions. VeroE6 cells were cultured in MEM containing 10% FBS, 1% penicillin–streptomycin and plated into 96-well plates for 16–24h at 20 000 cells/well. Pseudovirus, pre-activated with TPCK (Bioconcept) at 10 µg/mL for 1h at 37°, with or without serial dilution of antibodies was incubated for 1h and then added to the wells after washing 3X with MEM. A monoclonal antibody of unrelated specificity was used as a negative control. After 2–3h MEM containing 20% FBS and 2% penicillin–streptomycin was added to the cells for 48h. Following 48h of infection, culture medium was removed

from the cells and 50 µl/well of Bio-Glo (Promega) diluted 1:2 with PBS $Ca^{2+}Mg^{2+}$ was added to the cells and incubated in the dark for 5 min before reading on a Synergy H1 Hybrid Multi-Mode plate reader (Biotek). Measurements were done in duplicate and relative luciferase units were converted to percentage of neutralization and plotted with a nonlinear regression curve fit in Graph Prism.

Blockade of RBD binding to ACE2

Unlabeled mAbs or plasma/sera were serially diluted, mixed with RBD mouse Fc-tagged antigen (Sino Biological, final concentration 20 ng/ml) and incubated for 30 min at 37°C. The mix was added for 30 min to ELISA 96-well plates (Corning) pre-coated overnight at 4 °C with 2 µg/ml human ACE2 in PBS. Plates were washed and RBD binding was revealed using secondary goat anti-mouse IgG (Southern Biotech). After washing, pNPP substrate was added and plates were read at 405 nm. The percentage of inhibition was calculated as follow: (1−(OD sample−OD neg ctr)/(OD pos ctr−OD neg ctr)]) × 100.

Blockade of binding to RBD

Human anti-RBD full IgG1 mAbs were biotinylated using the EZ-Link NHS-PEO solid phase biotinylation kit (Pierce). Labelled mAbs were tested for binding to RBD by ELISA and the optimal concentration of each mAb to achieve 80% maximal binding was determined. Unlabeled mAbs or sera/plasma were serially diluted and added to ELISA 96-well plates (Corning) pre-coated overnight at 4 °C with 1 µg/ml of RBD mouse Fc-tagged antigen (Sino Biological) in PBS. After 30 min, biotinylated anti-RBD mAbs were added at the concentration achieving 80% maximal binding and the mixture was incubated at room temperature for 230 min. Plates were washed and antibody binding was revealed using alkaline phosphatase-comjugated streptavidin (Jackson ImmunoResearch). After washing, pNPP substrate (Sigma-Aldrich) was added and plates were read at 405 nm. The percentage of inhibition was calculated as follow: (1−(OD sample−OD neg ctr)/ (OD pos ctr−OD neg ctr)]) × 100.

Cell-surface mAb-mediated S_1 shedding

CHO cells stably expressing wild-type SARS-CoV-2 S were resuspended in wash buffer (PBS 1% BSA, 2 mM EDTA) and treated with 10 µg/ml TPCK-t (Bioconcept) for 30 min at 37°C. Cells were washed and aliquoted (90,000 cells/well). MAbs were added to cells at 15 µg/ml final concentration for 180 min at 37°C. Cells were collected at different time points (5, 15, 30, 60, 120, 180 and 240 min), washed at +4°C and incubated with 1.5 µg/ml secondary goat anti-human IgG, Fcγ fragment specific (Jackson ImmunoResearch) on ice for 20 min. Cells were washed and resuspended in wash buffer and analysed with ZE5 FACS (Bio-rad).

Western blot

SARS-CoV-2 S was incubated alone or with S2A4, S304 or S2X35 Fabs (molar ratio 1:1.2) during 0.5, 1 or 2 hr at room temperature. Laemmli loading buffer was added prior to boiling the samples for 5 min at 95°C. Samples were run on a 4%–20% gradient Tris-Glycine Gel (BioRad) and transferred to a PVDF membrane. Membrane was blocked in 5 % milk during 45 min at room temperature. An anti-S_2 SARS-CoV S monoclonal primary antibody (1:250 dilution) and an Alexa Fluor 680-conjugated goat anti-human secondary antibody (1:50,000; Jackson Laboratory) were used for Western-blotting. A LI-COR processor was used to develop images.

Measurement of effector functions

Determination of antibody-dependent activation of human FcγRIIIa was performed using SARS CoV-2 S stable transfected CHO cells as target, incubated with titrated concentrations of antibodies and after 10 min incubated with Jurkat expressing FcγRIIIa receptor on their surface and stable transfected with NFAT-driven luciferase gene (Promega, Cat. Nr. G9798 and G7018) at an effector to target ratio of 6:1. Activation of human FcγRIIIa (F158 or V158 variants) in this bioassay results in the NFAT-mediated expression of the luciferase reporter gene. Luminescence was measured after 21 hours of incubation at 37°C with 5% CO_2 with a luminometer using the Bio-Glo-TM Luciferase Assay Reagent according to the manufacturer's instructions.

Determination of antibody-dependent activation of human FcγRIIa was performed using SARS CoV-2 S stable transfected CHO cells as target, incubated with titrated concentrations of antibodies and after 10 min incubated with Jurkat expressing FcγRIIa receptor on their surface and stable transfected with NFAT-driven luciferase gene (Promega, Cat. Nr. G9995) at an effector to target ratio of 5:1. Activation of human FcγRIIa (H131 variant) in this bioassay results in the NFAT-mediated expression of the luciferase reporter gene. Luminescence was measured after 21 hours of incubation at 37°C with 5% CO_2 with a luminometer using the Bio-Glo-TM Luciferase Assay Reagent according to the manufacturer's instructions.

Complement-dependent cytotoxicity (CDC) assays were performed using SARS CoV-2 S stable transfected CHO cells as target, incubated with titrated concentrations of antibodies and after 10 min incubated at a concentration of 1:24 with Low-Tox M Rabbit Complement (Cedarlane Laboratories Limited, Cat. Nr.: CL3051) previously pre-absorbed with target cells alone in excess. Antibody dependent cell killing was measured using LDH release assay (Cytotoxicity Detection Kit (LDH) (Roche; Cat. Nr.: 11644793001) after 2 hours of incubation at 37°C.

Affinity and avidity determination by surface plasmon resonance (SPR)

SPR binding measurements were performed using a Biacore T200 instrument using either anti-AviTag pAb (for capturing S proteins) or StrepTactin XT (for capturing RBDs) covalently immobilized on CM5 chips. Running buffer for neutral pH experiments was Cytiva HBS-EP+ (pH 7.4) and for acidic pH experiments was 20 mM phosphate pH 5.4, 150 mM NaCl, 0.05% P-20. All measurements were performed at 25 °C. Acidic pH experiments were run as single-cycle kinetics. Antibody concentrations for all experiments are a 3-fold dilution series starting from 300 nM. Capture levels for neutral pH RBD experiments were ~75 RU and within 10% of each other except for S2H13 Fab data which was collected separately (capture level of ~60 RU) and scaled proportional to capture level to allow for comparison across datasets. Approximate capture levels for other data sets are: neutral pH Fab-Spike = 190 RU, neutral pH IgG-Spike = 165 RU, acidic Fab-RBD = 80 RU, acidic Fab-Spike = 205 RU, and acidic

IgG-Spike = 205 RU. Capture levels were within ~10% of each other within each neutral pH dataset, and within 3% of each other within each single-cycle, acidic pH dataset. Double reference-subtracted data were fit to a 1:1 binding model using Biacore Evaluation software, which yields an "apparent K_D" for the S-binding data because the kinetics also reflect Spike conformational dynamics and especially for the IgG binding data where the kinetics reflect avidity. RBD-binding data were fit with a Global Rmax. Spike-binding data for the tightly-associating S309 and S2X35 Fabs as well as all IgG were fit with local Rmax, since the Spike is undergoing conformational changes which can affect the accessibility of epitopes across different mAb concentrations (these $K_{D,app}$ are indicated to be approximate). For dissociation rates that were too slow to fit, $K_{D,app}$ are reported as an upper limit.

Competition experiments using biolayer interferometry (Octet)

The SARS-CoV-2 RBD was loaded for 3 min at 8 μg/ml in kinetics buffer onto anti-Penta-HIS (HIS1K) biosensors (Molecular Devices, ForteBio). Association of mAbs (full-length IgG) was performed in kinetics buffer (0.01% endotoxin-free BSA, 0.002% Tween-20, 0.005% NaN3 in PBS) at 15 μg/ml for 7 min.

Crystallization, data collection, structure determination and analysis

Crystals of the SARS-CoV-2 RBD-S304-S309-S2H14 Fab complex were obtained at 22°C by sitting drop vapor diffusion. A total of 200 nl complex were mixed with 200 nl mother liquor solution containing 16.2% (w/v) PEG 4000, 0.9 M sodium citrate pH 6.0, 0.18 M ammonium acetate, 0.02 M potassium acetate, 0.01 M MES pH 6 and 1.5% Pentaerythritol ethoxylate (15/4 EO/OH).

Data were collected at the Molecular Biology Consortium beamline 4.2.2 at the Advanced Light Source synchrotron facility in Berkeley, CA. Two individual datasets from the same crystal processed with the XDS software package (Kabsch, 2010), were merged for a final dataset at 2.65 Å in space group C2. The RBD-S304-S309-S2H14 Fab complex structure was solved by molecular replacement using Phaser (McCoy et al., 2007) and an X-ray structures of the RBD and Fabs as search models. Several

subsequent rounds of model building and refinement were performed using Coot (Emsley et al., 2010), Refmac5 (Murshudov et al., 2011), and MOE (www.chemcomp.com), to arrive at a final model for the ternary complex. Using the RBD-S304-S309-S2H14 Fab complex crystal structure, the S309, S304 and S2H14 binding epitopes on the RBD protein were determined by identifying all RBD residues within a 5.0Å distance from any Fab atoms. The analysis was performed using the Molecular Operating Environment (MOE) software package from the Chemical Computing Group (www.chemcomp.com) and the results were manually confirmed.

Optimal crystals of S2H14, S2A4 and S2X35 Fabs were obtained by the hanging-drop vapor diffusion method with a mosquito robot at 20°C. A total of 150 nl of Fabs at 20 mg per mL (for S2H14, S2A4) or at 12 mg per mL (for S2X35) in 20 mM Tris-HCl pH 8.0, 150 mM NaCl were mixed with 150nL mother liquor solution containing 0.2 M magnesium acetate and 20% (w/v) PEG 3350 (for S2H14 Fab), 1.2 M Ammonium sulfate, 0.1M Sodium cacodylate/Hydrochloric acid pH 6,5 (for S2A4 Fab) or 0.16 M $MgCl_2$, 0.08 M Tris-HCl, pH 8.5, 24% (w/v) PEG 4000 and 20% (v/v) glycerol (for S2X35 Fab). Drops were equilibrated against reservoir solutions for 1-2 weeks at room temperature after which crystals were flash cooled in liquid nitrogen using the mother liquor solution supplemented with 30% glycerol as a cryoprotectant. Diffraction data were remotely recorded on synchrotron beamline 5.0.2 at ALS, indexed and scaled using Mosfilm (Battye et al., 2011) and SCALA or aimless (Evans and Murshudov, 2013). Initial phases were obtained by molecular replacement in Phaser (McCoy et al., 2007) on the CCP4 suite, using homology models. Refinement was performed in iterations of manual model building in Coot (Emsley et al., 2010) and automatic refinement in Phenix (Liebschner et al., 2019).

CryoEM sample preparation, data collection and data processing

S2H13 Fab was generated by digestion of the corresponding monoclonal IgG with LysC (Thermo Fisher Scientific) at 1:2000 (w/w) ratio during 5 h at 37°C while Fabs S2A4, S2H14, S304 and S2X35 were recombinantly expressed as described above. SARS-CoV-2 S at 1.2 mg per mL was incubated with 1.2 molar excess of Fabs

at 4°C at least for 1 h. Three μL of 1-1.5 mg per mL of complexes was loaded onto a freshly glow discharged 1.2/1.3 UltrAuFoil grid (300 mesh) prior to plunge freezing using a vitrobot MarkIV (ThermoFisher Scientific) with a blot force of 0 and 6-7.5 s blot time at 100% humidity and 21°C.

Data were acquired on an FEI Titan Krios transmission electron microscope operated at 300 kV and equipped with a Gatan K2 Summit direct detector and Gatan Quantum GIF energy filter, operated in zero-loss mode with a slit width of 20 eV. Automated data collection was carried out using Leginon (Suloway et al., 2005) at a nominal magnification of 130,000x with a super-resolution pixel size of 0.525 Å and stage tilt angles up to 45° (Tan et al., 2017). The dose rate was adjusted to 8 counts/pixel/s, and each movie was fractionated in 50 frames of 200 ms. For the S/S304 dataset, 2,791 micrographs were collected with a defocus range comprised between -1.5 and -2.8 μm. For the S/S2H13 data set, 6,697 micrographs were collected with a defocus range comprised between -0.4 and -3.4 μm. For S2A4 data set, 1,995 micrographs were collected with a defocus range comprised between -0.4 and -2.4 μm. Movie frame alignment, estimation of the microscope contrast-transfer function parameters, particle picking and extraction were carried out using Warp (Tegunov and Cramer, 2019). Particle images were extracted with a box size of 800 binned to 400 yielding a pixel size of 1.05 Å.

For the S/S2H14 and S/S2X35 complexes, data were acquired on a FEI Glacios transmission electron microscope operated at 200 kV. Automated data collection was carried out using Leginon (Suloway et al., 2005) at a nominal magnification of 36,000x with a pixel size of 1.16 Å and stage tilt angle of 40° or 30° for S/S2H14 or S/S2X35 complexes, respectively (Tan et al., 2017). The dose rate was adjusted to 8 counts/pixel/s, and each movie was acquired in counting mode fractionated in 50 frames of 200 ms. For S/S2H14 complex, 1,886 micrographs were collected with a defocus range comprised between -1.0 and -2.5 μm. For S/S2X35 complex, 946 micrographs were collected with a defocus range comprised between -0.8 and -2.5 μm. Warp (Tegunov and Cramer, 2019) was also used for movie frame alignment,

estimation of the microscope contrast-transfer function parameters, particle picking and extraction.

For the S/S2H13, S/S2H14, S/S2A4 and S/S304 datasets, two rounds of reference-free 2D classification were performed using cryoSPARC (Punjani et al., 2017) to select well-defined particle images (only one round of reference-free 2D classification was performed for S/S2X35). Subsequently, two rounds of 3D classification with 50 iterations each (angular sampling 7.5° for 25 iterations and 1.8° with local search for 25 iterations), using our previously reported closed SARS-CoV-2 S structure as initial model (PDB 6VXX) or *ab initio* generated models for S2H14, S304 or S2X35 (Punjani et al., 2017), were carried out using Relion (Scheres, 2012b) without imposing symmetry. 3D refinements were carried out using non-uniform refinement along with per-particle defocus refinement in cryoSPARC (Punjani et al., 2019). Particle images were subjected to Bayesian polishing using Relion (Zivanov et al., 2018; Zivanov et al., 2019) before performing another round of non-uniform refinement in cryoSPARC followed by per-particle defocus refinement and again non-uniform refinement.

To further improve the density of the S2H13, S2A4 and S2X35 Fabs, the particles were symmetry-expanded and subjected to focus 3D classification without refining angles and shifts using a soft mask encompassing the RBM and S2H13 variable domains or RBD and S2A4 variable domains using a tau value of 60 (S2H13 and S2A4) or 40 for (S2X235). Particles belonging to classes with the best resolved local density were selected (all particles were retained for S2X35) and subjected to local refinement using cryoSPARC (Punjani et al., 2017; Punjani et al., 2019). Local resolution estimation, filtering, and sharpening were carried out using CryoSPARC (Cardone et al., 2013). Reported resolutions are based on the gold-standard Fourier shell correlation (FSC) of 0.143 criterion and Fourier shell correlation curves were corrected for the effects of soft masking by high-resolution noise substitution (Chen et al., 2013).

CryoEM model building and analysis.

UCSF Chimera (Pettersen et al., 2004) and Coot (Emsley et al., 2010) were used to fit atomic models (PDB 6VXX or PDB 6VYB) into the cryoEM maps and the Fab variable domains were manually built or the co-crystal structures of SARS-CoV-2 RBD with S304/S309 was used. Models were refined and relaxed using Rosetta using both sharpened and unsharpened maps (Frenz et al., 2019; Wang et al., 2016). Figures were generated using UCSF ChimeraX (Goddard et al., 2018).

Longitudinal Mixed-Effects Modeling

A non-linear mixed effects model was used to estimate parameters describing the kinetics of RBD, S- and N-specific IgG in individuals with longitudinal data following the onset of disease symptoms. Briefly, a one compartment direct response model with 1st order input and 1st order output was developed to describe the antibody response formation and decay. Individual parameters are assumed to be log-normally distributed and proportional residual error was employed in the modeling. Influence of gender, age and disease severity (hospitalized vs. symptomatic) in antibody response formation and decay were evaluated. The analyses were conducted using NONMEM, version 7.4 (ICON Development Solutions, Hanover, MD, USA). Graphical data presentations were conducted using R 4.0.2 (R Foundation for Statistical Computing).

QUANTIFICATION AND STATISTICAL ANALYSIS

Statistical analyses were performed using GraphPad Prism (v8) and Microsoft Excel for Windows 10 (v16.0.13001.20254). Statistical differences were analyzed with Mann-Whitney U-test. Nonparametric Kruskal-Wallis test was used to perform multiple comparisons between groups analyzed. Correction for multiple comparison was performed with Dunn's test. Nonparametric Spearman correlation was used to compute correlations between pairs of data. Statistical significance was defined as $P < 0.05$. ED50, IC50, ID80 and BD80 values were determined by non-linear regression analysis (log(agonist) vs. response - Variable slope (four parameters)).

References

Alshukairi, A.N., Khalid, I., Ahmed, W.A., Dada, A.M., Bayumi, D.T., Malic, L.S., Althawadi, S., Ignacio, K., Alsalmi, H.S., Al-Abdely, H.M., *et al.* (2016). Antibody Response and Disease Severity in Healthcare Worker MERS Survivors. Emerg Infect Dis *22*.

Alsoussi, W.B., Turner, J.S., Case, J.B., Zhao, H., Schmitz, A.J., Zhou, J.Q., Chen, R.E., Lei, T., Rizk, A.A., McIntire, K.M., *et al.* (2020). A Potently Neutralizing Antibody Protects Mice against SARS-CoV-2 Infection. J Immunol.

Barnes, C.O., West, A.P., Huey-Tubman, K.E., Hoffmann, M.A.G., Sharaf, N.G., Hoffman, P.R., Koranda, N., Gristick, H.B., Gaebler, C., Muecksch, F., *et al.* (2020). Structures of Human Antibodies Bound to SARS-CoV-2 Spike Reveal Common Epitopes and Recurrent Features of Antibodies. Cell.

Battye, T.G., Kontogiannis, L., Johnson, O., Powell, H.R., and Leslie, A.G. (2011). iMOSFLM: a new graphical interface for diffraction-image processing with MOSFLM. Acta Crystallogr D Biol Crystallogr *67*, 271-281.

Baum, A., Fulton, B.O., Wloga, E., Copin, R., Pascal, K.E., Russo, V., Giordano, S., Lanza, K., Negron, N., Ni, M., *et al.* (2020). Antibody cocktail to SARS-CoV-2 spike protein prevents rapid mutational escape seen with individual antibodies. Science.

Brouwer, P.J.M., Caniels, T.G., van der Straten, K., Snitselaar, J.L., Aldon, Y., Bangaru, S., Torres, J.L., Okba, N.M.A., Claireaux, M., Kerster, G., *et al.* (2020). Potent neutralizing antibodies from COVID-19 patients define multiple targets of vulnerability. Science.

Callow, K.A. (1985). Effect of specific humoral immunity and some non-specific factors on resistance of volunteers to respiratory coronavirus infection. J Hyg (Lond) *95*, 173-189.

Callow, K.A., Parry, H.F., Sergeant, M., and Tyrrell, D.A. (1990). The time course of the immune response to experimental coronavirus infection of man. Epidemiol Infect *105*, 435-446.

Cao, W.C., Liu, W., Zhang, P.H., Zhang, F., and Richardus, J.H. (2007). Disappearance of antibodies to SARS-associated coronavirus after recovery. N Engl J Med *357*, 1162-1163.

Cardone, G., Heymann, J.B., and Steven, A.C. (2013). One number does not fit all: mapping local variations in resolution in cryo-EM reconstructions. J Struct Biol *184*, 226-236.

Chen, S., McMullan, G., Faruqi, A.R., Murshudov, G.N., Short, J.M., Scheres, S.H., and Henderson, R. (2013). High-resolution noise substitution to measure overfitting and validate resolution in 3D structure determination by single particle electron cryomicroscopy. Ultramicroscopy *135*, 24-35.

Chi, X., Yan, R., Zhang, J., Zhang, G., Zhang, Y., Hao, M., Zhang, Z., Fan, P., Dong, Y., Yang, Y., *et al.* (2020). A neutralizing human antibody binds to the N-terminal domain of the Spike protein of SARS-CoV-2. Science.

Corti, D., Voss, J., Gamblin, S.J., Codoni, G., Macagno, A., Jarrossay, D., Vachieri, S.G., Pinna, D., Minola, A., Vanzetta, F., *et al.* (2011). A neutralizing antibody selected from plasma cells that binds to group 1 and group 2 influenza A hemagglutinins. Science *333*, 850-856.

Corti, D., Zhao, J., Pedotti, M., Simonelli, L., Agnihothram, S., Fett, C., Fernandez-Rodriguez, B., Foglierini, M., Agatic, G., Vanzetta, F., *et al.* (2015). Prophylactic and postexposure efficacy of a potent human monoclonal antibody against MERS coronavirus. Proc Natl Acad Sci U S A *112*, 10473-10478.

de Wit, E., Feldmann, F., Horne, E., Okumura, A., Cameroni, E., Haddock, E., Saturday, G., Scott, D., Gopal, R., Zambon, M., *et al.* (2019). Prophylactic efficacy of a human monoclonal antibody against MERS-CoV in the common marmoset. Antiviral Res *163*, 70-74.

DiLillo, D.J., Palese, P., Wilson, P.C., and Ravetch, J.V. (2016). Broadly neutralizing anti-influenza antibodies require Fc receptor engagement for in vivo protection. J Clin Invest *126*, 605-610.

DiLillo, D.J., and Ravetch, J.V. (2015). Differential Fc-Receptor Engagement Drives an Anti-tumor Vaccinal Effect. Cell *161*, 1035-1045.

DiLillo, D.J., Tan, G.S., Palese, P., and Ravetch, J.V. (2014). Broadly neutralizing hemagglutinin stalk-specific antibodies require FcγR interactions for protection against influenza virus in vivo. Nat Med *20*, 143-151.

Drosten, C., Meyer, B., Müller, M.A., Corman, V.M., Al-Masri, M., Hossain, R., Madani, H., Sieberg, A., Bosch, B.J., Lattwein, E., *et al.* (2014). Transmission of MERS-coronavirus in household contacts. N Engl J Med *371*, 828-835.

Duan, K., Liu, B., Li, C., Zhang, H., Yu, T., Qu, J., Zhou, M., Chen, L., Meng, S., Hu, Y., *et al.* (2020). Effectiveness of convalescent plasma therapy in severe COVID-19 patients. Proc Natl Acad Sci U S A *117*, 9490-9496.

Edridge, A.W., Kaczorowska, J.M., Hoste, A.C., Bakker, M., Klein, M., Jebbink, M.F., Matser, A., Kinsella, C., Rueda, P., Prins, M., *et al.* (2020). Coronavirus protective immunity is short-lasting. medRxiv, 2020.2005.2011.20086439.

Elbe, S., and Buckland-Merrett, G. (2017). Data, disease and diplomacy: GISAID's innovative contribution to global health. Glob Chall *1*, 33-46.

Emsley, P., Lohkamp, B., Scott, W.G., and Cowtan, K. (2010). Features and development of Coot. Acta Crystallographica Section D *66*, 486-501.

Evans, P.R., and Murshudov, G.N. (2013). How good are my data and what is the resolution? Acta Crystallogr D Biol Crystallogr *69*, 1204-1214.

Folegatti, P.M., Ewer, K.J., Aley, P.K., Angus, B., Becker, S., Belij-Rammerstorfer, S., Bellamy, D., Bibi, S., Bittaye, M., Clutterbuck, E.A., *et al.* (2020). Safety and immunogenicity of the ChAdOx1 nCoV-19 vaccine against SARS-CoV-2: a preliminary report of a phase 1/2, single-blind, randomised controlled trial. Lancet.

Frenz, B., Rämisch, S., Borst, A.J., Walls, A.C., Adolf-Bryfogle, J., Schief, W.R., Veesler, D., and DiMaio, F. (2019). Automatically Fixing Errors in Glycoprotein Structures with Rosetta. Structure *27*, 134-139.e133.

Gimson, A.E., Tedder, R.S., White, Y.S., Eddleston, A.L., and Williams, R. (1983). Serological markers in fulminant hepatitis B. Gut *24*, 615-617.

Goddard, T.D., Huang, C.C., Meng, E.C., Pettersen, E.F., Couch, G.S., Morris, J.H., and Ferrin, T.E. (2018). UCSF ChimeraX: Meeting modern challenges in visualization and analysis. Protein Sci *27*, 14-25.

Grifoni, A., Weiskopf, D., Ramirez, S.I., Mateus, J., Dan, J.M., Moderbacher, C.R., Rawlings, S.A., Sutherland, A., Premkumar, L., Jadi, R.S., *et al.* (2020). Targets of T Cell Responses to SARS-CoV-2 Coronavirus in Humans with COVID-19 Disease and Unexposed Individuals. Cell *181*, 1489-1501.e1415.

Guo, X., Guo, Z., Duan, C., chen, Z., Wang, G., Lu, Y., Li, M., and Lu, J. (2020). Long-Term Persistence of IgG Antibodies in SARS-CoV Infected Healthcare Workers. medRxiv, 2020.2002.2012.20021386.

He, W., Chen, C.J., Mullarkey, C.E., Hamilton, J.R., Wong, C.K., Leon, P.E., Uccellini, M.B., Chromikova, V., Henry, C., Hoffman, K.W., *et al.* (2017). Alveolar macrophages are critical for broadly-reactive antibody-mediated protection against influenza A virus in mice. Nat Commun *8*, 846.

Hensley, S.E., Das, S.R., Bailey, A.L., Schmidt, L.M., Hickman, H.D., Jayaraman, A., Viswanathan, K., Raman, R., Sasisekharan, R., Bennink, J.R., *et al.* (2009). Hemagglutinin receptor binding avidity drives influenza A virus antigenic drift. Science *326*, 734-736.

Hessell, A.J., Hangartner, L., Hunter, M., Havenith, C.E., Beurskens, F.J., Bakker, J.M., Lanigan, C.M., Landucci, G., Forthal, D.N., Parren, P.W., *et al.* (2007). Fc receptor but not complement binding is important in antibody protection against HIV. Nature *449*, 101-104.

Hoffmann, M., Kleine-Weber, H., and Pöhlmann, S. (2020a). A Multibasic Cleavage Site in the Spike Protein of SARS-CoV-2 Is Essential for Infection of Human Lung Cells. Mol Cell *78*, 779-784.e775.

Hoffmann, M., Kleine-Weber, H., Schroeder, S., Krüger, N., Herrler, T., Erichsen, S., Schiergens, T.S., Herrler, G., Wu, N.H., Nitsche, A., *et al.* (2020b). SARS-CoV-2 Cell Entry Depends on ACE2 and TMPRSS2 and Is Blocked by a Clinically Proven Protease Inhibitor. Cell *181*, 271-280.e278.

Huo, J., Zhao, Y., Ren, J., Zhou, D., Duyvesteyn, H.M.E., Ginn, H.M., Carrique, L., Malinauskas, T., Ruza, R.R., Shah, P.N.M., *et al.* (2020). Neutralisation of SARS-CoV-2 by destruction of the prefusion Spike. Cell Host & Microbe.

Johnson, R.F., Bagci, U., Keith, L., Tang, X., Mollura, D.J., Zeitlin, L., Qin, J., Huzella, L., Bartos, C.J., Bohorova, N., *et al.* (2016). 3B11-N, a monoclonal antibody against MERS-CoV, reduces lung pathology in rhesus monkeys following intratracheal inoculation of MERS-CoV Jordan-n3/2012. Virology *490*, 49-58.

Joyce, M.G., Sankhala, R.S., Chen, W.-H., Choe, M., Bai, H., Hajduczki, A., Yan, L., Sterling, S.L., Peterson, C.E., Green, E.C., *et al.* (2020). A Cryptic Site of Vulnerability on the Receptor Binding Domain of the SARS-CoV-2 Spike Glycoprotein. bioRxiv, 2020.2003.2015.992883.

Ju, B., Zhang, Q., Ge, X., Wang, R., Yu, J., Shan, S., Zhou, B., Song, S., Tang, X., Yu, J., *et al.* (2020). Potent human neutralizing antibodies elicited by SARS-CoV-2 infection. bioRxiv, 2020.2003.2021.990770.

Kabsch, W. (2010). XDS. Acta Crystallogr D Biol Crystallogr *66*, 125-132.

Ke, Z., Oton, J., Qu, K., Cortese, M., Zila, V., McKeane, L., Nakane, T., Zivanov, J., Neufeldt, C.J., Lu, J.M., *et al.* (2020). Structures, conformations and distributions of SARS-CoV-2 spike protein trimers on intact virions. bioRxiv, 2020.2006.2027.174979.

Kirchdoerfer, R.N., Wang, N., Pallesen, J., Wrapp, D., Turner, H.L., Cottrell, C.A., Corbett, K.S., Graham, B.S., McLellan, J.S., and Ward, A.B. (2018). Stabilized coronavirus spikes are resistant to conformational changes induced by receptor recognition or proteolysis. Sci Rep *8*, 15701.

Lan, J., Ge, J., Yu, J., Shan, S., Zhou, H., Fan, S., Zhang, Q., Shi, X., Wang, Q., Zhang, L., *et al.* (2020). Structure of the SARS-CoV-2 spike receptor-binding domain bound to the ACE2 receptor. Nature.

Lau, S.Y., Wang, P., Mok, B.W., Zhang, A.J., Chu, H., Lee, A.C., Deng, S., Chen, P., Chan, K.H., Song, W., *et al.* (2020). Attenuated SARS-CoV-2 variants with deletions at the S1/S2 junction. Emerg Microbes Infect *9*, 837-842.

Letko, M., Marzi, A., and Munster, V. (2020). Functional assessment of cell entry and receptor usage for SARS-CoV-2 and other lineage B betacoronaviruses. Nature Microbiology.

Li, L., Zhang, W., Hu, Y., Tong, X., Zheng, S., Yang, J., Kong, Y., Ren, L., Wei, Q., Mei, H., *et al.* (2020a). Effect of Convalescent Plasma Therapy on Time to Clinical Improvement in Patients With Severe and Life-threatening COVID-19: A Randomized Clinical Trial. JAMA.

Li, Q., Wu, J., Nie, J., Zhang, L., Hao, H., Liu, S., Zhao, C., Zhang, Q., Liu, H., Nie, L., *et al.* (2020b). The impact of mutations in SARS-CoV-2 spike on viral infectivity and antigenicity. Cell.

Liebschner, D., Afonine, P.V., Baker, M.L., Bunkóczi, G., Chen, V.B., Croll, T.I., Hintze, B., Hung, L.W., Jain, S., McCoy, A.J., *et al.* (2019). Macromolecular structure determination using X-rays, neutrons and electrons: recent developments in Phenix. Acta Crystallogr D Struct Biol *75*, 861-877.

Lindhardt, B.O., Gerstoft, J., Hofmann, B., Pallesen, G., Mathiesen, L., Dickmeiss, E., and Ulrich, K. (1989). Antibodies against the major core protein p24 of human immunodeficiency virus: relation to immunological, clinical and prognostic findings. Eur J Clin Microbiol Infect Dis *8*, 614-619.

Liu, L., Wang, P., Nair, M.S., Yu, J., Rapp, M., Wang, Q., Luo, Y., Chan, J.F., Sahi, V., Figueroa, A., *et al.* (2020a). Potent neutralizing antibodies directed to multiple epitopes on SARS-CoV-2 spike. Nature.

Liu, S.T.H., Lin, H.-M., Baine, I., Wajnberg, A., Gumprecht, J.P., Rahman, F., Rodriguez, D., Tandon, P., Bassily-Marcus, A., Bander, J., *et al.* (2020b). Convalescent plasma treatment of severe COVID-19: A matched control study. medRxiv, 2020.2005.2020.20102236.

Long, Q.X., Tang, X.J., Shi, Q.L., Li, Q., Deng, H.J., Yuan, J., Hu, J.L., Xu, W., Zhang, Y., Lv, F.J., *et al.* (2020). Clinical and immunological assessment of asymptomatic SARS-CoV-2 infections. Nat Med.

Luchsinger, L.L., Ransegnola, B., Jin, D., Muecksch, F., Weisblum, Y., Bao, W., George, P.J., Rodriguez, M., Tricoche, N., Schmidt, F., *et al.* (2020). Serological Analysis of New York City COVID19 Convalescent Plasma Donors. medRxiv.

Lund, J.M., Alexopoulou, L., Sato, A., Karow, M., Adams, N.C., Gale, N.W., Iwasaki, A., and Flavell, R.A. (2004). Recognition of single-stranded RNA viruses by Toll-like receptor 7. Proc Natl Acad Sci U S A *101*, 5598-5603.

McCoy, A.J., Grosse-Kunstleve, R.W., Adams, P.D., Winn, M.D., Storoni, L.C., and Read, R.J. (2007). Phaser crystallographic software. J Appl Crystallogr *40*, 658-674.

Menachery, V.D., Yount, B.L., Jr., Sims, A.C., Debbink, K., Agnihothram, S.S., Gralinski, L.E., Graham, R.L., Scobey, T., Plante, J.A., Royal, S.R., *et al.* (2016). SARS-like WIV1-CoV poised for human emergence. Proc Natl Acad Sci U S A *113*, 3048-3053.

Millet, J.K., and Whittaker, G.R. (2015). Host cell proteases: Critical determinants of coronavirus tropism and pathogenesis. Virus Res *202*, 120-134.

Murshudov, G.N., Skubák, P., Lebedev, A.A., Pannu, N.S., Steiner, R.A., Nicholls, R.A., Winn, M.D., Long, F., and Vagin, A.A. (2011). REFMAC5 for the refinement of macromolecular crystal structures. Acta Crystallogr D Biol Crystallogr *67*, 355-367.

Ng, K.W., Faulkner, N., Cornish, G.H., Rosa, A., Harvey, R., Hussain, S., Ulferts, R., Earl, C., Wrobel, A., Benton, D., *et al.* (2020). Pre-existing and de novo humoral immunity to SARS-CoV-2 in humans. bioRxiv, 2020.2005.2014.095414.

Ortiz, D.F., Lansing, J.C., Rutitzky, L., Kurtagic, E., Prod'homme, T., Choudhury, A., Washburn, N., Bhatnagar, N., Beneduce, C., Holte, K., *et al.* (2016). Elucidating the interplay between IgG-Fc valency and FcγR activation for the design of immune complex inhibitors. Sci Transl Med *8*, 365ra158.

Ou, X., Liu, Y., Lei, X., Li, P., Mi, D., Ren, L., Guo, L., Guo, R., Chen, T., Hu, J., *et al.* (2020). Characterization of spike glycoprotein of SARS-CoV-2 on virus entry and its immune cross-reactivity with SARS-CoV. Nat Commun *11*, 1620.

Pallesen, J., Wang, N., Corbett, K.S., Wrapp, D., Kirchdoerfer, R.N., Turner, H.L., Cottrell, C.A., Becker, M.M., Wang, L., Shi, W., *et al.* (2017). Immunogenicity

and structures of a rationally designed prefusion MERS-CoV spike antigen. Proc Natl Acad Sci U S A *114*, E7348-E7357.

Pettersen, E.F., Goddard, T.D., Huang, C.C., Couch, G.S., Greenblatt, D.M., Meng, E.C., and Ferrin, T.E. (2004). UCSF Chimera--a visualization system for exploratory research and analysis. J Comput Chem *25*, 1605-1612.

Pinto, D., Park, Y.J., Beltramello, M., Walls, A.C., Tortorici, M.A., Bianchi, S., Jaconi, S., Culap, K., Zatta, F., De Marco, A., *et al.* (2020). Cross-neutralization of SARS-CoV-2 by a human monoclonal SARS-CoV antibody. Nature *583*, 290-295.

Prévost, J., Gasser, R., Beaudoin-Bussières, G., Richard, J., Duerr, R., Laumaea, A., Anand, S.P., Goyette, G., Ding, S., Medjahed, H., *et al.* (2020). Cross-sectional evaluation of humoral responses against SARS-CoV-2 Spike. bioRxiv.

Punjani, A., Rubinstein, J.L., Fleet, D.J., and Brubaker, M.A. (2017). cryoSPARC: algorithms for rapid unsupervised cryo-EM structure determination. Nat Methods *14*, 290-296.

Punjani, A., Zhang, H., and Fleet, D.J. (2019). Non-uniform refinement: Adaptive regularization improves single particle cryo-EM reconstruction. bioRxiv, 2019.2012.2015.877092.

Robbiani, D.F., Gaebler, C., Muecksch, F., Lorenzi, J.C.C., Wang, Z., Cho, A., Agudelo, M., Barnes, C.O., Gazumyan, A., Finkin, S., *et al.* (2020). Convergent antibody responses to SARS-CoV-2 in convalescent individuals. Nature.

Rockx, B., Corti, D., Donaldson, E., Sheahan, T., Stadler, K., Lanzavecchia, A., and Baric, R. (2008). Structural basis for potent cross-neutralizing human monoclonal antibody protection against lethal human and zoonotic severe acute respiratory syndrome coronavirus challenge. J Virol *82*, 3220-3235.

Rogers, T.F., Zhao, F., Huang, D., Beutler, N., Burns, A., He, W.T., Limbo, O., Smith, C., Song, G., Woehl, J., *et al.* (2020). Isolation of potent SARS-CoV-2 neutralizing antibodies and protection from disease in a small animal model. Science.

Scheres, S.H. (2012a). A Bayesian view on cryo-EM structure determination. J Mol Biol *415*, 406-418.

Scheres, S.H. (2012b). RELION: implementation of a Bayesian approach to cryo-EM structure determination. J Struct Biol *180*, 519-530.

Seow, J., Graham, C., Merrick, B., Acors, S., Steel, K.J.A., Hemmings, O., O'Bryne, A., Kouphou, N., Pickering, S., Galao, R., *et al.* (2020). Longitudinal evaluation and decline of antibody responses in SARS-CoV-2 infection. medRxiv, 2020.2007.2009.20148429.

Seydoux, E., Homad, L.J., MacCamy, A.J., Parks, K.R., Hurlburt, N.K., Jennewein, M.F., Akins, N.R., Stuart, A.B., Wan, Y.-H., Feng, J., *et al.* (2020). Characterization of neutralizing antibodies from a SARS-CoV-2 infected individual. bioRxiv, 2020.2005.2012.091298.

Shang, J., Ye, G., Shi, K., Wan, Y., Luo, C., Aihara, H., Geng, Q., Auerbach, A., and Li, F. (2020). Structural basis of receptor recognition by SARS-CoV-2. Nature.

Shen, C., Wang, Z., Zhao, F., Yang, Y., Li, J., Yuan, J., Wang, F., Li, D., Yang, M., Xing, L., *et al.* (2020). Treatment of 5 Critically Ill Patients With COVID-19 With Convalescent Plasma. JAMA.

Song, W., Gui, M., Wang, X., and Xiang, Y. (2018). Cryo-EM structure of the SARS coronavirus spike glycoprotein in complex with its host cell receptor ACE2. PLoS Pathog *14*, e1007236.

Stettler, K., Beltramello, M., Espinosa, D.A., Graham, V., Cassotta, A., Bianchi, S., Vanzetta, F., Minola, A., Jaconi, S., Mele, F., *et al.* (2016). Specificity, cross-reactivity, and function of antibodies elicited by Zika virus infection. Science *353*, 823-826.

Suloway, C., Pulokas, J., Fellmann, D., Cheng, A., Guerra, F., Quispe, J., Stagg, S., Potter, C.S., and Carragher, B. (2005). Automated molecular microscopy: the new Leginon system. J Struct Biol *151*, 41-60.

Tan, C.W., Chia, W.N., Qin, X., Liu, P., Chen, M.I.C., Tiu, C., Hu, Z., Chen, V.C.-W., Young, B.E., Sia, W.R., *et al.* (2020). A SARS-CoV-2 surrogate virus neutralization test based on antibody-mediated blockage of ACE2–spike protein–protein interaction. Nature Biotechnology.

Tan, Y.Z., Baldwin, P.R., Davis, J.H., Williamson, J.R., Potter, C.S., Carragher, B., and Lyumkis, D. (2017). Addressing preferred specimen orientation in single-particle cryo-EM through tilting. Nat Methods *14*, 793-796.

Tang, A., Chen, Z., Cox, K.S., Su, H.P., Callahan, C., Fridman, A., Zhang, L., Patel, S.B., Cejas, P.J., Swoyer, R., *et al.* (2019). A potent broadly neutralizing human RSV antibody targets conserved site IV of the fusion glycoprotein. Nat Commun *10*, 4153.

Tegunov, D., and Cramer, P. (2019). Real-time cryo-electron microscopy data preprocessing with Warp. Nat Methods *16*, 1146-1152.

ter Meulen, J., van den Brink, E.N., Poon, L.L., Marissen, W.E., Leung, C.S., Cox, F., Cheung, C.Y., Bakker, A.Q., Bogaards, J.A., van Deventer, E., *et al.* (2006). Human monoclonal antibody combination against SARS coronavirus: synergy and coverage of escape mutants. PLoS Med *3*, e237.

Tian, X., Li, C., Huang, A., Xia, S., Lu, S., Shi, Z., Lu, L., Jiang, S., Yang, Z., Wu, Y., *et al.* (2020). Potent binding of 2019 novel coronavirus spike protein by a SARS coronavirus-specific human monoclonal antibody. Emerg Microbes Infect *9*, 382-385.

Tortorici, M.A., and Veesler, D. (2019). Structural insights into coronavirus entry. Adv Virus Res *105*, 93-116.

Traggiai, E., Becker, S., Subbarao, K., Kolesnikova, L., Uematsu, Y., Gismondo, M.R., Murphy, B.R., Rappuoli, R., and Lanzavecchia, A. (2004). An efficient method to make human monoclonal antibodies from memory B cells: potent neutralization of SARS coronavirus. Nat Med *10*, 871-875.

Walls, A.C., Park, Y.J., Tortorici, M.A., Wall, A., McGuire, A.T., and Veesler, D. (2020). Structure, Function, and Antigenicity of the SARS-CoV-2 Spike Glycoprotein. Cell *181*, 281-292.e286.

Walls, A.C., Tortorici, M.A., Bosch, B.J., Frenz, B., Rottier, P.J.M., DiMaio, F., Rey, F.A., and Veesler, D. (2016a). Cryo-electron microscopy structure of a coronavirus spike glycoprotein trimer. Nature *531*, 114-117.

Walls, A.C., Tortorici, M.A., Frenz, B., Snijder, J., Li, W., Rey, F.A., DiMaio, F., Bosch, B.J., and Veesler, D. (2016b). Glycan shield and epitope masking of a coronavirus spike protein observed by cryo-electron microscopy. Nat Struct Mol Biol *23*, 899-905.

Walls, A.C., Tortorici, M.A., Snijder, J., Xiong, X., Bosch, B.J., Rey, F.A., and Veesler, D. (2017). Tectonic conformational changes of a coronavirus spike glycoprotein promote membrane fusion. Proc Natl Acad Sci U S A *114*, 11157-11162.

Walls, A.C., Xiong, X., Park, Y.J., Tortorici, M.A., Snijder, J., Quispe, J., Cameroni, E., Gopal, R., Dai, M., Lanzavecchia, A., *et al.* (2019). Unexpected Receptor Functional Mimicry Elucidates Activation of Coronavirus Fusion. Cell *176*, 1026-1039.e1015.

Wang, C., Li, W., Drabek, D., Okba, N.M.A., van Haperen, R., Osterhaus, A.D.M.E., van Kuppeveld, F.J.M., Haagmans, B.L., Grosveld, F., and Bosch, B.-J. (2020a). A human monoclonal antibody blocking SARS-CoV-2 infection. bioRxiv, 2020.2003.2011.987958.

Wang, Q., Zhang, Y., Wu, L., Niu, S., Song, C., Zhang, Z., Lu, G., Qiao, C., Hu, Y., Yuen, K.Y., *et al.* (2020b). Structural and Functional Basis of SARS-CoV-2 Entry by Using Human ACE2. Cell *181*, 894-904.e899.

Wang, R.Y., Song, Y., Barad, B.A., Cheng, Y., Fraser, J.S., and DiMaio, F. (2016). Automated structure refinement of macromolecular assemblies from cryo-EM maps using Rosetta. Elife *5*.

Watanabe, Y., Allen, J.D., Wrapp, D., McLellan, J.S., and Crispin, M. (2020). Site-specific glycan analysis of the SARS-CoV-2 spike. Science.

Wec, A.Z., Wrapp, D., Herbert, A.S., Maurer, D.P., Haslwanter, D., Sakharkar, M., Jangra, R.K., Dieterle, M.E., Lilov, A., Huang, D., *et al.* (2020). Broad neutralization of SARS-related viruses by human monoclonal antibodies. Science.

Wrapp, D., Wang, N., Corbett, K.S., Goldsmith, J.A., Hsieh, C.L., Abiona, O., Graham, B.S., and McLellan, J.S. (2020). Cryo-EM structure of the 2019-nCoV spike in the prefusion conformation. Science *367*, 1260-1263.

Wu, Y., Wang, F., Shen, C., Peng, W., Li, D., Zhao, C., Li, Z., Li, S., Bi, Y., Yang, Y., *et al.* (2020). A noncompeting pair of human neutralizing antibodies block COVID-19 virus binding to its receptor ACE2. Science *368*, 1274-1278.

Yan, R., Zhang, Y., Li, Y., Xia, L., Guo, Y., and Zhou, Q. (2020). Structural basis for the recognition of SARS-CoV-2 by full-length human ACE2. Science *367*, 1444-1448.

Ying, T., Prabakaran, P., Du, L., Shi, W., Feng, Y., Wang, Y., Wang, L., Li, W., Jiang, S., Dimitrov, D.S., *et al.* (2015). Junctional and allele-specific residues are critical for MERS-CoV neutralization by an exceptionally potent germline-like antibody. Nat Commun *6*, 8223.

Yuan, M., Wu, N.C., Zhu, X., Lee, C.D., So, R.T.Y., Lv, H., Mok, C.K.P., and Wilson, I.A. (2020). A highly conserved cryptic epitope in the receptor-binding domains of SARS-CoV-2 and SARS-CoV. Science.

Yuan, Y., Cao, D., Zhang, Y., Ma, J., Qi, J., Wang, Q., Lu, G., Wu, Y., Yan, J., Shi, Y., *et al.* (2017). Cryo-EM structures of MERS-CoV and SARS-CoV spike glycoproteins reveal the dynamic receptor binding domains. Nat Commun *8*, 15092.

Zhou, P., Yang, X.L., Wang, X.G., Hu, B., Zhang, L., Zhang, W., Si, H.R., Zhu, Y., Li, B., Huang, C.L., *et al.* (2020a). A pneumonia outbreak associated with a new coronavirus of probable bat origin. Nature.

Zhou, T., Tsybovsky, Y., Olia, A.S., Gorman, J., Rapp, M.A., Cerutti, G., Katsamba, P.S., Nazzari, A., Schon, A., Wang, P.D., *et al.* (2020b). A pH-dependent switch mediates conformational masking of SARS-CoV-2 spike. bioRxiv.

Zivanov, J., Nakane, T., Forsberg, B.O., Kimanius, D., Hagen, W.J., Lindahl, E., and Scheres, S.H. (2018). New tools for automated high-resolution cryo-EM structure determination in RELION-3. Elife *7*.

Zivanov, J., Nakane, T., and Scheres, S.H.W. (2019). A Bayesian approach to beam-induced motion correction in cryo-EM single-particle analysis. IUCrJ *6*, 5-17.

EXAMPLE 3

ULTRAPOTENT HUMAN ANTIBODIES PROTECT AGAINST SARS-COV-2 CHALLENGE VIA MULTIPLE MECHANISMS

Isolation of ultra-potent SARS-CoV-2 neutralizing Abs.

Memory B cells from two individuals recovering from severe COVID-19 disease were sorted using biotinylated prefusion SARS-CoV-2 S ectodomain trimer as bait. Two mAbs, S2E12 and S2M11, stood out for their high neutralization potency against authentic SARS-CoV-2 virus and two different SARS-CoV-2 S pseudotyped viruses (using either murine-leukemia virus (MLV) or vesicular stomatitis virus (VSV) backbones). In an assay that measures inhibition of authentic SARS-CoV-2 entry (SARS-CoV-2-Nluc (*34*)), half-maximal inhibitory concentrations (IC_{50}) of 3-6 ng/ml (20-40 pM) were determined (Figures 35A-35B). IC_{50} values of 1.9-2.5 ng/ml for SARS-CoV-2 S-VSV (Figure 40A) and 10.3-30.4 ng/ml for SARS-CoV-2 S-MLV were determined (Figure 40B). In an authentic SARS-CoV-2 focus reduction neutralization test that measures inhibition of virus entry and spread (*35*), the IC_{50} values were 1.2-6.6 ng/ml (Figure 40C). The potency of these mAbs was demonstrated further by the concentrations necessary to inhibit 90% of authentic SARS-CoV-2-Nluc viral entry (IC_{90}), which was determined as 26.4±7.8 ng/mL and 12.7±3.1 ng/mL for S2E12 and S2M11, respectively. The higher neutralization potency of IgG compared to Fab observed for each mAb suggested that the distinct binding affinities and/or bivalent binding contribute to potency (Figure 35A). The S2E12 heavy chain uses VH1-58*01, D2-15*01 and JH3*02 genes whereas S2M11 derives from VH1-2*02, D3-3*01 and JH4*02 genes. The heavy chain variable gene nucleotide sequence germline identity is 96.53% for S2M11 and 97.6% for S2E12.

Both S2E12 and S2M11 bound to the SARS-CoV-2 RBD and prefusion-stabilized S ectodomain trimer (*6*) but not to the SARS-CoV RBD or S (*36*) by ELISA (Figures 35C-35F). Using surface plasmon resonance (SPR) and flow cytometry, it was observed that S2E12 and S2M11 compete for binding to the SARS-CoV-2 RBD or to

SARS-CoV-2 S, presented either as a recombinantly expressed prefusion-stabilized S ectodomain trimer or as full-length S expressed at the surface of ExpiCHO cells (Figures 41A-41B). When added first, S2M11 competed in a concentration-dependent manner with the sarbecovirus neutralizing S309 mAb for binding to SARS-CoV-2 S, whereas it could bind with minimal competition when added after S309 (Figure 41B). Whereas the S2E12 Fab (or IgG) bound to SARS-CoV-2 S and RBD similarly, the binding affinity of the S2M11 Fab (or IgG) for the S trimer was enhanced relative to the isolated SARS-CoV-2 RBD (Figure 35G and Figure 41C). Specifically, S2M11 binding kinetics to SARS-CoV-2 S were biphasic, including a first phase with identical binding kinetics and affinity as measured for binding to the isolated RBD, and a second phase with a much slower off-rate and therefore higher affinity. Binding of S2M11 Fab and IgG to S was increased at pH 5.4, a condition that favors the closed trimer conformation, compared to pH 7.4 (*37*) (Figure 35G, Figure 41C and Figure 49). Conversely, binding of the S2E12 Fab to S was diminished at pH 5.4 (and moderately reduced for S2E12 IgG), possibly due to the increased number of S trimers with closed RBDs (Figure 35G, Figures 41A and 41Cand Figure 49).

Collectively, these findings indicate that S2M11 and S2E12 target overlapping or partially overlapping SARS-CoV-2 RBD epitopes. The finding that S2M11 preferentially interacts with the S trimer relative to the RBD suggest that this mAb may bind to a quaternary epitope only exposed in the context of a native closed prefusion S. Finally, the enhanced binding of S2E12 to SARS-CoV-2 S in conditions favoring RBD opening (pH 7.4) indicates that this mAb may recognize a cryptic epitope not exposed in the closed S trimer.

S2E12 potently neutralizes SARS-CoV-2 by targeting the RBM

To understand the mechanism of S2E12-mediated potent neutralization of SARS-CoV-2, a complex between the SARS-CoV-2 S ectodomain trimer and the S2E12 Fab fragment was characterized using cryo-electron microscopy (cryoEM). 3D classification of the data showed the presence of S trimers with one, two or three Fabs bound to open RBDs for which structures were determined at 3.5 Å, 3.3Å and 3.3 Å

resolution, respectively (Figures 36A-36B, Figures 42A-42G and Figure 50). Local refinement was used to obtain a 3.7 Å map of the region corresponding to the S2E12 variable domains and RBD, which improved local resolution due to conformational dynamic relative to the rest of the S trimer, and this map was used along with a 1.4Å crystal structure of the S2E12 Fab to build a model (Figures 43D-43G, Figure 50 and Figure 51).

S2E12 recognizes an RBD epitope overlapping with the RBM (i.e. ACE2 receptor-binding site) that is partially buried at the interface between protomers in the closed S trimer (Figures 36A-36D and Figures 43A-43B). As a result, based on these data, S2E12 only interacts with open RBDs, as is the case for ACE2 as well as for several previously described neutralizing mAbs including S2H14 (*22, 25*) (Piccoli, Cell in Press). The concave S2E12 paratope recognizes the convex RBM tip through electrostatic and van der Waals interactions (Figures 36C-36D). Specifically, S2E12 utilizes the heavy chain complementary determining regions (CDR) 1-3 and the light chain CDR1 and CDR3, respectively accounting for 2/3 and 1/3 of the paratope buried surface area, to recognize residues 455-458 and 473-493 of the SARS-CoV-2 RBD (Figures 36C-36D). Most of the S2E12 contacts with the RBD are mediated by germline encoded residues, with only 1 out of 5 heavy chain (Gly109) and 1 out of 4 light chain (Gly94) mutated residues contributing to the paratope. The structural data explain that S2E12 binds efficiently to both the RBD and the prefusion S trimer (Figure 35G) and potently neutralizes SARS-CoV-2 (Figures 35A-35B and Figures 40A-40C): (i) S2E12 recognizes a tertiary 3D epitope, i.e. an epitope that is fully contained within one S protomer; (ii) ~50% of S trimers naturally harbor one open RBD at the viral surface or in recombinantly expressed S ectodomain trimers as observed by cryo-electron tomography and single particle cryoEM, respectively (*6, 38*), and (iii) S2E12 binding shifts the RBD conformational equilibrium toward open S trimers, as previously described for RBM-targeted mAbs (*22, 36*) (Piccoli, Cell in Press).

Further studies of S2E12 in complex with RBD achieved a resolution of 2.93 angstroms. Based on these studies, the S2E12 epitope is formed by amino acid residues 417, 453, 455, 456, 473, 475-480, 484-489, and 493.

S2M11 locks the SARS-CoV-2 S trimer in the closed state through binding to a quaternary epitope

CryoEM analysis of S2M11 in complex with SARS-CoV-2 S was carried out. 3D classification of the cryoEM data revealed the exclusive presence of S trimers adopting a closed conformation, which allowed determination of a 2.6Å structure of SARS-CoV-2 S bound to three S2M11 Fab fragments (Figures 37A-37B, Figures 44A-44F and Figure 50). S2M11 recognizes a quaternary epitope through electrostatic interactions and shape complementarity, comprising distinct regions of two neighboring RBDs within an S trimer (Figures 37C-37D). Specifically, S2M11 CDRH1, CDRH2 and the heavy chain framework region 3 (FR3) are docked into the RBM crevice (burying a surface of ~400Å^2), whereas CDRH3 spans the interface between the RBM and helices 339-343, and 367-374, as well as residue 436 of an adjacent RBD belonging to the neighboring protomer (i.e., burying a total surface of ~500Å^2) (Figures 37C-37F). S2M11 CDRL2 interacts with residues 440-441 and CDRL1 forms key contacts with the glycan at position N343, which is rotated ~45° compared to the orientation it adopts in the S309-bound S structure (*21*), both sets of interactions occurring with the neighboring RBD (quaternary epitope) (Figures 37C-37F and Figure 44G). Three out of eight S2M11 heavy chain residues that are mutated relative to germline contribute to epitope recognition (Ile54, Thr77 and Phe102) whereas none of the two light chain mutated residues participate in RBD binding. Further studies indicated that the S2M11 epitope is formed by: on a first RBD, amino acid residues 339, 342, 343, 367, 368, 371, 372, 373, 374, 436, 440, and 441, and, on a second RBD, amino acid residues 446, 447, 449, 452, 455, 456, 484, 485, 486, 487, 489, 490, 492, 493, 494, 496, and 498.

The observation that all particle images correspond to closed S trimers when bound to S2M11 contrasts with the previous finding of ~50%/50% of trimers closed or with one RBD open in the absence of bound mAb (*6*) or in complex with S309 (*21*) or S2H13 (Piccoli et al. Cell, in press), which do not select for any specific RBD conformation. Based on these data, it appears that S2M11 stabilizes the closed conformation of the S trimer by interacting with a composite epitope including two

neighboring RBDs (from two distinct protomers) that are close to each other in the closed state but spread apart upon RBD opening (*6*) (Figures 43C-43D). These results also explain the enhanced S2M11 binding affinity for S compared to the RBD (Figure 35G), as only the S trimer enables binding to the quaternary epitope which buries a ~60% greater paratope surface area compared to binding to the isolated RBM (Figures 37A-37F). The biphasic binding may be interpreted as S2M11 interacting with a tertiary epitope present in open RBDs (fast off-rate), based on the identical kinetics and affinity measured relative to isolated RBD, and S2M11 recognizing its full quaternary epitope (slow off-rate).

S2M11 and S2E12 inhibit SARS-CoV-2 attachment to ACE2 and trigger Fc-mediated effector functions

The present structural data indicate that both S2E12 and S2M11 would compete with ACE2 attachment to the RBD as they recognize epitopes overlapping with the RBM (Figures 38A-38B). Moreover, S2M11-induced stabilization of SARS-CoV-2 S in the closed conformational state yields S trimers with masked RBMs that are incompetent for receptor engagement, as previously shown for an engineered S construct covalently stabilized in the closed state (*39*). As expected based on the structures, both S2E12 and S2M11 blocked binding of SARS-CoV-2 S or RBD to immobilized human recombinant ACE2 measured by biolayer interferometry (Figures 38C-38D). Additionally, both S2E12 and S2M11 inhibited binding of ACE2 to SARS-CoV-2 S expressed at the surface of CHO cells (Figure 38E), validating this mechanism of neutralization using full-length native S trimers. The comparable efficiency of S2E12 and S2M11 to block S attachment to ACE2 correlates with their similar neutralization potencies.

To further investigate SARS-CoV-2 inhibition by S2E12 and S2M11, a cell-cell fusion assay was performed using VeroE6 cells (which endogenously express ACE2 at their surface) transiently transfected with full-length wildtype SARS-CoV-2 S. Although S2E12 and S2M11 bind and stabilize different conformations of the S protein, both mAbs efficiently blocked syncytia formation (Figure 38F), which results from S-

mediated membrane fusion. The absence of syncytia formation may be explained by S2E12- or S2M11-mediated disruption of ACE2 binding along with S2M11-induced inhibition of membrane fusion through conformational trapping of SARS-CoV-2 S in the closed state.

Ab-dependent cell cytotoxicity (ADCC) mediated by natural killer cells or Ab-dependent cell phagocytosis (ADCP) mediated by macrophages or monocytes are Fc-mediated effector functions that can contribute to protection by facilitating virus clearance and by supporting immune responses *in vivo,* independently of direct neutralization (*40*). As a prerequisite for ADCC to occur, it was validated that infected cells express SARS-CoV-2 S on their surface (Figures 45A-45B). To evaluate the ability of S2M11 and S2E12 to leverage ADCC and ADCP, these mAbs (IgG1 backbone) were tested for induction of FcγRIIa and FcγRIIIa-mediated signaling using a luciferase reporter assay. S2M11 promoted efficient, dose-dependent FcγRIIIa-mediated (but not FcγRIIa-mediated) signaling, in particular for the high affinity (V158) variant of the Fc receptor, to levels comparable to the cross-reactive mAb S309 (Figure 38G and Figures 45C-45D) (*21*). In contrast, S2E12 triggered FcγRIIa-mediated (but not FcγRIIIa-mediated) signaling, possibly as a result of the distinct orientation of the mAb relative to the membrane of the effector cells in comparison to S2M11 and S309. Accordingly, S2M11 but not S2E12 showed FcγRIIIa-dependent ADCC activity (Figure 38H and 45E) and ADCP activity (Figure 38I). As efficient activation of effector functions was observed when mixing S2M11 with S2E12 or S309 (Figures 38G, 38H and 45E), cocktails of these mAbs may leverage additional protective mechanisms *in vivo* besides inhibition of viral entry.

Formulation of ultra-potent neutralizing Ab cocktails against SARS-CoV-2

Surveillance efforts have led to the identification of a number of S mutants among circulating SARS-CoV-2 isolates. Several naturally occurring RBD mutations were shown to abrogate interactions with known mAbs and to reduce immune sera binding, raising concerns that viral neutralization escape mutants could emerge or be selected under pressure from mAb-based anti-viral treatments (*41*). To investigate if S2E12- and S2M11-mediated neutralization might be affected by SARS-CoV-2

polymorphism, binding of either mAb to 29 S protein variants (corresponding to mutations detected in circulating SARS-CoV-2 isolates) expressed at the surface of CHO cells was tested. The Y449N, E484K/Q, F490L and S494P RBD variants led to decreased S2M11 binding to S whereas none of the mutants tested affected interactions with S2E12, although several of them are found in the epitope of this latter mAb (Figure 52). The impact of these substitutions on S2M11 binding is explained by the structural data showing that the SARS-CoV-2 S Y449 and E484 side chains are hydrogen-bonded to the S2M11 heavy chain F29 backbone amide and the N52/S55 side chains, respectively, and the F490 and S494 residues are buried at the interface with S2M11. SARS-CoV-2 S-VSV pseudotyped virus entry assays with selected S variants confirmed these results and showed that the Y449N, E484K/Q, F490L/S and S494P individual substitutions abrogated S2M11-mediated neutralization whereas the L455F variant reduced neutralization potency by an order of magnitude (Figures 46A, 46C, 46E). S2E12 neutralized efficiently all variants tested except G476S that showed an order of magnitude decreased potency (Figures 46B, 46D, 46F). In agreement with deep mutational scanning data (*42*), it was found that the Y449N variant was impaired in its ability to bind ACE2 (Figure 47) which is expected to reduce viral fitness, likely explaining that this mutation has been reported to date in only one out of 90,287 complete SARS-CoV-2 genome sequences. Although rare, the G476S, E484K/Q, S494P and F490L mutations have been detected in 20, 10/17, 15 and 5 viral isolates across three continents and in theory could be selected under the selective pressure of S2E12 or S2M11. Overall, fifteen SARS-CoV-2 S variants with a single amino acid substitution within the S2M11 epitope were reported, with a prevalence of less than 0.1% as of September 2020. (Figure 46G).

To circumvent the risk of emergence or selection of neutralization escape mutants, the combination of S2M11, S2E12 and S309 in two-component mAb cocktails based on their complementary mechanisms of action was assessed. SARS-CoV-2 S-VSV pseudotyped virus entry assays showed that mAb cocktails potently neutralized the Y449N, S494P and G476S variants and overcame the neutralization escape phenotype observed with single mAbs (Figures 46H-46I). A concentration matrix of

S2E12 and S2M11 revealed their additive neutralization effects without antagonism, despite the fact that both Abs compete for binding to the RBM (Figures 48A-48C). Moreover, the combination of S309 with S2E12, which do not compete for binding to S, and S309 and S2M11, which partially compete (i.e. for attachment to the closed S trimer), also yielded additive neutralization effects (Figures 48D-48F), suggesting that two- (or three-) component mAb cocktails may prevent the emergence or the selection of viral mutants escaping mAb therapy.

S2M11 and S2E12 protect hamsters against SARS-CoV-2 challenge

To evaluate the protective efficacy of S2E12 and S2M11 against SARS-CoV-2 challenge *in vivo*, either mAb or a cocktail of both mAbs were tested in a Syrian hamster model (*43*). The mAbs were engineered with heavy and light chain constant regions from Syrian hamster IgG2 to allow optimal triggering of Fc-dependent effector functions. mAbs were administered via intraperitoneal injection 48h before intranasal challenge with 2 x 10^6 $TCID_{50}$ of SARS-CoV-2. Four days later, lungs were collected for the quantification of viral RNA and infectious virus. Either mAb alone or cocktails with 0.5 mg/kg or 1 mg/kg total mAb decreased the amount of viral RNA detected in the lungs by 2 to 5 orders of magnitude compared to hamsters receiving a control mAb (Figure 39A). The amounts of viral RNA detected at day 4 inversely correlated with serum mAb concentration measured at the time of infection (Spearman R -0.574, p=0.0052) (Figure 39B). Prophylactic administration of these mAbs at all doses tested completely abrogated viral replication in the lungs, with the exception of a single animal which received the low dose cocktail and was partially protected (Figure 39C). These data show protective efficacy of both mAbs at low doses, individually or as cocktails, in line with their ultra-potent *in vitro* neutralization.

Materials and Methods

Reagents

Cell lines were obtained from ATCC (HEK293T, Vero-E6), Thermo-Fisher Scientific (HEK293F) or Invitrogen (Expi-CHO cells). Expi-293 (Invitrogen) and Expi-

CHO cells (Invitrogen) were maintained in Expi-293 Expression Medium (Invitrogen) and ExpiCHO- Expression Medium (Gibco), respectively. All cell lines used in this study (except HEK293F) were routinely tested for mycoplasma and found to be mycoplasma-free.

Recombinant glycoprotein production

For B-cell sorting and cryoEM studies, a SARS-CoV-2 prefusion S ectodomain trimer was designed based on a previously described construct (*6*). Specifically, a gene encoding for the ectodomain of SARS-CoV-2 prefusion S ectodomain trimer (residues 14-1211, GenBank: YP_009724390.1) covering the region from the end of the signal peptide sequence (starting with QCVN) to the beginning of the transmembrane domain (ending with QYIK) was synthesized, codon optimized for human cell expression and placed into a pCVM vector by Genscript. To maximize protein expression, Kozak sequence was added as well as sequences encoding an exogenous N-terminal signal peptide: MGILPSPGMPALLSLVSLLSVLLMGCVAETGT (SEQ ID NO.:160) derived from μ-phosphatase, the K986P-V987P substitutions, the substitution of arginines at the S1/S2 cleavage site: R682S, R683G, R685G and a C-terminal extension:GSGR*ENLYFQG*GGGSGYIPEAPRDGQAYVRKDGEWVLLSTFLGSG**GLNDIFEAQKIEWHE**GSGHHHHHHHH (SEQ ID NO.:161) including a TEV cleavage site (italic), a T4 foldon trimerization motif (underlined), an avi-tag (bold) and 8 histidine residues (SARS-CoV-2 S avi**)**. The SARS-CoV-2 S hexapro construct was previously described (*57*). Both proteins were expressed in HEK293F cells grown in suspension using FreeStyle 293 expression medium (Life technologies) at 37˚C in a humidified 8 % CO2 incubator rotating at 130 rpm. The cultures were transfected using PEI (9 μg/mL) with cells grown to a density of 2.5 million cells per mL and cultivated for 4 days. Supernatants were harvested and cells resuspended for another 4 days in fresh media, yielding two harvests. SARS-CoV-2 S hexapro was purified from clarified supernatants using 1mL cobalt resin (Takara Bio TALON) and SARS-CoV-2 S avi was purified from supernatants using a 1mL HisTrap HP column. Both proteins were concentrated and flash frozen in a buffer containing 20 mM Tris pH 8.0 and 150 mM

NaCl prior to analysis. SDS-PAGE and negative stain EM was run to check purity and quality of the proteins.

For SPR and BLI, SARS-CoV-2 S (residues 13-1211) with a mu-phosphatase signal sequence and a C-terminal Avi-His8-EPEA-tag in a pD2610-V5 vector (ATUM Bio) was expressed in Expi293F cells at 37°C and 8% CO2 according to manufacturer's instructions (Thermo Fisher Scientific). Cell culture supernatant was collected after four days and purified over a 5 mL C-tag affinity matrix (Thermo Fisher Scientific). Elution fractions were concentrated and injected on a Superose 6 Increase 10/300 GL column with 1x PBS pH 7.4 as running buffer.

SARS-CoV-2 RBD (residues 328-531 with a C-terminal thrombin cleavage site-TwinStrep-8xHis-tag, and N-terminal signal sequence) was expressed in Expi293F cells at 37°C and 8% CO_2 in a humidified incubator. Transfection was performed using ExpiFectamine 293 reagent (Thermo Fisher Scientific). Cell culture supernatant was collected three days after transfection and supplemented with 10x PBS to a final concentration of 2.5x PBS (342.5 mM NaCl, 6.75 mM KCl and 29.75 mM phosphate) and sodium phosphate dibasic to adjust the pH. SARS-CoV-2 RBD was purified using a 1 ml HisTALON Superflow cartridge (Takara Bio) and subsequently buffer exchanged using a Zeba spin desalting column into Cytiva 1x HBS-N buffer.

Recombinant ACE2 (residues 19-615 from Uniprot Q9BYF1 with a C-terminal thrombin cleavage site-TwinStrep-10xHis-GGG-tag, and N-terminal signal sequence) was expressed in Expi293F cells at 37 °C and 8% CO2 in a humified incubator. Transfection was performed using ExpiFectamine 293 reagent (Thermo Fisher Scientific). Cell culture supernatant was collected seven days after transfection, supplemented with buffer to a final concentration of 80 mM Tris-HCl pH 8.0, 100 mM NaCl, and then incubated with BioLock solution for one hour. After filtration through a 0.22 μm filter, ACE2 was purified using a 1 ml StrepTrap High Performance column (Cytiva) followed by size exclusion chromatography using a Superdex 200 Increase 10/300 GL column and PBS as running buffer (Gibco 10010-023). ACE2 protein for BLI experiments was expressed in ExpiCHO-S cells. Cell culture supernatant was

collected nine days after transfection and protein was purified as described above using 20 mM Tris-HCl pH 7.5, 150 mM NaCl as size exclusion buffer.

Donors, B-cell isolation and mAb expression

Peripheral blood samples were obtained from two donors who have recovered from SARS-CoV-2 infection. Samples were collected 46 and 61 days after symptoms onset, respectively. Donors provided written informed consent. The study was approved by the Scientific and Ethical Committee of the Luigi Sacco Hospital, Milan, Italy. Peripheral blood mononuclear cells were isolated by Ficoll density gradient centrifugation and cryopreserved until use. Upon thawing of cells, B cells were enriched by staining with CD19 PE-Cy7 (BD Bioscience 341113) and incubation with anti-PE bead (Miltenyi Biotec, cat. 130-048-801), followed by positive selection using LS columns. Enriched B cells were stained with anti-IgM, anti-IgD, anti-CD14 and anti-IgA, all PE labelled, and prefusion SARS-CoV-2 S with a biotinylated avi tag conjugated to Streptavidin Alexa-Fluor 647 (Life Technologies). SARS-CoV-2 S-specific IgG+ memory B cells were sorted by flow cytometry via gating for PE-negative and Alexa-Fluor 647 positive cells. Cells were cultured for the screening of positive supernatants.

S2M11 and S2E12 VH and VL sequences were obtained by RT-PCR and mAbs (including S309) were expressed as recombinant human Fab fragment or as IgG1 (G1m3 allotype) carrying the half-life extending M428L/N434S (LS) mutation in the Fc . ExpiCHO cells were transiently transfected with heavy and light chain expression vectors as described previously (57). For in vivo experiments in Syrian hamsters, S2M11, S2E12 and a control mAb (specific to *Plasmodium falciparum* sporozoite) were produced with a Syrian hamster IgG2 Fc.

Affinity purification of recombinant antibodies was performed on ÄKTA Xpress FPLC (Cytiva) operated by UNICORN software version 5.11 (Build 407) using HiTrap Protein A columns (Cytiva) for full length human and hamster antibodies and CaptureSelect CH1-XL MiniChrom columns (ThermoFisher Scientific) for Fab

fragments, using PBS as mobile phase. Buffer exchange to the appropriate formulation buffer was performed with a HiTrap Fast desalting column (Cytiva).

Enzyme-linked immunosorbent assay (ELISA)

96-well ELISA plates were coated overnight at 4°C with 5 µg/ml of SARS-CoV2 RBD (produced in house; residues 331–550 of S glycoprotein from BetaCoV/Wuhan-Hu-1/2019, accession number MN908947) or 1 µg/ml of SARS-RBD (Sino Biological Europe GmbH), SARS-CoV-2 (6) or SARS-CoV S (36) trimers in PBS. Plates were blocked with a 1% w/v solution of Bovine Serum Albumin (BSA; Sigma) in PBS and incubated with serial dilutions of mAbs for 1 hour at room temperature. Subsequently, the plates were washed, and anti-human IgG coupled to alkaline phosphatase (Jackson Immunoresearch) were added and incubated for 1 hour. After further washing, the substrate (p-NPP, Sigma) was added and plates were read at 405 nm using a microplate reader (Biotek). The data have been plotted with Graphpad Prism software.

Binding measurements using SPR

Binding measurements were performed using a Biacore T200 instrument using either anti-AviTag pAb (for capturing S protein) or StrepTactin XT (for capturing RBD) covalently immobilized on CM5 chips. The running buffer was either Cytiva HBS-EP+ pH 7.4 (for neutral pH experiments) or 20 mM phosphate pH 5.4, 150 mM NaCl, 0.05% P-20 (for acidic pH experiments). All measurements were performed at 25 °C. Affinity/avidity determinations were run as single-cycle kinetics, with a 3-fold dilution series of mAb starting from 300 nM, and each concentration injected for 180 sec. Double reference-subtracted data were fit to either a 1:1 binding model or a heterogeneous ligand model (for S2M11), using Biacore Evaluation software. Fit results yielded apparent equilibrium dissociation constants ($K_{D,app}$) due to conformational dynamics of the RBDs in the context of the prefusion S trimer and due to avidity for IgG binding. For dissociation rates that were too slow to fit, $K_{D,app}$ are reported as an upper limit. For IgG competition experiments, the first injection contained 300 nM IgG; the second injection maintained the same 300 nM IgG as the first injection, plus an additional IgG at 300 nM. Each injection was carried out for 420 sec. For all

measurements, pH 5.4 data were normalized by capture level to the corresponding pH 7.4 data set to enable plotting the data on the same scale.

Biolayer Interferometry to test ACE2 binding inhibition

mAb-mediated inhibition of SARS-CoV-2 RBD or S binding to human recombinant ACE2 was assessed using biolayer interferometry with an Octet Red96 (ForteBio). Before the assay SARS-CoV2 RBD (1 μg/ml) or prefusion S ectodomain trimer (15 μg/ml) were incubated in kinetic buffer KB (PBS + 0.01% BSA) with S2M11, S2E12, S309 (30 μg/ml) or no mAb for 30 minutes at 37°C. Biotinylated recombinant human ACE2 protein in KB (2 μg/ml) was immobilized on High Precision Streptavidin SAX Biosensors (Sartorius). Next, an association step with the RBD/mAb or S/mAb complexes was performed for 6 and 10 minutes, respectively. Results were plotted using Graphpad Prism.

Inhibition of ACE2 binding to SARS-CoV-2 S expressed at the surface of ExpiCHO Cells using flow cytometry

S2M11, S2E12 and S309 were biotinylated using the EZ-Link NHS-PEO solid phase biotinylation kit (Pierce) and mAbs were subsequently buffer exchanged using a 7kDa MWCO Zeba Spin Desalting Columns into PBS. The concentration to achieve the 80 % maximal binding to ExpiCHO cells stably expressing wildtype, full-length spike SARS-CoV-2 S (strain MN908947.3) was determined by flow cytometry. Unlabeled S2M11, S2E12 and S309 were serially diluted from 10 to 0.056 μg/ml and added to ExpiCHO cells. After 20 minutes, biotinylated mAbs were added at the concentration achieving 80% maximal binding and incubated for additional 20 minutes. Cells were washed and incubated with Streptavidin Alexa Fluor 647 (Life 690Technologies). After 20 minutes and additional washing steps, cells were analyzed with a 855 ZE5 flow-cytometer (Bio-rad).

Flow cytometry of mAb and ACE2 binding on Spike Protein expressing ExpiCHO-S Cells

Transient Expression of SARS-CoV-2 Spike Protein on ExpiCHO-S Cells. The SARS-CoV-2 spike protein coding sequence (YP_009724390.1) was cloned into the pcDNA3.1(+) vector under control of the human CMV promoter to generate

pcDNA3.1(+) SARS-CoV-2 D19 spike. SARS-CoV-2 S and variants were generated using site-directed mutagenesis. Immediately before transfection, ExpiCHO-S cells were seeded at 6 x 10^6 cells cells/mL in a volume of 5 mL in a 50 mL bioreactor. S variant plasmids were diluted in iced OptiPRO SFM, mixed with ExpiFectamine CHO Reagent (Life Technologies) and added to the cells. Transfected cells were then incubated at 37°C, 8% CO_2 with an orbital shaking speed of 209 RPM (orbital diameter of 25 mm) for 42 hours.

Generation of fluorescently labeled ACE2

ACE2 was biotinylated by incubation with a 1.5 molar excess of Thermo EZ-Link NHS-PEG4-Biotin and was subsequently buffer exchanged using two successive 0.5 ml 7k MWCO Zeba Spin Desalting Columns into PBS; final concentration 1.1 mg/ml. Biotinylated-ACE2 was incubated with SA-BV421 (Biolegend) at a ratio of 1:1 by volume for 20 minutes at room temperature.

Binding to Cell Surface Expressed SARS-CoV-2 S

ExpiCHO cells expressing SARS-CoV-2 S variants were harvested, washed twice with FACS buffer (2% FBS), and dispensed into a 96-well V-bottom plate. Separately, the test antibody or ACE2-BV421 were serially diluted. As a positive control for SARS-CoV-2 S variants expression, a SARS-CoV-2 convalescent plasma sample was tested at a dilution of 1:500. Cells were stained with mAb for 30 mins on ice and then washed twice in FACS buffer. Alexa Fluor 647-labelled Goat Anti-Human IgG secondary Ab (Jackson Immunoresearch) was diluted 1:750 in FACS buffer to the cells for 15 min on ice. Cells were washed twice with FACS buffer and resuspended in 1% PFA (Alfa Aesar). Data was acquired by flow-cytometry (CytoFlex LX).

Competition of mAb and ACE2 for S binding

ExpiCHO cells transfected with wildtype or variant SARS-CoV-2 S were seeded in 96 well V bottom plates and incubated with the indicated anti-S mAbs diluted in FACS buffer for 15 minutes on ice. A final concentration of 20 µg/ml ACE2-SA-BV421 was then added to the cells and incubated for 30 minutes on ice. Cells were washed twice with FACS buffer, resuspended in FACS buffer containing Alexa Fluor 647-AffiniPure F(ab')2 Fragment Goat Anti-Human IgG (1:750 dilution), and incubated for 15 minutes

on ice. Cells were washed twice with FACS buffer and analyzed on a CytoFLEX LX Flow Cytometer (Beckman Coulter). Cells were also stained with anti-S mAbs in the absence of ACE2-SA-BV421 to determine the percent spike positive cells. Data were normalized to the percent spike positive cells.

Cell surface staining of SARS-CoV-2 infected Vero cells

Vero E6 cells were infected with authentic SARS-CoV-2 at an MOI 0.1. 24 hours later, cells were harvested, spun down, plated in a 96-well plate and incubated with mAbs in FACS buffer (PBS, 2%FCS). After a 20-minute incubation, cells were washed with FACS buffer and incubated with secondary antibody Alexa Fluor 647-labelled Goat Anti-Human IgG secondary Ab (Jackson Immunoresearch) at a dilution of 1:750 for 10 minutes. Cells were washed and fixed with BD fix/perm solution (BD Biosciences). Finally, cells were washed in FACS buffer and resuspended in FACS buffer for acquisition on a flow cytometer.

MLV-based pseudotyped virus production and neutralization

Pseudotyped viruses bearing the SARS-CoV-2 S-glycoprotein were generated as previously described (6). Briefly, HEK293T-17 cells were co-transfected with a plasmid encoding for SARS-CoV-2 S-glycoprotein harboring a C-terminal 19-residue truncation (*58*), the packaging and reverse transcriptase/integrase encoding-construct Gag-Pol, and the reporter vector pTG-Luc following X-tremeGENE HP (Merck) manufacturer's recommendations. Cells were incubated at 37°C with 5% CO2 for 72 hours before the supernatants containing the pseudotyped viruses were collected, cleared from cellular debris by centrifugation (1500g x 10 minutes at 4°C) and then stored at -80°C.

To evaluate the mAbs neutralization activity against MLV-based pseudotyped viruses, VeroE6 cells were seeded at 20000 cells/well in 96 well plates using MEM supplemented with 10% FBS, 1% penicillin–streptomycin. After 24 hours, pseudotyped viruses were pre-activated by incubation with 10 µg/ml TPCK-treated trypsin (Bioconcept) for 1 hour at 37°C. Next, serial dilutions of mAbs were mixed with the pseudotyped viruses and incubated for 1 hour at 37°C. VeroE6 cells were washed twice before addition of the mAb/pseudotyped virus mix and were incubated for 2 hours at

37°C. Cells were then supplemented with MEM containing 20% FBS and 2% penicillin–streptomycin and further incubated. After 48 hours culture media was removed and 50 μL/well of Bio-Glo (Promega) was added. Cells were then incubated in the dark for 5 minutes before the luminescence signal was recorded with Synergy H1 Hybrid Multi-Mode plate reader (Biotek). Relative luciferase units (RLU) were converted to neutralization percentage and plotted with a nonlinear regression curve fit using Graph Prism.

VSV-based pseudovirus production and neutralization

To generate SARS-CoV-2 pseudotyped vesicular stomatitis virus, Lenti-X 293T cells (Takara) were seeded in 10-cm dishes. The next day, cells were transfected with a plasmid encoding for SARS-CoV-2 S (YP_009724390.1) harboring a C-terminal 19-residue truncation using TransIT-Lenti (Mirus Bio) according to the manufacturer's instructions. One day post-transfection, cells were infected with VSV(G*ΔG-luciferase) (Kerafast) at an MOI of 3 infectious units/cell. Viral inoculum was washed off after one hour and cells were incubated for another day at 37°C. The cell supernatant containing SARS-CoV-2 pseudotyped VSV was collected at day 2 post-transfection, centrifuged at 1,000 x g for 5 minutes to remove cellular debris, aliquoted, and frozen at -80°C.

For viral neutralization, Vero E6 cells were seeded into clear bottom white walled 96-well plates at 20,000 cells/well and cultured overnight at 37°C. The next day, 9-point 4-fold serial dilutions of mAbs were prepared in media. SARS-CoV-2 pseudotyped VSV was diluted 1:25 in media and added 1:1 to each antibody dilution. Virus:mAb mixtures were incubated for 1 hour at 37°C. Media was removed from the Vero E6 cells and 50 μL of virus:mAb mixtures were added to the cells. One hour post-infection, 100 μL medium was added to all wells. After 17-20 hours incubation at 37°C, medium was removed and 50 μL Bio-Glo reagent (Promega) was added to each well. The plate was shaken on a plate shaker at 300 RPM at room temperature for 15 minutes and luminescence was read on an EnSight plate reader (Perkin-Elmer).

Neutralization of authentic SARS-CoV-2 by entry-inhibition assay

Neutralization was determined using SARS-CoV-2-Nluc, an infectious clone of SARS-CoV-2 (based on strain 2019-nCoV/USA_WA1/2020) encoding nanoluciferase

in place of the viral ORF7, which demonstrated comparable growth kinetics to wildtype virus (*34*). VeroE6 cells were seeded into black-walled, clear-bottom 96-well plates at 2 x 10^4 cells/well and cultured overnight at 37°C. The next day, 9-point 4-fold serial dilutions of mAbs were prepared in infection media (DMEM + 10% FBS). SARS-CoV-2-Nluc was diluted in infection media for a final MOI of 0.1 PFU/cell, added to the mAb dilutions and incubated for 30 minutes at 37°C. Media was removed from the VeroE6 cells, mAb-virus complexes were added, and cells were incubated at 37°C for 6 hours. Media was removed from the cells, Nano-Glo luciferase substrate (Promega) was added according to the manufacturer's recommendations, incubated for 10 minutes at room temperature and luciferase signal was quantified on a VICTOR Nivo plate reader (Perkin Elmer).

mAb combination studies

Individual antibodies were 3-fold serially diluted and mixed 1:1 in a checkerboard format before incubation with virus. Combinations of two mAbs were assessed in the respective neutralization assays for the individual viruses as described above. Analysis of drug combination effects was carried out in MacSynergy II (*59*). For normalization, values obtained from infected, untreated Vero E6 cells were used as positive controls and values from uninfected Vero E6 cells were used as negative controls. Synergy plots at 95% confidence were used for reporting.

Neutralization of authentic SARS-CoV-2 by focus-forming assay

SARS-CoV-2 strain 2019-nCoV/USA_WA1/2020 was obtained from the Centers for Disease Control and Prevention (gift of Natalie Thornburg). Virus was passaged once in Vero CCL81 cells (ATCC) and titrated by focus-forming assay on Vero E6 cells (*35*). Serial dilutions of indicated mAbs were incubated with 10^2 focus forming units (FFU) of SARS-CoV-2 for 1 hour at 37˚C. MAb-virus complexes were added to Vero E6 cell monolayers in 96-well plates and incubated for 1 hour at 37˚C. Subsequently, cells were overlaid with 1% (w/v) methylcellulose in MEM supplemented with 2% FBS. Plates were harvested 30 hours later by removing overlays and fixed with 4% PFA in PBS for 20 minutes at room temperature. Plates were washed and sequentially incubated with 1µg/mL of CR3022 anti-S antibody and HRP-

conjugated goat anti-human IgG in PBS supplemented with 0.1% saponin and 0.1% BSA. SARS-CoV-2-infected cell foci were visualized using TrueBlue peroxidase substrate (KPL) and quantitated on an ImmunoSpot microanalyzer (Cellular Technologies). Data were processed using Prism software (Graphpad Prism 8).

Fusion inhibition assay

Vero E6 cells were seeded in 96 well plates at 15,000 cells per well in 70µl DMEM High glucose + 2.4% Hyclone without antibiotics. After overnight culture the cells were transfected with CoV-2-Spike-D19_pcDNA3.1 as follows: for 10 wells, 0.57 µg plasmid CoV2-Spike-D19_pcDNA were mixed with 1.68ul X-tremeGENE HP in 30ul OPTIMEM. After 15min incubation time this solution was diluted 1:10 in DMEM medium and 30µl was added per well. A 4-fold serial dilution mAbs was prepared and was added to the cells, with a final starting concentration of 20 µg/ml. The following day, 30µl 5x concentrated Draq5 in DMEM was added per well and incubated for 2 hours at 37˚C. Nine images of each well were acquired with a Cytation 5 equipment for analysis.

Measurement of Fc-effector functions

mAb-dependent activation of human FcγRIIIa was performed with a bioluminescent reporter assay. ExpiCHO cells stably expressing full-length wild-type SARS-CoV-2 S (target cells) were incubated with different amounts of mAbs. After a 15-minute incubation, Jurkat cells stably expressing FcγRIIIa receptor (V158 or F158 variants) or FcγRIIa receptor (H131 variant) and NFAT-driven luciferase gene (effector cells) were added at an effector to target ratio of 6:1 for FcγRIIIa and 5:1 for FcγRIIa. Signaling was quantified by the luciferase produced as a result of NFAT pathway activation. Luminescence was measured after 20 hours of incubation at 37°C with 5% CO2 with a luminometer using the Bio-Glo-TM Luciferase Assay Reagent according to the manufacturer's instructions (Promega, Cat. Nr.: G9798, G7018 and G9995)
To test for ADCC, ExpiCHO cells stably expressing SARS-CoV-2 S were used as target cells. NK cells were isolated from the blood of healthy donors with the MACSxpress NK Isolation Kit (Miltenyi Biotec, Cat. Nr.: 130-098-185). Target cells were incubated with mAbs for 10 minutes before addition of NK cells at an

effector:target ratio of 9:1. After a 4 hour-incubation at 37°C, LDH release as a readout of cellular cytotoxicity was detected with the Cytotoxicity Detection Kit (LDH) (Roche; Cat. Nr.: 11644793001).

To test for ADCP, PMBCs from healthy donors were used as a source of phagocytic cells. PBMCs were stained with Cell Trace Violet (Invitrogen). ExpiCHO cells stably expressing SARS-CoV-2 S were used as target cells and were fluorescently labelled with PKH67 (Sigma Aldrich). Labelled target cells (7500 cells/well) were incubated with serially diluted antibodies. After 10 minutess, stained PBMCs (150,000 cells/well) were added. The next day, cells were washed with FACS buffer (PBS, 1%FBS). Cells were stained with APC-labelled anti-CD14 mAb (BD Pharmingen) for the identification of monocytes. After 20 minutes, cells were washed with FACS buffer and fixed with 4% paraformaldehyde in PBS, 1% FBS. Cells were washed and resuspended in FACS buffer for acquisition on a ZE5 Cell Analyzer (Biorad). Data were analyzed using FlowJo software. The percentage of ADCP was calculated as the % of monocytes ($CD14^+$ cells) that were positive for PKH67.

CryoEM sample preparation, data collection and data processing

S2M11 and S2E12 Fabs were generated by digestion of the corresponding mAbs with LysC (Thermo Fisher Scientific) at 1:4000 (w/w) ratio at 37°C during an overnight digestion. SDS-PAGE in reducing and non-reducing condition was used to check quality of digestion. SARS-CoV-2 S avi at 1.2 mg per mL was incubated with a 1.2 molar excess of Fab S2M11 at 4°C for 1 hour. SARS-CoV-2 hexaPro was incubated at 1 mg per ml with a 1.5 molar excess of Fab S2E12 during 1 hour at 4°C after which the complex was further purified by size exclusion chromatography using a Superose 6 increase 10/300 column (GE Healthcare). 3 µL of 1-1.2 mg per mL of complexes were loaded onto a freshly glow discharged R 2/2 UltrAuFoil grids (200 mesh) prior to plunge freezing using a vitrobot MarkIV (ThermoFisher Scientific) with a blot force of 0 and 7-7.5 second blot time at 100% humidity and 21°C.

Data were acquired on a FEI Titan Krios transmission electron microscope operated at 300 kV and equipped with a Gatan K2 Summit direct detector and Gatan Quantum GIF energy filter, operated in zero-loss mode with a slit width of 20 eV.

Automated data collection was carried out using Leginon (60) at a nominal magnification of 130,000x with a super-resolution pixel size of 0.525 Å. The dose rate was adjusted to 8 counts/pixel/s, and each movie was fractionated in 50 frames of 200 ms. For the S/S2M11 dataset, 4,932 micrographs were collected with a defocus range comprised between -0.8 and -2 μm. For the S/S2E12 data set, 6,697 micrographs were collected also with a defocus range comprised between -0.8 and -2 μm. Movie frame alignment, estimation of the microscope contrast-transfer function parameters, particle picking and extraction were carried out using Warp (*60*). Particle images were extracted with a box size of 800 pixels2 (S/S2M11) or 1024 pixels^2 and respectively binned to 400 or 512 yielding a pixel size of 1.05 Å.

For S/S2M11 and S/S2E12 datasets, one round of reference-free 2D classification were performed using cryoSPARC (*61*). Subsequently, for both datasets one round of 3D classification with 50 iterations (angular sampling 7.5° for 25 iterations and 1.8° with local search for 25 iterations), using *ab initio* generated models in cryoSPARC (*61*), were carried out using Relion (*62, 63*) without imposing symmetry. 3D refinements were carried out using non-uniform refinement (*64*). Particle images were subjected to Bayesian polishing (*65*) using Relion before performing another round of non-uniform refinement in cryoSPARC followed by per-particle defocus refinement and again non-uniform refinement.

To improve the density of the S/S2E12 interface, the particles were symmetry-expanded and subjected to focus 3D classification without refining angles and shifts using a soft mask encompassing the RBD and S2E12 variable domains in Relion. Particles belonging to classes with the best resolved local density were selected and subjected to local refinement using cryoSPARC . Local resolution estimation, filtering, and sharpening were carried out using CryoSPARC. Reported resolutions are based on the gold-standard Fourier shell correlation (FSC) of 0.143 criterion and Fourier shell correlation curves were corrected for the effects of soft masking by high-resolution noise substitution (*66*).

CryoEM model building and analysis.

UCSF Chimera (*67*) and Coot (*68*) were used to fit atomic models (PDB 6VXX or PDB 6VYB) into the cryoEM maps and the Fab variable domains were manually built. S2E12 was built in the locally refined map and subsequently validated using the Fab crystal structure. Models were refined and relaxed using Rosetta using both sharpened and unsharpened maps (*69-71*). Validation used Phenix (*72*), Molprobity (*73*) and Privateer (*74*). Figures were generated using UCSF ChimeraX (*75*).

S2E12 crystallization and structure solution

Crystals of S2E12 Fab were obtained by the sitting-drop vapor diffusion method. A total of 200 nl Fab at approximately 7 mg/ml in 20 mM Tris-HCl pH 7.5, 150 mM NaCl were mixed with 200 nl mother liquor solution containing 0.2 M magnesium chloride hexahydrate, 0.1 M Tris pH 8.5 and 30% (w/v) PEG 4000. Crystals were flash cooled in liquid nitrogen using the mother liquor solution supplemented with 20% glycerol as a cryoprotectant. Diffraction data were collected on synchrotron beamline X10SA at the Swiss Light Source, and processed with the XDS software package (*76*). Initial phases were obtained by molecular replacement using Phaser (*77*) on the CCP4 suite, using a homology model. Several subsequent rounds of model building and refinement were performed using Coot (*68*) and Refmac5 (*78*).

Conservation analysis

Conservation analysis was performed as described previously (*21*), using a GISAID EpiCov dump obtained on September 12th 2020 (n=90,287). We required at least 4 supporting sequences to call a variant.

In vivo mAb testing using a Syrian hamster model

KU LEUVEN R&D has developed and validated a SARS-CoV-2 Syrian Golden hamster infection model (*43*).

SARS-CoV-2: the SARS-CoV-2 strain used in this study, BetaCov/Belgium/GHB-03021/2020 (EPI ISL 109 407976|2020-02-03), was recovered from a nasopharyngeal swab taken from a RT-qPCR confirmed asymptomatic patient who returned from Wuhan, China in the beginning of February 2020. A close relatedness with the prototypic Wuhan-Hu-1 2019-nCoV (GenBank accession 112 number MN908947.3)

strain was confirmed by sequencing and phylogenetic analysis. Infectious virus was isolated by serial passaging on Huh7 and Vero E6 cells (*43*); passage 6 virus was used for the study described here. The titer of the virus stock was determined by end-point dilution on Vero E6 cells by the Reed and Muench method. This work was conducted in the high-containment A3 and BSL3+ facilities of the KU Leuven Rega Institute (3CAPS) under licenses AMV 30112018 SBB 219 2018 0892 and AMV 23102017 SBB 219 20170589 according to institutional guidelines.

Cells: Vero E6 cells (African green monkey kidney, ATCC CRL-1586) were cultured in minimal essential medium (Gibco) supplemented with 10% fetal bovine serum (Integro), 1% L- glutamine (Gibco) and 1% bicarbonate (Gibco). End-point titrations were performed with medium containing 2% fetal bovine serum instead of 10%.

SARS-CoV-2 infection model in hamsters: Wildtype Syrian hamsters (Mesocricetus auratus) were purchased from Janvier Laboratories and were housed per two in ventilated isolator cages (IsoCage N Biocontainment System, Tecniplast) with ad libitum access to food and water and cage enrichment (wood block). Housing conditions and experimental procedures were approved by the ethical committee of animal experimentation of KU Leuven (license P065-2020). Female hamsters of 6-10 weeks old were anesthetized with ketamine/xylazine/atropine and inoculated intranasally with 50 µL containing 2×106 TCID50. mAb treatment (S2M11 (1 mg/kg), S2E12 (1 mg/kg) or their combinations (1 or 0.5 mg/kg)) was initiated 48 hours before infection by intraperitoneal injection. Hamsters were monitored for appearance, behavior and weight. At day 4 post infection (pi), hamsters were euthanized by intraperitoneal injection of 500 µL Dolethal (200mg/mL sodium pentobarbital, Vétoquinol SA). Lungs were collected, and viral RNA and infectious virus were quantified by RT-qPCR and end-point virus titration, respectively. Blood samples were collected before infection for PK analysis.

SARS-CoV-2 RT-qPCR: Hamster tissues were collected after sacrifice and were homogenized using bead disruption (Precellys) in 350 µL RLT buffer (RNeasy Mini kit, Qiagen) and centrifuged (10,000 rpm, 5 minutes) to pellet the cell debris. RNA was extracted according to the manufacturer's instructions. To extract RNA from serum, the

NucleoSpin kit (Macherey-Nagel) was used. Of 50 µL eluate, 4 µL was used as a template in RT-qPCR reactions. RT-qPCR was performed on a LightCycler96 platform (Roche) using the iTaq Universal Probes One-Step RT-qPCR kit (BioRad) with N2 primers and probes targeting the nucleocapsid (*43*). Standards of SARS-CoV2 cDNA (IDT) were used to express viral genome copies per mg tissue or per mL serum.

End-point virus titrations: Lung tissues were homogenized using bead disruption (Precellys) in 350 µL minimal essential medium and centrifuged (10,000 rpm, 5min, 4°C) to pellet the cell debris. To quantify infectious SARS-CoV-2 particles, endpoint titrations were performed on confluent Vero E6 cells in 96-well plates. Viral titers were calculated by the Reed and Muench method (*79*) and were expressed as 50% tissue culture infectious dose ($TCID_{50}$) per mg tissue.

References

1. P. Zhou *et al.*, A pneumonia outbreak associated with a new coronavirus of probable bat origin. *Nature*, (2020).
2. N. Zhu *et al.*, A Novel Coronavirus from Patients with Pneumonia in China, 2019. *N Engl J Med*, (2020).
3. H. Zhou *et al.*, A Novel Bat Coronavirus Closely Related to SARS-CoV-2 Contains Natural Insertions at the S1/S2 Cleavage Site of the Spike Protein. *Curr Biol* **30**, 2196-2203.e2193 (2020).
4. C. Drosten *et al.*, Identification of a novel coronavirus in patients with severe acute respiratory syndrome. *N Engl J Med* **348**, 1967-1976 (2003).
5. T. G. Ksiazek *et al.*, A novel coronavirus associated with severe acute respiratory syndrome. *N Engl J Med* **348**, 1953-1966 (2003).
6. A. C. Walls *et al.*, Structure, Function, and Antigenicity of the SARS-CoV-2 Spike Glycoprotein. *Cell* **181**, 281-292.e286 (2020).
7. D. Wrapp *et al.*, Cryo-EM structure of the 2019-nCoV spike in the prefusion conformation. *Science* **367**, 1260-1263 (2020).
8. J. Lan *et al.*, Structure of the SARS-CoV-2 spike receptor-binding domain bound to the ACE2 receptor. *Nature*, (2020).
9. J. Shang *et al.*, Structural basis of receptor recognition by SARS-CoV-2. *Nature*, (2020).
10. R. Yan *et al.*, Structural basis for the recognition of SARS-CoV-2 by full-length human ACE2. *Science* **367**, 1444-1448 (2020).
11. M. Hoffmann *et al.*, SARS-CoV-2 Cell Entry Depends on ACE2 and TMPRSS2 and Is Blocked by a Clinically Proven Protease Inhibitor. *Cell* **181**, 271-280.e278 (2020).
12. Q. Wang *et al.*, Structural and Functional Basis of SARS-CoV-2 Entry by Using Human ACE2. *Cell* **181**, 894-904.e899 (2020).

13. M. Letko, A. Marzi, V. Munster, Functional assessment of cell entry and receptor usage for SARS-CoV-2 and other lineage B betacoronaviruses. *Nature Microbiology*, (2020).
14. M. A. Tortorici, D. Veesler, Structural insights into coronavirus entry. *Adv Virus Res* **105**, 93-116 (2019).
15. P. M. Folegatti *et al.*, Safety and immunogenicity of the ChAdOx1 nCoV-19 vaccine against SARS-CoV-2: a preliminary report of a phase 1/2, single-blind, randomised controlled trial. *Lancet*, (2020).
16. J. Yu *et al.*, DNA vaccine protection against SARS-CoV-2 in rhesus macaques. *Science*, (2020).
17. F. C. Zhu *et al.*, Safety, tolerability, and immunogenicity of a recombinant adenovirus type-5 vectored COVID-19 vaccine: a dose-escalation, open-label, non-randomised, first-in-human trial. *Lancet* **395**, 1845-1854 (2020).
18. L. A. Jackson *et al.*, An mRNA Vaccine against SARS-CoV-2 - Preliminary Report. *N Engl J Med*, (2020).
19. U. Sahin *et al.*, Concurrent human antibody and T_H1 type T-cell responses elicited by a COVID-19 RNA vaccine. *medRxiv*, 2020.2007.2017.20140533 (2020).
20. M. J. Mulligan *et al.*, Phase 1/2 Study to Describe the Safety and Immunogenicity of a COVID-19 RNA Vaccine Candidate (BNT162b1) in Adults 18 to 55 Years of Age: Interim Report. *medRxiv*, 2020.2006.2030.20142570 (2020).
21. D. Pinto *et al.*, Cross-neutralization of SARS-CoV-2 by a human monoclonal SARS-CoV antibody. *Nature* **583**, 290-295 (2020).
22. C. O. Barnes *et al.*, Structures of Human Antibodies Bound to SARS-CoV-2 Spike Reveal Common Epitopes and Recurrent Features of Antibodies. *Cell*, (2020).
23. D. F. Robbiani *et al.*, Convergent antibody responses to SARS-CoV-2 in convalescent individuals. *Nature*, (2020).
24. C. Wang *et al.*, A human monoclonal antibody blocking SARS-CoV-2 infection. *bioRxiv*, 2020.2003.2011.987958 (2020).
25. Y. Wu *et al.*, A noncompeting pair of human neutralizing antibodies block COVID-19 virus binding to its receptor ACE2. *Science* **368**, 1274-1278 (2020).
26. P. J. M. Brouwer *et al.*, Potent neutralizing antibodies from COVID-19 patients define multiple targets of vulnerability. *Science*, (2020).
27. E. Seydoux *et al.*, Characterization of neutralizing antibodies from a SARS-CoV-2 infected individual. *bioRxiv*, 2020.2005.2012.091298 (2020).
28. W. B. Alsoussi *et al.*, A Potently Neutralizing Antibody Protects Mice against SARS-CoV-2 Infection. *J Immunol*, (2020).
29. T. F. Rogers *et al.*, Isolation of potent SARS-CoV-2 neutralizing antibodies and protection from disease in a small animal model. *Science*, (2020).
30. S. J. Zost *et al.*, Potently neutralizing and protective human antibodies against SARS-CoV-2. *Nature*, (2020).
31. J. Hansen *et al.*, Studies in humanized mice and convalescent humans yield a SARS-CoV-2 antibody cocktail. *Science*, (2020).
32. R. Shi *et al.*, A human neutralizing antibody targets the receptor-binding site of SARS-CoV-2. *Nature* **584**, 120-124 (2020).

33. B. Ju *et al.*, Human neutralizing antibodies elicited by SARS-CoV-2 infection. *Nature* **584**, 115-119 (2020).
34. X. Xie *et al.*, A nanoluciferase SARS-CoV-2 for rapid neutralization testing and screening of anti-infective drugs for COVID-19. *bioRxiv*, 2020.2006.2022.165712 (2020).
35. J. B. Case *et al.*, Neutralizing Antibody and Soluble ACE2 Inhibition of a Replication-Competent VSV-SARS-CoV-2 and a Clinical Isolate of SARS-CoV-2. *Cell Host Microbe* **28**, 475-485.e475 (2020).
36. A. C. Walls *et al.*, Unexpected Receptor Functional Mimicry Elucidates Activation of Coronavirus Fusion. *Cell* **176**, 1026-1039.e1015 (2019).
37. T. Zhou *et al.*, A pH-dependent switch mediates conformational masking of SARS-CoV-2 spike. *bioRxiv*, (2020).
38. Z. Ke *et al.*, Structures, conformations and distributions of SARS-CoV-2 spike protein trimers on intact virions. *bioRxiv*, 2020.2006.2027.174979 (2020).
39. M. McCallum, A. C. Walls, J. E. Bowen, D. Corti, D. Veesler, Structure-guided covalent stabilization of coronavirus spike glycoprotein trimers in the closed conformation. *Nat Struct Mol Biol*, (2020).
40. S. Bournazos, T. T. Wang, J. V. Ravetch, The Role and Function of Fcγ Receptors on Myeloid Cells. *Microbiol Spectr* **4**, (2016).
41. Q. Li *et al.*, The impact of mutations in SARS-CoV-2 spike on viral infectivity and antigenicity. *Cell*, (2020).
42. T. N. Starr *et al.*, Deep Mutational Scanning of SARS-CoV-2 Receptor Binding Domain Reveals Constraints on Folding and ACE2 Binding. *Cell* **182**, 1295-1310.e1220 (2020).
43. R. Boudewijns *et al.*, STAT2 signaling as double-edged sword restricting viral dissemination but driving severe pneumonia in SARS-CoV-2 infected hamsters. *bioRxiv*, 2020.2004.2023.056838 (2020).
44. L. Liu *et al.*, Potent neutralizing antibodies against multiple epitopes on SARS-CoV-2 spike. *Nature* **584**, 450-456 (2020).
45. M. Schoof *et al.*, An ultra-potent synthetic nanobody neutralizes SARS-CoV-2 by locking Spike into an inactive conformation. *bioRxiv*, 2020.2008.2008.238469 (2020).
46. C. O. Barnes *et al.*, Structural classification of neutralizing antibodies against the SARS-CoV-2 spike receptor-binding domain suggests vaccine and therapeutic strategies. *bioRxiv*, 2020.2008.2030.273920 (2020).
47. X. Brochet, M. P. Lefranc, V. Giudicelli, IMGT/V-QUEST: the highly customized and integrated system for IG and TR standardized V-J and V-D-J sequence analysis. *Nucleic Acids Res* **36**, W503-508 (2008).
48. J. Snijder *et al.*, An Antibody Targeting the Fusion Machinery Neutralizes Dual-Tropic Infection and Defines a Site of Vulnerability on Epstein-Barr Virus. *Immunity* **48**, 799-811.e799 (2018).
49. G. Fibriansah, S. M. Lok, The development of therapeutic antibodies against dengue virus. *Antiviral Res* **128**, 7-19 (2016).
50. W. Dejnirattisai *et al.*, A new class of highly potent, broadly neutralizing antibodies isolated from viremic patients infected with dengue virus. *Nat Immunol* **16**, 170-177 (2015).

51. E. N. Gallichotte *et al.*, Human dengue virus serotype 2 neutralizing antibodies target two distinct quaternary epitopes. *PLoS Pathog* **14**, e1006934 (2018).
52. D. G. Widman *et al.*, Transplantation of a quaternary structure neutralizing antibody epitope from dengue virus serotype 3 into serotype 4. *Sci Rep* **7**, 17169 (2017).
53. F. Long *et al.*, Structural basis of a potent human monoclonal antibody against Zika virus targeting a quaternary epitope. *Proc Natl Acad Sci U S A* **116**, 1591-1596 (2019).
54. B. R. West *et al.*, Structural Basis of Pan-Ebolavirus Neutralization by a Human Antibody against a Conserved, yet Cryptic Epitope. *mBio* **9**, (2018).
55. B. Kaufmann *et al.*, Neutralization of West Nile virus by cross-linking of its surface proteins with Fab fragments of the human monoclonal antibody CR4354. *Proc Natl Acad Sci U S A* **107**, 18950-18955 (2010).
56. E. T. Crooks *et al.*, Vaccine-Elicited Tier 2 HIV-1 Neutralizing Antibodies Bind to Quaternary Epitopes Involving Glycan-Deficient Patches Proximal to the CD4 Binding Site. *PLoS Pathog* **11**, e1004932 (2015).
57. C. L. Hsieh *et al.*, Structure-based design of prefusion-stabilized SARS-CoV-2 spikes. *Science*, (2020).
58. X. Ou *et al.*, Characterization of spike glycoprotein of SARS-CoV-2 on virus entry and its immune cross-reactivity with SARS-CoV. *Nat Commun* **11**, 1620 (2020).
59. M. N. Prichard, C. Shipman, A three-dimensional model to analyze drug-drug interactions. *Antiviral Res* **14**, 181-205 (1990).
60. D. Tegunov, P. Cramer, Real-time cryo-electron microscopy data preprocessing with Warp. *Nat Methods* **16**, 1146-1152 (2019).
61. A. Punjani, J. L. Rubinstein, D. J. Fleet, M. A. Brubaker, cryoSPARC: algorithms for rapid unsupervised cryo-EM structure determination. *Nat Methods* **14**, 290-296 (2017).
62. J. Zivanov *et al.*, New tools for automated high-resolution cryo-EM structure determination in RELION-3. *Elife* **7**, (2018).
63. D. Kimanius, B. O. Forsberg, S. H. Scheres, E. Lindahl, Accelerated cryo-EM structure determination with parallelisation using GPUs in RELION-2. *Elife* **5**, (2016).
64. A. Punjani, H. Zhang, D. J. Fleet, Non-uniform refinement: Adaptive regularization improves single particle cryo-EM reconstruction. *bioRxiv*, 2019.2012.2015.877092 (2019).
65. J. Zivanov, T. Nakane, S. H. W. Scheres, A Bayesian approach to beam-induced motion correction in cryo-EM single-particle analysis. *IUCrJ* **6**, 5-17 (2019).
66. S. Chen *et al.*, High-resolution noise substitution to measure overfitting and validate resolution in 3D structure determination by single particle electron cryomicroscopy. *Ultramicroscopy* **135**, 24-35 (2013).
67. E. F. Pettersen *et al.*, UCSF Chimera--a visualization system for exploratory research and analysis. *J Comput Chem* **25**, 1605-1612 (2004).
68. P. Emsley, B. Lohkamp, W. G. Scott, K. Cowtan, Features and development of Coot. *Acta Crystallographica Section D* **66**, 486-501 (2010).
69. B. Frenz *et al.*, Automatically Fixing Errors in Glycoprotein Structures with Rosetta. *Structure* **27**, 134-139.e133 (2019).

70. R. Y. Wang *et al.*, Automated structure refinement of macromolecular assemblies from cryo-EM maps using Rosetta. *Elife* **5**, (2016).
71. F. DiMaio *et al.*, Atomic-accuracy models from 4.5-Å cryo-electron microscopy data with density-guided iterative local refinement. *Nat Methods* **12**, 361-365 (2015).
72. D. Liebschner *et al.*, Macromolecular structure determination using X-rays, neutrons and electrons: recent developments in Phenix. *Acta Crystallogr D Struct Biol* **75**, 861-877 (2019).
73. V. B. Chen *et al.*, MolProbity: all-atom structure validation for macromolecular crystallography. *Acta Crystallogr D Biol Crystallogr* **66**, 12-21 (2010).
74. J. Agirre *et al.*, Privateer: software for the conformational validation of carbohydrate structures. *Nat Struct Mol Biol* **22**, 833-834 (2015).
75. T. D. Goddard *et al.*, UCSF ChimeraX: Meeting modern challenges in visualization and analysis. *Protein Sci* **27**, 14-25 (2018).
76. W. Kabsch, XDS. *Acta Crystallogr D Biol Crystallogr* **66**, 125-132 (2010).
77. A. J. McCoy *et al.*, Phaser crystallographic software. *J Appl Crystallogr* **40**, 658-674 (2007).
78. G. N. Murshudov *et al.*, REFMAC5 for the refinement of macromolecular crystal structures. *Acta Crystallogr D Biol Crystallogr* **67**, 355-367 (2011).
79. L. J. Reed, H. Muench, A SIMPLE METHOD OF ESTIMATING FIFTY PER CENT ENDPOINTS12. *American Journal of Epidemiology* **27**, 493-497 (1938).

The various embodiments described above can be combined to provide further embodiments. All of the U.S. patents, U.S. patent application publications, U.S. patent applications, foreign patents, foreign patent applications and non-patent publications referred to in this specification and/or listed in the Application Data Sheet, including U.S. Patent Application No. 63/034,326, filed June 3, 2020, U.S. Patent Application No. 63/055,861, filed July 23, 2020, U.S. Patent Application No. 63/058,368, filed July 29, 2020, U.S. Patent Application No. 63/066,093, filed August 14, 2020, U.S. Patent Application No. 63/070,803, filed August 26, 2020, U.S. Patent Application No. 63/078,157, filed September 14, 2020, and U.S. Patent Application No. 63/166,874, filed March 26, 2021, are incorporated herein by reference, in their entirety. Aspects of the embodiments can be modified, if necessary to employ concepts of the various patents, applications and publications to provide yet further embodiments.

These and other changes can be made to the embodiments in light of the above-detailed description. In general, in the following claims, the terms used should not be

construed to limit the claims to the specific embodiments disclosed in the specification and the claims, but should be construed to include all possible embodiments along with the full scope of equivalents to which such claims are entitled. Accordingly, the claims are not limited by the disclosure.

CLAIMS

What is claimed is:

1. An antibody, or an antigen-binding fragment thereof, that competes with an antibody or antigen-binding fragment comprising a VH amino acid sequence according to SEQ ID NO: 16 and a VL amino acid sequence according to SEQ ID NO: 26 for binding to a SARS-CoV-2 S glycoprotein of a S glycoprotein trimer.

2. An antibody, or an antigen-binding fragment thereof, that is capable of binding to a SARS CoV-2 S glycoprotein of a S glycoprotein trimer, wherein:

(a) binding comprises contacting one or more of amino acid residues 369-386, 404-411, and 499-508 of SEQ ID NO: 3; and/or

(b) binding comprises binding an epitope formed by amino acid residues 369-386, 404-411, and 499-508 of SEQ ID NO: 3.

3. The antibody or antigen-binding fragment of claim 2, which does not contact one or more of amino acids 406, 409, 410, 411, 499, 500, 505, and 507 of SEQ ID NO.:3 when binding to the S glycoprotein.

4. The antibody or antigen-binding fragment of any one of claims 1-3, which is capable of binding to a SARS-CoV-2 S glycoprotein of a S glycoprotein trimer wherein two or three receptor binding domains (RBDs) of the trimer are in an open conformation and one or zero RBDs of the trimer is in a closed conformation, and optionally is not capable of binding to the S glycoprotein when only one RBD of the trimer is in an open conformation and two RBDs of the trimer are in a closed conformation.

5. An antibody, or an antigen-binding fragment thereof, which is capable of binding to a SARS-CoV-2 S glycoprotein of a S glycoprotein trimer wherein two or

three receptor binding domains (RBDs) of the trimer are in an open conformation and one or zero RBDs of the trimer is in a closed conformation, and optionally is not capable of binding to the S protein when only one RBD of the trimer is in an open conformation and two RBDs of the trimer are in a closed conformation.

6. An antibody, or an antigen-binding fragment thereof, that competes with an antibody or antigen-binding fragment comprising a VH amino acid sequence according to SEQ ID NO: 31 and a VL amino acid sequence according to SEQ ID NO: 35 for binding to a SARS-CoV-2 S glycoprotein of a S glycoprotein trimer.

7. An antibody, or an antigen-binding fragment thereof, that is capable of binding to a SARS CoV-2 S glycoprotein of a S glycoprotein trimer, wherein:

(a) binding comprises contacting one or more of amino acid residues 444-449 and 472-498 of SEQ ID NO: 3; and/or

(b) the antibody or antigen-binding fragment recognizes an epitope formed by amino acid residues 444-449 and 472-498 of SEQ ID NO: 3; and/or

(c) binding comprises binding within a crevice formed by a receptor binding motif (RBM) β-hairpin in a receptor binding domain (RBD) of the S glycoprotein.

8. The antibody or antigen-binding fragment of claim 7, which does not contact one or more of amino acids 448, 473-478, 487, 491, 492, 495, 496, and 497 of SEQ ID NO.:3 when binding to the SARS-CoV-2 S glycoprotein.

9. The antibody or antigen-binding fragment of any one of claims 6-8, which is capable of binding to a SARS-CoV-2 S glycoprotein of a S glycoprotein trimer wherein one or zero receptor binding domains (RBDs) of the trimer are in an open conformation and two or three RBDs of the trimer are in a closed conformation.

10. An antibody, or an antigen-binding fragment thereof, which is capable of binding to a SARS-CoV-2 S glycoprotein protein of a S glycoprotein trimer wherein

one or zero receptor binding domains (RBDs) of the trimer are in an open conformation and two or three RBDs of the trimer are in a closed conformation.

11. An antibody, or an antigen-binding fragment thereof, that competes with an antibody or antigen-binding fragment comprising a VH amino acid sequence according to SEQ ID NO: 47 and a VL amino acid sequence according to SEQ ID NO: 51 for binding to a SARS-CoV-2 S glycoprotein of a S glycoprotein trimer.

12. An antibody, or an antigen-binding fragment thereof, that is capable of binding to a SARS CoV-2 S glycoprotein, wherein:

(a) binding comprises contacting one or more of amino acid residues 403, 444-456, 475, and 485-505 of SEQ ID NO: 3; and/or

(b) the antibody or antigen-binding fragment recognizes an epitope formed by amino acid residues 403, 444-456, 475, and 485-505 of SEQ ID NO: 3.

13. The antibody or antigen-binding fragment of claim 12, which does not contact one or more of amino acids 448, 450, 451, 452, 454, 486, 488, 490, 491, 492, 497, 503, and 504 of SEQ ID NO.:3 when binding to the S glycoprotein.

14. The antibody or antigen-binding fragment of any one of claims 11-13, which is capable of binding to a SARS-CoV-2 S glycoprotein of a S glycoprotein trimer wherein one, two, or three receptor binding domains (RBDs) of the trimer are in an open conformation.

15. An antibody, or an antigen-binding fragment thereof, that competes with an antibody or antigen-binding fragment comprising a VH amino acid sequence according to SEQ ID NO: 64 and a VL amino acid sequence according to SEQ ID NO: 68 for binding to a SARS-CoV-2 S glycoprotein of a S glycoprotein trimer.

16. An antibody, or an antigen-binding fragment thereof, that is capable of binding to a SARS CoV-2 S glycoprotein of a S glycoprotein trimer, wherein:

(a) binding comprises contacting one or more of amino acid residues 368-388 and 407-414 of SEQ ID NO: 3; and/or

(b) the antibody or antigen-binding fragment recognizes an epitope formed by amino acid residues 368-388 and 407-414 of SEQ ID NO: 3.

17. The antibody or antigen-binding fragment of claim 15 or 16, which is capable of binding to a SARS-CoV-2 S glycoprotein of a S glycoprotein trimer wherein two or three receptor binding domains (RBDs) of the trimer are in an open conformation and zero or one RBDs of the trimer is in a closed conformation.

18. An antibody, or an antigen-binding fragment thereof, that competes with an antibody or antigen-binding fragment comprising a VH amino acid sequence according to SEQ ID NO: 150 and a VL amino acid sequence according to SEQ ID NO: 154 for binding to a SARS-CoV-2 S glycoprotein of a S glycoprotein trimer.

19. An antibody, or an antigen-binding fragment thereof, that is capable of binding to a SARS CoV-2 S glycoprotein of a S glycoprotein trimer, wherein:

(a) binding comprises contacting one or more of amino acid residues 369-392, 411-414, 427-430, and 515-517 of SEQ ID NO: 3; and/or

(b) the antibody or antigen-binding fragment recognizes an epitope formed by amino acid residues 369-392, 411-414, 427-430, and 515-517 of SEQ ID NO: 3.

20. The antibody or antigen-binding fragment of claim 18 or 19, which is capable of binding to a SARS-CoV-2 S protein of a S protein trimer wherein two or three receptor binding domains (RBDs) of the trimer are in an open conformation and zero or one RBDs of the trimer is in a closed conformation.

21. The antibody or antigen-binding fragment of any one of claims 15-20, wherein binding of the antibody or antigen-binding fragment to the S glycoprotein promotes or leads to release of the S1 subunit from the S glycoprotein.

22. An antibody, or an antigen-binding fragment thereof, that competes with an antibody or antigen-binding fragment comprising a VH amino acid sequence according to SEQ ID NO: 123 and a VL amino acid sequence according to SEQ ID NO: 138 for binding to a SARS-CoV-2 S glycoprotein of a S glycoprotein trimer.

23. An antibody, or an antigen-binding fragment thereof, that is capable of binding to a SARS CoV-2 S glycoprotein of a S glycoprotein trimer, wherein:

(a) binding comprises contacting one or more of amino acid residues 417, 453, 455, 456, 473, 475-480, 484-489, and 493 of SEQ ID NO: 3; and/or

(b) the antibody or antigen-binding fragment recognizes an epitope formed by amino acid residues 417, 453, 455, 456, 473, 475-480, 484-489, and 493of SEQ ID NO.: 3.

24. The antibody or antigen-binding fragment of claim 22 or 23, which is capable of binding to a SARS-CoV-2 S glycoprotein of a S glycoprotein trimer wherein one, two, or three receptor binding domains (RBDs) of the trimer are in an open conformation and zero, one, or two RBDs of the trimer are in a closed conformation.

25. An antibody, or an antigen-binding fragment thereof, that competes with an antibody or antigen-binding fragment comprising a VH amino acid sequence according to SEQ ID NO: 142 and a VL amino acid sequence according to SEQ ID NO: 146 for binding to a SARS-CoV-2 S glycoprotein trimer.

26. An antibody, or an antigen-binding fragment thereof, that is capable of binding to a SARS CoV-2 S glycoprotein trimer, wherein:

(a) binding comprises contacting one or more of amino acid residues on each of two receptor binding domains (RBDs), wherein binding comprises contacting, on a first RBD, one or more of amino acid residues 339, 342, 343, 367, 368, 371, 372, 373, 374, 436, 440, and 441, and, on a second RBD, one or more of amino acid residues 446, 447, 449, 452, 455, 456, 484, 485, 486, 487, 489, 490, 492, 493, 494, 496, and 498, wherein the amino acid numbering is according to SEQ ID NO.:3; and/or

(b) the antibody or antigen-binding fragment recognizes an epitope formed by the following:

(b)(i) on a first RBD, amino acid residues 339, 342, 343, 367, 368, 371, 372, 373, 374, 436, 440, and 441, and,

(b)(ii) on a second RBD, amino acid residues 446, 447, 449, 452, 455, 456, 484, 485, 486, 487, 489, 490, 492, 493, 494, 496, and 498, wherein the amino acid numbering is according to SEQ ID NO.:3.

27. The antibody or antigen-binding fragment of claim 25 or 26, which is capable of binding to the S glycoprotein trimer wherein three receptor binding domains (RBDs) of the trimer are in a closed conformation.

28. The antibody or antigen-binding fragment of any one of claims 25-27, wherein binding of the antibody or antigen-binding fragment to the S glycoprotein trimer inhibits or prevents an RBD of the trimer from assuming an open conformation.

29. The antibody or antigen-binding fragment of any one of claims 1-28, wherein binding of the antibody or antigen-binding fragment to the S glycoprotein or S glycoprotein trimer, respectively, blocks an interaction between the S glycoprotein and a human ACE2.

30. The antibody or antigen-binding fragment of any one of claims 1-28, wherein binding of the antibody or antigen-binding fragment to the S glycoprotein or S

glycoprotein trimer, respectively, does not block an interaction between the S glycoprotein and a human ACE2.

31. The antibody or antigen-binding fragment of any one of claims 1-30, which is capable of neutralizing an infection by a SARS-CoV-2.

32. An isolated polynucleotide encoding the antibody or antigen-binding fragment of any one of claims 1-31.

33. A vector comprising the polynucleotide of claim 32.

34. A recombinant host cell that: (i) expresses the antibody or antigen-binding fragment of any one of claims 1-31; (ii) comprises the polynucleotide of claim 32; and/or (iii) comprises the vector of claim 33.

35. A composition comprising:

(i) the antibody or antigen-binding fragment of any one of claims 1-31;

(ii) the polynucleotide of claim 32;

(iii) the vector of claim 33; and/or

(iv) the host cell of claim 34, and

a pharmaceutically acceptable carrier, excipient, or diluent.

36. A combination comprising (i) any two or more of the antibodies or antigen-binding fragments of any of claims 1-31 or (ii) a first antibody or antigen-binding fragment of any of claims 1-31 and a second antibody or antigen-binding fragment that is antibody S309 or an antibody that competes with antibody S309 for binding to a SARS CoV-2 S glycoprotein.

37. A composition comprising (i) any two or more of the antibodies or antigen-binding fragments of any of claims 1-31 or (ii) a first antibody or antigen-

binding fragment of any of claims 1-31 and a second antibody or antigen-binding fragment that is antibody S309 or that competes with antibody S309 for binding to a SARS-CoV-2 S glycoprotein and a pharmaceutically acceptable carrier, excipient, or diluent.

38. A method for treating a SARS-CoV-2 infection in a subject, the method administering to the subject an effective amount of:

(i) the antibody or antigen-binding fragment of any one of claims 1-31;

(ii) the polynucleotide of claim 32;

(iii) the vector of claim 33;

(iv) the host cell of claim 34;

(v) the composition of claim 35;

(vi) the combination of claim 36;

(vii) the composition of claim 37;

(viii) any two or more of the antibodies or antigen-binding fragments of any one of claims 1-31; or

(ix) any combination of (i)-(viii).

39. The antibody or antigen-binding fragment of any one of claims 1-31, the polynucleotide of claim 32, the vector of claim 33, the host cell of claim 34, the composition of claim 35, the combination of claim 36, the composition of claim 37, and/or the any two or more of the antibodies or antigen-binding fragments of any one of claims 1-31, for use in a method of treating a SARS-CoV-2 infection in a subject.

40. An immunogenic composition comprising:

(a) a SARS-CoV-2 nucleocapsid (N) protein (SEQ ID NO.:170), or an immunogenic fragment thereof;

(b) a SARS-CoV-2 S polypeptide or multimer thereof comprising (i) one, two, or three Receptor Binding Domains (RBDs) in an open conformation and (ii) a Site Ia polypeptide, the Site Ia polypeptide capable of being bound by antibody S2H14;

(c) a SARS-CoV-2 Spike (S) polypeptide comprising (i) a RBD in an open conformation or in a closed conformation and (ii) a Site Ib polypeptide, the Site Ib polypeptide capable of being bound by antibody S2H13;

(d) a SARS-CoV-2 S polypeptide or multimer thereof comprising (i) two or three Receptor Binding Domains (RBDs) in an open conformation and (ii) a Site IIa polypeptide, the Site IIa polypeptide capable of being bound by antibody S2X35;

(e) a SARS-CoV-2 S polypeptide or multimer thereof comprising (i) two adjacent RBDs in an open conformation and (ii) a Site IIb polypeptide, the Site IIb polypeptide capable of being bound by antibody S2A4;

(f) a SARS-CoV-2 S polypeptide or multimer thereof comprising (i) two adjacent RBDs in an open conformation and (ii) a Site IIc polypeptide, the Site IIc polypeptide capable of being bound by antibody S304;

(g) a SARS-CoV-2 S polypeptide capable of being bound by antibody CR3022;

(h) a SARS-CoV-2 Spike (S) polypeptide or multimer thereof comprising (i) a RBD in an open conformation or in a closed conformation and (ii) a Site IV polypeptide, the Site IV polypeptide capable of being bound by antibody S309;

(i) a polynucleotide encoding the SARS-CoV-2 N or S protein polypeptide of any one or more of (a)-(h); or

(j) any combination of (a)-(i) above.

41. The immunogenic composition of claim 40, further comprising a pharmaceutically acceptable carrier, excipient, or diluent, and/or comprising an adjuvant.

42. The immunogenic composition of claim 40 or claim 41, wherein the SARS-COV-2 S polypeptide comprises a prefusion-stabilized S ectodomain and/or does not comprise a R1 domain, a CH domain, a CD domain, a HR1 domain, a HR2 domain, a TM domain, and/or a CT domain.

43. A method comprising administering the immunogenic composition or composition of any one of claims 40-42 to a subject having, suspected of having, or at risk for having a SARS-CoV-2 infection.

44. Use of:

(a) (a)(i) antibody S2H14, or an antigen-binding fragment thereof, or (a)(ii) an antibody or antigen-binding fragment thereof that competes with (a)(i) for binding to a SARS-CoV-2 S glycoprotein;

(b) (b)(i) antibody S2H13, or an antigen-binding fragment thereof, or (b)(ii) an antibody or antigen-binding fragment thereof that competes with (b)(i) for binding to a SARS-CoV-2 S glycoprotein;

(c) (c)(i) antibody S2X35, or an antigen-binding fragment thereof, or (c)(ii) an antibody or antigen-binding fragment thereof that competes with (i) for binding to a SARS-CoV-2 S glycoprotein;

(d) (d)(i) antibody S2A4 or an antigen-binding fragment thereof, or (d)(ii) an antibody or antigen-binding fragment thereof that competes with (d)(i) for binding to a SARS-CoV-2 S glycoprotein;

(e) (e)(i) antibody S304 or an antigen-binding fragment thereof, or (e)(ii) an antibody or antigen-binding fragment thereof that competes with (e)(i) for binding to a SARS-CoV-2 S glycoprotein;

(f) (f)(i) antibody S309 or an antigen-binding fragment thereof, or (f)(ii) an antibody or antigen-binding fragment thereof that competes with (f)(i) for binding to a SARS-CoV-2 S glycoprotein; and/or

(g) (g)(i) antibody CR3022, or an antigen-binding fragment thereof, or (g)(ii) an antibody or antigen-binding fragment thereof that competes with (g)(i) for binding to a SARS-CoV-2 S glycoprotein,

in the diagnosis of a SARS-CoV-2 infection, wherein the diagnosis comprises contacting the antibody or antigen-binding fragment thereof with a sample from a subject, and detecting the presence or absence of a complex comprising the antibody or antigen-binding fragment with an antigen.

45. Use of:

(a) (a)(i) antibody S2H14, or an antigen-binding fragment thereof, or (a)(ii) an antibody or antigen-binding fragment thereof that competes with (a)(i) for binding to a SARS-CoV-2 S glycoprotein;

(b) (b)(i) antibody S2H13, or an antigen-binding fragment thereof, or (b)(ii) an antibody or antigen-binding fragment thereof that competes with (b)(i) for binding to a SARS-CoV-2 S glycoprotein;

(c) (c)(i) antibody S2X35, or an antigen-binding fragment thereof, or (c)(ii) an antibody or antigen-binding fragment thereof that competes with (c)(i) for binding to a SARS-CoV-2 S glycoprotein;

(d) (d)(i) antibody S2A4 or an antigen-binding fragment thereof, or (d)(ii) an antibody or antigen-binding fragment thereof that competes with (d)(i) for binding to a SARS-CoV-2 S glycoprotein;

(e) (e)(i) antibody S304 or an antigen-binding fragment thereof, or (e)(ii) an antibody or antigen-binding fragment thereof that competes with (e)(i) for binding to a SARS-CoV-2 S glycoprotein;

(f) (f)(i) antibody S309 or an antigen-binding fragment thereof, or (f)(ii) an antibody or antigen-binding fragment thereof that competes with (f)(i) for binding to a SARS-CoV-2 Spike S glycoprotein; and/or

(g) (g)(i) antibody CR3022, or an antigen-binding fragment thereof, or (g)(ii) an antibody or antigen-binding fragment thereof that competes with (g)(i) for binding to a SARS-CoV-2 S glycoprotein,

in determining whether a SARS-CoV-2 vaccine composition comprises an epitope in a correct conformation for binding by the antibody or antigen-binding fragment thereof.

46. A method comprising detecting, in sera from one or more subject having (hospitalized, symptomatic, or asymptomatic) or recovered from a SARS-CoV-2 infection:

(a) the titer of antibody (e.g., IgG, IgA, and/or IgM) that binds to SARS-CoV-2 S glycoprotein;

(b) the titer of antibody that binds to SARS-CoV-2 RBD and optionally neutralizes the SARS-CoV-2 infection;

(c) the titer of antibody that binds to SARS-CoV-2 Domain A and optionally neutralizes the SARS CoV-2 infection;

(d) the titer of antibody that binds to SARS-CoV-2 S2 and optionally neutralizes the SARS CoV-2 infection; and/or

(e) the titer of antibody that binds to SARS-CoV-2 N protein and optionally neutralizes the SARS-CoV-2 infection.

47. The method of claim 45, further comprising preparing an immunogenic composition comprising whichever of SARS-CoV-2 S glycoprotein, RBD, Domain A, or N protein that resulted in the highest titer of antibody.

48. The method of claim 46 or 47, wherein the sera is from a subject who experienced a symptom of a SARS-CoV-2 infection and the method further comprises preparing an immunogenic composition comprising whichever of the SARS-CoV-2 S protein, RBD, Domain A, or N protein against which the highest titer of antibody is detected at 25, preferably 50, more preferably 75, still more preferably 100, even more preferably 125, still more preferably 150 days after the onset of the symptom.

49. A composition or combination comprising any two, any three, or all four of (a)-(d):

(a) (a)(i) an antibody or antigen-binding fragment thereof (*e.g.*, Fv, scFv, Fab, scFab, or the like) that is capable of binding to a SARS CoV-2 S glycoprotein and comprises a CDRH1 comprising the sequence set forth in SEQ ID NO: 143, a CDRH2

comprising the sequence set forth in SEQ ID NO:144, a CDRH3 comprising the sequence set forth in SEQ ID NO:145, a CDRL1 comprising the sequence set forth in SEQ ID NO:147, a CDRL2 comprising the sequence set forth in SEQ ID NO:148, and a CDRL3 comprising the sequence set forth in SEQ ID NO:149, or (a)(ii) an antibody or antigen-binding fragment thereof that competes with the antibody or antigen-binding fragment of (a)(i) for binding to the SARS CoV-2 S glycoprotein;

(b) (b)(i) an antibody or antigen-binding fragment thereof that is capable of binding to a SARS CoV-2 S glycoprotein and comprises a CDRH1 comprising the sequence set forth in SEQ ID NO: 109, a CDRH2 comprising the sequence set forth in SEQ ID NO:110, a CDRH3 comprising the sequence set forth in SEQ ID NO:111, a CDRL1 comprising the sequence set forth in SEQ ID NO:133, a CDRL2 comprising the sequence set forth in SEQ ID NO:134, and a CDRL3 comprising the sequence set forth in SEQ ID NO:135, or (b)(ii) an antibody or antigen-binding fragment thereof that competes with the antibody or antigen-binding fragment of (b)(i) for binding to the SARS CoV-2 S glycoprotein;

(c) (c)(i) an antibody or antigen-binding fragment thereof that is capable of binding to a SARS CoV-2 S glycoprotein and comprises a CDRH1 comprising the sequence set forth in SEQ ID NO: 102, a CDRH2 comprising the sequence set forth in SEQ ID NO:103, a CDRH3 comprising the sequence set forth in SEQ ID NO:104, a CDRL1 comprising the sequence set forth in SEQ ID NO:106, a CDRL2 comprising the sequence set forth in SEQ ID NO:107, and a CDRL3 comprising the sequence set forth in SEQ ID NO:108, or (c)(ii) an antibody or antigen-binding fragment thereof that competes with the antibody or antigen-binding fragment of (c)(i) for binding to the SARS CoV-2 S glycoprotein;

(d) (d)(i) an antibody or antigen-binding fragment thereof that is capable of binding to a SARS CoV-2 S glycoprotein and comprises a CDRH1 comprising the sequence set forth in SEQ ID NO: 94, a CDRH2 comprising the sequence set forth in SEQ ID NO:95, a CDRH3 comprising the sequence set forth in SEQ ID NO:96, a CDRL1 comprising the sequence set forth in SEQ ID NO:98, a CDRL2 comprising the sequence set forth in SEQ ID NO:99, and a CDRL3 comprising the sequence set forth

in SEQ ID NO:100, or (d)(ii) an antibody or antigen-binding fragment thereof that competes with the antibody or antigen-binding fragment of (d)(i) for binding to the SARS CoV-2 S glycoprotein.

50. The composition of claim 49, further comprising a pharmaceutically acceptable carrier, excipient, or diluent.

51. The composition of claim 49 or 50, wherein:

(1) the antibody or antigen-binding fragment of (a)(i) comprises a VH comprising or consisting of an amino acid sequence having at least 80%, 85%, 90%, 91%, 92%, 93%, 94%, 95%, 96,%, 97%, 98%, or 99% identity (*e.g.*, as determined using BLAST) (*e.g.*, 100% identity) to the amino acid sequence set forth in SEQ ID NO:142 and a VL comprising or consisting of an amino acid sequence having at least 80%, 85%, 90%, 91%, 92%, 93%, 94%, 95%, 96,%, 97%, 98%, or 99% identity to the amino acid sequence set forth in SEQ ID NO:146;

(2) the antibody or antigen-binding fragment thereof of (b)(i) comprises a VH comprising or consisting of an amino acid sequence having at least 80%, 85%, 90%, 91%, 92%, 93%, 94%, 95%, 96,%, 97%, 98%, or 99% identity to the amino acid sequence set forth in SEQ ID NO:123 and a VL comprising or consisting of an amino acid sequence having at least 80%, 85%, 90%, 91%, 92%, 93%, 94%, 95%, 96,%, 97%, 98%, or 99% identity to the sequence set forth in SEQ ID NO:138;

(3) the antibody or antigen-binding fragment thereof of (c)(i) comprises a VH comprising or consisting of an amino acid sequence having at least 80%, 85%, 90%, 91%, 92%, 93%, 94%, 95%, 96,%, 97%, 98%, or 99% identity to the amino acid sequence set forth in SEQ ID NO:101 and a VL comprising or consisting of an amino acid sequence having at least 80%, 85%, 90%, 91%, 92%, 93%, 94%, 95%, 96,%, 97%, 98%, or 99% identity to the amino acid sequence set forth in SEQ ID NO:105; and/or

(4) the antibody or antigen-binding fragment thereof of (d)(i) comprises a VH comprising or consisting of an amino acid sequence having at least 80%, 85%, 90%, 91%, 92%, 93%, 94%, 95%, 96,%, 97%, 98%, or 99% identity to the amino acid

sequence set forth in SEQ ID NO:93 and a VL comprising or consisting of an amino acid sequence having at least 80%, 85%, 90%, 91%, 92%, 93%, 94%, 95%, 96,%, 97%, 98%, or 99% identity to the amino acid sequence set forth in SEQ ID NO:97.

52. A composition comprising:

(a) (a)(i) antibody S2M11, or an antigen-binding fragment thereof, or (a)(ii) an antibody or antigen-binding fragment thereof that competes with (a)(i) for binding to a SARS-CoV-2 S glycoprotein;

(b) (b)(i) antibody S2E12, or an antigen-binding fragment thereof, or (b)(ii) an antibody or antigen-binding fragment thereof that competes with (b)(i) for binding to a SARS-CoV-2 S glycoprotein;

(c) (c)(i) antibody S309, or an antigen-binding fragment thereof, or (c)(ii) an antibody or antigen-binding fragment thereof that competes with (c)(i) for binding to a SARS-CoV-2 S glycoprotein; or

(d) any combination of (a)-(c) above.

53. The composition of claim 52, further comprising a pharmaceutically acceptable carrier, excipient, or diluent.

54. The antibody or antigen-binding fragment of any one of claims 1-31, the combination of claim 36, or the composition of any one of claims 37, 38, and 49-53, wherein any one or more of the antibodies or antigen binding fragments comprises a Fc polypeptide comprising:

(i) a mutation that enhances binding to a human FcRn and/or extends an *in vivo* half-life of antibody or antigen-binding fragment, optionally a M428L mutation, a N434S mutation, YTE mutation, or any combination thereof; and/or

(ii) a mutation that that enhances binding to a human FcγR, optionally a G236A mutation, a A330L mutation, a I332E, a S239D mutation, or any combination thereof.

55. The composition of any one of claims 49-54 for use in treating or preventing SARS-CoV-2 infection.

56. A method of treating or preventing SARS-CoV-2 infection in a subject, comprising administering to the subject an effective amount of the composition of any one of claims 49-54.

57. A method of treating or preventing a SARS-CoV-2 infection in a subject, comprising administering to the subject an effective amount of any one or more of:

(a) (i) an antibody or antigen-binding fragment thereof (*e.g.*, Fv, scFv, Fab, scFab, or the like) that is capable of binding to a SARS CoV-2 S protein and comprises a CDRH1 comprising the sequence set forth in SEQ ID NO: 143, a CDRH2 comprising the sequence set forth in SEQ ID NO:144, a CDRH3 comprising the sequence set forth in SEQ ID NO:145, a CDRL1 comprising the sequence set forth in SEQ ID NO:147, a CDRL2 comprising the sequence set forth in SEQ ID NO:148, and a CDRL3 comprising the sequence set forth in SEQ ID NO:149, or (ii) an antibody or antigen-binding fragment thereof that competes with the antibody or antigen-binding fragment of (i) for binding to the SARS CoV-2 S protein;

(b) (i) an antibody or antigen-binding fragment thereof that is capable of binding to a SARS CoV-2 S protein and comprises a CDRH1 comprising the sequence set forth in SEQ ID NO: 109, a CDRH2 comprising the sequence set forth in SEQ ID NO:110, a CDRH3 comprising the sequence set forth in SEQ ID NO:111, a CDRL1 comprising the sequence set forth in SEQ ID NO:133, a CDRL2 comprising the sequence set forth in SEQ ID NO:134, and a CDRL3 comprising the sequence set forth in SEQ ID NO:135, or (ii) an antibody or antigen-binding fragment thereof that competes the antibody or antigen-binding fragment of (i) for binding to the SARS CoV-2 S protein;

(c) (i) an antibody or antigen-binding fragment thereof that is capable of binding to a SARS CoV-2 S protein and comprises a CDRH1 comprising the sequence set forth in SEQ ID NO: 102, a CDRH2 comprising the sequence set forth in SEQ ID

NO:103, a CDRH3 comprising the sequence set forth in SEQ ID NO:104, a CDRL1 comprising the sequence set forth in SEQ ID NO:106, a CDRL2 comprising the sequence set forth in SEQ ID NO:107, and a CDRL3 comprising the sequence set forth in SEQ ID NO:108, or (ii) an antibody or antigen-binding fragment thereof that competes the antibody or antigen-binding fragment of (i) for binding to the SARS CoV-2 S protein;

(d) (i) an antibody or antigen-binding fragment thereof that is capable of binding to a SARS CoV-2 S protein and comprises a CDRH1 comprising the sequence set forth in SEQ ID NO: 94, a CDRH2 comprising the sequence set forth in SEQ ID NO:95, a CDRH3 comprising the sequence set forth in SEQ ID NO:96, a CDRL1 comprising the sequence set forth in SEQ ID NO:98, a CDRL2 comprising the sequence set forth in SEQ ID NO:99, and a CDRL3 comprising the sequence set forth in SEQ ID NO:100, or (ii) an antibody or antigen-binding fragment thereof that competes the antibody or antigen-binding fragment of (i) for binding to the SARS CoV-2 S protein.

58. The method of claim 57, wherein:

(1) the antibody or antigen-binding fragment of (a)(i) comprises a VH comprising or consisting of an amino acid sequence having at least 80%, 85%, 90%, 91%, 92%, 93%, 94%, 95%, 96,%, 97%, 98%, or 99% identity (*e.g.*, as determined using BLAST) (*e.g.*, 100% identity) to the amino acid sequence set forth in SEQ ID NO:142 and a VL comprising or consisting of an amino acid sequence having at least 80%, 85%, 90%, 91%, 92%, 93%, 94%, 95%, 96,%, 97%, 98%, or 99% identity to the amino acid sequence set forth in SEQ ID NO:146;

(2) the an antibody or antigen-binding fragment thereof of (b)(i) comprises a VH comprising or consisting of an amino acid sequence having at least 80%, 85%, 90%, 91%, 92%, 93%, 94%, 95%, 96,%, 97%, 98%, or 99% identity to the amino acid sequence set forth in SEQ ID NO:123 and a VL comprising or consisting of an amino acid sequence having at least 80%, 85%, 90%, 91%, 92%, 93%, 94%, 95%, 96,%, 97%, 98%, or 99% identity to the sequence set forth in SEQ ID NO:138;

(3) the an antibody or antigen-binding fragment thereof of (c)(i) comprises a VH comprising or consisting of an amino acid sequence having at least 80%, 85%, 90%, 91%, 92%, 93%, 94%, 95%, 96,%, 97%, 98%, or 99% identity to the amino acid sequence set forth in SEQ ID NO:101 and a VL comprising or consisting of an amino acid sequence having at least 80%, 85%, 90%, 91%, 92%, 93%, 94%, 95%, 96,%, 97%, 98%, or 99% identity to the amino acid sequence set forth in SEQ ID NO:105; and/or

(4) the antibody or antigen-binding fragment thereof of (d)(i) comprises a VH comprising or consisting of an amino acid sequence having at least 80%, 85%, 90%, 91%, 92%, 93%, 94%, 95%, 96,%, 97%, 98%, or 99% identity to the amino acid sequence set forth in SEQ ID NO:93 and a VL comprising or consisting of an amino acid sequence having at least 80%, 85%, 90%, 91%, 92%, 93%, 94%, 95%, 96,%, 97%, 98%, or 99% identity to the amino acid sequence set forth in SEQ ID NO:97.

59. A method of treating or preventing a SARS-CoV-2 infection in a subject, comprising administering to the subject an effective amount of one of (a)-(d):

(a) (i) an antibody or antigen-binding fragment thereof (*e.g.*, Fv, scFv, Fab, scFab, or the like) that is capable of binding to a SARS CoV-2 S protein and comprises a CDRH1 comprising the sequence set forth in SEQ ID NO: 143, a CDRH2 comprising the sequence set forth in SEQ ID NO:144, a CDRH3 comprising the sequence set forth in SEQ ID NO:145, a CDRL1 comprising the sequence set forth in SEQ ID NO:147, a CDRL2 comprising the sequence set forth in SEQ ID NO:148, and a CDRL3 comprising the sequence set forth in SEQ ID NO:149, or (ii) an antibody or antigen-binding fragment thereof that competes with the antibody or antigen-binding fragment of (i) for binding to the SARS CoV-2 S protein;

(b) (i) an antibody or antigen-binding fragment thereof that is capable of binding to a SARS CoV-2 S protein and comprises a CDRH1 comprising the sequence set forth in SEQ ID NO:109, a CDRH2 comprising the sequence set forth in SEQ ID NO:110, a CDRH3 comprising the sequence set forth in SEQ ID NO:111, a CDRL1 comprising the sequence set forth in SEQ ID NO:133, a CDRL2 comprising the sequence set forth in SEQ ID NO:134, and a CDRL3 comprising the sequence set forth

in SEQ ID NO:135, or (ii) an antibody or antigen-binding fragment thereof that competes the antibody or antigen-binding fragment of (i) for binding to the SARS CoV-2 S protein;

(c) (i) an antibody or antigen-binding fragment thereof that is capable of binding to a SARS CoV-2 S protein and comprises a CDRH1 comprising the sequence set forth in SEQ ID NO: 102, a CDRH2 comprising the sequence set forth in SEQ ID NO:103, a CDRH3 comprising the sequence set forth in SEQ ID NO:104, a CDRL1 comprising the sequence set forth in SEQ ID NO:106, a CDRL2 comprising the sequence set forth in SEQ ID NO:107, and a CDRL3 comprising the sequence set forth in SEQ ID NO:108, or (ii) an antibody or antigen-binding fragment thereof that competes the antibody or antigen-binding fragment of (i) for binding to the SARS CoV-2 S protein;

(d) (i) an antibody or antigen-binding fragment thereof that is capable of binding to a SARS CoV-2 S protein and comprises a CDRH1 comprising the sequence set forth in SEQ ID NO:94, a CDRH2 comprising the sequence set forth in SEQ ID NO:95, a CDRH3 comprising the sequence set forth in SEQ ID NO:96, a CDRL1 comprising the sequence set forth in SEQ ID NO:98, a CDRL2 comprising the sequence set forth in SEQ ID NO:99, and a CDRL3 comprising the sequence set forth in SEQ ID NO:100, or (ii) an antibody or antigen-binding fragment thereof that competes the antibody or antigen-binding fragment of (i) for binding to the SARS CoV-2 S protein;

wherein the subject has received, or is receiving, any one or more of the other of (a)-(d) (*e.g.*, administering an effective amount of (a) to a subject who has received or is receiving (b), (c), and/or (d).

60. The method of claim 59, wherein:

(1) the antibody or antigen-binding fragment of (a)(i) comprises a VH comprising or consisting of an amino acid sequence having at least 80%, 85%, 90%, 91%, 92%, 93%, 94%, 95%, 96,%, 97%, 98%, or 99% identity (*e.g.*, as determined using BLAST) (*e.g.*, 100% identity) to the amino acid sequence set forth in SEQ ID NO:142 and a VL comprising or consisting of an amino acid sequence having at least

80%, 85%, 90%, 91%, 92%, 93%, 94%, 95%, 96,%, 97%, 98%, or 99% identity to the amino acid sequence set forth in SEQ ID NO:146;

(2) the antibody or antigen-binding fragment thereof of (b)(i) comprises a VH comprising or consisting of an amino acid sequence having at least 80%, 85%, 90%, 91%, 92%, 93%, 94%, 95%, 96,%, 97%, 98%, or 99% identity to the amino acid sequence set forth in SEQ ID NO:123 and a VL comprising or consisting of an amino acid sequence having at least 80%, 85%, 90%, 91%, 92%, 93%, 94%, 95%, 96,%, 97%, 98%, or 99% identity to the sequence set forth in SEQ ID NO:138;

(3) the antibody or antigen-binding fragment thereof of (c)(i) comprises a VH comprising or consisting of an amino acid sequence having at least 80%, 85%, 90%, 91%, 92%, 93%, 94%, 95%, 96,%, 97%, 98%, or 99% identity to the amino acid sequence set forth in SEQ ID NO:101 and a VL comprising or consisting of an amino acid sequence having at least 80%, 85%, 90%, 91%, 92%, 93%, 94%, 95%, 96,%, 97%, 98%, or 99% identity to the amino acid sequence set forth in SEQ ID NO:105; and/or

(4) the antibody or antigen-binding fragment thereof of (d)(i) comprises a VH comprising or consisting of an amino acid sequence having at least 80%, 85%, 90%, 91%, 92%, 93%, 94%, 95%, 96,%, 97%, 98%, or 99% identity to the amino acid sequence set forth in SEQ ID NO:93 and a VL comprising or consisting of an amino acid sequence having at least 80%, 85%, 90%, 91%, 92%, 93%, 94%, 95%, 96,%, 97%, 98%, or 99% identity to the amino acid sequence set forth in SEQ ID NO:97.

61. The method of any one of claims 57-60, wherein an antibody or antigen-binding fragment administered to the subject comprises a Fc polypeptide comprising:

(i) a mutation that enhances binding to a human FcRn and/or extends an *in vivo* half-life of antibody or antigen-binding fragment, optionally a M428L mutation, a N434S mutation, YTE mutation, or any combination thereof; and/or

(ii) a mutation that that enhances binding to a human FcγR, optionally a G236A mutation, a A330L mutation, a I332E, a S239D mutation, or any combination thereof.

62. A method of diagnosing a SARS-CoV-2 infection, comprising contacting the composition of any one of claims 49-54 with a sample from a subject and detecting the presence or absence of a complex comprising the antibody or antigen-binding fragment and an antigen.

63. The composition of any one of claims 49-54 for use in determining whether a SARS-CoV-2 vaccine composition comprises an epitope in a correct conformation for binding by the antibody(ies) or antigen-binding fragment(s) thereof.

64. An immunogenic composition comprising:

(a) a SARS-CoV-2 S polypeptide or multimer thereof that comprises two or three receptor binding domains (RBDs) in a closed-conformation, wherein two adjacent RBDs are in a closed conformation;

(b) a SARS-CoV-2 S polypeptide or multimer thereof capable of being bound by an antibody or antigen-binding fragment thereof comprising a CDRH1 comprising the sequence set forth in SEQ ID NO: 143, a CDRH2 comprising the sequence set forth in SEQ ID NO:144, a CDRH3 comprising the sequence set forth in SEQ ID NO:145, a CDRL1 comprising the sequence set forth in SEQ ID NO:147, a CDRL2 comprising the sequence set forth in SEQ ID NO:148, and a CDRL3 comprising the sequence set forth in SEQ ID NO:149;

(c) a SARS-CoV-2 S polypeptide or multimer thereof capable of being bound by an antibody or antigen-binding fragment thereof comprising a CDRH1 comprising the sequence set forth in SEQ ID NO: 109, a CDRH2 comprising the sequence set forth in SEQ ID NO:110, a CDRH3 comprising the sequence set forth in SEQ ID NO:111, a CDRL1 comprising the sequence set forth in SEQ ID NO:133, a CDRL2 comprising the sequence set forth in SEQ ID NO:134, and a CDRL3 comprising the sequence set forth in SEQ ID NO:135;

or any combination of (a)-(c).

65. The immunogenic composition of claim 64, further comprising:

(d) a SARS-CoV-2 S polypeptide or multimer thereof capable of being bound by an antibody or antigen-binding fragment thereof comprising a CDRH1 comprising the sequence set forth in SEQ ID NO: 102, a CDRH2 comprising the sequence set forth in SEQ ID NO:103, a CDRH3 comprising the sequence set forth in SEQ ID NO:104, a CDRL1 comprising the sequence set forth in SEQ ID NO:106, a CDRL2 comprising the sequence set forth in SEQ ID NO:107, and a CDRL3 comprising the sequence set forth in SEQ ID NO:108;

(e) a SARS-CoV-2 S polypeptide or multimer thereof capable of being bound by an antibody or antigen-binding fragment thereof comprising a CDRH1 comprising the sequence set forth in SEQ ID NO:94, a CDRH2 comprising the sequence set forth in SEQ ID NO:95, a CDRH3 comprising the sequence set forth in SEQ ID NO:96, a CDRL1 comprising the sequence set forth in SEQ ID NO:98, a CDRL2 comprising the sequence set forth in SEQ ID NO:99, and a CDRL3 comprising the sequence set forth in SEQ ID NO:100;

or a combination thereof.

66. An immunogenic composition comprising:

(a) a SARS-CoV-2 S polypeptide or multimer thereof capable of being bound by an antibody or antigen-binding fragment thereof comprising a VH comprising the sequence set forth in SEQ ID NO:142 and a VL comprising the sequence set forth in SEQ ID NO:146;

(b) a SARS-CoV-2 S polypeptide or multimer thereof capable of being bound by an antibody or antigen-binding fragment thereof comprising a VH comprising the sequence set forth in SEQ ID NO:123 and a VL comprising the sequence set forth in SEQ ID NO:138;

or a combination thereof.

67. The immunogenic composition of claim 66, further comprising:

(c) a SARS-CoV-2 S protein polypeptide capable of being bound by an antibody or antigen-binding fragment thereof comprising a CDRH1 comprising the

sequence set forth in SEQ ID NO: 102, a CDRH2 comprising the sequence set forth in SEQ ID NO:103, a CDRH3 comprising the sequence set forth in SEQ ID NO:104, a CDRL1 comprising the sequence set forth in SEQ ID NO:106, a CDRL2 comprising the sequence set forth in SEQ ID NO:107, and a CDRL3 comprising the sequence set forth in SEQ ID NO:108;

(d) a SARS-CoV-2 S protein polypeptide capable of being bound by an antibody or antigen-binding fragment thereof comprising a CDRH1 comprising the sequence set forth in SEQ ID NO: 94, a CDRH2 comprising the sequence set forth in SEQ ID NO:95, a CDRH3 comprising the sequence set forth in SEQ ID NO:96, a CDRL1 comprising the sequence set forth in SEQ ID NO:98, a CDRL2 comprising the sequence set forth in SEQ ID NO:99, and a CDRL3 comprising the sequence set forth in SEQ ID NO:100;

or a combination thereof.

68. An immunogenic composition comprising:

(a) a SARS-CoV-2 S polypeptide capable of being bound by antibody S2M11, or an antigen-binding fragment thereof;

(b) a SARS-CoV-2 S polypeptide capable of being bound by antibody S2E12, or an antigen-binding fragment thereof;

(c) a SARS-CoV-2 S polypeptide capable of being bound by antibody S309, or an antigen-binding fragment thereof; or

(d) any combination of (a)-(c) above.

69. The immunogenic composition of any one of claims 64-68, further comprising a pharmaceutically acceptable carrier, excipient, or diluent, and/or comprising an adjuvant.

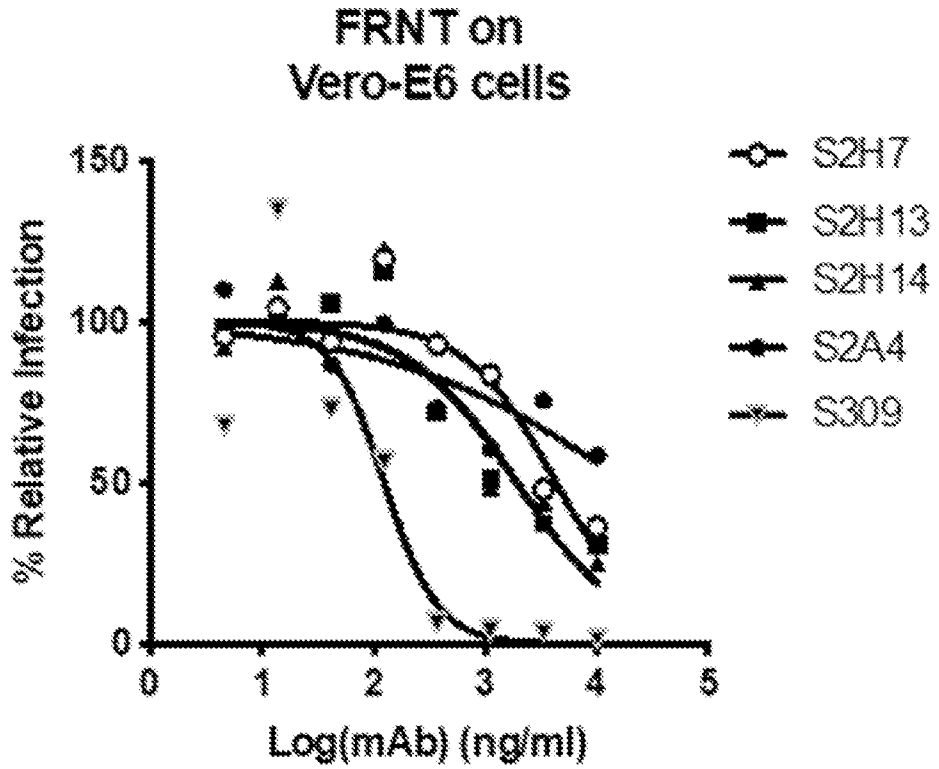

FRNT on
Vero-E6 cells
% Relative Infection
150
100
50
0
0
1
2
3
4
5
Log(mAb) (ng/ml)
S2H7
S2H13
S2H14
S2A4
S309

FIG. 1A

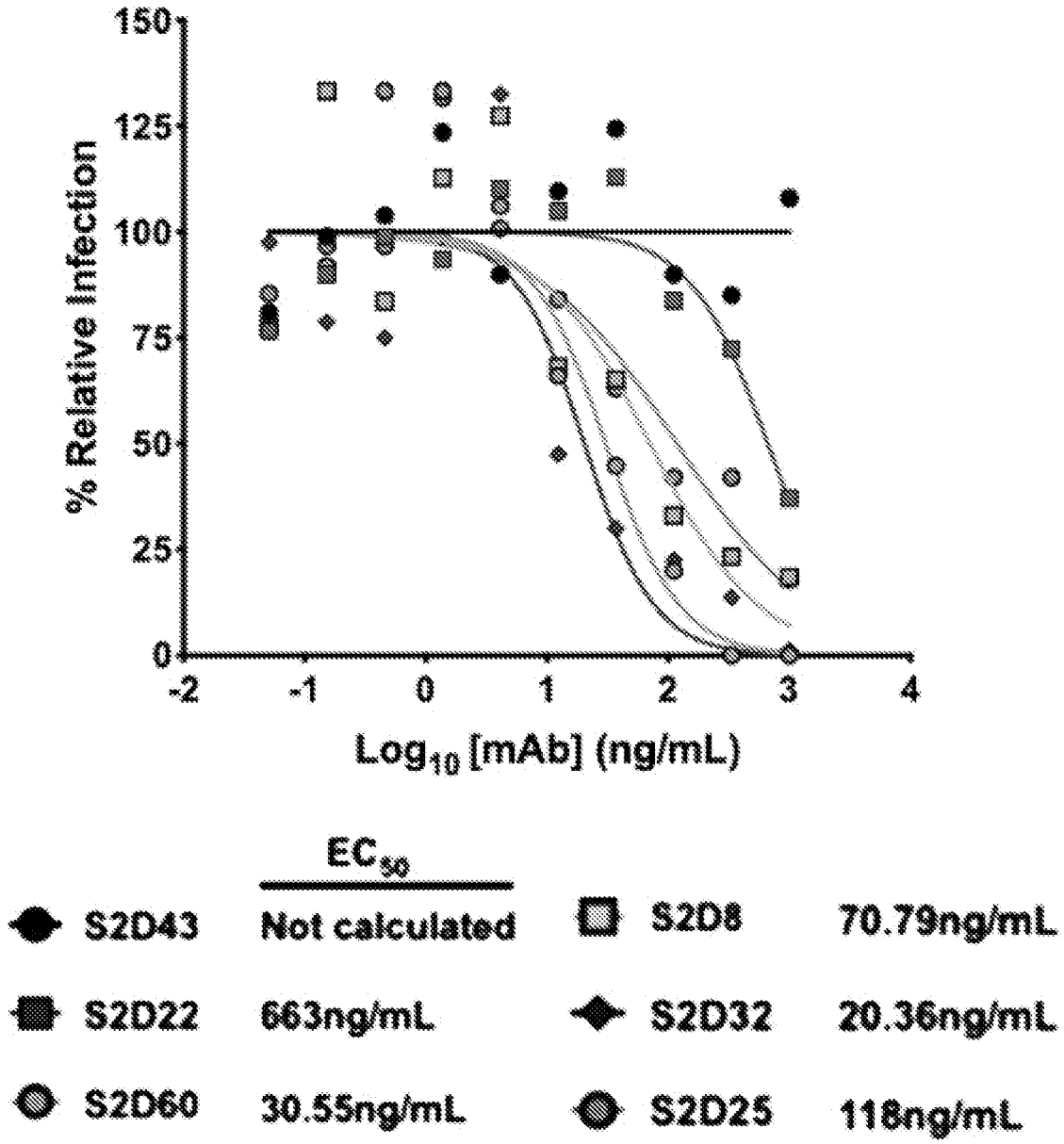

% Relative Infection
150
125
100
75
50
25
0
-2
-1
0
1
2
3
4
Log10 [mAb] (ng/mL)
EC50
S2D43 Not calculated
S2D8 70.79ng/mL
S2D22 663ng/mL
S2D32 20.36ng/mL
S2D60 30.55ng/mL
S2D25 118ng/mL

FIG. 1B

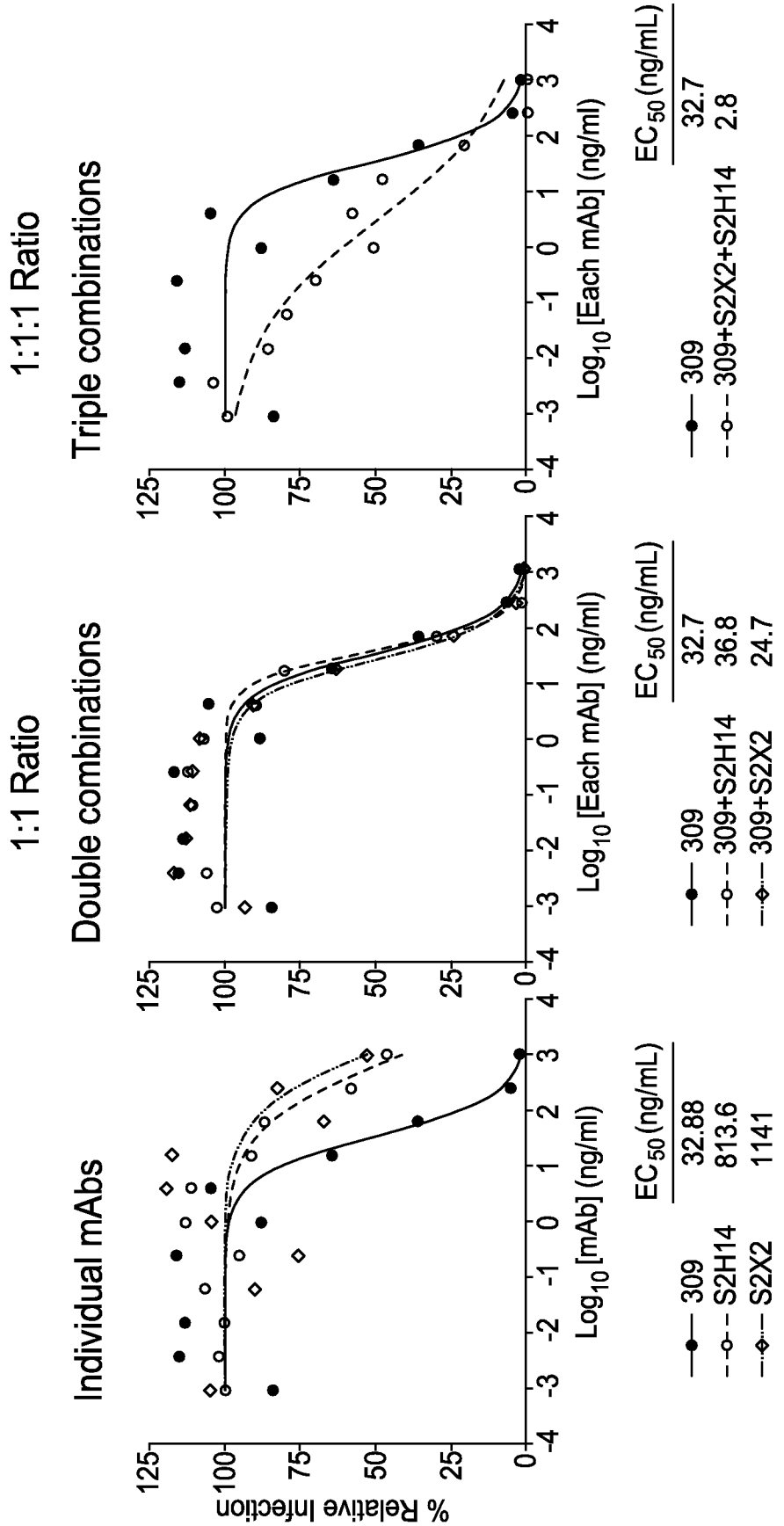

Individual mAbs
1:1 Ratio
Double combinations
1:1:1 Ratio
Triple combinations
% Relative Infection
Log10 [mAb] (ng/ml)
Log10 [Each mAb] (ng/ml)
309
S2H14
S2X2
309+S2H14
309+S2X2
309+S2X2+S2H14
EC50 (ng/mL)
32.88
813.6
1141
32.7
36.8
24.7
32.7
2.8

FIG. 2

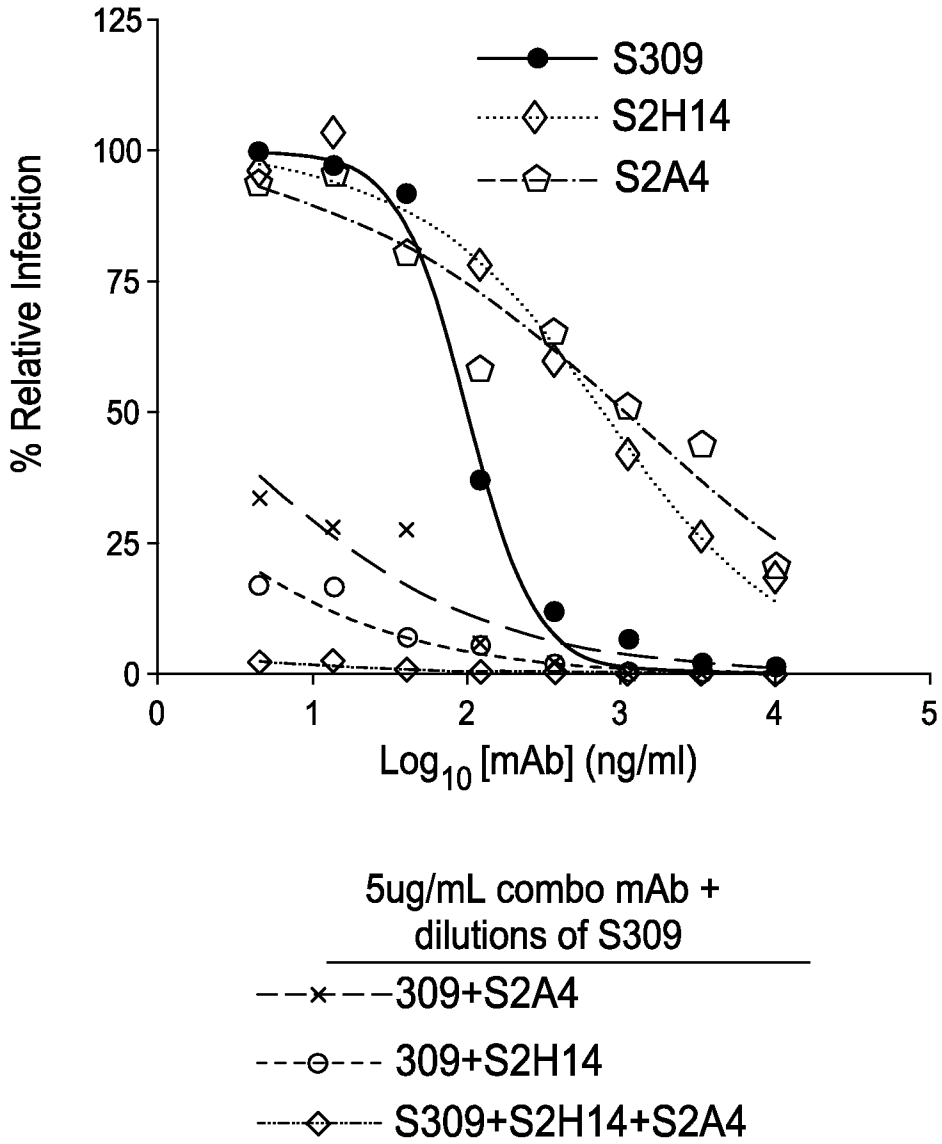

125
100
75
50
25
0
% Relative Infection
S309
S2H14
S2A4
0
1
2
3
4
5
Log10 [mAb] (ng/ml)
5ug/mL combo mAb +
dilutions of S309
309+S2A4
309+S2H14
S309+S2H14+S2A4

FIG. 3

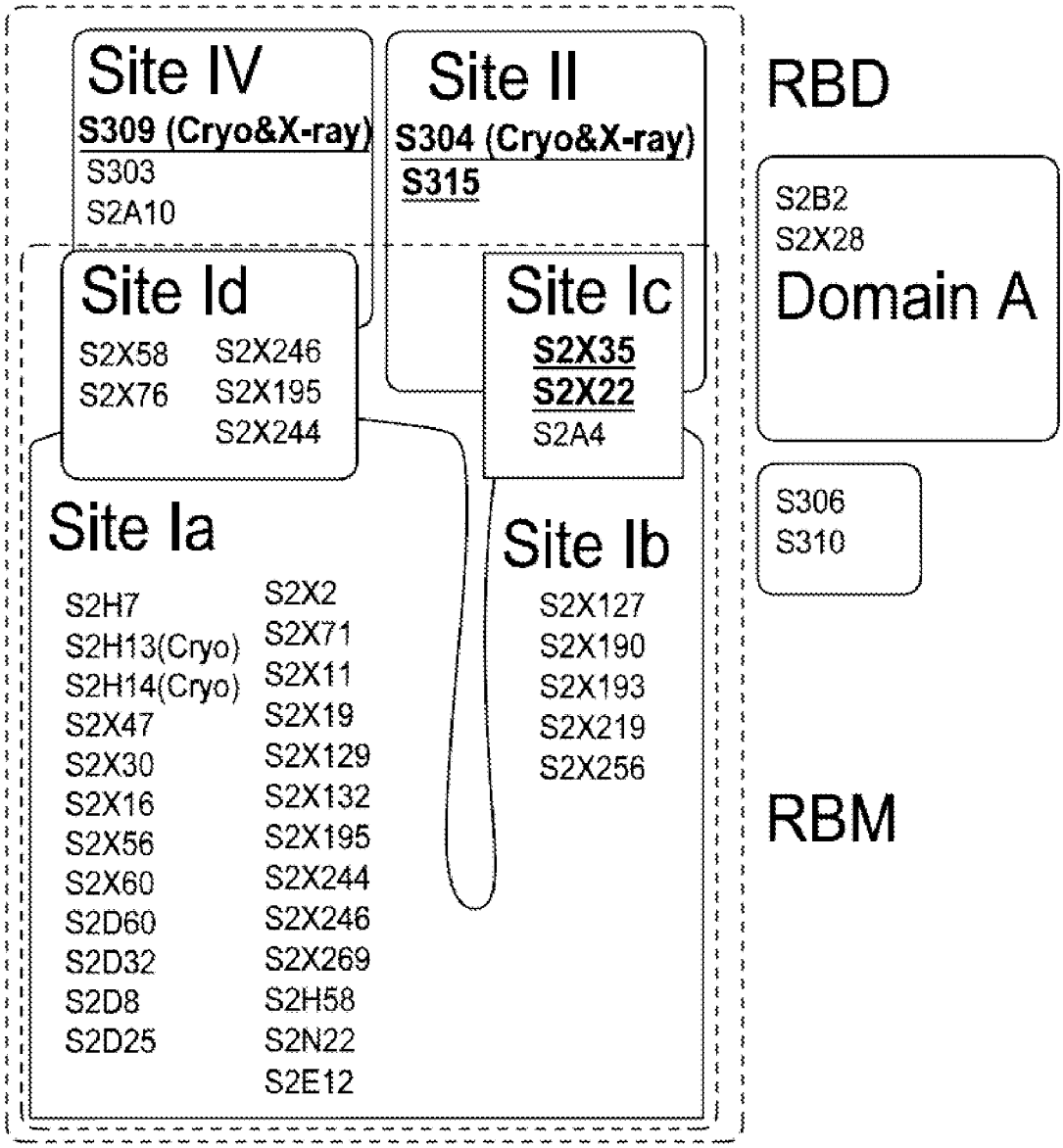

Site IV
S309 (Cryo&X-ray)
S303
S2A10
Site II
S304 (Cryo&X-ray)
S315
RBD
S2B2
S2X28
Domain A
Site Id
S2X58
S2X76
S2X246
S2X195
S2X244
Site Ic
S2X35
S2X22
S2A4
S306
S310
Site Ia
S2H7
S2H13(Cryo)
S2H14(Cryo)
S2X47
S2X30
S2X16
S2X56
S2X60
S2D60
S2D32
S2D8
S2D25
S2X2
S2X71
S2X11
S2X19
S2X129
S2X132
S2X195
S2X244
S2X246
S2X269
S2H58
S2N22
S2E12
Site Ib
S2X127
S2X190
S2X193
S2X219
S2X256
RBM
"compete with S309; bold underlined, cross-reactive to SARSI

FIG. 4

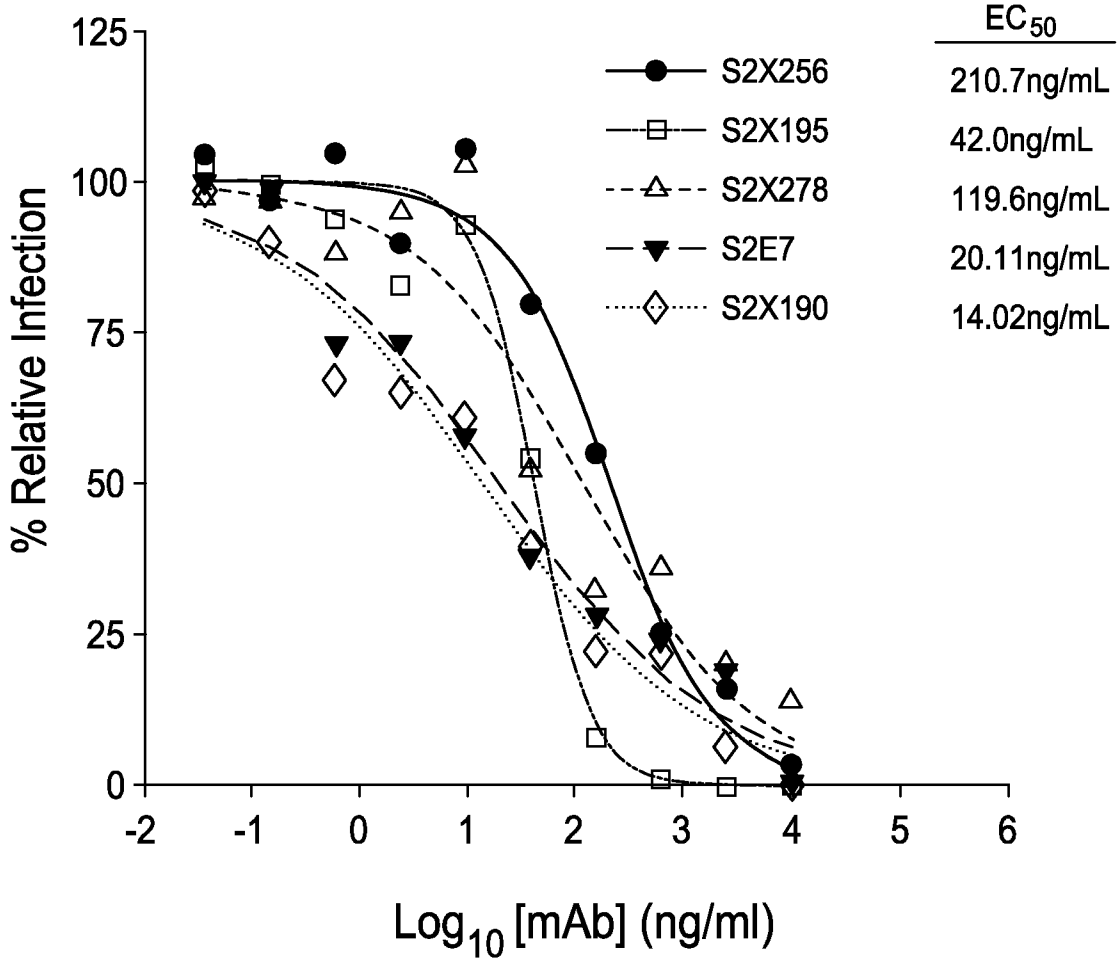

125
100
75
50
25
0
% Relative Infection
-2
-1
0
1
2
3
4
5
6
Log10 [mAb] (ng/ml)
EC50
S2X256
210.7ng/mL
S2X195
42.0ng/mL
S2X278
119.6ng/mL
S2E7
20.11ng/mL
S2X190
14.02ng/mL

FIG. 5A

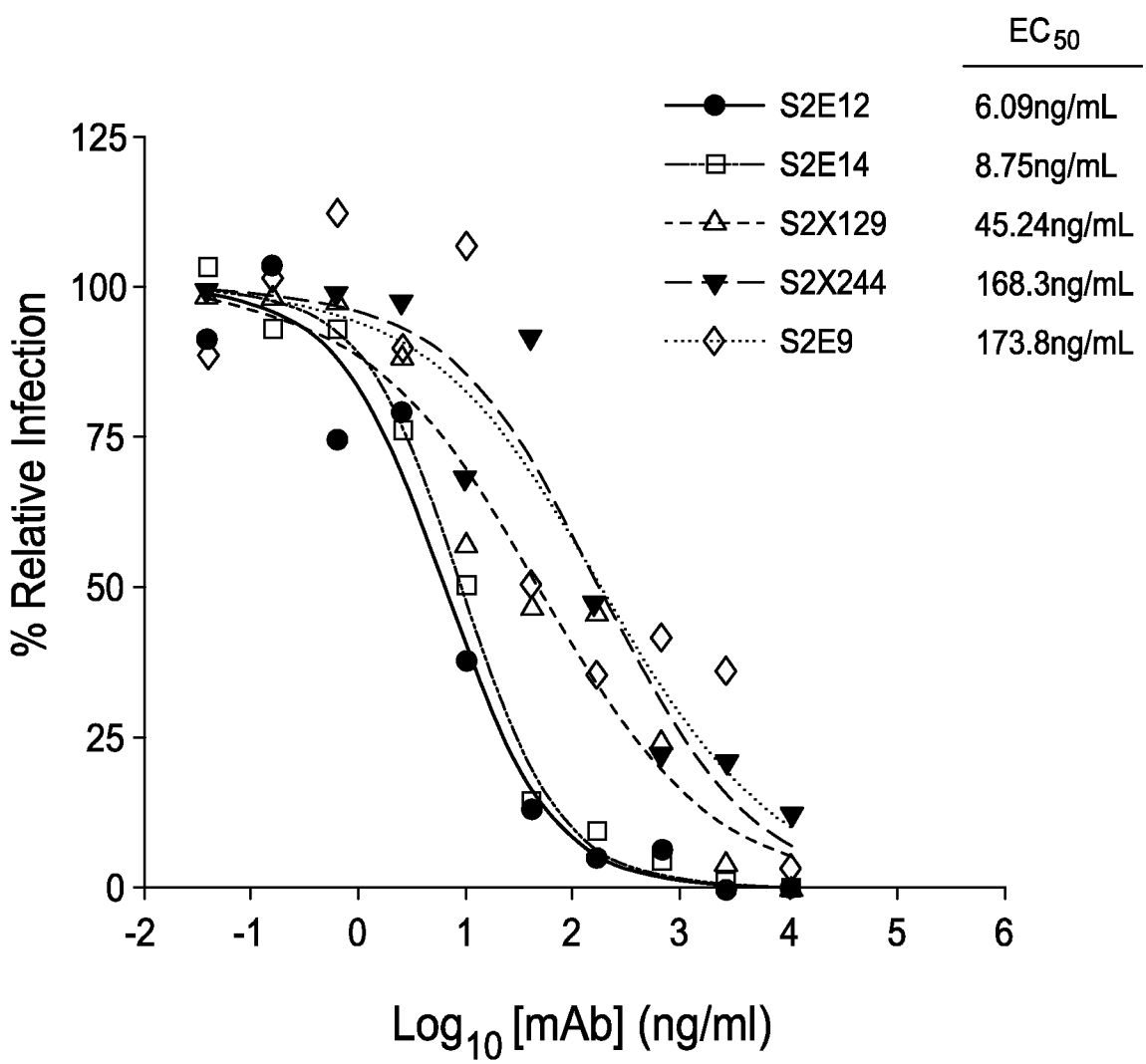

EC50
S2E12 6.09ng/mL
S2E14 8.75ng/mL
S2X129 45.24ng/mL
S2X244 168.3ng/mL
S2E9 173.8ng/mL
% Relative Infection
125
100
75
50
25
0
-2
-1
0
1
2
3
4
5
6
Log10 [mAb] (ng/ml)

FIG. 5B

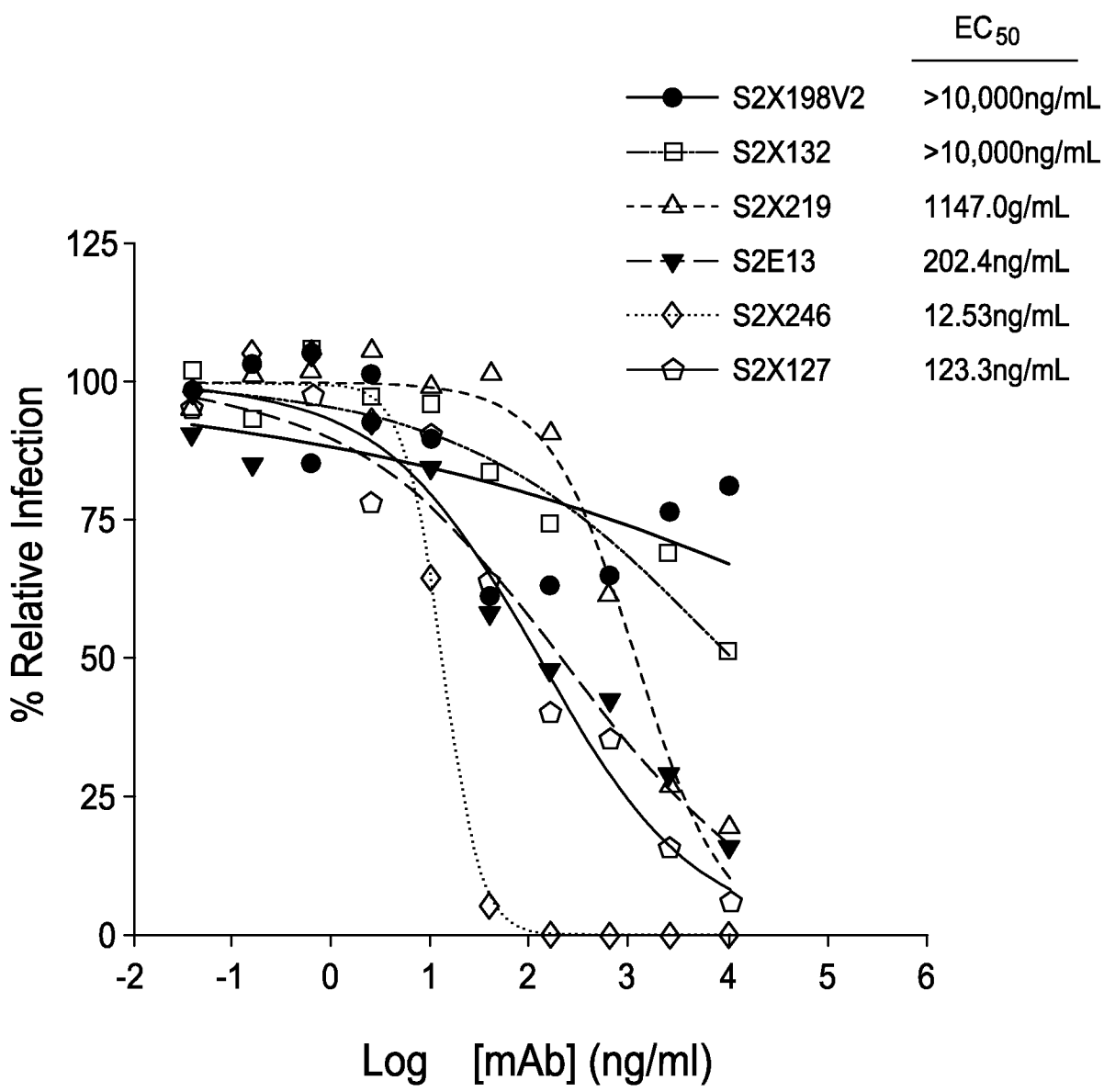

EC50
S2X198V2 >10,000ng/mL
S2X132 >10,000ng/mL
S2X219 1147.0g/mL
S2E13 202.4ng/mL
S2X246 12.53ng/mL
S2X127 123.3ng/mL
% Relative Infection
125
100
75
50
25
0
-2
-1
0
1
2
3
4
5
6
Log [mAb] (ng/ml)

FIG. 5C

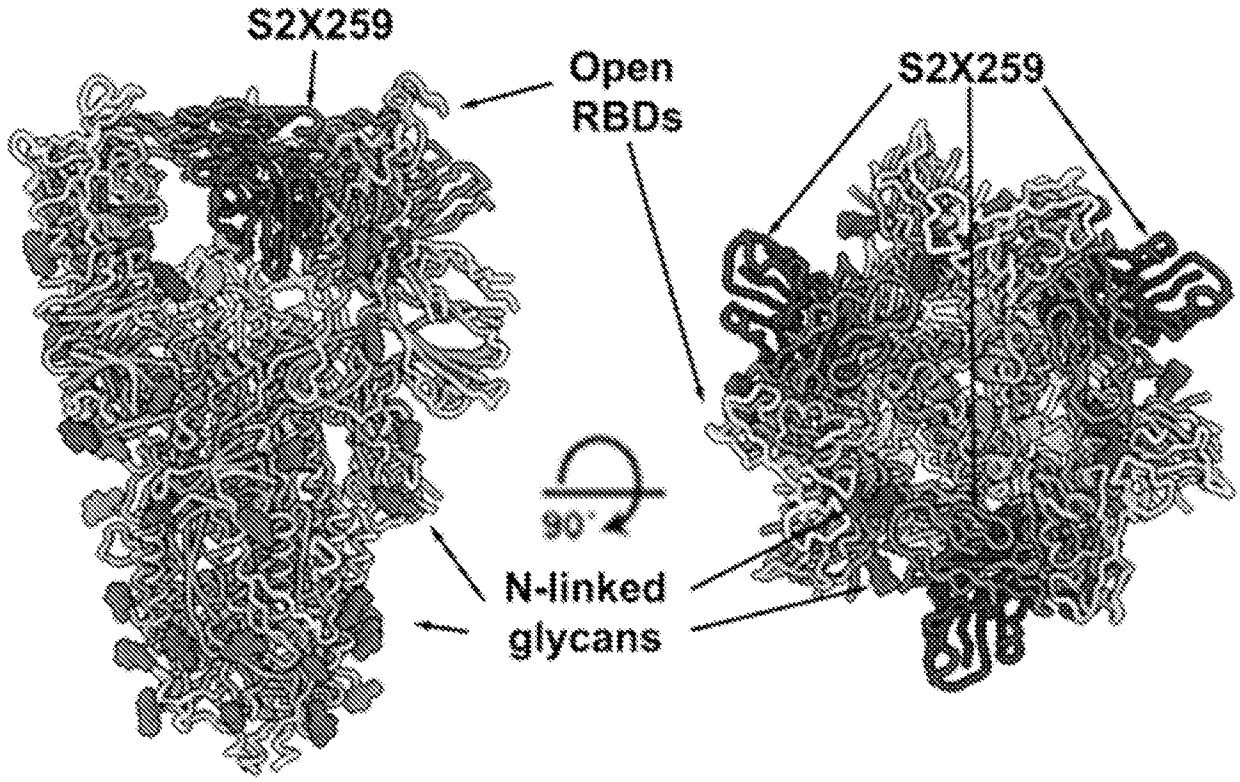


FIG. 6

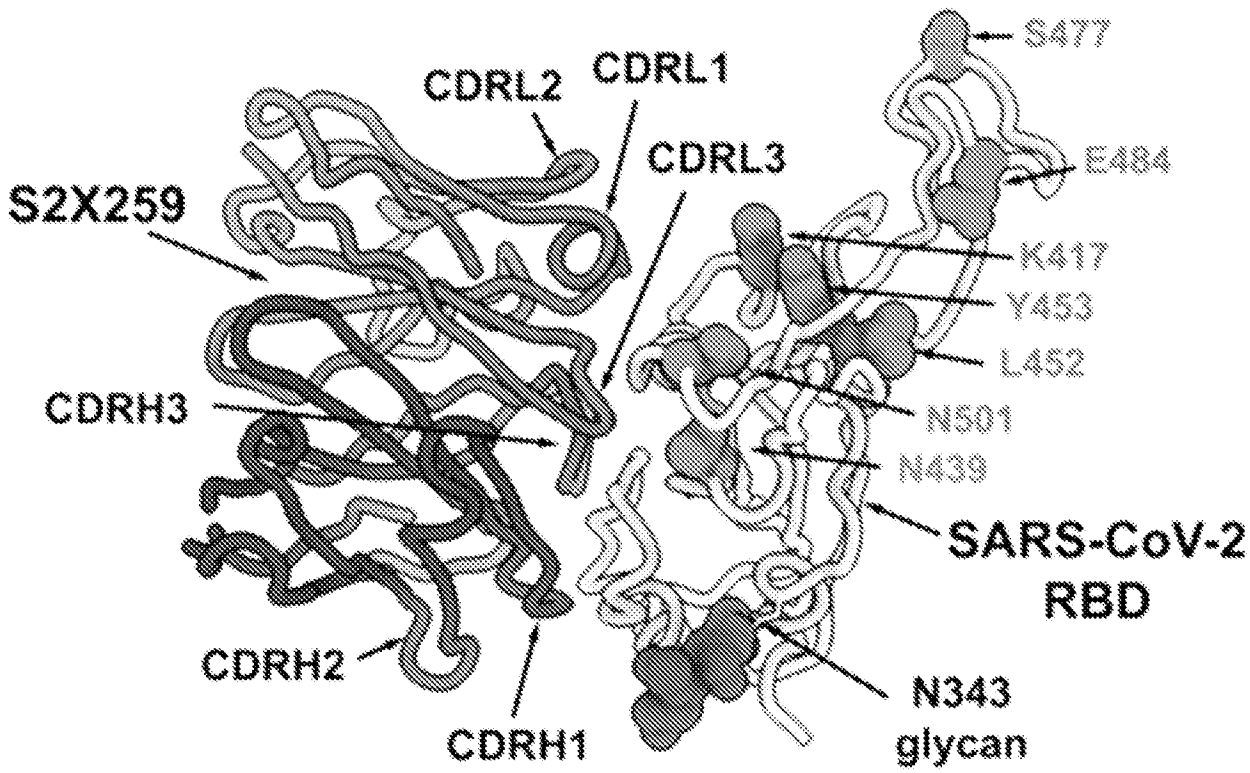

S477
CDRL2
CDRL1
E484
CDRL3
S2X259
K417
Y453
L452
CDRH3
N501
N439
SARS-CoV-2
RBD
CDRH2
N343
glycan
CDRH1

FIG. 7

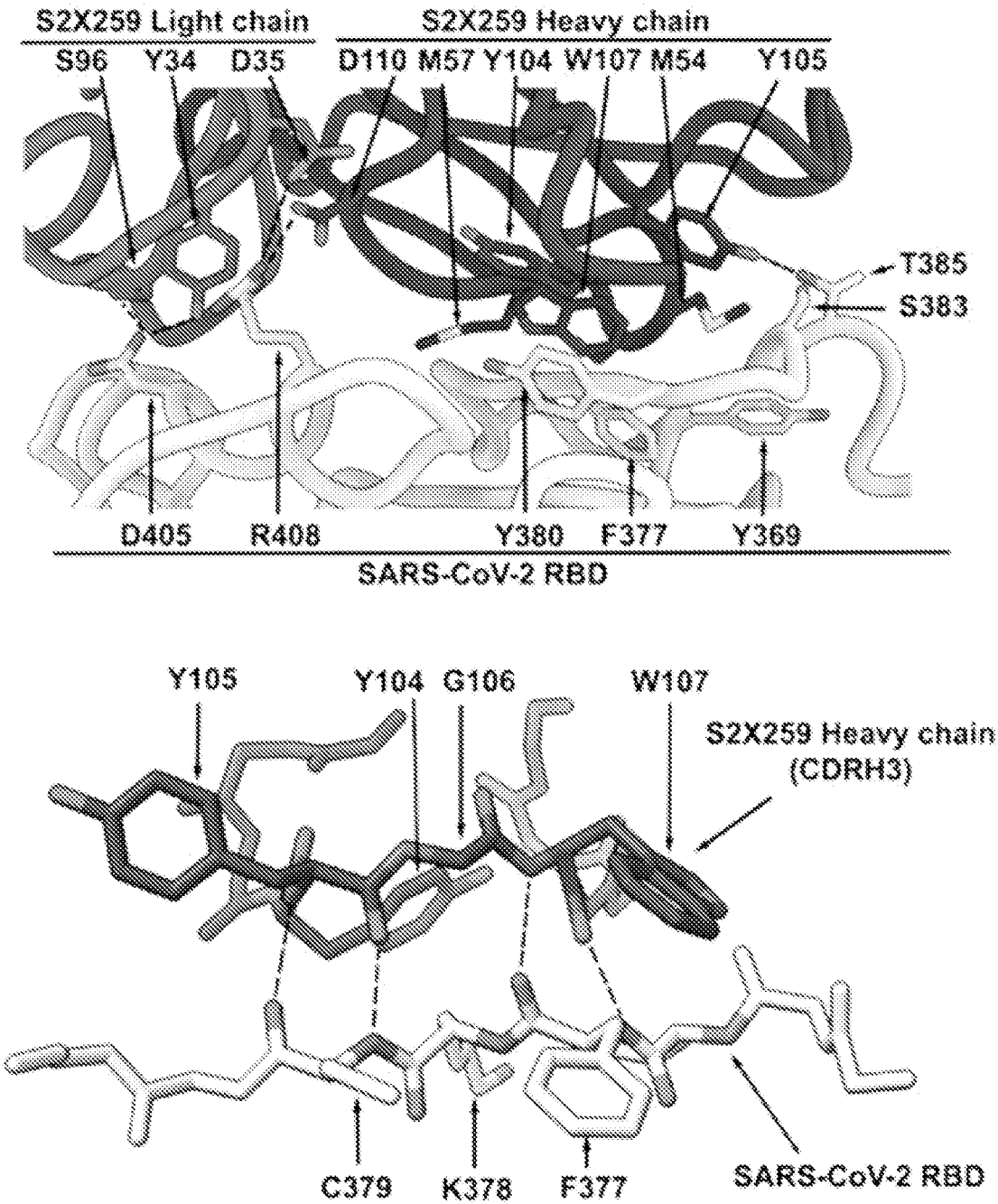

S2X259 Light chain
S2X259 Heavy chain
S96
Y34
D35
D110
M57
Y104
W107
M54
Y105
T385
S383
D405
R408
Y380
F377
Y369
SARS-CoV-2 RBD
Y105
Y104
G106
W107
S2X259 Heavy chain
(CDRH3)
C379
K378
F377
SARS-CoV-2 RBD

FIG. 8

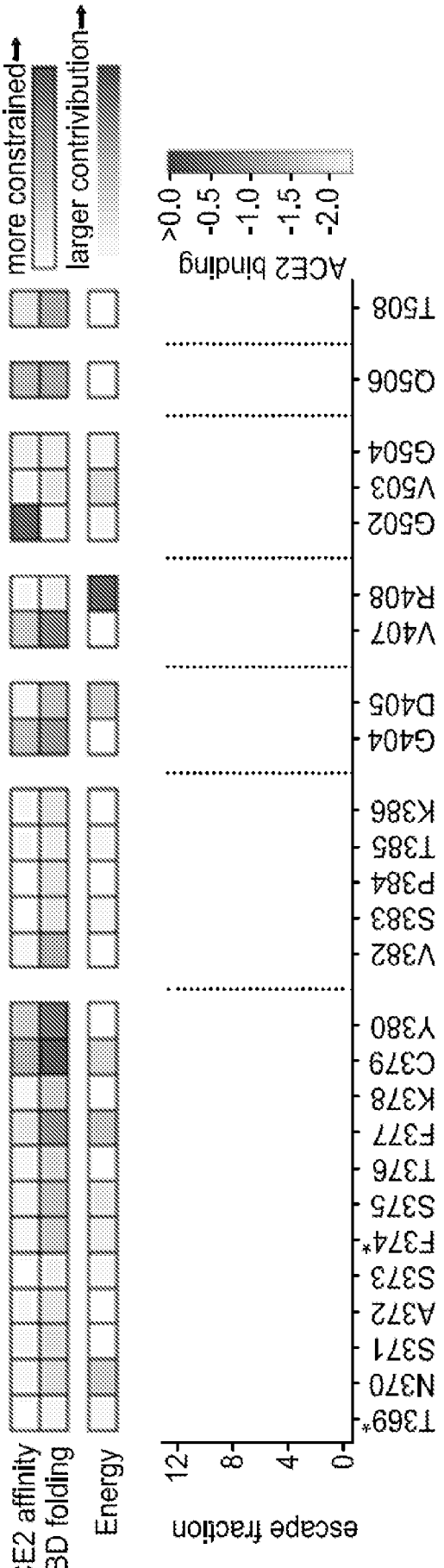

more constrained
larger contribution
ACE2 binding
>0.0
-0.5
-1.0
-1.5
-2.0
T508
Q506
G504
V503
G502
R408
V407
D405
G404
K386
T385
P384
S383
V382
Y380
C379
K378
F377
T376
S375
F374*
S373
A372
S371
N370
T369*
escape fraction
12
8
4
0
ACE2 affinity
RBD folding
Energy

FIG. 9



FIG. 10

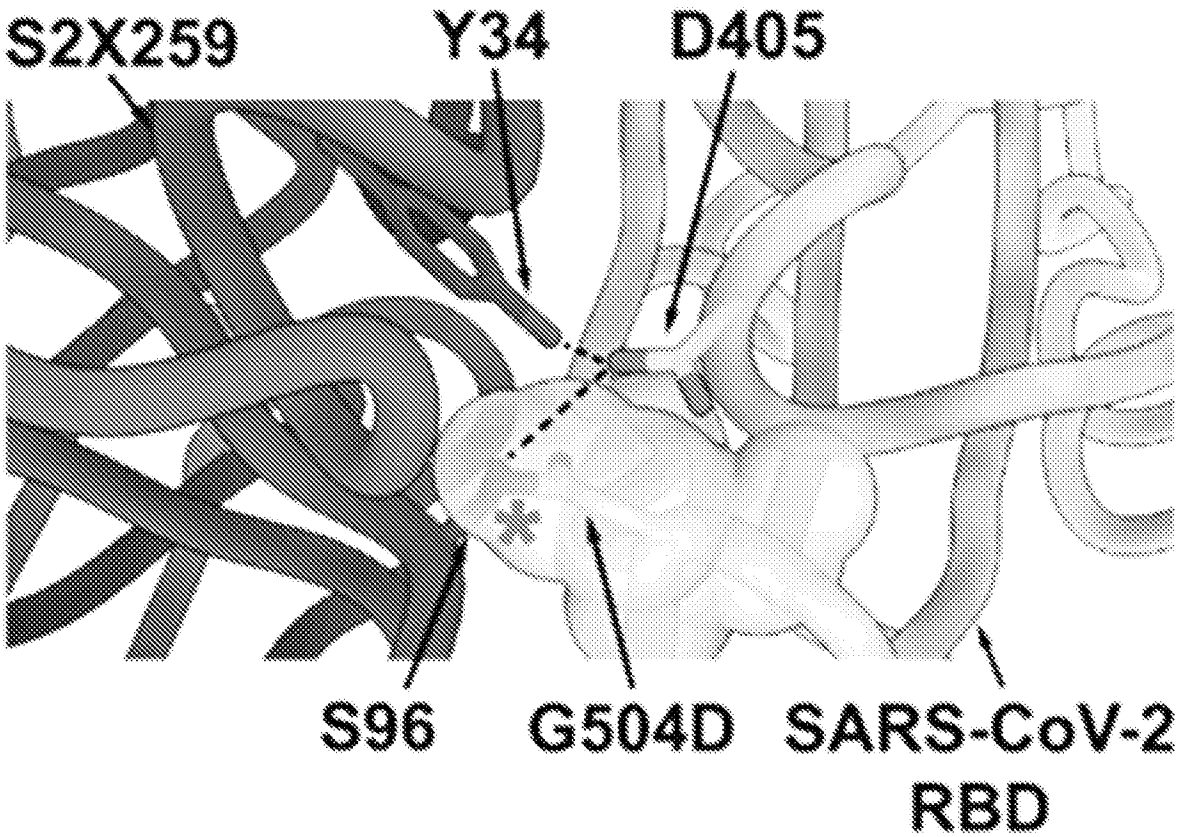


FIG. 11

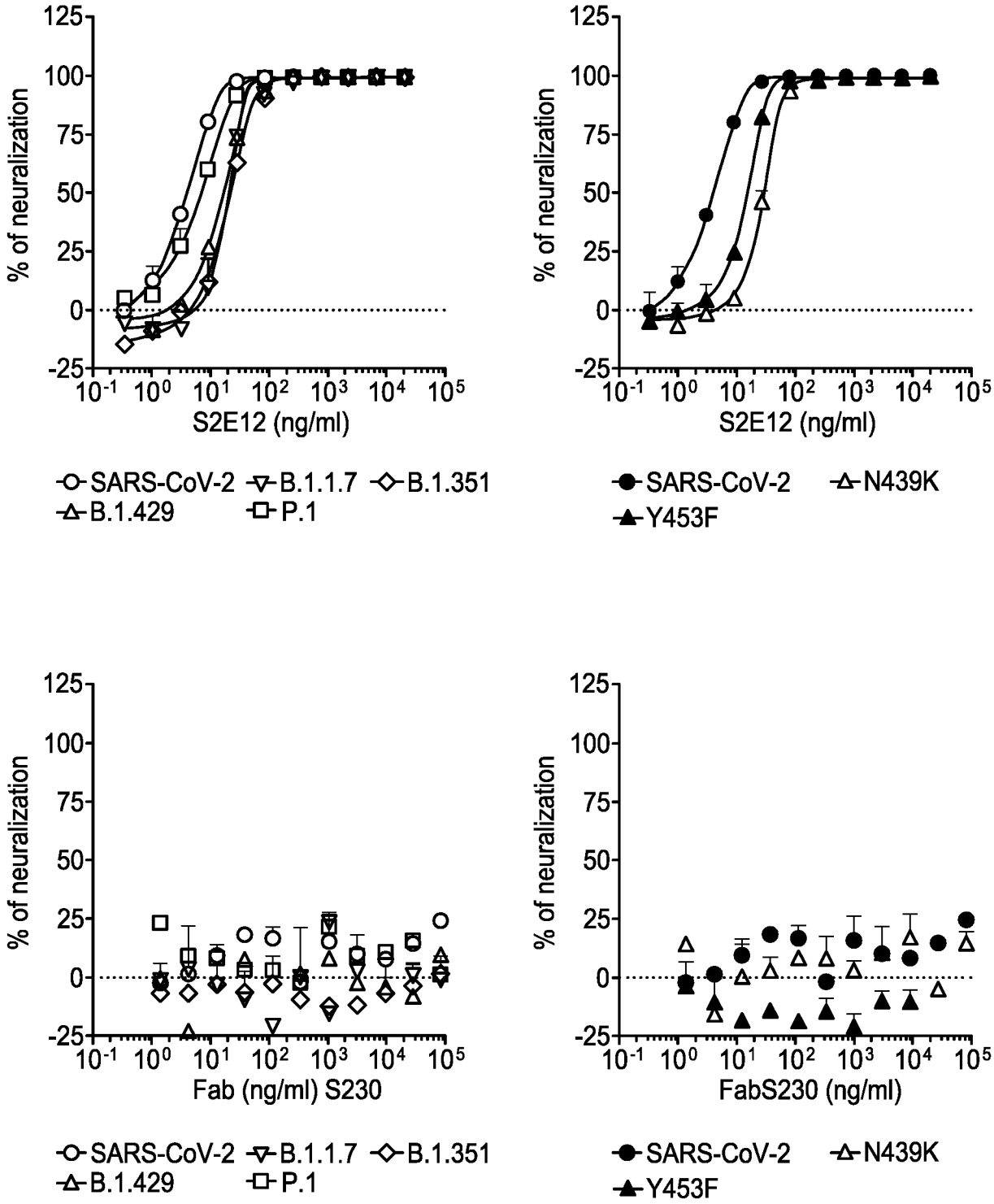

125
100
75
50
25
0
-25
% of neuralization
10^{-1} 10^{0} 10^{1} 10^{2} 10^{3} 10^{4} 10^{5}
S2E12 (ng/ml)
SARS-CoV-2
B.1.1.7
B.1.351
B.1.429
P.1
SARS-CoV-2
N439K
Y453F
Fab (ng/ml) S230
FabS230 (ng/ml)

FIG. 12A

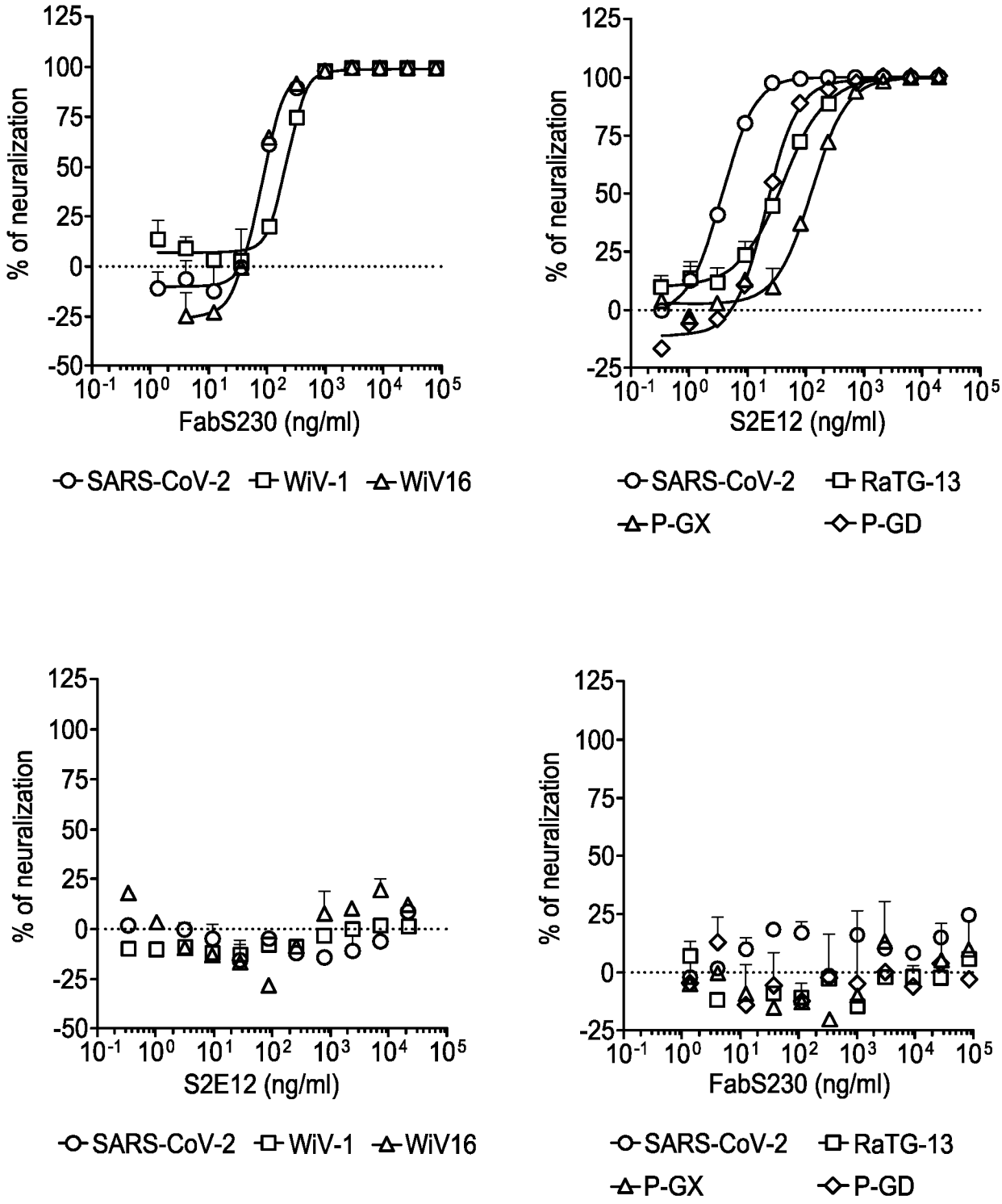

% of neuralization
FabS230 (ng/ml)
SARS-CoV-2
WiV-1
WiV16
S2E12 (ng/ml)
RaTG-13
P-GX
P-GD

FIG. 12B

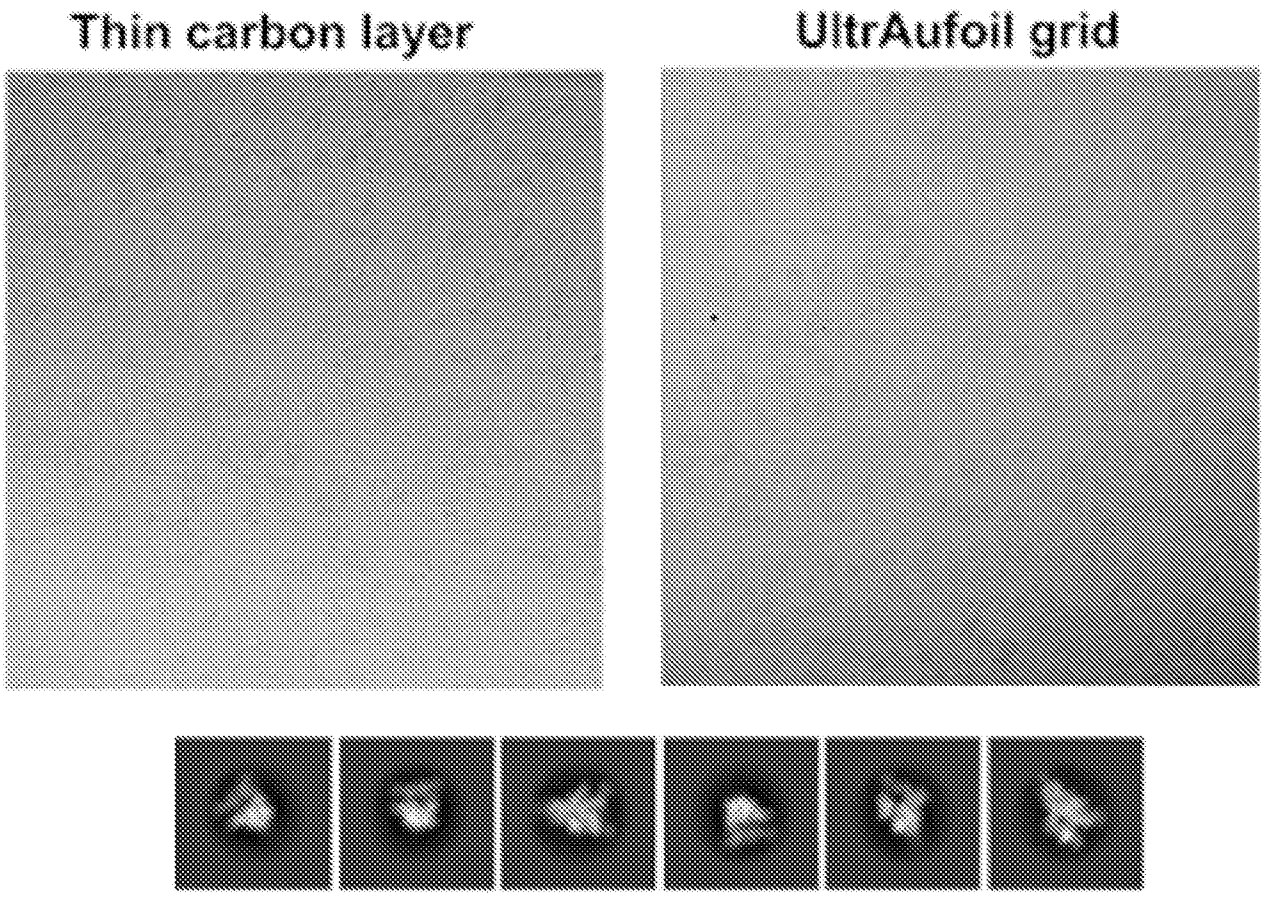


FIG. 13

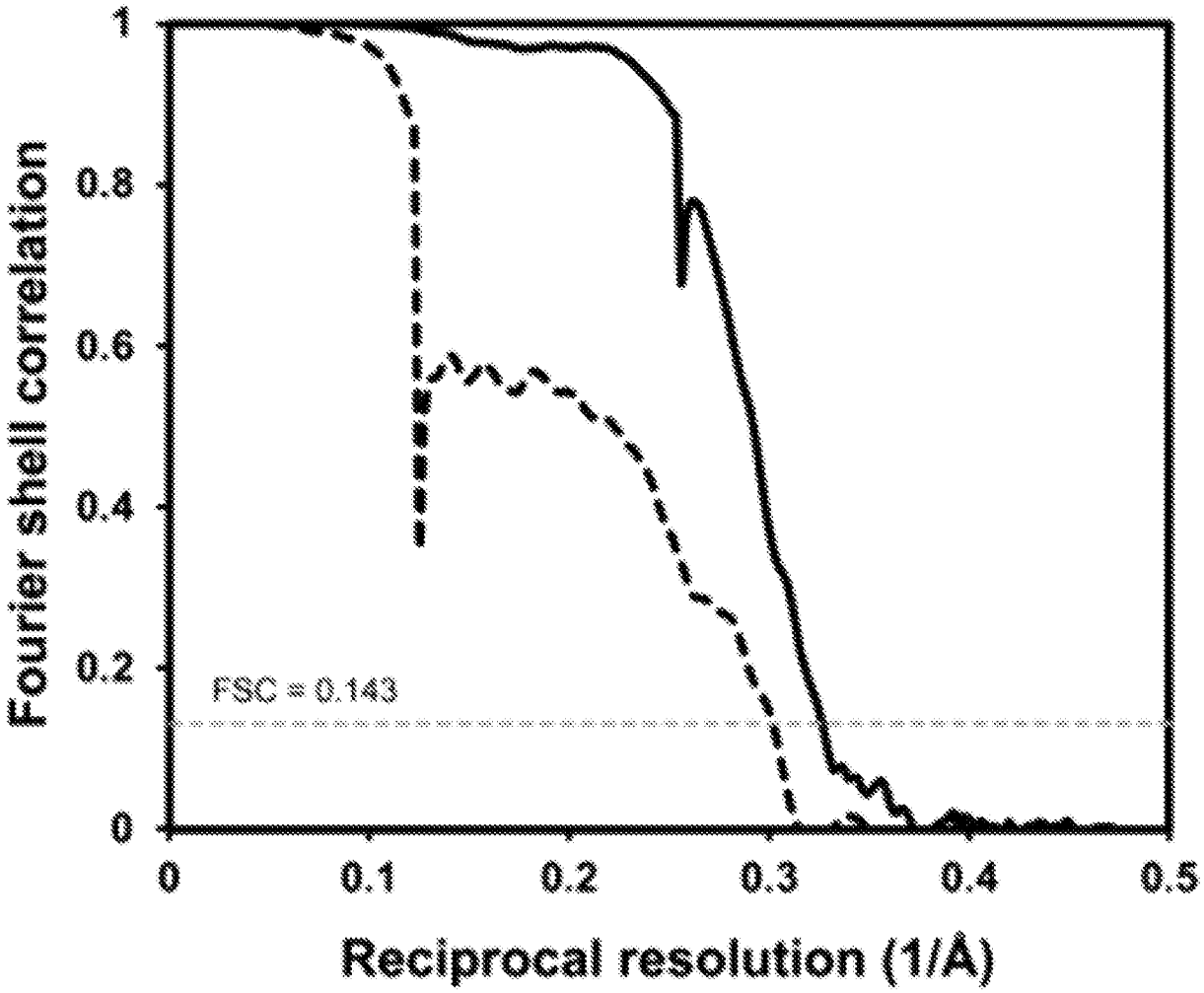

Fourier shell correlation
1
0.8
0.6
0.4
0.2
0
FSC = 0.143
0
0.1
0.2
0.3
0.4
0.5
Reciprocal resolution (1/Å)

FIG. 14

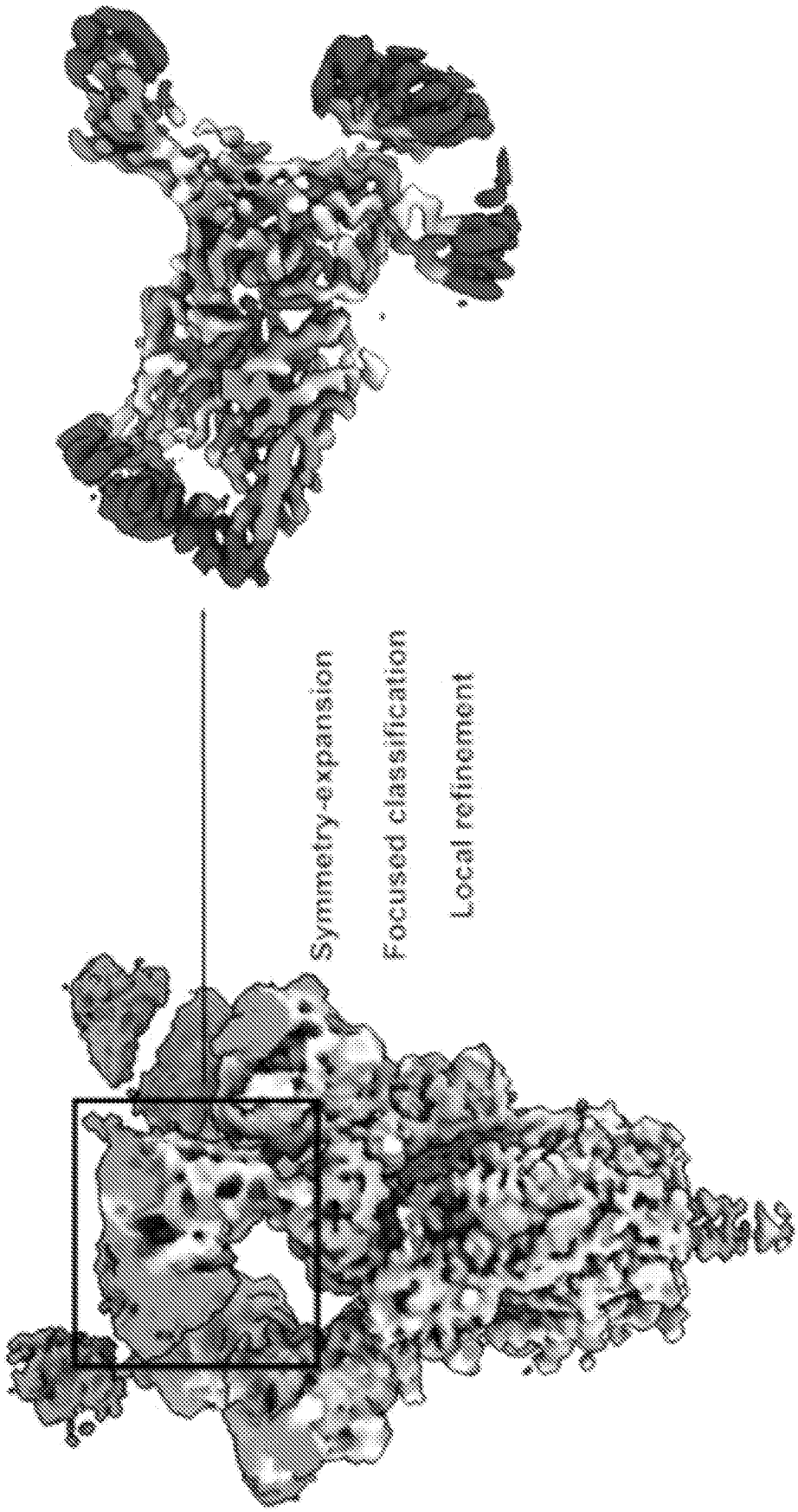

Symmetry-expansion
Focused classification
Local refinement

FIG. 15

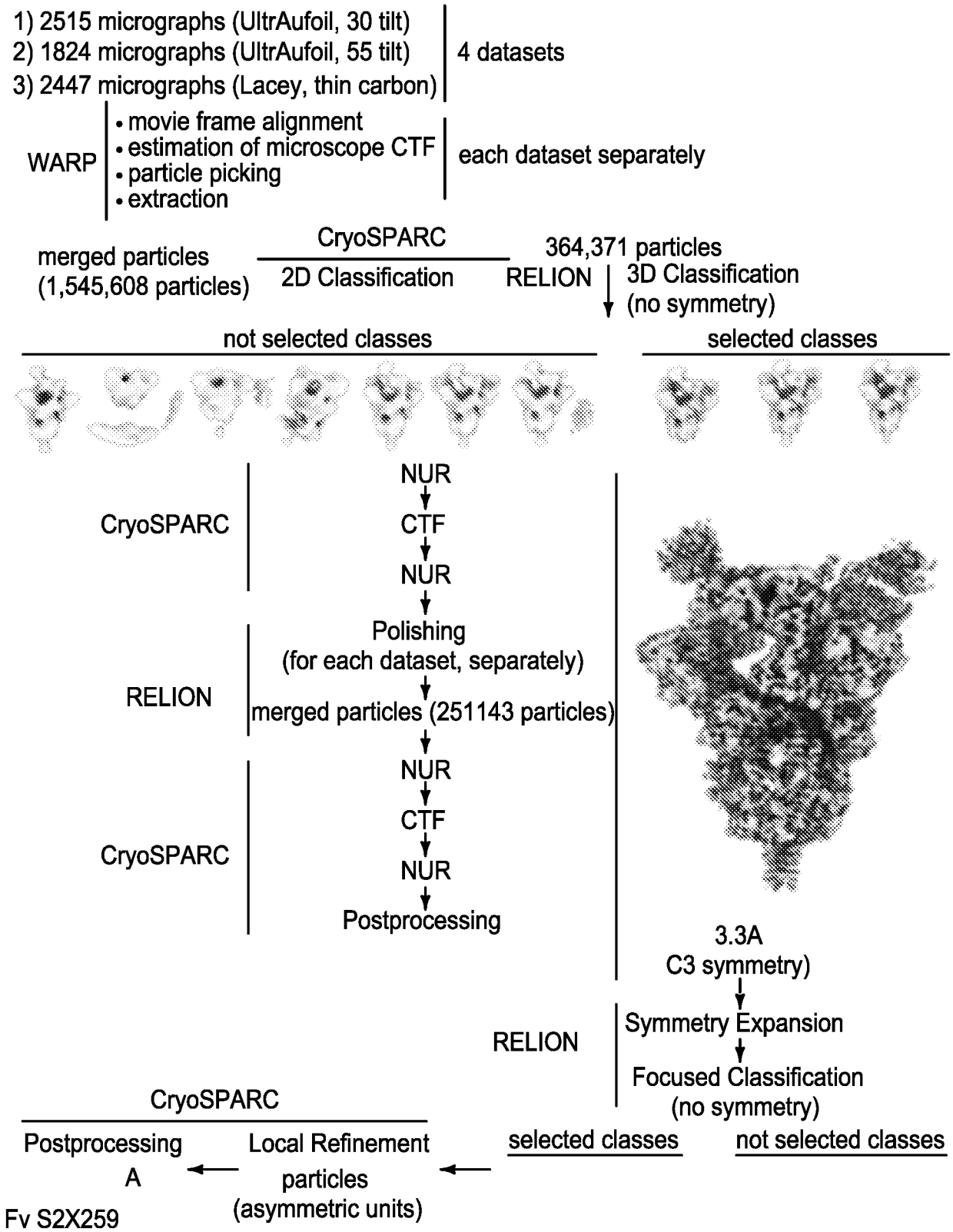

1) 2515 micrographs (UltrAufoil, 30 tilt)
2) 1824 micrographs (UltrAufoil, 55 tilt)
3) 2447 micrographs (Lacey, thin carbon)
4 datasets
WARP
• movie frame alignment
• estimation of microscope CTF
• particle picking
• extraction
each dataset separately
merged particles
(1,545,608 particles)
CryoSPARC
2D Classification
364,371 particles
RELION
3D Classification
(no symmetry)
not selected classes
selected classes
CryoSPARC
NUR
CTF
NUR
RELION
Polishing
(for each dataset, separately)
merged particles (251143 particles)
CryoSPARC
NUR
CTF
NUR
Postprocessing
3.3A
C3 symmetry)
RELION
Symmetry Expansion
Focused Classification
(no symmetry)
CryoSPARC
Postprocessing
Local Refinement
selected classes
not selected classes
A
particles
(asymmetric units)
Fv S2X259
RBD

FIG. 16

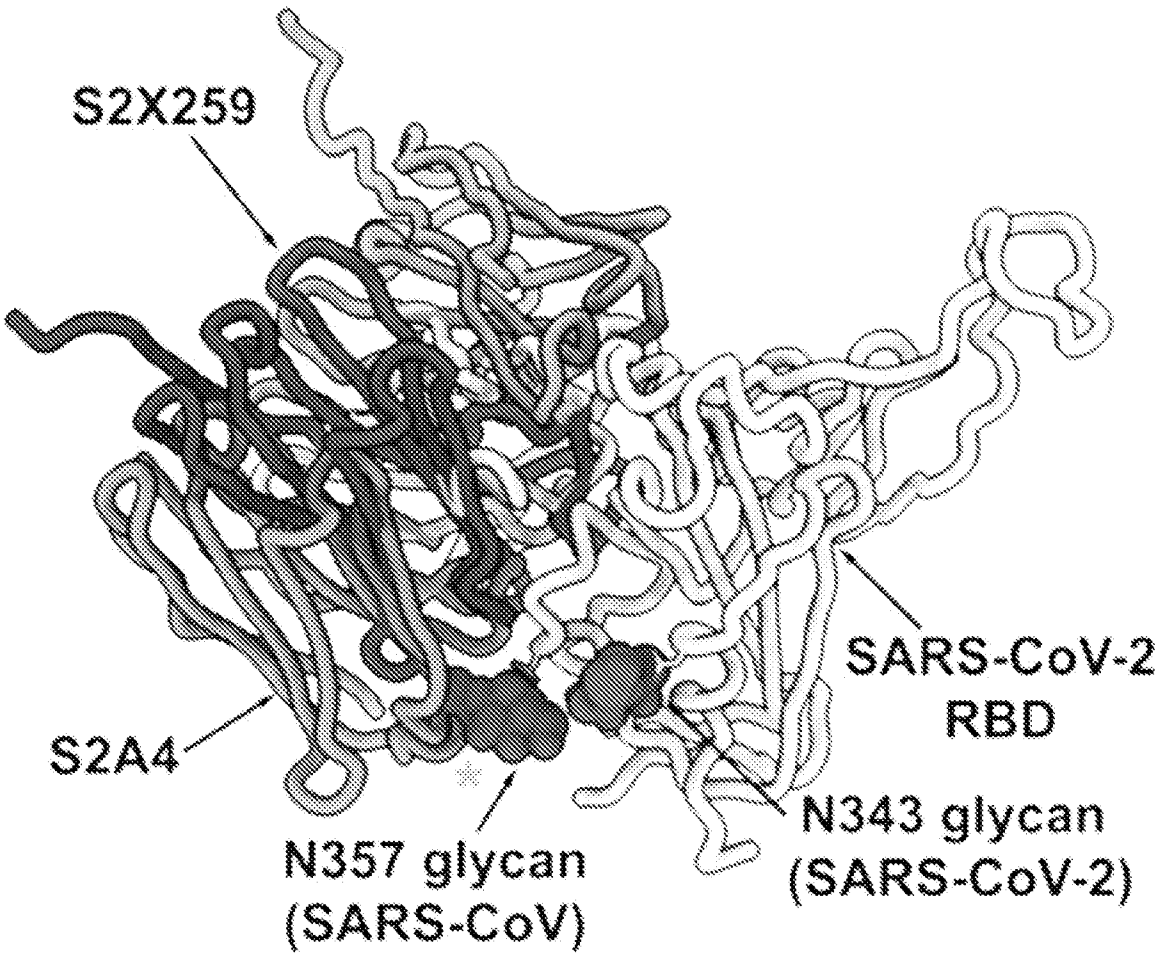

S2X259
SARS-CoV-2
RBD
S2A4
N343 glycan
(SARS-CoV-2)
N357 glycan
(SARS-CoV)

FIG. 17

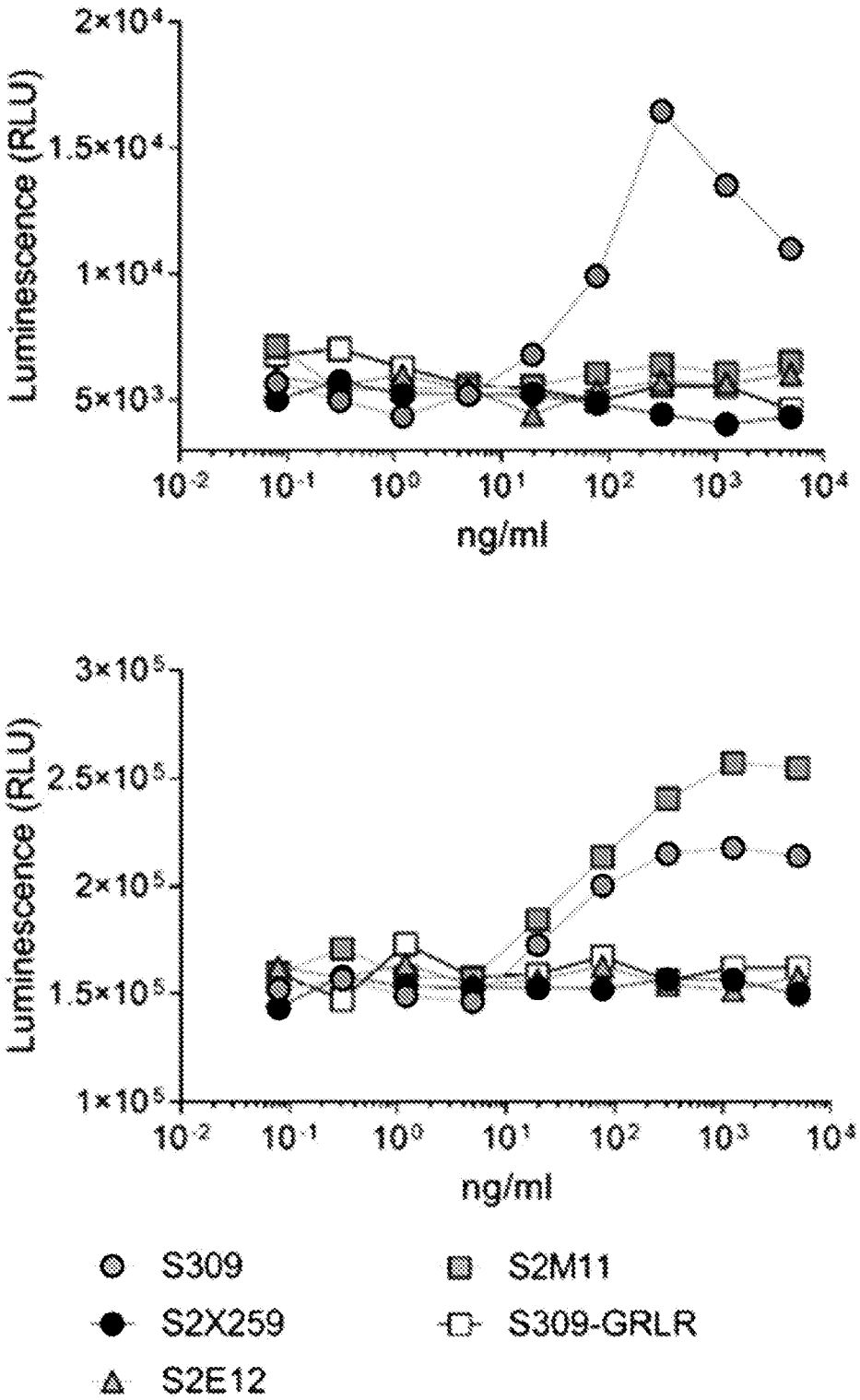

Luminescence (RLU)
2×10⁴
1.5×10⁴
1×10⁴
5×10³
10⁻² 10⁻¹ 10⁰ 10¹ 10² 10³ 10⁴
ng/ml
Luminescence (RLU)
3×10⁵
2.5×10⁵
2×10⁵
1.5×10⁵
1×10⁵
10⁻² 10⁻¹ 10⁰ 10¹ 10² 10³ 10⁴
ng/ml
S309
S2X259
S2E12
S2M11
S309-GRLR

FIG. 18

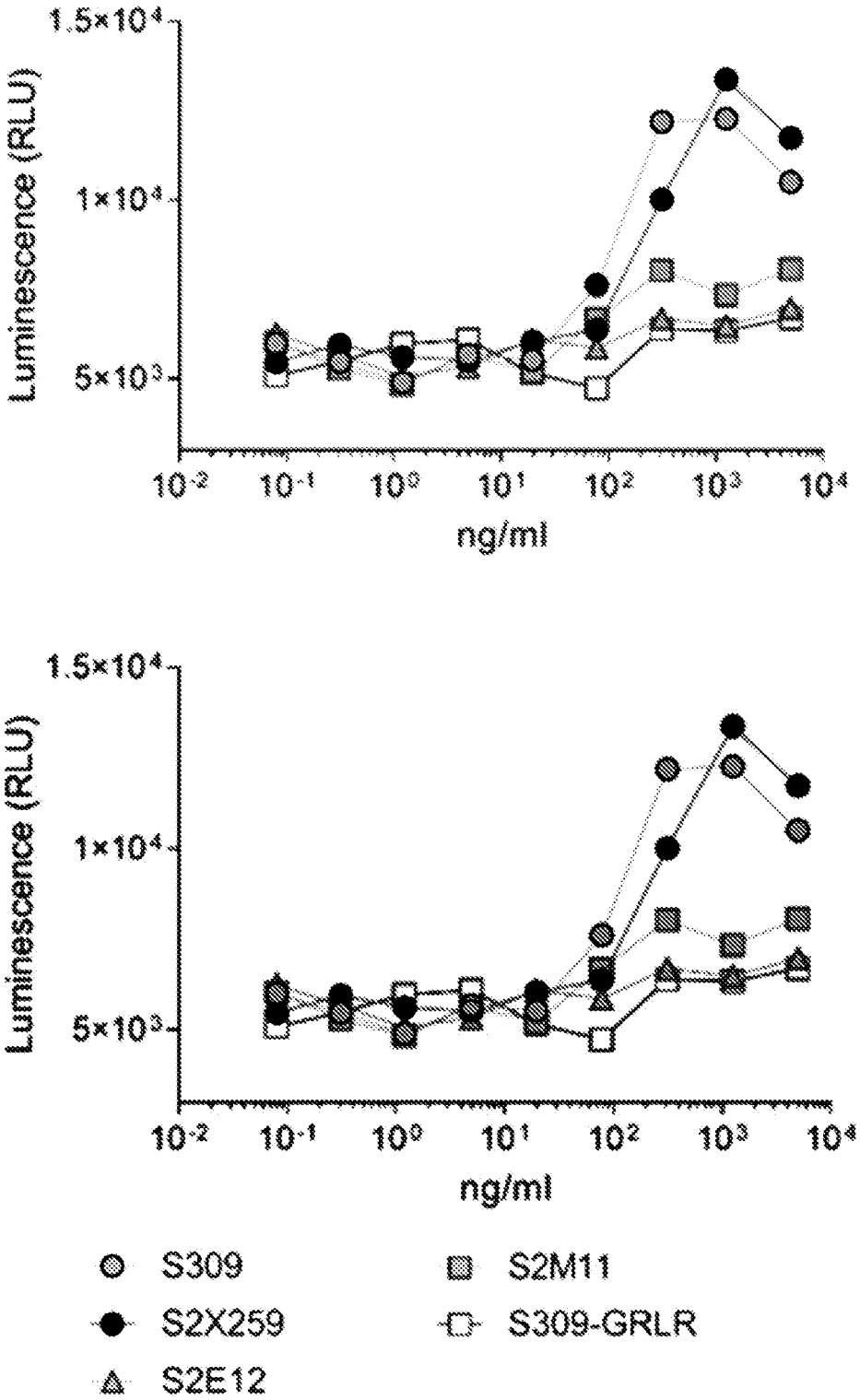

1.5×10⁴
1×10⁴
5×10³
Luminescence (RLU)
10⁻²
10⁻¹
10⁰
10¹
10²
10³
10⁴
ng/ml
S309
S2X259
S2E12
S2M11
S309-GRLR

FIG. 19

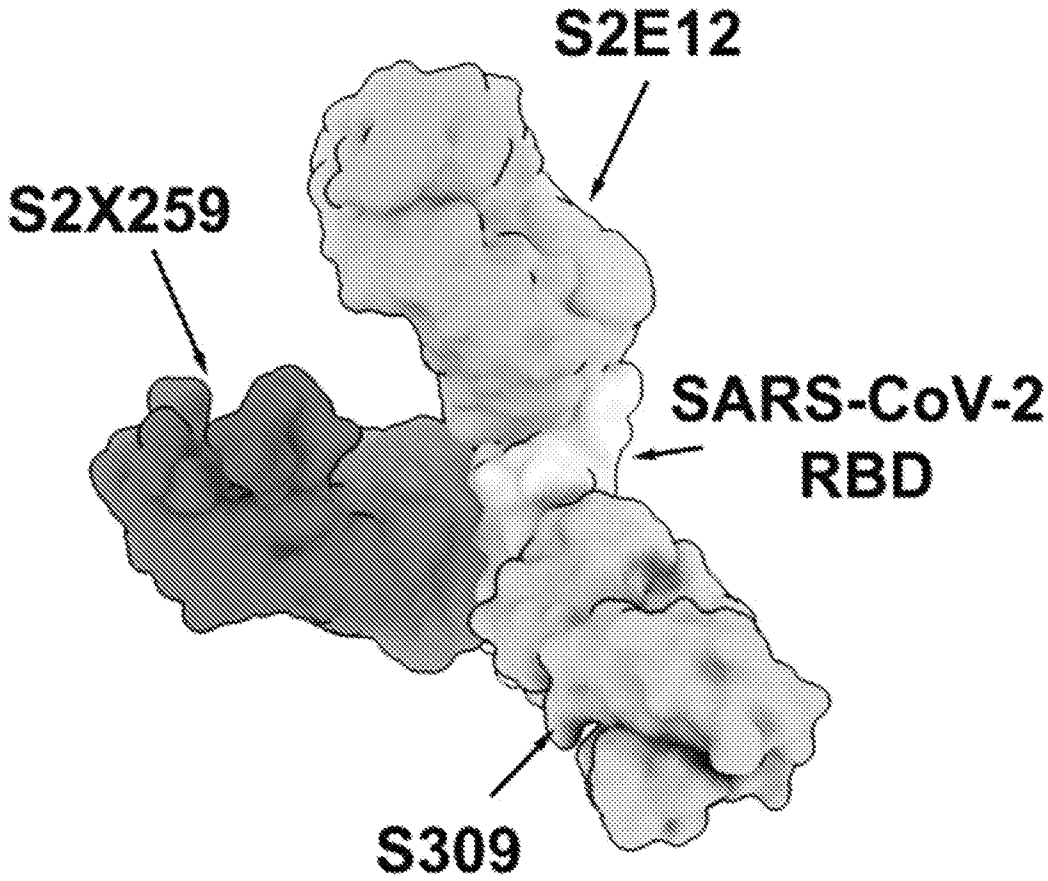


FIG. 20

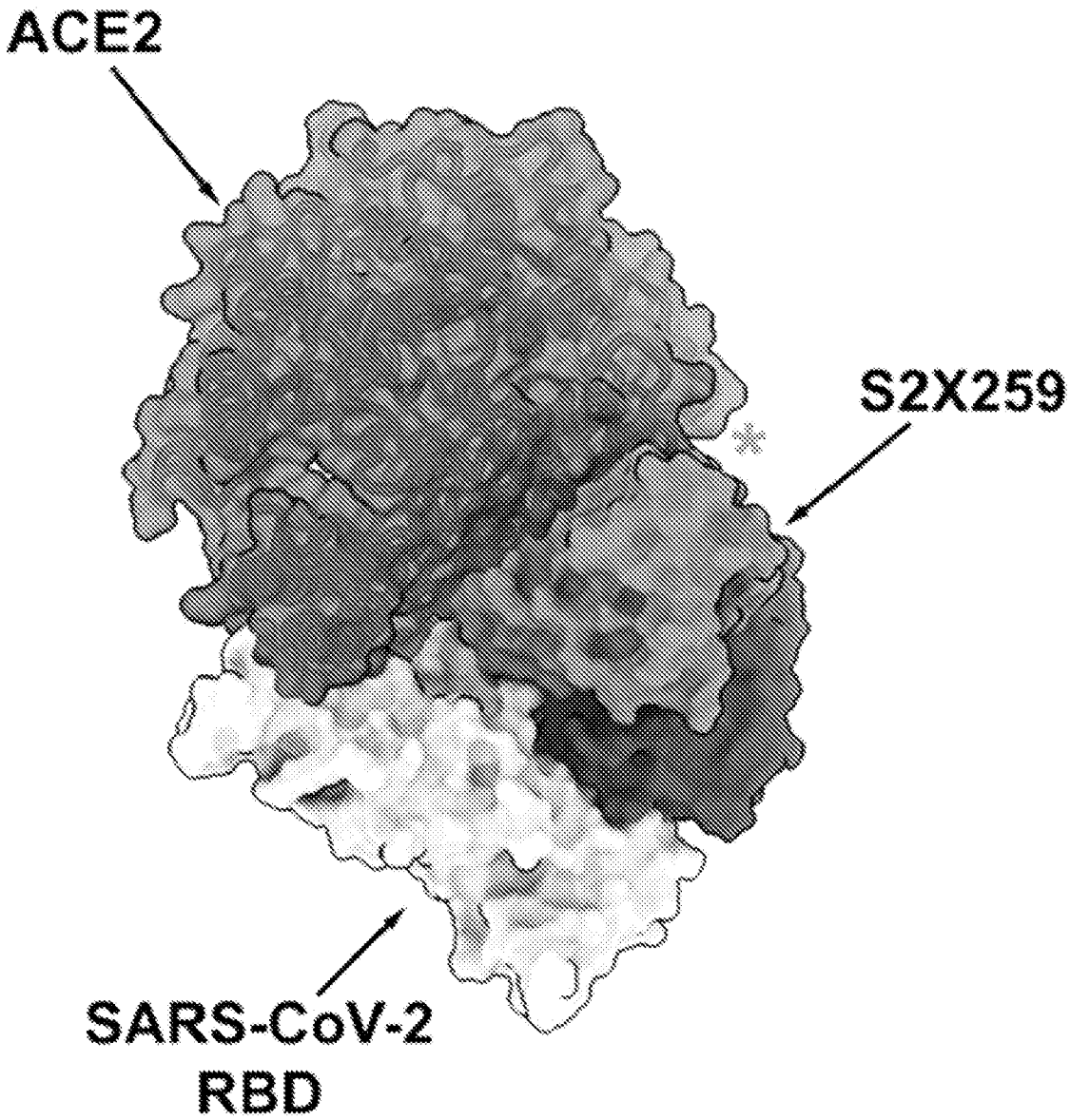


FIG. 21

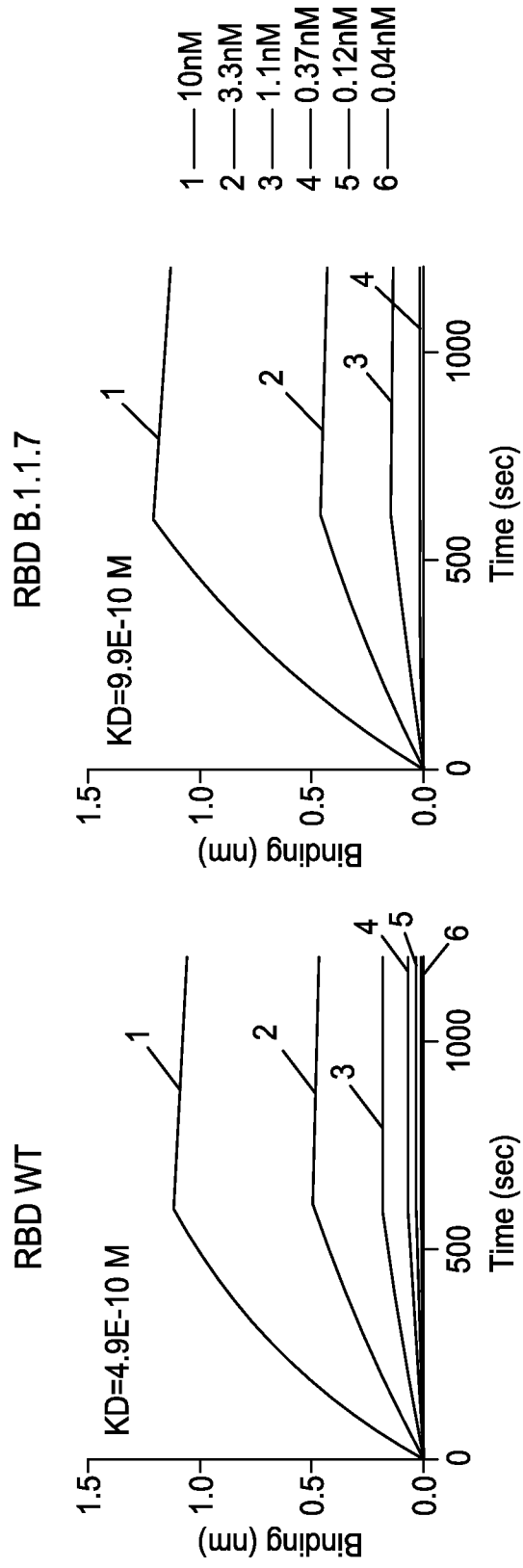

RBD WT
KD=4.9E-10 M
Binding (nm)
Time (sec)
RBD B.1.1.7
KD=9.9E-10 M
1 — 10nM
2 — 3.3nM
3 — 1.1nM
4 — 0.37nM
5 — 0.12nM
6 — 0.04nM

FIG. 22A

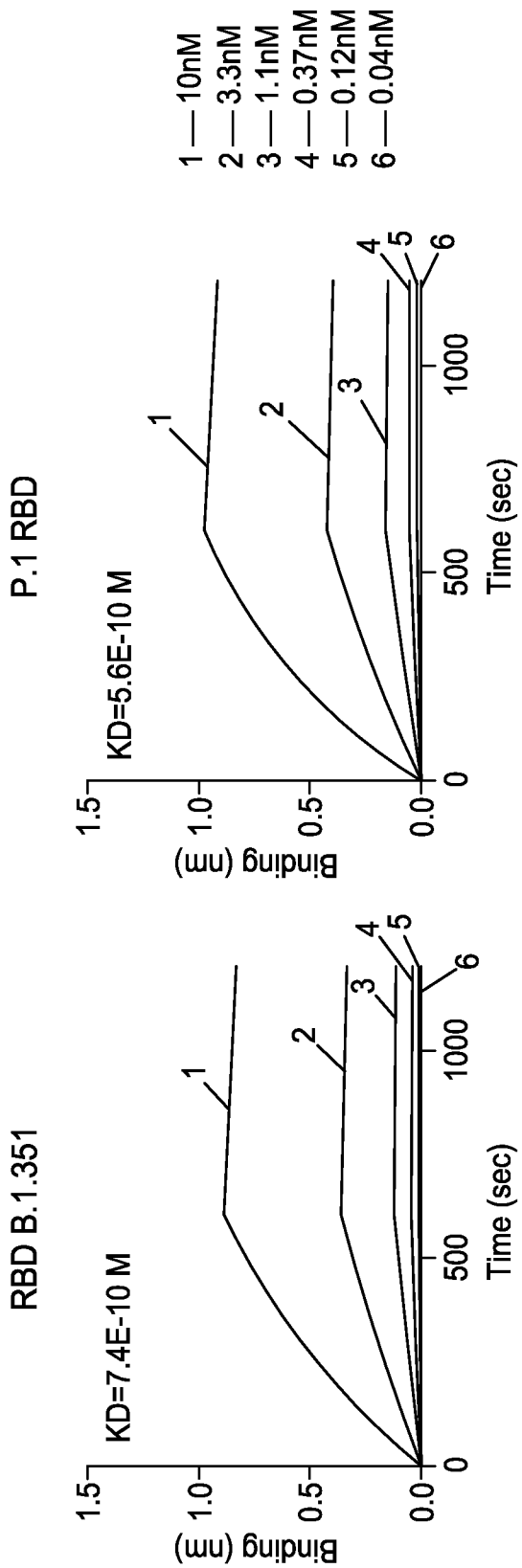
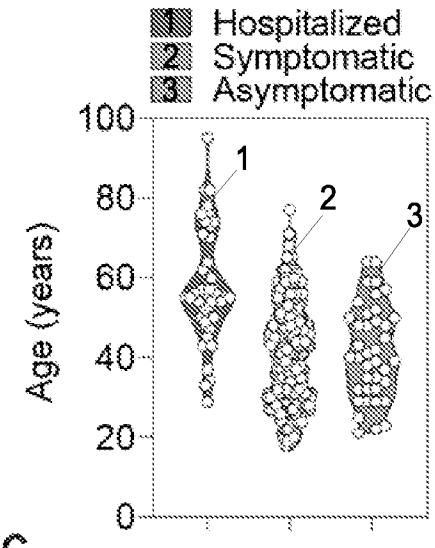

RBD B.1.351
KD=7.4E-10 M
P.1 RBD
KD=5.6E-10 M
Binding (nm)
Time (sec)
1.5
1.0
0.5
0.0
0
500
1000
1 — 10nM
2 — 3.3nM
3 — 1.1nM
4 — 0.37nM
5 — 0.12nM
6 — 0.04nM

FIG. 22B

A

Patients demographics	
Participants	647
Female	411
Male	229
N/A	7
Average age	42
Range	18-95
Positive PCR for SARS-CoV-2	271
Average days post-symptom onset	42
Range	10-147
Hospitalized	47
Clinica Luganese Moncucco	31
Luigi Sacco Hospital	16
Symptomatic	556
Clinica Luganese Moncucco	9
Luigi Sacco Hospital	1
US - San Francisco	100
Ticino healthcare workers	423
Swiss volunteers	23
Asymptomatic	44
Luigi Sacco Hospital	4
US - San Francisco	2
Ticino healthcare workers	36
Swiss volunteers	2
Subjects with multiple time points	368
Hospitalized	11
Symptomatic	329
Asymptomatic	28
Pre-pandemic healthy donors (controls)	32

B



C

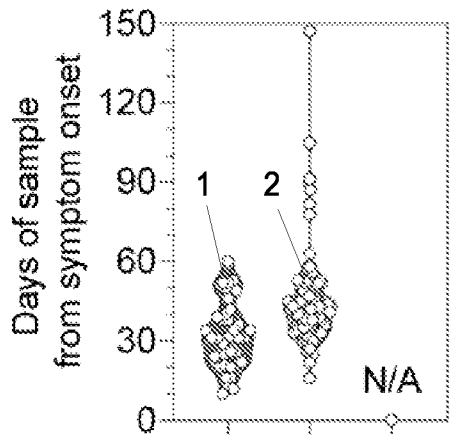


FIG. 23

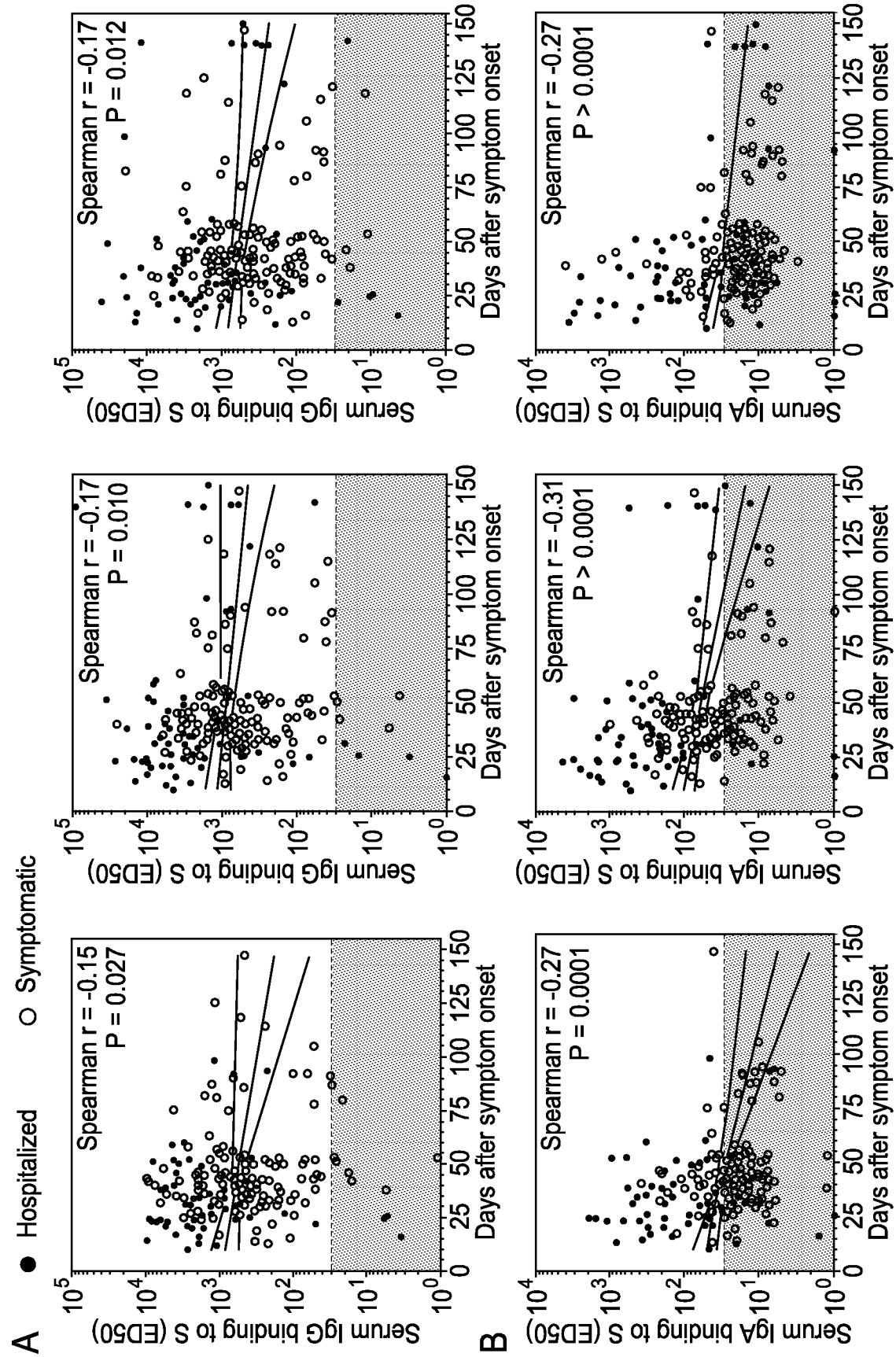

A
B
● Hospitalized
○ Symptomatic
Serum IgG binding to S (ED50)
Serum IgA binding to S (ED50)
Days after symptom onset
Spearman r = -0.15
P = 0.027
Spearman r = -0.17
P = 0.010
Spearman r = -0.17
P = 0.012
Spearman r = -0.27
P = 0.0001
Spearman r = -0.31
P > 0.0001
Spearman r = -0.27
P > 0.0001

FIG. 24

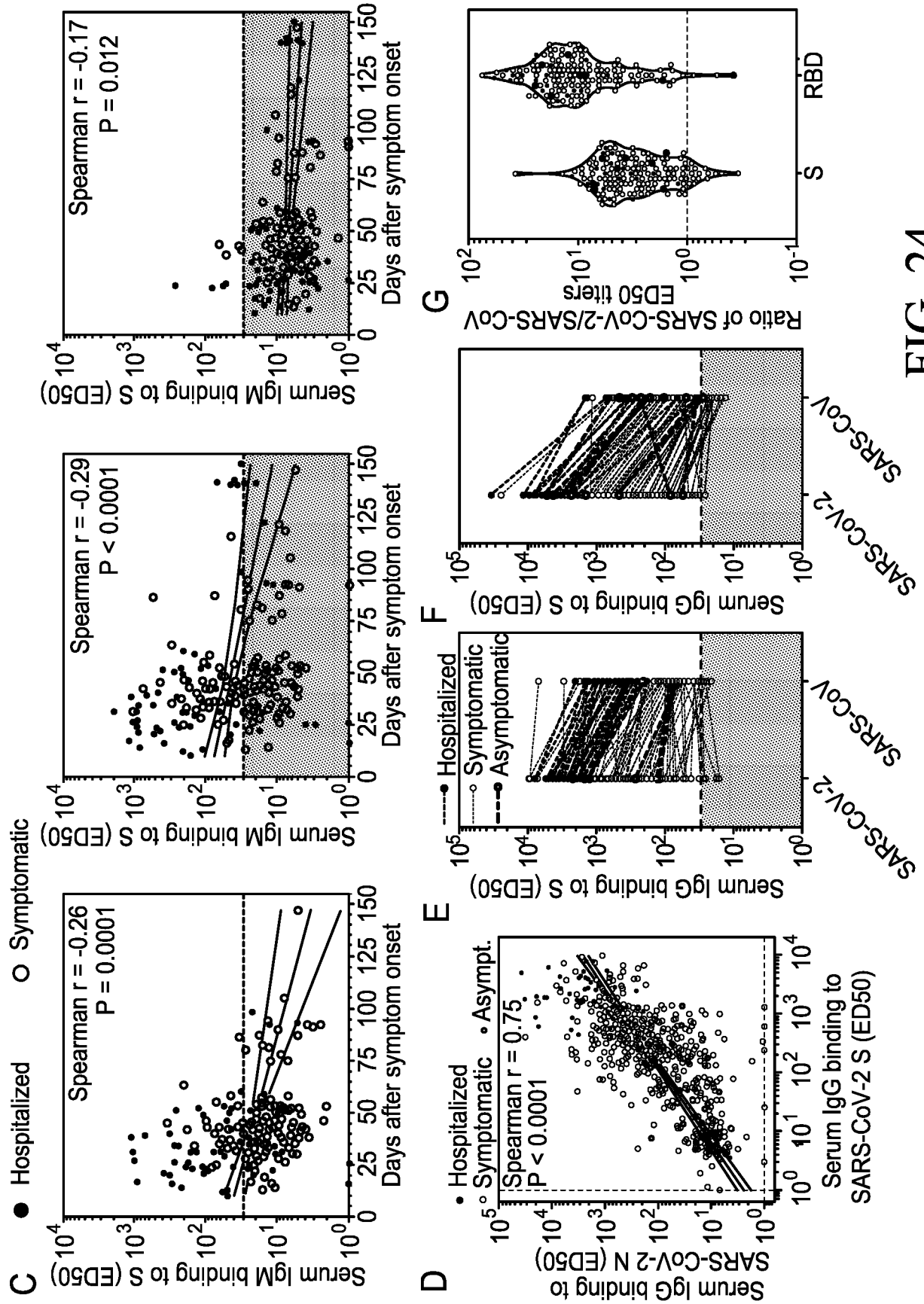
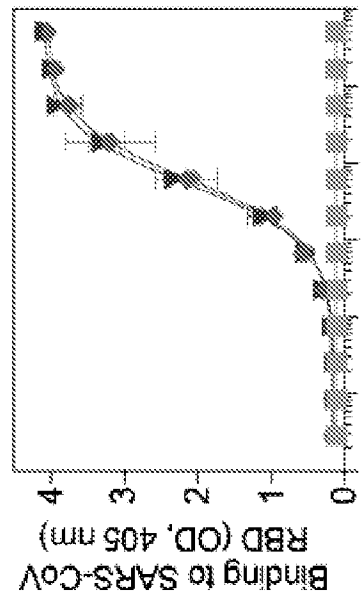

C
● Hospitalized
○ Symptomatic
Spearman r = -0.26
P = 0.0001
Spearman r = -0.29
P < 0.0001
Spearman r = -0.17
P = 0.012
Serum IgM binding to S (ED50)
Days after symptom onset
D
● Hospitalized
○ Symptomatic
● Asympt.
Spearman r = 0.75
P < 0.0001
Serum IgG binding to SARS-CoV-2 N (ED50)
Serum IgG binding to SARS-CoV-2 S (ED50)
E
Hospitalized
Symptomatic
Asymptomatic
Serum IgG binding to S (ED50)
SARS-CoV-2
SARS-CoV
F
Serum IgG binding to S (ED50)
SARS-CoV-2
SARS-CoV
G
Ratio of SARS-CoV-2/SARS-CoV ED50 titers
S
RBD

FIG. 24

mAb	VH (% identity nts; aa differences)	VL (% identity nts; aa differences)	Source	Time point from disease onset	RBD site	Neutralization (IC50, ng/ml)
S2H14	VH3-15 (100; 0)	VL6-57 (100; 0)	Plasma cells	17 days	Ia	900
S2H13	VH3-7 (97.92; 4)	VL7-46 (98.96; 1)	Plasma cells	17 days	Ib	500
S2X35	VH1-18 (98.61; 4)	VL1-40 (98.96; 1)	Memory B cells	48 days	IIa	500
S2A4	VH3-7 (99.31; 2)	VL2-23 (100; 0)	Memory B cells	24 days	IIb	3500
S304	VH3-13 (98.60; 5)	VK1-39 (97.13; 6)	Memory B cells	10 years	IIc	>5000 (Pinto et al.)
S309	VH1-18 (97.22; 8)	VK3-20 (97.52; 6)	Memory B cells	10 years	IV	120-180 (Pinto et al.)

nts, nucleotides; aa, amino acids; ^{a}FcγRIIa activation

FIG. 25A



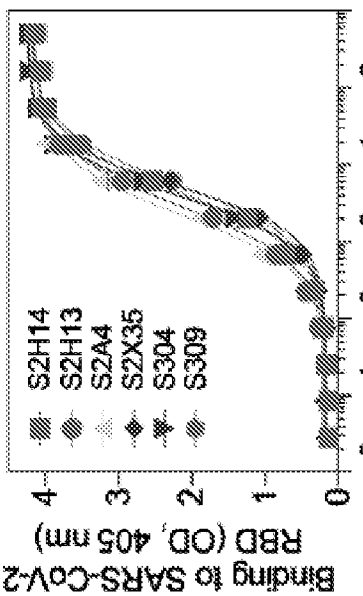


FIG. 25B

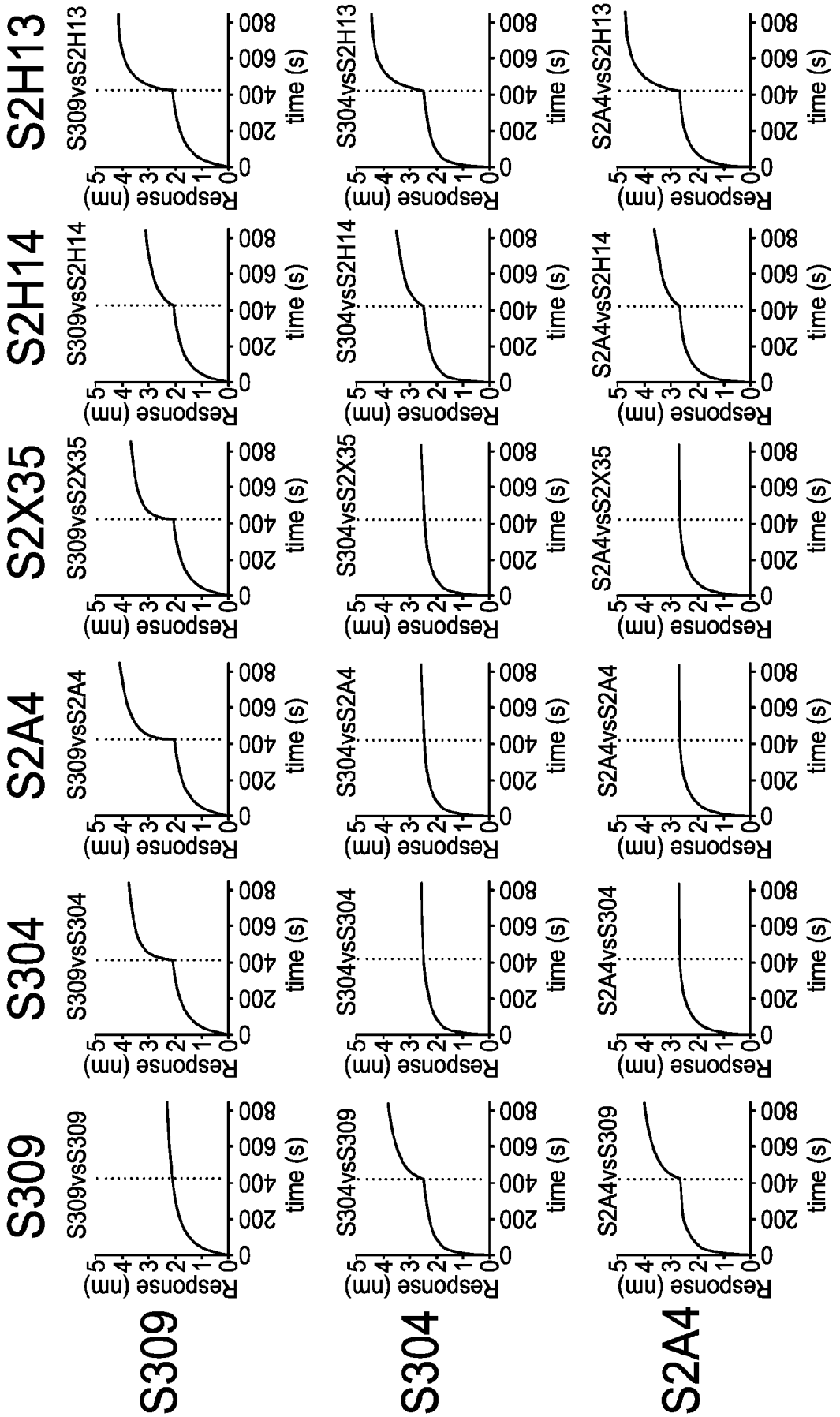

S309
S304
S2A4
S2X35
S2H14
S2H13
S309vsS309
S309vsS304
S309vsS2A4
S309vsS2X35
S309vsS2H14
S309vsS2H13
S304vsS309
S304vsS304
S304vsS2A4
S304vsS2X35
S304vsS2H14
S304vsS2H13
S2A4vsS309
S2A4vsS304
S2A4vsS2A4
S2A4vsS2X35
S2A4vsS2H14
S2A4vsS2H13
Response (nm)
time (s)
0
1
2
3
4
5
0
200
400
600
800

FIG. 25C

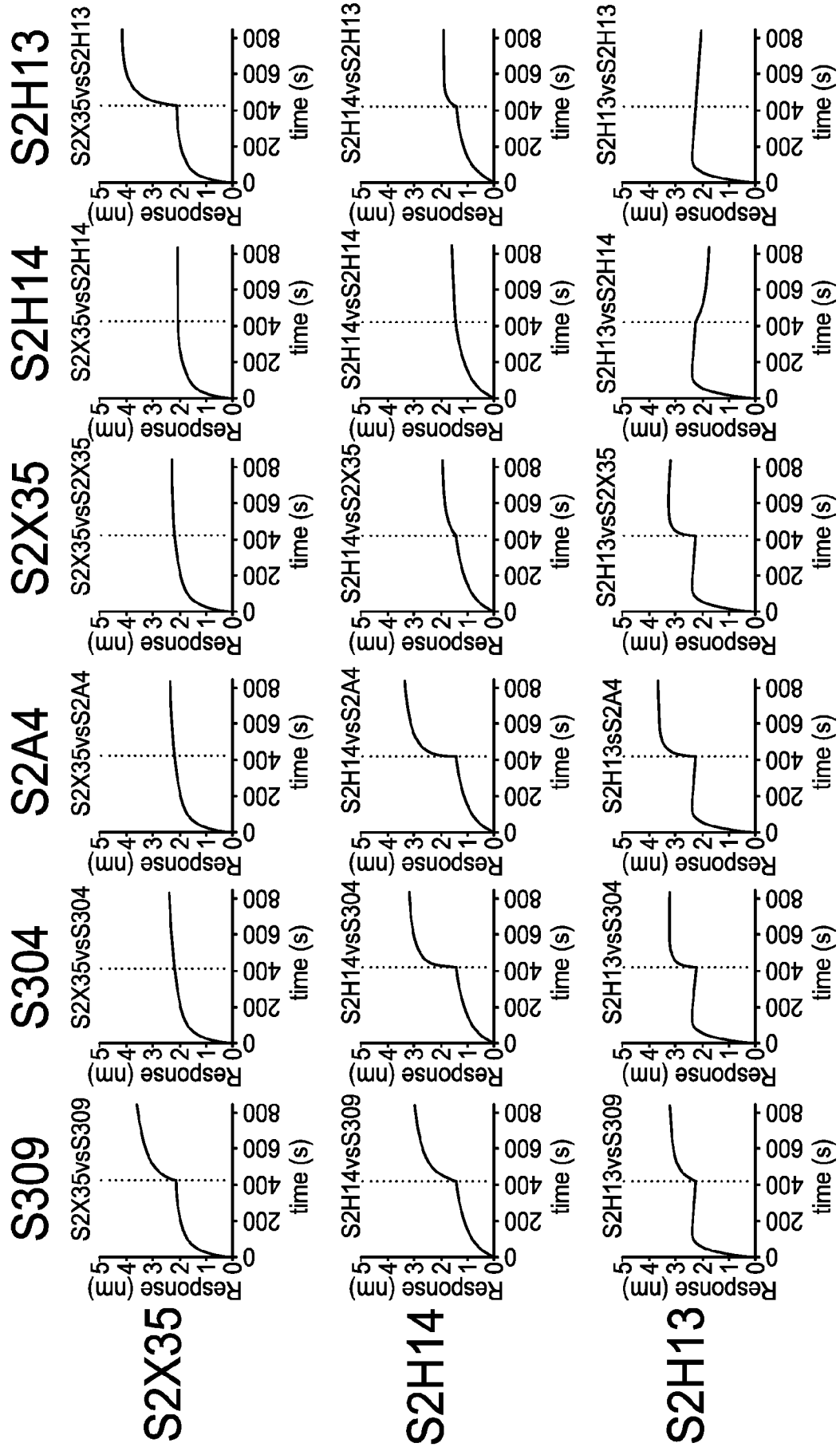

S309
S304
S2A4
S2X35
S2H14
S2H13
S2X35
S2H14
S2H13
S2X35vsS309
S2X35vsS304
S2X35vsS2A4
S2X35vsS2X35
S2X35vsS2H14
S2X35vsS2H13
S2H14vsS309
S2H14vsS304
S2H14vsS2A4
S2H14vsS2X35
S2H14vsS2H14
S2H14vsS2H13
S2H13vsS309
S2H13vsS304
S2H13vsS2A4
S2H13vsS2X35
S2H13vsS2H14
S2H13vsS2H13
Response (nm)
time (s)
0
200
400
600
800
1
2
3
4
5

FIG. 25C cont.

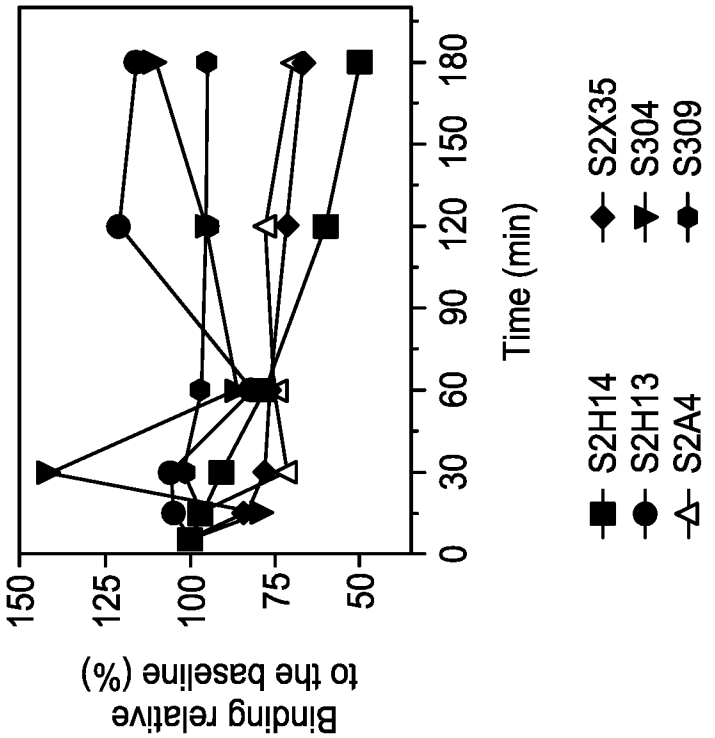


FIG. 25E

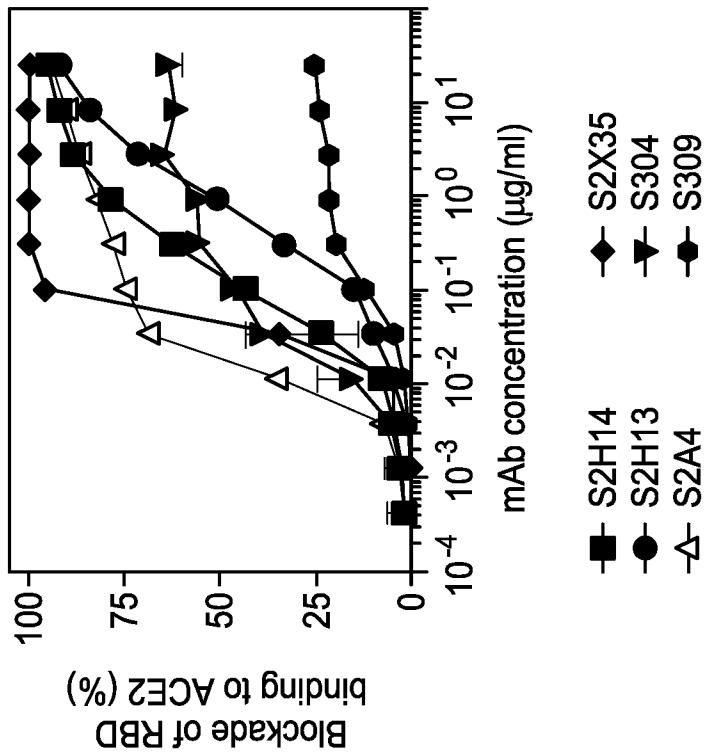


FIG. 25D

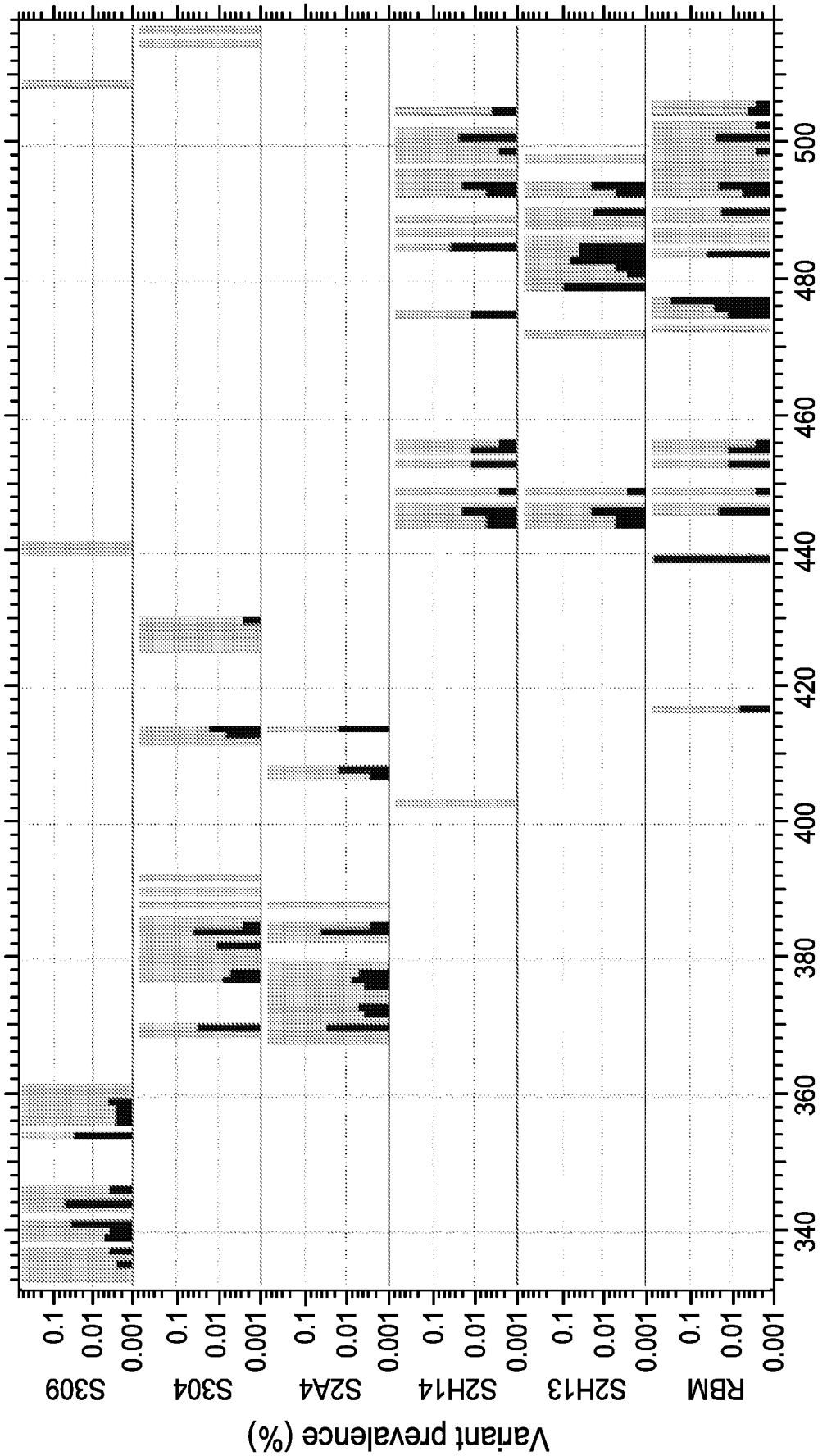

Variant prevalence (%)
RBM
S2H13
S2H14
S2A4
S304
S309
0.1
0.01
0.001
340
360
380
400
420
440
460
480
500
RBD Residues

FIG. 25F

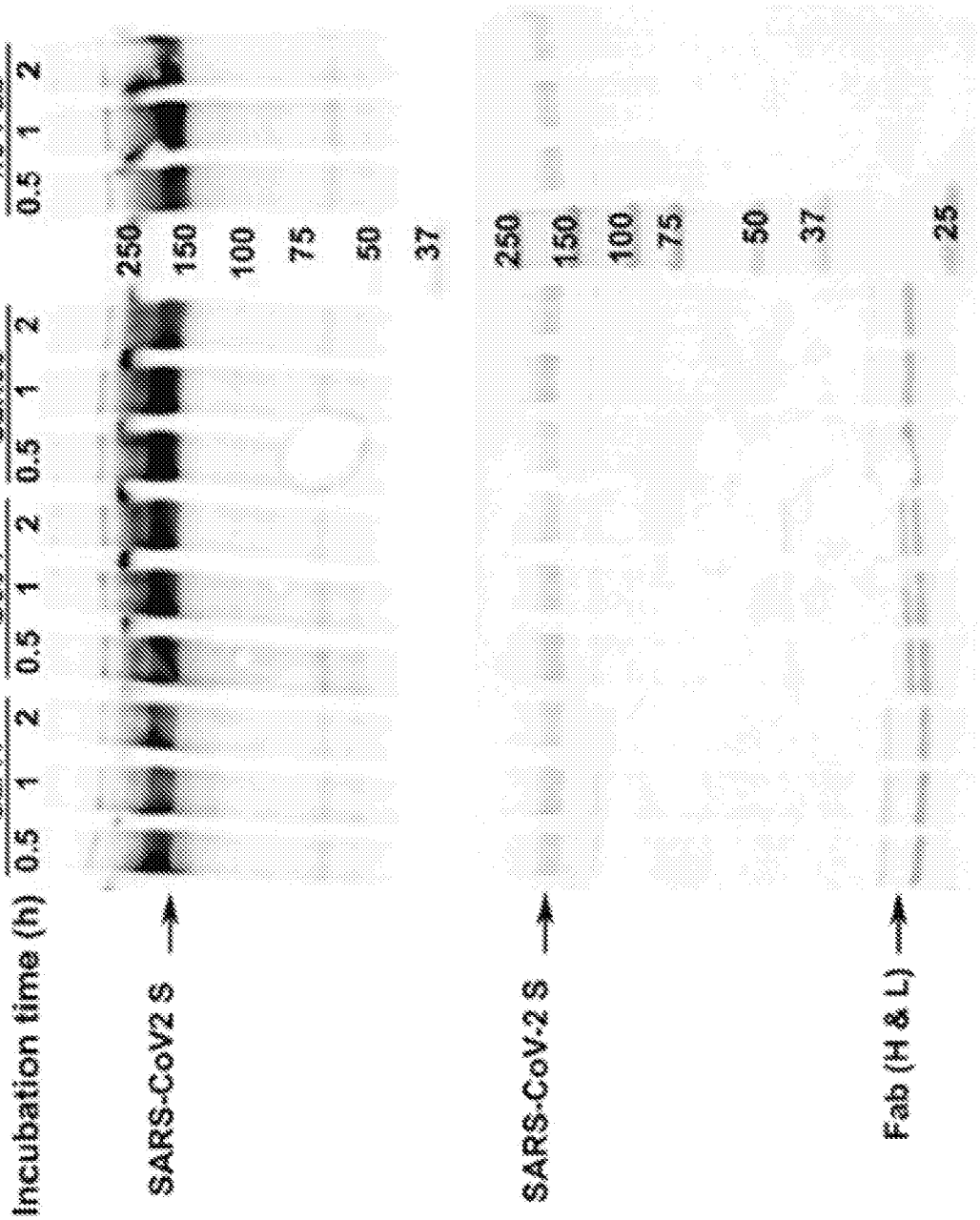

Incubation time (h)
S2A4
S304
S2X35
no Fab
0.5 1 2 0.5 1 2 0.5 1 2 0.5 1 2
SARS-CoV2 S
250
150
100
75
50
37
SARS-CoV-2 S
250
150
100
75
50
37
Fab (H & L)
25

FIG. 25G

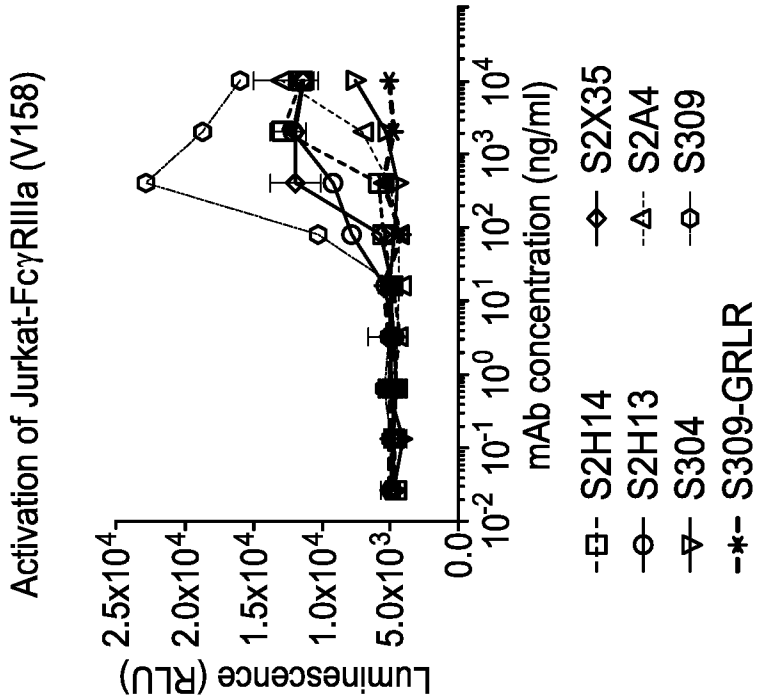


FIG. 25I

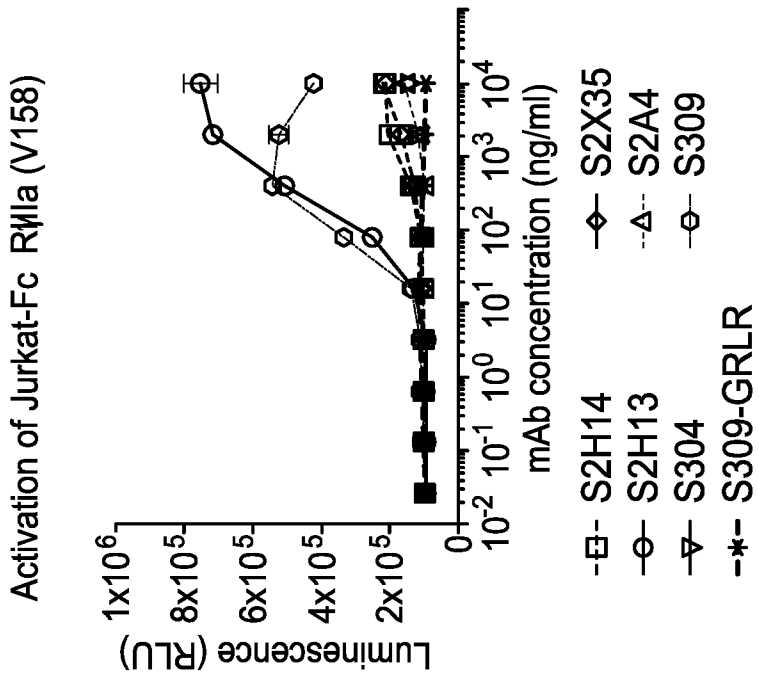


FIG. 25H

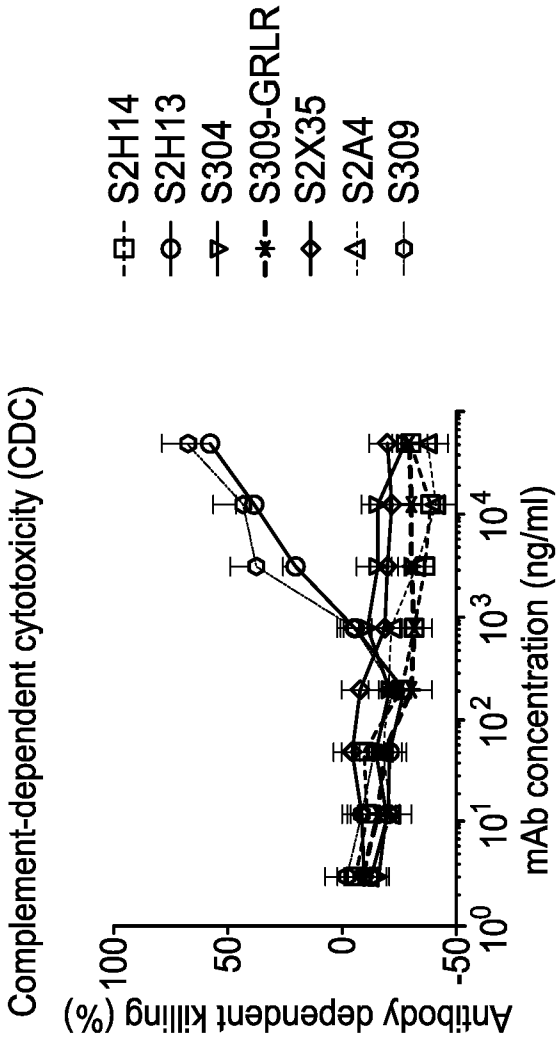

S2H14
S2H13
S304
S309-GRLR
S2X35
S2A4
S309
Complement-dependent cytotoxicity (CDC)
Antibody dependent killing (%)
100
50
0
-50
10^0
10^1
10^2
10^3
10^4
mAb concentration (ng/ml)

FIG. 25J

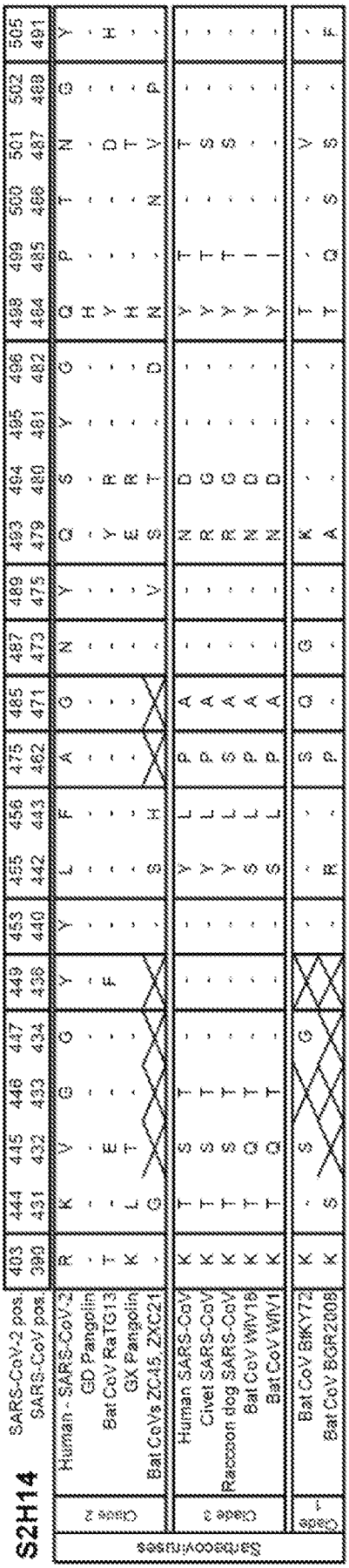


FIG. 26A-1

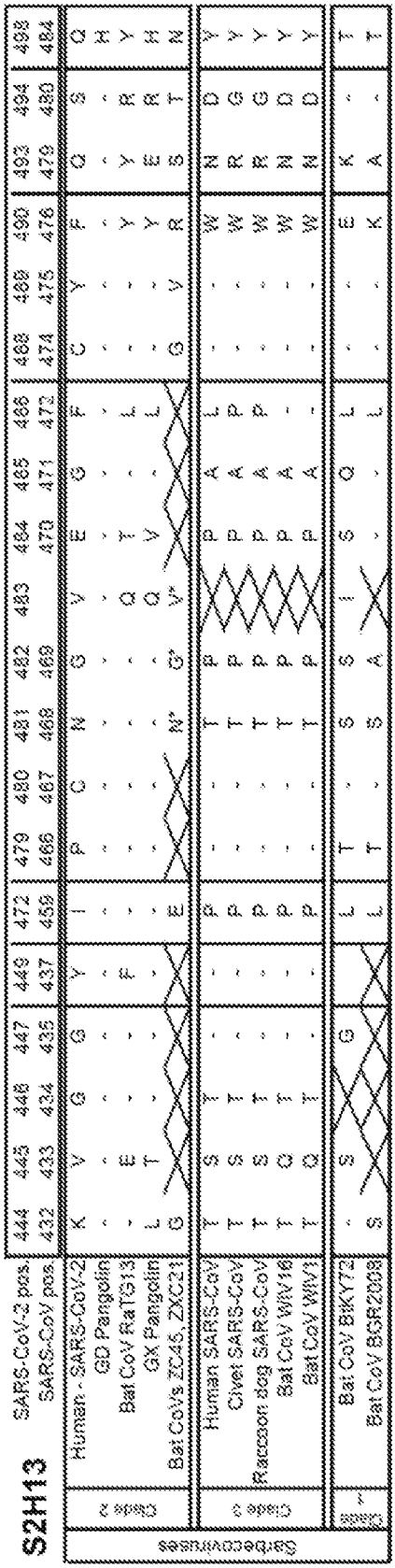


FIG. 26A-2

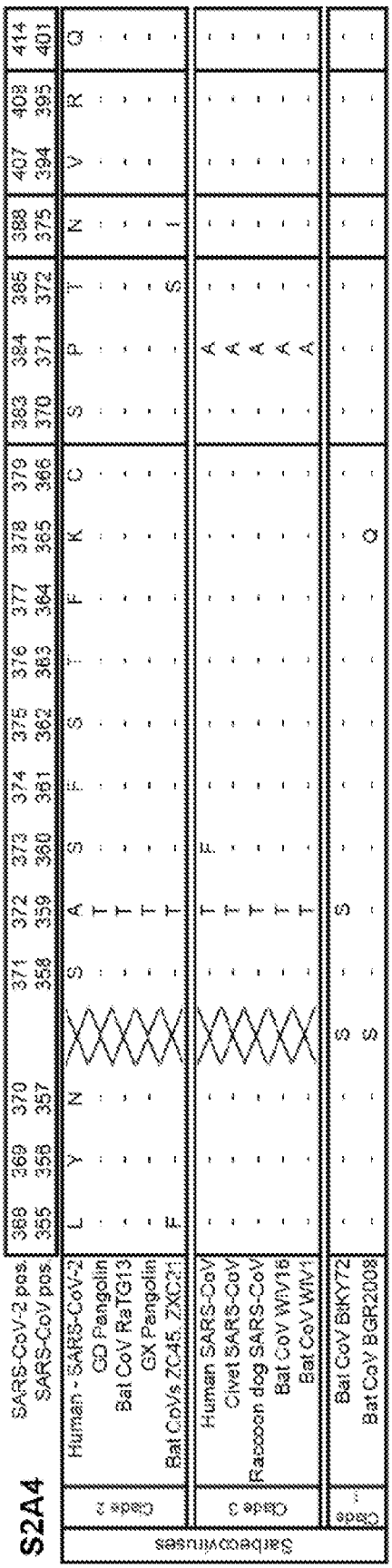


FIG. 26A-3

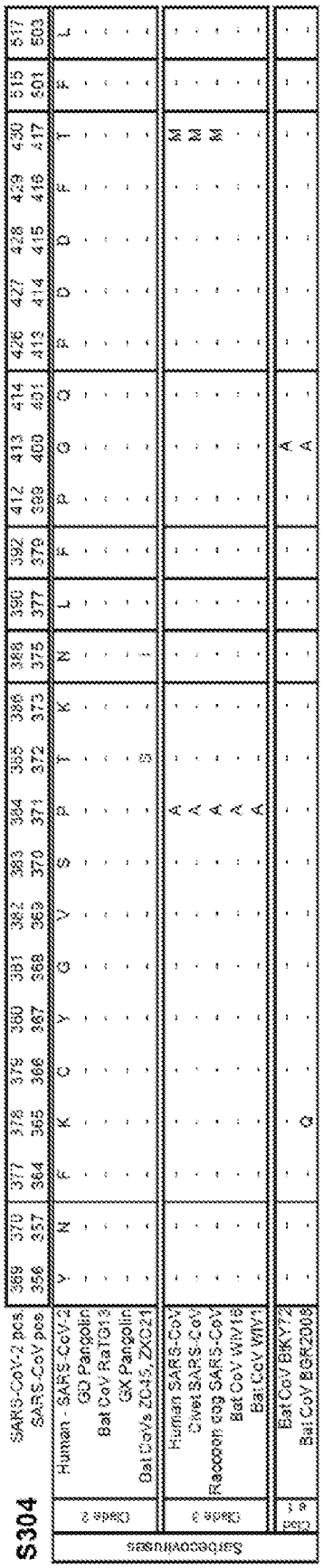


FIG. 26A-4

	Spike	RBD	RBM	S309	S304	S2H13	S2H14	S2A4
Bat CoV BtKY72 (Clade 1)	72/84%	73/85%	46/54%	62/86%	96/96%	30/50%	57/70%	95/100%
Bat CoV RaTG13 (Clade 2)	97/98%	90/94%	67/83%	86/95%	100/100%	55/65%	65/78%	95/95%
SARS- (Clade 3)	76/87%	74/82%	42/50%	81/95%	92/92%	30/35%	44/48%	84/84%

FIG. 26B

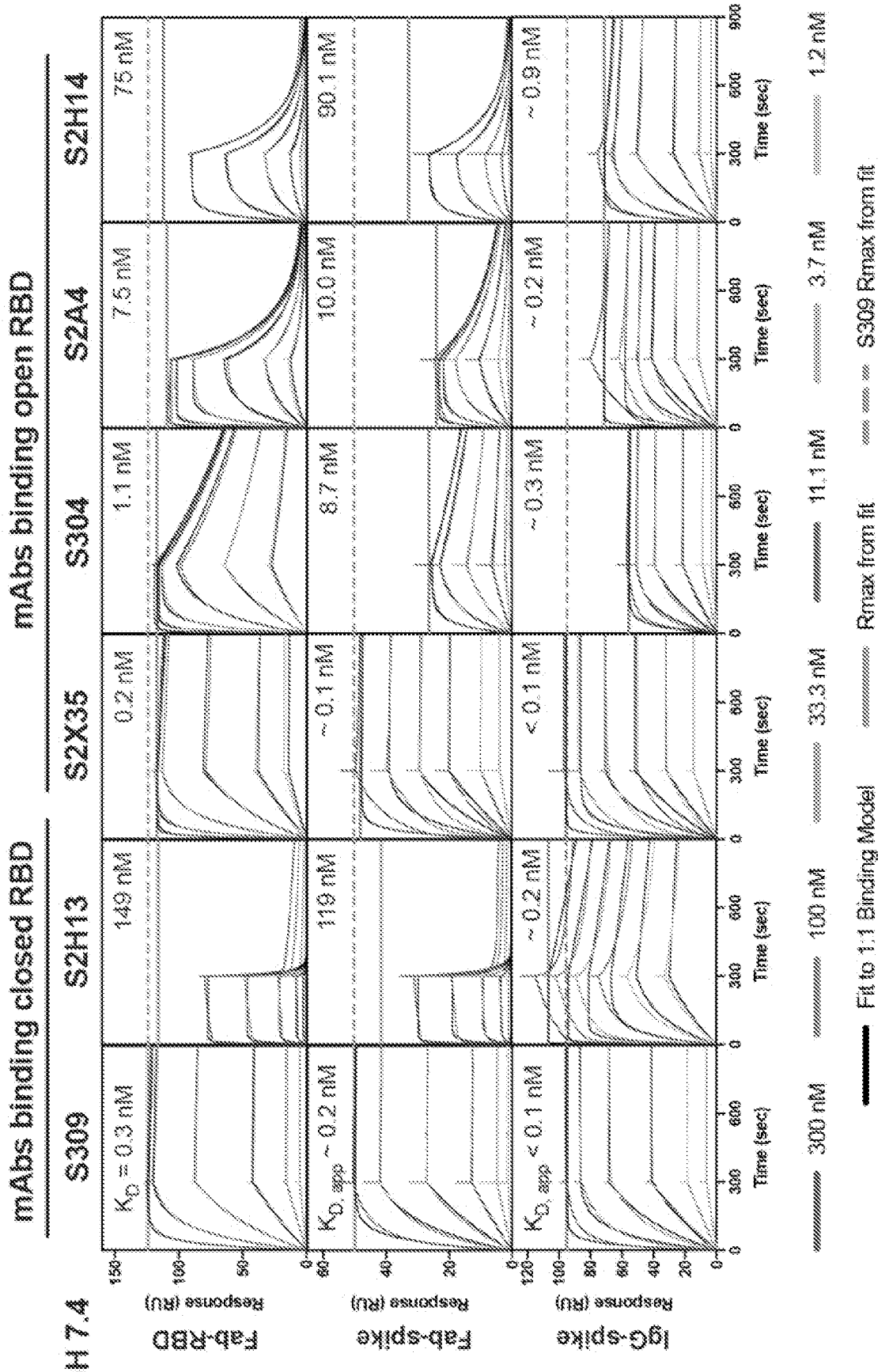

pH 7.4
mAbs binding closed RBD
mAbs binding open RBD
S309
S2H13
S2X35
S304
S2A4
S2H14
Fab-RBD
Fab-spike
IgG-spike
Response (RU)
Time (sec)
K_D = 0.3 nM
149 nM
0.2 nM
1.1 nM
7.5 nM
75 nM
$K_{D,\ app}$ ~ 0.2 nM
119 nM
~ 0.1 nM
8.7 nM
10.0 nM
90.1 nM
$K_{D,\ app}$ < 0.1 nM
~ 0.2 nM
< 0.1 nM
~ 0.3 nM
~ 0.2 nM
~ 0.9 nM
300 nM
100 nM
33.3 nM
11.1 nM
3.7 nM
1.2 nM
Fit to 1:1 Binding Model
Rmax from fit
S309 Rmax from fit

FIG. 27A

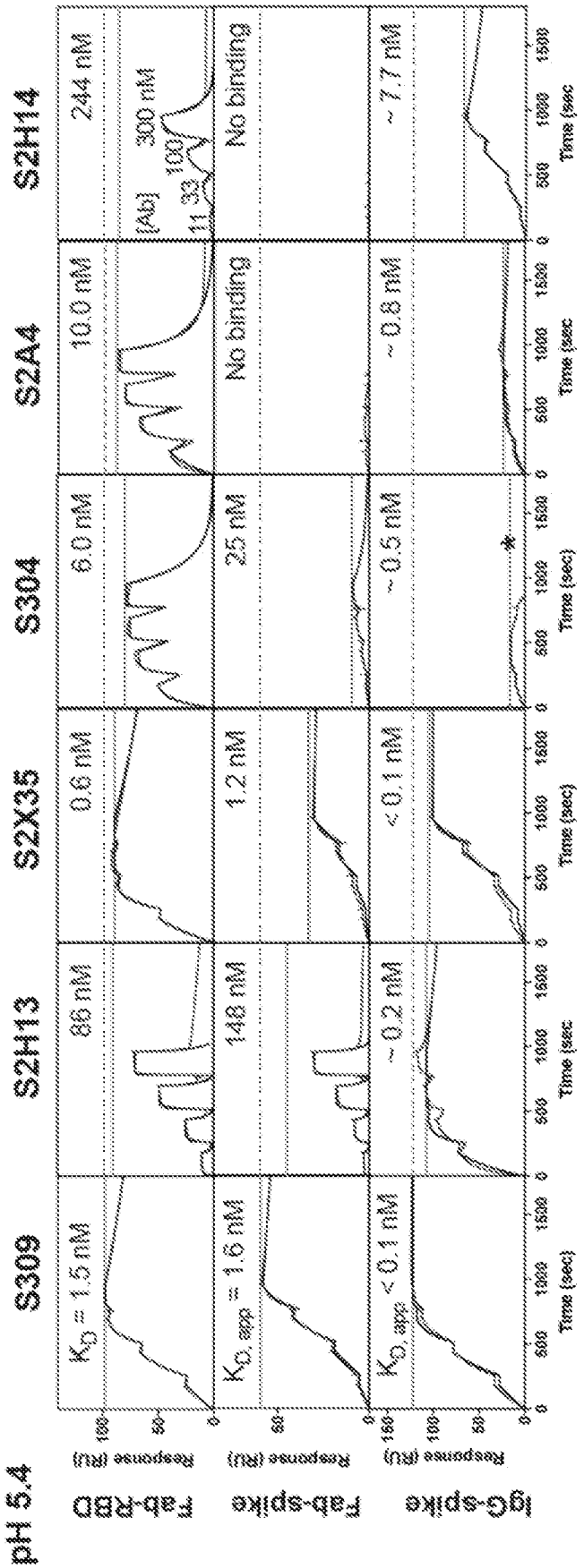

pH 5.4
S309
S2H13
S2X35
S304
S2A4
S2H14
IgG-spike
Fab-spike
Fab-RBD
Response (RU)
Time (sec)
K_D = 1.5 nM
$K_{D, app}$ = 1.6 nM
$K_{D, app}$ < 0.1 nM
86 nM
148 nM
~ 0.2 nM
0.6 nM
1.2 nM
< 0.1 nM
6.0 nM
25 nM
~ 0.5 nM
10.0 nM
No binding
~ 0.8 nM
244 nM
No binding
~ 7.7 nM
[Ab] 300 nM 100 33 11

FIG. 27B

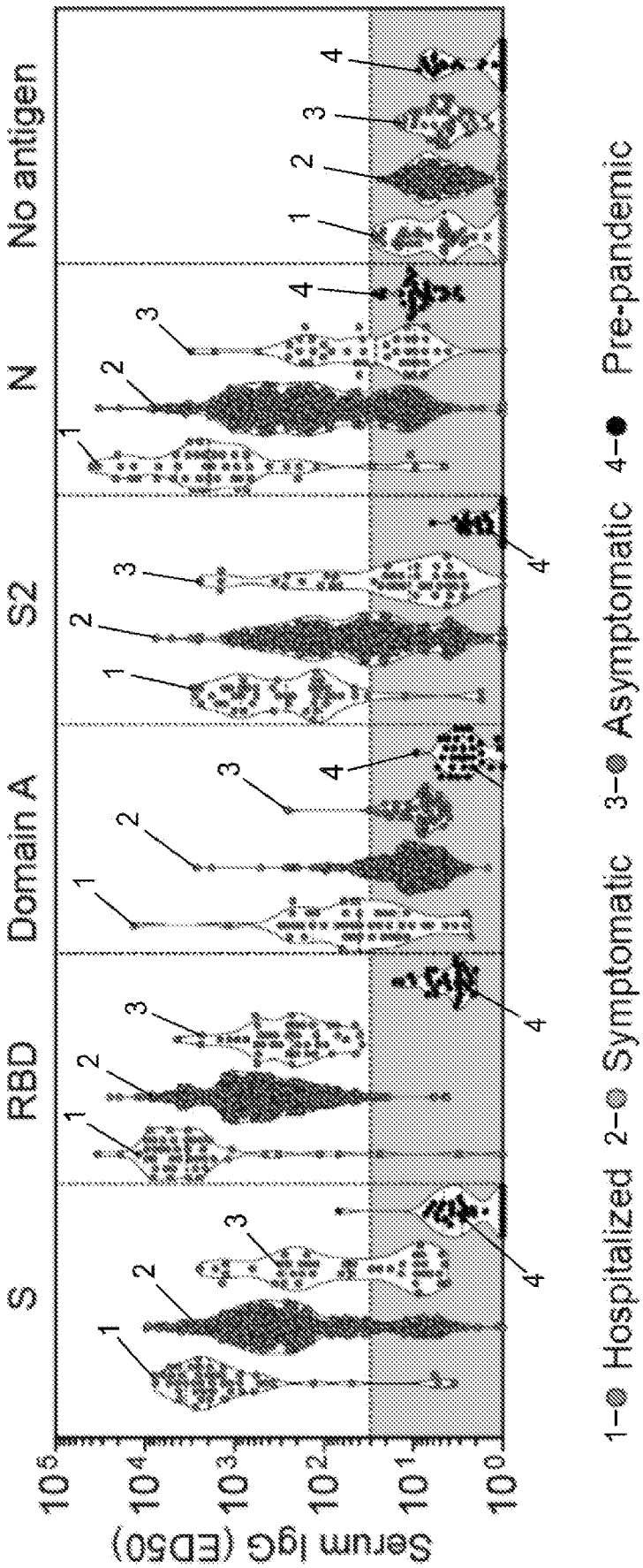

S
RBD
Domain A
S2
N
No antigen
Serum IgG (ED50)
10^5
10^4
10^3
10^2
10^1
10^0
1–● Hospitalized 2–● Symptomatic 3–● Asymptomatic 4–● Pre-pandemic

FIG. 28A

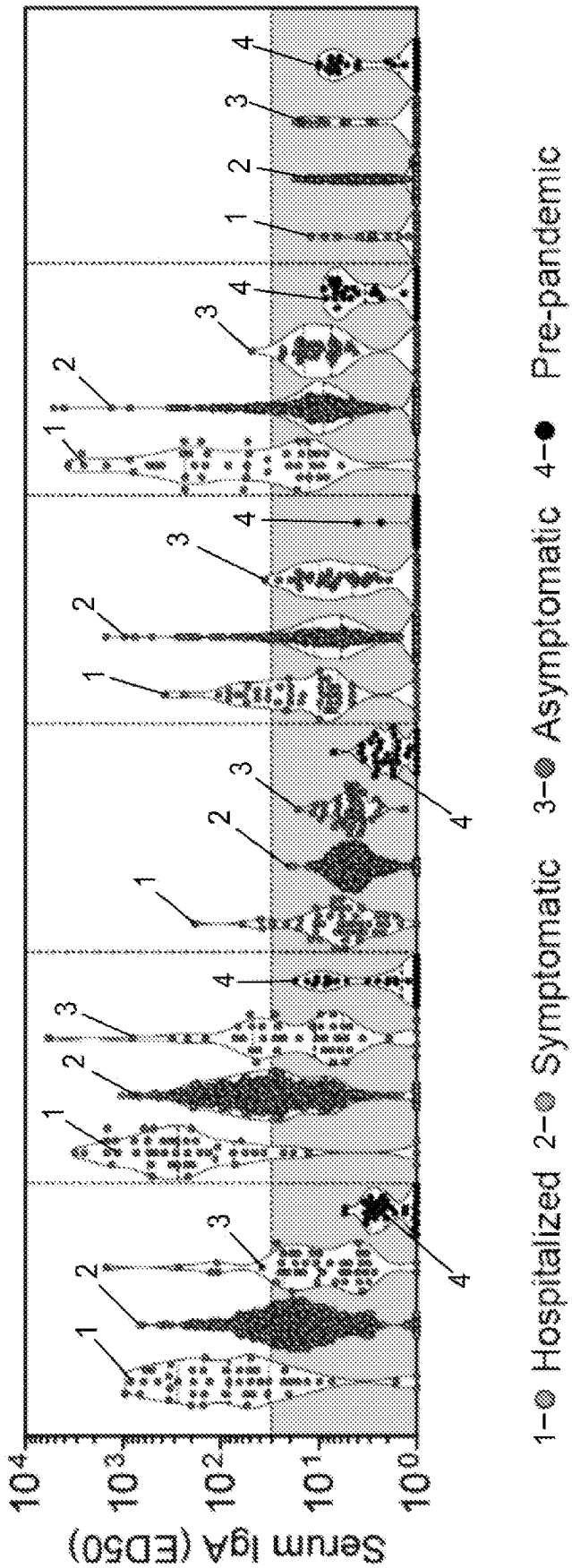

Serum IgA (ED50)
10^4
10^3
10^2
10^1
10^0
1–● Hospitalized 2–● Symptomatic 3–● Asymptomatic 4–● Pre-pandemic

FIG. 28B

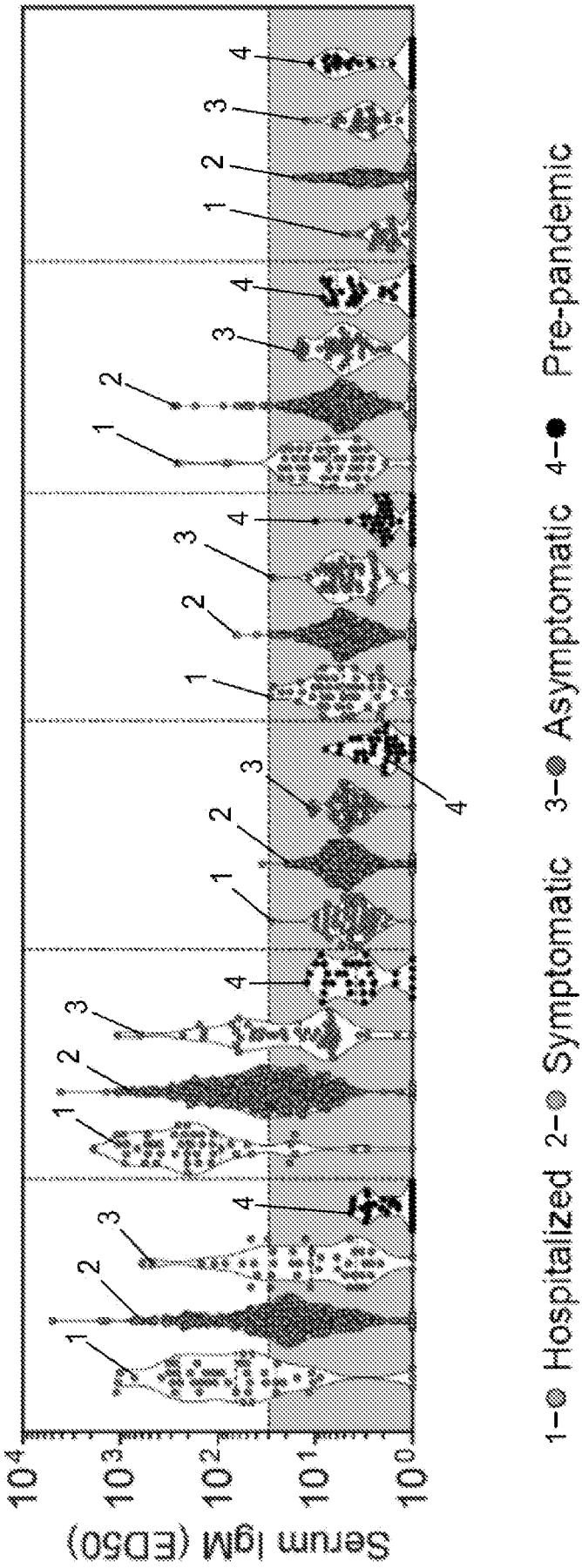

Serum IgM (ED50)
10^4
10^3
10^2
10^1
10^0
1–● Hospitalized 2–● Symptomatic 3–● Asymptomatic 4–● Pre-pandemic

FIG. 28C

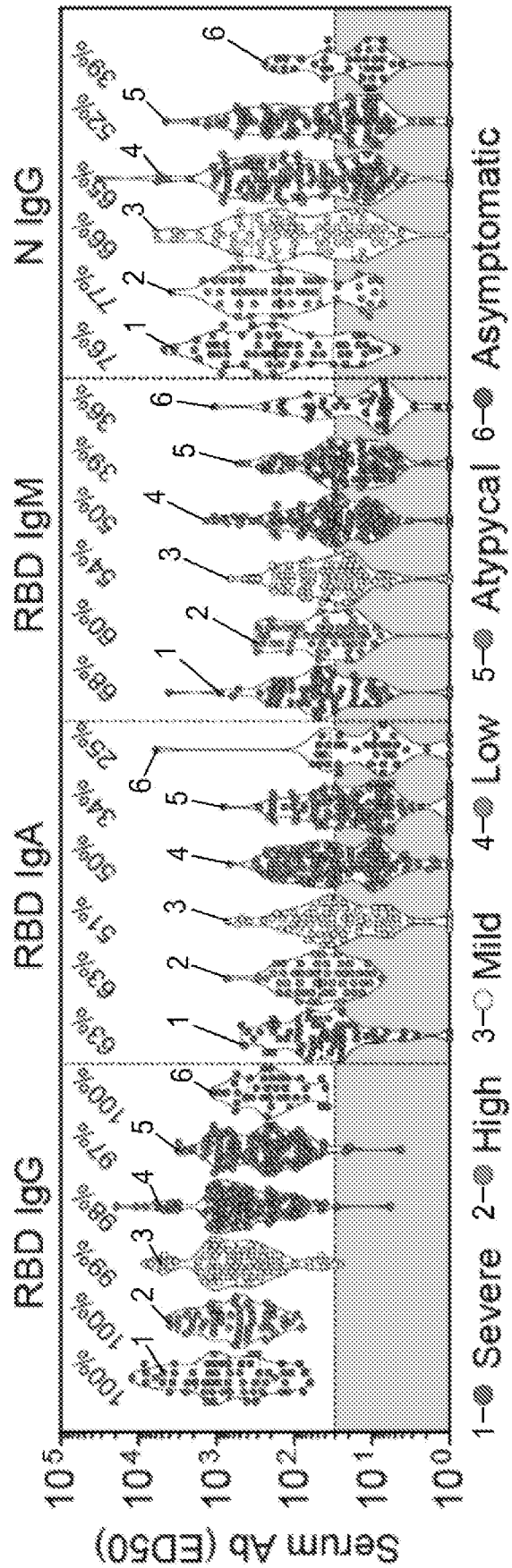

RBD IgG
RBD IgA
RBD IgM
N IgG
Serum Ab (ED50)
1—● Severe 2—● High 3—○ Mild 4—● Low 5—● Atypycal 6—● Asymptomatic

FIG. 28D

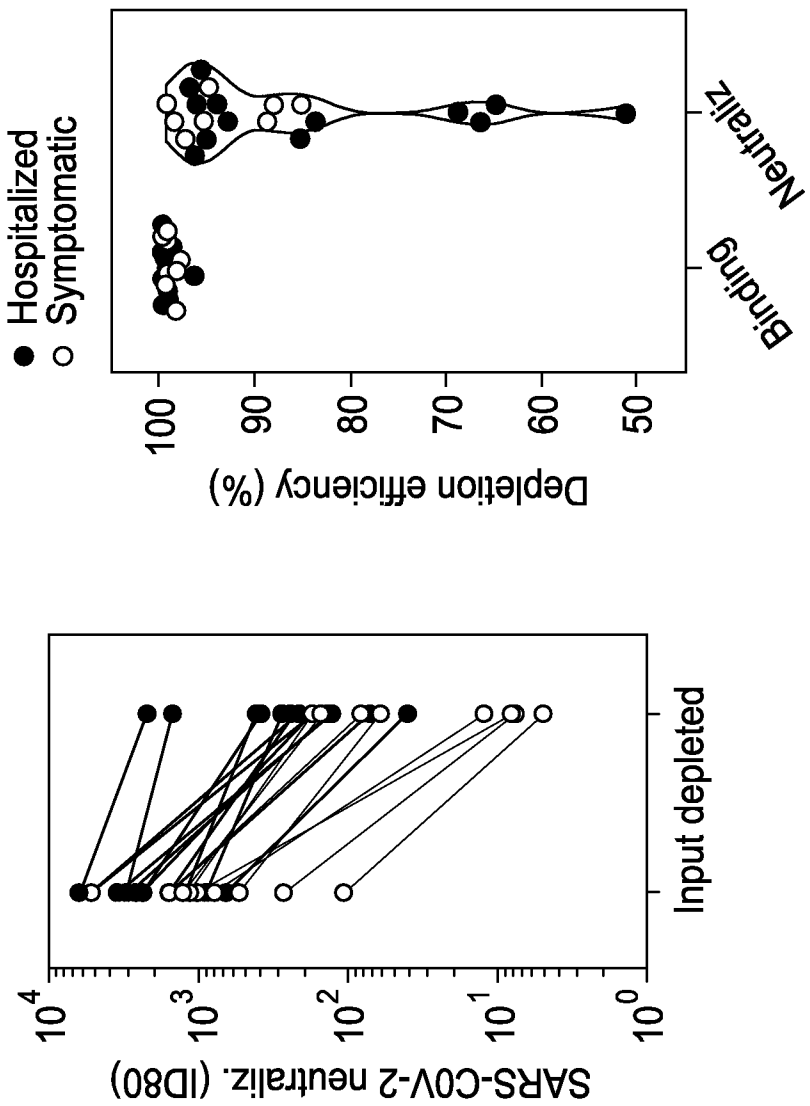

Hospitalized
Symptomatic
Depletion efficiency (%)
100
90
80
70
60
50
Binding
Neutraliz
SARS-C0V-2 neutraliz. (ID80)
10^4
10^3
10^2
10^1
10^0
Input depleted
IgG binding to RBD (ED50)
10^5
10^4
10^3
10^2
10^1
10^0
Input depleted

FIG. 28E

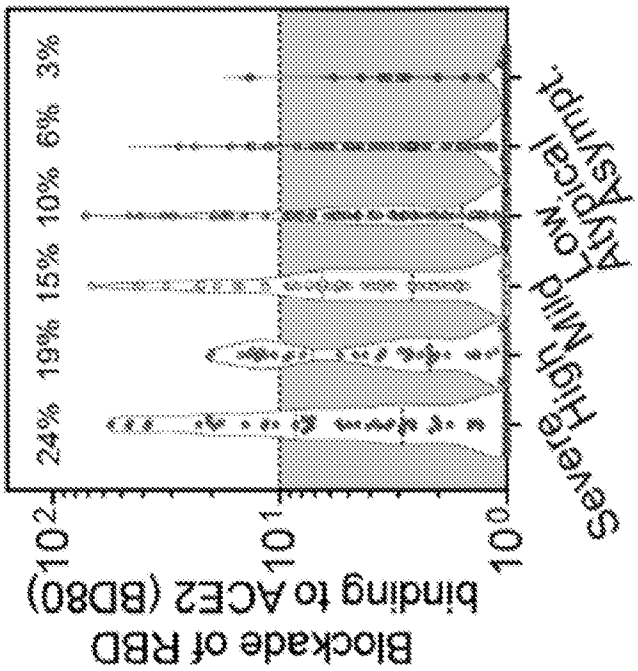


FIG. 28G

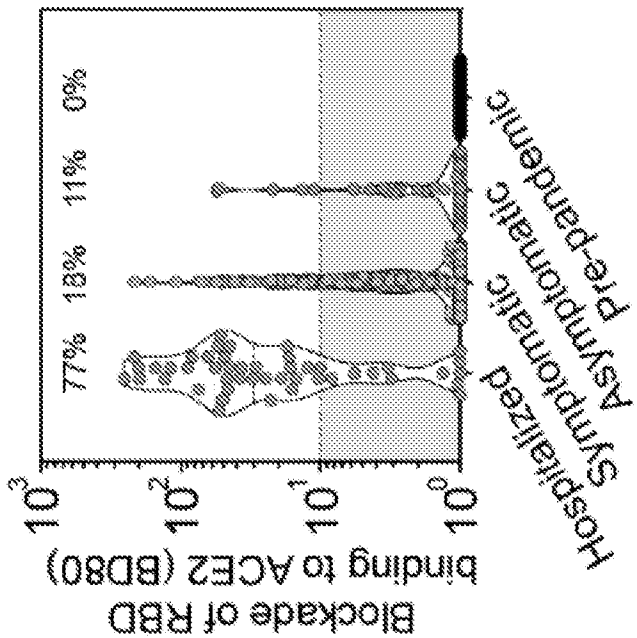


FIG. 28F

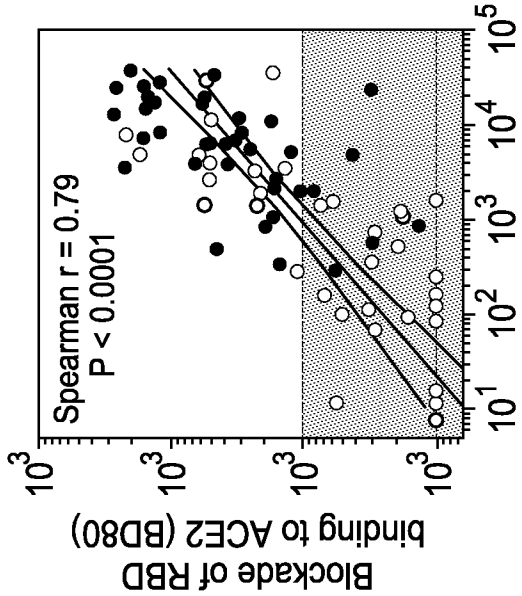


FIG. 28I

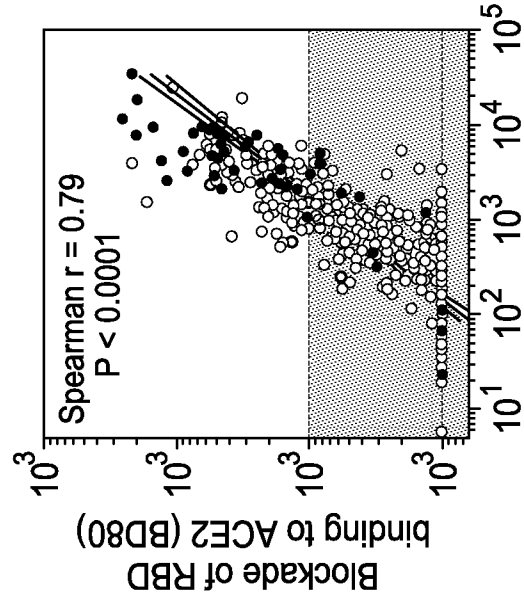


FIG. 28H

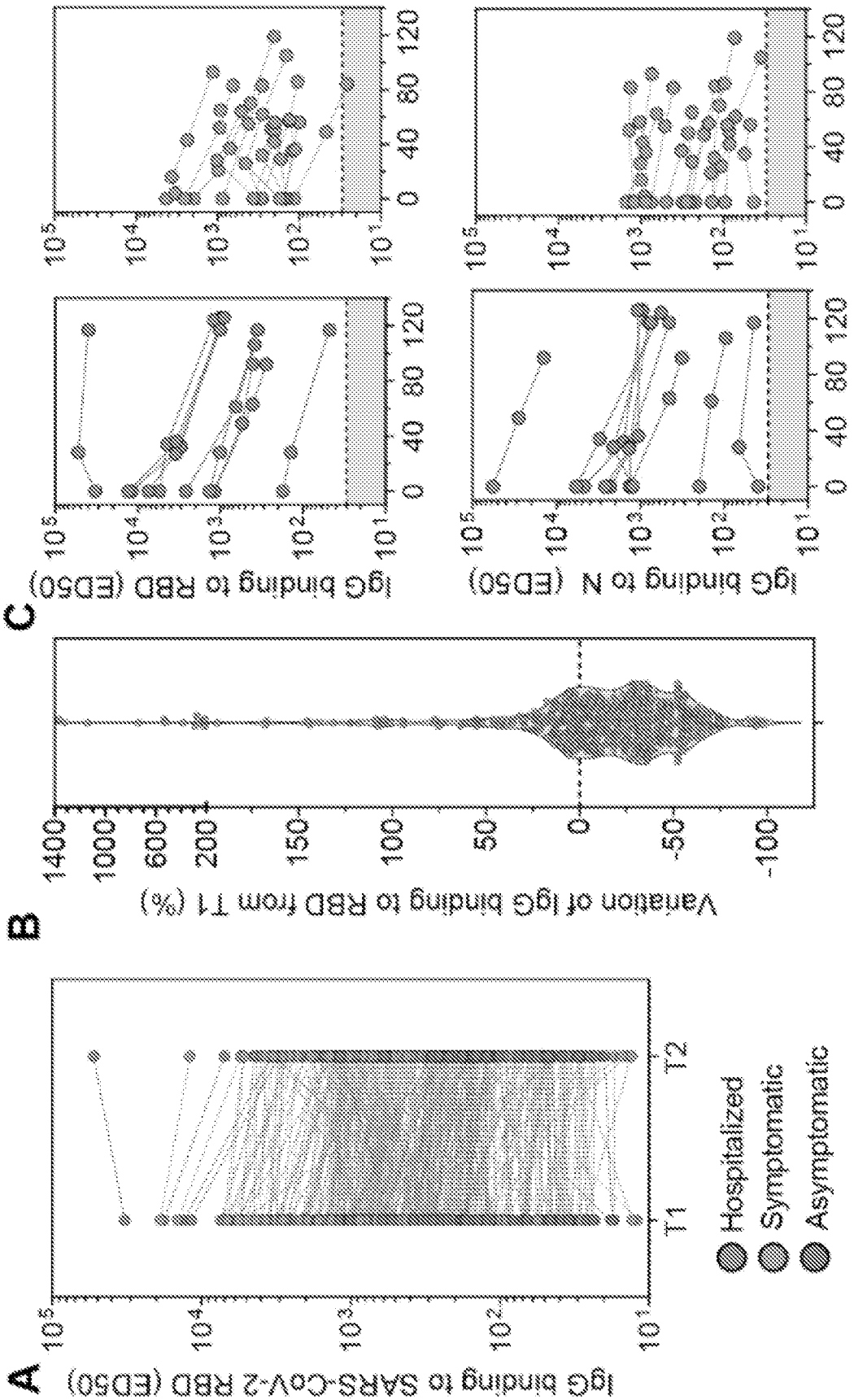
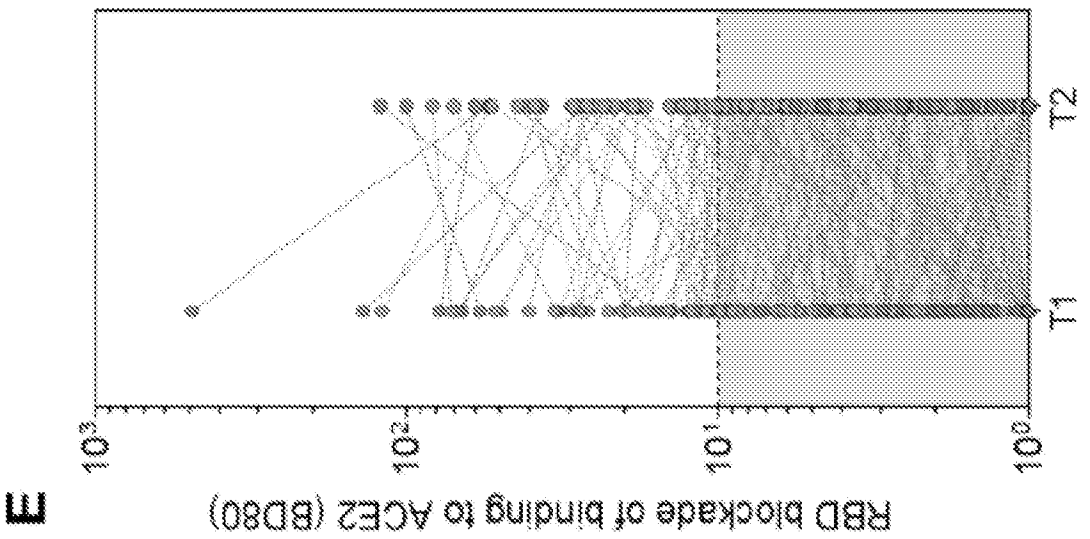

A
IgG binding to SARS-CoV-2 RBD (ED50)
T1
T2
Hospitalized
Symptomatic
Asymptomatic
B
Variation of IgG binding to RBD from T1 (%)
C
IgG binding to RBD (ED50)
IgG binding to N (ED50)

FIG. 29


E
RBD blockade of binding to ACE2 (BD80)
10^3
10^2
10^1
10^0
T1
T2

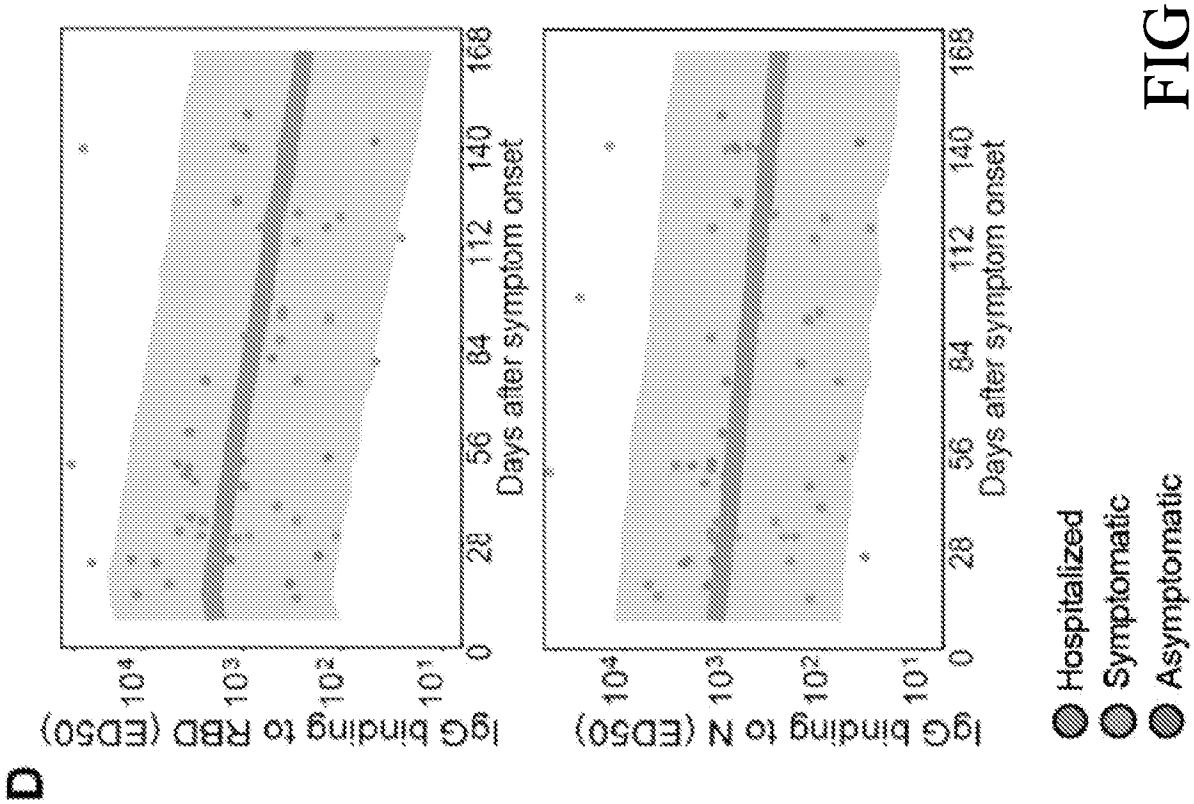

D
IgG binding to RBD (ED50)
IgG binding to N (ED50)
10^4
10^3
10^2
10^1
0
28
56
84
112
140
168
Days after symptom onset
Hospitalized
Symptomatic
Asymptomatic

FIG. 29

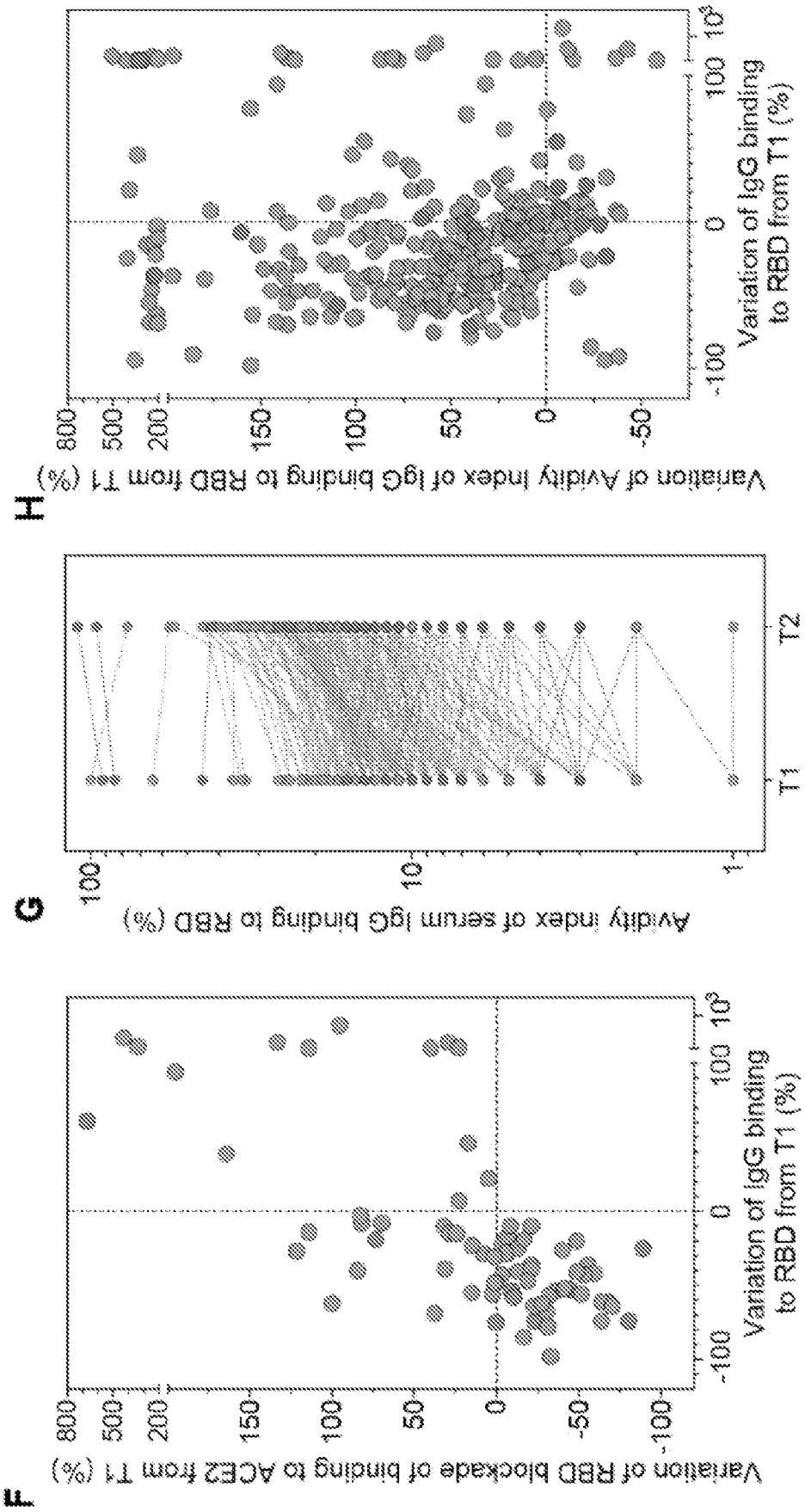

F
Variation of RBD blockade of binding to ACE2 from T1 (%)
800
500
200
150
100
50
0
-50
-100
-100
0
100
10³
Variation of IgG binding to RBD from T1 (%)
G
Avidity index of serum IgG binding to RBD (%)
100
10
1
T1
T2
H
Variation of Avidity Index of IgG binding to RBD from T1 (%)
800
500
200
150
100
50
0
-50
-100
0
100
10³
Variation of IgG binding to RBD from T1 (%)

FIG. 29

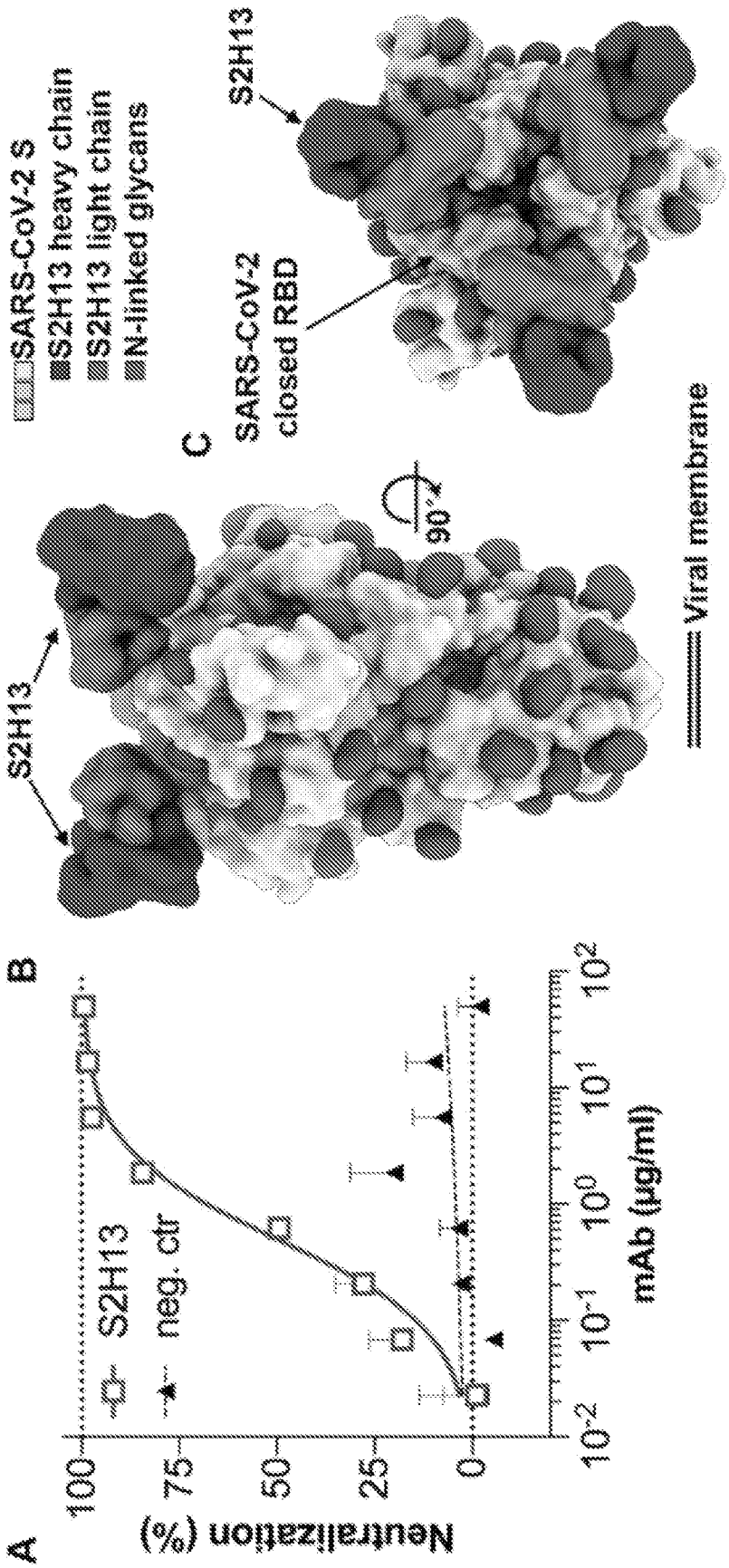

A
Neutralization (%)
100
75
50
25
0
S2H13
neg. ctr
10^{-2}
10^{-1}
10^{0}
10^{1}
10^{2}
mAb (µg/ml)
B
S2H13
90°
Viral membrane
C
SARS-CoV-2 S
S2H13 heavy chain
S2H13 light chain
N-linked glycans
SARS-CoV-2
closed RBD
S2H13

FIG. 30

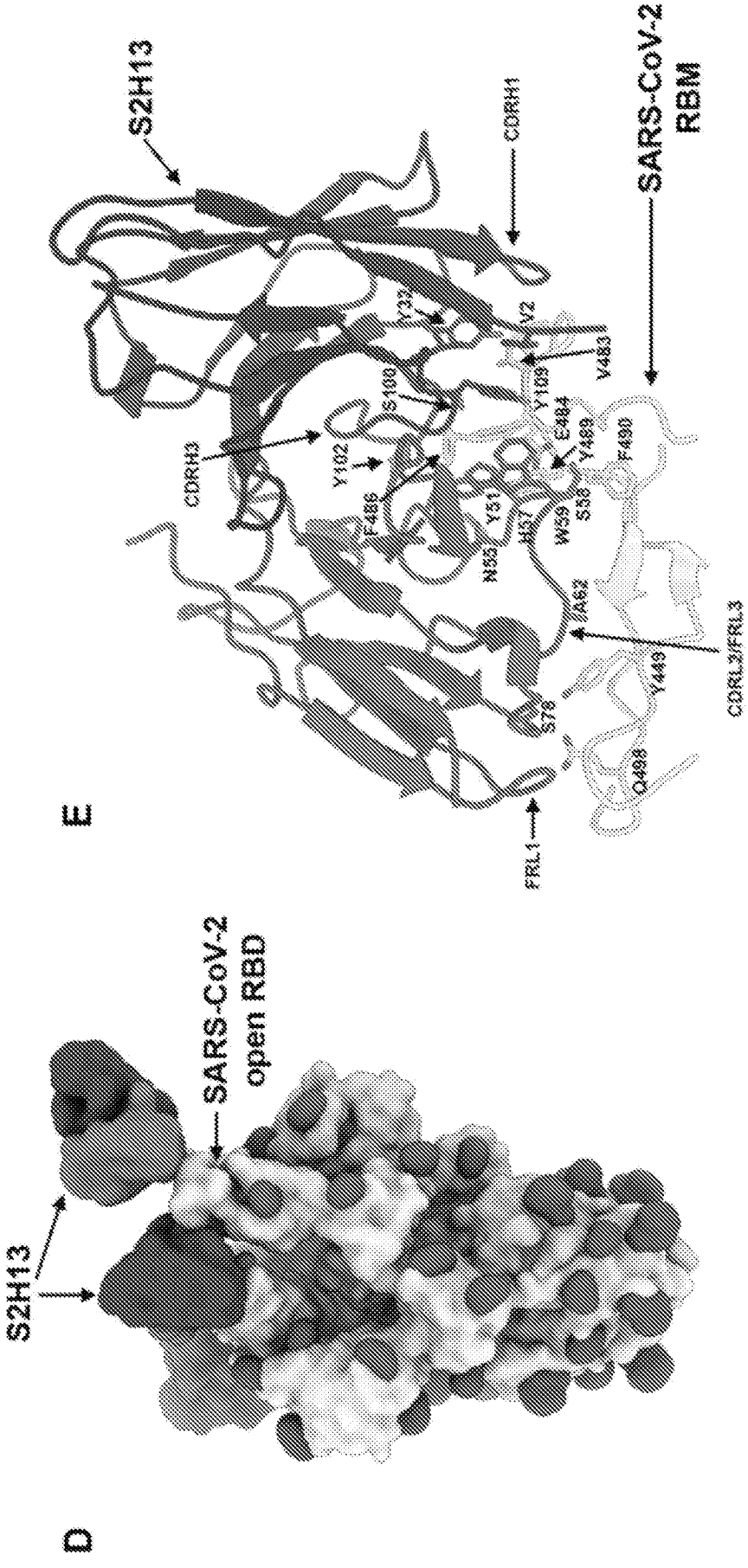

D
S2H13
SARS-CoV-2
open RBD
E
S2H13
CDRH1
SARS-CoV-2
RBM
CDRH3
FRL1
CDRL3/FRL3
Y33
V2
Y109
V483
S100
Y102
E484
Y489
F490
F486
Y51
N53
W59
S56
A62
S76
Y449
Q498

FIG. 30

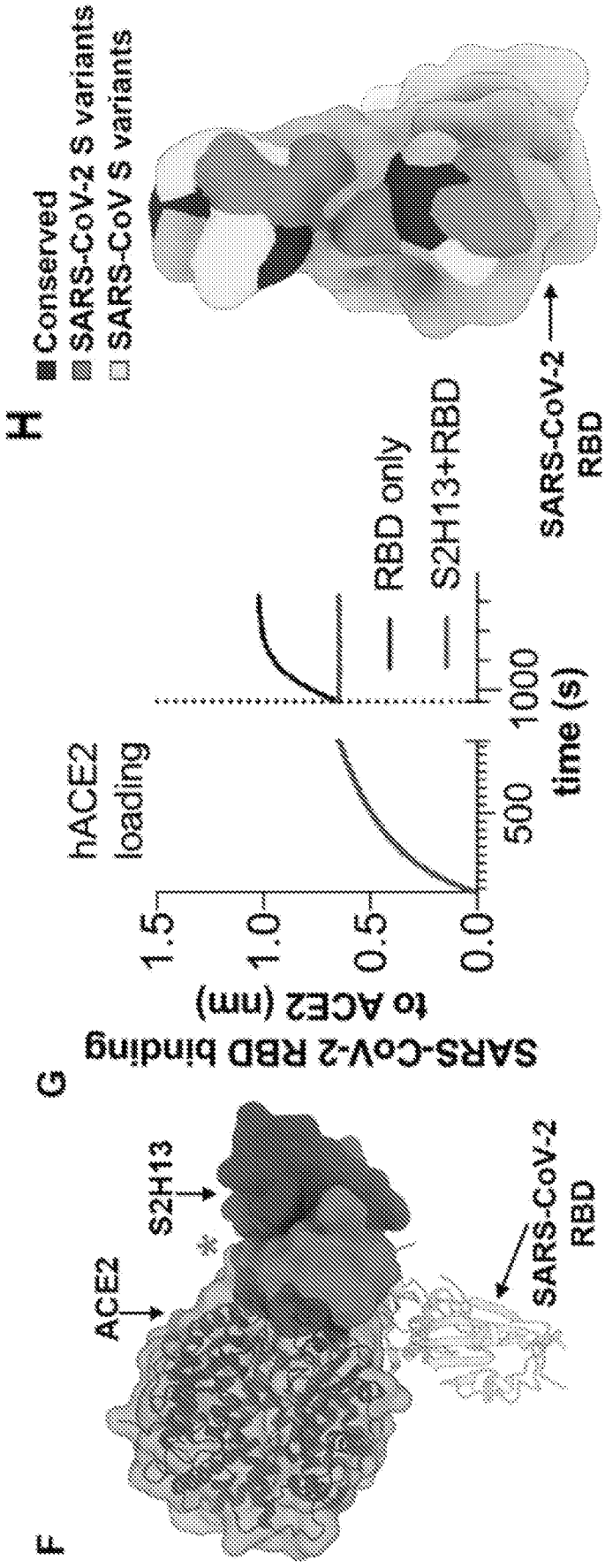

H
Conserved
SARS-CoV-2 S variants
SARS-CoV S variants
SARS-CoV-2 RBD
RBD only
S2H13+RBD
time (s)
500
1000
hACE2 loading
SARS-CoV-2 RBD binding to ACE2 (nm)
1.5
1.0
0.5
0.0
G
S2H13
ACE2
SARS-CoV-2 RBD
F

FIG. 30

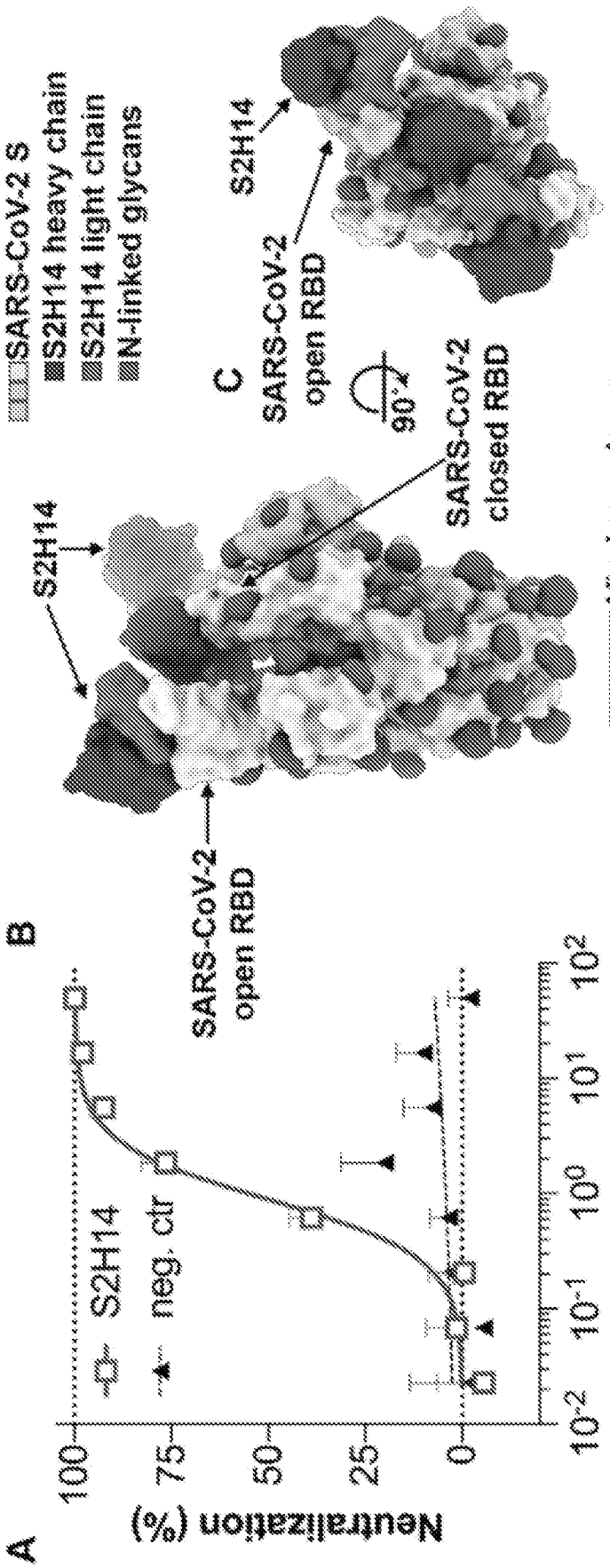

A
Neutralization (%)
100
75
50
25
0
S2H14
neg. ctr
10^{-2} 10^{-1} 10^{0} 10^{1} 10^{2}
mAb (µg/ml)
B
SARS-CoV-2 open RBD
S2H14
SARS-CoV-2 closed RBD
Viral membrane
C
SARS-CoV-2 open RBD
S2H14
90°
SARS-CoV-2 S
S2H14 heavy chain
S2H14 light chain
N-linked glycans

FIG. 31

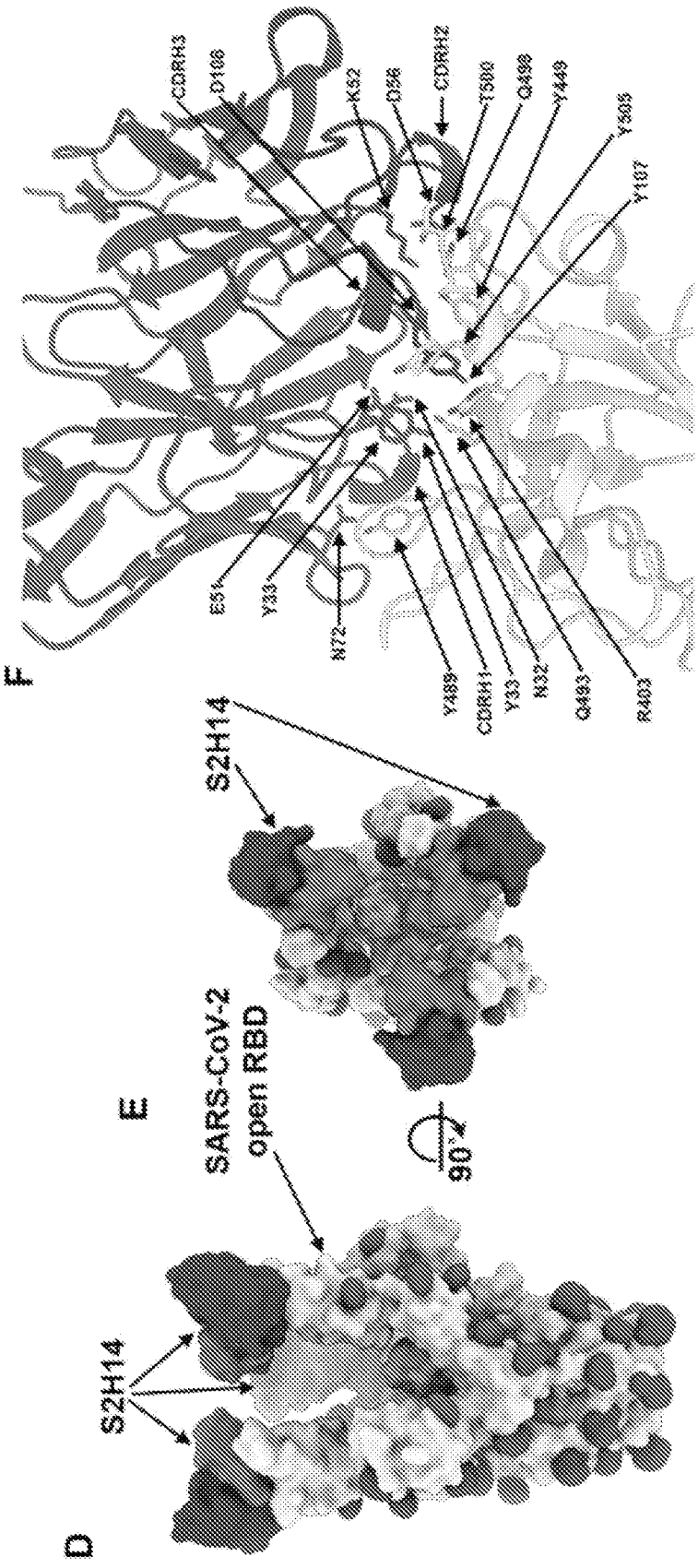

D
S2H14
SARS-CoV-2
open RBD
E
90°
S2H14
F
CDRH3
D106
K52
D58
CDRH2
T500
Q498
Y449
Y505
Y107
E51
Y33
N72
Y489
CDRH1
Y33
N32
Q493
R403

FIG. 31

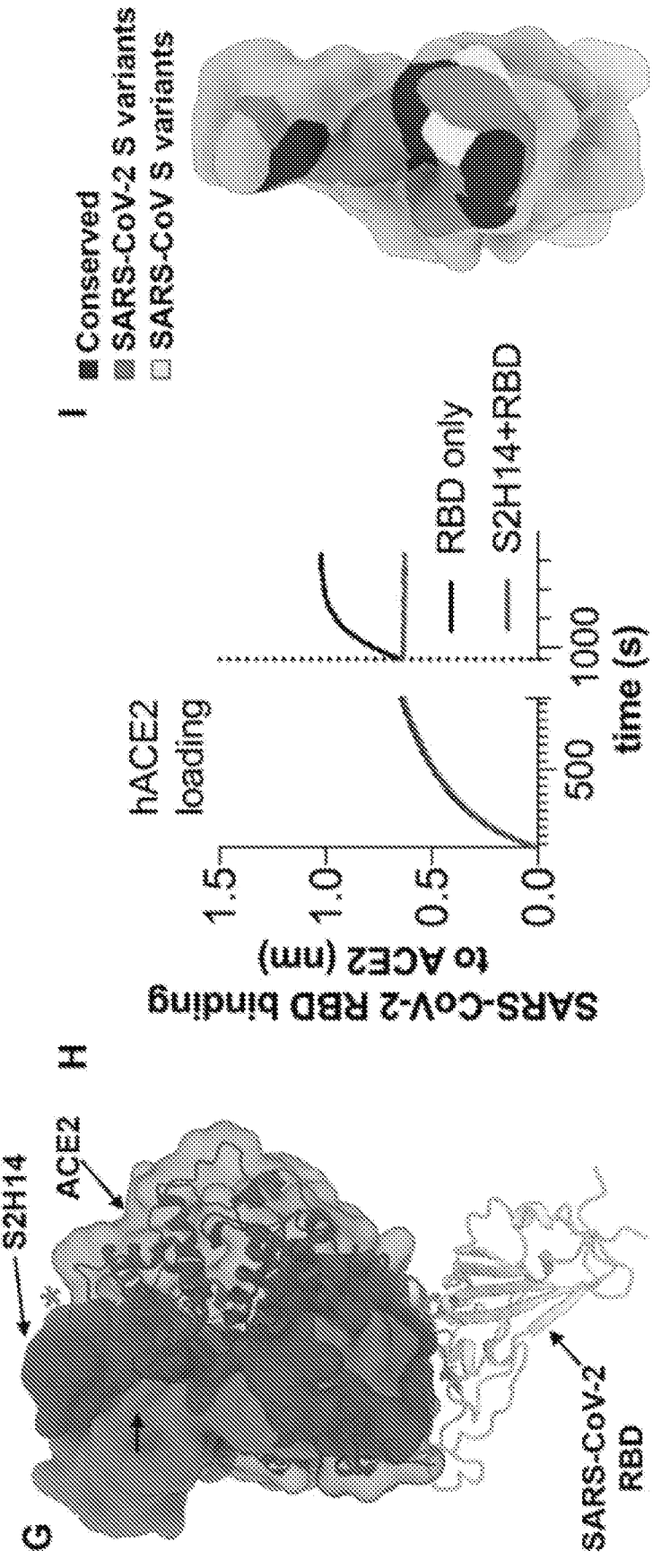

G
S2H14
ACE2
SARS-CoV-2
RBD
H
SARS-CoV-2 RBD binding
to ACE2 (nm)
1.5
1.0
0.5
0.0
hACE2
loading
500
1000
time (s)
RBD only
S2H14+RBD
I
Conserved
SARS-CoV-2 S variants
SARS-CoV S variants

FIG. 31

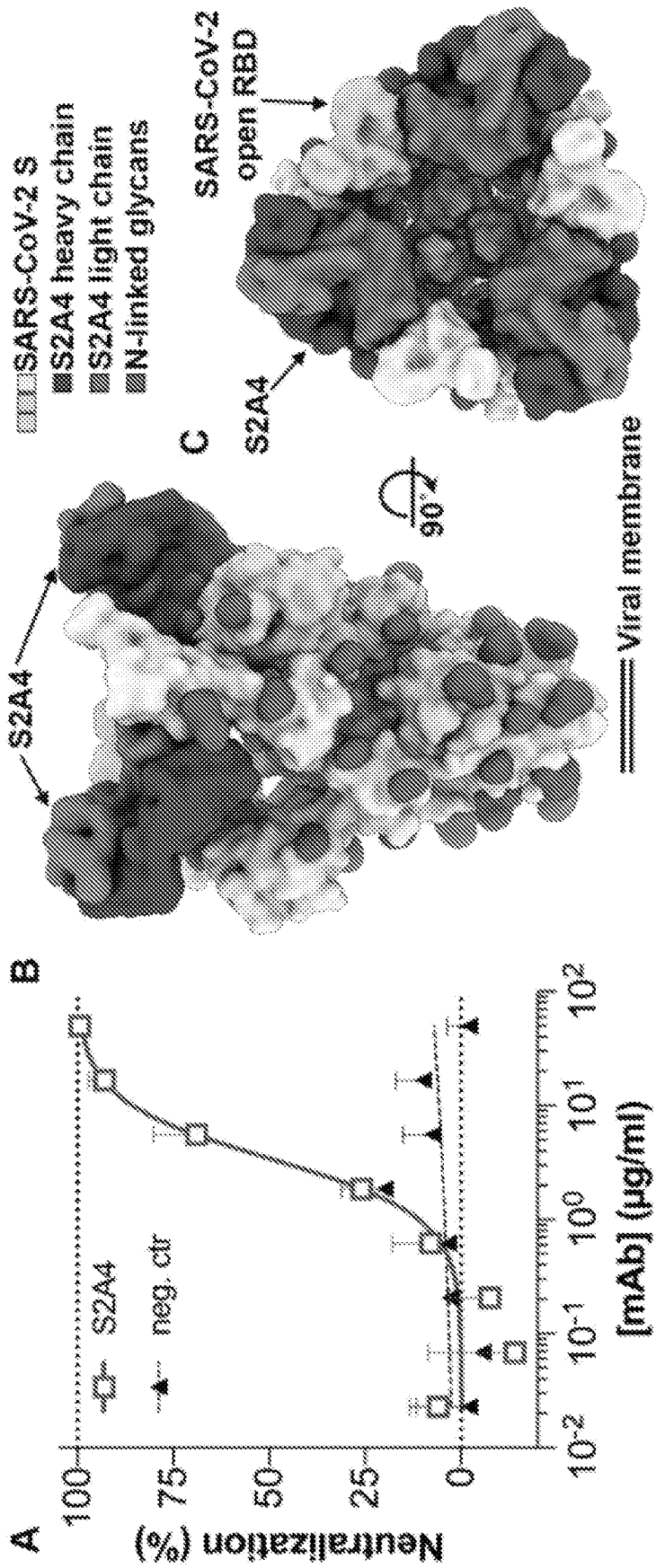

A
Neutralization (%)
100
75
50
25
0
S2A4
neg. ctr
10^{-2}
10^{-1}
10^{0}
10^{1}
10^{2}
[mAb] (µg/ml)
B
S2A4
C
SARS-CoV-2 S
S2A4 heavy chain
S2A4 light chain
N-linked glycans
SARS-CoV-2
open RBD
S2A4
90°
Viral membrane

FIG. 32

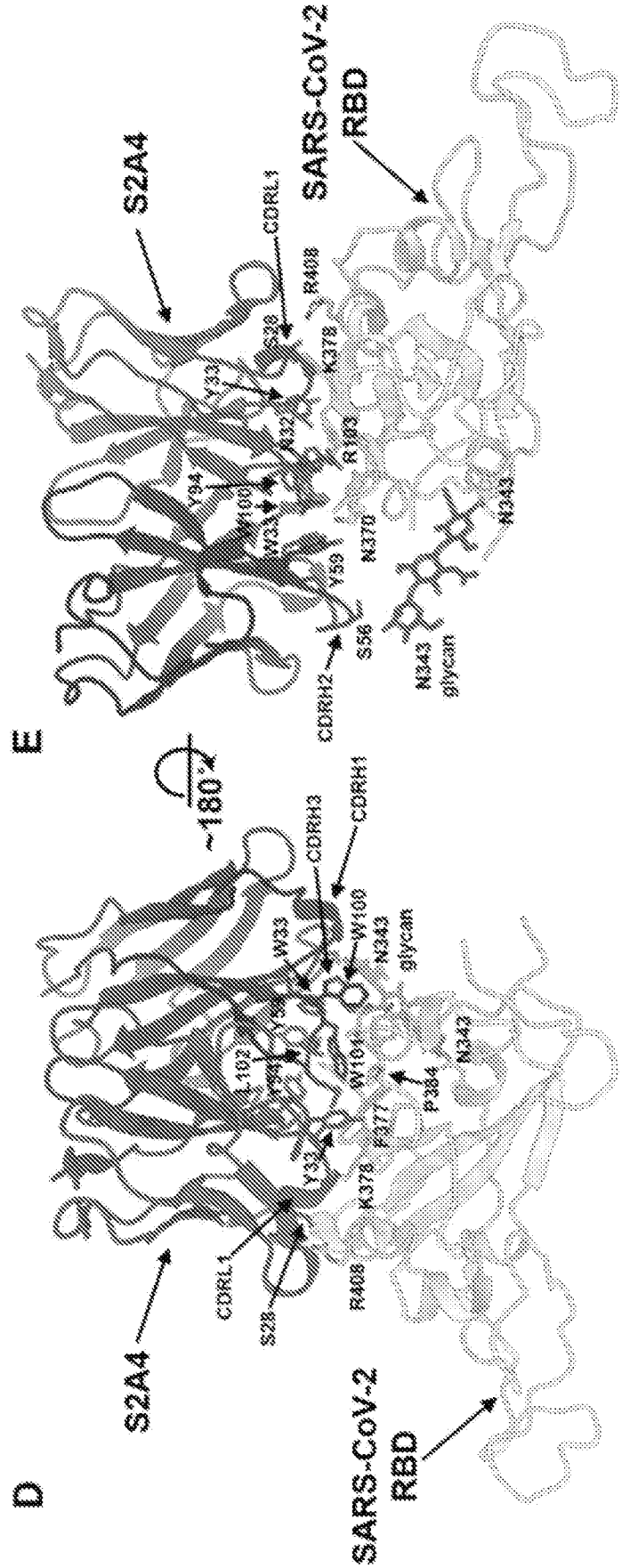

D
S2A4
SARS-CoV-2 RBD
~180°
E
S2A4
SARS-CoV-2 RBD
CDRH1
CDRH2
CDRH3
CDRL1
N343 glycan
S28
S56
W33
Y33
Y59
W100
R408
K378
N370
N343
P384
F377

FIG. 32

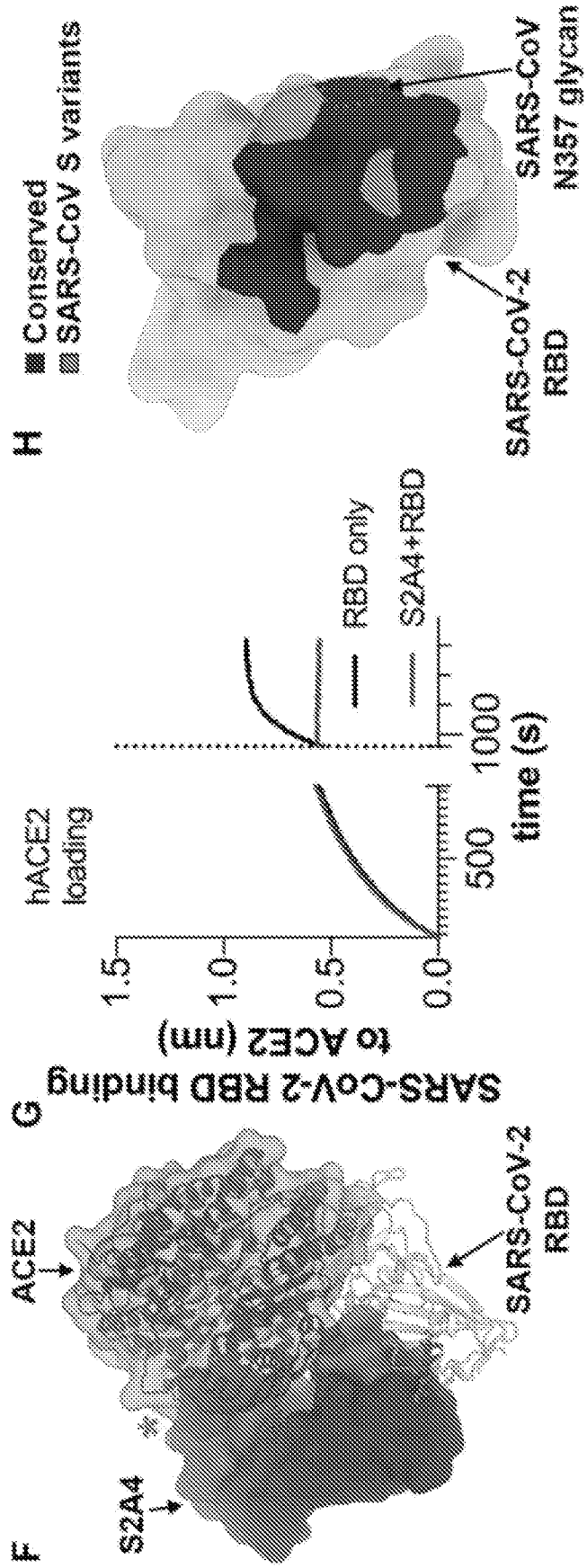

F
S2A4
ACE2
SARS-CoV-2 RBD
G
SARS-CoV-2 RBD binding to ACE2 (nm)
1.5
1.0
0.5
0.0
hACE2 loading
500
1000
time (s)
RBD only
S2A4+RBD
H
Conserved
SARS-CoV S variants
SARS-CoV-2 RBD
SARS-CoV N357 glycan

FIG. 32

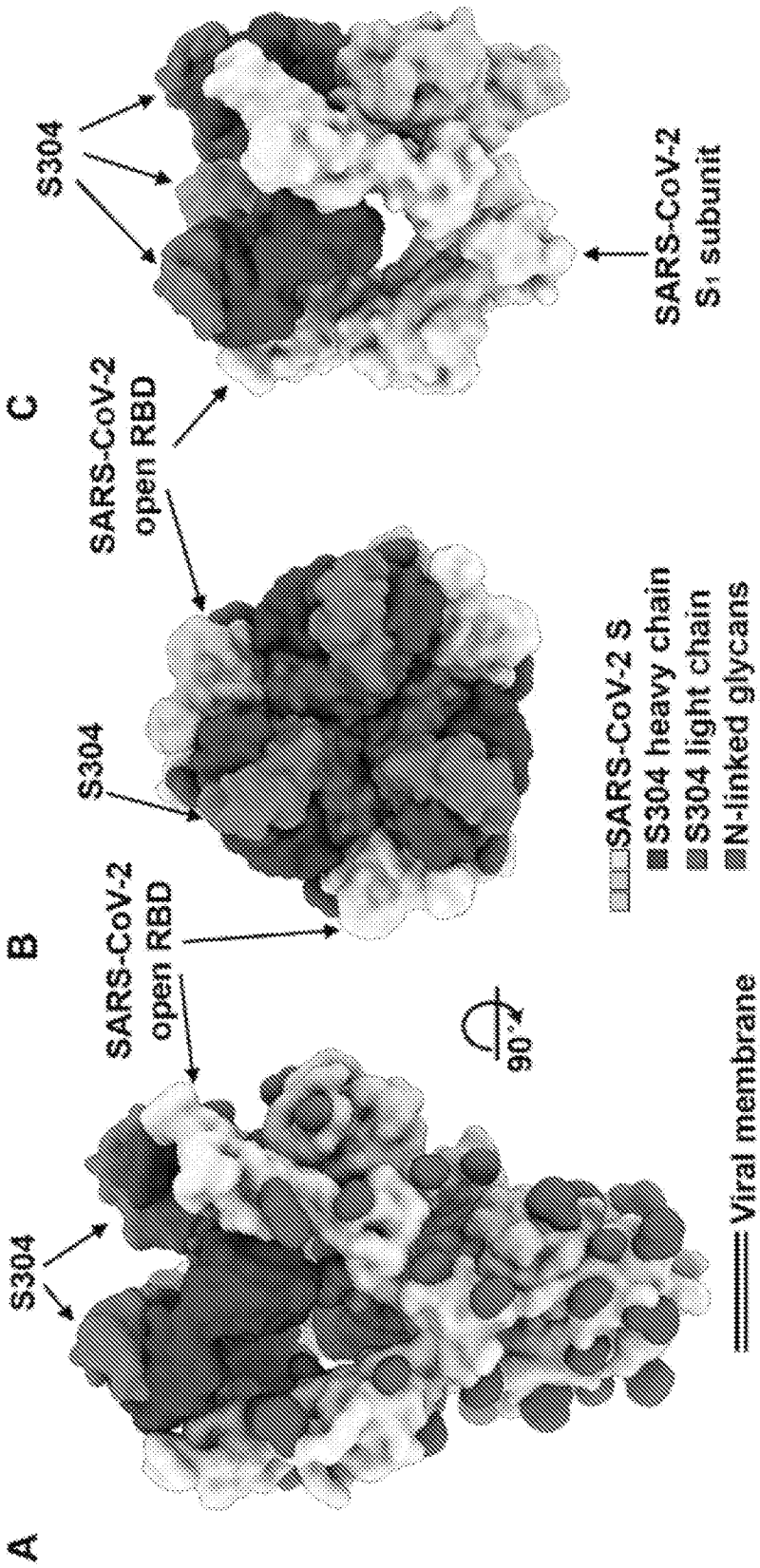

A
S304
SARS-CoV-2
open RBD
90°
B
S304
SARS-CoV-2
open RBD
C
S304
SARS-CoV-2
S1 subunit
SARS-CoV-2 S
S304 heavy chain
S304 light chain
N-linked glycans
Viral membrane

FIG. 33

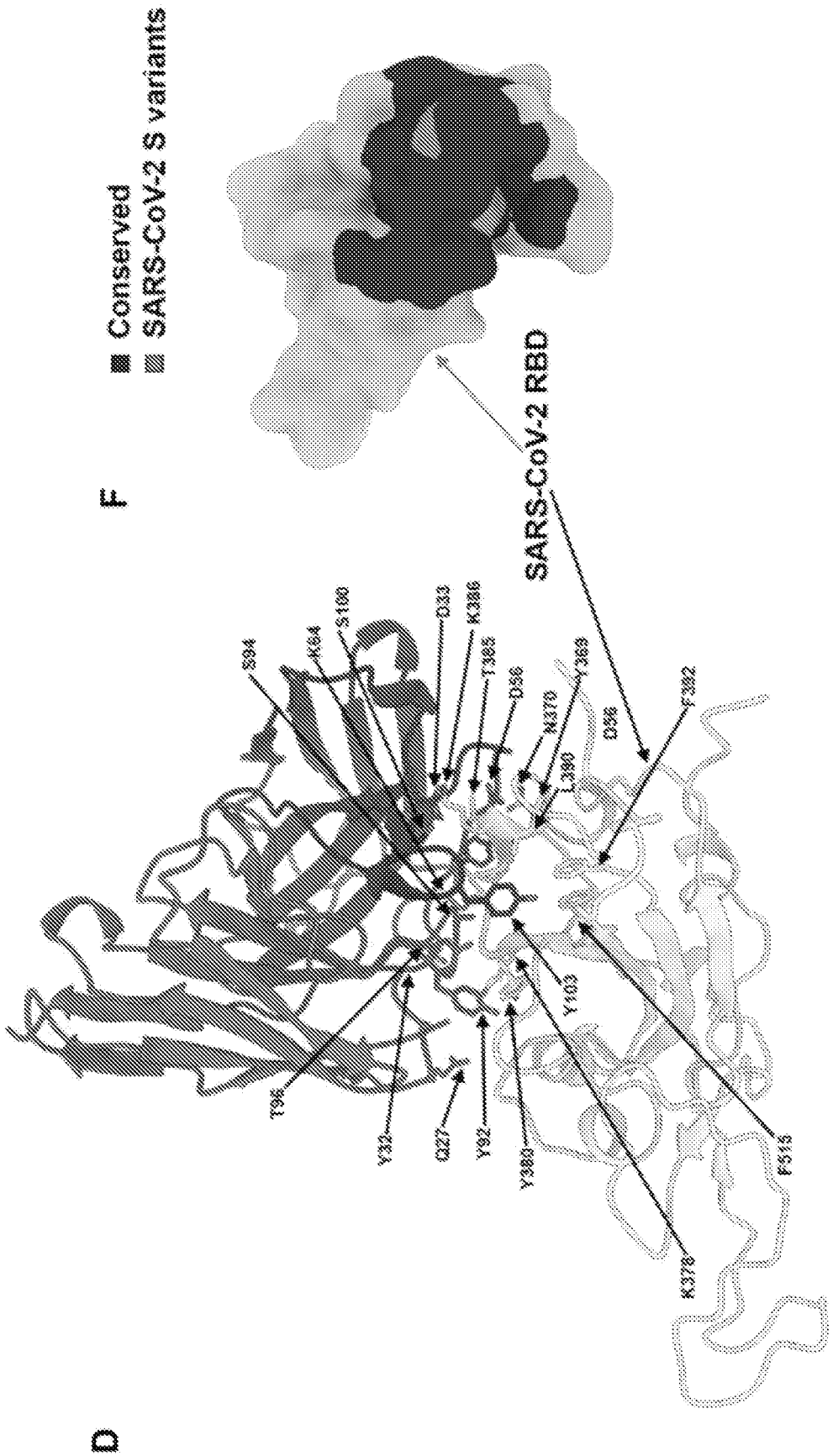

F
Conserved
SARS-CoV-2 S variants
SARS-CoV-2 RBD
D
S94
K64
S100
D33
K386
T385
D56
N370
Y369
D56
F392
L390
T96
Y32
Q27
Y92
Y380
Y103
F515
K378

FIG. 33

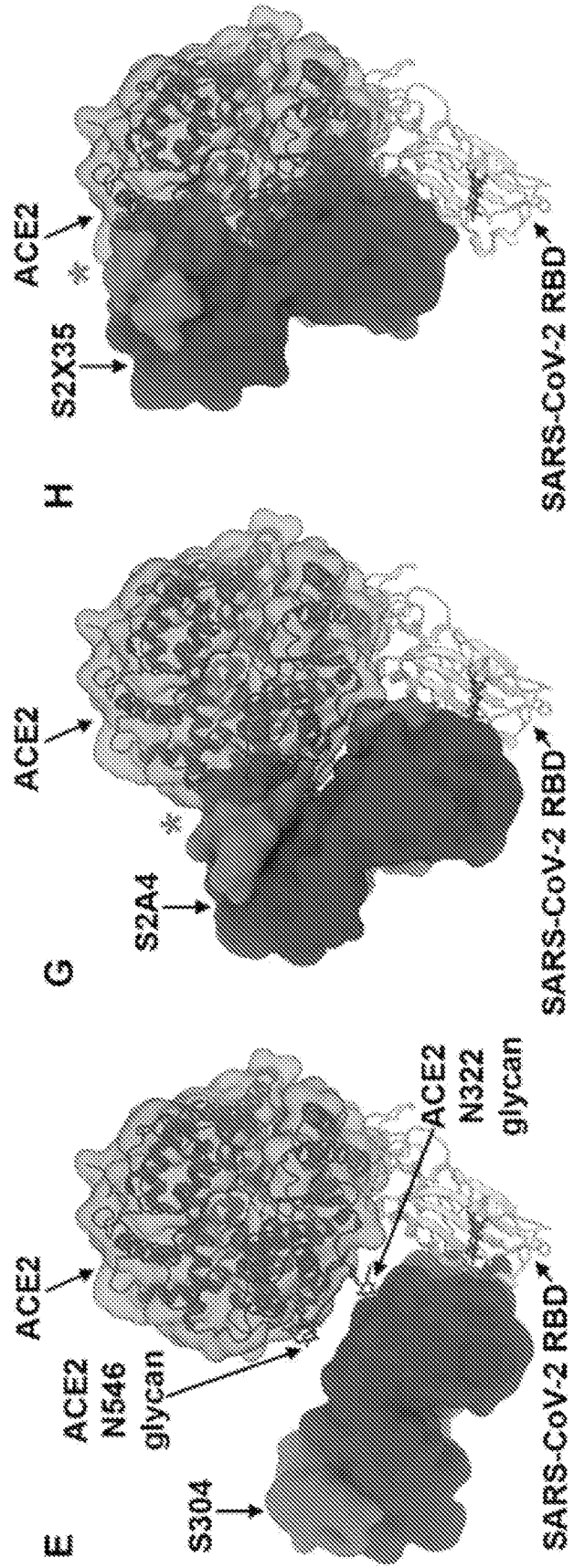

H
S2X35
ACE2
SARS-CoV-2 RBD
G
S2A4
ACE2
SARS-CoV-2 RBD
E
S304
ACE2
N546
glycan
ACE2
ACE2
N322
glycan
SARS-CoV-2 RBD

FIG. 33

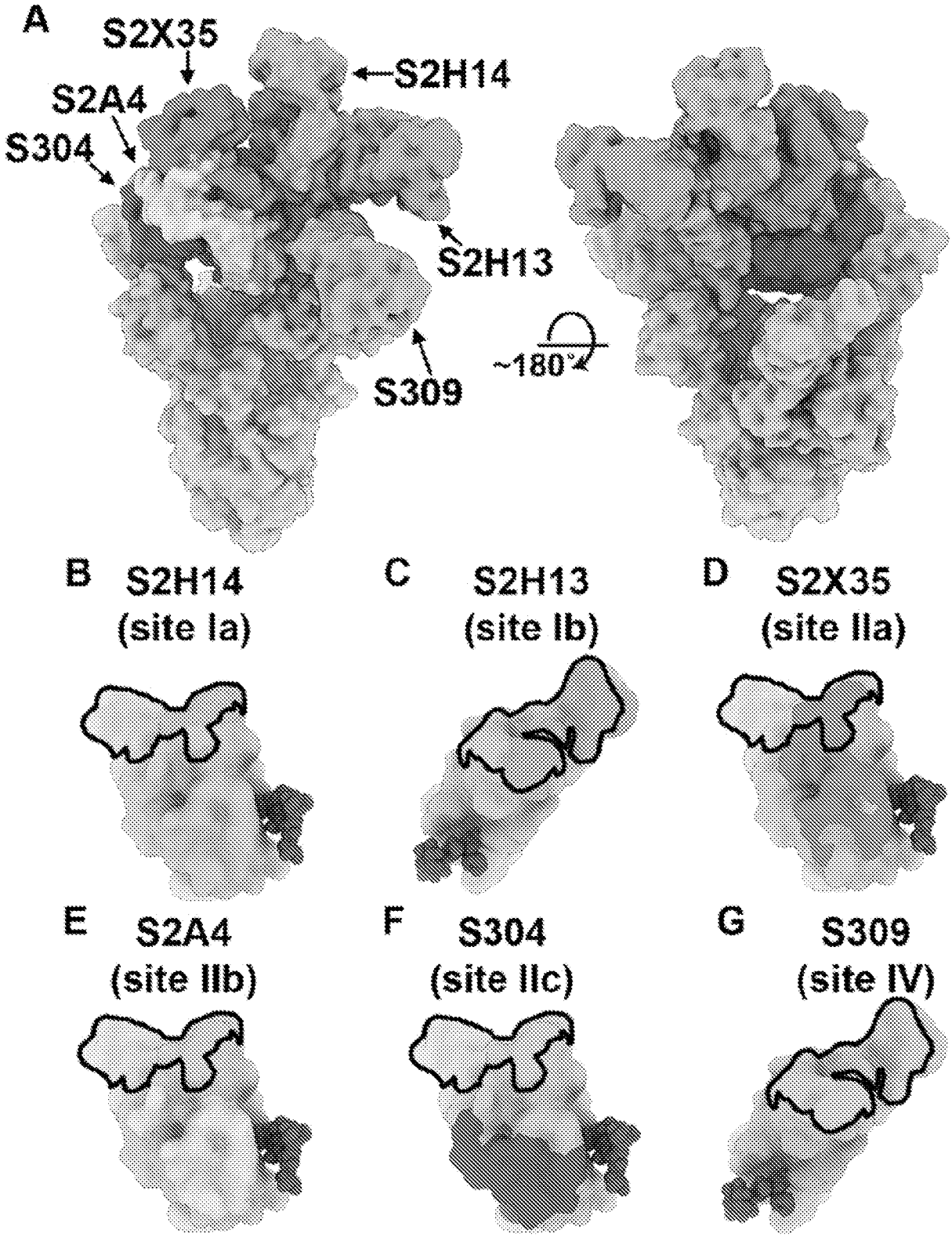

A
S2X35
S2H14
S2A4
S304
S2H13
~180°
S309
B
S2H14
(site Ia)
C
S2H13
(site Ib)
D
S2X35
(site IIa)
E
S2A4
(site IIb)
F
S304
(site IIc)
G
S309
(site IV)

FIG. 34

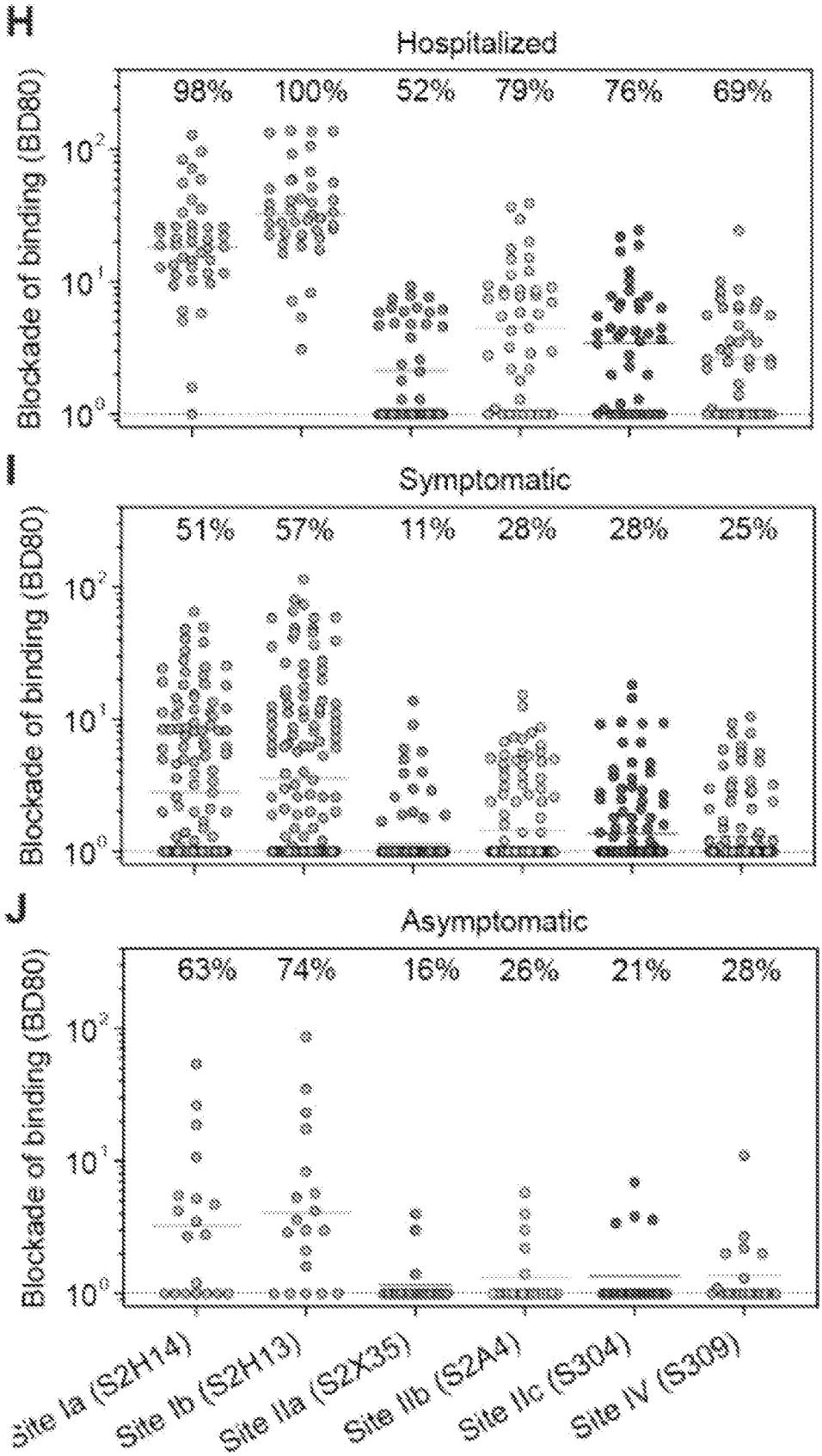

H
Hospitalized
98%
100%
52%
79%
76%
69%
Blockade of binding (BD80)
I
Symptomatic
51%
57%
11%
28%
28%
25%
Blockade of binding (BD80)
J
Asymptomatic
63%
74%
16%
26%
21%
28%
Blockade of binding (BD80)
Site Ia (S2H14)
Site Ib (S2H13)
Site IIa (S2X35)
Site IIb (S2A4)
Site IIc (S304)
Site IV (S309)

FIG. 34

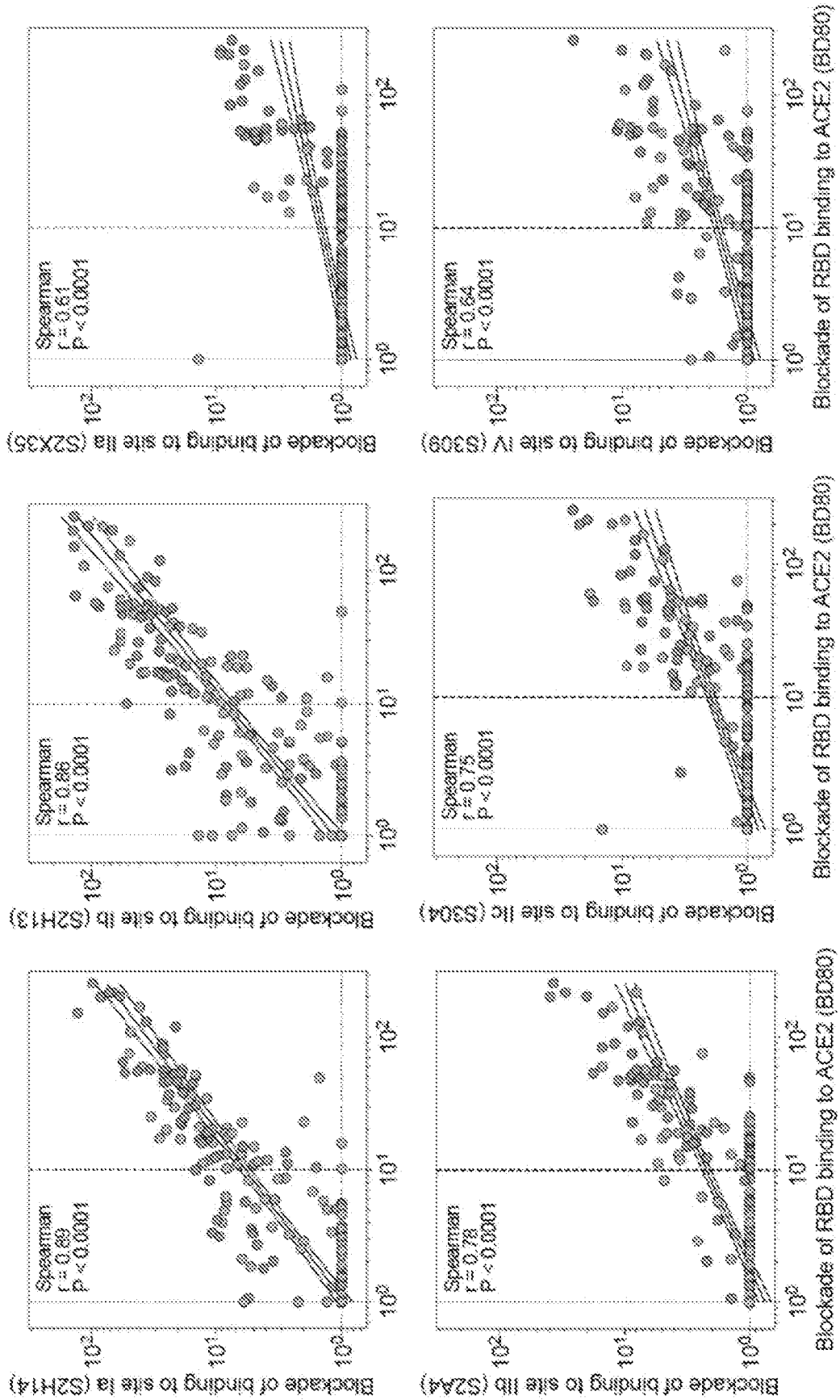

Blockade of binding to site Ia (S2H14)
Blockade of binding to site Ib (S2H13)
Blockade of binding to site IIa (S2X35)
Blockade of binding to site IIb (S2A4)
Blockade of binding to site IIc (S304)
Blockade of binding to site IV (S309)
Blockade of RBD binding to ACE2 (BD80)
Spearman
r = 0.89
P < 0.0001
Spearman
r = 0.86
P < 0.0001
Spearman
r = 0.61
P < 0.0001
Spearman
r = 0.78
P < 0.0001
Spearman
r = 0.75
P < 0.0001
Spearman
r = 0.84
P < 0.0001
10^0
10^1
10^2

FIG. 34K

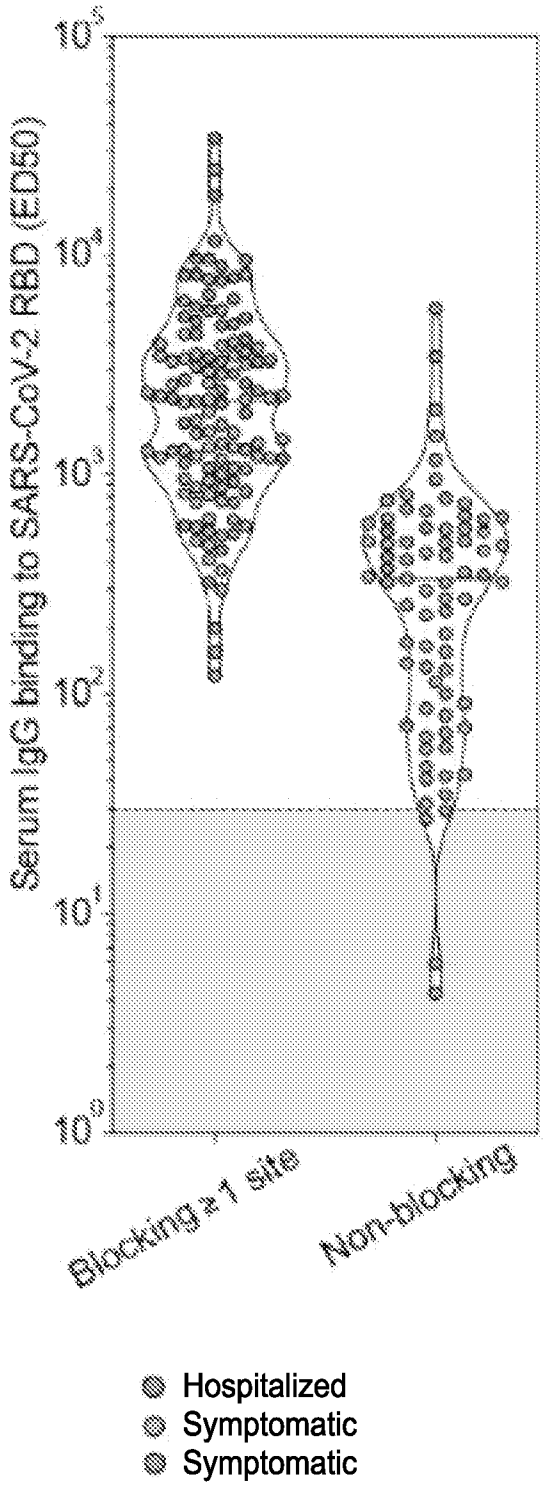

Serum IgG binding to SARS-CoV-2 RBD (ED50)
10^5
10^4
10^3
10^2
10^1
10^0
Blocking ≥ 1 site
Non-blocking
Hospitalized
Symptomatic
Symptomatic

FIG. 34L

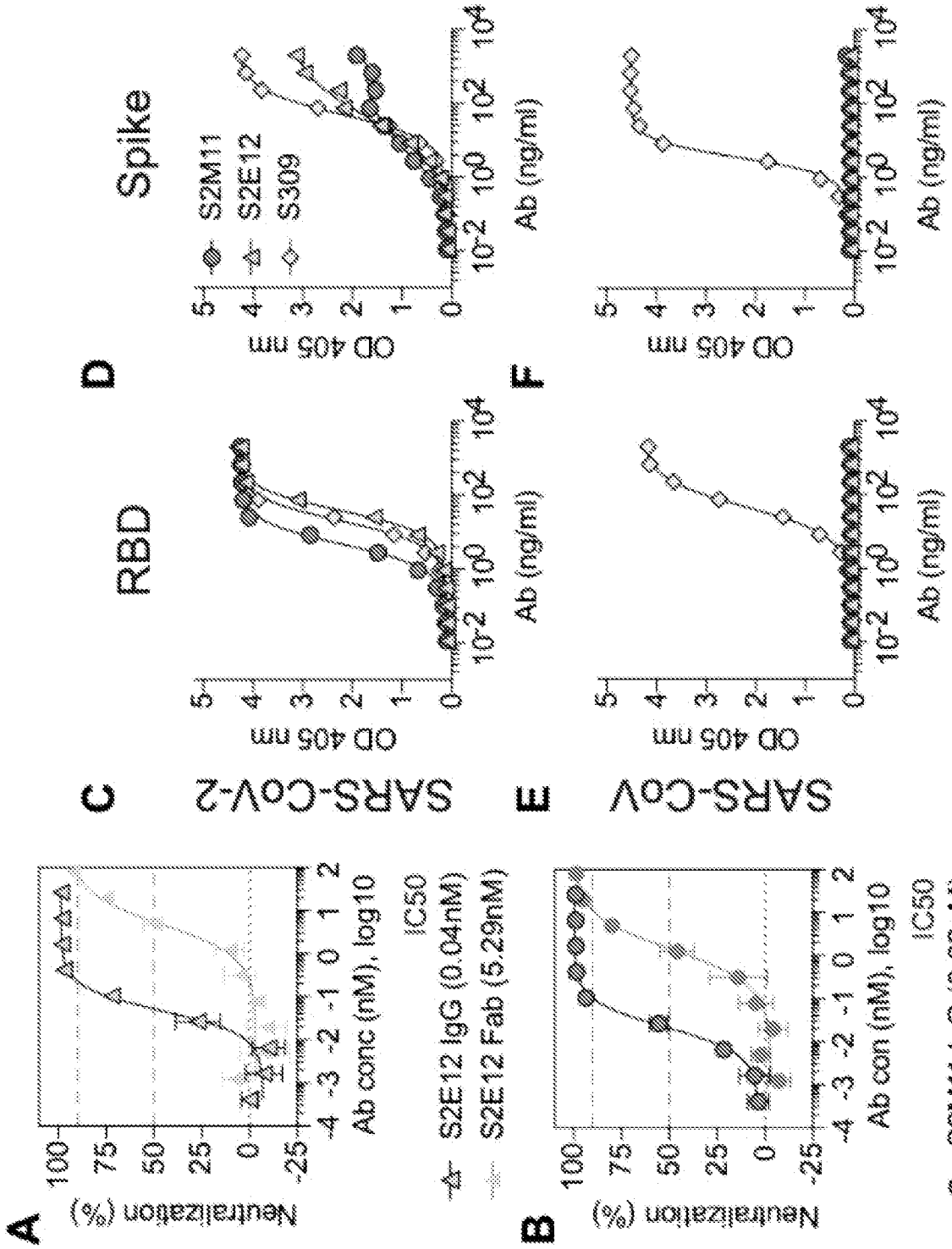

A
Neutralization (%)
Ab conc (nM), log10
IC50
S2E12 IgG (0.04nM)
S2E12 Fab (5.29nM)
B
Neutralization (%)
Ab con (nM), log10
IC50
S2M11 IgG (0.02nM)
S2M11 Fab (1.66nM)
C
SARS-CoV-2
RBD
OD 405 nm
Ab (ng/ml)
D
Spike
S2M11
S2E12
S309
OD 405 nm
Ab (ng/ml)
E
SARS-CoV
OD 405 nm
Ab (ng/ml)
F
OD 405 nm
Ab (ng/ml)

FIG. 35

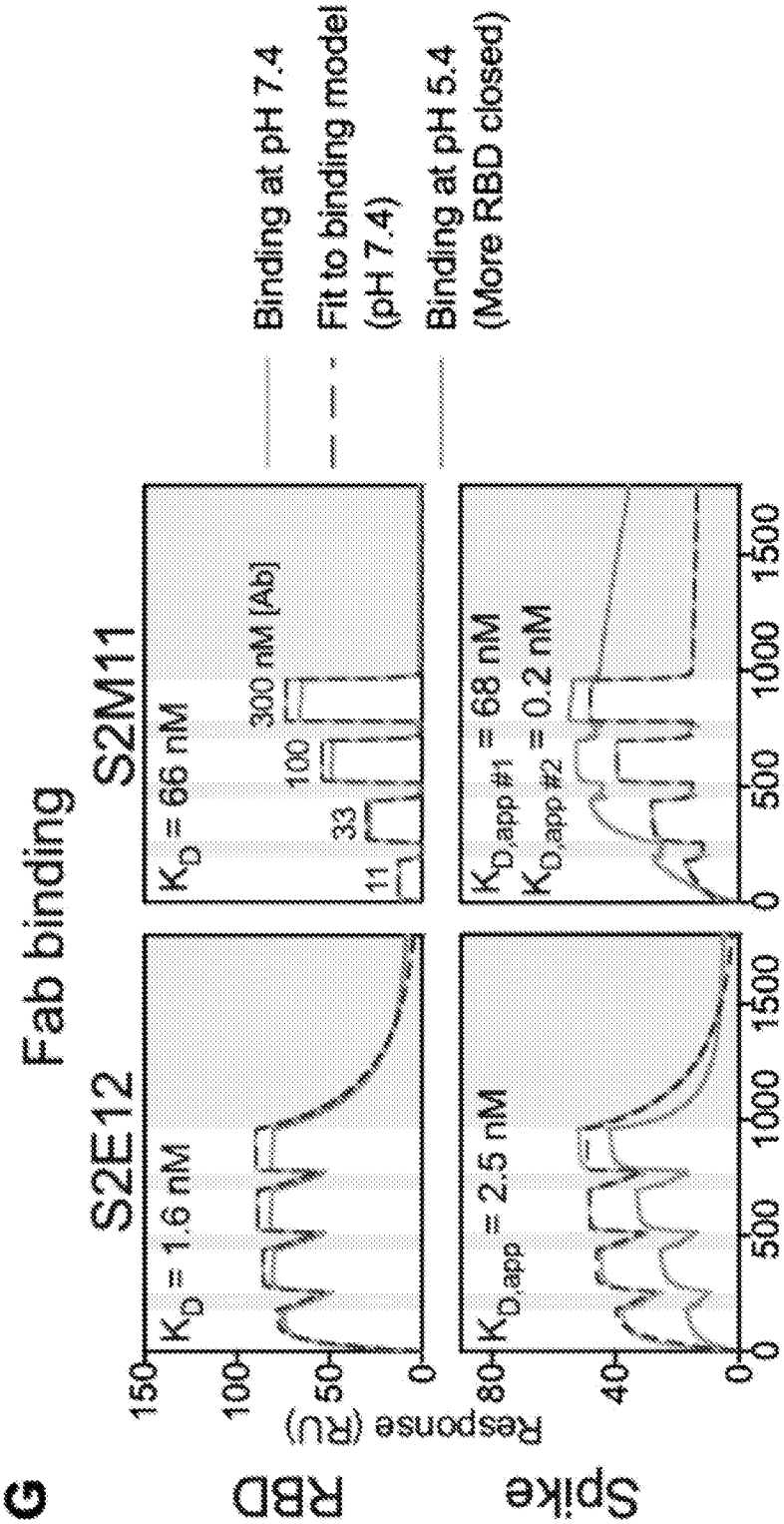

G
Fab binding
S2E12
S2M11
RBD
Spike
Response (RU)
150
100
50
0
80
40
0
K_D = 1.6 nM
K_D = 66 nM
$K_{D,app}$ = 2.5 nM
$K_{D,app\ \#1}$ = 68 nM
$K_{D,app\ \#2}$ = 0.2 nM
300 nM [Ab]
100
33
11
0
500
1000
1500
Binding at pH 7.4
Fit to binding model (pH 7.4)
Binding at pH 5.4 (More RBD closed)

FIG. 35

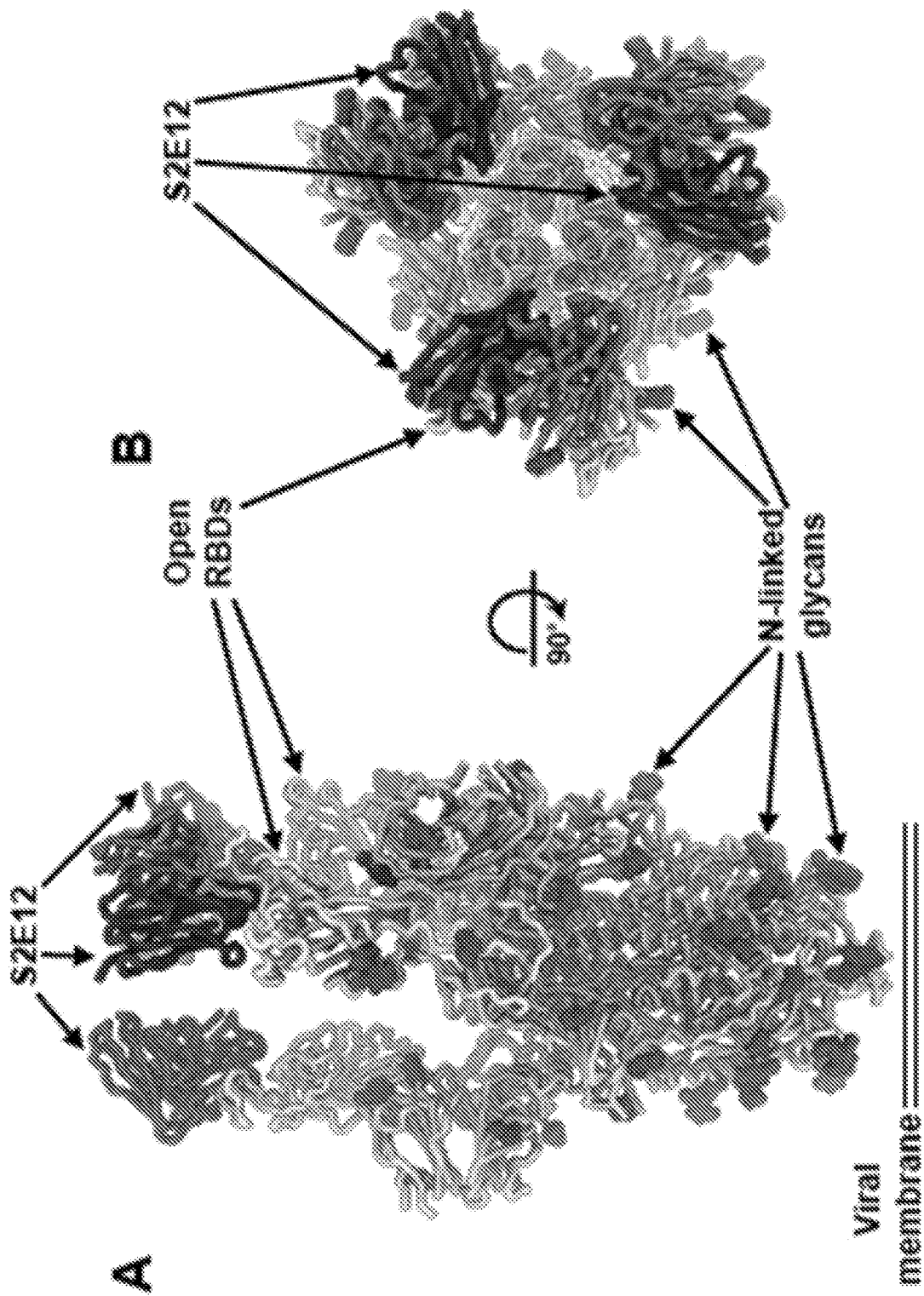


FIG. 36

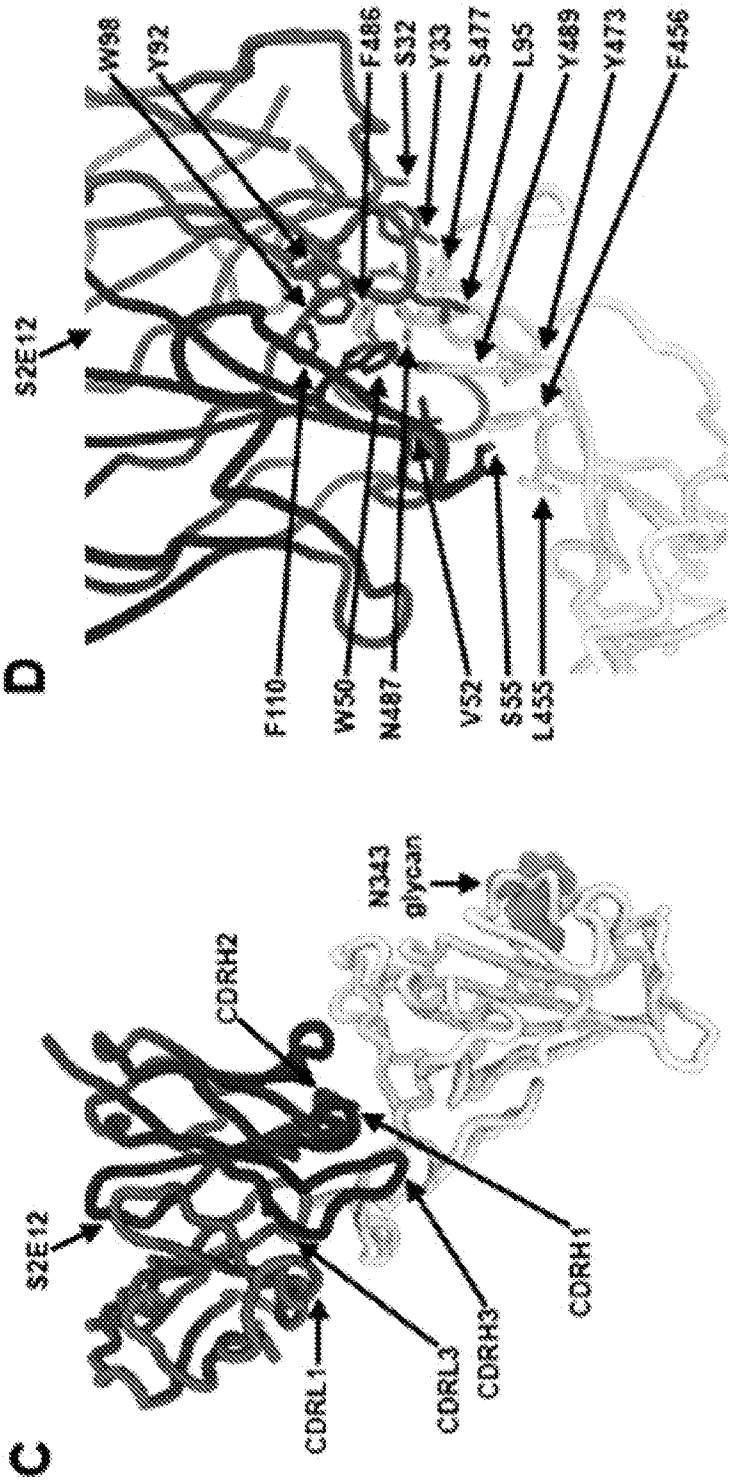

C
S2E12
CDRH2
N343
glycan
CDRL1
CDRL3
CDRH3
CDRH1
D
S2E12
W98
Y92
F486
S32
Y33
S477
L95
Y489
Y473
F456
F110
W50
N487
V52
S55
L455

FIG. 36

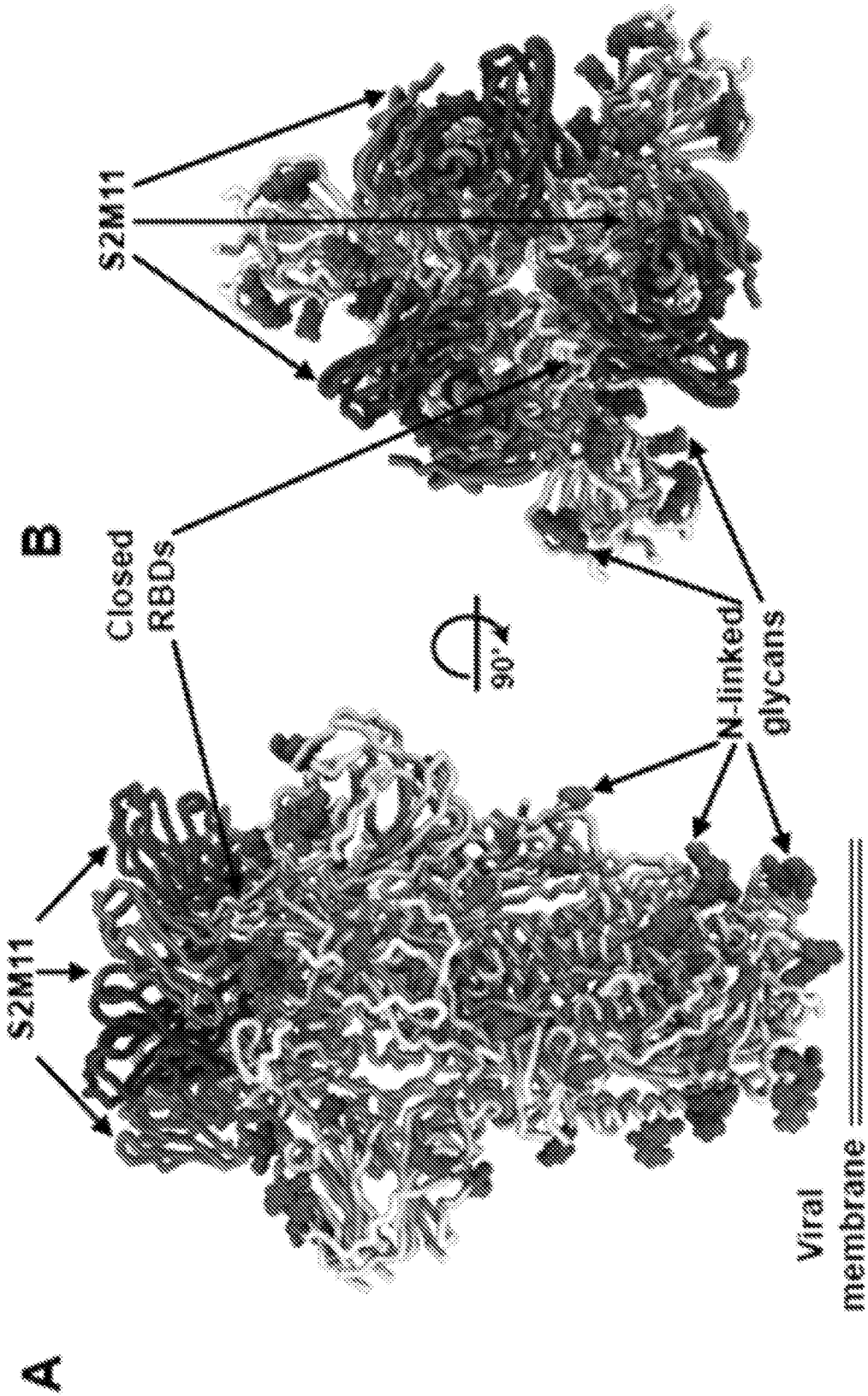

A
S2M11
Viral membrane
B
Closed RBDs
90°
S2M11
N-linked glycans

FIG. 37

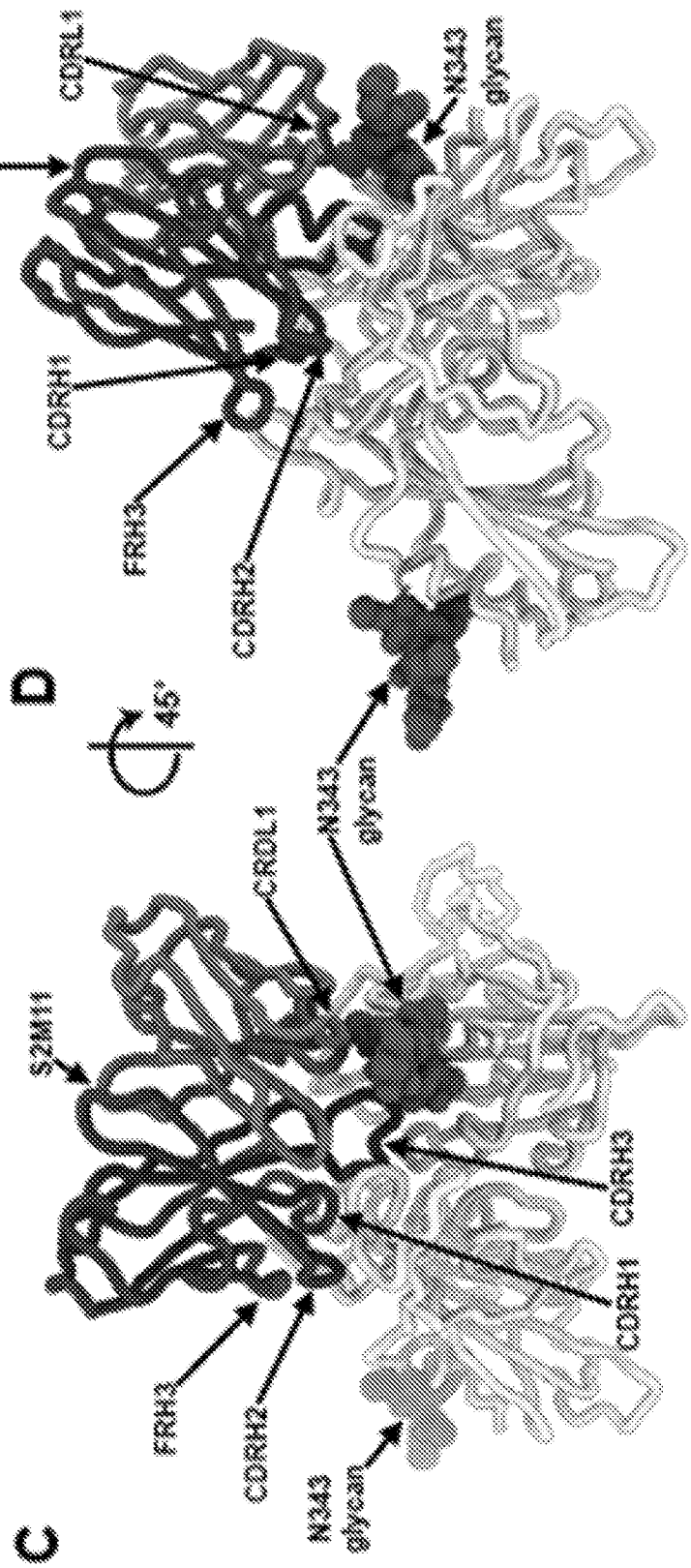

C
S2M11
CDRL1
FRH3
CDRH2
N343
glycan
45°
D
S2M11
CDRL1
N343
glycan
FRH3
CDRH2
CDRH3
CDRH1
N343
glycan

FIG. 37

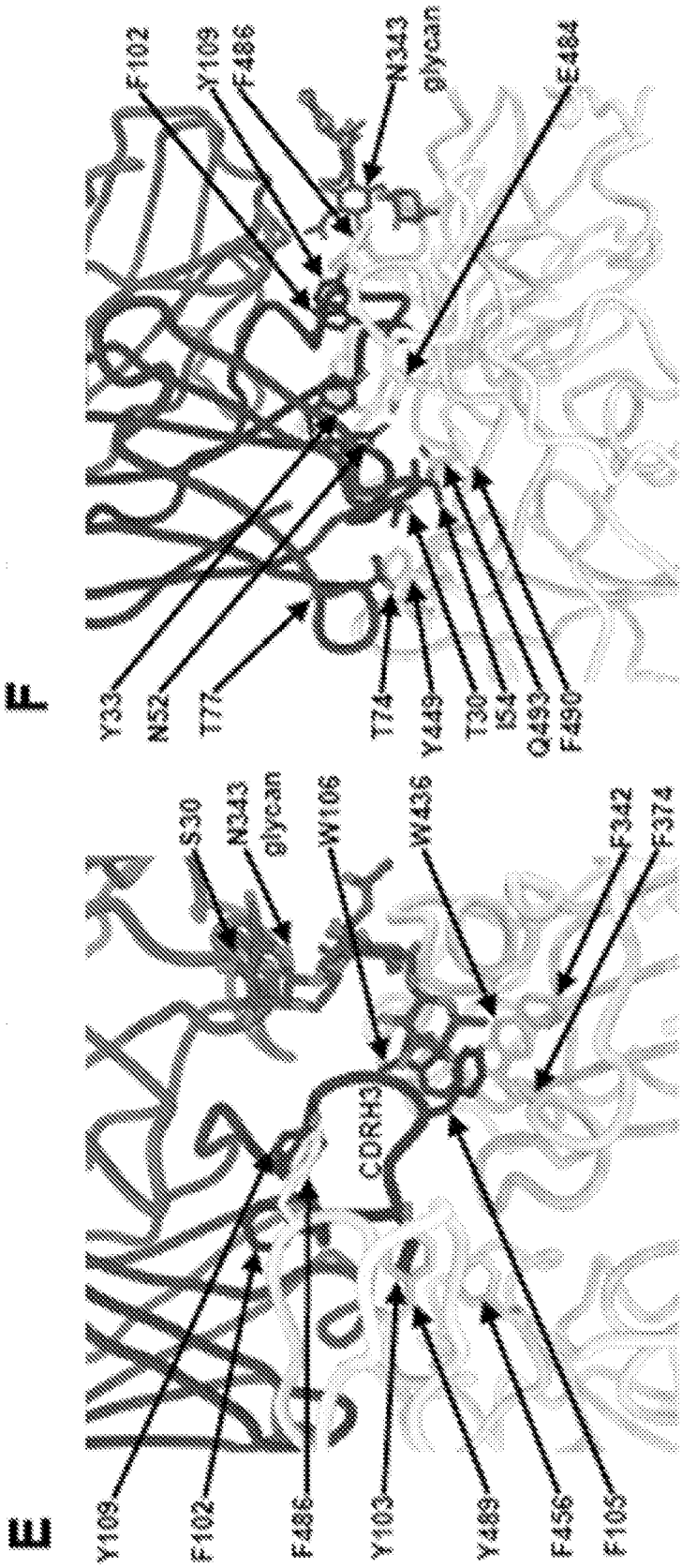

E
Y109
F102
F486
Y103
Y489
F456
F105
CDRH3
S30
N343 glycan
W106
W436
F342
F374
F.
Y33
N52
T77
T74
Y449
T30
I54
Q493
F490
F102
Y109
F486
N343 glycan
E484

FIG. 37

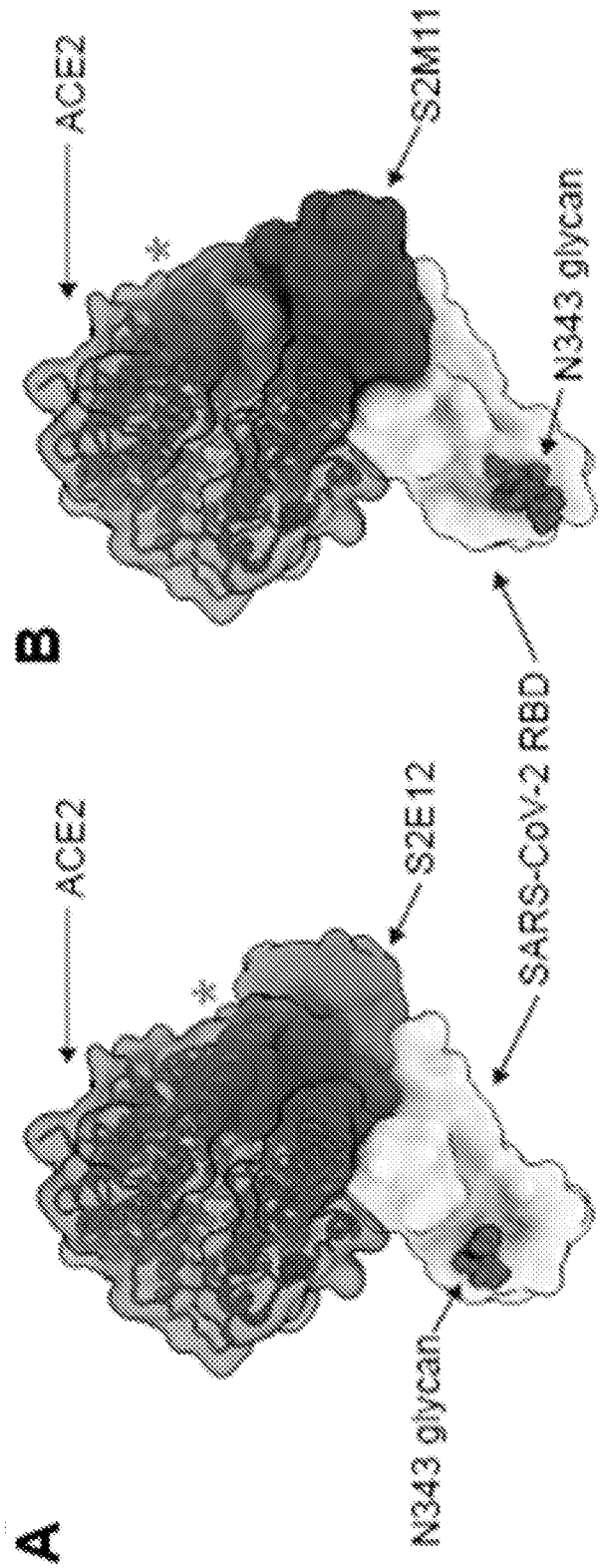

A
ACE2
S2E12
SARS-CoV-2 RBD
N343 glycan
B
ACE2
S2M11
N343 glycan

FIG. 38

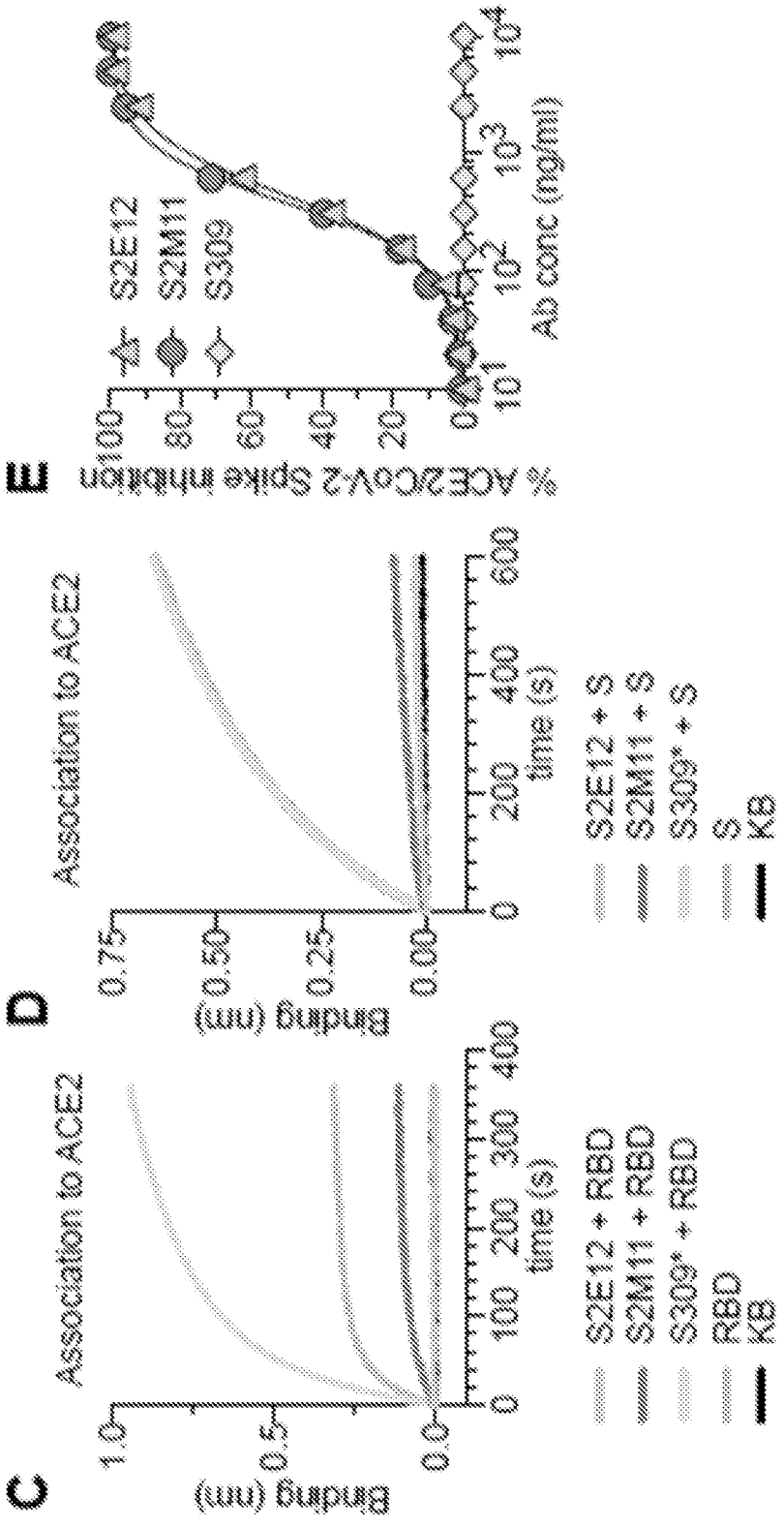

C
Association to ACE2
Binding (nm)
1.0
0.5
0.0
0
100
200
300
400
time (s)
S2E12 + RBD
S2M11 + RBD
S309* + RBD
RBD
KB
D
Association to ACE2
Binding (nm)
0.75
0.50
0.25
0.00
0
200
400
600
time (s)
S2E12 + S
S2M11 + S
S309* + S
S
KB
E
% ACE2/CoV-2 Spike inhibition
100
80
60
40
20
0
S2E12
S2M11
S309
10^1
10^2
10^3
10^4
Ab conc (mg/ml)

FIG. 38

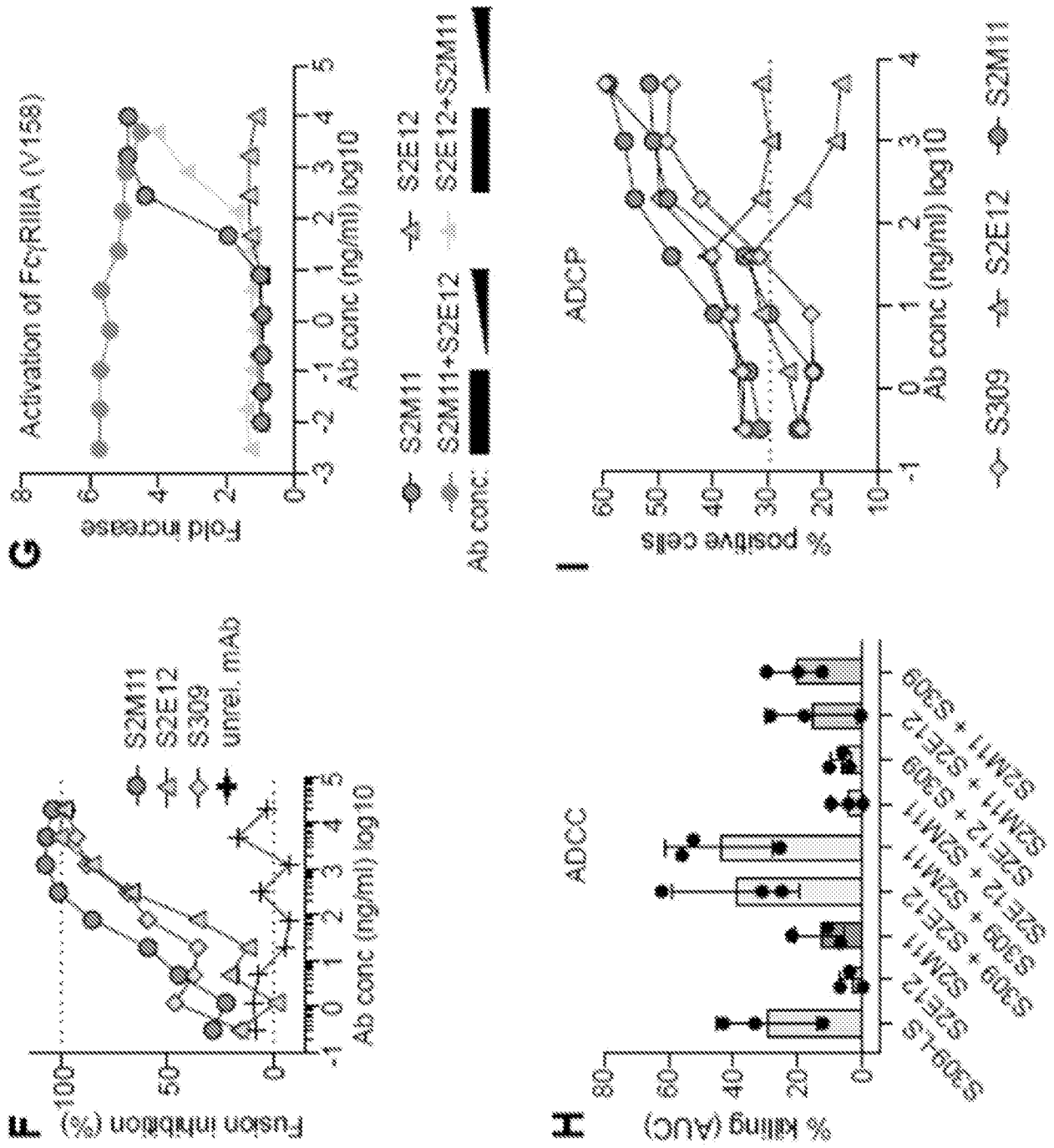

G
Activation of FcγRIIIA (V158)
Fold increase
Ab conc (ng/ml) log10
S2M11
S2E12
S2M11+S2E12
S2E12+S2M11
Ab conc:
I
ADCP
% positive cells
Ab conc (ng/ml) log10
S309
S2E12
S2M11
F
Fusion inhibition (%)
S2M11
S2E12
S309
unrel. mAb
Ab conc (ng/ml) log10
J
ADCC
% killing (AUC)
S309-LS
S2E12
S2M11
S309 + S2E12
S309 + S2M11
S2E12 + S2M11
S309 + S2E12 + S2M11

FIG. 38

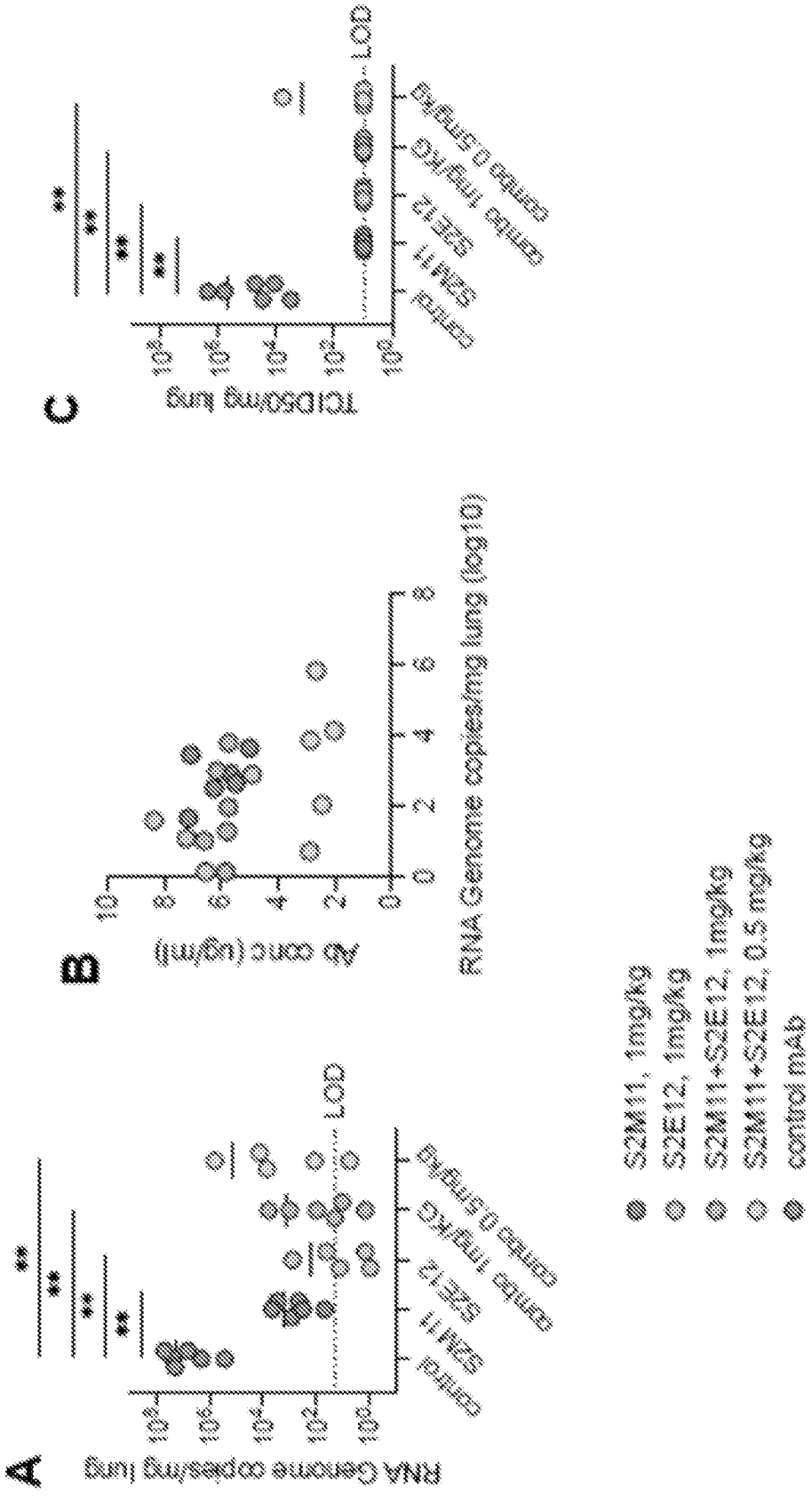

A
RNA Genome copies/mg lung
LOD
Control
S2M11
S2E12
Combo 1mg/kg
Combo 0.5mg/kg
B
Ab conc (ug/ml)
RNA Genome copies/mg lung (log10)
C
TCID50/mg lung
LOD
S2M11, 1mg/kg
S2E12, 1mg/kg
S2M11+S2E12, 1mg/kg
S2M11+S2E12, 0.5 mg/kg
control mAb

FIG. 39

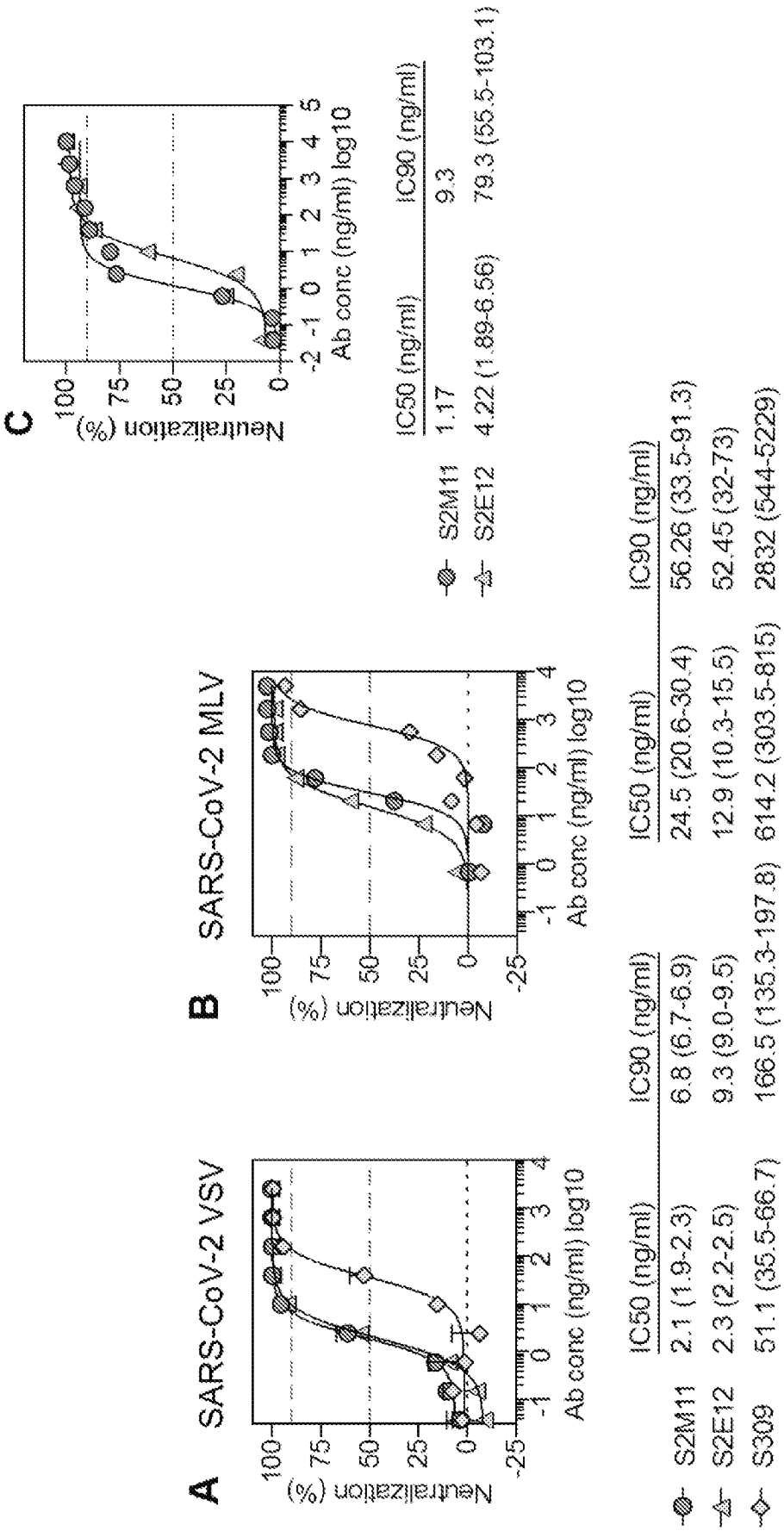

A
SARS-CoV-2 VSV
Neutralization (%)
Ab conc (ng/ml) log10
B
SARS-CoV-2 MLV
Neutralization (%)
Ab conc (ng/ml) log10
C
Neutralization (%)
Ab conc (ng/ml) log10
S2M11
S2E12
S309
IC50 (ng/ml) IC90 (ng/ml)
2.1 (1.9-2.3) 6.8 (6.7-6.9)
2.3 (2.2-2.5) 9.3 (9.0-9.5)
51.1 (35.5-66.7) 166.5 (135.3-197.8)
IC50 (ng/ml) IC90 (ng/ml)
24.5 (20.6-30.4) 56.26 (33.5-91.3)
12.9 (10.3-15.5) 52.45 (32-73)
614.2 (303.5-815) 2832 (544-5229)
IC50 (ng/ml) IC90 (ng/ml)
S2M11 1.17 9.3
S2E12 4.22 (1.89-6.56) 79.3 (55.5-103.1)

FIG. 40

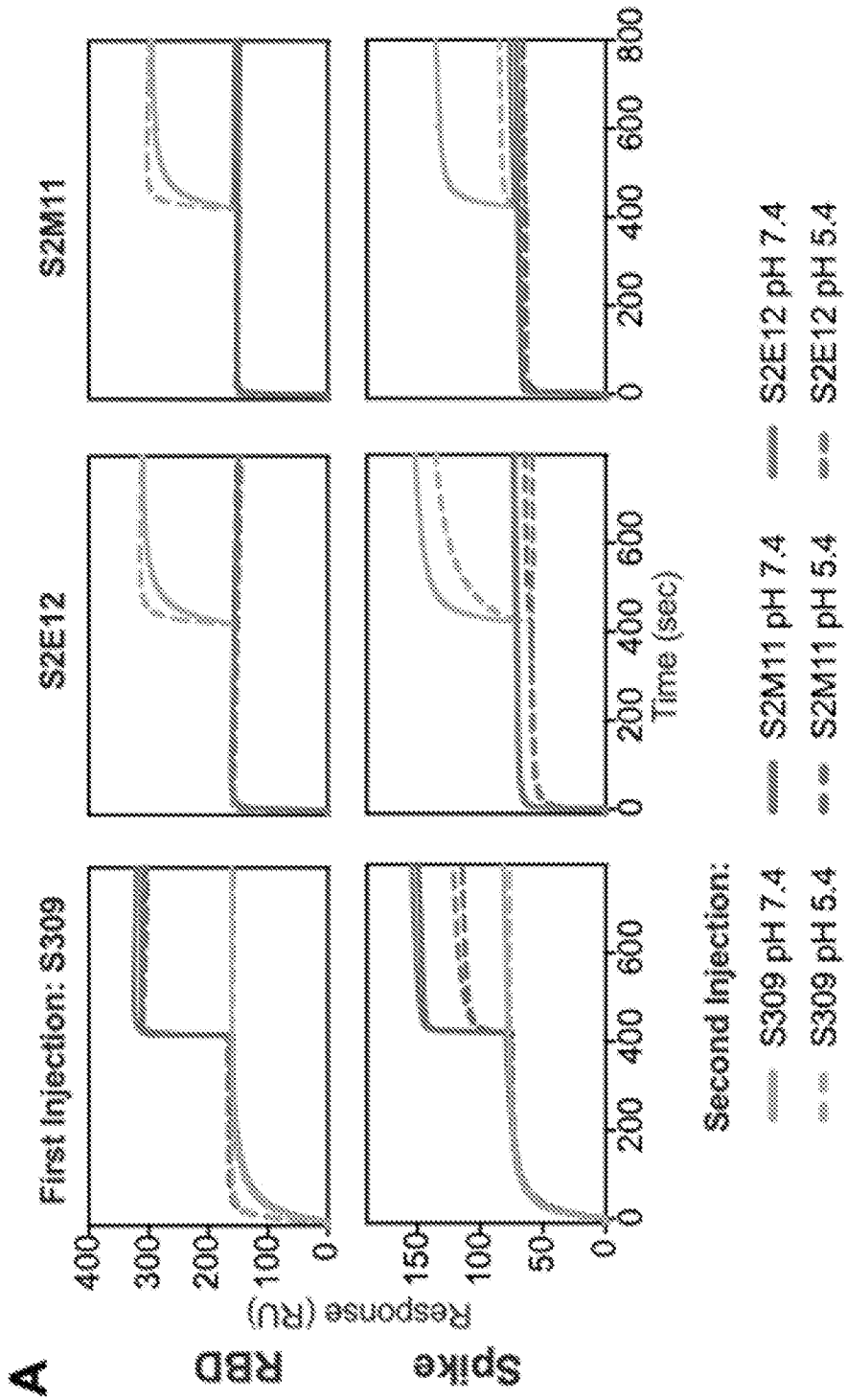

A
RBD
Spike
Response (RU)
First Injection: S309
S2E12
S2M11
Time (sec)
Second Injection:
S309 pH 7.4
S309 pH 5.4
S2M11 pH 7.4
S2M11 pH 5.4
S2E12 pH 7.4
S2E12 pH 5.4

FIG. 41

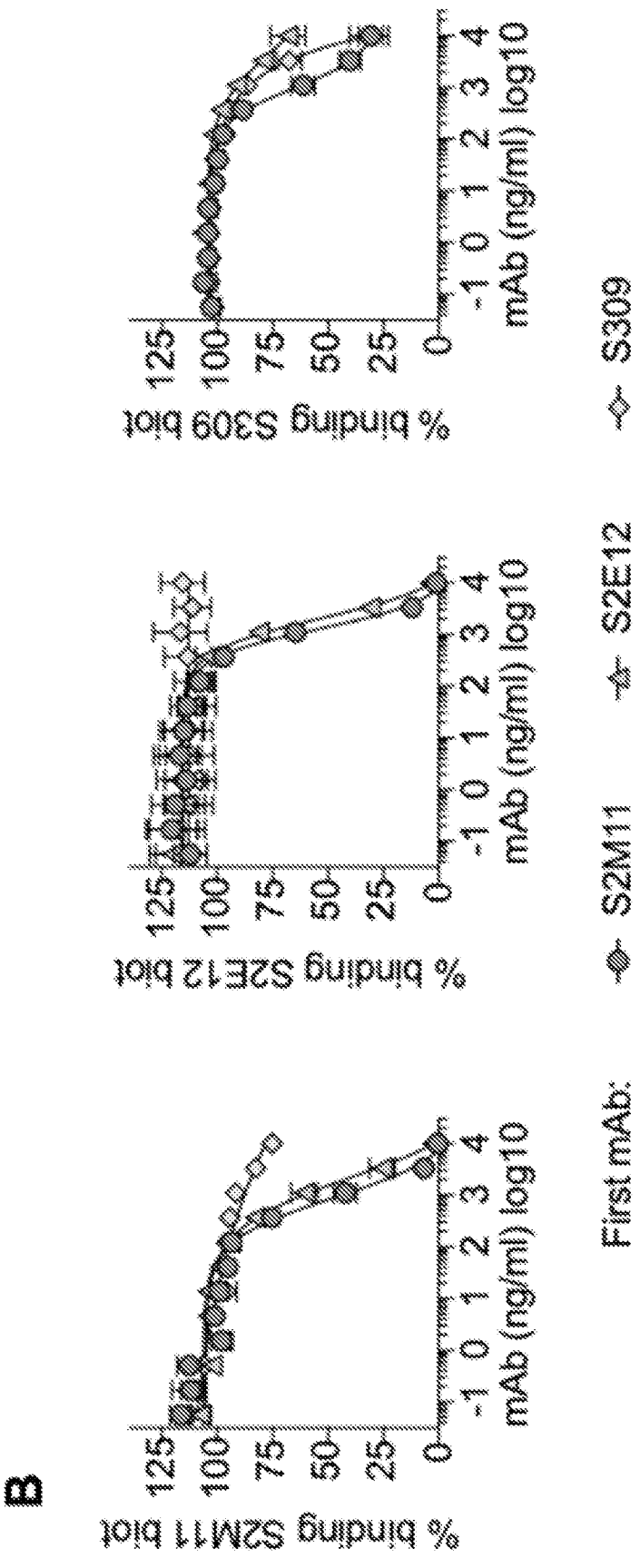

B
% binding S2M11 biot
% binding S2E12 biot
% binding S309 biot
125
100
75
50
25
0
-1 0 1 2 3 4
mAb (ng/ml) log10
First mAb:
S2M11
S2E12
S309

FIG. 41

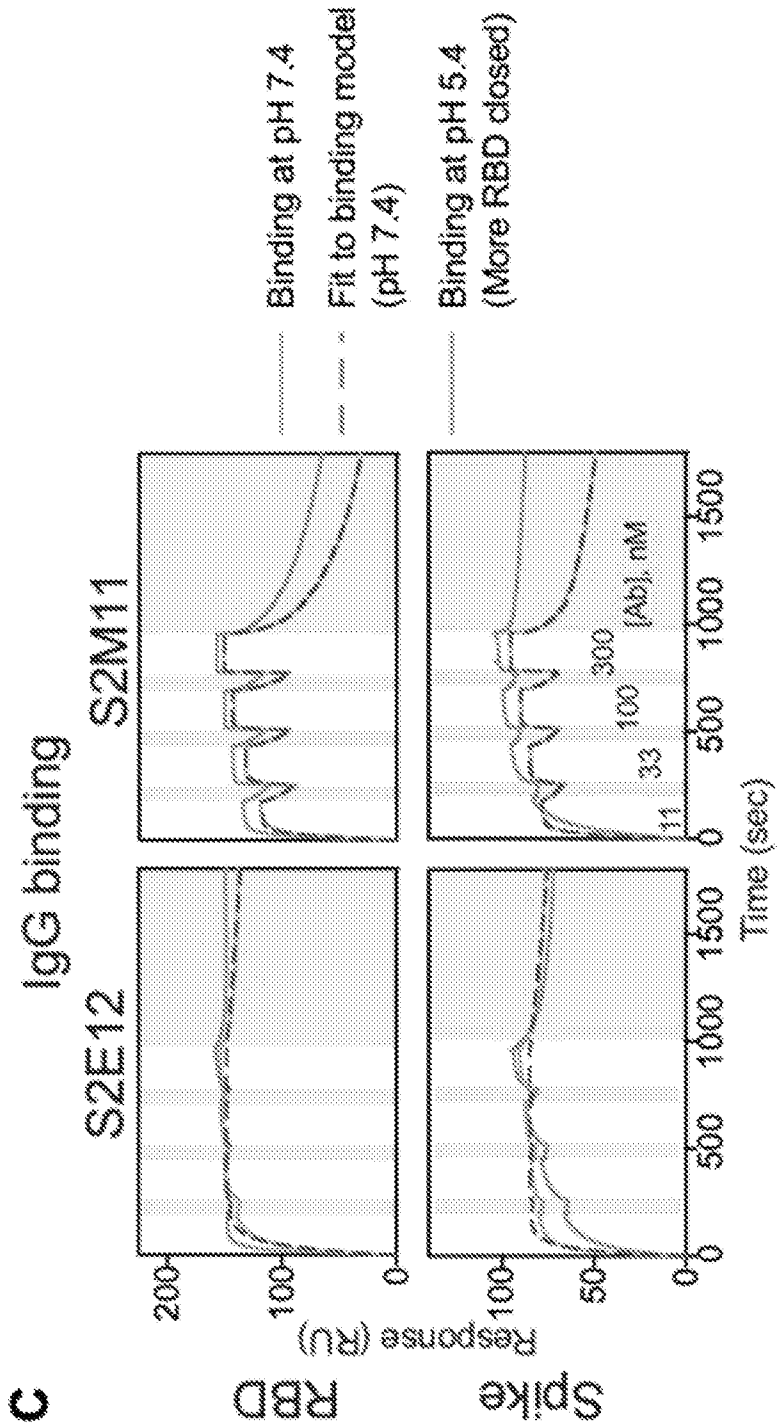

c
RBD
Spike
Response (RU)
200
100
0
100
50
0
IgG binding
S2E12
S2M11
0
500
1000
1500
Time (sec)
11
33
100
300
[Ab], nM
Binding at pH 7.4
Fit to binding model (pH 7.4)
Binding at pH 5.4 (More RBD closed)

FIG. 41

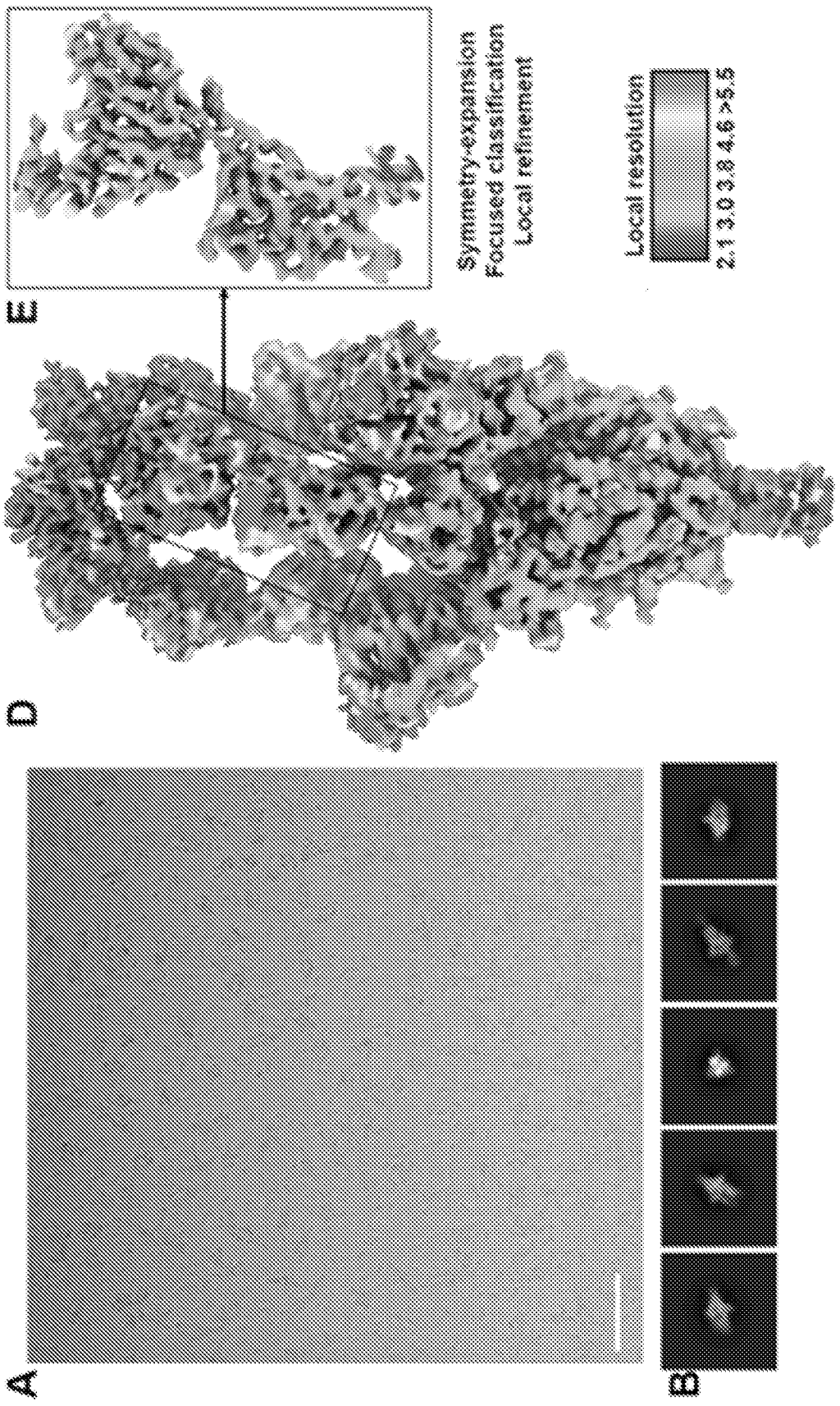

A
B
D
E
Symmetry-expansion
Focused classification
Local refinement
Local resolution
2.1 3.0 3.8 4.6 >5.5

FIG. 42

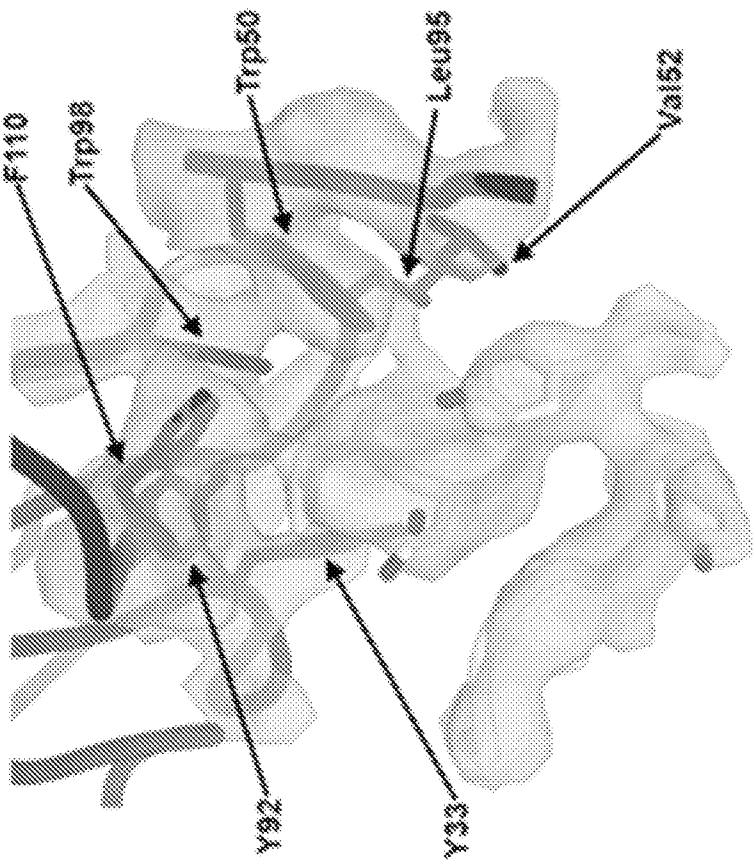


FIG. 42F

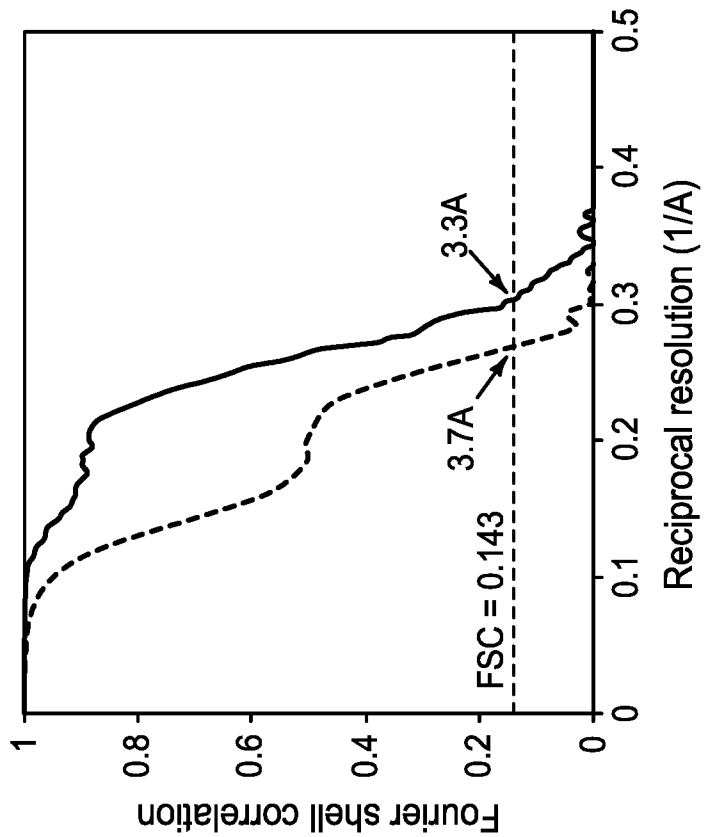


FIG. 42C

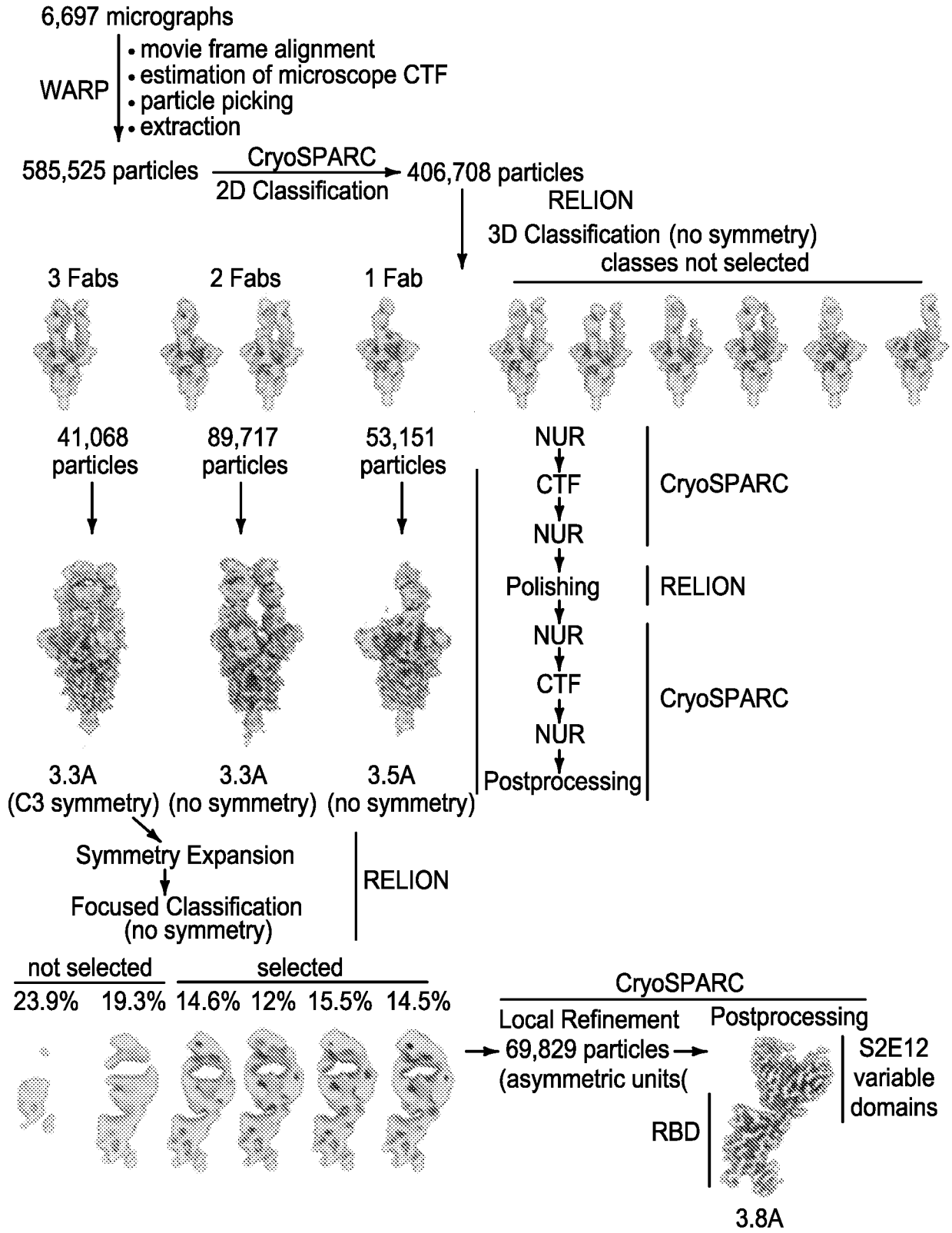

6,697 micrographs
WARP
• movie frame alignment
• estimation of microscope CTF
• particle picking
• extraction
585,525 particles
CryoSPARC
2D Classification
406,708 particles
RELION
3D Classification (no symmetry)
classes not selected
3 Fabs
2 Fabs
1 Fab
41,068 particles
89,717 particles
53,151 particles
NUR
CTF
NUR
Polishing
NUR
CTF
NUR
Postprocessing
CryoSPARC
RELION
CryoSPARC
3.3A (C3 symmetry)
3.3A (no symmetry)
3.5A (no symmetry)
Symmetry Expansion
Focused Classification (no symmetry)
RELION
not selected
selected
23.9% 19.3% 14.6% 12% 15.5% 14.5%
CryoSPARC
Local Refinement
69,829 particles (asymmetric units)
Postprocessing
RBD
S2E12 variable domains
3.8A

FIG. 42G

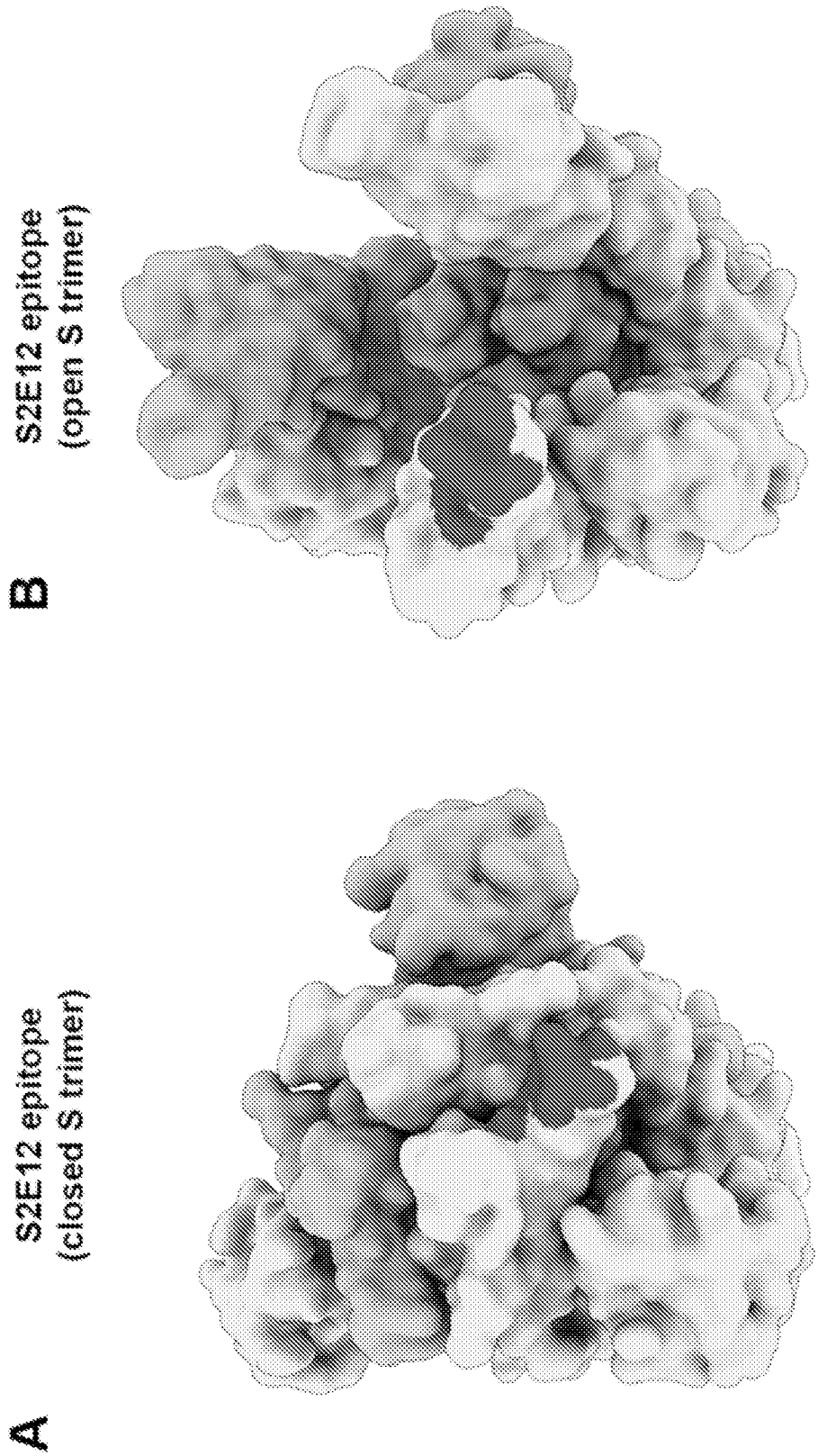

A
S2E12 epitope
(closed S trimer)
B
S2E12 epitope
(open S trimer)

FIG. 43

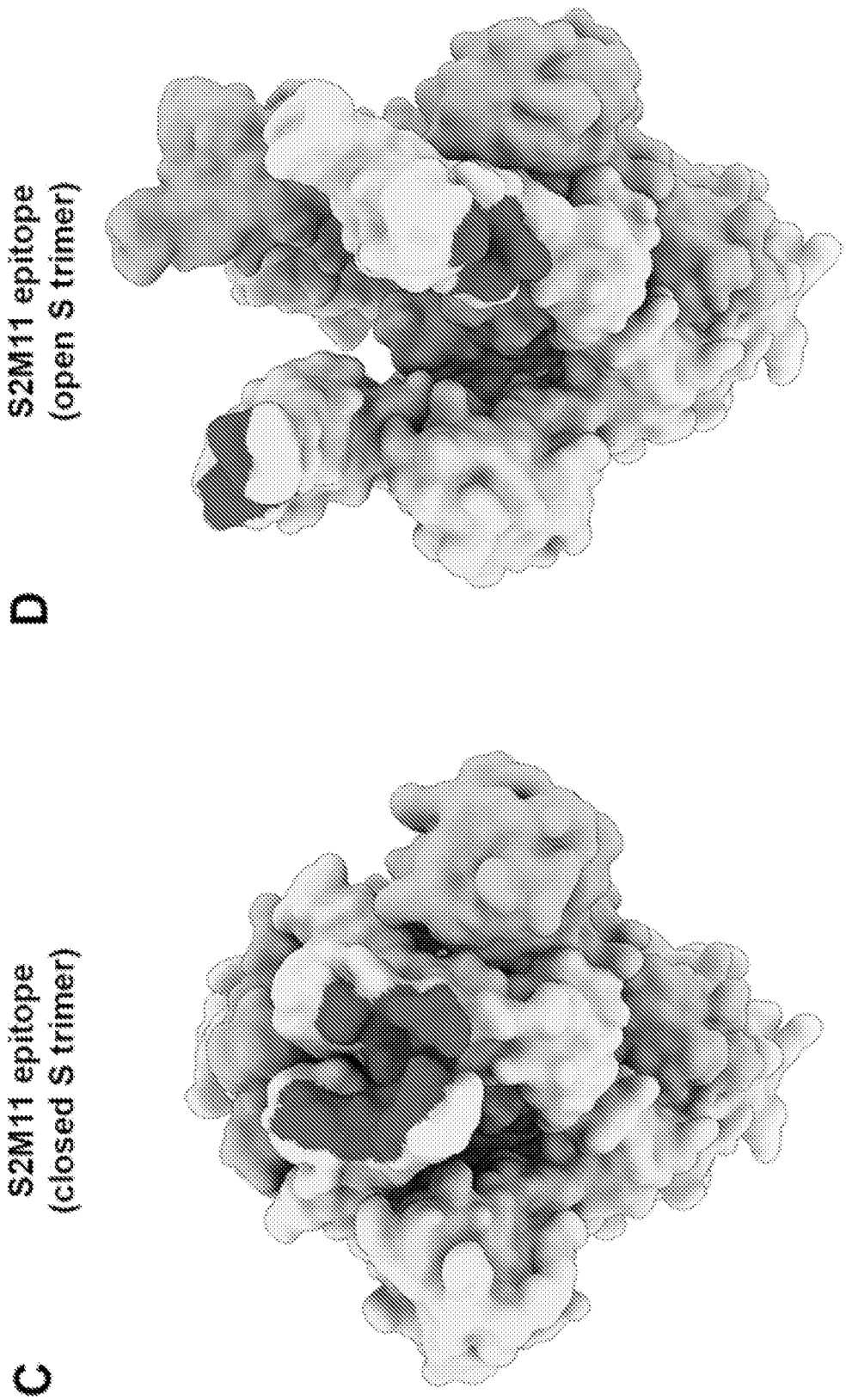

C
S2M11 epitope
(closed S trimer)
D
S2M11 epitope
(open S trimer)

FIG. 43

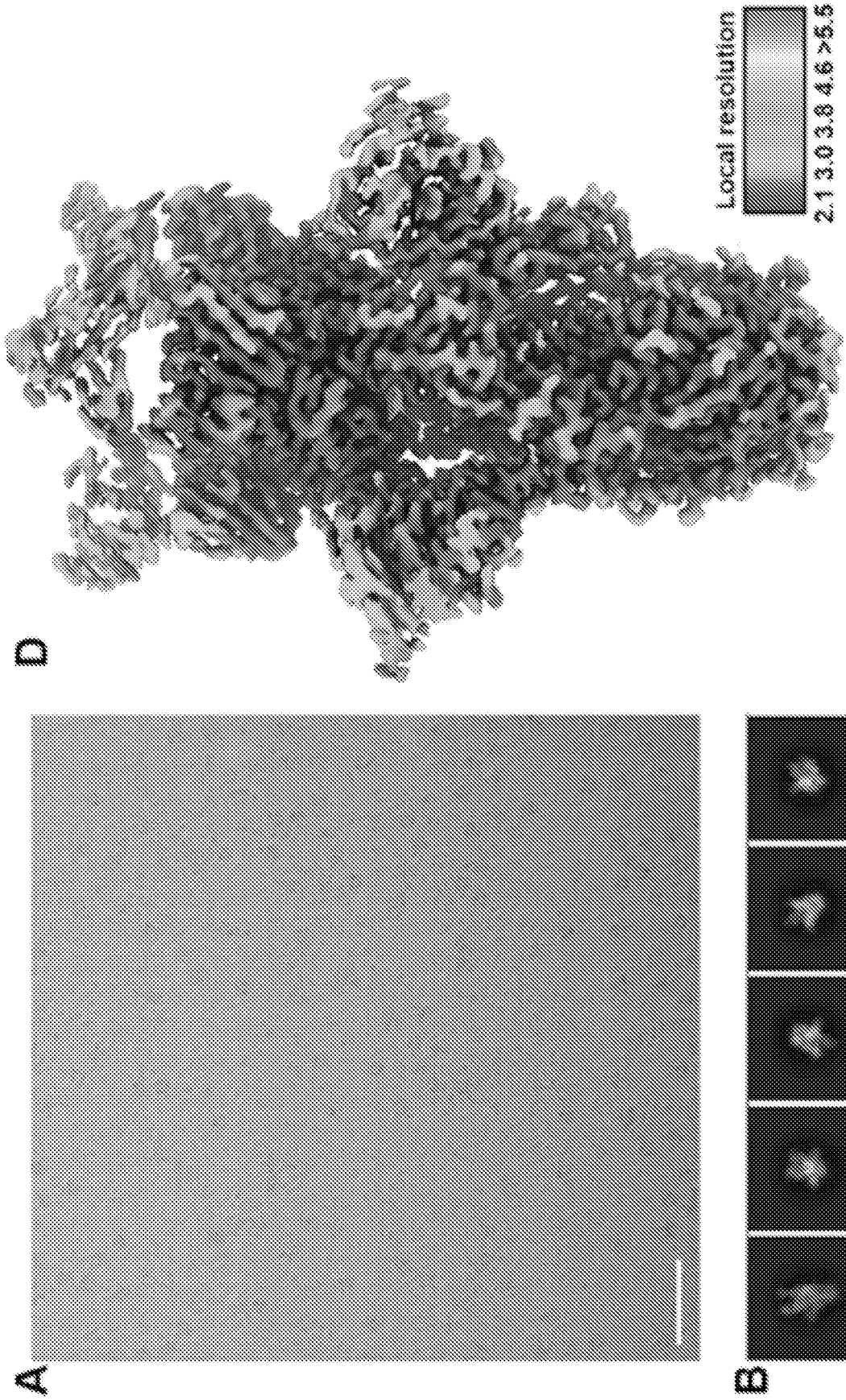


FIG. 44

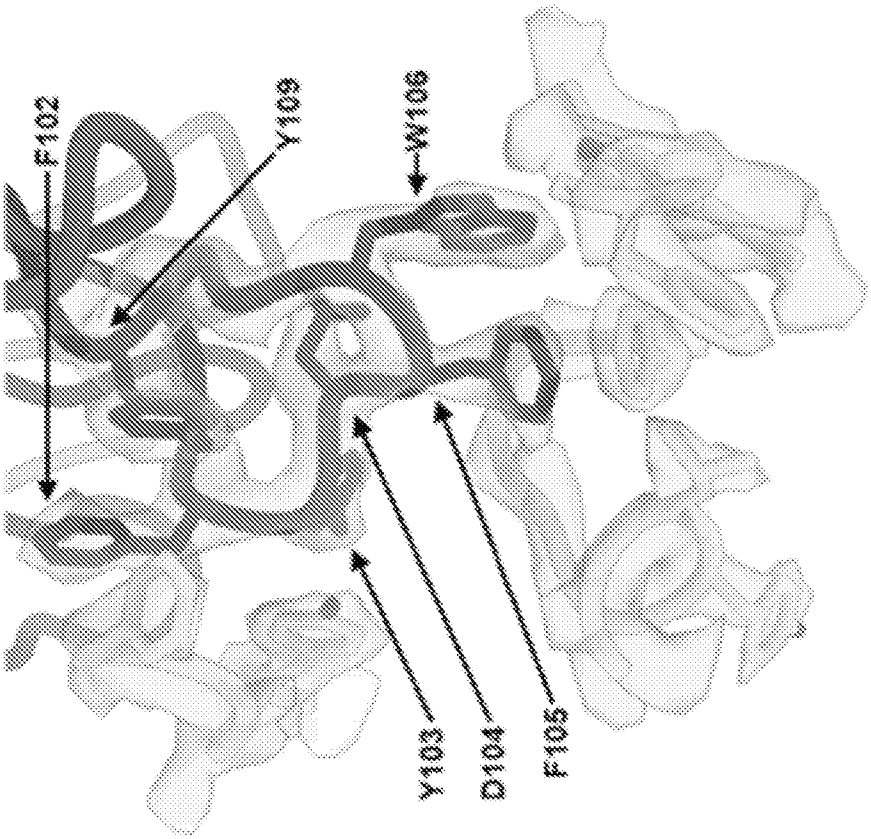


FIG. 44E

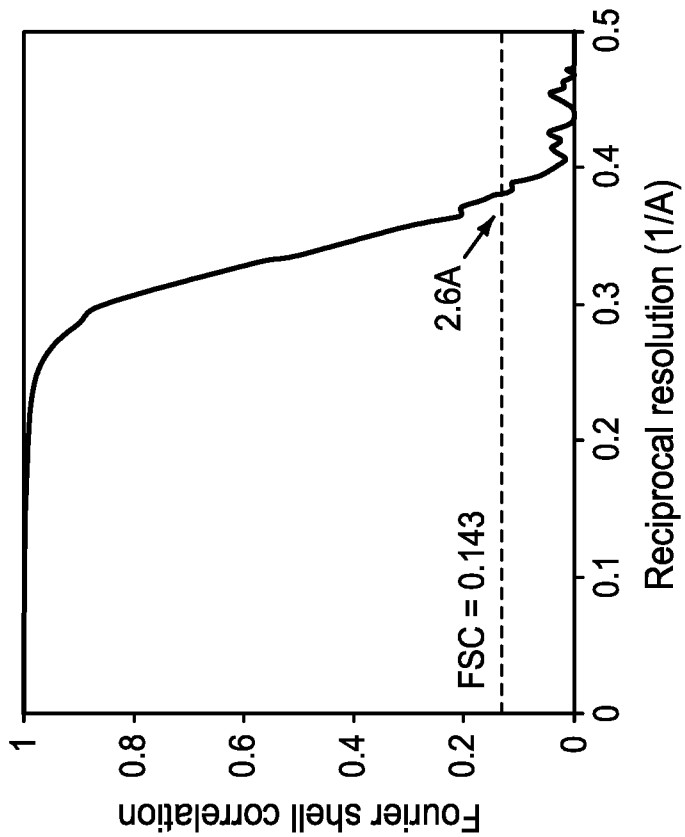


FIG. 44C

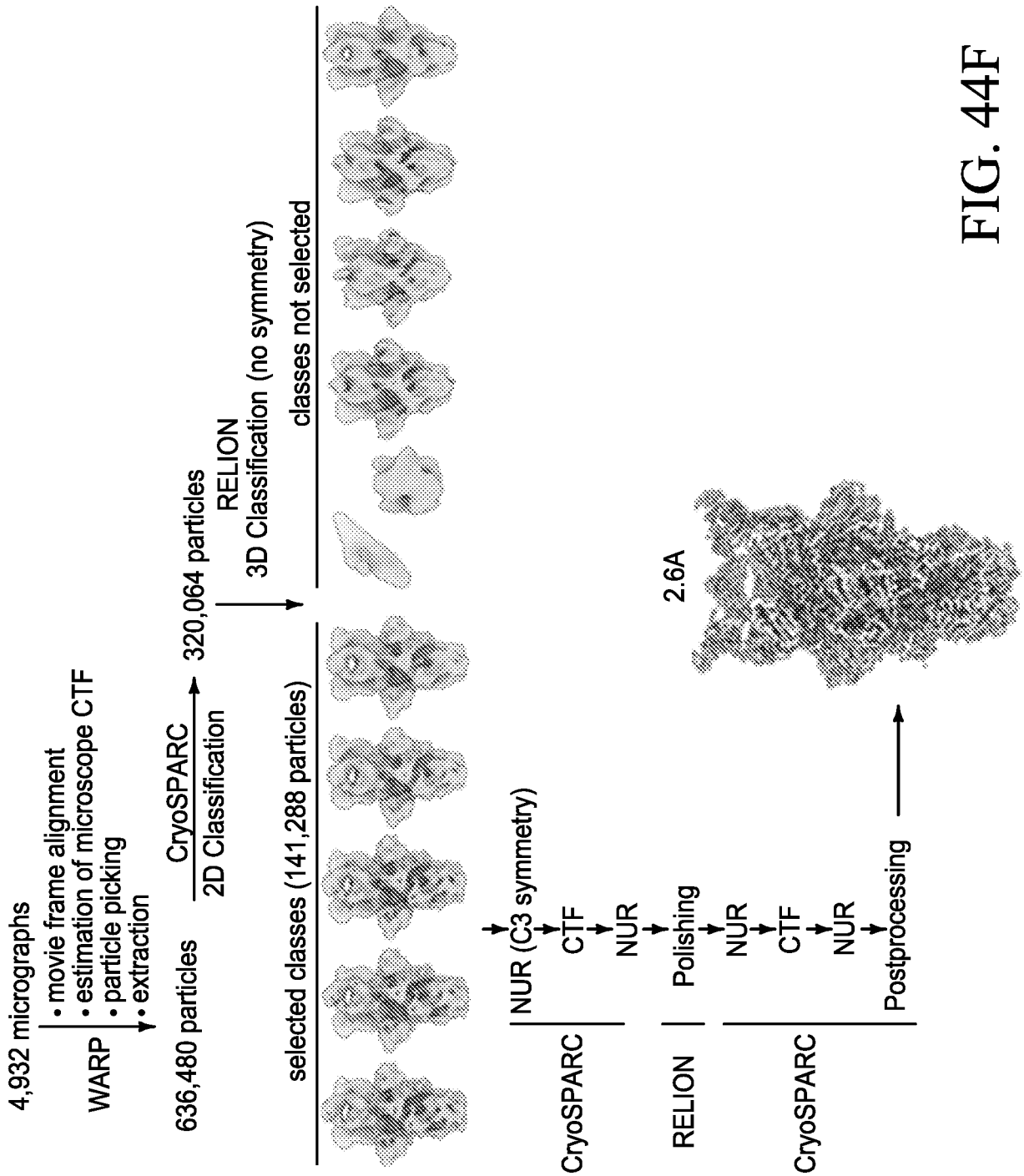

4,932 micrographs
WARP
• movie frame alignment
• estimation of microscope CTF
• particle picking
• extraction
636,480 particles
CryoSPARC
2D Classification
320,064 particles
RELION
3D Classification (no symmetry)
selected classes (141,288 particles)
classes not selected
CryoSPARC
NUR (C3 symmetry)
CTF
NUR
RELION
Polishing
CryoSPARC
NUR
CTF
NUR
Postprocessing
2.6A

FIG. 44F

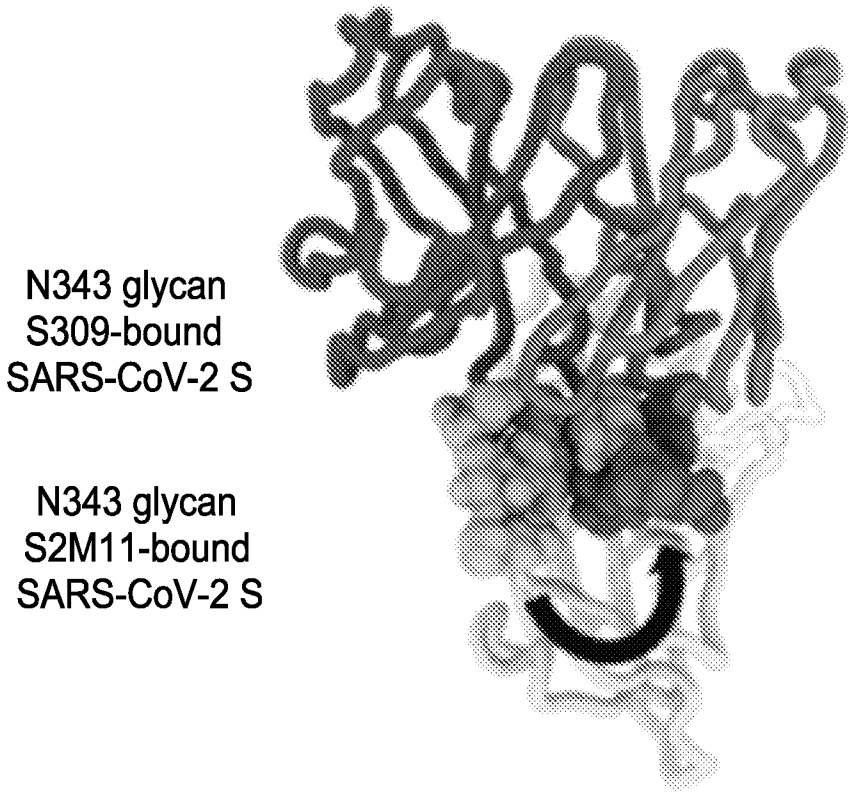

N343 glycan
S309-bound
SARS-CoV-2 S
N343 glycan
S2M11-bound
SARS-CoV-2 S

FIG. 44G

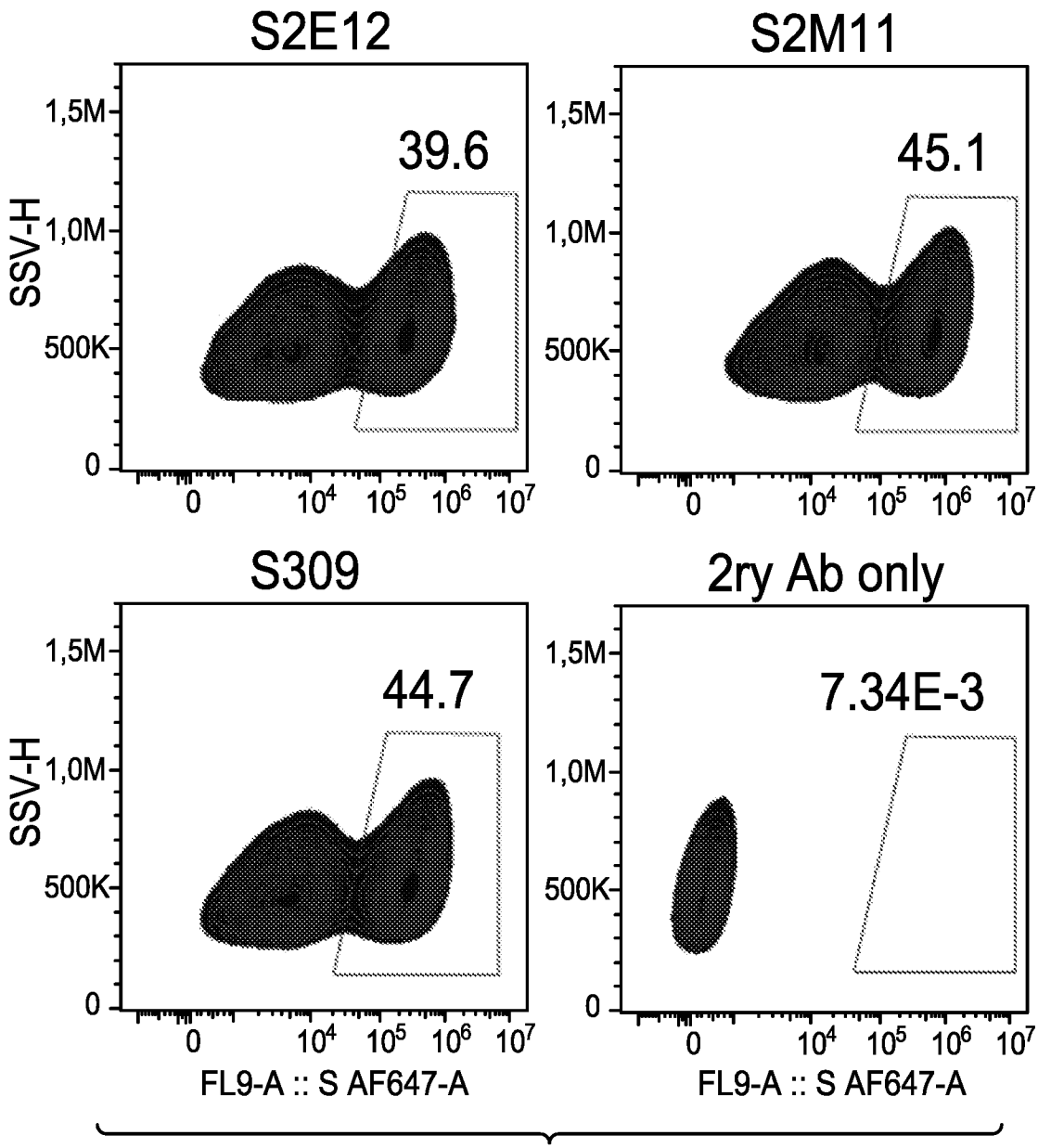


FIG. 45A

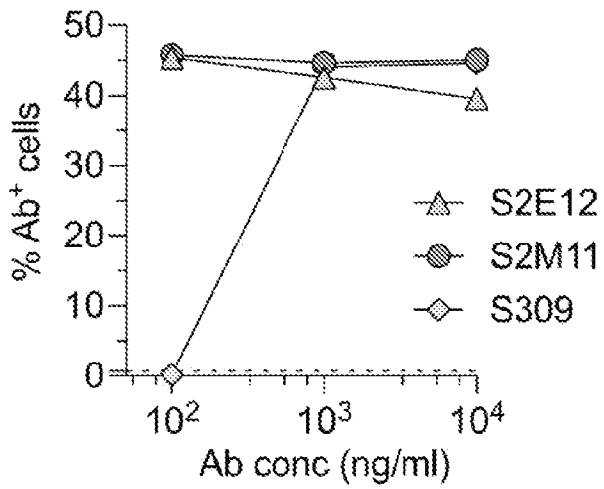


FIG. 45B

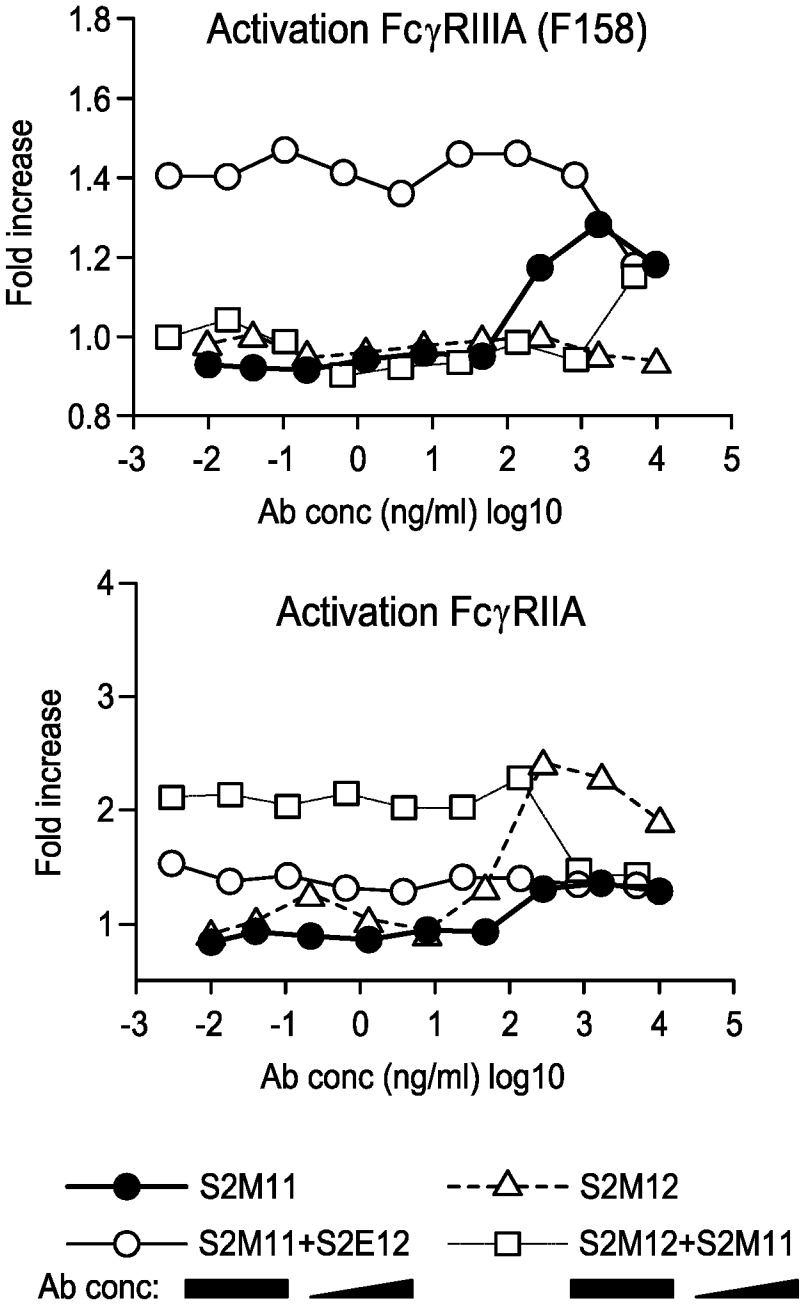

Activation FcγRIIIA (F158)
Fold increase
1.8
1.6
1.4
1.2
1.0
0.8
-3 -2 -1 0 1 2 3 4 5
Ab conc (ng/ml) log10
Activation FcγRIIA
Fold increase
4
3
2
1
-3 -2 -1 0 1 2 3 4 5
Ab conc (ng/ml) log10
S2M11
S2M12
S2M11+S2E12
S2M12+S2M11
Ab conc:

FIG. 45C

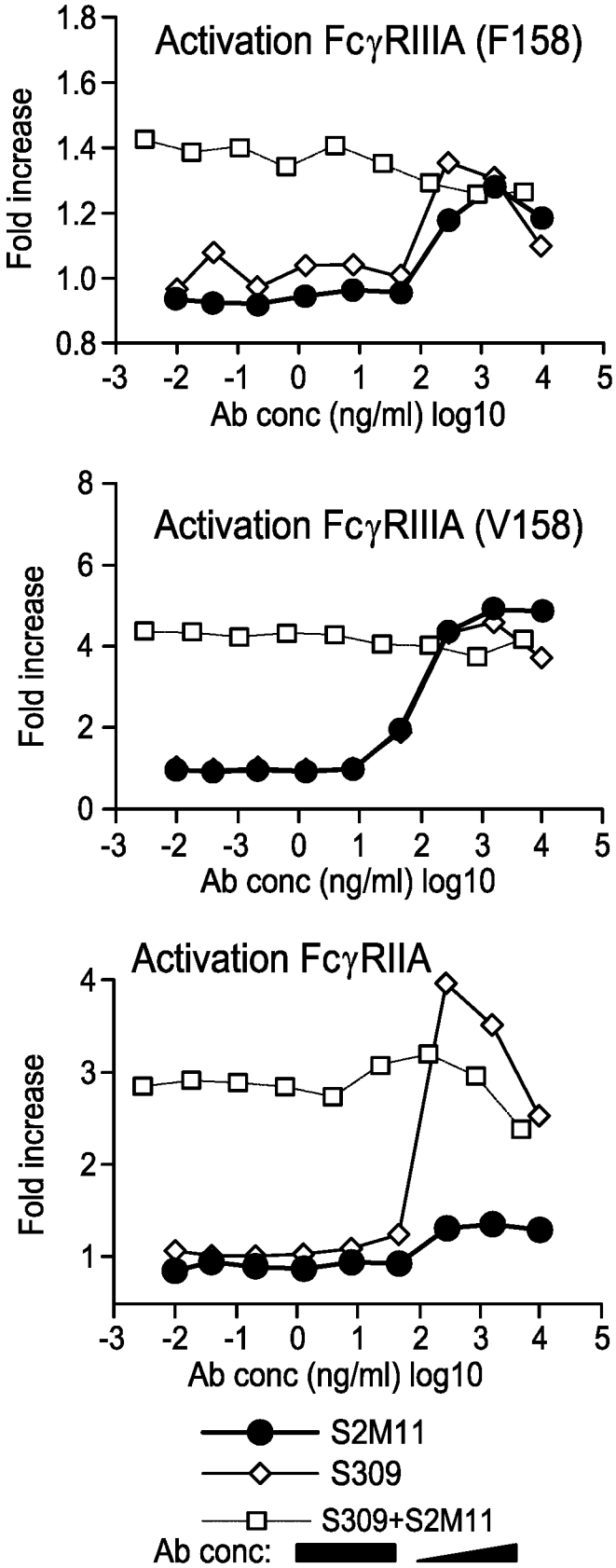

Activation FcγRIIIA (F158)
Fold increase
1.8
1.6
1.4
1.2
1.0
0.8
-3 -2 -1 0 1 2 3 4 5
Ab conc (ng/ml) log10
Activation FcγRIIIA (V158)
Fold increase
8
6
4
2
0
-3 -2 -3 0 1 2 3 4 5
Ab conc (ng/ml) log10
Activation FcγRIIA
Fold increase
4
3
2
1
-3 -2 -1 0 1 2 3 4 5
Ab conc (ng/ml) log10
S2M11
S309
S309+S2M11
Ab conc:

FIG. 45D

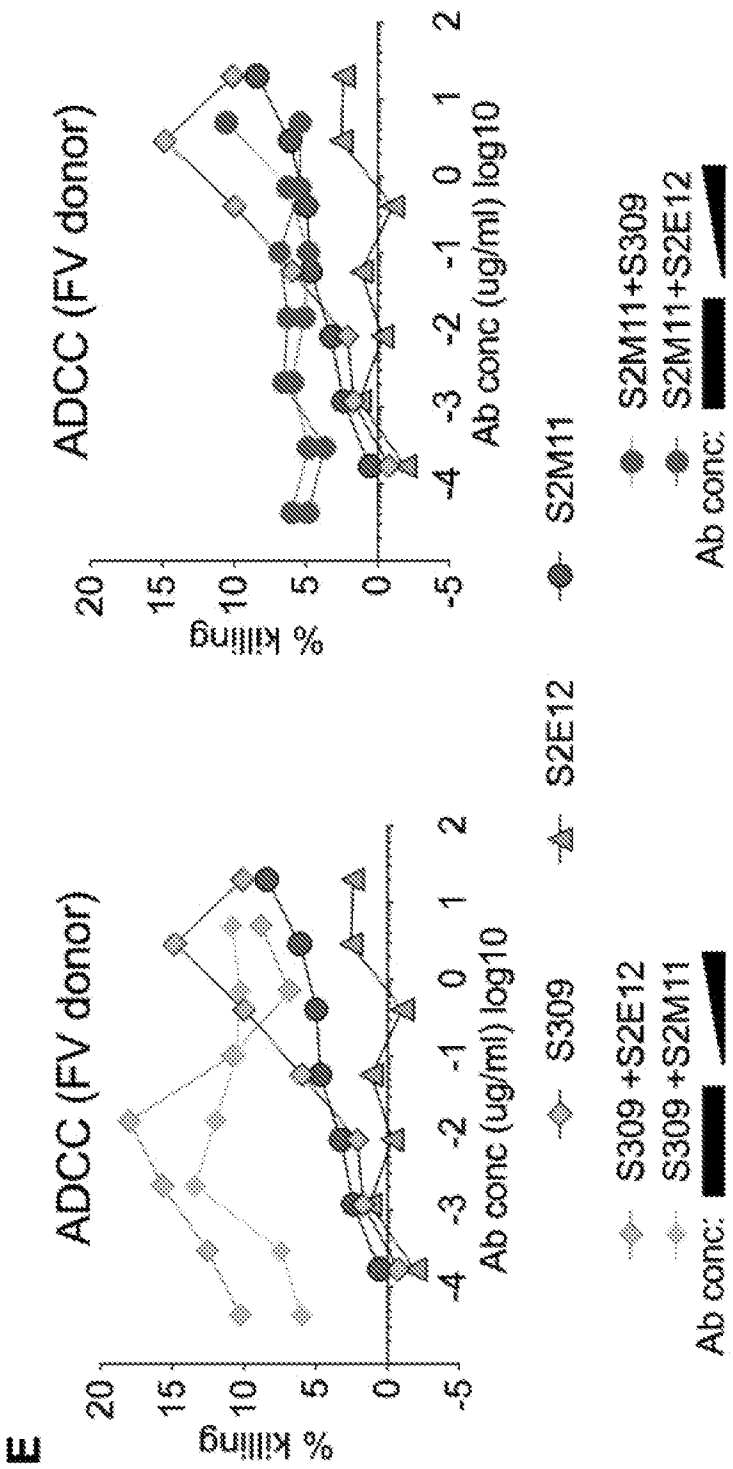

E
ADCC (FV donor)
% killing
20
15
10
5
0
-5
-4
-3
-2
-1
0
1
2
Ab conc (ug/ml) log10
S309
S2E12
S2M11
S309 +S2E12
S309 +S2M11
Ab conc:
ADCC (FV donor)
% killing
Ab conc (ug/ml) log10
S2M11+S309
S2M11+S2E12
Ab conc:

FIG. 45

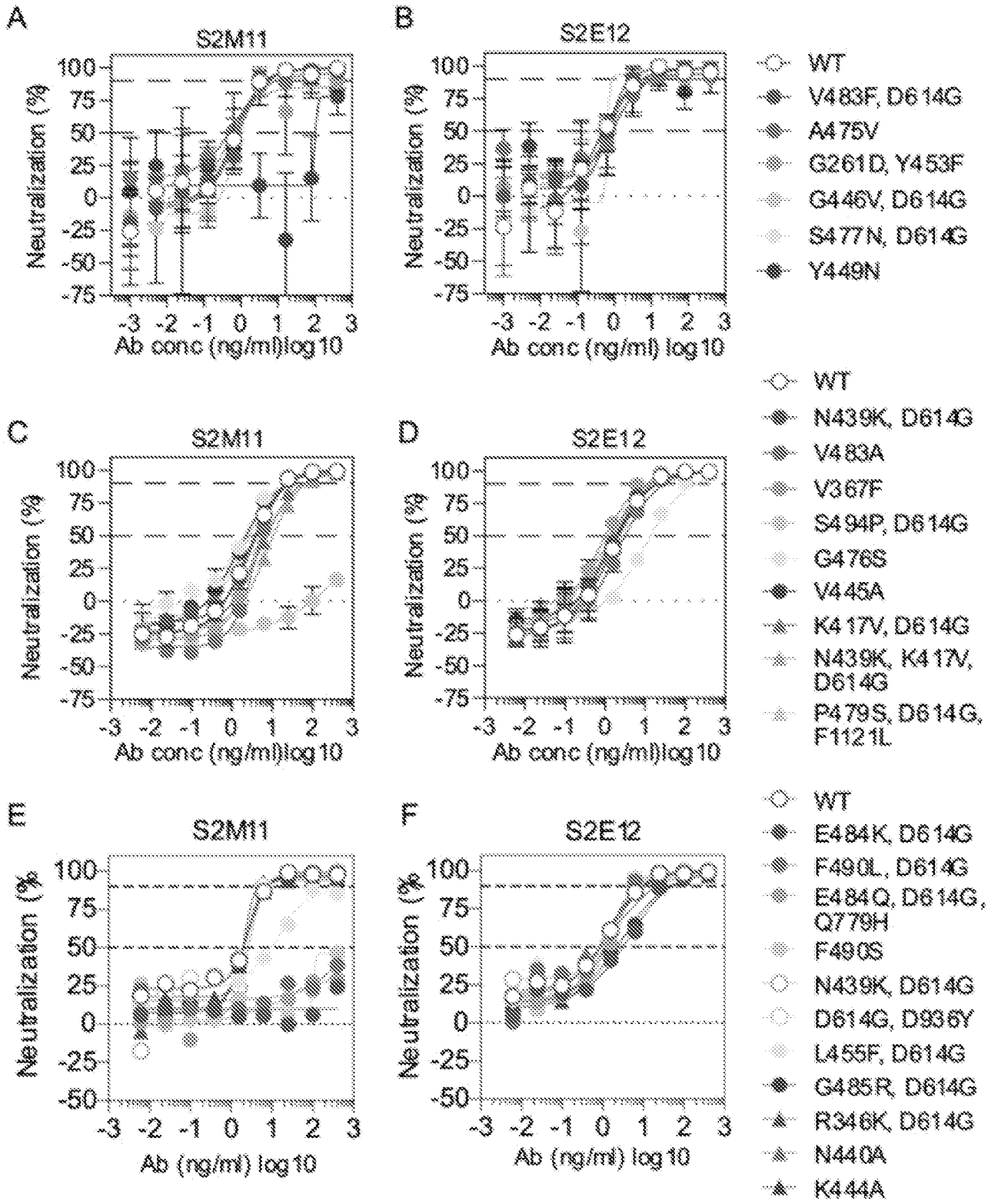

A
S2M11
Neutralization (%)
Ab conc (ng/ml)log10
B
S2E12
Neutralization (%)
Ab conc (ng/ml) log10
WT
V483F, D614G
A475V
G261D, Y453F
G446V, D614G
S477N, D614G
Y449N
C
S2M11
Neutralization (%)
Ab conc (ng/ml)log10
D
S2E12
Neutralization (%)
Ab conc (ng/ml)log10
WT
N439K, D614G
V483A
V367F
S494P, D614G
G476S
V445A
K417V, D614G
N439K, K417V, D614G
P479S, D614G, F1121L
E
S2M11
Neutralization (%)
Ab (ng/ml) log10
F
S2E12
Neutralization (%)
Ab (ng/ml) log10
WT
E484K, D614G
F490L, D614G
E484Q, D614G, Q779H
F490S
N439K, D614G
D614G, D936Y
L455F, D614G
G485R, D614G
R346K, D614G
N440A
K444A

FIG. 46

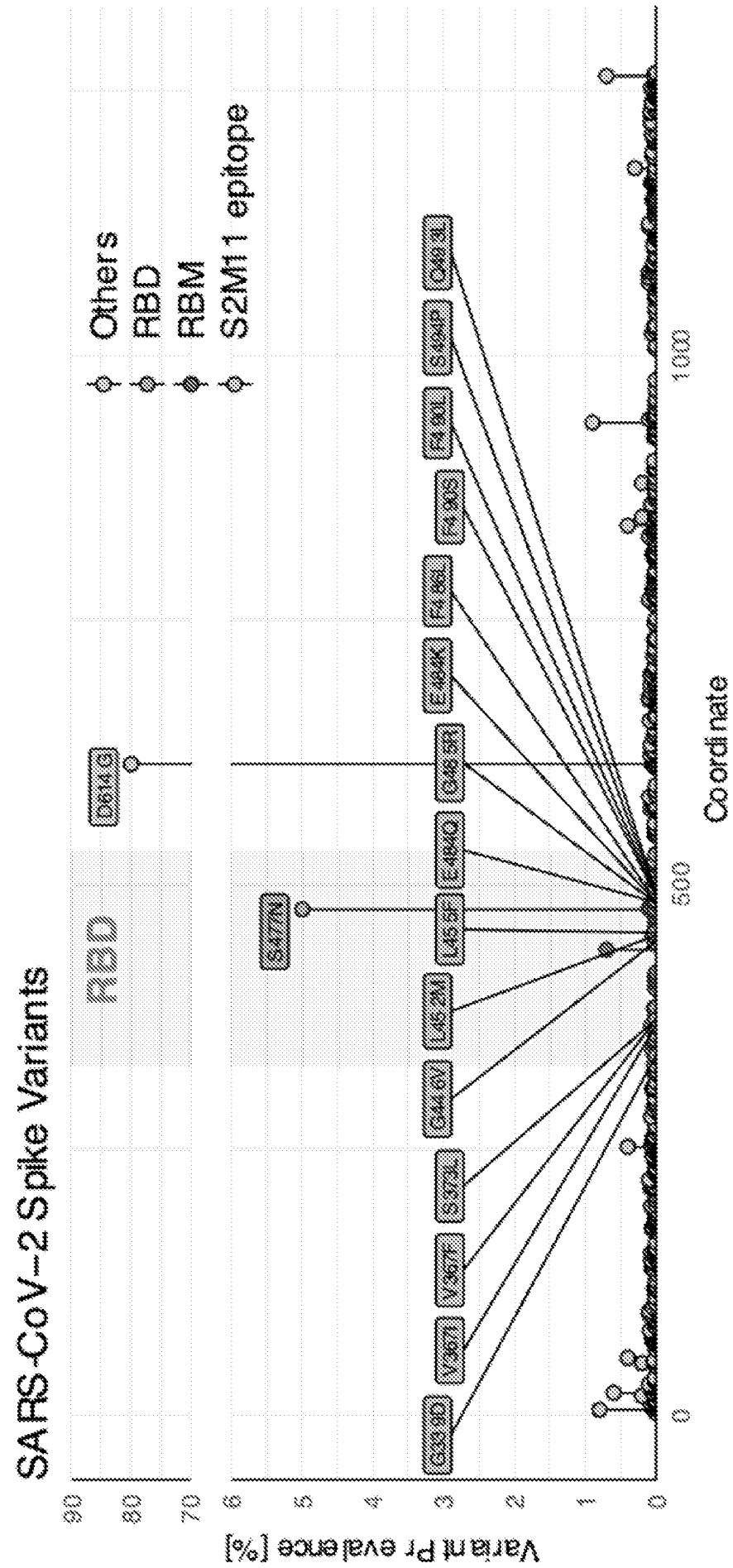

SARS-CoV-2 Spike Variants
Others
RBD
RBM
S2M11 epitope
RBD
D614G
S477N
L452R
E484Q
G446S
E484K
F490L
F486L
F456L
S494P
Q498R
G339D
V367F
V367F
S373P
G446V
L452M
Variant Pr evalence [%]
Coordinate
0
500
1000
0
1
2
3
4
5
6
70
80
90

FIG. 46G

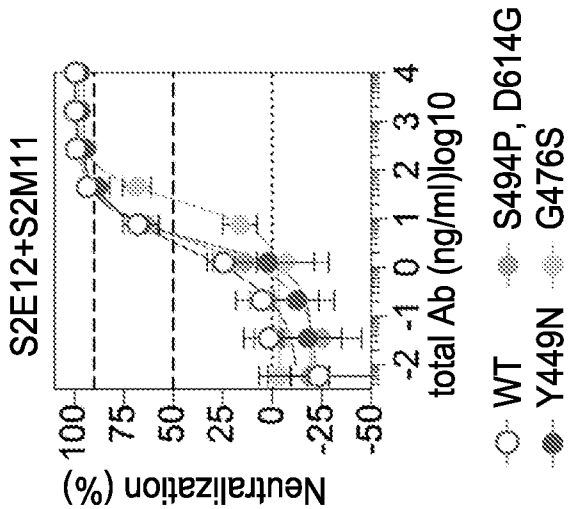


FIG. 46J

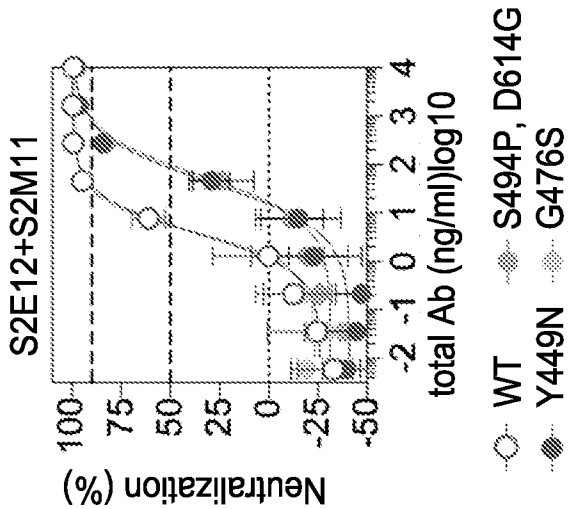


FIG. 46I

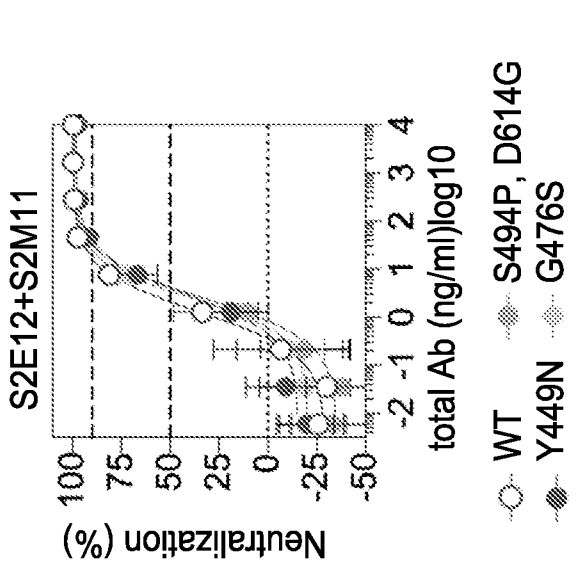


FIG. 46H

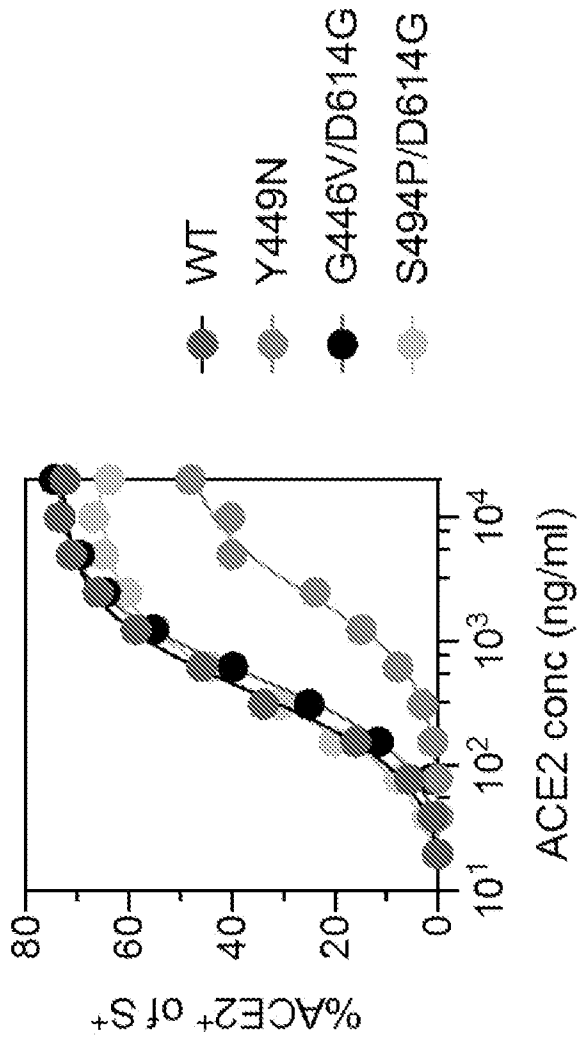

WT
Y449N
G446V/D614G
S494P/D614G
%ACE2+ of S+
0
20
40
60
80
10^1
10^2
10^3
10^4
ACE2 conc (ng/ml)

FIG. 47

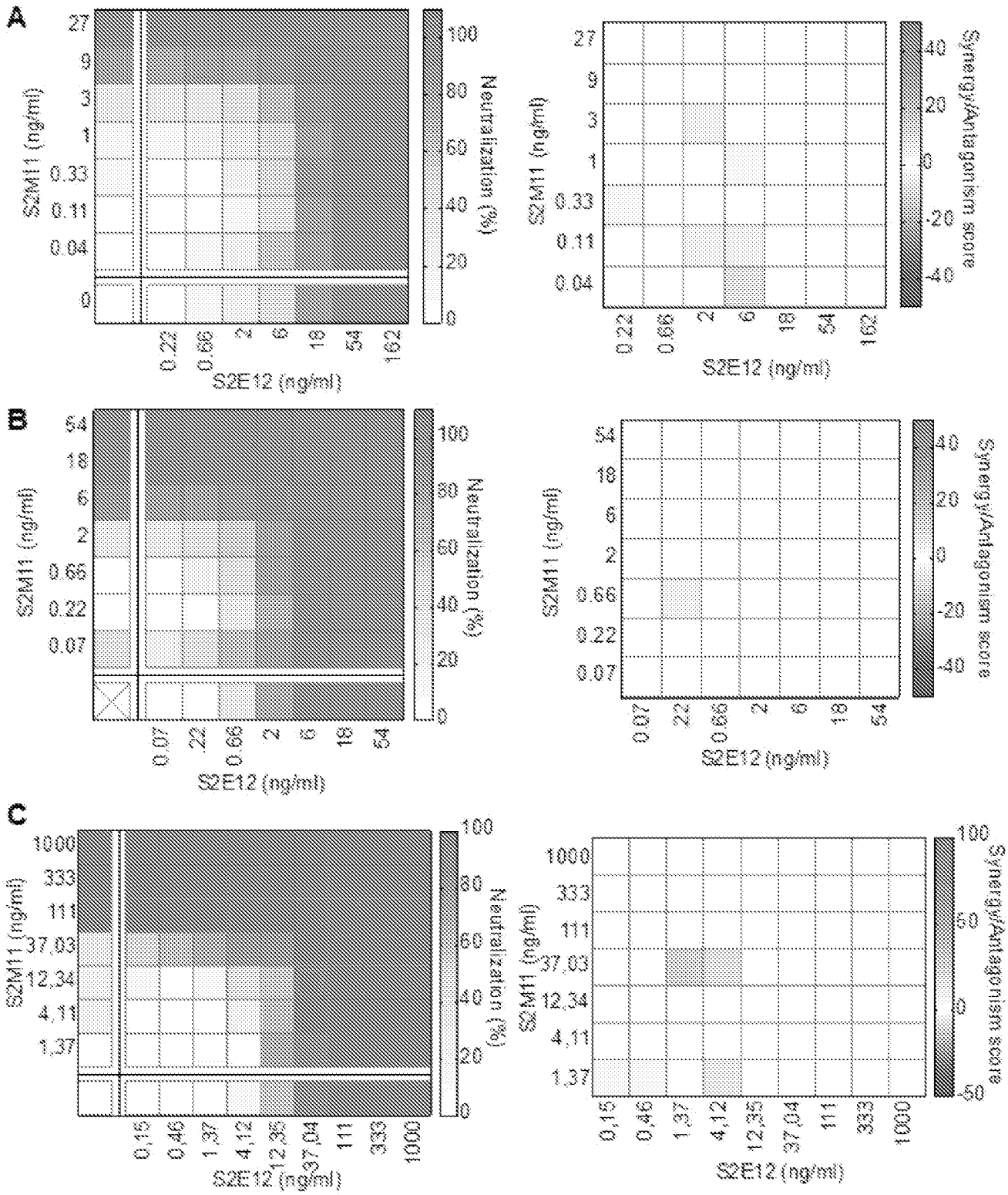

A
S2M11 (ng/ml)
27
9
3
1
0.33
0.11
0.04
0
S2E12 (ng/ml)
0.22
0.66
2
6
18
54
162
Neutralization (%)
100
80
60
40
20
0
Synergy/Antagonism score
40
20
0
-20
-40
B
S2M11 (ng/ml)
54
18
6
2
0.66
0.22
0.07
S2E12 (ng/ml)
0.07
0.22
0.66
2
6
18
54
Neutralization (%)
Synergy/Antagonism score
C
S2M11 (ng/ml)
1000
333
111
37,03
12,34
4,11
1,37
S2E12 (ng/ml)
0,15
0,46
1,37
4,12
12,35
37,04
111
333
1000
Neutralization (%)
Synergy/Antagonism score
100
50
0
-50

FIG. 48

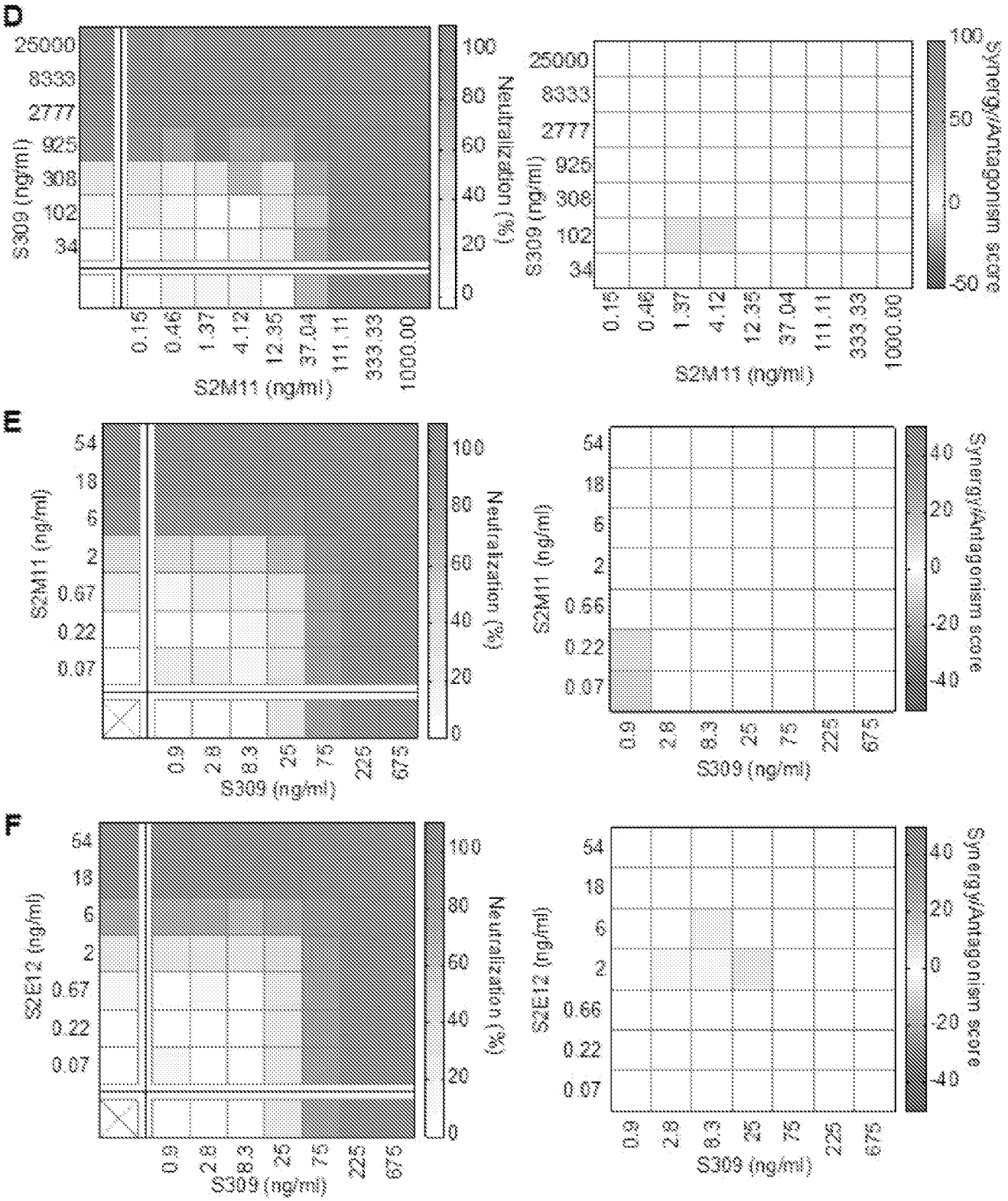

D
S309 (ng/ml)
25000
8333
2777
925
308
102
34
S2M11 (ng/ml)
0.15
0.46
1.37
4.12
12.35
37.04
111.11
333.33
1000.00
Neutralization (%)
100
80
60
40
20
0
Synergy/Antagonism score
50
0
-50
E
S2M11 (ng/ml)
54
18
6
2
0.67
0.22
0.07
S309 (ng/ml)
0.9
2.8
8.3
25
75
225
675
Neutralization (%)
Synergy/Antagonism score
0.66
-20
-40
F
S2E12 (ng/ml)

FIG. 48

			(1/Ms)		(1/s)	
S2E12 Fab	RBD	7.4	4.4e6	7.1e-3	90.2
		5.4	1.6	7.4e6	8.4e-3	110.5
	Spike	7.4	1.1	2.5e6	6.2e-3	49.6
		5.4	2.5	5.0e5	5.8e-3	42.5
S2E12 IgG	RBD	7.4	11.6	2.1e6	1.0e-4	148.4
		5.4	0.05	4.5e6	<1e-4	209
	Spike	7.4	<0.05	2.9e6	1.4e-4	85.0
		5.4	0.05	9.2e5	2.2e-4	96.0
S2M11 Fab	RBD	7.4	0.2	2.4e6	0.16	89.8
		5.4	66	2.3e6	0.14	108
	Spike	7.4 (biphasic fit)	60	2.0e6	0.14	40.4
			68	7.8e5	1.4e-4	15.2
		5.4 (biphasic fit)	0.2	3.3e6	0.14	9.8
			42	4.4e5	3.2e-4	51.9
			0.7			
S2M11 IgG	RBD	7.4 (biphasic fit)	28	1.3e6	3.7e-2	46.7
			0.3	9.1e6	2.7e-3	107.6
		5.4 (biphasic fit)	31	1.5e6	4.8e-2	47.8
			0.1	1.5e7	1.4e-3	175.5
	Spike	7.4 (biphasic fit)	12	1.4e6	1.7e-2	21.7
			0.05	8.0e6	4.3e-4	66.9
		5.4	0.1	1.2e6	1.4e-4	109

FIG. 49

	SARS-CoV-2 S/S2M11 (PDB EMD-	SARS-CoV-2 S/S2E12 (3 RBDs open) PDB EMD	SARS-CoV-2 S/S2E12 (local refinement) PDB EMD
Data collection and processing			
Magnification	130,000	130,000	130,000
Voltage (kV)	300	300	300
Electron exposure (e^-/Å^2)	70	70	70
Defocus range (μm)	0.8-2.0	0.8-2.0	0.8-2.0
Pixel size (Å)	0.525	0.525	0.525
Symmetry imposed	C3	C3	C1
Final particle images (no.)	141,243	41,068	69,829
Map resolution (Å)	2.6	3.3	3.8
FSC threshold	0.143	0.143	0.143
Map sharpening *B* factor (Å^2)	-74	-46	-24
Validation			
MolProbity score	0.61	1.62	0.87
Clashscore	0.25	7.92	0.52
Poor rotamers (%)	0.18	0.38	0
Ramachandran plot			
Favored (%)	97.93	96.90	96.84
Allowed (%)	1.99	2.85	2.43
Disallowed (%)	0.08	0.25	0.73

FIG. 50

	S2E12 Fab
Data collection	
X-ray source	SLS X10SA
Space group	$P2_12_12_1$
Cell dimensions	
a, *b*, *c* (Å)	58.01, 85.72, 86.31
α, β, γ (°)	90, 90, 90
Resolution (Å)	48.15-1.38 (1.4-1.38)
R_{sym} or R_{merge}	0.059 (2.16)
$CC_{1/2}$	0.999 (0.74)
$I / \sigma I$	19.1 (1.2)
Completeness (%)	99.3 (87.8)
Redundancy	13.1 (13.1)
Refinement	
Resolution (Å)	1.38
No. reflections	84581
R_{work} / R_{free}	0.20/0.215
No. atoms	
Protein	3736
Ligand	
B-factors (Å^2)	
Protein	27.2
Ligand	
R.m.s. deviations	
Bond lengths (Å)	0.004
Bond angles (°)	1.03

FIG. 51

Variant mutations:	S2M11	S2E12	S309
G261D, Y453F	+	+	+
R346K, D614G	+	+	+
V367F	+	+	+
K417V, D614G	+	+	+
N439K, D614G	+	+	+
N440A	+	+	+
K444A	+	+	+
V445A	+	+	+
G446V, D614G	+	+	+
Y449N	-	+	+
N450A	+	+	+
Y453F, G261D	+	+	+
L455F, D614G	+	+	+
F456V	+	+	+
A475V	+	+	+
G476S	+	+	+
S477N, D614G	+	+	+
T478I, D614G	+	+	+
P479S, D614G, F1121L	+	+	+
V483A	+	+	+
V483F, D614G	+	+	+
E484K, D614G	-	+	+
E484Q, D614G, Q779H	-	+	+
G485R, D614G	+	+	+
F486A	+	-	+
F490L, D614G	-	+	+
Q493A	+	+	+
S494P, D614G	-	+	+
D614G	+	+	+

FIG. 52

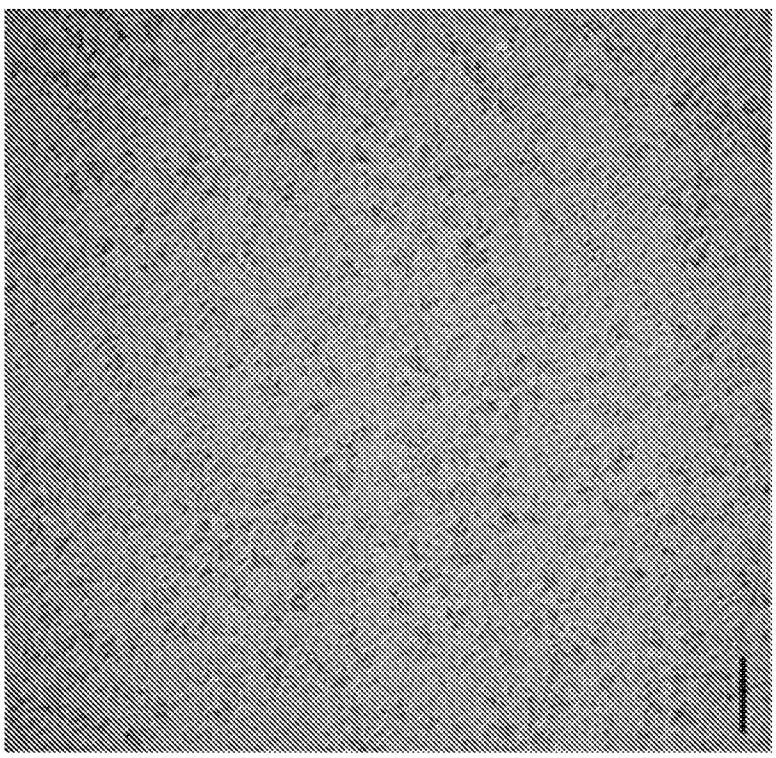


FIG. 53A



FIG. 53B

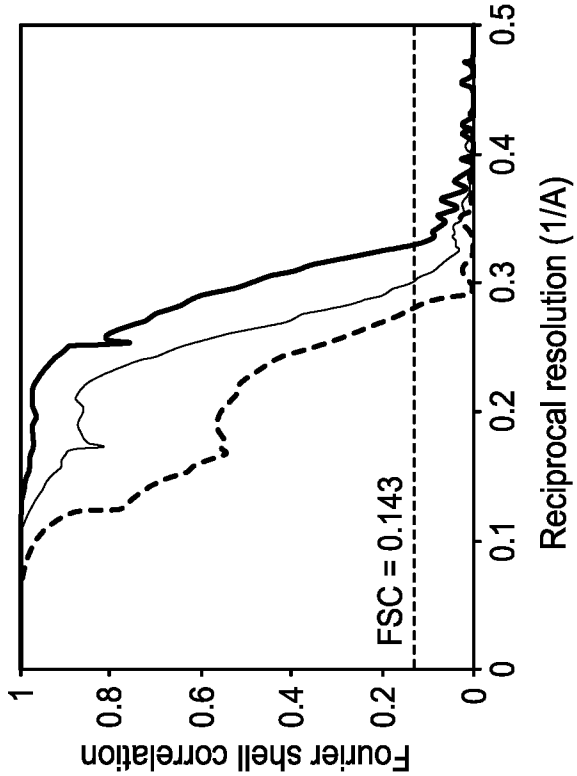


FIG. 53C

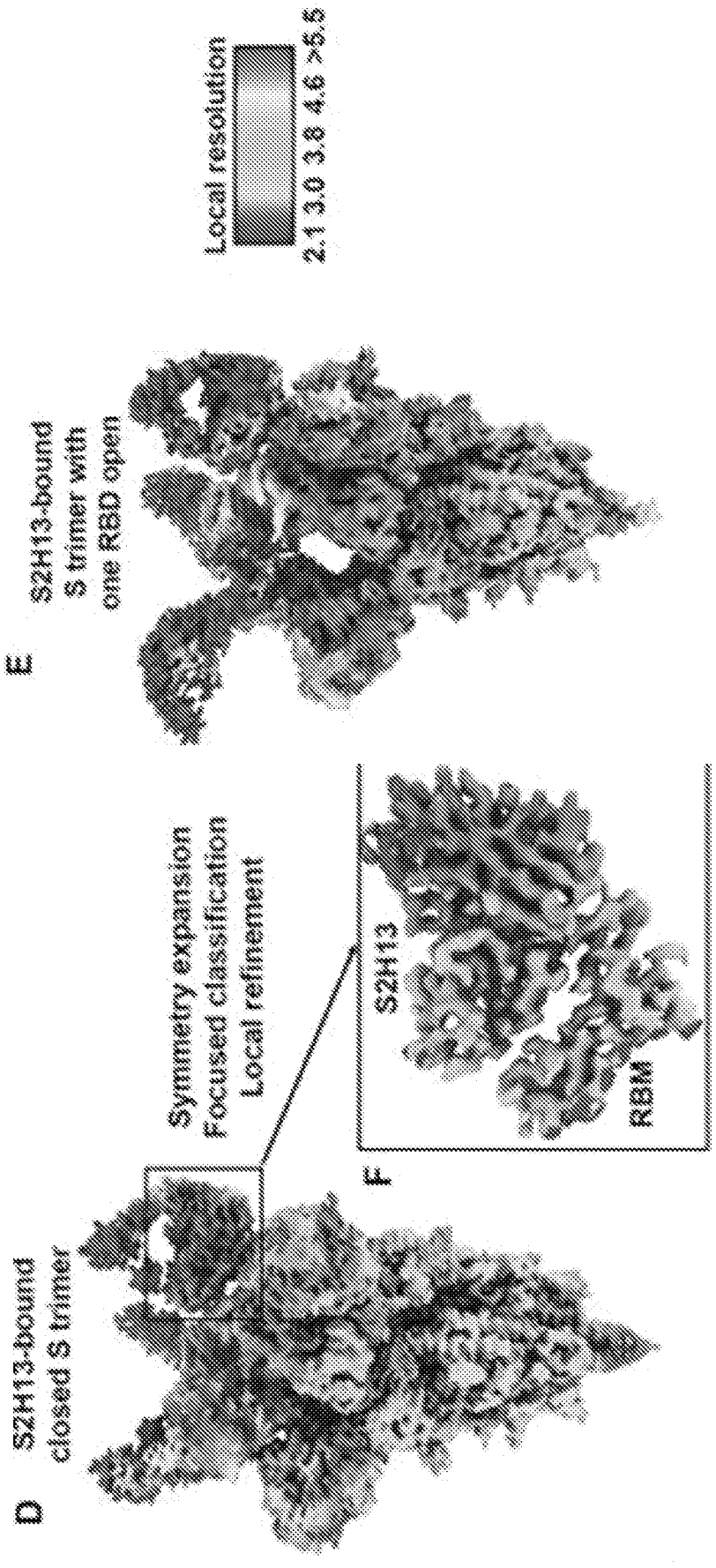

D
S2H13-bound
closed S trimer
Symmetry expansion
Focused classification
Local refinement
F
S2H13
RBM
E
S2H13-bound
S trimer with
one RBD open
Local resolution
2.1 3.0 3.8 4.6 >5.5

FIG. 53

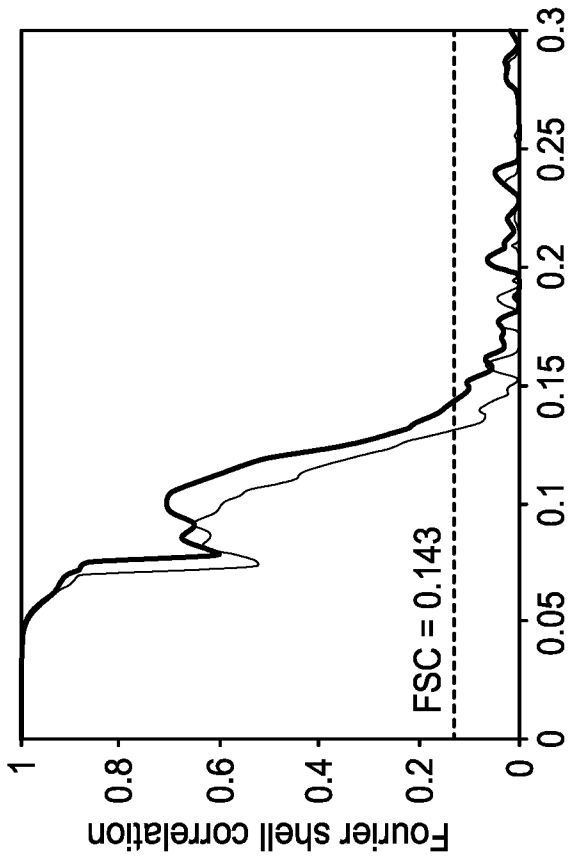


FIG. 53I

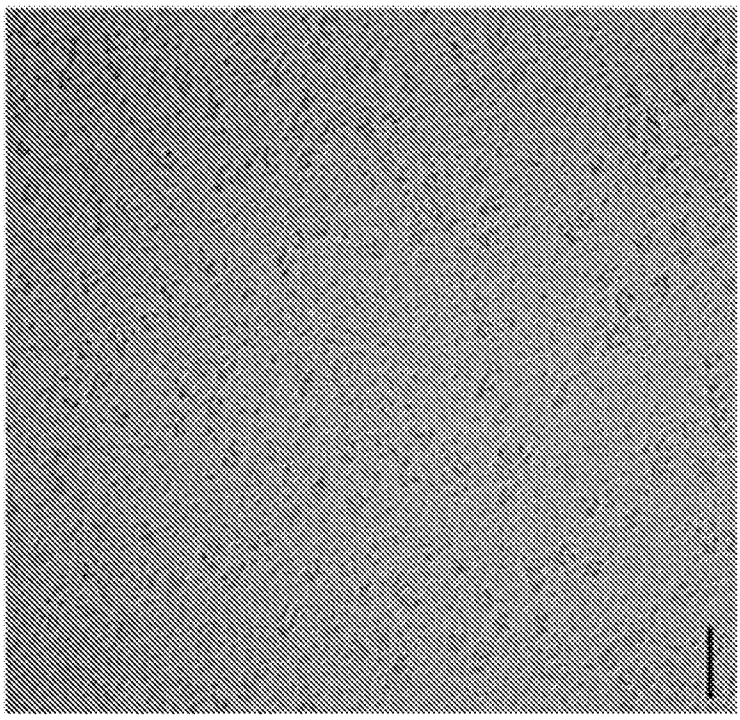


FIG. 53G



FIG. 53H

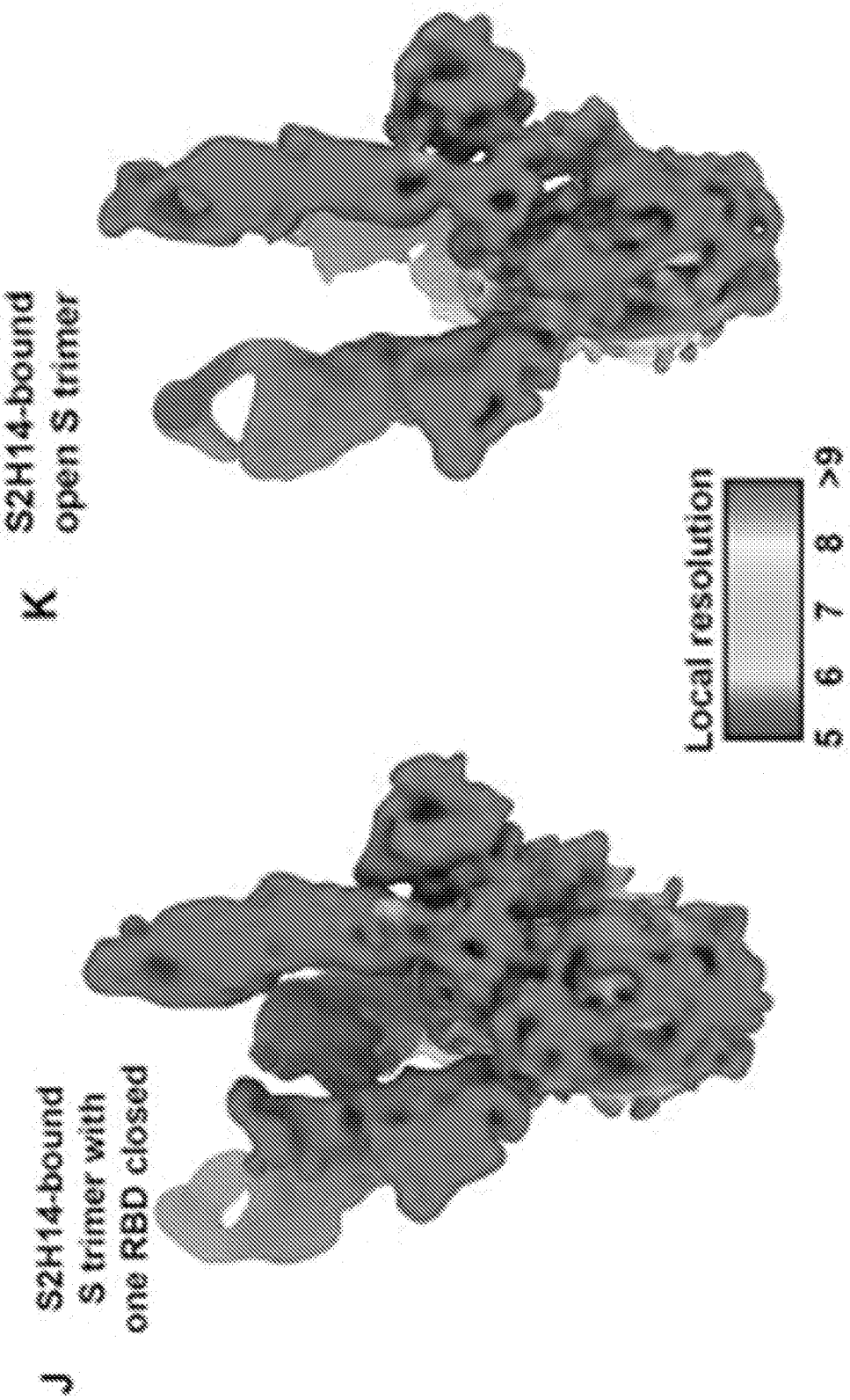

J
S2H14-bound
S trimer with
one RBD closed
K
S2H14-bound
open S trimer
Local resolution
5 6 7 8 >9

FIG. 53

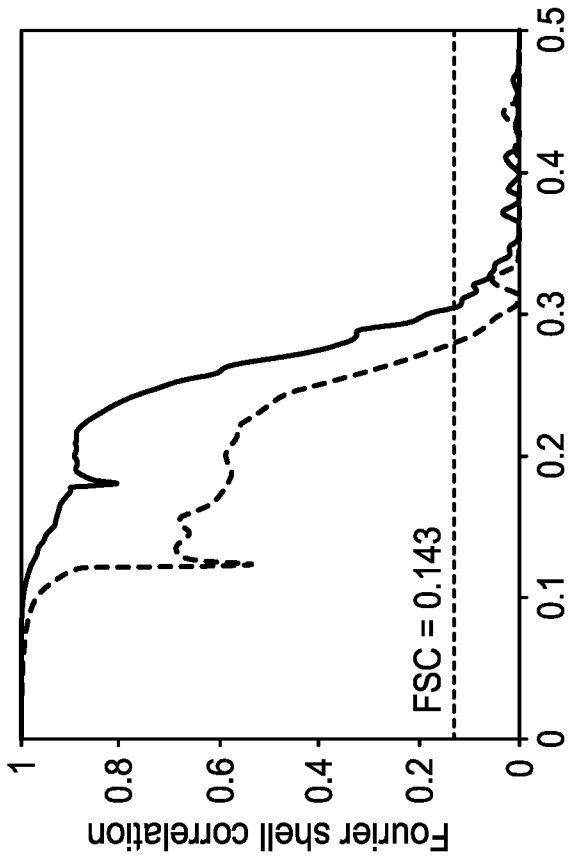


FIG. 54C

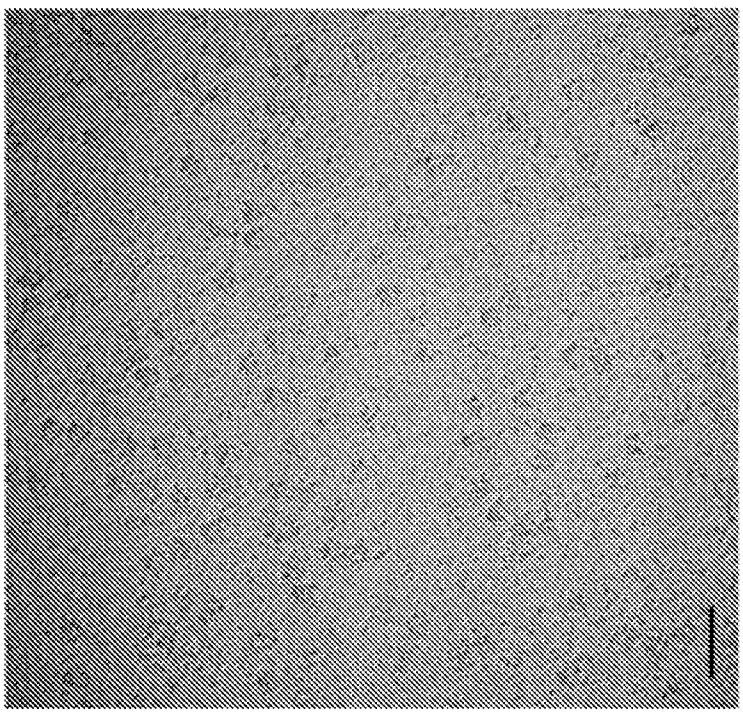


FIG. 54A



FIG. 54B

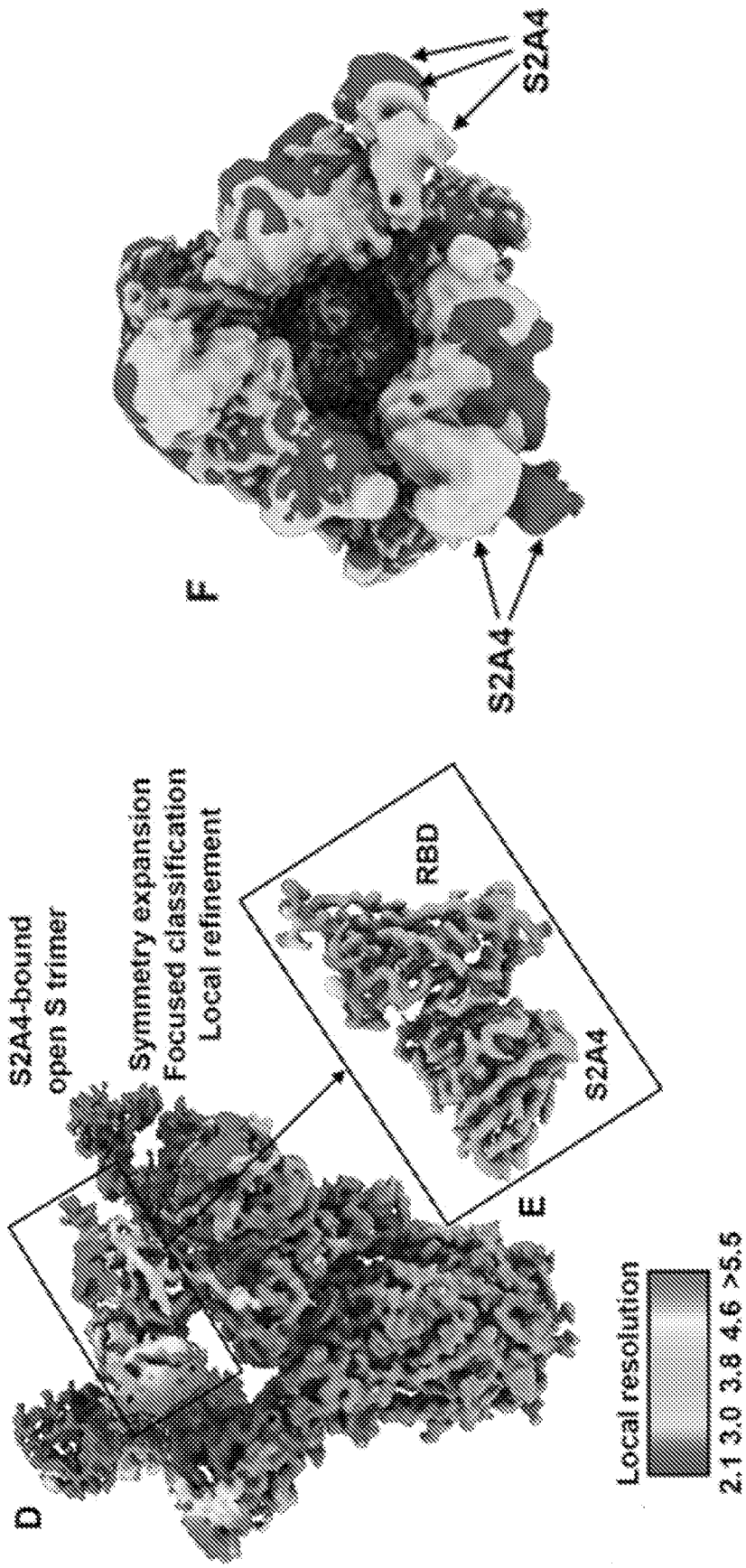

S2A4
F
S2A4
S2A4-bound
open S trimer
Symmetry expansion
Focused classification
Local refinement
RBD
S2A4
E
D
Local resolution
2.1 3.0 3.8 4.6 >5.5

FIG. 54

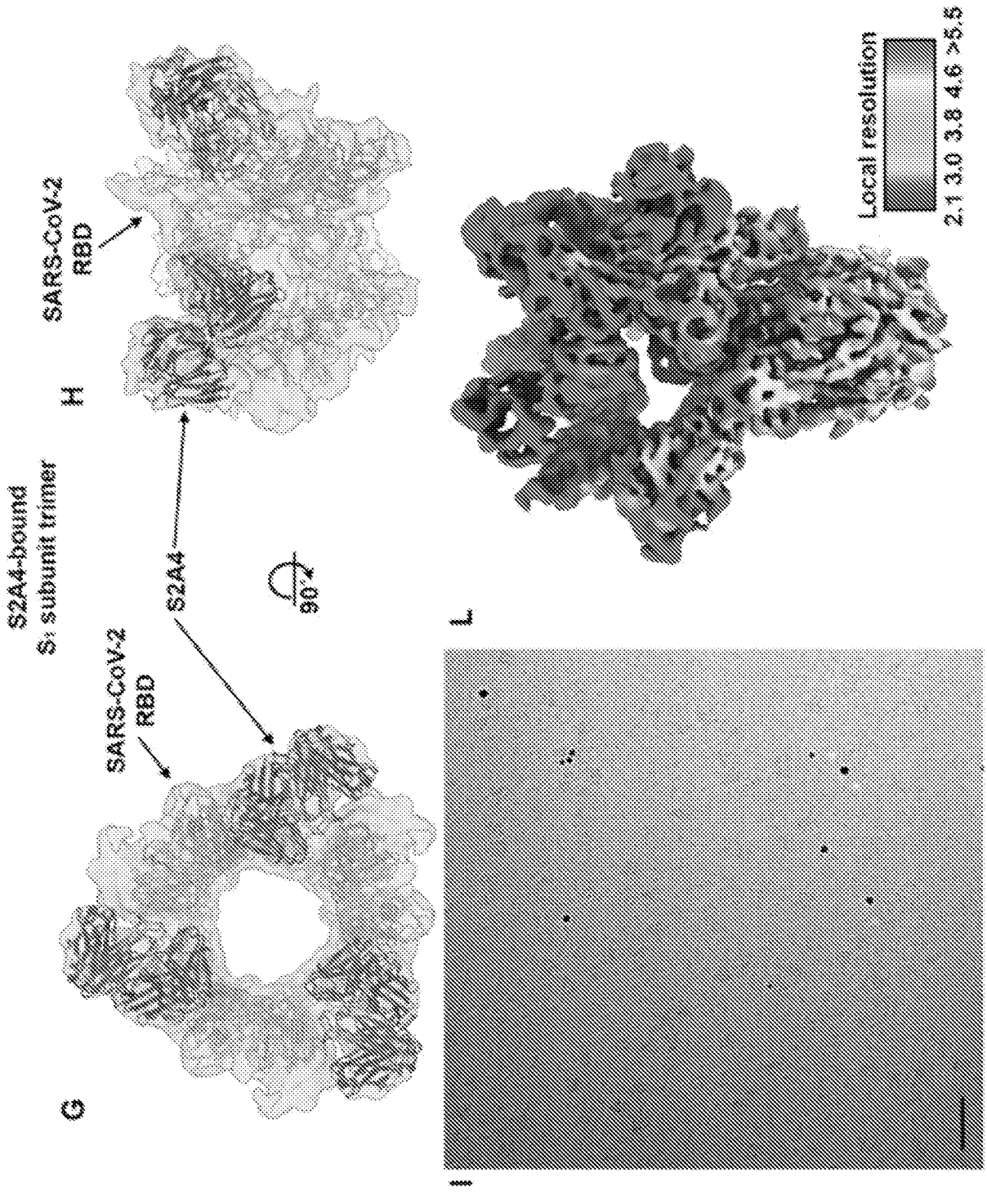

G
SARS-CoV-2 RBD
S2A4
S2A4-bound S1 subunit trimer
90°
H
SARS-CoV-2 RBD
I
J
L
Local resolution
2.1 3.0 3.8 4.6 >5.5

FIG. 54

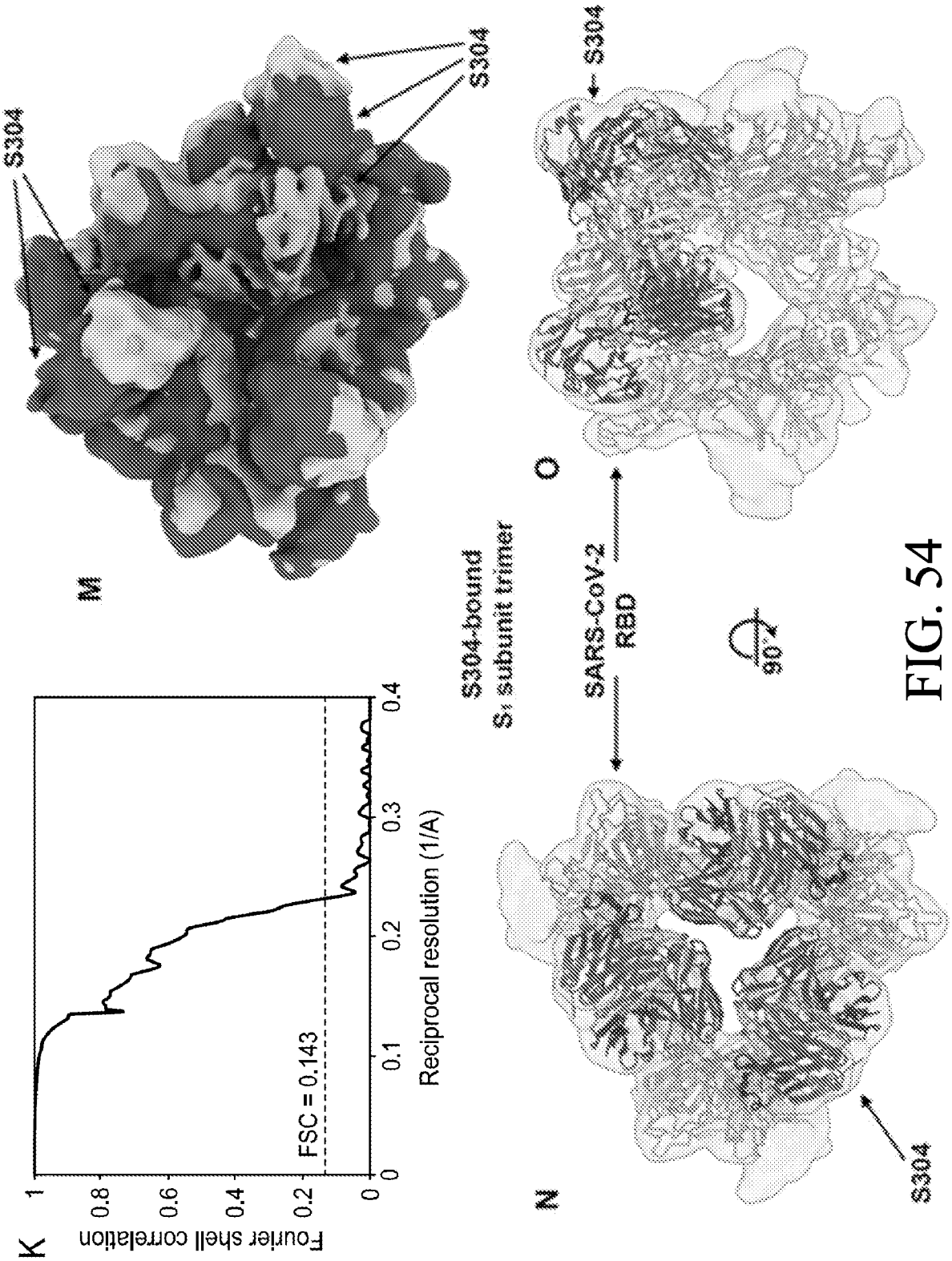

K
Fourier shell correlation
1
0.8
0.6
0.4
0.2
0
0
0.1
0.2
0.3
0.4
Reciprocal resolution (1/A)
FSC = 0.143
M
S304
S304
S304-bound
S1 subunit trimer
SARS-CoV-2
RBD
90°
N
O
S304
S304

FIG. 54

INTERNATIONAL SEARCH REPORT

International application No
PCT/US2021/035782

A. CLASSIFICATION OF SUBJECT MATTER
INV. A61P31/14 C07K16/10
ADD.

According to International Patent Classification (IPC) or to both national classification and IPC

B. FIELDS SEARCHED

Minimum documentation searched (classification system followed by classification symbols)
A61P A61K C07K

Documentation searched other than minimum documentation to the extent that such documents are included in the fields searched

Electronic data base consulted during the international search (name of data base and, where practicable, search terms used)
EPO-Internal, BIOSIS, EMBASE, WPI Data

C. DOCUMENTS CONSIDERED TO BE RELEVANT

Category*	Citation of document, with indication, where appropriate, of the relevant passages	Relevant to claim No.
X	MENG YUAN ET AL: "A highly conserved cryptic epitope in the receptor binding domains of SARS-CoV-2 and SARS-CoV", SCIENCE, vol. 368, no. 6491, 8 May 2020 (2020-05-08), pages 630-633, XP055707792, DOI: DOI: 10.1126/science.abb7269 figures 1,2,4 ----- -/--	2

[X] Further documents are listed in the continuation of Box C. [ ] See patent family annex.

* Special categories of cited documents :

"A" document defining the general state of the art which is not considered to be of particular relevance

"E" earlier application or patent but published on or after the international filing date

"L" document which may throw doubts on priority claim(s) or which is cited to establish the publication date of another citation or other special reason (as specified)

"O" document referring to an oral disclosure, use, exhibition or other means

"P" document published prior to the international filing date but later than the priority date claimed

"T" later document published after the international filing date or priority date and not in conflict with the application but cited to understand the principle or theory underlying the invention

"X" document of particular relevance; the claimed invention cannot be considered novel or cannot be considered to involve an inventive step when the document is taken alone

"Y" document of particular relevance; the claimed invention cannot be considered to involve an inventive step when the document is combined with one or more other such documents, such combination being obvious to a person skilled in the art

"&" document member of the same patent family

Date of the actual completion of the international search	Date of mailing of the international search report
5 October 2021	14/10/2021

Name and mailing address of the ISA/	Authorized officer
European Patent Office, P.B. 5818 Patentlaan 2 NL - 2280 HV Rijswijk Tel. (+31-70) 340-2040, Fax: (+31-70) 340-3016	Cilensek, Zoran

1

Form PCT/ISA/210 (second sheet) (April 2005)

INTERNATIONAL SEARCH REPORT

International application No.
PCT/US2021/035782

Box No. I Nucleotide and/or amino acid sequence(s) (Continuation of item 1.c of the first sheet)

1. With regard to any nucleotide and/or amino acid sequence disclosed in the international application, the international search was carried out on the basis of a sequence listing:

   a. [X] forming part of the international application as filed:

      [X] in the form of an Annex C/ST.25 text file.

      [ ] on paper or in the form of an image file.

   b. [ ] furnished together with the international application under PCT Rule 13*ter*.1(a) for the purposes of international search only in the form of an Annex C/ST.25 text file.

   c. [ ] furnished subsequent to the international filing date for the purposes of international search only:

      [ ] in the form of an Annex C/ST.25 text file (Rule 13*ter*.1(a)).

      [ ] on paper or in the form of an image file (Rule 13*ter*.1(b) and Administrative Instructions, Section 713).

2. [ ] In addition, in the case that more than one version or copy of a sequence listing has been filed or furnished, the required statements that the information in the subsequent or additional copies is identical to that forming part of the application as filed or does not go beyond the application as filed, as appropriate, were furnished.

3. Additional comments:

C(Continuation). DOCUMENTS CONSIDERED TO BE RELEVANT

Category*	Citation of document, with indication, where appropriate, of the relevant passages	Relevant to claim No.
X	SHI RUI ET AL: "A human neutralizing antibody targets the receptor-binding site of SARS-CoV-2", NATURE, MACMILLAN JOURNALS LTD., ETC, LONDON, vol. 584, no. 7819, 26 May 2020 (2020-05-26), pages 120-124, XP037211681, ISSN: 0028-0836, DOI: 10.1038/S41586-020-2381-Y [retrieved on 2020-05-26] figure 4f	2
A	PINTO DORA ET AL: "Cross-neutralization of SARS-CoV-2 by a human monoclonal SARS-CoV antibody", NATURE, MACMILLAN JOURNALS LTD., ETC, LONDON, vol. 583, no. 7815, 18 May 2020 (2020-05-18), pages 290-295, XP037289888, ISSN: 0028-0836, DOI: 10.1038/S41586-020-2349-Y [retrieved on 2020-05-18] the whole document	2
T	TORTORICI M. ALEJANDRA ET AL: "Broad sarbecovirus neutralization by a human monoclonal antibody", NATURE, vol. 597, no. 7874, 2 September 2021 (2021-09-02), pages 103-108, XP055845075, London ISSN: 0028-0836, DOI: 10.1038/s41586-021-03817-4 Retrieved from the Internet: URL:https://www.nature.com/articles/s41586-021-03817-4.pdf> the whole document	2
A,P	PICCOLI LUCA ET AL: "Mapping Neutralizing and Immunodominant Sites on the SARS-CoV-2 Spike Receptor-Binding Domain by Structure-Guided High-Resolution Serology", CELL, ELSEVIER, AMSTERDAM NL, vol. 183, no. 4, 16 September 2020 (2020-09-16), page 1024, XP086341451, ISSN: 0092-8674, DOI: 10.1016/J.CELL.2020.09.037 [retrieved on 2020-09-16] the whole document	2

-/--

1

INTERNATIONAL SEARCH REPORT

International application No
PCT/US2021/035782

C(Continuation). DOCUMENTS CONSIDERED TO BE RELEVANT

Category*	Citation of document, with indication, where appropriate, of the relevant passages	Relevant to claim No.
A,P	WEC ANNA Z. ET AL: "Broad neutralization of SARS-related viruses by human monoclonal antibodies", SCIENCE, vol. 369, no. 6504, 15 June 2020 (2020-06-15), pages 731-736, XP055845076, US ISSN: 0036-8075, DOI: 10.1126/science.abc7424 figures 3,4 -----	2

1

INTERNATIONAL SEARCH REPORT

International application No.
PCT/US2021/035782

Box No. II Observations where certain claims were found unsearchable (Continuation of item 2 of first sheet)

This international search report has not been established in respect of certain claims under Article 17(2)(a) for the following reasons:

1. ☐ Claims Nos.:
because they relate to subject matter not required to be searched by this Authority, namely:

2. ☒ Claims Nos.: 1, 3-69
because they relate to parts of the international application that do not comply with the prescribed requirements to such an extent that no meaningful international search can be carried out, specifically:
see FURTHER INFORMATION sheet PCT/ISA/210

3. ☐ Claims Nos.:
because they are dependent claims and are not drafted in accordance with the second and third sentences of Rule 6.4(a).

Box No. III Observations where unity of invention is lacking (Continuation of item 3 of first sheet)

This International Searching Authority found multiple inventions in this international application, as follows:

1. ☐ As all required additional search fees were timely paid by the applicant, this international search report covers all searchable claims.

2. ☐ As all searchable claims could be searched without effort justifying an additional fees, this Authority did not invite payment of additional fees.

3. ☐ As only some of the required additional search fees were timely paid by the applicant, this international search report covers only those claims for which fees were paid, specifically claims Nos.:

4. ☐ No required additional search fees were timely paid by the applicant. Consequently, this international search report is restricted to the invention first mentioned in the claims; it is covered by claims Nos.:

Remark on Protest

☐ The additional search fees were accompanied by the applicant's protest and, where applicable, the payment of a protest fee.

☐ The additional search fees were accompanied by the applicant's protest but the applicable protest fee was not paid within the time limit specified in the invitation.

☐ No protest accompanied the payment of additional search fees.

FURTHER INFORMATION CONTINUED FROM PCT/ISA/ 210

Continuation of Box II.2

Claims Nos.: 1, 3-69

The present application contains multiple independent claims in the same category.
The claims also cover subject-matter which cannot be meaningfully searched, as explained herein below.
Claim 1 is directed to an antibody, or an antigen-binding fragment thereof, that competes with an antibody or antigen-binding fragment comprising a VH amino acid sequence according to SEQ ID NO: 16 and a VL amino acid sequence according to SEQ ID NO: 26 for binding to a SARS-CoV-2 S glycoprotein of a S glycoprotein trimer.
However, if an antibody comprising SEQ ID NO:16 and 26 does not form part of the state of the art, the prior art antibodies could not be, even theoretically, characterized in respect of this property.
Similar considerations apply to claims 2 and 3. In the absence of evidence to the contrary, the prior art antibodies can be considered to bind or not bind "one or more" of said amino acids.
In the same vein, similar considerations apply to claims 4 and 5.
Claims 6-20 and 22-29 suffer from similar defects.
Claim 21 is considered to lack clarity, since it is not apparent under which conditions said binding takes place and what is meant by the feature " promotes or leads to release of the S1 subunit"
Claim 31 is regarded to lack clarity, since it is open what is mean by the feature "neutralizing an infection by a SARS-CoV-2" and under which conditions and how is said effect determined.
By way of dependency, claims 32- 39 suffer from similar defects.
Similar considerations apply to claim 40, items (d)-(h), since the claim relies on the internal designations. In addition, proteins are commonly defined by their sequence, rather than by the ability of being recognized by this or another agent, such as an antibody.
At least some of said defects are recognized in claims 41-45.
Claim 46 appears prima facie not to suffer from the above effects but it is not immediately apparent how it relates to the remaining subject-matter.
Claims 47-50 and 52 appear to suffer from at least some of the defects discussed herein above.
Claim 54 does not only suffer from the above defects by way of dependency but also suffers from further defects. In the absence of a reference point to compare the required enhancement in binding, it is not possible to ascertain, even theoretically, what is covered by the

FURTHER INFORMATION CONTINUED FROM PCT/ISA/ 210

claim.
Claims 55-57 and 59-69 suffer from similar defects.
With their
submissions dated 09-09-2021, the Applicant indicated that the subject-matter of claim 2 be searched. The search is carried out accordingly.

The applicant's attention is drawn to the fact that claims relating to inventions in respect of which no international search report has been established need not be the subject of an international preliminary examination (Rule 66.1(e) PCT). The applicant is advised that the EPO policy when acting as an International Preliminary Examining Authority is normally not to carry out a preliminary examination on matter which has not been searched. This is the case irrespective of whether or not the claims are amended following receipt of the search report or during any Chapter II procedure. If the application proceeds into the regional phase before the EPO, the applicant is reminded that a search may be carried out during examination before the EPO (see EPO Guidelines C-IV, 7.2), should the problems which led to the Article 17(2) PCT declaration be overcome.